Toshio Yamaguchi

26th International Conference on Solution Chemistry

26ICSC

Abstracts of Papers

26th
I.C.S.C.

July 26-31, 1999

Fukuoka, Japan

Welcome Message

Distinguished Guests, Ladies and Gentlemen:

On behalf of the Organizing Committee of the 26th International Conference on Solution Chemistry, I wish to express our hearty welcome to all participants from abroad and Japan.

Solutions, especially aqueous solutions, are a very familiar and daily used substance of human beings and have attracted interests of scientists from their unique properties and the important role as a field of chemical reactions. When we look back the history of solution chemistry, we find many names of pioneers of modern chemistry in the field of solution chemistry started at the end of the 19th Century; they are, for instance, van't Hoff, Arrhenius, Ostwald, Nernst, and even Werner.

In Japan, solution chemistry was the most important and fashionable chemistry at the beginning of the 20th Century. Professor Joji Sakurai of the Imperial University of Tokyo, who was a leading scientist of Japan at the Meiji Era, was a physical chemist who studied chemistry of solutions. Both Prof. Ikeda and Prof. Ohsaka studied chemistry at the laboratory of Prof. Ostwald in Germany. After the initial rapid development of solution chemistry in the early 20th Century as a part of physical chemistry in Japan, the subjects to be involved were extended to those of inorganic and analytical chemistry and even biochemistry and polymer chemistry in recent years.

The first challenge of Japanese group of solution chemistry to join the international society was undertaken in 1982 by organizing the 6th International Symposium on Solute-Solute-Solvent Interactions at Minoo, Osaka. Even now, some of the participants may remember the success of the symposium, and since then, Japan has been accepted as a member of solution chemistry society of the world.

After the 6th ISSSSI Japan has organized many international conferences related to solution chemistry, and then, Japan becomes one of the most active members with the world-leading scientific standard of solution chemistry. The 26th International Conference on Solution Chemistry was thus organized to show the trace of the progress of Japan's Solution Chemistry to the world after 1982, and to exchange most recent knowledge about chemistry of solutions among scientists in the world.

Now, Ladies and Gentlemen; we have the 26th International Conference on Solution Chemistry in Fukuoka City, which was the gate of the oriental culture from Korea and China, and even India and Pakistan through these countries. The venue is most suitable to be the new gate to new solution chemistry of the 21st Century. I hope that all participants will look forward to aiming at new targets of solution chemistry in the next century in order to create new scopes of science and technology of water and solutions through discussions, and they will also enjoy the culture and landscape of Kyushu and delicious foods from the Japan Sea.

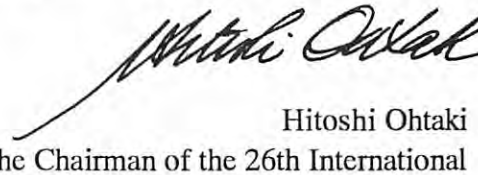

Hitoshi Ohtaki
The Chairman of the 26th International
Conference on Solution Chemistry

26th International Conference on Solution Chemistry

has been organized under the auspices of

The Science Council of Japan
The Chemical Society of Japan
Association of Japanese Solution Chemists

and under the sponsorship of

International Union of Pure and Applied Chemistry

We express sincere gratitude to the following organizations for financial support:

The Commemorative Association for the Japan World Exposition (1970)
The Asahi Glass Foundation
Uehara Memorial Foundation
The Ogasawara Foundation for the Promotions of Science and Engineering
The Kumagai Foundation for the Promotions of Science and Engineering
Tokyo Ohka Foundation for the Promotions of Science and Engineering
The Kao Foundation for Arts and Science
Suntory Institute for Bioorganic Research
The Chemical Society of Japan (Kyushu Branch)
The Japan Society for Analytical Chemistry
Yokatopia Foundation
Promotion Council of Northern Kyushu Science Cities' Development Plan
Fukuoka Industry, Science & Technology Foundation
Research Institute of Innovative Technologies for the Earth
Osaka Pharmaceutical Manufacturers Association
The Pharmaceutical Manufacturers Association of Tokyo

and many private companies.

1. Organization

National Organizing Committee

H. Ohtaki (Ritsumeikan University) *Chair*
H. Nomura (Nagoya University) *Vice-chair*
S. Ishiguro (Kyushu University) *Secretary*

H. Akaiwa (Gunma University)
T. Akiyoshi (Shionogi & Co. Ltd.) *Chair of Fund Raising Subcommittee*
M. Aratono (Kyushu University)
F. Hirata (Institute for Molecular Science)
M. Kai (Daicel Chemical Industries, Ltd.) *Vice- Chair of Fund Raising Subcommittee*
S. Kaizaki (Osaka University)
H. Kanno (National Defense Academy)
H. Maeda (Kyushu University)
T. Miyajima (Kyushu University) *Chair of Tour Program Subcommittee*
A. Morita (The University of Tokyo)
M. Nakahara (Kyoto University) *Chair of Publication Subcommittee*
I. Okada (Sofia University) *Vice- Chair of Fund Raising Subcommittee*
H. Ogawa (Tokyo Denki University)
T. Ogawa (Kyushu University)
K. Ozutsumi (Ritsumeikan University)
Y. Sasaki (Hokkaido University)
K. Sawada (Niigata University)
M. Tabata (Saga University) *Chair of Public Relations Subcommittee*
I. Taniguchi (Kumamoto University) *Vice- Chair of Fund Raising Subcommittee*
Y. Taniguchi (Ritsumeikan University)
T. Tominaga (Okayama University of Science) *Chair of Program Subcommittee*
T. Tomura (The Chemical Society of Japan) *Chair of Treasury Subcommittee*
T. Yamaguchi (Fukuoka University) *Chair of Local Arrangement Subcommittee*
H. Yokoyama (Yokohama City University)
K. Yoshihara (Japan Advanced Institute of Science and Technology, Hokuriku)
H. Wakita (Fukuoka University) *Chair of Financial Subcommittee*

International Steering Committee

J. B. Gill (UK) *Chair*
Late V. Gutmann (Austria) *Honorary Member*
A. I. Popov (USA) *Honorary Member*
J. Barthel (Germany)
L. Blum (USA)
G. Gritzner (Austria)
H. Ohtaki (Japan)
I. Persson (Sweden)
P. Turq (France)
C. A. N. Viana (Portugal)
M. Zeidler (Germany)

National Advisory Board

Prof. Emeritus M. Tanaka (Nagoya University) *Chair*
Prof. Emeritus S. Ikeda (Osaka University)
Prof. Emeritus H. Inokuchi (Institute for Molecular Science)
Late Prof. Emeritus K. Saito (Tohoku University)
Prof. Emeritus K. Suzuki (Ritumeikan University)
Prof. Emeritus S. Seki (Osaka University)
Prof. Emeritus N. Tanaka (Tohoku University)
Prof. Emeritus H. Yamatera (Nagoya University)
Prof. Emeritus T. Yamamoto (Kyoto University)
Prof. Emeritus Y. Yamamoto (Hiroshima University)

Program Subcommittee

T. Tominaga (Okayama University of Science), *Chair*

Sessions

(S1) *Theoretical approaches and computer simulations*
Susumu Okazaki (Tokyo Institute of Technology, Japan)

(S2) *Structure, dynamics, and fluctuations*
Masaru Nakahara (Kyoto University)

(S3) *Structure thermodynamics, kinetics and reaction mechanisms of coordination compounds in solution*
Masaaki Tabata (Saga University)

(S4) *Chemical thermodynamics in solution*
Takayoshi Kimura (Kinki University)

(S5) *Analytical and environmental aspects in solution chemistry*
Tohru Miyajima (Saga University)

(S6) *Bioinorganic and pharmaceutical chemistry*
Akira Odani (Nagoya University) and Helmut Sigel (University of Basel)

(S7) *Polymers, colloids and interfaces in the solution phase*
Hiroshi Maeda (Kyushu University)

(S8) *The role of the reaction field in organic chemistry: Theory and experiment*
Hiroshi Yamataka (Osaka University)

(S9) *Industrial applications of solution chemistry*
Isao Taniguchi (Kumamoto University)

Minisymposia

(M1) *Equilibrium and non-equilibrium theories of molecular liquids*
Fumio Hirata (Institute of Molecular Science)

(M2) *Fast reaction dynamics in solution*
Tadashi Okada (Osaka University)

(M3) *Recent progress in redox chemistry of coordination compounds and metalloenzymes*
Yoichi Sasaki (Hokkaido University)

(M4) *Hydrophobic interactions in complex and organized systems*
Shinobu Koda (Nagoya University)

(M5) *Recent progress of nonaqueous and mixed solvents in analytical and inorganic chemistry*
Haruhiko Yokoyama (Yokohama City University)

(M6) *How much do we know about water at the molecular level?*
Hiroyasu Nomura (Nagoya University)

Contents

Plenary Lectures

ELECTRON TUNNELING IN BIOLOGICAL MOLECULES

Harry B. GRAY
Beckman Institute, California Institute of Technology, Pasadena, CA, 91125 USA

Electron transfers are key steps in photosynthesis, respiration, drug metabolism, and many other biological processes. These reactions commonly occur between protein-bound prosthetic groups that are separated by large molecular distances (often greater than 10 Å). Although the electron donors and acceptors are expected to be weakly coupled, the reactions are remarkably fast and proceed with high specificity. Our work in this area, which has utilized ruthenium-modified heme (**Figure 1**) and copper proteins, has shown that the structure of the intervening polypeptide potentially can control many of these reaction rates. This work has been extended to include the use of substrate-linker-ruthenium sensitizers to trigger redox reactions at enzyme active sites. By rapid flash-quench oxidation of bound ruthenated substrates, it has been possible to generate high-valent forms of cytochrome P450.

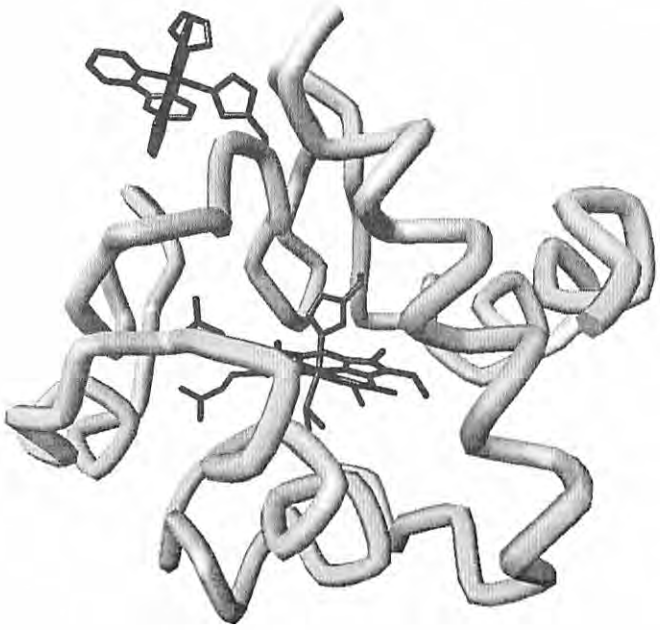

Figure 1. Structure of Ru(His33)-cytochrome *c*

SOLUTION STRUCTURE OF PARAMAGNETIC METALLOPROTEINS

IVANO BERTINI

University of Florence, Magnetic Resonance Center, Via Luigi Sacconi 6, 50019 Sesto F.no, Florence. Italy

The solution structure of several Fe-S proteins and cytochromes, which are electron transfer proteins, will be presented in thc oxidized and reduced species. It will be shown that the reduced forms of high potential Fe-S proteins and cytochromes have a smaller mobility than when they are in the oxidized species. This is true both in the milli- to micro-seconds and in the nano- to pico-seconds ranges. Changes associated with the electron transfer process will be discussed.

NEW HORIZONS IN HYDROGEN BONDED CLUSTERS IN SOLUTION

Toshio YAMAGUCHI
Department of Chemistry, Fukuoka University, Fukuoka 814-0180, Japan

Over the last two decades the advent of intense synchrotron radiation and pulsed neutron sources and two dimensional area detectors of imaging plate and CCD has developed X-ray and neutron diffraction and X-ray absorption spectroscopy for microscopic investigations of the structure and dynamic properties of liquids and solutions over a wide range of temperatures, pressures, and concentrations from glassy and supercooled to supercritical states, and furthermore computer simulation techniques based on the experiment data have enabled us to reveal three-dimensional pictures of the liquids and solutions.

With the help of these breakthroughs in solution structural chemistry, a lot of efforts have recently been made to manifest the structure of hydrogen bonded clusters in solution on the molecular level and to explicate various anomalies in physico-chemical quantities of liquid and liquid mixtures and characteristic behaviors in chemical reactions taking place in solution from the microscopic structures of the clusters.

Several of the examples will be described, such as disproportionation-type reactions in aqueous glassy and supercooled solution, decomposition reactions of organic wastes in supercritical water, micelle formation and protein folding in water-alcohol binary mixtures.

Some perspectives of structural solution chemistry in the 21st century will be briefly mentioned.

M. Matsumoto, N. Nishi, T. Furusawa, M. Saita, T. Takamuku, M. Yamagami, and T. Yamaguchi, *Bull. Chem. Soc. Jpn.*, **68**, 1775-1783 (1995).

M. Nakahara, T. Yamaguchi, and H. Ohtaki, *Recent Research Development in Physical Chemistry*, **1**, 17-49 (1997).

H. Ohtaki, T. Radnai, and T. Yamaguchi, *Chem. Soc. Rev.*, 41-51 (1997).

T. Yamaguchi, *J. Mol. Liq.*, **78**, 43-50 (1998).

T. Yamaguchi and A. K. Soper, *J. Chem. Phys.*, **110**, 3529-3535 (1999).

HYDRATION AND ELECTROSTATIC INTERACTIONS BETWEEN HYDROPHILIC MOLECULES AND SURFACES IN AQUEOUS SOLUTIONS

J. N. Israelachvili

Department of Chemical Engineering, and Materials Department,
University of California, Santa Barbara, California 93106, USA.

The Surface Forces Apparatus (SFA) allows one to measure various interaction forces between surfaces as a function of their separation in aqueous solutions. In addition, the optical technique used allows one to directly visualize various interfacial phenomena (such as slow structural rearrangements) that may be occurring during an interaction. In this way, complex colloidal interactions – such as typically occur in gels, polyelectrolyte solutions and biocolloidal systems – may be studied at the molecular level both in space and time. Recent SFA (and other) results on a variety of hydrocolloidal and biopolymer systems show that these have much more complex and time-dependent interaction potentials than normally occur between simpler colloidal surfaces, i.e., their interactions are not simply described by van der Waals attraction and electrostatic repulsion which are the two principal forces of the Derjaguin-Landau-Verwey-Overbeek (DLVO) theory [1].

After briefly describing how such interactions can be measured and visualized, a review will be given of the various types of forces that can arise, sometimes simultaneously, between complex biomolecules and surfaces in aqueous solutions. These include van der Waals, ionic, electrostatic, structural, hydration, hydrophobic, polymer-mediated, thermal fluctuation and bio-specific interactions, and specific examples are given of how of these arises.

These recent results show that – even though all forces have a common origin – biocolloidal interactions can differ from normal, non-specific "colloidal" interactions in three important ways: (1) biological, especially bio-specific, interactions are qualitatively different in that many molecular groups are often involved "sequentially" (in different regions of space and time) in such a way that "the whole is greater than the sum of the parts", (2) interacting bio-colloidal surfaces are usually 'asymmetric' which, as will be shown, gives rise to very different interactions than those that arise between similar (symmetric) surfaces, and (3) non-equilibrium and time effects often play a crucial role in regulating biological interactions.

It is unlikely that a single, generic interaction potential can be written that covers all possible situations, but careful consideration of the surfaces, the molecules and solution conditions should allow reasonable predictions to be made in many cases.

NEW RESULTS FOR NMR RELAXATION IN LIQUIDS

M. D. ZEIDLER

Institute of Physical Chemistry, RWTH, Templergraben 59, D-52056 Aachen, Germany

NMR relaxation provides a powerful method for the study of molecular motion in liquids. Depending on the specific relaxation mechanism either the translational or the rotational motion may be studied. In some cases, like the dipolar relaxation mechanism, both motions contribute to the mechanism, and consequently the contributions must be separated from each other. For this purpose isotopic substitution experiments prove to be very useful. Since temperature and pressure dependence of the relaxation can be studied, we obtain information on how the molecular motion depends on these external parameters.

Examples of such recent studies in our laboratory will be presented. In particular I will report on the following topics: For water, ammonia and acetonitrile the isotopy effect between hydrogen and deuterium substituted compounds on the rotational motion was measured. The rotational motion of X-H bonds, where X may be oxygen or nitrogen, was studied with the aim to get information on the strength of the hydrogen bond. In addition, when making use of the quadrupolar relaxation, the nuclear quadrupole coupling constant can be extracted which also reflects the hydrogen bond strength. Inclusion compounds like water clathrates are interesting objects in order to study the highly mobile liquid-like motion of the organic guest molecules. In this case the guest which determines the water structure of its cage can be varied in size, and the influence on the mobility can be followed.

Oral Presentations

Many-body interactions and the properties of molten ionic mixtures

Paul A. Madden
Physical and Theoretical Chemistry Laboratory, University of Oxford, South Parks Road, Oxford OX1 3QZ, UK.

Many binary systems (and their mixtures) which might be expected to be "ionic", from electronegativity considerations, are found to exhibit pronounced "covalent effects" in their condensed phase structure and dynamical properties. An extreme example is $AlCl_3$, which melts from an ionic crystal to form a non-conducting molecular liquid. Uncertainty as to the origin of the "covalent" interactions responsible for this behaviour has inhibited attempts to explore these liquids theoretically and with computer simulations. Recent work [1], involving both electronic structure calculations and computer simulation, has suggested that the interactions arise and are describeable within the ionic model – provided that it is realised that anions in the condensed phase have profoundly different properties from their free counterparts as a consequence of the strong confining potential exerted on the anionic electron density by surrounding ions. Depending on the precise shape of the potential (which, in thermal motion, will vary from one instant to the next), the anion may be more-or-less compressed, deformed and polarized and hence its interaction potential with the other ions in the system will also vary. Only for the simplest ionic systems (*e.g.* alkali halides) can this variation be neglected and the interactions described by some average pair potential.

In systems where they are substantial, the many-body effects promote remarkably rich changes in the intermediate-range structure of the liquid. $AlCl_3$ becomes molecular [2], $BeCl_2$ a "living polymer" of extended chains [3], and the distinctive IRO of the 3-d network, glass-forming systems $ZnCl_2$ [4], BeF_2 and SiO_2 is reproduced. The structural changes have considerable dynamical consequences; for $ZnCl_2$ the slow structural relaxation, leading to the glass transition, may be traced back to the relaxation of the IRO. On shorter timescales (higher frequency) these liquids exhibit spectroscopic bands usually assigned to quasi-molecular units. The validity of this viewpoint, and its relationship to the "ionic" picture of these melts, more frequently adopted in diffraction studies, may be explored [5].

1. M. Wilson and P.A. Madden *Chem. Soc. Rev.* **25**, 339 (1996).
2. F. Hutchinson *et al J. Chem. Phys.* **110**, 5821 (1999).
3. M. Wilson and P.A. Madden *Molec. Phys.* **92**, 197 (1997).
4. M. Wilson and P.A. Madden *Phys. Rev. Lett.* **80**, 532 (1998).
5. M. C. C. Ribeiro *et al J. Chem. Phys.* **110**, 4803 (1999).

IMPORTANCE OF INTERFACIAL PHENOMENA IN LIQUID-LIQUID EXTRACTION: COMPUTER SIMULATIONS ON THE DEMIXING OF WATER - OIL SOLUTIONS OF SALTS AND IONOPHORES

Marc BAADEN and Georges WIPFF *
Institut de Chimie, Université Louis Pasteur, 4, rue B. Pascal, Strasbourg, 67000, France

Computer simulations contribute to our understanding of phase separation in liquid-liquid extraction of ions by ionophores. [1,2] We describe results of molecular dynamics (MD) simulations on the demixing of "perfectly mixed" binary water-chloroform solutions of cations and ionophores, which demonstrate the importance of interfacial phenomena during the early steps of liquid separation. In all cases, microscopic phase separation is rapid (about 1 nanosecond), leading to water-oil interfaces where the extractants adsorb. The outcome of the phase separation is compared with MD simulations at the preformed liquid-liquid interface.

Two important systems are investigated. The first one deals with Cs^+ extraction by calixarenes. The effect of counterions and "synergism" at the interface are addressed by computations where TBP is added to the system. The second system concerns uranyl extraction by TBP, in relation with the PUREX process. Spontaneous formation of $(TBP)_2(UO_2)(NO_3)_2$ complexes at the interface, which gradually forms during the demixing process, has been observed (see Figure below). Some mechanistic issues raised by the simulations will be addressed.

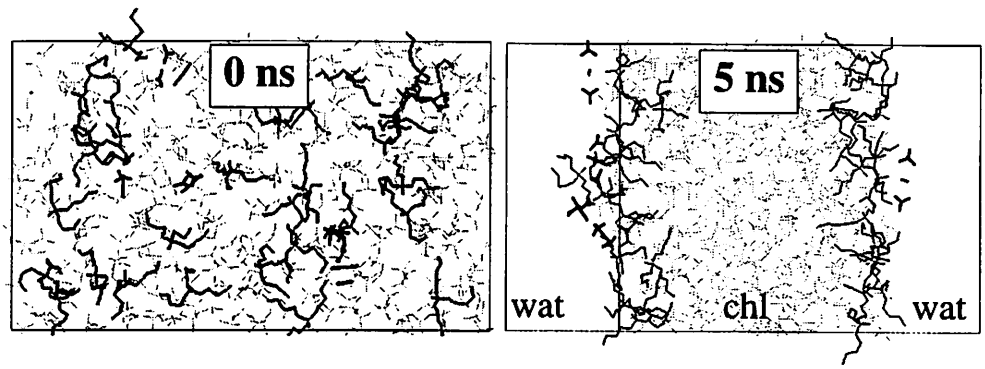

The TBP_{30}, $[UO_2(NO_3)_2]_5$ system, "perfectly mixed" (0 ns; left) and after 5 ns of MD simulation (right). $(TBP)_2(UO_2)(NO_3)_2$ complexes remain trapped at the interface instead of diffusing to the organic phase. Water molecules are omitted for clarity.

1. Berny, F.; Muzet, N.; Troxler, L.; Wipff, G., in "Supramolecular Chemistry: where it is and where it is going ", Kluwer Acad. Pub., Dordrecht, 1999, 95-125.
2. Muzet, N.; Engler, E.; Wipff, G., *J. Phys. Chem. B*, 1998, **102**, 10772.

THE INFLUENCE OF MOLECULAR STRUCTURE IN NONAQUEOUS SOLVENTS ON ION SOLVATION AND ASSOCIATION

H. KRIENKE [1]

[1] Institut für Physikalische und Theoretische Chemie der Universität Regensburg, D-93040 Regensburg, Germany

Polarizable interaction site model (ISM) potentials are used to represent the molecular interactions in certain classes of polar solvents and in model ionic solutions on Born-Oppenheimer (BO) level. With Monte Carlo (MC) and molecular Ornstein - Zernike (MOZ) integral equation techniques the intermolecular correlations and structural parameters are calculated for several often used organic solvents. The solvation of alkali and halide ions in acetonitrile and acetone has been investigated. The local structure of solvents around the ions is discussed in terms of various spatial distribution functions. We calculate these functions as well as solvation numbers and -energies for different ISM and compare the results of the MC and MOZ calculations with experimental findings [1,2]. The connection between ionic pair distribution functions and the association constant is discussed in the framework of different chemical model descriptions of electrolyte solutions on McMillan-Mayer (MM) level [3,4].

References:
1. Richardi, J.; Fries, P.H.; Krienke, H., *J.Chem.Phys.*, 1998, **108**, 4079.
2. Krienke, H.; Fischer, R., *J.Molec.Liquids*, 1999, to appear.
3. Krienke, H.; Barthel, J., *J.Molec.Liquids*, 1998, **78**, 123.
4. Krienke, H.; Barthel, J.; Holovko, M.; Protsykevich, I.; Kalyushnyi,Yu., *J.Molec.Liquids*, 1999, to appear.

QUANTUM DYNAMICS IN CONDENSED PHASES AND THE CASE OF THE EXCESS PROTON IN WATER

Gregory A. VOTH
Department of Chemistry and Henry Eyring Center for Theoretical Chemistry, University of Utah, Salt Lake City, Utah, 84112, USA

A general theoretical discussion of proton translocation in water and biophysical systems will be given. The modeling of the interactions which mediate the translocation process will be described, including an accurate multi-state empirical valence bond treatment. The method of centroid molecular dynamics to include the nuclear quantum effects will also be discussed. In all cases, the microscopic features which affect the quantum dynamical proton translocation process will be elaborated.

A path integral centroid molecular dynamics method for Bose and Fermi statistics

Kenichi KINUGAWA[1], Hidemi NAGAO[2], and Koji OHTA[3]

[1] Department of Chemistry, Faculty of Science, Nara Women's University, Nara 630-8506, Japan

[2] Department of Chemistry, Graduate School of Science, Osaka University, Toyonaka, Osaka 560-0043, Japan

[3] Department of Optical Materials, Osaka National Research Institute, AIST, MITI, Ikeda, Osaka, 563-8577, Japan

Path integral centroid molecular dynamics (CMD) method proposed by Cao and Voth in 1994 is a promising simulation method for the investigation of the real-time semi-classical dynamics of quantum systems. The centroid degrees of freedom are, however, treated as Boltzmann particles in the original CMD. Here we propose an extended CMD method applicable to many-body systems obeying Bose/Fermi statistics. It is formulated on the basis of the "pseudo-Boltzmann" canonical partition function of quantum statistical mechanics. The centroid in the present scheme is defined as an average position of a closed necklace of each quantum particle, while the Bose/Fermi statistical-mechanical effect is separated from the effect of quantum dispersion of each particle by mapping onto the "permutation potential". There exist the attractive and repulsive forces due to the permutation potential in Bose and Fermi system, respectively, aside from the forces due to the interactomic interaction potential.

In parallel, a path integral molecular dynamics (PIMD) method extended to Bose/Fermi statistics is further presented to calculate thermodynamic properties as a simulation method alternative to conventional path integral Monte Carlo algorithm. This extended PIMD technique is used in Bose/Fermi CMD simulation to evaluate the centroid mean force by which centroid degrees of freedom are driven.

Bosonic PIMD and CMD simulations have been performed for bulk ^{4}He and ideal Bose gas, respectively. The remnant of λ transition is observed for ^{4}He, while it is shown that Bose statistics causes a decay of the centroid velocity autocorrelation function of ideal Bose gas in nanosecond scale owing to the permutation forces.

Further results and discussion will be presented.

A path integral centroid molecular dynamics study of dynamic structure of the liquid helium-4

Shinichi Miura[1], Susumu Okazaki[1], Kenichi Kinugawa[2]
[1]Department of Electronic Chemistry, Tokyo Institute of Technology, 4259 Nagatsuta, Yokohama 226-8502, Japan.
[2]Department of Chemistry, Nara Women's University, Nara 630-8506, Japan.

Path integral centroid molecular dynamics (CMD) calculation for normal liquid ^{4}He has been performed. Dynamical behavior of the liquid at 4 K, which can not be reproduced by classical approximation, was well described by the CMD formalism. The calculated self-diffusion coefficient was found to be $5.06 \pm 0.04 \times 10^{-5}$ cm^2/s, which is in the same order of magnitude as that of ordinary liquids. Relaxation function of density fluctuation has also been calculated within the CMD approximation. Detailed comparison between the static susceptibility function $\chi(k)$ and the static structure factor of the centroid density $S^{(c)}(k)$ has been made. These correspond to the initial value of the exact and the centroid relaxation functions, respectively. For small k ($\leq$ 1.0 Å^{-1}), $\chi(k)$ is well approximated by $S^{(c)}(k)$. For larger k, both the correlation functions have identical peak position. However, the intensity of $S^{(c)}(k)$ is systematically larger than that of $\chi(k)$. The calculated dynamic structure factor has been compared with the spectrum obtained from neutron scattering experiment. The agreement is satisfactory for $0.2 < k < 2.2$ Å^{-1}. The calculated peak frequency as a function of k, i.e., the dispersion relation, has a minimum around 1.9 Å^{-1}, where the static correlation function shows maximum intensity. This behavior has also been experimentally observed for the dispersion relation for superfluid ^{4}He. The peak continuously loses collective character and shows single-particle behavior with increasing k around the minimum. This behavior gives rise to the minimum in the dispersion relation for normal liquid ^{4}He. The spectrum becomes narrow as the peak approaches the minimum, showing that the single-particle contribution becomes dominant in the dynamic structure factor. This narrowing is widely found among classical liquids; but not observed in the spectrum of the superfluid ^{4}He indicating that the excitation around the minimum for the superfluid may have a different molecular origin than that for normal liquid ^{4}He.

Nonlinear dynamics of molecular liquids

Akira Yoshimori
Department of Physics, Kyushu University, Fukuoka, 812-8581, Japan.

The time dependent density functional method (TDDFM) is extended to the reference interaction site method (RISM) to study nonlinear dynamics[1] of molecular liquids. This is also the nonlinear extension of the linear Langevin theory of the RISM.[2]

The nonlinear Langevin equation theory[3] is applied to the calculation of the streaming velocity term of the TDDFM. The projection is constructed by the delta functions of the site density, $\rho_a(\mathrm{r}) \equiv \sum_i \delta(\mathrm{r}-\mathrm{r}_i^a)$, and linear terms of the site current density, $\mathbf{J}_a(\mathrm{r}) \equiv \sum_i \mathrm{v}_i^a \delta(\mathrm{r}-\mathrm{r}_i^a)$. Here, r_i^a and v_i^a are the position and velocity of site a of molecule i. The projection permits the inclusion of linear terms of $\mathbf{J}_a(\mathrm{r})$ and all the nonlinearity of $\rho_a(\mathrm{r})$.

Using the theory and some approximations, the obtained equations are

$$\dot{\rho}_a(\mathrm{r}) = -\nabla \cdot \mathbf{J}_a(\mathrm{r}) \tag{1}$$

$$\dot{\mathbf{J}}_a(\mathrm{r}) = -\sum_b \int d\mathrm{r}' \mathbf{M}_{ab}(\mathrm{r},\mathrm{r}') \nabla \frac{\delta \beta F}{\delta \rho_b(\mathrm{r}')} - \sum_b L_{ab} \mathbf{J}_b(\mathrm{r}) + \mathbf{R}_a, \tag{2}$$

where βF is the nondimensinal free energy functional, L_{ab} is the irreversible transport coefficient, and $\mathbf{R}_a$ is the random force. The 3-dimensional tensor, $\mathbf{M}_{ab}(\mathrm{r},\mathrm{r}')$, is given by

$$\mathbf{M}_{ab}(\mathrm{r},\mathrm{r}') = \frac{k_B T}{M} \rho_a(\mathrm{r}) w_{ab}(\mathrm{r}-\mathrm{r}') - \{S_{ab}\mathbf{U} + (1-\delta_{ab})\mathbf{T}_{ab}\}, \tag{3}$$

where

$$S_{ab} = -\frac{2}{3}\rho_a(\mathrm{r}) w_{ab}(\mathrm{r}-\mathrm{r}') C_{ab} \tag{4}$$

$$\mathbf{T}_{ab} = \frac{1}{3}\rho_a(\mathrm{r}) s_{ab}(\mathrm{r}-\mathrm{r}') C_{ab} \mathbf{D}(\mathrm{r}-\mathrm{r}'). \tag{5}$$

Here, M is the total mass of the molecule, $w_{ab}(\mathrm{r}) = \delta_{ab}\delta(\mathrm{r}) + (1-\delta_{ab}) s_{ab}(\mathrm{r})$, and $s_{ab}(\mathrm{r}) = \delta(r - l_{ab})/4\pi l_{ab}^2$ where l_{ab} is the bond length between sites a and b. In addition, $\mathbf{U}$ is the unit tensor and $\mathbf{D}(\mathrm{r}) = 3\mathrm{rr}/r^2 - \mathbf{U}$. The constant C_{ab} depends on the intramolecular structure. For diatomic molecules, $C_{ab} = z_a z_b k_B T/I$, where z_a is the distance between site a and the center of mass and I is the moment of inertia.

1. Yoshimori, A., *J. Chem. Phys.*, 1996, 104, 9586. *ibid.* 1998, 105, 5971. Yoshimori, A.; Day, T. J. F.; Patey, G. N., *ibid.* 1988, 108, 6378.
2. Chong, S.-H.; Hirata, F., *Phys. Rev. E*, 1998, 57, 1691.
3. Zwanzig, R., *Phys. Rev.*, 1961, 124, 983. Mori, H.; Fujisaka, H., *Prog. Theor. Phys.*, 1973, 49, 764. Kawasaki, K., *J. Phys. A*, 1973, 6, 1289.

The concentration fluctuations and the mutual diffusion coefficient in the supercritical solutions

Yosuke Kataoka

Department of Materials Chemistry, Faculty of Engineering, Hosei University, 3-7-2 Kajino-cho, Koganei, 184-8584, Japan

Molecular dynamics simulations on Lennard-Jones mixture in the supercritical region are performed at many state points. We estimate the critical point by pressure-volume-temperature curves at the mole fraction $x = 0.50$. The number of the molecule in the unit cell is 1600(2-dimensional case) or 62500(3-dimensional). The mutual diffusion coefficient D is written as a product of the thermodynamic factor Q and the kinematic one L.[1] $D=QL$. The kinematic factor L is obtained by the mean square displacement of the center of mass of the component 1. The thermodynamic factor Q is calculated by the radial distribution functions $g_{ab}(R)$ according to the Kirkwood-Buff theory. The constant volume, constant temperature molecular dynamics method is used to obtain the density dependence of the mutual diffusion coefficient in a solution where the mole fraction is fixed as 0.5. And the concentration dependence is also examined under the pressure constant condition. The concentration fluctuations near the critical point are large compared to the ideal mixing. The mutual diffusion coefficient normalized by the self diffusion coefficient has small value near the critical point because of the large concentration fluctuation. The joint diffusion coefficients between the different species are compared to discuss the molecular motion in the supercritical region and that in the normal state.

1. Jolly, D. L.; Bearman, R. J., *Mol. Phys.*, 1980, **41** 137.

WATER CHARACTERISTICS DEPEND ON THE IONIC ENVIRONMENT. THERMODYNAMICS AND MODELISATION OF THE AQUO IONS

F. David[1], V. Vokhmin[2] and G. Ionova[2]

1: IPN, 91406 Orsay Cedex, France, 2: IPC Moscow, 31 Leninski Prospekt, Russia.

We have characterized the aquo ion in solution by five parameters: charge z and crystallographic radius R_c of the ion with the coordination number N, radius R_w of the water molecule in the aquo complex and number H of water molecules in the second hydration shell. From an analysis of experimental determinations of the cation-oxygen distance and evaluation of electrostriction phenomena, we have concluded that the radius R_w of the water molecule depends on the charge of the central ion and on his crystallographic radius. A "packing factor", PF, of the water molecule is also deduced from these experimental and computed data. Finally, we will show that the number H corresponding to different ions with charge -1, +1, +2 and +3 varies smoothly with the charge existing on the primary hydration sphere.

The different ion–water interactions will be discussed, and we will propose a general relation which gives the free hydration enthalpy, ΔG(hyd), of a monatomic ion with ionic character. It depends on the five fundamental characteristics of the aquo ion and reproduces the experimental data with standard deviation less than 0.3%.

In order to try to extend this model of hydration to ions with covalent character we will consider the effective charge of these species obtained by a quantum chemical computation (REX program taking into account relativistic effects). After an evaluation of the covalent contribution to ΔG(hyd), and evaluation of the ionic part of ΔG(hyd) using the ionic model, we conclude that the radius of the water molecule should be also affected by the covalent effect. The variation of R_w should be linearly correlated with the variation of the charge. In order to verify this linear correlation, we will consider experimental determination by EXAFS of the radius of the water molecule. EXAFS data[1] were obtained recently on 14 trivalent lanthanides and 5 trivalent actinides (U^{3+}, Np^{3+}, Pu^{3+}, Am^{3+} and Cf^{3+}). Since the experimental conditions and the analysis of the spectra are systematically similar for the two series of elements a consistent comparison of the water radius can be achieved and a covalent effect has been observed for several ions.

We will conclude that the proposed hydration model could be extended to monatomic ions with covalent character if one introduces in the equation the effective charge of the ion in solution and the decrease of the water radius due to covalent effect. Finally, we will stress that the hydration model and the properties of water molecules in the vicinity of the ion could be a powerful tool to evaluate the size of the aquo ions in solution and consequently to predict transport properties of the ions. We propose also to reexamine activity coefficient models taking into account realistic properties of the aquo ions and to deduce a general model of the entropy of aquo ions by derivation with temperature of the hydration relation.

[1]Aquo ions of some trivalent lanthanide and actinides. EXAFS data and thermodynamic consequences. F. David, R. Revel, B. Fourest, S. Hubert, J.F. Le Du, C. Den Auwer, C. Madic, L.R. Morss.. 26ICSC Fukuoka, Japan, 26-31 July 1999.

EQUILIBRIUM PROPERTIES AND DISSOCIATION DYNAMICS IN LIQUID $N_2O_4 = 2\,NO_2$

Toshiko KATO[1], Soichi HAYASHI[2] and Katsunosuke MACHIDA[3]
[1]Seibo Jogakuin Jr. College, Fukakusa, Fushimi-ku, Kyoto, 612-0878, Japan
[2]Tohjiin, Naka-machi, 51-2, Kita-ku, Kyoto, 603-8347, Japan
[3]Tatsugaoka, 2-1-308, Ohtu, 520-0803, Japan

Equilibrium properties and dissociation dynamics of $N_2O_4 = 2NO_2$ in liquid state are studied by classical molecular dynamics simulations. *ab initio* MO calculation has been carried out to elucidate NO2-NO2 potential, and a modified Morse potential which can reproduce highly anisotropic character of covalent bonding between N-N has been formulated. The reactive liquid N_2O_4 is modeled as liquid NO_2 (250 NO_2 in a cubic cell with periodic boundary condition) which interact with the orientation-sensitive attractive pairwise potential (OSPP) between N-N atoms and Lennard-Jones potentials between N-O and O-O atoms. The simulation is initiated from an equilibrium configuration of liquid N_2O_4.

Equilibrium properties of the reactive liquid N_2O_4 were found to be very sensitive to the anisotropy factor of OSPP: the populations of more than NO_2 dimer (3-mer, 4-mer,...) are considerable when the anisotropy of the NN bond is small, while the equilibrium liquid $N_2O_4=2NO_2$ is formed, that is, most NO_2 form monomer or dimer and the population of more than 3-mer is small when considerable anisotropy of the NN bond as to rocking angle between NN bond and ONO direction is included. Torsional anisotropy of the NN bond is also found to play an important role in determining the equilibrium constant and dissociation rate in liquid state. Temperature dependence of the equilibrium constant and dissociation dynamics shows that dimer dissociates and equilibrium shifts to monomer side as the temperature increases, which accords with the experimental observation.

The dissociation dynamics in reactive liquid N_2O_4 are compared with those of a reactant NO_2 pair activated above the dissociation threshold in the gas phase and in inert solvent N_2O_4. The dissociation reactions in the latter are viewed as energy excitation process of the reactive mode to cross the dissociation limit. A completely different dissociation process is observed in reactive liquid N_2O_4. A bound pair in the initial equilibrium configuration of pure liquid N_2O_4 is not stable and dissociates without any excitation of the system, and the fragment NO_2 associates to another NO_2 of other N_2O_4. The dependence of the lifetime of N_2O_4 and the time-scale of the change of bound partner on the anisotropy factor of the OSPP potential will also be discussed.

Toshiko Kato, Soichi Hayashi and Katsunosuke Machida, J. Mol. Liq. 1995 65/66, 405.
Toshiko Kato, J. Chem. Phys. 1996, 105, 4511.
Toshiko Kato, J. Chem. Phys. 1998, 108, 6611.

TOPOLOGY CHANGE OF THE REGION EXCLUDED BY THE SOLUTE MOLECULE WHILE THE SOLUTE MOLECULE IS HYPOTHETICALLY SCALED UP IN THE EXTENDED SCALED PARTICLE THEORY

M. IRISA, S. GONDO, and T. TAKASAKI
Faculty of Biochemical science and engineering, Department of Computer science and Systems engineering, Kyushu Institute of Technology, 680-4, Iizuka, 820-8502, Japan

One of the quantitative methods for fast calculation of the hydrophobic effect on the hydration free energy of the large molecule, e.g. protein, is the extended scaled particle theory[1]. In the statistical mechanics, chemical potential of the molecule is calculated by integrating probability function in the phase space while the target molecule is hypothetically scaled up. The extended scaled particle theory uses an assumption for the integration of the probability function accompanying the scaling up of the solute molecule from the material point (scaling parameter λ=0) to the real size (λ=1). In the extended scaled particle theory, topology of the region excluded by the solute molecule modeled as the fused spheres is changed during the hypothetical scaling up of the solute molecule because the size of the solvent molecule modeled as the sphere is fixed.

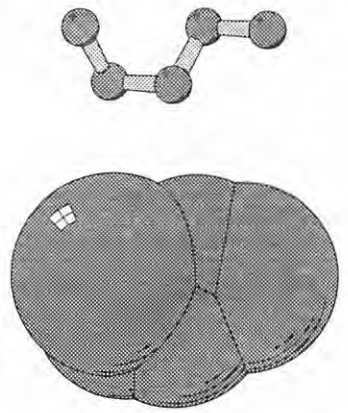

Figure 1

In order to strengthen the mathematical basis of the topology change of the region excluded by the solute molecule during the scaling up of the solute molecule, we have tried to solve the geometry problem which have the one-to-one correspondence to the alpha shape[2] in the computational geometry. In the alpha shape, the fused spheres is scaled up by adding the same value (α value) to the radii of all the spheres in the fused spheres. Scaling up of the α value exactly corresponds to the scaling down of the scaling parameter λ in the extended scaled particle theory. The elements of the topology which affects to the excluded volume are intersection circle (IC), exposed vertex (EV), and buried vertex (BV) of the solute molecule[3]. The topological elements IC and EV correspond to the edge and the tetrahedron in the alpha shape which is the subset of the dual figure of the Voronoi diagram.

We have examined changes of the topology of alkanes (methane, ethane, propane, butane, and pentane) during decreasing the scaling parameter λ to zero. Radii of the heavy atom (united atom) and water is 1.9Å and 1.375Å. It was found that only pentane has the conformation in which topology change occures (Fig. 1).

1. Irisa, M.; Takahashi, T.; Nagayama, K.; Hirata, F., *Molecular Physics*, 1995, **85**, 1227.
2. Edelsbrunner, H.; Facello, M.; Fu, P.;Liang, J., *Proceedings of the 28th Annual Hawaii International Conference on System Science*, 1995, 256.
3. Irisa, M., *Computer Physics Communications*, 1996, **98**, 317.

ENERGY DISSIPATION IN SUPERCRITICAL FLUID SOLUTIONS

Okitsugu KAJIMOTO[1], Atsuhiko SHIMOJIMA[2], and Kentaro SEKIGUCHI[1]

[1]Department of Chemistry, Graduate School of Science, Kyoto University, Kyoto, 606-8502, Japan

[2]Japan Science and Technology Corporation

No energy dissipation occurs for an isolated molecule except for the radiative energy loss while a solute molecule in solution rapidly loses its internal energy to solvent molecules. In supercritical fluid solutions, the efficiency of energy dissipation from the hot molecule depends on the density of fluid. In a very low density region, the energy dissipation rate should increase linearly with the increase in the fluid density, simply reflecting the increase in the collision number. In a high density region, the isolated binary collision (IBC) model as well as the time-dependent perturbation theory has been applied successfully to interpret the density dependence of the energy dissipation. Around the critical density, the cluster formation comes into play in the energy dissipation process and the peculiar density dependence is often observed. The interpretation is, however, still controversial.[1,2]

In the present study, we measured the rate of energy dissipation from the hot molecules formed by overtone excitation and interpreted the observed rate with the aid of simple molecular dynamics calculations. Phenylacetylene or naphthalene molecules in supercritical CO_2 or CF_3H were vibrationally excited by a pump pulse through their C-H overtone absorption. The second laser pulse after a short delay monitored the population of molecules in the prepared state by exciting them into the fluorescing electronically excited state. Intramolecular vibrational energy redistribution (IVR) also depleted the molecules in the initial vibronic state. The rates of energy dissipation and IVR depended on both the excess vibrational energy and the fluid density.

To evaluate the applicability of the two theoretical models, IBC and time-dependent perturbation, a simple MD simulation has been carried out and both the radial distribution function and the time-correlation function were estimated at several densities. Based on these key functions, we discuss the density dependence of the energy dissipation process in relation to the experimental data obtained in supercritical CO_2 in the present study and those reported by other groups.[1,2]

1. Schwarzer ,D.; Troe, J.; Zerezke, M. *J. Chem. Phys.*1977, **107**, 8380.
2. Urdahl, R.S.; Myers, D.J.; Rector, K.D.; Davis, P.H.; Cherayil, B.J.; Fayer, M.D. *J. Chem. Phys.* 1997, **107**, 3747.

VIBRATIONAL ENERGY RELAXATION IN THE ELECTRONIC EXCITED STATE IN FLUIDS OVER THE WIDE DENSITY REGION

Y. KIMURA, T. YAMAGUCHI, and N. HIROTA
Department of Chemistry, Graduate School of Science, Kyoto University, Kyoto 606-8502, Japan

It is an important and still open problem on the vibrational energy relaxation whether the isolated binary collision model holds or not in solution. In this model, the vibrational energy relaxation rate is described by the product of the collision frequency and the energy dissipation rate per collision. Supercritical fluid is a suitable solvent to study this problem, since we can continuously change the collision frequency by changing the solvent density. In this work, we present new results on the vibrational energy relaxation rates in the S_2 state of azulene in supercritical fluids measured by the time-dependent fluorescence spectrum. Since the fluorescence lineshape is dependent on the vibrational excess energy in the S_2 state, we can estimate the excess energy in the S_2 state of azulene in solution at each time after the photo-excitation by analyzing the fluorescence lineshape .

The time-dependent fluorescence spectrum has been measured by a streak camera after the excitation of the second harmonic of the output (566 nm) of a pulsed dye laser. Figure 1 shows time profiles of the fluorescence intensity and the excess energy estimated from the lineshape. Assuming a single exponential decay of the excess energy, we have got good fits to the signals (solid lines). Figure 2 shows the density dependence of the excess energy decay (○) in CO_2 thus estimated together with the results for the ground state (■) from the literature[1]. The density dependence is very similar to that in the ground state, although the rate is about three times faster in the excited state. From this result we consider that the density dependence of the vibrational energy relaxation rate is dominated by the density dependence of the collisional frequency, and that the different rates between two electronic states are due to the difference in the efficiency of the energy loss per collision. The details including other solvent fluids and other systems will be discussed in the presentation.

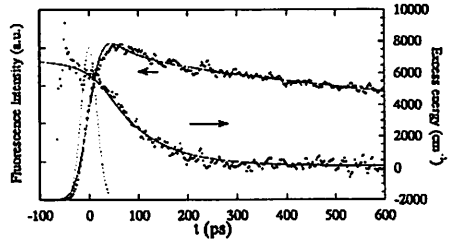

Fig. 1. Time profiles of the fluorescence intensity and the excess energy in CO_2 at $\rho_r = 0.1$ at 323K.

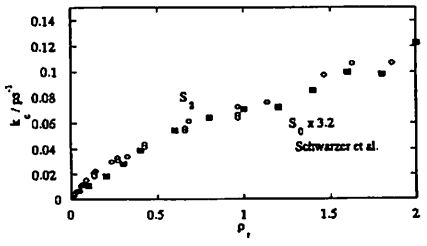

Fig. 2 Density dependence of the excess energy decay rate (k_e) in CO_2.

1 . Schwarzer, D.; Troe, J.; Votsmeier, M.; Zerezke, M.; *J. Chem. Phys.* 1996, **105**, 3121.

FRACTAL NATURE OF SALT-INDUCED FLUCTUATION IN 1-PROPANOL AQUEOUS SOLUTION

M. MISAWA[1], K. YOSHIDA[2], H. MUNEMURA[2], Y. HOSOKAWA[2], K. MARUYAMA[1], M. FURUSAKA[3] and M. IMAI[4]

[1]Department of Chemistry, Faculty of Science, Niigata University, Niigata 950-2181, Japan
[2]Graduate School of Science and Technology, Niigata University, Niigata 950-2181, Japan
[3]Institute of Materials Structure Science, KEK, Tsukuba 305-0801, Japan
[4]Department of Physics, Ochanomizu University, Tokyo 112-0012, Japan

Water and 1-propanol can mix in any proportion and at any temperature between 0 and 100°C. However, when a small amount of salt such as KCl is added into the solution, the phase separation occurs at a finite temperature range defined by a lower temperature T_L and an upper one T_H[1]. We examined the structural evolution of concentration fluctuation induced by salt in the solution by means of small-angle neutron scattering in order to study the microscopic origin of the salt induced phase separation phenomena.

Figure 1 shows the scattered intensity I(Q) measured for the $(C_3H_7OD)_1$-$(D_2O)_5$ solution including about 2mol% KCl in the lower one phase region. The curve (a) is just below the T_L, while the curve (b) is far below the T_L. We carried out the similar measurements for the same solution at various temperatures between 20 and 37°C in the lower one phase region and furthermore between 63 and 76°C in the upper one phase region. All I(Q) curves studied are fitted very well with the scattering function[2] for a fractal structure given by a correlation function $g(r)=\delta(r)+(A/r^{3-d_f})\exp(-r/\xi)$ with a fractal dimension d_f and a correlation length ξ. A common fractal dimension of $d_f=1.9$ is obtained despite of the lower and upper one phase regions. Furthermore, the correlation length ξ diverges similarly in both regions. It is concluded that the structural evolution of the concentration fluctuation has a common fractal nature in both the lower and upper one phase regions.

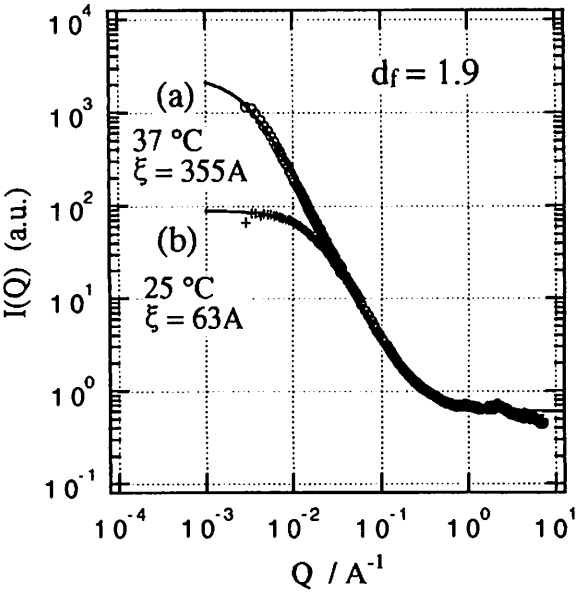

Fig. 1 Small-angle neutron scattering intensity I(Q). Solid curves show fitted results.

1. G. M. Schneider, *Ber. Bunsenges. Physk. Chem.* 1972, 76, 325.
2. T. Freltoft, K. Kjems and S. K. Sinha, *Phys. Rev.*,1986, **B33**, 269.

Structure and Dynamics of Water: from Ambient to Supercritical

Masaru NAKAHARA, Nobuyuki MATUBAYASI, Chihiro WAKAI, and Yasuo TSUJINO
Institute for Chemical Research, Kyoto University, Uji, Kyoto, 611-0011, Japan

Over a wide range of temperature and pressure, water acts as the most unique solvent and serves as the central substance of physical chemistry. As is well known, the unique properties of water are caused by the hydrogen bonding. When water and aqueous solutions are concerned in ambient conditions, there have been uncountable number of research devoted to the hydrogen bonding structures since the pioneering works by Pauling, Bernal and Fowler, and Frank and Evans. It is then natural to focus on the hydrogen bonding when the structure of water at nonambient conditions, either supercooled or supercritical, is to be characterized. The first work performed at the molecular level to characterize the hydrogen bonding in supercritical water employed the neutron scattering.[1] Although this is an important and stimulating work, of course, it studied only one state point in the supercritical region of water. In view of the fact that supercritical water is attractive due to the wide availability of the density, it is necessary to employ an experimental method which can cover a wide range of the density. The nuclear magnetic resonance (NMR) spectroscopy meets this necessity. In our laboratory, we have been employing NMR to quantitatively investigate the structure and dynamics of the hydrogen bonding in supercritical water.

The experimental techniques used in our high-temperature NMR measurements are described in previous papers.[2,3] A most distinguishing feature of our techniques is that an aqueous sample is sealed in a capillary and that isochoric measurements are possible. In order to characterize the hydrogen bonding structure of supercritical water, we determined the proton chemical shift of water from the ambient to supercritical conditions. The chemical shifts were then related to the average number of hydrogen bonds per water molecule through the help of computer simulations. The number of hydrogen bonds were further used to estimate the average dipole moment of the water molecule in the supercritical conditions, which is the key quantity to perform computer simulations of aqueous systems.[2,3,4]

The dynamical counterpart of our structural study of supercritical water has been performed by NMR relaxation measurements. Using D_2O, we measured the spin-lattice relaxation time. The spin-lattice relaxation time was then found to be related to the rotational relaxation time of a single water molecule. In Fig. 1, we show the rotational relaxation time τ_{2R} at super- and subcritical conditions. It is seen that while τ_{2R} decreases rapidly with the temperature in the subcritical condition, it is a weak function of the density in the supercritical conditions.[5] The relationship of this result to the previous relaxation studies of water in ambient organic solvents is to be discussed.

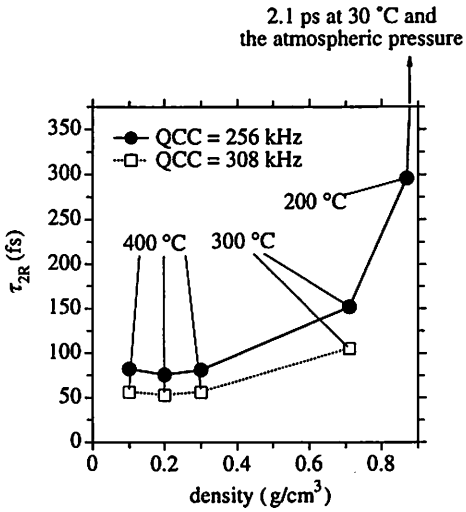

Fig. 1. The rorational correlation time τ_{2R} of water at super- and subcritical conditions as a function of the density. Note that the mass density of D_2O is obtained when 1.1 is multiplied to the density shown.

1. Postorino, P.; Tromp, R. H.; Ricci, M. A.; Soper, A. K.; Neilson, G. W., *Nature*, 1993, **366**, 668.
2. Matubayasi, N.; Wakai, C.; Nakahara, M., *Phys. Rev. Lett.*, 1997, **78**, 2573.
3. Matubayasi, N.; Wakai, C.; Nakahara, M., *J. Chem. Phys.*, 1997, **107**, 9133.
4. Matubayasi, N.; Wakai, C.; Nakahara, M., *J. Chem. Phys.*, 1999, **110**, Apr 22 issue.
5. Matubayasi, N.; Tsujino, Y.; Nakahara, M., 1999, to be submitted.

NMR CHEMICAL SHIFT STUDY OF THE BINARY METHANOL – BENZENE-d_6 SYSTEM

Nobuyoshi ASAHI[1] and Yoshio NAKAMURA[2]

[1]Research Institute for Solvothermal Technology, 2217-43 Hayashi, Takamatsu, 761-0431, Japan

[2]Division of Chemistry, Graduate School of Science, Hokkaido University, Kita 10 Nishi 8, Kita-ku, Sapporo 060-0810, Japan

In the past decade, much attention has been paid to supercritical fluids as solvents of chromatography, extraction and reaction. Supercritical fluids having the OH group such as water or methanol, in particular, have been attracted to investigate the unusual solvent properties due to hydrogen bonding. In the present study, we have measured the chemical shifts of methanol in the binary methanol – benzene-d_6 system in order to elucidate the hydrogen-bonded structure and solute-solvent interaction.

Chemical shifts of methanol were determined as the shift difference of the OH proton referred to the CH_3 proton. Measurements were made with a Bruker CXP NMR spectrometer operating at 38.3 MHz. The resolution of spectra obtained by Fourier transformation after a FID acquisition was 1 Hz (0.025 ppm). The density of the methanol – benzene-d_6 mixtures studied was 3.30×10^3 molm^{-3} and kept constant. The compositions of the mixtures were 25, 50 and 75 in methanol mol%.

The chemical shifts decrease with increasing temperature, and decrease with decreasing the methanol concentration, i.e., the methanol density. The present results for methanol in mixtures are similar to those of pure methanol in our previous study.[1,2] The change in the chemical shifts of the OH proton can be interpreted in terms of change in the hydrogen bonding in methanol. The chemical shift results in the supercritical region are in good agreement with those of the same density of pure methanol within experimental errors. Thus, we calculated the n-mer mole fractions as a function of cluster size n by using the thermodynamic aggregation model, assuming that the observed chemical shift δ is the sum of the chemical shift of the non-hydrogen-bonded OH proton $\delta_{N\text{-}HB}$ and the hydrogen-bonded proton δ_{HB}. The results for 75 mol% at 575 K show that the monomer mole fraction and the energy ΔE of hydrogen bond formation are 0.8 and 20.8 kJmol^{-1}, respectively. We concluded that the existence of benzene has no effect on the hydrogen-bonded structure of methanol over the temperature and concentration range studied.

1.Asahi, N.; Nakamura, Y., *Chem.Phys.Lett.*, 1998, **290**, 63.

2.Asahi, N.; Nakamura, Y., *J.Chem.Phys.*, 1998, **109**, 9879.

ACETIC ACID CLUSTERS IN AQUEOUS SOLUTION: PRESENCE OF MICRO-PHASES IN THE MIXTURES

Nobuyuki NISHI Takakazu NAKABAYASHI, and Kentaroh KOSUGI
Institute for Molecular Science, Myodai/ji, Okazaki 444-8585, Japan

Acetic acid is thought to be strongly associated with water molecules, since it is a typical hydrophilic molecule. Kaatze and his coworkers found the presence of two relaxation terms and attributed to the existence of two microphases, one with high and the other one with low water content. The water-rich phase was assumed to fill the space between the acid-rich microphase aggregates. Their observation suggested the dominance of acid-acid association in aqueous solution.

Low frequency Raman $R(\bar{\nu})$ spectra of acetic acid-water binary solutions exhibits isosbestic points in the region of $0 \leq x_A$(mole fraction of acetic acid) ≤ 0.5 and $0.5 \leq x_A \leq 1.0$, suggesting the presence of three states in the mixtures. We first attributed these intermolecular complexes to the acid-water clusters in the mixtures. However, the $R(\bar{\nu})$ spectrum of the aqueous mixture at $x_A = 0.5$ bears a very close resemblance to that of the acetic acid-methanol mixture with $x_A = 0.5$, indicating that the molecular complexes responsible to the Raman spectra are acetic acid clusters. The observed spectral pattern is explained satisfactorily with a side-on type open dimer structure by ab initio molecular orbital calculation at HF/6-31G(d,p) level. The contribution to the low frequency Raman spectra is clearly seen in the diluted solution at $x_A = 0.0075$. In the spectrum, spectral intensity of water-water interaction component at $185cm^{-1}$ is found to be more enhanced compared with the intensity in the pure water spectrum. This is in accord with the idea of hydrophobic hydration.

Interesting spectral changes are also found in the intramolecular vibrational region. With decreasing acetic acid concentration, the peak of the C=O stretching vibrational band shows high frequency shift from 1665 cm^{-1} at x_A =0.7 to 1705 cm^{-1} at x_A =0.3. This means that the increase of water content breaks the hydrogen bond of the C=O group of acetic acid even for the pairs of acid-water complexes. The hydrogen bonds in acetic acids polymers are dissociated with the addition of water leaving free C=O groups in aqueous environment. The side-on type dimer unit can explain the observation. On the other hand, increase of acetic acid in water decreases the intensity of the hydrogen-bonded O-H stretching band at 3200 cm^{-1} relative to that of the O-H band of weakly associated species at 3410 cm^{-1}. These results suggest that acetic acids in water break the hydrogen-bond networks of water due to the self association increasing the number of the acid-acid hydrogen-bonds at the C=O sites. The present results support the microphase model of the mixtures: one is solute rich phase and the other is water rich one.

FORMATION OF A PSEUDO CLUSTER IN THE POLYPHOSPHATE SYSTEM

T.NAKASHIMA[1] AND H.WAKI [2]

[1]Faculty of Education and Welfare Science, Oita University, 870-1192,Oita,Japan

[2]Department of Chemistry, Faculty of Science, Kyushu University, 812-8581,Fukuoka, Japan

Indirect evidences may suggest the presence of a kind of cluster in solutions in which two large polyvalent anions are loosely associated. This structure can be kept by a mediating motion of a few numbers of monovalent cations between the two polyvalent anions. This phenomena can first be interpreted by an electrostatic model for hexavalent dodecaoxohexaphosphates (III)(DOHP) anion. A simple model calculation gave a clear potential minimum at the distance of 6Å~ between DOHP, if three monovalent cations are participated. It was recognized that the mediation by less or more numbers of the cations is inconvenient to produce such a cluster.

A simplified molecular dynamics simulation by a Hyper Chem.. R5.0 also displayed similar phenomena on DOHP(Fig). A potentiometric measurement on the interaction between DOHP and potassium ions indicated the cation invasion into the space between these two DOHP anions associated.

The absorption spectra for the DOHP solutions containing copper(II) ions rendered a broad peak at 400~500 nm, reflecting the presence of a special solution localized between adjacent DOHP anions.

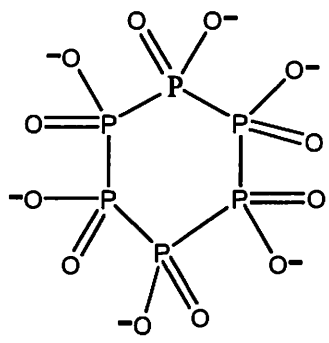

Structure of DOHP

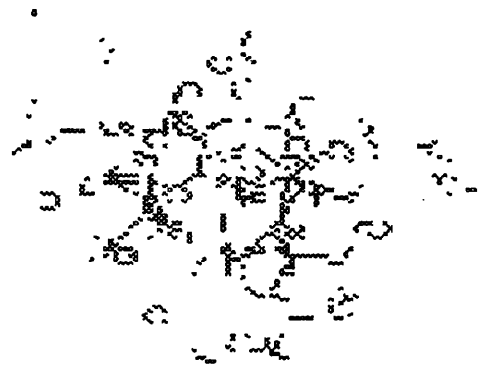

Association of DOHP anions mediated by K^+

A MOLECULAR DYNAMICS STUDY OF THE LIPID BILAYER

Susumu OKAZAKI
Department of Electronic Chemistry, Tokyo Institute of Technology,
4259 Nagatsuta, Midori-ku, Yokohama 226-8502, Japan

Lipid bilayers in the liquid crystal phase have a very complex structure. It is heterogeneous showing a kind of microscopic phase separation between the membrane layer and water. In the membrane, orientation of the lipid molecule has an order with its molecular axis aligned to the bilayer normal, while the projection of molecules to the bilayer plane possesses a liquid like disordered structure. The system is, thus, anisotropic, too. The purpose of the present study[1~5] is to establish a simulation technique for a realistic membrane and to clarify molecular based picture of a number of interesting physical properties of the membrane resulting from these complicated structures. Very long-time calculations in a suitable ensemble as well as a number of techniques in the calculations were needed to acomplish the above.

First, a large membrane area fluctuation has been investigated in detail defining a single-molecular area based upon Voronoi tesselation analysis for the center of mass of the lipid molecules projected on the bilayer plane. Statistics of the fluctuation and its molecular origin will be presented. Second, charges on the head groups lining up at the interface produce an electric field, which is thought to play an essential role in the physical properties of the membrane. It influences much the permeability of polar small molecules and ions across the membrane as well as the conformation of proteins in the membrane. Here, dielectric property, electric potential profile, and structure and dynamics of water have been investigated. Third, free energy profile of a small molecule transport across the membrane has been evaluated based upon thermodynamic integration method. This will present a thermodynamic mechanism of the small molecule permiation.

1. W. Shinoda, T. Fukada, S. Okazaki, and I. Okada, *Chem. Phys. Lett.*, 232, 308 (1995).
2. W. Shinoda, N. Namiki, and S. Okazaki, *J. Chem. Phys.*, 106, 5731 (1997).
3. W. Shinoda and S. Okazaki, *J. Chem. Phys.*, 109, 1517 (1998).
4. W. Shinoda, M. Shimizu, and S. Okazaki, *J. Phys. Chem.*, B102, 6647 (1998).
5. Z. Fang, A. D. J. Haymet, W. Shinoda, and S. Okazaki, *Comp. Phys. Commun.*, 116, 295 (1999).

DIFFUSION AND STRUCTURE IN WATER-AMPHIPHILE MIXTURES

Kenneth R. HARRIS[1] and Paula J. NEWITT[1],
[1]School of Chemistry, University College, University of New South Wales,
Australian Defence Force Academy, Canberra, ACT 2600, Australia.
(email: k-harris@adfa.edu.au)

High-pressure diffusion studies can give important information in aqueous systems. Easteal and Woolf [1] have demonstrated that the infinite-dilution tracer diffusion coefficients of methanol and ethanol in water were enhanced much more than the self-diffusion coefficient of the solvent water by the application of high pressure (100-200 MPa) at low temperatures (5-15 °C).

Results for the intra-diffusion water (D_w) in aqueous solutions of several amphiphiles as a function of pressure, temperature and composition have been obtained. At low temperatures, we have shown that for 2-methylpropan-2-ol [2,3] (TBA) and 2-propanol as solutes, D_w shows a maximum with increasing pressure to a greater relative extent than does the self-diffusion coefficient in pure water under the same conditions. This is consistent with the concept that the water is more structured in under these conditions.

At higher concentrations, and at higher temperatures, the normal behaviour of a diminution of the diffusion coefficient with increasing pressure occurs. This is inconsistent with ordering of hydration water suggested by certain models based on the presence of clathrate-like hydrates at these compositions.

Results for other systems, particularly water-acetonitrile[4] and water-ethanol, are discussed. At low solute concentrations the enhancement of D_{rel} (= $D(p)/D(0.1\ \text{MPa})$) is never higher than in pure water under the same conditions. We find no evidence in the diffusion results for structural enhancement of water by the solute in these systems, though this has been proposed by some past workers in interpreting certain experimental results and molecular dynamics simulations.

1. Easteal, A. J.; Woolf, L. A., *J. Phys. Chem.*, 1985, **89**, 1066.
2. Harris, K. R.; Newitt, P. J., *J. Phys. Chem. B*, 1998, **102**, 8874.
3. Harris, K. R.; Newitt, P. J., 1999, submitted for publication.
4. Harris, K. R.; Newitt, P. J., 1999, submitted for publication.

ATOMIC RESOLUTION FOR NON-EQULIBRIUM STRUCTURES IN THE STEADY STATE AND FOR CHLORIDE-ION-ASSISTED ORDERED-ARRAY OF THE CHLORIDE RECEPTORS AT THE INTERFACE BETWEEN NaCl (c)/ KBr (c) AND WATER

K. ICHIKAWA
Graduate School of Environmental Earth Science, Hokkaido University , Sapporo 060-0810, Japan

Despite the considerable theoretical and experimental activities on ionic-crystal growth in aqueous solution over the years, little is known about the two-dimensional array and motion of water molecules and ions at the interface between ionic crystal and water.

The observed AFM images have allowed us to sort out the non-equilibrium atomic array in stationary state on terraces and at steps of the interface between NaCl(c)/ KBr(c) and water. One can expect to see progress in the transformation to the non-equilibrium atomic array at the interface between the ionic crystal and water. The new configuration may be more easily attainable by the two-dimentional translation of ions through energetically favourable diffusion paths at the interface.[1)]

The atomic-resolution AFM images at the interface between KBr(c) and water showed the two-dimentional array of potassium ions and water molecules which were located one another at same vertical height. Because (1) the non-equilibrium structure at the interface between KBr(c) and water showed the extremely short separation 0.20nm between bright spots and (2) both Na^+ or K^+ can go upright to the same vertical height of chloride/bromide ions and above their height at the interface under water. Thus, the ordered array of monolayer of water molecules has been established by their own strong hydrogen bonds with Br^- (i.e., $Br^- \cdots H-O-H, \angle Br^- HO = 0°$) and their interaction with K^+ ions (i.e., $K^+OwK^+OwK^+$ and Ow stands for oxygen atom in H_2O). The above-mentioned geometry of the hydrogen bond of water molecule with anion or cation was also observed for incompletely hydrated solution of LiCl using the neutron diffraction and isotopic substitution technique.[2)]

The ordered array of cage hosts as chloride receptor was established via their encapsulation of Cl^- belonging to the above-mentioned non-equilibrium layer at the interface under water.[3)]

1. Ichikawa, K.; Yamada, M., *J. Phys.: Condens. Matter,* 1996, 8, 4889.
2. Ichikawa, K.; Kameda, Y.; Matsumoto, T.; Misawa, M., *J. Phys. C:Solid State Phys.,* 1984,17, L725.
3. Ichikawa, K.; Yamada, M.; Ito, T., *Chem. European J.,* 1998, 4, 914.
E-mail: ichikawa@ees.hokudai.ac.jp

STOKES-EINSTEIN RELATION FOR A MASSIVE SOLUTE PARTICLE

M. Fushiki[1] and K. Miyazaki[2]
[1] National Institute of Material and Chemical Research, Tsukuba, Ibaraki 305-8565, Japan
[2]Theoretical Studies Division,Institute for Molecular Science,Myoudaiji, Okazaki 444-8585, Japan

Stokes-Einstein (SE) relation relates the diffusion coefficient D of a solute particle with the solvent viscosity η as $D = k_B T / c\pi\eta(\sigma_0+\sigma_1)$, where σ_0 and σ_1 are, respectively, solute and solvent diameters and constant c is determined by the hydrodynamic condition, being 2 for slip and 3 for stick boundary condition. An old hard sphere MD simulation revealed that the SE relation with the slip boundary condition was hold when the mass and size of a solute particle were the same as those of solvents[1]. However, a recent MD simulation for hard sphere fluids with an infinite mass solute particle showed the results which was consistent with the SE relation with the stick boundary condition[2]. In this work we study the mechanism which causes this change from slip to stick value by using MD simulations.

1. B. J. Alder, D. M. Gass, and T. E. Wainwright, J. Chem. Phys. **53**, 3813(1970).
2. L. Bocquet, J. P. Hansen, and J. Piasecki, J. Stat. Phys. **76**, 527(1994).

Molecular Behaviors in The Translational Diffusions of Fatty Acids in Their Liquids

Makio IWAHASHI[1], Yasutoshi KASAHARA[1], Hideyuki MINAMI[1], Hideyo MATSUZAWA[1], Kenji NOMURA[2], Hikaru TERAUCHI[2], and Yukihiro OZAKI[2]
[1] School of Science, Kitasato University, Sagamihara, 228-8555, Japan
[2] School of Science, Kwansei Gakuin University, Nishinomiya, 662-8501, Japan

Fatty acids are characteristic building-block components of most of lipids such as phospholipid and glycolipid which construct biomembrances; they play important role in membrane functions such as flexibility, fluidity, and material transfer. The functions seems to depend mainly on the property as a liquid rather than that as a solid. The molecular and liquid structures for the acids in the liquid states, however, have not been studied because the liquid state of the acids has hitherto been believed to be merely isotropic irrespective of temperature or pressure. In a previous study, mainly by NIR spectroscopic method we have revealed that *cis*-9-octadecenoic acid in its liquid exists as dimers even at relatively high temperatures. Namely, the dimers of the acids are the units in intra- or intermolecular movements. In this study, the dynamic molecular structures and the assembly structures of the fatty acids in the liquid states have been studied through the observations of density, viscosity, η, translational self-diffusion coefficient, D, ^{13}C NMR spin-lattice relaxation time, T_1, and X-ray diffraction.

Experimental. Samples of tetradecane (99.9 %, Wako Pure Chemical Industry Co.), octanoic, nonanoic, and decanoic acids (>99.9 %, Nippon Oil and Fats Co.) were used without further purification. D and T_1 for the samples of the acids were obtained by the pulsed-gradient NMR and the inversion recovery methods, respectively, using a JEOL EX-400 NMR spectrometer. X-ray diffraction experiments for all the samples were carried out with AgKα or MoKα radiation.

Results and Discussion. Stokes radius, a, was calculated using the obtained D and η values. The a values (ca. 3.0 Å) are almost irrespective of the number of carbon atoms for the fatty acids. The radial distribution function curves for nonanoic acid and tetradecane were obtained through the Fourier transformation of the X-ray diffraction data. The clear distribution patterns in the both curves mean that the acid and tetradecane molecules highly aggregate in parallel. The distances between the molecules neighboring directly each other are 5.4 Å and 5.5 Å, respectively. Namely, rodlike molecules such as fatty acids or tetradecane tend to aggregate with each other, and may make clusters resembling bundles of straw. As no optical anisotropy such as streaming birefringence has ever been observed for pure liquids of the fatty acids, the bundles, whose sizes may be smaller than the wavelength of the visible light, would therefore be randomly oriented and make a liquid. As the rotational (end-over-end), as well as transverse, motion of each rod in the bundles may be severely restricted, the rods (the dimers of the fatty acid molecules) seem to translate only longitudinally.

HYDRATION AND SOLVATION OF METAL IONS
A COORDINATION CHEMISTRY OVERVIEW

Ingmar PERSSON
Department of Chemistry
Swedish University of Agricultural Sciences
P.O.Box 7015
S-750 07 Uppsala, Sweden

The structure of the hydrated and solvated metal ions in solution is very important for the understanding of the reactivity and reaction mechanisms of ions in different media. In order to get a more detailed picture of the hydration and solvation of metal ion a number of structural, thermodynamic and spectroscopic techniques must be applied. In this presentation the structural aspect of the hydrated and solvated metal ions in solution will be emphasized. The structures of hydrated and solvated metal ions in solution, as determined by means of large angle X-ray scattering (LAXS) and EXAFS (extended X-ray absorption fine structure) spectroscopy will be reviewed; Solvents coordinating through oxygen (water, dimethylsulfoxide, *N,N*-dimethylformamide, *N,N*-dimethylpropylene urea), nitrogen (acetonitrile, pyridine, liquid ammonia), sulfur (*N,N*-dimethylthioformamide, tetrahydrothiophene) and phosphorus (triethylphosphite) and metal ions from the entire periodic table will be discussed.

NEW FAMILY OF NAKED PLATINUM-THALLIUM BONDED SMALL CYANO CLASTERS: STRUCTURE, EQUILIBRIUM AND KINETICS

Imre Tóth

Department of Inorganic and Analytical Chemistry, Lajos Kossuth University (KLTE), H-4010 Debrecen Pf.21, Hungary.

Recently, we have reported studies on the formation, structure and equilibrium of a new family of oligometallic platinum-thallium cyano compounds containing a direct metal-metal bond.[1,2] The complexes are synthesised according to the reaction:

$$mPt(CN)_4^{2-} + Tl^{3+} + nCN^- \rightleftharpoons [Pt_mTl(CN)_{4+n}]^{(n-1)-}$$

Four binuclear species represented by a general formula $[(NC)_5Pt\text{-}Tl(CN)_{n-1}]^{(n-1)-}$ (n=1-4) and a trinuclear complex $[(NC)_5Pt\text{-}Tl\text{-}Pt(CN)_5]^{3-}$ are formed in aqueous solution.

The complexes exist in an equilibrium, which also includes the parent complexes $Pt(CN)_4^{2-}$ and $Tl(CN)_n^{3-n}$ (n=0-4), and can be controlled by varying the cyanide concentration and/or pH of the solution.

Multinuclear NMR- (^{13}C, ^{195}Pt, ^{205}Tl), IR-, Raman-, ESCA-spectroscopy, X-ray and EXAFS studies confirm direct, sort (2,60-2,64 Å) Pt-Tl bonds, formed by the overlapping of d_{z^2} and $(d^{10})s^0$ orbitals of Pt(II) and Tl(III), respectively.

Formation kinetics of the complexes involve at least two steps: (i) Pt-Tl bond formation by an one electron transfer reaction and (ii) formation of the $-Pt(CN)_5$ unit by entering a cyanide ligand. Mechanism of the reaction is suggested.

The compounds are usually inert towards redox decomposition and can be kept in solution for years in the dark at room temperature. Under certain conditions a two-electron transfer reaction between the bound platinum and thallium atoms takes place. The only product of thallium reduction is Tl(I), while oxidation of platinum leads to different complexes of either Pt(IV) or Pt(III), including two new compounds:[3] $(CN)_5Pt^{IV}(H_2O)^-$ and $(CN)_5Pt^{III}Pt^{III}(CN)_5^{4-}$.

The work was supported by the NFR, INTAS 96-1162 and OTKA T26116 research grants.

1. Maliarik M., Berg K. E., Glaser J., Sandström M., Tóth I. *Inorg. Chem.* 1998, **37**, 2910.
2. Maliarik M., Glaser J., Tóth I., Webba da Silva M., Zékány L. *Eur. J. Inorg. Chem.* 1998, 565.
3. Maliarik M., Glaser J., Tóth I. *Inorg. Chem.* 1998, **37**, 5452.

Structural Study for the Interaction between Polyaza Macrocyclic Metal Complex Ions and Halide Ions in Aqueous Solution

Hisanobu WAKITA, Toshio YAMAGUCHI, Tsutomu KURISAKI,
Mitsutoshi YOKOMIZO, Shuji MATSUO, and Makoto INUZUKA
Department of Chemistry, Faculty of Science, Fukuoka University
Nanakuma, Jonan-ku, Fukuoka 814-80, JAPAN

The chemistry of polyaza macrocyclic metal complexes has been a fascinating area of current research. The formation of transition metal(II) complexes with some saturated polyaza macrocycles has been investigated in aqueous solution in spite of experimental difficulties, especially, multinuclear complexes with them are very popular since the research interests stem mainly from their use as models for protein, as synthetic ionophores, as models to study the magnetic exchange phenomena, and as metal complex catalysts. In these formations the halide ions are, sometimes, secondary in importance to nitrogen and oxygen as ligands to the Ni(II) and Cu(II) ions.

To understand the role of halide ions in the mixed ligand complexes, we have investigated the complex formation of Ni(II) or Cu(II) ion with some saturated tetraza macrocycles (cyclam[1], N,N', N'',N'''-tetrakis(2-aminoethyl)-1,4,8,11-tetraazacyclohexadecane(taeh)[2], 1,4,7-tris(2-o-hydroxy phenyl propyl)1,4,7-triazacyclononane(tppt)) and halide ions in aqueous solution. We have investigated the complex structures in aqueous solution by EXAFS and XANES analyses, and the coverency of the interaction between the metal and halide ions by use of the molecular oribital calculation[3].

The aqueous solutions of $[CuBr_2(cyclam)]$ and $[Cu(cyclam)(H_2O)_2]F_2 \cdot 4H_2O$ were subjected to the XANES analysis, and the results show the existence of $[CuBr(cyclam)(H_2O)]^+$ in the solution of $[CuBr_2(cyclam)]$, and also that of covalency between Cu^{2+} and Br^- ions in the complex $[CuBr(cyclam)(H_2O)]^+$.

The structures of $[Cu_2(taeh)X](ClO_4)_3$ complexes in aqueous solution are divided in two types. $[Cu_2(taeh)Cl](ClO_4)_3$ and $[Cu_2(taeh)Br](ClO_4)_3$ have a Cu-X-Cu bridged structure. $[Cu_2(taeh)I](ClO_4)_3$ and $[Cu_2(taeh)N_3](ClO_4)_3$ have a structure without metal-metal bridge. The structure formations are influenced by the size of the bridged atom (halogen atom) or molecule(N_3).

The nobel polyaza macrocyclic ligand tppt form a dinuclear Cu(II) complex with chloride ion in solid and in aqueous solution by X-ray diffraction and XAFS analysis. The short metal-metal and metal-halogen ditances in the comlex are also discussed.

1, S.Matsuo, T.Yamaguchi, and H.Wakita, to be submitted in "Advances in Quntum Chemistry".
2, M. Yokomizo, T. Kurisaki, T. Yamaguchi, and H. Wakita, Bull. of the Society for Discrete Variational Xα, 11, No.1, 90(1998).
3, S.Yamashita, H.Adachi, M.Fujiwara, Y.Kato, T.Yamaguchi, and H.Wakita, in "Advances in Quntum Chemistry"(Lowdin P., ed.)Vol.29, pp357-371(1997), Academic Press, San Diego,USA.

ELECTRONIC AND SPATIAL STRUCTURE OF COMPLEX SPECIES FORMING IN SOLUTIONS OF COORDINATION COMPOUNDS (BY XAFS SPECTROSCOPY)

S.B. ERENBURG, N.V. BAUSK, L.N. MAZALOV, S.M. ZEMSKOVA, M.K. DROZDOVA
Institute of Inorganic Chemistry RAS, Lavrentiev av.3, Novosibirsk 630090, RUSSIA.

The classes of objects that have been of special interest to inorganic chemists in recent time are difficult or impossible to characterize by the traditional X-ray structural methods because they have no or a limited long-range order. In particular we have studied various complex-solvent systems containing species whose structures are determined by the processes of complexation in solutions. To study the effect of solvent on the electronic and spatial structure of the complex species forming in solutions we have measured PdK EXAFS and XANES spectra for the complexes of $PdCl_2$ with dialkylsulfides and CdK, ZnK and CuK spectra for the dialkyldithiocarbamate complexes of cadmium, zinc and copper in organic solvents with different donor properties. We have also measured SK_α, SK_β, ClK_α X-ray fluorescence spectra for this complex-solvent systems. EXAFS and XANES spectra were measured using synchrotron radiation of the VEPP-3 storage ring at the Budker Institute of Nuclear Physics in Novosibirsk. On the basis of the EXAFS, XANES and X-ray fluorescence data models have been proposed to describe the spatial structure of the complex species in nonaqueous solutions. The parameters of Pd, Cd, Zn and Cu local spatial structure were determined from EXAFS data using EXCURV92 program.

The coordination of aromatic solvent molecules to the palladium atom with the formation of weak π-bond has been revealed for the solutions of $PdCl_2$ complexes with various dialkylsulfides in benzene and pseudocumene. The distances from palladium atoms to the carbon atoms of aromatic solvents vary in the range from 2.44Å to 2.49Å. Analysis of the obtained data has indicated that the interaction mechanism of the complexes with aromatic solvents differs from that with dichloroethane. This allowed us to explain the earlier discovered differences in the extraction constant variations in a series of solvents in the extraction of silver and palladium with dialkylsulfides [1].

The models of spatial structure of complex forms for the metal chelates nonaqueous solvents have been suggested (in accordance with results of NMR spectra measurements of ^{113}Cd for cadmium complexes [2]). It was determined that $[Cd(Et_2Dtc)_2]_2$, $[Cd(nBu_2Dtc)_2]_2$ and $[Zn(nBu_2Dtc)_2]_2$ molecules in benzene solution are dimers which serve as a base unit for the solid complexes, but their spatial structure is differ in comparison with the solid state one. Zinc coordinates five sulfur atoms at a distance of 2,36Å, Zn-Zn distance is 3,80Å and the whole molecule geometry is fixed harder than in solid state. The additional coordination of phosphorus and nitrogen atoms to cadmium, zinc and copper atoms was determined for the complexes in tributhylphosphine and pyridine. Valuable changes in pre-edge and above the edge region of CuK XANES spectra in the tributylphosphine and pyridine solution in comparison with the solid complex gives an indication of changes of the $4p_z$- orbitals energy and occupancy. The coordination of solvent molecules by metal atoms of dialkyldithiocarbamate complexes Cd, Zn and Cu was not found in benzene solution.

It was shown that specific solvation of the transition metal complexes and their spatial structure in nonaqueous solutions are determined by electronic and spatial structures of molecules of the complexes as well as by donating abilities of solvents.

1. Erenburg S.B., Bausk N.V., Mazalov L.N. *et al.*, *Russian J. Struct. Chem.* 1995, **36**(6), 941.
2. Mazalov L.N., Erenburg S.B., Bausk N.V. *et al.*, *Russian J. Struct. Chem.* 1997, **38**(4), 601.

A LIQUID-TYPE QUASI-CLOSE PACKING IN CONCENTRATED AQUEOUS SOLUTIONS OF LANTHANUM CHLORIDE AND BROMIDE. X-RAY DIFFRACTION INVESTIGATIONS

Cabaço, M. I.; Gaspar, A. M.; Morais, C. M.; Marques, M. I.; and Alves Marques, M.
Centro de Física da Matéria Condensada da Universidade de Lisboa, Av. Prof. Gama Pinto, 2, 1649-003 Lisboa, Portugal and Departamento de Física do Instituto Superior Técnico, Av. Rovisco Pais, 1049-001 Lisboa, Portugal

X-ray diffraction patterns in concentrated aqueous solutions of lanthanum bromide and chloride are compared in the region of the momentum transfer $Q = (4 \pi / \lambda) \sin \theta$ (θ the diffracting angle) from $Q \sim 0.7$ up to 1.5 $Å^{-1}$. The large difference between the profiles of the scattered intensity is interpreted by the existence of molecular and ionic correlations in these solutions. A liquid-type quasi-close-packing of lanthanum cations is a reasonable approach of the network and represents a balance between tight local coordination around each cation and medium range statistical coordination dominated (both?) by electrostatic effects. Previous investigations about the same theme, using the same technique, will also be revised and discussed (1, 2, 3, 4). Experiments with concentrated aqueous solutions of copper nitrate will be, plausibly, reported and discussed.

References:

[1] M. Alves Marques and M.I. de Barros Marques, Proc. Koninkl. Ned. Akad. Wetensch., **B77** (1974) 286.

[2] M.I. de Barros Marques, M.I. Cabaço, M.A. de Sousa Oliveira and M.Alves Marques, Chem. Phys. Lett., **91** (1982) 222 and references therein.

[3] M.I. Cabaço, M.Alves Marques, M.I. de Barros Marques, G.Bushnell-Wye, M.M. Costa, M.J. Almeida and L.C. Andrade, J.Phys. Cond. Matter., **7** (1995) 7409.

[4] M.I. Cabaço, A.M. Gaspar, C.M. de Morais and M. Alves Marques, submitted to J.Mol. Liquids.

STRUCTURE OF PLATINUM AND THALLIUM CYANO COMPOUNDS WITH A DIRECT METAL-METAL BOND

Farideh JALILEHVAND, Mikhail MALIARIK, Magnus SANDSTRÖM, Ingmar PERSSON, Per PERSSON, Julius GLASER, Lars ERIKSSON and Imre TÓTH

Department of Chemistry, Royal Institute of Technology, S-100 44 Stockholm, Sweden

The structure of a family of three binuclear complexes, $[(NC)_5Pt\text{-}Tl(CN)_n]^{n-}$ with n = 1 - 3, previously characterized by spectroscopic methods,[1] has been studied in aqueous solution by means of EXAFS methods. This has been made possible by the recent development in the EXAFS data treatment which allows modeling of the excessive multiple scattering of the linearly coordinated cyano ligands. For a full structural description data were recorded both at the Pt-L_{III} and Tl-L_{III} edges. Short Pt-Tl bond distances were found, 2.598(3), 2.618(4), and 2.638(4) Å, which increase with the number of cyano ligands on the thallium atom, n = 1, 2, and 3, respectively. The platinum atom coordinates five cyano ligands with the thallium atom completing a somewhat distorted octahedron. Thallium coordinates one cyano ligand in the hydrated $[(NC)_5Pt\text{-}Tl(CN)]^-$ complex in a linear Pt-Tl-CN entity and probably four water molecules loosely bound to thallium with the Tl-O distance 2.51 Å. In the species $[(NC)_5Pt\text{-}Tl(CN)_n]^{n-}$, n = 2 and 3, the thallium atom is probably tetrahedrally four-coordinated.

A combination of X-ray powder diffraction and EXAFS methods was used to reveal the crystal structure of a powder of composition $(NC)_5PtTl$ (space group P4/nmm (No. 129), a = 7.647(3), c = 8.049(3) Å, Z = 2. In the structure $(NC)_5PtTl$ entities are linked in linear -Tl···NC-Pt-Tl··· chains; the Pt-Tl distance is 2.627(2) Å. A three-dimensional network is formed by cyano groups forming bridges between the platinum and thallium atoms of neighboring antiparallel chains. The Pt-Tl bonds can be considered as stable intermediates in a two-electron transfer between Pt^{II} and Tl^{III}.

The structures of the pentacyano $[(NC)_5Pt(OH)]^{2-}$, $[(NC)_5Pt(OH_2)]^-$, $[(NC)_5PtI]^{2-}$ complexes, and the binuclear $[Pt_2(CN)_{10}]^{4-}$ species with a Pt(III)-Pt(III) bond of 2.726 Å, have been determined in solution.

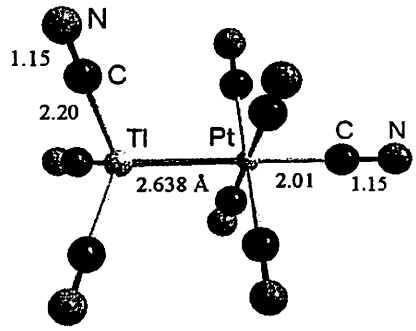

The structure of the $[(NC)_3Tl\text{-}Pt(CN)_5]^{3-}$ complex

1. M.Maliarik; K.Berg; J.Glaser, M.Sandström, I.Tóth, *Inorg.Chem.*, 1998, **37**, 2910, 5452.

A ^{15}N NMR STUDY ON THE INTRAMOLECULAR HYDROGEN BOND FORMATION IN *CYCLO*-μ-IMIDOTRIPHOSPHATE ANIONS

Hideshi Maki[1], Yoshiki Ueda[1], Hiroyuki Nariai[1], Itaru Motooka[1] and Tohru Miyajima[2]

[1]Department of Chemical Science and Engineering, Faculty of Engineering, Kobe University, 1-1 Rokkodai-cho, Nada-ku, Kobe 657-8501, Japan

[2]Department of Chemistry, Faculty of Science and Engineering, Saga University, 1-Honjo, Saga 840-8502, Japan

Cyclic imidopolyphosphate anions, involving P-NH-P linkages, i.e., *cyclo*-μ-triimidotriphosphate, $cP_3(NH)_3$, and *cyclo*-μ-tetraimidotetraphosphate, $cP_4(NH)_4$, contain non-bridging oxygen atoms as well as bridging nitrogen atoms as donor atoms for metal complexation. In addition to this interesting feature as ligand molecules, they have tautomerism equilibria. However, quite little has been known on intermolecular hydrogen bond formation in these ligands. A ^{15}N NMR technique is expected to provide deep insights into the microscopic hydrogen bond formation. ^{15}N enriched samples of these anions have been prepared and the hydrogen bond formation in the cyclic anions have been investigated precisely.

^{1}H decoupled ^{15}N NMR spectrum of $cP_4(NH)_4$ anions(Fig. 1) consists of a triplet peak, indicating equivalent coupling due to two adjacent ^{31}P nucleus; $^{1}J(^{15}N\text{-}^{31}P)$ = 24 Hz, whereas spectrum of $cP_3(NH)_3$ anions(Fig. 2) is composed of nine peaks, which may originate due to intramolecular hydrogen bond formation between imido groups and phosphate groups in the molecules. The pH profile of the ^{1}H coupled ^{15}N NMR spectra of both anions gives most straight forward evidence for the tautomerism equilibria in these cyclic anions. At extremely low and high pH regions, no ^{1}H coupling has been observed for both anions, whereas at medium pH region, i.e., pH = 6 - 8 for $cP_3(NH)_3$, and pH = 5.5 - 9.5 for $cP_4(NH)_4$, ^{1}H coupling with ^{15}N nucleus has become appreciable.

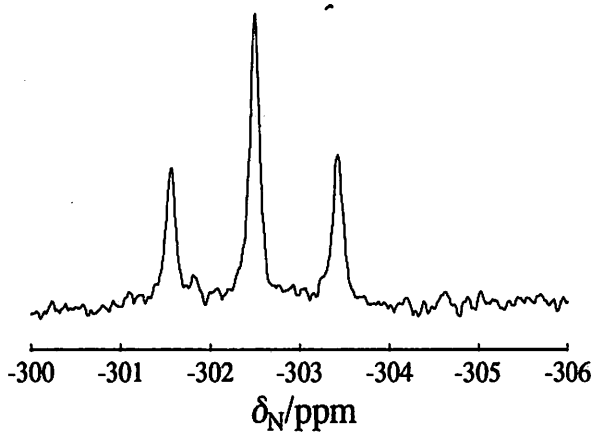

Fig.1 ^{1}H-decoupled ^{15}N NMR spectrum of $cP_4(NH)_4$ at pH=7.37.

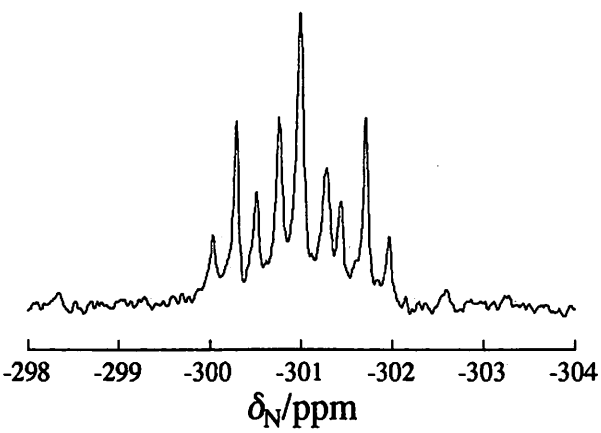

Fig.2 ^{1}H-decoupled ^{15}N NMR spectrum of $cP_3(NH)_3$ at pH=6.82.

Ternary Complexation of Metal Ions with 1,10-Phenanthroline and Halide or Thiocyanate Ions in *N,N*-Dimethylformamide

M. KOMIYA,[1] and S. ISHIGURO[1*]

[1] Department of Chemistry, Faculty of Science, Kyushu University, Hakozaki, Higashi-ku, Fukuoka, 812-8581, Japan

Binary and ternary complexation of metal(II) or metal(III) ion with 1,10-phennthroline (phen) or 2,2'-bipyridine and halide (chloride and bromide) or pseudo-halide (thiocyanate) ions has been studied by precise titration calorimetry in *N,N*-dimethylformamide (DMF) or *N,N*-dimethylacetamide (DMA) at 298K. All data obtained in ternary M^{n+}-X^--L (M = Cd(II), Zn(II) or Ln(III), X = Cl, Br or SCN, L = phen or bipy) systems were analysed on the basis of the thermodynamic quantities in binary M^{n+}-L and M^{n+}-X^- systems. All the titration curves are explained well in terms of formation of mononuclear complexes of the type $[MX_pL_q]^{(n-p)+}$. Formation of $[MXL]^{(n-1)+}$, $[MX_2L]^{(n-2)+}$, $[MX_3L]^{(n-3)+}$, $[M^{II}XL_2]^{(n-1)+}$ or $[MX_2L_2]^{(n-2)+}$ has been established in the chloride, bromide or thiocyanate systems, and their formation constants and reaction enthalpies and entropies were extracted.

In the M^{2+}-X^--phen systems, formation constants and reaction enthalpies are significantly positive and negative compared with those in the corresponding 2,2'-bipyridine systems, respectively. This indicates a stronger affinity of 1,10-phenanthroline, as the affinity of halide (or thiocyanate) ions to metal ions is almost the same in both systems. In addition, obtained reaction entropies are appreciably more positive than those in the corresponding 2,2'-bipyridine systems. In the 1,10-phenanthroline systems, ternary complexes are sufficiently formed in solution even at a high concentration of the anions and 1,10-phenanthroline, despite that 2,2'-bipyridine molecules bound to metal ion are practically expelled by the aions. Species distribution in the M^{2+}-X^--phen systems is thus different from those in the corresponding M^{2+}-X^--bipy systems.

Formation constants and reaction enthalpies of ternary $[ZnX(bipy)]^+$ and $[ZnX_2(bipy)]$ formed in DMA are significantly positive and negative compared with those in DMF, respectively, and the coordination geometry in DMA is more shifted toward the tetrahedral side than that in DMF. These may primarily originate from the steric hindrance of the acetyl methyl group of DMA coordinated to the metal ion, which weakens solvation and makes the complexation more favorable and exothermic.

SPECTROSCOPIC DETERMINATIONS OF ION ASSOCIATED STRUCTURES IN ELECTROLYTE SOLUTIONS

J. B. GILL and P. GANS,
School of Chemistry, University of Leeds, UK, LS2 9JT.

Under appropriate conditions vibrational spectroscopy is an excellent tool for the qualitative identification of the ion-paired species present in an electrolyte solution. Some of the authors' past work on the assignments made to produce structural details of various types of ion associate to be found in these solutions will be reviewed in this lecture. Examples will be provided of the use of both infrared and Raman spectra, often used in a complementary manner, to indicate the existence of contact ion-pairs (sometimes in isomeric forms), solvent-shared ion-pairs (or outer-sphere complexes), and ion aggregates.

With specific regard to metal complex ions vibrational spectroscopy has provided us with many examples of the existence of ion associates formed between complex anions and "simple" solvated cations. Also, in the particular case where a metal cation is strongly solvated/complexed by the solvent, simple monatomic anions like the halides can form "inclusion" or "penetration" ion-pairs in which the anion appears to be embedded within the sheath of the solvating molecules around the cation.

The lecture will also illustrate how vibrational spectroscopy of electrolyte solutions has indicated that contact ion-pair formation is not normally an enthalpically favourable process; it is actually an entropically driven one.

FIXATION OF LIQUID SOLUTIONS FOR THE USE OF MÖSSBAUER SPECTROSCOPY IN SOLUTION CHEMISTRY

Kálmán BURGER[1] and Attila VÉRTES[2]

[1]Research Group for Biocoordination Chemistry of the Hungarian Academy of Sciences, PO Box 440, 6701 Szeged, Hungary
[2]Department of Nuclear Chemistry of the L. Eötvös University, Budapest, Hungary

Comparison of experimental Mössbauer quadrupole splitting values with those calculated on the basis of the assumption of different stereochemistries of the Mössbauer active central atom of complexes are used to determine not only the coordination number and symmetry of the coordination sphere but also the steric position (e.g. equatorial, apical) of the single donor groups in latter[1]. To apply this procedure for the study of complexes formed in liquid solutions, latter have to be fixed strong enough to achieve recoilless γ-ray resonance absorption (the Mössbauer effect) in the system.

Fixing liquids for Mössbauer studies was performed by quenching them[2]. This has the disadvantage that due to decrease of temperature during the quick-freezing process the complex formation equilibria may shift changing the concentration ratio of the step-wise formed complexes in solution, eventually even altering the composition of some of them.

To overcome this difficulty the following new procedure was elaborated. The liquid solution, containing the Mössbauer active solute, was fixed as submicroscopic droplets in the nanosize holes of solid carriers. Latters consisted either of silicium dioxide (thirsty glass, silica tubes, etc.) or of an organic microemulsion[3]. Both types having holes of uniform pore size.

To study the effect of the internal surfaces of these pores on the structure and electronic structure of the solute, which may be reflected in the Mössbauer parameters, analogous carriers with hydrophilic and hydrophobic surfaces and with smaller (< 4 nm) and larger (> 4 nm) pore sizes were prepared.

Mössbauer investigations of aqueous solutions of different model compounds ($FeSO_4$, $SnCl_4$, $Sn(OH)_6^{2-}$, Me_2Sn-glyuconylglycine, etc.) have shown that in the carriers with strongly hydrogen bonding (hydrophylic) internal surfaces the solvent water covers latter surface preventing direct connection between the Mössbauer active solute and the surface.

On the other hand the solvated solute, situated in the H-bonded water cluster of the aqueous solution, is connected through this cluster by H-bonds to the surface bound water layer. Latter connection proved to be strong enough to fix the solution for achieving recoilless γ-ray resonance absorption above the freezing temperate of the solution.

Comparison of the Mössbauer parameters measured for solutions trapped in the carrier with those recorded for the corresponding solid model compounds, both containing the Mössbauer active central atom in the same surrounding, has shown that the fixation of the solution caused significant changes in the Mössbauer parameters in those system only, which are sensitive to water activity changes of the solution (e.g. when protonation of weak basic donors are involved etc.)

Combination of equilibrium measurements and Mössbauer investigations made possible the deconvolution of Mössbauer spectra reflecting the presence of several species of different composition and structure in the same solution and assigne the resulting spectrum parts to the corresponding species. In this way Mössbauer spectroscopy can contribute to the structural study of species formed in overlapping coordination processes in solution.

1.Burger, K., Nagy, L., Buzás, N., Vértes, A., Mehner, H., *J. Chem. Soc. Dalton Trans.*, 1993, 2499–2504.
2. Vértes, A., Nagy, D. L., *Mössbauer Spectroscopy of Frozen Solutions*, Academy Publ., Budapest, 1990.
3. Burger, K., Buzás, N., Gajda-Schrantz, K., Gajda, T., Nemes-Vetéssy, Zs., Vértes, A., Dékány, I., *Spectrochimica Acta Part A.*, 1997, 53, 2525–2536.

SELECTIVE LITHIUM ION TRANSPORT UNDER TWO-PHASE SYSTEM. MECHANISM OF ION-PAIR EXTRACTION OF ALKALI METAL IONS WITH HIGHLY LIPOPHILIC PHTHALOCYANINES SUBSTITUTED WITH MANY POLYFLUOROALKOXYL GROUPS

Takaaki SONODA, Yoichi KAMINAGA*, Kazuhiko MATSUMOTO, and Hiroshi KOBAYASHI
Institute of Advanced Material Science, Kyushu University, Kasuga 816, Japan
*Interdiciplinary Graduate School of Sciences, Kyushu University, Kasuga 816, Japan

Phthalocyanine derivatives, $H_2Pc(TFE)_n$ (n = 8, 16) and $H_2Pc(PFP)_{16}$, substituted with a large number of trifluoroethoxyl (OCH_2CF_3; TFE) and pentafluoropropoxyl ($OCH_2C_2F_5$; PFP) groups, respectively, and their metal complexes are very stable and soluble in aprotic polar solvents.

The mechanism of selective lithium ion transport from aqueous phase to organic phase under AcOEt-H_2O two-phase system was investigated by experimetal and computational methods in the ion-pair extraction reaction of alkali metal ions with the phthalocyanine derivatives, where alkali metal ions were transported in the following order: $Li^+ >> Cs^+ > Rb^+ > K^+ > Na^+$.

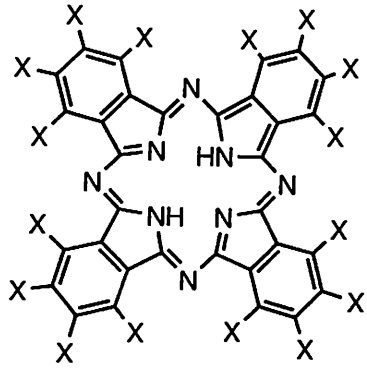

$H_2Pc(TFE)_{16}$ (X =TFE = CF_3CH_2O)
$H_2Pc(PFP)_{16}$ (X =PFP= $C_2F_5CH_2O$)

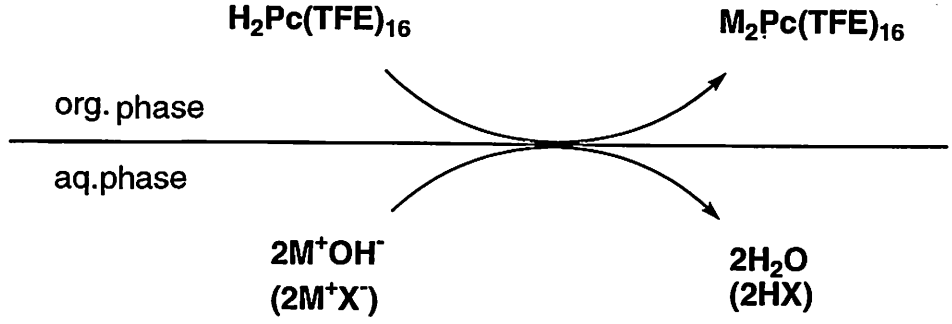

metal ion (M^+) transport : $Li^+ >> Cs^+ > Rb^+ > K^+ > Na^+$

Kinetics and Mechanism of the reactions of *trans*-(diaqua)(N,N′-ethylene-bis-salicylidiniminato)metal(III) ions with sulphur(IV) in aqueous medium: a comparative study for chromium(III), manganese(III), iron(III) and cobalt(III).

A.C. Dash and **Arabinda Das**
Department of Chemistry, Utkal University,
Bhubaneswar - 751004, Orissa (India).

ABSTRACT

The reactions of $SO_2/HSO_3^-/SO_3^{2-}$ with *trans*-$[M(salen)(OH_2)_2]^+$ (M = Cr(III), Mn(III), Fe(III), Co(III), Salen = N,N′-ethylene-bis-salicylidiniminate) under varying conditions of pH, [S(IV)] and temperature have been investigated in aqueous medium. In all cases, the reaction involves the formation of (aquo) sulphito complex, observed in the stopped flow time scale. While O-bonded sulphito complex is sole product for Cr(III), (trans-$[(OH_2)Cr(salen)(OSO_2O)]^-$, in all other cases S-bonded sulphito complex (*trans*-$[(OH_2)M(salen)(SO_3\text{-}S)]^-$ (M = Mn(III), Fe(III), Co(III)) is formed. This occures by direct substitution of the diaqua or aqua hydroxo forms of the parent complex by HSO_3^- and/or SO_3^{2-} in the case of Mn(III) and Fe(III). The $[S^{IV}]_T$ and pH dependence, however, suggest that *trans*-$[Co(salen)(OH_2)_2]^+$ and *trans*-$[Co(salen)(H_2O)(OH)]$ react with SO_2 to generate the *trans*-$[Co(Salen)(OH_2)(SO_3\text{-}S)]^-$ (S-bonded isomer) without intervention of the O-bonded sulphito complex. The *trans*-$[(OH_2/OH)Cr(salen)(OSO_2\text{-}O)]^{-/2-}$ exerts a small *trans*-labilising effect as demonstrated in the aqua-hydroxo ligand substitution by py, imidazole, N_3^- and NCS^-. The *trans* effect of the S-bonded sulphite in *trans*-$[Co(salen)(OH_2)(SO_3\text{-}S)]^-$ is also not substantial. Unlike the *trans*-$[Co(salen)(OH_2)(SO_3\text{-}S)]^-$, the complexes of Mn(III) and Fe(III) undergo redox reactions. While the redox reactions of Fe(III) complex involves both inner and outer sphere type, the corresponding Mn(III) complex involve essentially outersphere type.

A SHORT-LIVED INTERMEDIATE IN THE REACTION OF MERCURY(II)-PORPHYRIN WITH SILVER(I)

M. TABATA, W. MIYATA and K. NAKATAKI
Deapartment of Chemistry, Faculty of Science and Engineering, Saga University,
1 Honjo-machi, Saga, 840-8502, Japan

The kinetics and mechanism of metal-substitution reaction of 5,10,15,20-tetrakis(4-sulfonatophenyl)porphyrinatomercury(II) with silver(I) ion was studied at pH 6-7.5, I = 0.1 ($NaNO_3$) and 25°C in a large excess of silver(I). The reaction was started by mixing two solutions: one contains $[Hg_2(tpps)]^{2-}$ ($1x10^{-6}$ - $4x10^{-6}$ M), Hg^{2+} ($1x10^{-5}$ - 10^{-4} M), PIPES buffer (10^{-2} M) and $NaNO_3$ (0.1 M), and other contains Ag^+ ($1x10^{-3}$-10^{-2} M), PIPES buffer and $NaNO_3$. and followed by a UNISOK RSP-601 stopped-flow/rapid-scan spectrophotometer, where M = mol dm^{-3}.

Figure 1 shows the change in absorption spectra and clearly indicates the formation of an intermediate. After the mixing of the solution of $[Hg_2(tpps)]^{2-}$with Ag^+, absroption maxima (λmax = 434 nm)) of $[Hg_2(tpps)]^{2-}$shifted to 445 nm and reached to a maximum absorbance during the reaction time of 0-2s (the first-step reaction). The aborbance at 445nm then decreased and reached to a constant absorbance for a reaction time of 10-60s (the second step reaction). Finally, the absorbance at 445nm decreased gradually and that at 421 nm increased for 1-60 min (the third step). The each reaction path was analyzed at various concentrations of the porphyrin, Hg^{2+}, Ag^+ and pH. From the results, the following reaction processes are proposed:

$$[Hg_2(tpps)]^{2-} + Ag^+ \longrightarrow [Hg(tpps)Ag]^+ + Hg^{2+}$$

$$[Hg(tpps)Ag]^+ \longrightarrow [Ag(tpps)]^{5-} + Hg^{2+}$$

$$[Ag(tpps)]^{5-} + O_2 + 4H^+ \longrightarrow [Ag(II)tpps)]^{4-} + 2H_2O$$

In the heterodinuclear metalloporphyrin, Hg^{2+} and Ag^+ bond to the porphyrin simultaneously. Due to the large ionic radii of Hg^{2+} and Ag^+, these metals of $[Hg(tpps)Ag]^{2-}$ are located in out of plane and the intermediate is stable and gives a large spectral change compared with the intermediate ($[Hg(tpps)Cu]^{2-}$) reported previously for the reaction of $[Hg_2(tpps)]^{2-}$ with Cu^{2+}.[1]

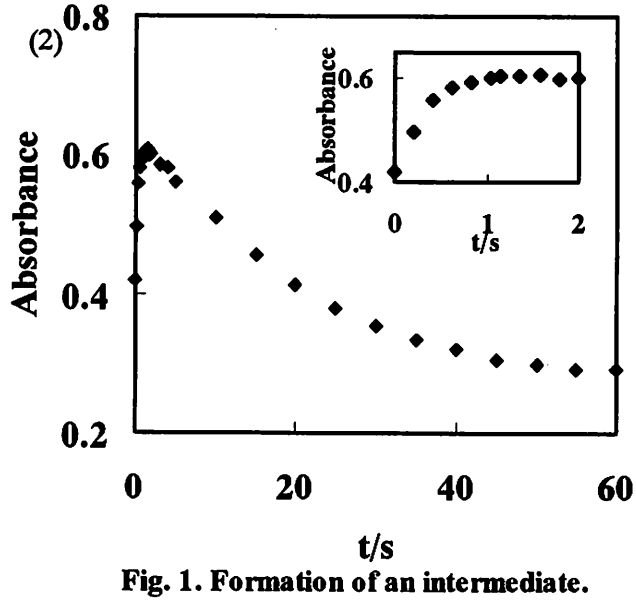

Fig. 1. Formation of an intermediate.

1. M. Tabata, W. Miyata, and N.Nahar, *Inorg. Chem.* **1995**, *34*, 6492.

SOLUTION THERMODYNAMICS. IMPORTANCE OF THERMOPHYSICAL DATA FOR MODELLING NON-ELECTROLYTE MIXTURES PROPERTIES

Jean-Pierre E. GROLIER
Laboratoire de Thermodynamique et Génie Chimique, Université Blaise Pascal, 24 avenue des Landais, 63177 Aubière, France

When dealing with mixtures or solutions, two types of information are of major importance for theoretical as well as engineering calculations : pure phase thermophysical properties and, more generally, phase-equilibrium data. Theoretical models of molecular interactions can be developed from *ab initio* calculations to estimate excess quantities of mixtures, as well as phase equilibrium data. However, such calculations are possible only for mixtures of rather simple molecules and are restricted to limited ranges of the p-T-x variables. Accurately measured thermophysical properties are then essential to improve model calculations and also to validate prediction procedures.

Taking into consideration the great number of possible mixtures obtained by combining the large number of (existing or available) substances an approach based on functional group contribution methods is certainly the best way to deal with non-electrolyte mixtures. In this context direct experimental data must be obtained on selected key systems in order to characterize functional group pair-wise interactions.

New concepts and novel designs of calorimetric techniques[1,2] have extended the accessible ranges of temperature and pressure; in addition automated and faster procedures facilitate data acquisition. Remarkably sophisticated instruments are now available, which provide heats of mixing and derived quantities, like heat capacities and thermomechanical coefficients[3,4], to considerably enlarge reliable databases.

Recent measurements on selected organic mixtures will serve to illustrate how physico-chemical interpretation of molecular interactions and predictive methods of excess quantities and phase equilibria have gained from experimental achievements[5].

1. Randzio, S.L.; Grolier, J-P.E.; Quint, J.R., *Rev. Sci. Instruments*, 1994, **65**, 960.

2. Mathonat, C.; Hynek, V.; Majer, V.; Grolier, J-P.E., *J. Solution Chem.*, 1994, **23**, 1161.

3. Grolier, J-P.E.; Randzio, S.L., *Fluid Phase Equilibria*, 1997, **133**, 35.

4. Randzio, S.L.; Grolier, J-P.E.; Quint, J.R., *High Temperatures-High Pressures*, 1998, **30**, 645.

5. Grolier, J-P.E., *Pure & Applied Chemistry*, 1997, **11**, 2231.

HEAT CAPACITIES OF THE CONSTITUENT GROUPS OF UNFOLDED PROTEINS IN AQUEOUS SOLUTION

Gavin R. HEDWIG
Institute of Fundamental Sciences – Chemistry, Massey University, Palmerston North, New Zealand

The partial molar heat capacity of the fully unfolded form of a protein in aqueous solution is an important quantity in discussions of the thermodynamic stability of proteins. As this form of a protein is often experimentally inaccessible, its heat capacity is usually evaluated using a group additivity scheme. In this approach it is assumed that the heat capacity of the protein can be obtained using a simple summation of the partial molar heat capacities of the constituent groups such as the amino acid side-chains, the backbone peptide group and the ionic end-groups. These group contributions are derived using heat capacity data for solutes of low molar mass that are chosen to model the various constituent groups of proteins.

In current studies we have used tripeptides of sequence glycyl-X-glycine, where X is one of the naturally occurring amino acids, as compounds to model the amino acid side-chains of proteins. The partial molar heat capacities at infinite dilution, $C^{o}_{p,2}$, over the temperature range 10 to 100 °C have been determined for 20 tripeptides using high sensitivity differential scanning calorimetry. These heat capacities were used to derive group contributions for all the amino acid side-chains. For several of the hydrophobic side-chains, group contributions were also derived from heat capacity data for neutral N-acetyl amino acid amides determined over the temperature range 15 to 55 °C using flow calorimetry.

These side-chain heat capacities, along with that of the backbone peptide group, which was derived from heat capacity data for a homologous series of peptides of sequence alanyl(glycyl)$_x$glycine, x = 1 – 3[1], were used to calculate the partial molar heat capacities of some oligopeptides and unfolded proteins in aqueous solution. These results will be presented and compared with those obtained using heat capacity data for alternative model compounds.

Although group additivity schemes to calculate the heat capacities of oligopeptides and proteins have been widely used for many years, the principle of group additivity has, hitherto, not been verified experimentally for these systems. We have determined recently $C^{o}_{p,2}$ values over the temperature 10 to 100 °C for several tetrapeptides of sequence glycyl-X-Y-glycine, where X and Y are different amino acids. These results will be presented and compared with those calculated using group contributions.

1. Häckel, M.; Hedwig, G.R.; Hinz, H.-J., *Biophys. Chem.*, 1998, 73, 163.

EXCESS MOLAR ENTHALPIES FOR BINARY MIXTURES OF HEXANE + 1-HEXANOL NEAR THE CRITICAL POINT

H. OGAWA[1], J.-Y. COXAM[2], J.-P. E. GROLIER[2] and S. L. RANDZIO[3]
[1]Department of Natural Sciences, Faculty of Science and Engineering, Tokyo Denki University, Hatoyama, Hiki-gun, Saitama, 350-0311, Japan
[2]Laboratoire de Thermodynamique et Génie-Chimique, Université Blaise Pascal, 63177 Aubière, France
[3]Polish Academy of Sciences, Institute of Physical Chemistry, ul. Kasprzaka 44/52, PL-01-224 Warszawa, Poland

Introduction

Recently, the pressure variables of the thermodynamic properties for binary mixtures of hexane + 1-hexanol have been calculated by Grolier and Randzio[1] from the isobaric thermal expansivities and the molar volume isotherm. The results of the calculated pressure derivatives of excess molar enthalpy show fairly large and positive value in the vicinity of the critical points of hexane. In order to check the validity of such calculation method using density data and to explain the behavior of the component molecules of the mixture, excess enthalpies, H^E were estimated by direct calorimetry.

Experimental

Apparatus used in this study was flow calorimeter which has been remodeled by Mathonat et al[2] from the commercial product of differential heat flux calorimeter (C-80, SETARAM). Procedure adopted was ordinary method in the flow calorimetry. Materials were special grade reagents. Hexane was used without further purification, 1-hexanol was stored over the 4A molecular sieves.

Results and Discussion

H^E were evaluated at 9 temperatures between 323 and 533K and at 4 pressures between 3.5 and 15MPa. These temperature range include the critical temperature of hexane (507.68K). All pressure conditions exceed the critical pressure of both component liquids of hexane (3.035Mpa) and 1-hexanol (3.46Mpa). At lower pressure than those critical values, measurement has been impossible by extremely unstable output signal from the calorimeter.

Enthalpy changes on mixing were positive (endothermic) for all temperatures and pressures. The small pressure dependence of H^E at low temperature became remarkably large positive near the critical point of hexane. Temperature dependence of H^E was large and positive at lower temperature and large and negative near the critical point. The complicated concentration dependence of H^E at lower temperature became monotonous and parabolic with increasing temperature.

The tendencies on pressure dependence of H^E were agreed with those calculated from volume behavior, however, small differences appeared in the magnitude especially at the higher pressure. These discrepancies will be resulted from the problem in the polynomial equation to express the properties as function of pressure and temperature.

These phenomena will be explained qualitatively considering decrease of free volume at higher pressure and decrease of local concentration fluctuation at higher temperature. In the vicinity of the critical point of the one component, reduced temperature and reduced pressure are much different between pure state and mixing state corresponding to the difference in critical points. At lower pressure near the critical temperature, the gas-like volume of hexane decrease by mixing with liquid-like 1-hexanol, and this effect brings negative contribution to positive H^E of this system. But, this positive contribution become small rapidly as increase of pressure by decrease of volume of hexane.

References

1. Grolier, J.-P. E.; Randzio, S. L., *Fluid Phase Equilibria*, 1997, **133**, 35.
2. Mathonat, C.; Hynek, V.; Majer, V.; Grolier, J.-P. E., *J. Solution Chem.*, 1994, **23**, 1161.

CONSECUTIVE COMPLEX FORMATION REVISITED.

Claus E. Schäffer, ces@kiku.dk
Chemical Laboratory I (Department of Chemistry,
University of Copenhagen), H.C.Ørsted Institute,
Universitetsparken 5, DK 2100 Copenhagen Ø

We shall be concerned with stepwise complex formation involving unidentate, neutral ligands and a central ion whose coordination number remains constant during the complexation process. Under these circumstances this process can from a thermodynamic point of view by using standard notation be described by one **primary parameter**

$$\mathbf{logK_{av}} \equiv Av_i\,(logK_i) = [\Sigma_i\,(logK_i)]/N = (log\beta_N)/N$$

where av represents geometrical average and Av arithmetrical average.[1] Approximate values for the individual $logK_i$ ($i = 1,2 \ldots N$) can be obtained by applying parameter-free statistical corrections to $\mathbf{logK_{av}}$. The purely statistical constants K_i' are given by[1]

$$K_i'/K_{av} = (N - i + 1)/i$$

and the corrections to $\mathbf{logK_{av}}$ are accordingly equal to $\log[(N - i + 1)/i]$ where it should be noted that $\Sigma_i\,\{\log[(N - i + 1)/i]\} = 0$ so that the logarithms of the statistical constants K_i', $logK_i'$, are symmetrically distributed around $logK_{av}$.

The normal observation is that the consecutive constants decrease more than would be expected from this statistical point of view. This can be qualitatively understood by a charge accumulation effect. When, for example, ammonia ligands stepwise replace water molecules, the more covalent metal-ammine bond causes in each step an increased charge donation from the ligand sphere to the metal ion. In order to try to quantify this phenomenon, we assume that the consecutive constants K_i can be corrected for the effect of charge accumulation by the following expression:
$K_i'' = a^{(i-1)}K_1$, where a is a positive quantity, usually smaller than unity. This expression, or $logK_i'' = \log[a^{(i-1)}] + logK_1$, leads, for N=4, by barycentration to the correction vector, $\{\Delta logK_4', \Delta logK_3', \Delta logK_2', \Delta logK_1'\} = \log(a^{1/2})\{3, 1, -1, -3\}$, which is to be added to the vector $\{logK_4', logK_3', logK_2', logK_1'\}$ in order to obtain the results of our two-parameter model. Evaluation of these results thus depends on **the secondary parameter** a.

It is found that certain chemical systems, e.g. Cu^+-NH_3 (N = 2), Cu^{2+}-NH_3 (N = 4), and Ni^{2+}-NH_3 (N = 6), can be described almost within the experimental uncertainty by our two-parameter model. For the Cu^+-NH_3 system this description is tautological and trivial..

1. Schäffer, C. E., Coordination Chemistry, ACS Symposium Series 565, Ed. George B. Kauffman, 1994, Chapter 8.

DILUTE NONELECTROLYTE SOLUTIONS : THERMODYNAMICS, HIGH-PRECISION EXPERIMENTS, DATA REDUCTION AND THEORY

Emmerich WILHELM

Institut für Physikalische Chemie, Universität Wien, Währinger Straße 42,

Wien, A-1090, Austria

Dilute nonelectrolyte solutions form only a subset of fluid mixtures, yet they are of fundamental importance for the foundations of mixture thermodynamics, and are also of considerable interest in a multitude of areas in the applied sciences,[1-3] such as chemical technology, oceanography, geochemistry and biophysics, to name but a few. In this conference contribution I will be concerned with

(I) the concise formulation of the relevant thermodynamics with the focus being on vapor-liquid equilibria involving noncondensable solutes (gases),

(II) the practical implementation of thermodynamic theory in high-precision experiments, and

(III) the semi-theoretical estimation of several auxiliary quantities needed in rigorous data reduction.

Henry fugacities (also known as Henry's law constants), Ostwald coefficients, and mole fraction solubilities will be considered as well as various quantities derived via the temperature dependence of the Henry fugacities (van't Hoff analysis), such as partial molar enthalpy changes and partial molar heat capacity changes on solution.[4-6] Some of the main problems encountered in data reduction and data correlation over large temperature and pressure ranges will be critically discussed and illustrated by selected results obtained for aqueous and nonaqueous dilute solutions.

1. Hildebrand, J.H.; Prausnitz, J.M.; Scott, R.L., *Regular and Related Solutions,* Van Nostrand Reinhold, New York, **1970**.
2. Wilhelm, E., *CRC Crit. Rev. Analyt. Chem.*, **1985**, 16, 129-175.
3. Prausnitz, J.M.; Lichtenthaler, R.N.; Azevedo, E.G., *Molecular Thermodynamics of Fluid-Phase Equilibria*, 2nd edition, Prentice-Hall, Englewood Cliffs, N.J., **1986**.
4. Wilhelm, E., in : *Molecular Liquids: New Perspectives in Physics and Chemistry,* Teixeira-Dias, J.J.: editor. Kluwer Academic Publishers, Amsterdam, **1992**, 175-206.
5. Wilhelm, E., *Thermochim. Acta*, **1997**, 300, 159-168.
6. Wilhelm, E., *High Temp. - High Press.*, **1997**, 29, 613-630.

THE USE OF DENSIMETRY AND FIXED-CELL SCANNING CALORIMETRY TO PROBE SOLUTE AND SOLUTION STRUCTURE AND REACTIONS FROM 270 TO 400 K

E. M. Woolley, M. Stark, M. L. Origlia, T. D. Ford, T. G. Call, and K. Ballerat-Busserolles
Department of Chemistry & Biochemistry, Brigham Young University, Provo, Utah 84602, U.S.A.

Apparent and partial molar heat capacities and volumes can be sensitive indicators of the structure of solutions and solutes. Recent advances have been made in the design and use of fixed-cell, power-compensation, differential-output, temperature-scanning calorimeters that permit the measurement of precise heat capacities of solvents and solutions at temperatures from about 260 to 400 K and at pressures from ambient to 0.4 MPa. We have shown that these new calorimeters can be used to determine aqueous solution volumic heat capacities that are precise and accurate to between 5 and 50 ppm. Densities of the solutions are also required with the same precision and accuracy over the same range of temperatures in order to obtain the more useful apparent and partial molar heat capacities from the calorimetric results. A carefully thermostated vibrating-tube densimeter has been interfaced for computer control to efficiently provide solution densities of this quality at temperatures from 273 to 370 K. Thus, the heat capacity and density measurements from these two instruments facilitate the determination of apparent molar heat capacities and apparent molar volumes of aqueous solutions at solute molalities as low as 10^{-3} mol·kg^{-1} and at temperatures from 273 to 400 K.

In this paper we will present new densimetric and calorimetric results for a variety of aqueous solutions that illustrate the effects of solute structure, concentration, and temperature on apparent molar volumes and apparent molar heat capacities. Solutes investigated include the following: (a) surfactants, where "hydrophobic interactions" are important, (b) neutral weak acids and bases, (c) neutralized acids and bases, (d) neutral, protonated, and de-protonated amino acids, (e) sugars, and (f) both strong and ion-paired electrolytes. The heat capacity results for structurally-related species can be combined to obtain precise derived properties as functions of temperature and solute concentration, such as changes in enthalpies and free energies for proton dissociation and precise pH values for buffer solutions.

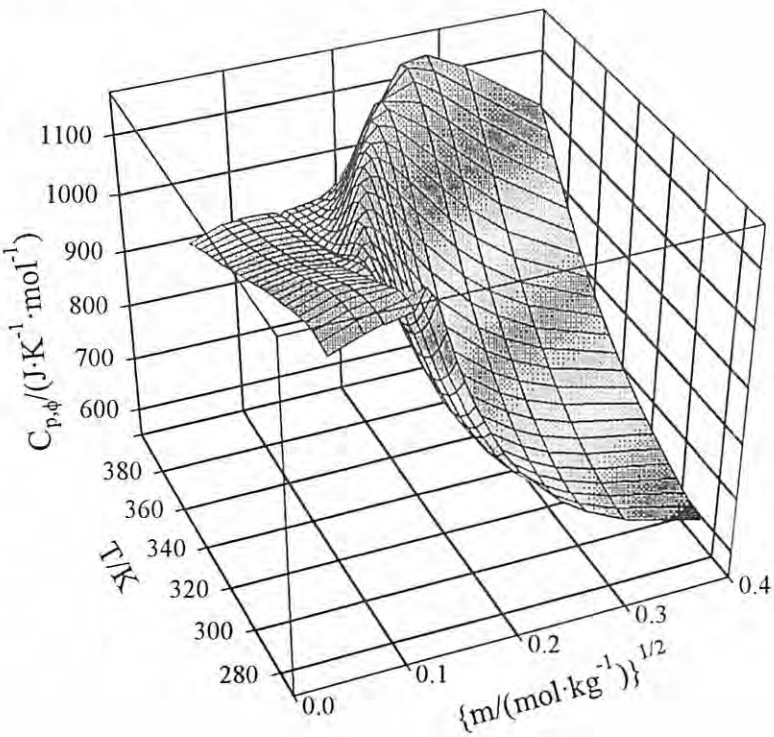

Surface of apparent molar heat capacity *vs* molality and temperature for aqueous *n*-dodecylpyridinium chloride. Intersections of lines on the surface represent experimental values. The "humps" at low and high temperatures result from changes in speciation, and the steep decrease occurs as micelles form above the "critical micelle concentration." This figure illustrates the remarkable sensitivity of heat capacities as an indicator of solute-solute and solute-solvent interactions.

SOLUTION THERMODYNAMIC ASPECTS OF LIQUID AND SUPERCRITICAL CO_2 FOR PRECISION CLEANING

Rajiv KOHLI
RKAssociates, 2450 Airport Road, D-238, Longmont, Colorado 80503, USA

On the pressure-temperature phase diagram for CO_2 the liquid phase exists above the triple point (0.52 MPa, 216.45 K) and supercritical phase exists above the critical point (7.38 MPa, 304.45 K). Liquid and supercritical CO_2 are finding increasing use for a wide variety of precision cleaning and processing applications as replacements for ozone-depleting solvents. In these fluid states, CO_2 exhibits very low surface tension and viscosity that enable CO_2 in these states to penetrate tight spaces in parts with complex geometries. Also, CO_2 is inexpensive, it is widely available and it is non-toxic. Although CO_2 in these fluid states is well suited to remove organic compounds and films due to its excellent solvating properties for nonpolar organic compounds, CO_2 has very limited solubility for inorganics and particulates. However, the presence of co-solvents, including water, low molecular weight alcohols, and fluorinated ligands, enhances the cleaning efficiency of CO_2 in these fluid states for inorganic compounds and particulates.

By applying solution thermodynamics considerations of solute behavior in the fluid solvents, better understanding can be gained of the behavior of co-solvents in liquid and supercritical CO_2. For this purpose, the thermodynamic properties have been estimated for species of interest from 10-50 MPa in the temperature range 273 K into the critical region. The estimation techniques are based on the Born equation for the absolute standard partial molal Gibbs free energy of solvation $\Delta\overline{G}^0$, which can be written for the jth ion as

$$\Delta\overline{G}_j^0 = \frac{N^0 Z_j^2 e^2}{2r_{e,j}}\left(\frac{1}{\varepsilon} - 1\right)$$

where N^0 denotes Avogadro's number, ε is the relative permittivity of H_2O, e represents the electronic charge, $r_{e,j}$ is the effective electrostatic radius of the jth ion, and Z_j is the formal charge on the jth ion.

The thermodynamic properties have been estimated using revised equations of state in the Shock-Helgeson approach. This approach is more generally applicable than other estimation techniques based on solely electrostatic or density models of the thermodynamic properties. The estimated values are in good agreement (within ~5%) with the relatively few available experimental data in the critical region for CO_2. The thermodynamic data are being employed to understand the behavior of co-solvents in liquid and supercritical fluids CO_2 that may lead to the development of new formulations for enhanced precision cleaning applications.

VOLUMETRIC PROPERTIES CONCERNING QUATERNIZATION OF TRIETHYLPHOSPHINE

César A. N. Viana [1], António R. T. Calado [2,*] and Lídia M. V. Pinheiro [2,*]
[1] CECUL-IBRC - Cç. Bento da Rocha Cabral, 14, 1200-Lisboa.
[2] Faculdade de Farmácia da Universidade de Lisboa - CECUL-IBRC, Av. das Forças Armadas, 1649-019 Lisboa, Portugal.
* To whom correspondence should be addressed.

Pressure effects on the amines and phosphines quaternization reactions in solution has been studied for several years.[1-3] Following the kinetics and thermodynamic research studies on Menshutkin and Menshutkin-type reactions, [4,5] (particularly, the high pressure ones), the results related to the pressure effect on rate constants of the triethylphosphine quaternization in six protic and dipolar aprotic solvents, at 313,15 K, are presented.

Several mathematical models were experimented,[5] and two equations were selected, namely the Asano [6] (Figure 1) and the Golinkin-Laidlaw-Hyne equation,[7] from which the results were analysed. The pressure dependence of rate constants is discussed in terms of activation volumes, extrasolvation numbers and isothermal compression of activation, allowing the dissecting of the mechanistics contribuitions.

Calculated activation parameters (Table 1) reflects the change in solvation between initial and transition state, indicating a superior solvation state in the quaternization of triethyphosphine, when compared with the correspondent Menshutkin reaction. In general, activation volumes are far more negative and the charge development index shows a later transition state in the phosphine reaction.

Differential analyses of the pseudo-thermodinamic activation functions between the different solvents were also performed, confirming the relevant paper of the hydrogen bond effects upon solvation.

Figure 1
Et_3P + EtI (Asano equation)

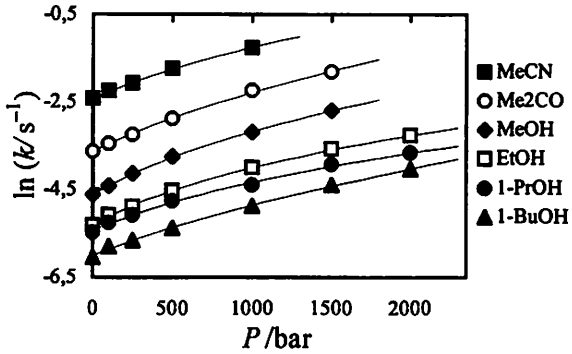

Table 1

	$-\Delta^{\ddagger}V^{0}_{Et_3N+EtI}$	$-\Delta^{\ddagger}V^{0}_{Et_3P+EtI}$
MeOH	37,3 (1,7)	55,7 (1,9)
EtOH	32,4 (1,3)	52,2 (1,6)
1-PrOH	29,1 (1,4)	42,2 (0,3)
1-BuOH	28,1 (1,0)	38,7 (3,2)
MeCN	31,6 (1,3)	43,4 (3,5)
Me_2CO	55,1 (5,0)	48,9 (4,1)

1. Forster, W.; Laird, R. M., *J. Chem Soc. Perkin Trans. 2*, 1991, 1033.
2. Abboud, J.-L. M.; Notario, R.; Bertrán, J.; Solà, M., *Prog. Phys. Org. Chem.*, 1993, **19**, 1.
3. Kondo, Y.; Zanka, A.; Kusabayashi, S., *J. Chem. Soc., Perkin Trans. 2*, 1985, 827.
4. Viana, C.A.N.; Calado, A.R.T.; Pinheiro, L.M.V., *J Chem. Res. (S)*, 1992, 6; *(M)*, 1992, 173.
5. Viana, C. A. N.; Calado, A. R. T.; Pinheiro, L. M. V., *J. Phys. Org. Chem.*, 1995, **8**, 63.
6. Asano, T.; Yano, T.; Okada, T., *J. Am. Chem. Soc.*, 1982, **104**, 4900.
7. Golinkin, H. S.; Laidlaw, W. G.; Hyne, J. B., *Can. J. Chem.*, 1966, **44**, 2193.

THEORETICAL ESTIMATION OF EXCESS THERMODYNAMIC QUANTITIES FOR SUPER CRITICAL FLUID MIXTURES

Masaharu Ohba[1], Takahide Goto[1], Hideo Ogawa[2] and Sachio Murakami[3]
[1]Faculty of Agriculture, Meijo University, Shiogamaguchi, Tenpaku-ku, Nagoya, 468-0073, Japan
[2]Faculty of Science and Engineering, Tokyo Denki University, Hatoyama, Saitama 350-03, Japan
[3]Faculty of Science, Osaka City University, Sumiyoshi-ku, Osaka, 558 Japan

[Introduction] Recently, much attention has been paid to the properties of super critical fluid mixtures, because of the development of industrial applications of fluids such as the super critical fluid extraction. Therefore, it is the urgent subject to study the thermodynamic properties of fluid mixtures near and at the critical point. The investigations of excess thermodynamic properties of fluid mixtures near the critical point have been steadily increasing during the past decade. In this work, we will calculate the excess thermodynamic quantities for model fluid mixtures near the critical point by using the PY integral equation, and compare the results with some experimental data.

[Model] Model system is the two component fluid mixture interacting through the 12-6 Lennard-Jones potentials. The values of interaction parameters for component A are fixed at ε_{AA}=1 and σ_{AA}=1. Those of the component B are determined so that the ratio of the critical temperature and pressure of two components for model fluids will be equal to those of real fluids to be compared. The Lorentz-Berthelot rule is used for interaction parameters between unlike molecules.

[Results and Discussions] We calculated the excess enthalpies H^E of the model fluid mixture with ε_{BB}=1.846 and σ_{BB}=1.227. This system is corresponds to the mixture of ethane and 1-propanol, whose experimental values of excess enthalpies and volumes were reported by Ott *et al.*[1] Figure 1 shows the phase diagrams of ethane and 1-propanol (lower figure) and the pure components of the model system(upper figure). The p, T values of the measured and calculated systems shown in Fig.2 are also plotted in Fig.1. The curves of H^E for the model system at T=1.5 and 1.6 are not drawn near x_1=0.8～0.9, because the PY equation cannot be solved in this range. The H^E curves of the model system quite resemble those of the ethane and 1-propanol system in spite of no hydrogen bond and dipolar interaction in our model systems. For the mixture composed of the liquids whose state are near the triple point, the neglect of the hydrogen bond and dipolar interaction does not give the agreement as shown in this calculations. As is not shown here, we have also obtained the good agreement between the model system and the mixture of ethane and ethene near the critical point. This indicates that the most important factor to determine the behavior of excess thermodynamic quantities near the critical point is the relative position of the measured state to its critical point of each component.

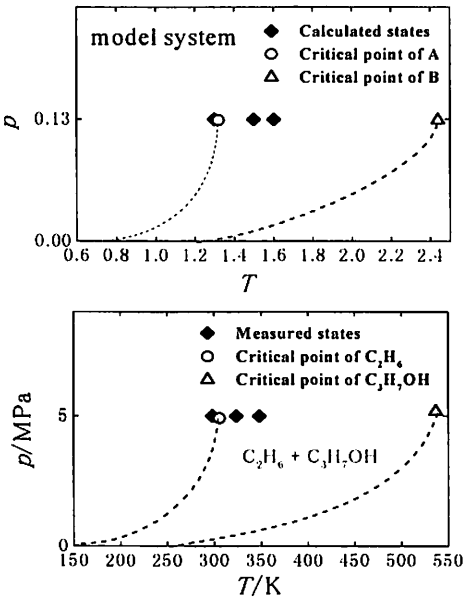

Figure 1. Calculated Measured states of the mode and ethane+1-propanol.

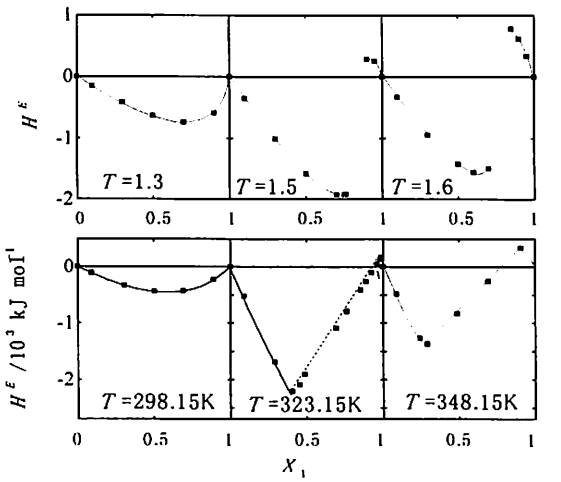

Figure 2. Excess enthalpies of the model fluid mixture (upper figure) and ethane+1-propanol (lower figure). X_1 means the mole fraction of A or ethane.

(1) Ott, J.B., Lemon, L.R., Sipowska, J.T., Brown, P.R., *J.Chem. Thermodynamics*, **27**, (1995) 1033.

Investigation of the metal ion speciation at trace level in complex aqueous solution by separation methods.

M. PESAVENTO
Department of General Chemistry, University of Pavia, Via Taramelli 12, 27100 Pavia, Italy

The distribution of a metal ion in an aqueous sample among different chemical species (speciation) is of paramount importance in determining its actual toxicity, bioavailability and transport mechanism, which is essentially due to precipitation/adsorbtion/dissolution processes. Many methods exist for the characterization of metal complexes in solution, but the detection limits of the different techniques and the presence of interfering substances can limit their application in the case of real samples with low metal ions concentration. An example of this are the potentiomentric methods with ion selective electrodes. Actually the most widely diffused methods for the experimental investigation of the speciation of trace metal ions in real samples are those based on the separation of one species, before preconcentration and determination.

The ion exchange complexing resins are often used to this aim, since they have a high selectivity towards those metal ions which are complexed by the active groups in the resin. The species sorbed is the free metal ion, but of course not only that originally present as such in the sample, but also that dissociated from the complex present in the solution phase, if any. As a matter of fact the complexation equilibrium in solution, $M + I \leftrightarrow MI$, is shifted to the left when the free metal ion is sorbed on the resin, since this complexation and the sorption equilibrium on the resin are concomitant. Thus not the free metal ion fraction, but the "labile fraction" is sorbed on the resin and experimentally determined. While being related, the two quantities are well different, and, moreover, the labile fraction strongly depends on the experimental conditions, and has only an operational meaning.

Only recently it has been shown[1] that the concentration of the free metal ion in solution [M], in the presence of a sorbing material, and at equilibrium, can be calculated from the sorbed metal ion concentration, c, by the relationship $[M] = cV/K^*w$. K^* is the ratio of the metal ion concentration in the solid phase to the free metal ion in solution, and can be evaluated independently.

The stability of the complexes in equilibrium with the resin can be globally evaluated by determining the side reaction coefficient of the metal ion, α, i.e. the ratio of total to free metal ion in solution ($\alpha = (c_{tot}-c)/[M]$). Only those complexes which are in equilibrium with the resin, being at least partially and not completely dissociated by the resin, are detected. Weaker or stronger complexes are respectively quantitatively dissociated, or not dissociated at all, so that they can be investigated by the same approach, but only using a resin with different sorbing properties towards that metal ion.

Also the concentration of the ligands can be evaluated by titration with the metal ion of interest in the presence of a proper complexing resin. [M] is evaluated from the concentration of sorbed metal ion by the relation reported above. The total ligand concentration and the conditional stability constant are obtained according to a procedure previously described[2].

Samples of environmental interst, freshwater and seawater, were examined by the methods proposed, using different resins. Sometimes unexpectedly steady complexes of heavy metal ions were detected. Of course their nature could not be determined by the proposed methods, but interesting informations could be obtained by comparing the side reaction coefficients, concentration and conditional constants obtained experimentally, with the corresponding values of known ligands.

1. M. Pesavento; R. Biesuz, *Anal. Chem.*, 1995, **67**, 3558.
2. I. Ruzic, *Anal. Chim. Acta*, 1982, **140**, 99.

ADSORPTION EQUILIBRIA OF TETRAVALENT METAL IONS ON IDA-TYPE CHELATING RESINS

Akio YUCHI and Norihito YOSHIDA
Department of Applied Chemistry, Nagoya Institute of Technology, Gokiso, Showa, Nagoya 466-8555, Japan

In a previous study,[1] we have determined the adsorption curves for seven trivalent metal ions(M^{3+}) on the chelating resins containing iminodiacetic acid groups(-LH_2), under the conditions of metal ions excess against chelating groups. Such adsorption curves unambiguously indicated the presence of two adsorption species, [$(-L)_2HM$] and [$(-L)_3H_3M$]. We have extended this work to the adsorption of tetravalent metal ions(M^{4+}: Th^{4+}, Zr^{4+}, Hf^{4+}).

The adsorption of Zr^{4+} and Hf^{4+} steeply increased with a decrease in an acidity between 0.5 and 2.5 mol dm^{-3}. The acidity-dependence and no effect of coexisting anions suggested the adsorbed species of [$-LM(OH)_2$].

The adsorption of Th^{4+}, on the other hand, gradually increased with an increase in pH between 0.5 and 3.5 and approached to a limiting value, which corresponded to half that of the total amount of [$-LH_2$]. Equilibrium analysis identified three species, [$(-L)_4H_4Th$], [$(-L)_3H_2Th$] and [$(-L)_2Th$].

The adsorption constants for [$(-L)_a(H)_bM$] (a-b=1; M: trivalent metal and Th ions), K_{ab}= [$(-L)_a(H)_bM$][H^+]$^{2a-b}$/[M^{m+}][-LH_2]$_a$, agreed well with the stability constants of these metal ions with methyliminodiacetic acid in aqueous solutions, K=[$ML^{(m-2)+}$][H^+]^2/[M^{m+}] [H_2L], irrespective of the presence of monoanionic species, [-LH^-] in the resin phase.

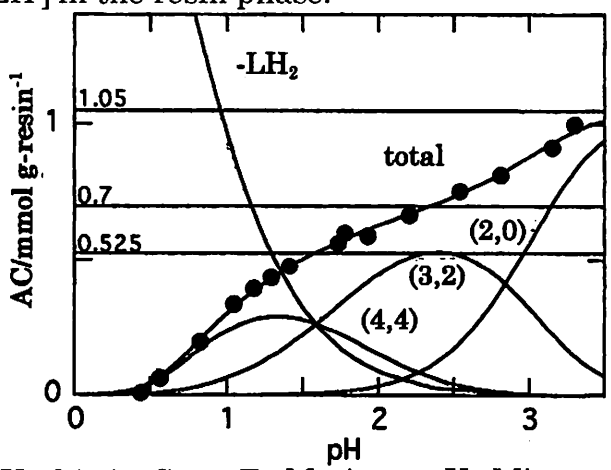

Fig. Adsorption curves of Th^{4+}.
Total amount/mol: 10^{-4}(Th);5.25x10^{-5}(-LH_2).
Each curve designated by (a,b) indicates the contribution of the species [$(-L)_a(H)_bTh$].
Horizontal lines correspond to 50, 33 and 25% occupation of IDA groups, respectively

1. Yuchi, A.; Sato, T.; Morimoto, Y.; Mizuno, H.; Wada, H., *Anal. Chem.*, 1997, **69**, 2941.

Intercalation to DNA and its sensory application

Makoto TAKAGI
Department of Chemical Systems and Engineering, Kyushu University, Fukuoka 812-8581, Japan

Intercalation to DNA is an insertion of a certain family of condensed, polycyclic, aromatic molecules into the base stacks of double stranded DNA. From physico-chemical point of view, the intercalation is featured with a variety of such interactions between DNA and the intercalator as electrostatic, hydrophobic stacking, and steric interactions. When the intercalators or DNA ligands are modified with additional functional groups that allow further interactions with DNA, the resultant ligands are given peculiar features that can be of interest in their physiological activity and in such analytical applications as gene detection and diagnosis.

One of the present topics is our recent study on a threading type of intercalation. The threading intercalators are a class of intercalators that carry two very bulky substituents that are to be placed in the major and minor grooves when the ligand is bound to DNA by intercalation mode. The bulky substituents serve like steric stoppers in both the association and dissociation steps for intercalation, and the intercalated complexes are prone to be kinetically stable as compared with the non-threading counterparts.

When the bulky substituent contains added intercalating units, the resultant DNA-ligand complex is now featured with poly-intercalation through threading. This gives some interesting topological varieties in poly-intercalation, which depends on the molecular construction in assembling the intercalating units in the ligand.

While most of the binding study of intercalating DNA ligands have made use of UV/VIS spectrophotometry taking advantage of intercalating aromatic unit, electrochemical methods can also be of choice if electrochemically active functional groups are introduced in the ligand. As to the molecular detection sensitivity, the electrochemical method can be comparable under favorable conditions to that of spectrofluorometry. Binding study of electro-active DNA ligands and their application to gene detection is another topic of the present paper. The combination of electro-active and threading features within a single ligand assures particularly good performance for specific gene detection on a microelectrode.

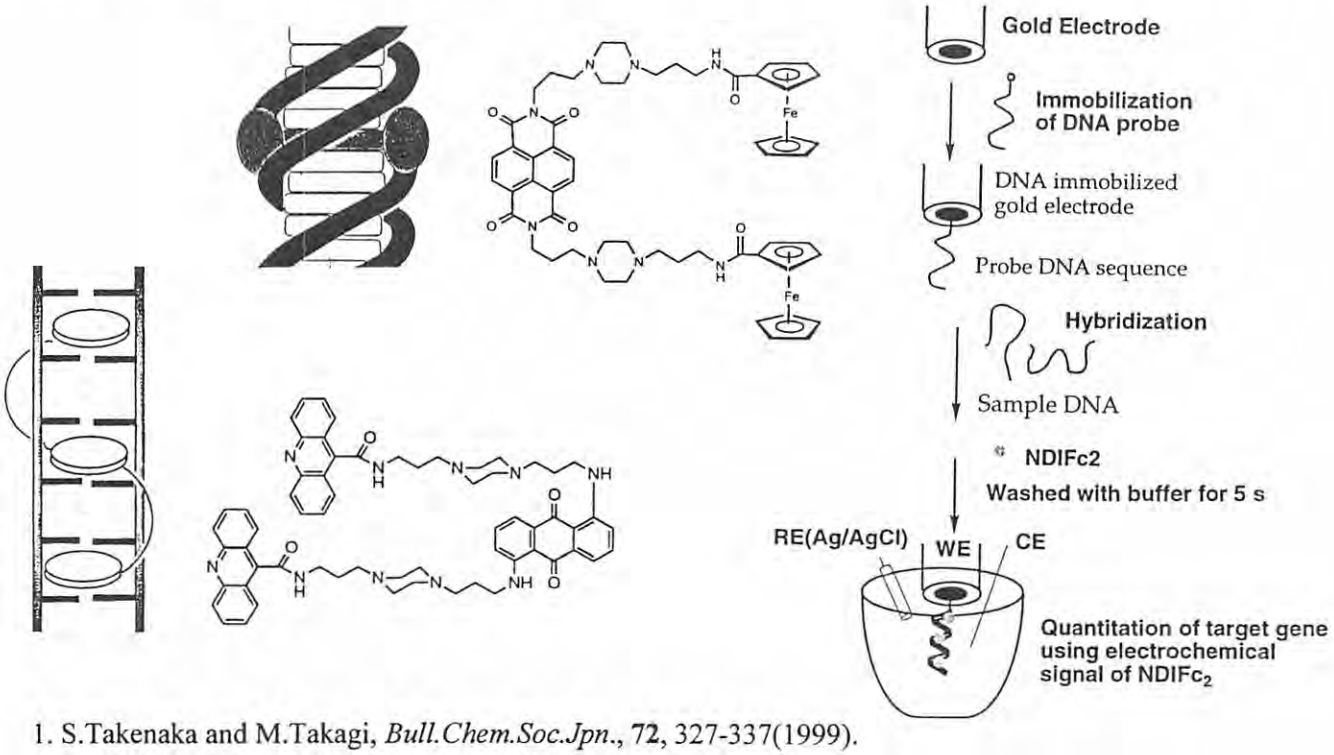

1. S.Takenaka and M.Takagi, *Bull.Chem.Soc.Jpn.*, 72, 327-337(1999).
2. S.Takenaka, *et al.*, *Chem. Lett.*, 319-320, 321-322(1999).

ANION SENSING BY CHROMOIONOPHORES IN AQUEOUS VESICLE SOLUTION

Takashi HAYASHITA, Tsunenobu ONODERA, Ryo KATO, Seiichi NISHIZAWA, and Norio TERAMAE

Department of Chemistry, Graduate School of Science, Tohoku University, Aramaki, Sendai 980-8578, Japan

We have shown that tiourea based chromoionophore (C_1-TU) binds strongly with anions *via* hydrogen bonding in non-aqueous media and produces an effective color change with a selectivity of $OAc^- > H_2PO_4^- > Cl^- >> ClO_4^-$, reflecting the basicity of anions.[1] For anion sensing in aqueous media, however, the hydrogen bonding interaction is strongly weakened by hydration of anions. A simple strategy to achieve anion recognition in water is to incorporate the chromoionophore into hydrophobic regions such as vesicle media to shield the binding site from water. In this study, we have designed novel thiourea based chromoionophores having various length of alkyl chains (C_n-TU) to control the positioning in the vesicle assembly and examined their anion recognition function in aqueous vesicle solution.

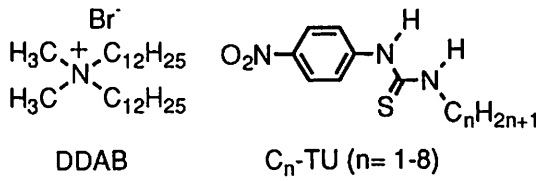

DDAB C_n-TU (n= 1-8)

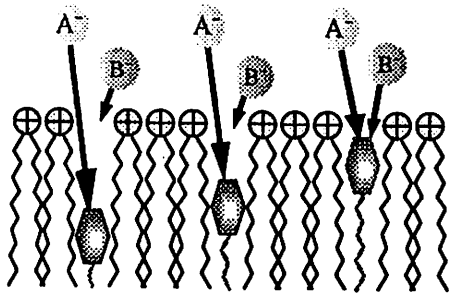

Fig. 1 Positioning of C_n-TU in aqueous vesicle solution.

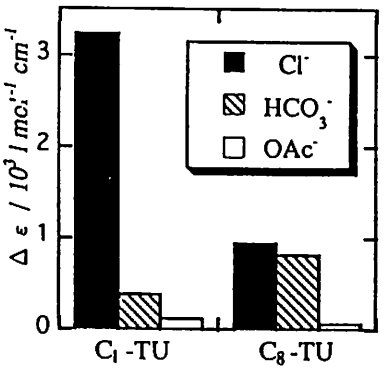

Fig.2 Effect of anion species on spectral response of C_n-TU. C_1-TU(348.0 nm), C_8-TU(366.0 nm), [NaX] = 5.0 mM

The chromoionophores (C_n-TU, 0.05 mM) were solubilized into cationic vesicle (DDAB, 0.5 mM) by ultrasonic probe method and the changes in UV-Vis spectra upon addition of anions (Na^+ salts) were assessed. The shifts in λ_{max}, pK_a values, and ^1H NMR reveal that the positioning of chromophore binding sites are successfully controlled by the alkyl chain length; the binding site of C_n-TU bearing long alkyl chain locates at the surface of the cationic vesicle, and that of C_n-TU bearing short alkyl chain positions at the deep side of the vesicle (Fig. 1). At pH 7.5 adjusted by HEPES buffer, DDAB/C_n-TU assemblies in water exhibit no response for OAc^-, which differs from the C_n-TU function in non-aqueous media. The response selectivity is strongly affected by the positioning of C_n-TU in DDAB vesicle, and high selectivity for Cl^- over HCO_3^- and OAc^- is only achieved for C_1-TU which locates at the deep side of the vesicle (Fig. 2). This is a first example that depth dependent anion recognition is performed in aqueous vesicle solution.

1. S. Nishizawa, R. Kato, T. Hayashita, N. Teramae, *Anal. Sci.*, **1998**, 14, 595-597.

THE RECOVERY OF CHROMIUM FROM WASTE STREAMS USING HOLLOW FIBRE CONTAINED LIQUID MEMBRANES

P.J.HARRINGTON, G.W. STEVENS
Department of Chemical Engineering, The University of Melbourne, Parkville, Victoria, 3052, Australia

Precipitation is the most common treatment process of heavy metals; however, industrial companies are under increasing pressure from water authorities to reduce the solid waste generated by precipitation through the use of recycling methods. In addition to the tightening of government regulations, heavy metal plating companies are looking to recycling processes to save money on plating chemicals and disposal costs.

An effective heavy metal recycling process requires two stages; a process to selectively remove the ions of interest and a subsequent concentrating stage. Typically, ion exchange and evaporation are used in combination to selectively remove and concentrate heavy metals. A relatively new technique known as contained liquid membranes combines both requirements in a single stage operation, and therefore represents a significant and cost saving to the process.

Generally, the installation of liquid membrane process in industry has been limited. This is because of the problems encountered with the first type liquid membrane developed, the supported liquid membrane (SLM), namely organic entrainment in the aqueous phase, and low mass flux. This paper investigates the feasibility of using hollow fibre membrane units as liquid-liquid contactors or contained liquid membranes. Such process are believed to be more robust than supported liquid membrane technology; however, experimental verification is not available in the literature. This work develops the understanding required for the design and implementation of these contained liquid membrane systems in the electroplating industry. The potential of liquid membrane processes for the plating industry is evaluated through the implementation of a commercial scale operation in the electroplating works.

MECHANISM OF INTERFACIAL COMPLEXATION IN METAL EXTRACTION SYSTEMS

Hitoshi WATARAI
Department of Chemistry, Graduate School of Science, Osaka University, Toyonaka 560-0043 JAPAN

Development of measurement techniques of interfacial reactions:

Complexation at the liquid-liquid interface is an essential subject for understanding the mechanisms in solvent extraction as well as in liquid membrane separation, counter current chromatography and ion-selective electrode. The difficulty in the study of interfacial complexation was how to determine the concentration of reactant or product at the interface as a function of time. We have developed various techniques for the measurement of interfacial reaction, especially for the interfacial complexation; they included a high-speed stirring method[1], a two-phase stopped flow method[2], a centrifugal liquid membrane method[3], and an interfacial relaxation method with ATR optical mode[4]. Electro-spray mass spectrometry has also been applied for the detection of the interfacial complexes.

Facilitation of interfacial adsorption of ligand:

Primary process of the interfacial complexation in solvent extraction is the adsorption of an extractant. We proved experimentally that the interfacial concentration of the extractant governed the formation rate of metal complex at the interface for the extraction systems with 2-hydroxy oxime[5] and pyridylazo-ligands[6]. Protonation or dissociation of the extractant by a change of pH facilitated the interfacial complexation as well as the interfacial adsorption of extractant. It has been shown that molecular dynamics simulation is very useful to draw possible molecular pictures of the structure of liquid-liquid interface and the configuration of an adsorbed extractant molecule[7].

Facilitation of formation of intermediate complex at the interface:

The most attractive role of the interface is the catalytic function which facilitates the extraction rate by the stabilization of an extractant and/or intermediate complex at the interface. We definitely observed that the formation of a charged complex at the interface was the essential step governing the synergistic extraction rate in the extraction systems of Ni(II) with pyridylazo-ligands[6]. The formation of charged complex at the interface was also found in the extraction systems including μ-oxo dimer of Fe(III) porphyrin.[8] The interfacial adsorption of μ-oxo dimer was facilitated by the protonation at dodecane/acid solution interface. Europium(III)-2-thenoyltrifluoroacetonate (tta) complex was trapped at the toluene/water interface, when bathophenanthrolinedisulfonic acid (bps) was added. In this case, monomeric and dimeric complexes of Eu(III)-tta-bps were formed at the interface.

1. Watarai, H., *Trends in Analytical Chemistry*, 1993, **12**, 313.
2. Nagatani, H.; Watarai, H., *Anal. Chem.*, 1996, **68**, 1250.
3. Nagatani, H.; Watarai, H., *Anal. Chem.*, 1998, **70**, 2860.
4. Tsukahara, S.; Watarai, H., *Chem. Lett.*, **1999**, 89.
5. Watarai, H.; Saitoh, K., *Langmuir*, 1994, **10**, 3913.
6. Onoe, Y.; Tsukahara, S.; Watarai, H., *Bull. Chem. Soc. Jpn.*, 1998, **71**, 603.
7. Watarai, H.; Gotoh, M.; Gotoh, N., *Bull. Chem. Soc. Jpn.*, 1997, **70**, 957.
8. Nagatani, H.; Watarai, H., *J. Chem. Soc., Faraday Trans.*, 1998, **94**, 247.

ECOLOGICAL ASPECTS OF THE ORGANIC SOLUTION CHEMISTRY IN UNSATURATED SYSTEMS SUCH AS SOILS

Ádám Zsolnay[1] and Bernd Steinweg[1]
[1] Institute for Soil Ecology, GSF- Research Centre for Environment and Health, D-85764 Neuherberg bei München, Germany

A great number of ecological and environmental processes in soils are a function of solution chemistry (Zsolnay[1]):

1. substrate utilisation, which is essential to maintain soil life and which can also have an effect on the production of greenhouse gases such as CO_2 and N_2O;
2. the making available to the biosphere of noxious organic and inorganic compounds. This can have a toxic effect on the one hand but on the other hand can be a significant process for soil remediation;
3. the transporting directly or indirectly via co-transport of undesirable compounds to the hydrosphere, including to groundwater; and
4. the sequestration of organic compounds, which can have a pronounced effect on the physical quality of soils and can also help mitigate CO_2 loads in the atmosphere.

Because of the complicated matrix structure of soils and sediments and because of the continuously changing water content of the former, solution chemistry in soils can by no means be regarded as a homogeneous process. One can envision at least three different solution environments in unsaturated soils in which the dissolved organic material is exposed to and participates in different processes (modified from Zsolnay[1]):

	micro-pores	meso-pores	macro-pores
pore size (µm)	<0.2	0.2 to 6	>6
water "type"	cohesive/adhesive	cohesive	gravitational/cohesive
water tension (kPa)	<-1500	-1500 to -50	>-50
% of water at WHC[a]	~30	~50	~20
transport mechanism	diffusion	diffusion>convection	convection>diffusion
metabolism	abiotic, exo-enzymes	microbial	biotic
relative turn over	slow	moderate	rapid
matrix influence	very strong	strong	weak
effect of drought	weak	moderate	strong

[a] WHC is the water holding capacity. The values in this row are extremely approximate.

Therefore, one of the greatest challenges in soil solution chemistry is the obtaining of samples, which are representative of the *in situ* conditions and processes. For example, research at our laboratory has shown that *in situ* concentrations are generally over an order of magnitude greater than those obtained with extraction techniques. Furthermore, solutions obtained with suction cups can only give information in regards to the relatively small macro-pore environment. The above points with appropriate experimental results will be discussed in detail.

1. Zsolnay, Á., *Humic Substances in Terrestrial Ecosystems*, Piccolo, A., Ed.; Elsevier: Amsterdam, 1996; pp. 171-223.

SPECTROSCOPIC AND THERMODYNAMIC APPROACHES TO THE APPRAISAL OF HUMIC ACID BORNE ACTINIDE MIGRATION

JAE-IL KIM

Forschungszentrum Karlsruhe, Institut für Nukleare Entsorgungstechnik,

76021 Karlsruhe, Germnany

The paper comprises, in the first part, the spectroscopic speciation in the actinide complexation with humic acid and thermodynamic modelling of binary and ternary species formation in a wide range of pH. For the low actinide concentration range, i.e. nano-mole range, laser spectroscopy is used to speciate their pertinent complexation reactions with humic acid or humic colloids. The second part deals with the application of the model to appraise the migration behaviour of actinide ions in natural aquifer systems. Discussion also takes into account the competitive geo-chemical reactions involved, e.g. hydrolysis and complexation of actinide ions with other water constituent ligands

EFFECT OF HUMIC SUBSTANCES ON THE GENERATION OF HYDROGEN PEROXIDE BY PHOTOSENZITIZATION OF TRIS(2,2'-BIPYRIDINE) RUTHENIUM(II) COMPLEX

Masami FUKUSHIMA and Kenji TATSUMI
Hydrospheric Environmental Protection Department, National Institute for Resources and Environment (NIRE), 16-3 Onogawa, Tsukuba 305-8569, Japan

Introduction: The photocatalytic production of H_2O_2 has been investigated using photosensitized dyes, such as the tris(2, 2'-bipyridine) ruthenium(II) complex ($Ru(bpy)_3^{2+}$) [1,2]. The photoinduced electron transfer reaction of $Ru(bpy)_3^{2+}$ with the redox mediators, such as methyl viologen (MV^{2+}), cannot occur without an electron donor, such as EDTA. Since the redox potential of $Ru(bpy)_3^{3+/2+}$ is known to be +1.29 V, EDTA (+0.4 V) could be effectively used as an electron donor for the reduction of $Ru(bpy)_3^{3+}$. HSs, which are widely distributed in aqueous environments, function as reducing agents. It has been reported that the redox potentials of HS are in the range of +0.5 ~ +0.7 V, and it is well-known that HS are capable of reducing chromium(VI). This redox potential (+1.33 V) is near that of $Ru(bpy)_3^{3+/2+}$. This suggests that $Ru(bpy)_3^{3+}$ may be also reduced by HS. The present study describes attempts to enhance H_2O_2 production in aqueous systems, which contain HS, by taking advantage of the reducing abilities of HS to the $Ru(bpy)_3^{2+}$-photosensitized production of H_2O_2.

Experimental: The test solutions usually contained 50 μM $Ru(bpy)_3^{2+}$, 2.5 mM MV^{2+}, 100 mg L^{-1} HS and 0.01 M formate buffer (pH 3.6). Photoirradiation was carried out by 500 W Xenon short arc lamp after passing through a color glass filter. An L-42 color glass filter, which cut off light below 420 nm, was routinely used. After O_2 gas was bubbled into the test solution, and the solution was then irradiated for 60 min. H_2O_2 was analyzed by a colorimetric method, and HCOOH was measured by an HPLC [2].

Results and Discussion: It was demonstrated that the photosensitized production of H_2O_2 by $Ru(bpy)_3^{2+}$ was enhanced in the presence of HS. Figure 1 shows the electron pathways for the generation of H_2O_2 in the present system. The HS assisted the photocatalytic reaction of $Ru(bpy)_3^{2+}$, and MV^{2+} as a redox mediator was required to produce H_2O_2. Moreover, H_2O_2 was not produced in the absence of HCOOH. The putative role of HCOOH is to reduce the oxidized HS. Figure 2 shows the relationship between the HS concentration and the ratio of $[H_2O_2]$ to $[H_2O_2]_0$ ($[H_2O_2]$: in the presence of HS, $[H_2O_2]_0$: in the absence of HS). The $[H_2O_2]/[H_2O_2]_0$ ratio indicates the degree of enhancement, and shows that the photosensitized production of H_2O_2 is enhanced approximately 120-fold by HS. The increase of $[H_2O_2]/[H_2O_2]_0$ up to [HS] = 75 mg L^{-1} is due to the local accumulation of $Ru(bpy)_3^{2+}$ and MV^{2+} into HS, and the decrease above 100 mg L^{-1} can be attributed to the spreading of the reactants over the HS polymer domain. These results indicate that the enhancement of H_2O_2 production is related to the binding of $Ru(bpy)_3^{2+}$ and MV^{2+} with the HS.

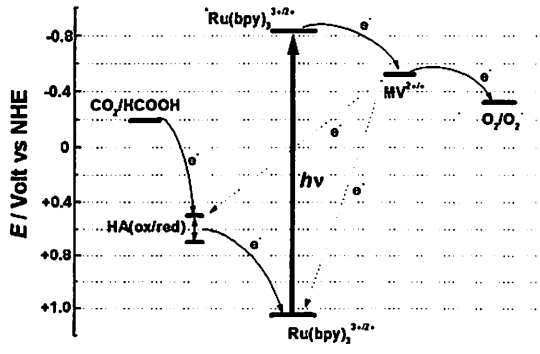

Figure 1 Electron pathways for the production of H_2O_2

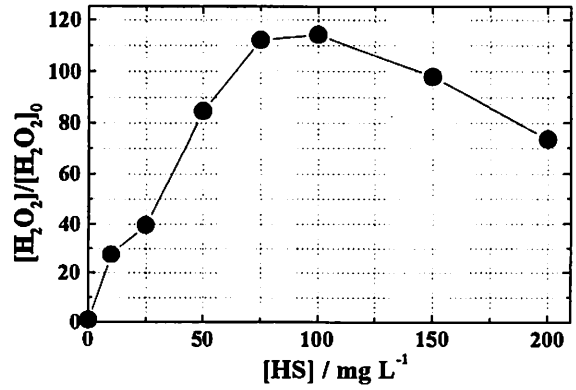

Figure 2 Effect of the concentration of HS

1. Kurimura, Y.; Nagashima, M.; Takato, K.; Tsuchida, E.; Kaneko, M.; Yamada, A. *J. Phys. Chem.* **1982**, *86*, 2432-2437.
2. Fukushima, M.; Tatsumi, K.; Tanaka, S.; Nakamura, H. *Environ. Sci. Technol.* **1998**, *32*, 3948-3953.

USE OF IMMOBILISED HUMIC ACID ON DIFFERENT SOLID SUPPORTS FOR INVESTIGATION OF COMPLEXATION OF AMERICIUM(III) BY HUMIC ACID

Gyula Szabó[1], Judit Guczi[1], Tohru Miyajima[2] and Robert A. Bulman[3]
[1]"Frédéric Joliot-Curie" National Research Institute for Radiobiology and Radiohygiene, PO Box 101, Budapest, H-1775, Hungary
[2]Department of Chemistry, Faculty of Science and Engineering, Saga University, 1-Honjo, Saga 840-8502, Japan
[3]National Radiological Protection Board, Didcot, United Kingdom, OX11 ORQ

Humic substances form complexes with a wide variety of metal ions and thus mediate their bioavailability, biotoxicity and transport in the biosphere. A detailed understanding of the influence of humic substances on the speciation of metal ions is beyond our reach owing to the complicated, heterogeneous and variable nature of these polydispersed, polyelectrolytic substances. Thus to predict humate-mediated movement of transuranic radionuclides through the environment, it is necessary to understand the chemistry of the interactions of transuranic elements with humic substances in fine detail.

This presentation reports the immobilisation of humic acid (Aldrich) on silica gel and alumina[1] and the characterisation of the resulting materials by CHN element analysis, potentiometric titration and IR spectrometry. The interaction between a trivalent actinide, Am(III), and the two forms of immobilised humic acid have been investigated at pH 6 by titrating the suspended materials in 0.1 M $NaClO_4$. This same media also used when evaluating the sorption of Am(III) by the parent silica gel and alumina. The Am(III)-humic acid stability constants have been evaluated from data obtained from these experiments by using charge neutralisation model[2], continuous multiligand model[3] and non-linear regression of binding isotherms[4]. The results have been interpreted in terms of complexes of 1:1 stoichiometry. The evaluated stability constants vary slightly and show similarity to values reported by others who have used other methods.

Our results demonstrate that it is possible to study the nature of the complexation chemistry of humic acids without resorting to sophisticated instrumental procedures.

1. Szabo, Gy.; Farkas, Gy.; Bulman, R.A., *Chemosphere*, 1992, **24**, 403.
2. Kim, J.I.; Czerwinski, K.R., *Radiochimica Acta*, 1996, **73**, 5.
3. Giesy, J.P.; Geiger, R.A.; Kevern, N.R., *J. Environ. Radioactivity*, 1986, **4**, 39.
4. Sposito, G., *CRC Crit. Rev. Environ. Control*, **15**, 1.

DETERMINATION OF SILICA COMPLEXES IN SODIUM AND CALCIUM CHLORIDE SOLUTIONS USING A FAB-MS

Miho TANAKA[1] and Kazuya TAKAHASHI[2]

1)The Tokyo University of Fisheries, Konan, Minato, Tokyo 108-8477, Japan

2)The Institute of Physical and Chemical Research (RIKEN), Hirosawa, Wako, Saitama 351-0198, Japan

FAB-MS (Fast Atom Bombardment Mass Spectrometry, negative ion mode) allows us to analyze species in solution directly under the relatively moderate ionizing condition. When the chemical species of silica was attempt to be identified by 29-Si NMR, the required detection limit of the concentration of silica is, at least, 0.1 mol dm^{-3}(M). As the naural water contains, at most, 2mM of silicon, the chemical species of silica in the natural water have not been indentified. In our study, the FAB-MS was applied to direct detection of silica species dissolved in alkali, alkaline earth chloride solutions in order to investigate its dissolution processes in LiCl, NaCl, $MgCl_2$, $CaCl_2$ and $SrCl_2$ solutions, which is main component in the natural waters. From the results the following features were obtained; several species of dissolved silica in the solution were detected and it was found that Na^+ , Ca^{2+} and Sr^{2+} form complexes with silica (such as $[SiO_2(OH)_2Na]^-$, $[SiO_3(OH)Ca]^-$, and $[SiO_3(OH)Sr]^-$) but Li^+ and Mg^{2+} do not form such complexes with silica in the solution. This suggested that Na^+, Ca^{2+} and Sr^{2+} accelerated the dissolution of silica forming complexes under the solution equilibrium. FAB-MS is useful to identify the chemical species in solution.

The chemical states of silica dissolved in sodium chloride (NaCl) and calcium chloride ($CaCl_2$) solutions were identified by measurements with FAB-MS spectroscopy. An apparent peak at m/z=95, which corresponds to $SiO(OH)_3^-$ in 0.1M NaCl solution, was not confirmed due to the interference of the peaks corresponds to $NaCl_2^-$; however, the peaks for complexes such as $SiO_2(OH)_2Na^-$, $Si_2O_2(OH)_5^-$, $Si_2O_3(OH)_4Na^-$, $Si_2O_4(OH)_3Na_2^-$, $Si_2O_5(OH)_2Na_3^-$, $Si_3O_3(OH)_7^-$, $Si_3O_4(OH)_6Na^-$, $Si_3O_5(OH)_5Na_2^-$, $Si_4O_5(OH)_7^-$, $Si_4O_6(OH)_6Na^-$, $Si_4O_7(OH)_5Na_2^-$, were detected. These complexes can be confirned not only in the form of the anion itself (e.g., $Si_2O_2(OH)_5^-$), but also in the form of some complexes with sodium ions, such as $Si_2O_2(OH)_4Na^-$.

The species dissolved in $CaCl_2$ solution were compared with those in the sodium chloride (NaCl) solution to discuss the stability of the complex in $CaCl_2$ solution. In 0.1 mol/l(M) $CaCl_2$ solution, some new species of silica complexes were identified. The species of silica dissolved in $CaCl_2$ solution were as follows: silica monomer, $SiO_3(OH)^-$ and $SiO_3(OH)Ca^-$, the dimer species such as $Si_2O_2(OH)_5^-$, $Si_2O_4(OH)_3Ca^-$, the linear tetramer such as $Si_4O_4(OH)_9^-$, $Si_4O_6(OH)_7Ca^-$, $Si_4O_8(OH)_5Ca_2^-$, $Si_4O_{10}(OH)_3Ca_3^-$ and $Si_4O_{12}(OH)Ca_4^-$, and the cyclic tetramer such as $Si_4O_5(OH)_7^-$, $Si_4O_7(OH)_5Ca^-$, $Si_4O_9(OH)_3Ca_2^-$ and $Si_4O_{11}(OH)Ca_3^-$. The linear tetramer silica complexes were contained in the 0.1 M $CaCl_2$ solution, and the 8 protons of the linear tetramer silicate $Si_4O_4(OH)_9^-$ are all exchangeable with Ca^{2+}, while the linear tetramer silicate complexes were not identified in 0.1 M NaCl solution. This indicates that the Ca-silica complex is more stable than Na-silica complex in each chloride solution, and that Ca^{2+} should assist in the two intra-molecular bondings of $Si\text{-}O^-$.

AN INTERPRETATION OF THE UNIQUE COMPLEXATION BEHAVIOR IN ION-EXCHANGERS

T. MIYAJIMA[1], H. KODAMA[2], K. TAJIRI[3], S. ISHIGURO[3], and J. A. MARINSKY[4]

[1]Department of Chemistry, Faculty of Science and Engineering, Saga University, Saga, 840-8502, Japan
[2]Department of Biological Resource Chemistry, Faculty of Agriculture, Kyoto Pref. University, Kyoto, 606-8201, Japan
[3]Department of Chemistry and Physics, Graduate School of Science, Kyushu University, Fukuoka, 812-8581, Japan
[4]Department of Chemistry, Natural Sciences and Mathematics Complex, SUNY at Buffalo, Buffalo, 14260-3000, USA

Despite a large number of studies on the peculiar complexation behavior in ion-exchangers and ionic micelles, the mechanism of the extraordinary high complexability still remains unclear. For example, the complexation of Co^{2+} ions with SCN^- ions is enhanced in strong basic anion exchange resins, such as Dowex 1. This enhancement has been attributed to the characteristic features of the ion-exchange resin, such as a low dielectric constant and high internal pressure.

In order to gain a much deeper insight into the unique complexation behavior in the ion exchanger phase, the complexation behavior of the Co^{2+}/SCN^- system has been monitored spectrophotometrically in the presence of polyvinylbenzyltrimethylammonium ions, the linear polymer analog of Dowex 1. The magnitude of the complexability has been expressed as a function of the concentrations of SCN^- ions, supporting electrolyte, and the polymer. It has been revealed that 1) the fully coordinated complex, $[Co(NCS)_4]^{2-}$, is the only complexed species present in the polymer domain, 2) the degree of complexation is highly dependent on the hydrophobicity/hydrophilicity nature of both cations and anions, and 3) the polymer concentration effect can be quantified by a "binding equilibrium" between hydrophobic complexes, $[Co(NCS)_4]^{2-}$, and trimethylammonium groups in the polymer domain.

Abnormally high degree of complexability of a metal ion with hydrophobic ligand anions in the ion-exchange resin phase can be interpreted as hydrophobic adsorption of anionic complexes to the polymer backbone.

METAL ION-BINDING PROPERTIES OF THE ANTIVIRAL NUCLEOTIDE ANALOGUE 9-[2-(PHOSPHONOMETHOXY)ETHYL]ADENINE (PMEA). WHY IS ITS DIPHOSPHORYLATED FORM ($PMEApp^{4-}$) INITIALLY AN EXCELLENT SUBSTRATE FOR NUCLEIC ACID POLYMERASES?

Helmut SIGEL
Institute of Inorganic Chemistry, University of Basel, Spitalstrase 51,
CH-4056 Basel, Switzerland

PMEA, an acyclic analogue of (2'-deoxy)-adenosine 5'-monophosphate ($dAMP^{2-}/AMP^{2-}$), is a potent prodrug with selective antiviral activity against herpes simplex viruses (HSV) and retroviruses, including human immunodeficiency viruses (HIV-1 and HIV-2).[1] It is active after its diphosphorylation by kinases, i.e., $PMEApp^{4-}$ is recognized by nucleic acid polymerases as substrate and incorporated in the growing nucleic acid chain, which is then terminated due to the lack of a 3'-hydroxy group present in the parent (2'-deoxy)-adenosine 5'-triphosphate ($dATP^{4-}/ATP^{4-}$). In fact, $PMEApp^{4-}$ is initially an excellent substrate, e.g. reverse transcriptases are effectively inhibited even in the presence of a 20-fold excess of dATP.[2] Why? -- Equilibrium studies revealed[3] that metal ions like Mg^{2+}, Mn^{2+} or Zn^{2+} coordinate not only to the phosphonate group of $PMEA^{2-}$ but they interact also with the ether oxygen giving rise to an intramolecular equilibrium; the formation degree of the 5-membered chelates varies between about 30-50%.[3] Furthermore, measurements with methyl phosphonylphosphate, $CH_3\text{-}P(O)_2^-\text{-}O\text{-}PO_3^{2-}$, show that its complexes are somewhat more stable (ca. 0.1-0.2 log unit) than those with methyl diphosphate, $CH_3\text{-}OP(O)_2^-\text{-}O\text{-}PO_3^{2-}$, and this increased stability is to be attributed to the increased basicity of a phosphonate compared to a phosphate group.[4] Both effects together, i.e. chelate formation and increased basicity,[4] favour metal ion binding at the P_α group of $PMEApp^{4-}$ compared to that of ATP^{4-}; i.e., $M_2(PMEApp)$ is expected to reach a higher formation degree than $M_2(ATP)$ and consequently nucleophilic attack at the P_α will also be facilitated.

Nucleophilic attack of $\bar{N}$ at $M_2(PMEApp)$

Supported by the Swiss Nat. Sci. Found. and the Swiss Fed. Office for Educ. & Sci. (COST D8).

1. Tsai, C.-C.; Follis, K. E.; Sabo, A.; Beck, T. W.; Grant, R. F.; Bischofberger, N.; Benveniste, R. E.; Black, R., *Science*, 1995, **270**, 1197-1199.
2. Holý, A.; Votruba, I.; Merta, A.; Černý, J.; Veselý, J.; Vlach, J.; Šedivá, K.; Rosenberg, I.; Otmar, M.; Hřebabecký, H.; Trávniček, M.; Vonka, V.; Snoeck, R.; De Clercq, E., *Antiviral Res.*, 1990, **13**, 295-311.
3. Sigel, H., *Coord. Chem. Rev.*, 1995, **144**, 287-319; *J. Indian Chem. Soc.*, 1997, **74**, 261-271 (*P. Ray Award Lecture*).
4. Sigel, H.; Song, B.; Blindauer, C. A.; Kapinos, L. E.; Gregáň, F.; Prónayová, N., *Chem. Commun.*, 1999, in press.

THE ELECTRON TRANSFER REACTION MECHANISM FROM $Fe(CN)_6^{4-}$ OR $W(CN)_8^{4-}$ TO THE CUPRIC ION IN HUMAN-COPPER, ZINC-SUPEROXIDE DISMUTASE

Junzo Hirose, Miki Ishikawa, Yoshie Kitsutaka, Kouhei Settsu, Hiroyuki Iwamoto
Department of Applied Biological Science, Faculty of Engineering, Fukuyama University, Fukuyama City, Hiroshima 729-0292 Japan; email:hirose@fubac.fukuyama-u.ac.jp

Copper, zinc superoxide dismutase (SOD) catalyzes the dismutation of superoxide anion with high efficiency. Hirose et al. reported that the electron transfer proceeded from bulky $Fe(CN)_6^{4-}$ to copper(II) ion of SOD which is present at the bottom of the narrow active site (Hirose et al., Inorg. Chem *27*, 3746-3751 (1988)). By using mutants of human-SOD and ^{13}C NMR of $Co(CN)_6^{4-}$, Bertini et al. (Inorg. Chem. *32*, 1106-1110 (1993)) have pointed out the possibility that $Fe(CN)_6^{4-}$ approaches the copper ion at the entrance of the cavity and the electron of $Fe(CN)_6^{4-}$ jump to the cupric ion in SOD for ~4Å.

The detail kinetic mechanism of the electron transfer from $Fe(CN)_6^{4-}$ to the cupric ion in human-SOD is unknown, so that the electron transfer rate from $Fe(CN)_6^{4-}$ or $W(CN)_8^{4-}$ to the cupric ion in human-SOD were followed by micro-stopped flow. The redox potential of $Fe(CN)_6^{4-}$ and $W(CN)_8^{4-}$ were 468 and 556 mV obtained by cyclic volutammetry, respectively.

The relationship between the pseudo-first order rate constants (k_{obs}) of the electron transfer reaction and the concentration of $Fe(CN)_6^{4-}$ or $W(CN)_8^{4-}$ gave the hyperbolic functions. This behavior indicates that the electron transfer reaction proceeds through the adduct formed by $Fe(CN)_6^{4-}$ or $W(CN)_8^{4-}$ and human-SOD:

$$ECu(II) + M(CN)_n^{4-} \overset{K_f}{\rightleftarrows} ECu(II) \cdot M(CN)_n^{4-} \overset{k_1}{\rightarrow} ECu(I) + M(CN)_n^{3-} \quad (1)$$

where ECu(II) is human-SOD and $M(CN)_n^{4-}$ is $Fe(CN)_6^{4-}$ or $W(CN)_8^{4-}$. The formation constants (K_f) of the adducts with $Fe(CN)_6^{4-}$ and $W(CN)_8^{4-}$ were 250 and 468 M^{-1} in 0.02 M MES buffer at 25 ℃(pH 6.0). The electron transfer rate (k_1) of $Fe(CN)_6^{4-}$ or $W(CN)_8^{4-}$ were 0.15 and 0.073 sec^{-1}. The enthalpy of the formation constants(K_f) and the activation energy of the electron transfer rates(k_1) in the electron transfer reaction from $Fe(CN)_6^{4-}$ or $W(CN)_8^{4-}$ to the cupric ion of SOD were obtained by the temperature dependence of K_f and k_1. The values of the enthalpy of the formation constant and the activation energy of $Fe(CN)_6^{4}$ were almost consistent with those of $W(CN)_8^{4-}$, respectively.

It is known that the redox potentials of the copper ions in SOD are depend on the pH. The pH dependence of the electron transfer rates from $Fe(CN)_6^{4-}$ to the cupric ions in SOD was measured at various pHs from 4.8 to 8.0. At all pHs from pH 4.8 to 8.0, the electron transfer reactions from $Fe(CN)_6^{4-}$ to the cupric ions in SOD proceeded through Eq. 1. The formation constants (K_f) of the adduct were decreased by increasing of pH but the electron transfer rate constants (k_1)were constant between pH 4.8 and 8.0 in spite of the change of the redox potential of the copper ion in SOD.

These results indicate that the electron transfer rate constant does not be governed by the redox potential differences between the cupric ion in SOD and metal complexes. It implies that the electron transfer reaction from $Fe(CN)_6^{4-}$ or $W(CN)_8^{4-}$ to the cupric ions in SOD may proceeds through the inner sphere reaction mechanism.

CROSS-LINKING NUCLEOBASES WITH *trans*-a_2Pt^{II} : FROM MODELS TO OLIGONUCLEOTIDES

Bernhard Lippert, Matthias Janik, Jens Müller, Roland K. O. Sigel
Fachbereich Chemie, Universität Dortmund, 44221 Dortmund, Germany

In the so-called 'antisense' and 'antigene' approach synthetic oligonucleotides capable of hybridizing with target sequences in either single-stranded RNA or double-stranded DNA are applied in order to block expression of crucial, disease-related proteins.[1] As we have proposed,[2] monofunctionally *trans*-a_2Pt^{II} (a = NH_3 or amine) - modified oligonucleotides could be useful in this apporach by providing a lasting cross-link between the synthetic oligonucleotide and the target, thereby leading to metalated duplex and triplex structures. It has been demonstrated,[3,4] that this idea works in principle. Rules underlying these reactions are expected to be similar to those seen in model chemistry of metal-modified base pairs, triples and quartets.[5] The synthesis of specifically platinated oligonucleotides on a preparative scale[6] still presents a major challenge.

The lecture will provide an up-to-date account of this approach.

Support by the BIOMED programme of the EU (Contract BMH4-CT98-2485) and the Deutsche Forschungsgemeinschaft, DFG, is gratefully acknowledged.

1. Chadwick, D.J.; Cardew, G. (Eds), *Oligonucleotides as Therapeutic Agents*, Wiley: Chichester, UK, 1997.
2. Krizanovic, O.; Sabat, M.; Beyerle-Pfnür, R.; Lippert, B., *J. Am. Chem. Soc.*, 1993, **115**, 5538.
3. Colombier, C.; Lippert, B.; Leng. M., *Nucleic Acids Res.*, 1997, **24**, 4519.
4. Dalbiès, R.; Payet, D.; Leng, M., *Proc. Natl. Acad. Sci. USA*, 1994, **91**, 8147.
5. Lippert, B., *J. Chem. Soc., Dalton Trans.*, 1997, 3971; Sigel, R.K.O.; Thompson, S.M.; Freisinger, E.; Lippert, B., *J. Chem. Soc., Chem. Commun.*, 1999, 19; Lüth, M.S.; Freisinger, E.; Glahé, F.; Lippert, B., *Inorg. Chem.*, 1998, **37**, 5044.
6. Berghoff, U.; Schmidt, K.; Janik, M.; Schröder, G.; Lippert, B., *Inorg. Chim. Acta*, 1998, **269**, 135.

BIOLOGICAL IMPORTANCE OF SOLUTION SPECIATION OF AL(III) AND VO(IV)

Tamás KISS
Department of Inorganic and Analytical Chemistry, József Attila University, P.O.Box 440, H-6701 Szeged, Hungary

The chemical form of an element essential or toxic in which it enters to body, is absorbed, transported or it reaches a target organ or tissue is basically important as it may influence its physiological activity. Partly independently on how a metal ion containing drug is administered it undergoes transformations because of the possible ligand exchange reactions with many potential metal ion binder biomolecules of biofluids or tissues.

The paper will give examples on the importance of biospeciation of Al(III) and VO(IV) and the application of speciation results in understanding the biological effects of these elements.

The neurotoxic Al [1] is transported through the blood stream bound mostly to the iron transport protein transferrin. However, a small fraction of Al (~10–15%) is bound to low molecular mass (l.m.m.) constituents of serum. Among these citrate and phosphate seem to be the most important. pH-potentiometric and multinuclear (^{1}H, ^{13}C, ^{31}P, ^{27}Al) NMR studies served to assess the solution state of Al(III) including the effect of time on speciation. The results suggest that besides the tridentate citrate the monodentate phosphate also participates actively in Al(III) binding under serum conditions.

Since the discovery in 1979 that vanadium can exert insulin-mimetic activity, great efforts have been made to prepare vanadium(IV) and vanadium(V) complexes of high activity and low toxicity [2]. The interactions of several promising insulin-mimetic drugs such as $VO(maltolate)_2$, $VO(picolinate)_2$ and $VO(6\text{-Me-picolinate})_2$ with various l.m.m. binders of biofluids (e.g. inorganic phosphates, nucleotides, oxalate, lactate, citrate and catecholamines) have been studied and their participation in VO(IV) binding considered. As an example the estimated species distribution of the above mentioned 3 potential drugs in blood serum revealed that the ternary complexes with citrate are the most important VO(IV) binders of these potential drugs.

Vanadium in its high oxidation states is a rather hard metal ion and has fairly low affinity to N-donors, hence in the absence of a suitable anchoring donor its strong binding to oligopeptides *via* the promotion of peptide amide deprotonation and coordination is considerably hindered. Salicylic-amino acid derivatives such as SalGly and SalGlyAla, having phenolate anchoring donors proved to be very efficient VO(IV)-binders, and the formation of amide deprotonated species proved to be predominant in the physiological pH range.

Acknowledgements. The works were supported by the National Research Fund (OTKA 23776/97) and the Hungarian Ministry of Education (FKFP 0013/97).

[1] R.B. Martin, *Acc. Chem. Res.*, **27**, 204 (1994).
[2] Metal Ions in Biological Systems, (Eds. H. Sigel and A. Sigel), Vol 31, Marcell Dekker, Basel, 1995.

STRUCTURE—INSULIN MIMETIC ACTIVITY RELATIONSHIP OF VANADYL-PYCOLINATE COMPLEXES

Hiromu Sakurai, Toshikazu Takino and Asuka Tamura

Department of Analytical and Bioinorganic Chemistry, Kyoto Pharmaceutical University, 5 Nakauchi-cho, Misasagi, Yamashina-ku, Kyoto 607-8414, Japan
Fax: 81-75-595-4753, e-mail: sakurai@mb.kyoto-phu.ac.jp

Insulin-dependent diabetes mellitus (IDDM) and non-insulin-dependent diabetes mellitus (NIDDM) are characterized by hyperglycemia due to the absolute deficiency of insulin and the deterioration of sensitivity of insulin-receptor of the cells, respectively. Although many therapeutics for NIDDM are known, no therapeutics for IDDM have been developed except insulin which is injected intramuscularly every day. Therefore, orally active therapeutic agents, which replace by insulin, are expected.

Vanadium, an essential trace element in living systems, exhibits insulin-mimetic action in animals and human. When vanadyl sulfate is administered orally to STZ-induced hyperglycemic rats, it induces normoglycemic state. However, its long-term administration causes kidney toxicity. Therefore, we are developing new vanadyl complexes with higher effectiveness and less toxicity than vanadyl sulfate. In *in vitro* experiment, we examine insulin-mimetic activity of vanadyl complexes by evaluating the inhibitory effect of free fatty acid release from rat adipocytes treated with epinephrine. Based on the *in vitro* results, we have found several vanadyl complexes that show good blood glucose normalizing effect on the STZ-induced diabetic rats.

Among the vanadyl complexes with different coordination mode such as $VO(O_4)$, $VO(N_4)$, $VO(S_4)$, $VO(O_2N_2)$, $VO(S_2O_2)$ and $VO(S_2N_2)$, vanadyl-picolinate with $VO(N_2O_2)$ coordination mode was found to be one of the most effective complex in *in vitro* and *in vivo* evaluations. Then we have developed many types of vanadyl-picolinate complexes.

Introduction of substituents with electron pushing or pulling character to the pyridine ring of picolinate enhanced the insulin-mimetic activity in the *in vitro* evaluations. We examined the solution characteristics of the complexes involving optical absorption and electron spin resonance (ESR) spectra, and discussed *in vitro* and *in vivo* insulin-mimetic activities of the new synthesized complexes with respect to their structures.

Ref.: Sakurai, H. *et al.*, ACS Symposium Series **711**, 344-352 (1998).

INTRA- AND INTERMOLECULAR INTERACTIONS INVOLVING AMINO ACID SIDE CHAINS OF SMALL COMPLEXES AND METALLOPROTEINS

Osamu YAMAUCHI[1,2], Akira ODANI[1], Shun HIROTA[1], and Masako TAKANI[3]

[1]Department of Chemistry, Graduate School of Science, Nagoya University, Nagoya 464-8602, Japan

[2]Research Center for Materials Science, Nagoya University, Nagoya 464-8602, Japan

[3]Faculty of Pharmaceutical Sciences, Kanazawa University, Kanazawa 920-0934, Japan

Charged, polar, and aromatic side chain groups of amino acid residues of peptides and proteins are involved in hydrogen bonding, aromatic ring stacking, and other weak interactions and thus contribute to specificity and efficiency of biological reactions. When coordinated around a metal center, amino acids and peptides offer their side chain groups for noncovalent interactions with other groups within the same complex molecule or between different molecules. Metal complexes containing amino acid residues may therefore simulate the site of interaction between proteins *etc.* and provide information on the mode and stability of side chain–side chain interactions and molecular recognition in biological systems.

In order to obtain information on specific noncovalent interactions involving side chains of amino acid residues in proteins, we studied the solution equilibria and noncovalent interactions in Cu(II)–dipeptide (L) and Cu(II)–dipeptide–amino acid ternary systems with L composed of N-terminal arginine (Arg), lysine (Lys), or glycinate (Gly) and C-terminal aspartate (Asp), glutamate (Glu), or Gly. We also studied the adduct formation between metalloproteins and oligopeptides of Lys (Lysptd) or Asp (Aspptd). The stability of the complexes CuL and $CuLH_{-1}$ (H_{-1} denotes deprotonation from the peptide moiety) has been found to be in the order XAsp≥XGlu>XGly (X = Arg, Lys, or Gly), and from the thermodynamic parameters, $CuLH_{-1}$ involving oppositely charged side chains such as $Cu(ArgAspH_{-1})$ is more stabilized than that with only one charged side chain such as $Cu(ArgGlyH_{-1})$ probably due to the hydrogen bonds between the side chains. $Cu(ArgAspH_{-1})$ and $Cu(ArgGluH_{-1})$ isolated as crystals have been shown to have guanidinium-carboxylate hydrogen bonds between neighboring complex molecules, supporting the conclusion from the stability constants. Adduct formation due to interactions of similar nature has been shown to occur between Lysptd and negatively charged plastocyanin, a copper-containing electron transfer protein, and between Aspptd and positively charged cytochrome *c*.

Detailed information on hydrogen bonds and aromatic ring stacking in chemical systems may be important for understanding biological functions and developing biomimetic systems.

Kinetic Studies of the Reassembly of the Water Oxidation Complex in Apo-WOC-Photosystem II

Y. Abe,* G. M. Ananyev, A. Murphy, L. Zaltsman, J. Mincer and G. C. Dismukes
*Nara Women's University, Department of Chemistry, Nara 630-8506, Japan
Princeton University, Department of Chemistry, Princeton, New Jersey 08540, U.S.A.

Photoactivation is the process of binding and photooxidation of the inorganic cofactores (Mn^{2+}, Ca^{2+}, Cl^-) within the apoprotein components of Photosystem II (apo-WOC-PSII) of green plants and cyanobacteria. We have reported that photoassembly of the inorganic core involves binding of Mn^{2+} and Ca^{2+} and photooxidation via a sequence of assembly intermediates: $[Mn(OH)]^+$, $[Mn(OH)_2]^+$, $[Mn(OH)_2]^+Ca^{2+}$, $[Mn(\mu\text{-}OH)_2Mn]^{3+}Ca^{2+}$ on the pathway to formation of the functional $Mn_4O_yCa_1Cl_x$ core.[1-5] Competitive inhibition of Mn^{2+} binding by M^{2+} dications correlates directly with the ease of $M(OH)^+$ formation. Oxo-metal cations (VO^{2+}, UO_2^{2+}) and Cs^+ are strong competitive inhibitors, consistent with formation of $Mn(OH)^+$ as the initial intermediate. Cs^+ binds with high affinity and remarkable selectivity (Cs^+/Li^+ >5000), features which could find use removal of ^{137}Cs from nuclear fuels/wastes.

In order to further identify the intermediates we studied the pH dependence of Mn^{2+} binding to apo-WOC-PSII and its inhibition by Cs^+, using the kinetics of PSII-mediated electron transfer from Mn^{2+} to an electron acceptor (DCIP) to assay binding. We confirmed published work showing the presence of both high- and low-affinity Mn^{2+} binding sites in apo-WOC-PSII. Ca^{2+} was shown to competitively prevent Mn^{2+} electron donation only at the low affinity site, thus identifying it as the potential native Ca^{2+} site. The Michaelis-Menten rate parameters (K_m^{-1} and V_{max}) both increase modestly in the pH range 6.0-7.5, at both the high- and low-affinity Mn^{2+} sites, while the binding constant for Cs^+ (at the high affinity site) decreases enormously in this range. Because Cs^+ does not hydrolyze in this pH range, the drop in inhibition constant may be due to deprotonation of an amino acid residue in the site or increased competition from $Mn(OH)^+$. The rate of electron transfer in the range pH 4-9 exhibits a maximum at 7.0-7.5 and decreases above this pH. We attribute this decrease to deprotonation of Y_Z, the redox-active tyrosine-Z.

(Research supported by the NIH (GM-39932) and the JSPS.)

* This research was performed at Princeton University

1) G. M. Ananyev and G. C. Dismukes, *Biochemistry*, 1996, **35**, 4102.
2) G. M. Ananyev and G. C. Dismukes, *Biochemistry*, 1996, **35**, 14608.
3) L. Zaltsman, G. M. Ananyev, E. Bruntrager, and G. C. Dismukes, *Biochemistry*, 1997, **36**, 8914.
4) G. M. Ananyev and G. C. Dismukes, *Biochemistry*, 1997, **36**, 11342.
5) G. M. Ananyev, A. Murphy, Y. Abe, and G. M. Dismukes, *Biochemistry*, 1999, in press.

THE FOUR-ELECTRON REDUCTION PROCESS OF DIOXYGEN AT THE TRINUCLEAR COPPER CENTER IN LACCASE

Giorgio ZOPPELLARO, Hong-wei HUANG, Takeshi SAKURAI
Graduate School of Natural Science and Technology, Kanazawa University, Kakuma, Kanazawa,920-1192, Japan

Laccase (diphenol : dioxygen oxidoreductase) is a member of multicopper oxidases which contains four coppers in a single protein molecule and utilize dioxygen as the final electron acceptor from its substrate such as urushiol. Nevertheless the complete mechanism concerning the four-electron reduction process hasn't been estabilished yet. We succeded to detect 3e- reduced intermediates (oxygen anion radical and hydroxyl radical in equilibrium) and characterize them using UV-Vis absorption, stopped-flow, EPR spectroscopies and SQUID measurements. Soon after mixing the reduced laccase with oxygen-containing buffer both type I and type III Cu's have been fully oxidized (within 15 ms) giving the strong absorption bands at 614 nm and 330 nm. However the difference absorption spectrum between laccase during reoxidation and resting laccase gave the transient absorption bands arising from an intermediate at 370 nm (ε = 1000), 420 nm (sh), and 650 nm (weak), with a decay that followed the same first-order process. The rate costants for the decay of the intermediate have been determined by stopped-flow measurements bethween pH 4.0 and 7.4. The intermediate could be detected for ca. 2 min at pH 7.4, while it was observable for less then 5 s at pH 4.2.The rate was decreased in D_2O, giving the isotope effect k_H/k_D of 1.4 indipendent of pH. The thermodinamic parameters enthalpy and entropy of activation relative to the decay of the intermediate were measured within pH 4.4 and 7.4. The large positive values for the enthalpy (47.7 ± 0.42 kJmol^{-1} at pH 4.4 and 36.70 ± 0.20 kJmol^{-1} at pH 7.4) and the large negative values for the entropy (-84.4 ± 0.70 Jmol^{-1}K^{-1} at pH 4.4 and -143.0 ± 0.70 Jmol^{-1}K^{-1} at pH 7.4) suggest that strong structural changes should take place into the active site, that are apparently coupled with the proton transfer. The EPR spectra at cryogenic temperature (< 27 K) showed two novel signals around 370 mT and 420 mT (**Fig.1**). The signal at 370 mT was detected only at pH less than 6, while both were detected at pH 7.4. Taking into consideration that both of absorption bands at 614 nm and 330 nm were recovered and the apparence of the EPR signals of type II copper was coupled with the decay of the intermediate, it was concluded that the intermediates were derived from dioxygen as the electron acceptor (i.e. the oxygen and hydroxyl radical) bound to the trinuclear copper center. According to the magnetic properties detected by the SQUID measurements, the oxygen radical in the intermediate was found to be magnetically coupled with type III coppers weakly, forming a three spin sistem. Based on all magnetic and spectroscopic data we propose the mechanism (**Fig.2**) of the dioxygen reduction by laccase.

Fig. 1

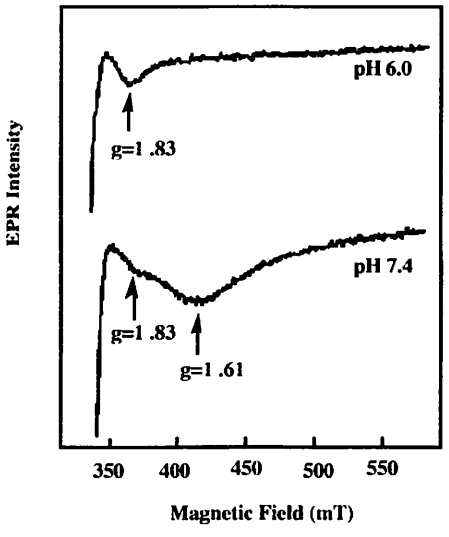

Fig. 2

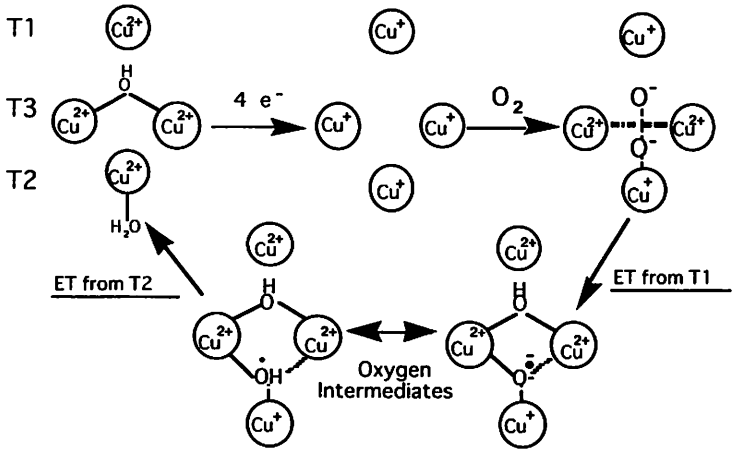

STRUCTURE, SOLUTION BEHAVIOR, AND PHARMACOLOGICAL IMPORTANCE OF SOME WATER-SOLUBLE BISMUTH(III) COMPLEXES

Eiji ASATO

Department of Chemistry, Biology, and Marine Science, College of Science, University of the Ryukyus, 1 Senbaru Nishihara-cho, Okinawa, 903-0213, Japan

Many of bismuth(III) compounds have pronounced antimicrobial activity and were once widely used in medical applications. Some bismuth compounds, *e.g.* the nitrate and the subsalicylate, are still used against a variety of gastrointestinal disorder. However, solution chemistry of the pharmacologically important Bi compounds has been poorly understood, because most Bi compounds are insoluble in water or undergo rapid hydrolysis giving insoluble bismuth-oxy salts.

Antimicrobial drugs CBS, which are bismuth complexes of citric acid, are highly soluble in water and are now widely used in many countries to treat peptic ulcers. Although the detailed mechanism of action of CBS is still unclear, its bactericidal activity against *Helicobacter pylori*, a pathogenic factor of clonic gastritis and peptic ulcer, is now well known. In this contribution, the author will report crystal structures and solution chemistry of several water-soluble Bi complexes including CBS models.[1,2]

The antibacterial activities toward *H.pylori* and inhibitory effect toward *H.pylori*-produced urease were tested for many Bi compounds.[3] From the *in vitro* experiments (see Table 1), no significant difference in the MIC values were observed between all the Bi compounds tested, suggesting that anti-*H.pylori* activity is a general property for Bi compounds. However, the urease inhibition activity was found to depend on the ligand bound to the metal ions. Based on the anti-*H.pylori* activity and the urease inhibition effect, some examples of Bi complexes potentially applicable to new antiulcer drugs will be discussed.

Table 1. *In vitro* Minimum Inhibitory Concentrations of Bismuth Compounds against *H.pylori*, Determined by the Agar Dilution Method : MIC (μg/mL)

Compound	Range	MIC_{50}	MIC_{90}
$[Bi(SCH_2CH_2OH)_2](NO_3)\cdot H_2O$	1.56 ~ 6.25	3.13	6.25
$[Bi(SCH_2CH_2O)(SCH_2CH_2OH)]$	1.56 ~ 6.25	3.13	6.25
$[Bi(SCH_2CH_2OH)_3]$	1.56 ~ 6.25	3.13	3.13
Bismuth oxide salicylate [BiO(sal)]	1.56 ~ 6.25	6.25	6.25
$(NH_4)_3[Bi(Tsal)_3]\cdot 2H_2O\cdot EtOH$	1.56 ~ 6.25	6.25	6.25
$(NH_4)_8[Bi_2(cit)_2(Hcit)_2(H_2O)_4]\cdot 2H_2O$ (CBS-model)	1.56 ~ 6.25	3.13	6.25

Hsal: salicylic acid, H_2Tsal; thiosalicylic acid, H_4cit: citric acid

1) Asato, E.; Katsura, K.; Mikuriya, M.; Fujii, T.; Reedijk, J., *Inorg. Chem.*, 1993, **32**, 5322. 2) Asato, E.; Katsura, K.; Mikuriya, M.; Turpeinen, U.; Mutikainen, I.; Reedijk, J., *Inorg. Chem.*, 1995, **34**, 2447. 3) Asato, E.; Kamanruta, K.; Akamine, Y.; Fukami, T.; Nukada, R.; Mikuriya, M.; Deguchi, S.; Yokota, Y., *Bull. Chem. Soc. Jpn.*, 1997, **70**, 639.

WEAK INTERACTIONS BETWEEN ARG, GLU, AND TYR SIDE CHAINS

Akira ODANI[1], Waheeda Jahan PUSPITA[1], Noriaki SUZUKI[1], and Osamu YAMAUCHI[1,2]

[1] Department of Chemistry, Graduate School of Science, Nagoya University, Nagoya 464-8602, Japan

[2]Research Center for Materials Science, Nagoya University, Nagoya 464-8602, Japan

Noncovalent interactions are important for molecular recognition and specificity of reactions in biological and chemical systems. We have been studying formations of ternary metal complexes involving various weak interactions between two functional groups such as aromatic rings and charged groups. Here we report specific interactions between three different groups of arginine(Arg), glutamate(Glu), and tyrosinate (Tyr) side chains in ternary Cu(II)-dipeptide-amino acid and Pt(phen)-(Arg)•••hydroxybenzoate systems (phen = 1,10-phenanthroline) (Fig. 1).

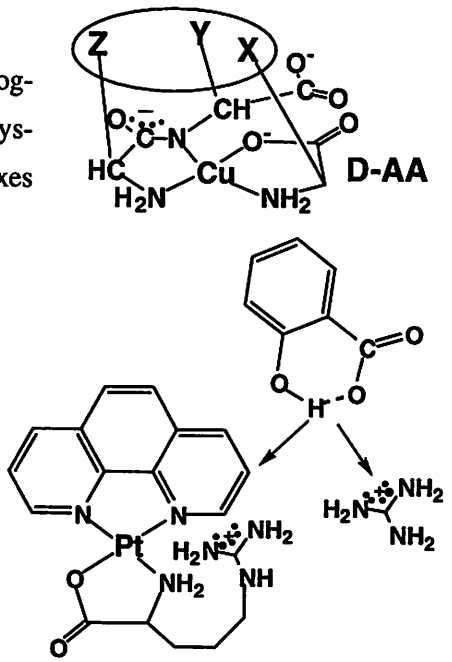

Fig. 1. Systems studied.

Stereoselective binding of amino acids toward a Cu(II)-dipeptide complex was studied by pH titrations at 25°C and I = 0.1(KNO_3). Tyrosine exhibited large stereoselectivity (0.22 log unit, D > L) toward Cu(L-Arg•L-Glu)(H_{-1}), whereas phenylalanine, serine, and alanine showed no stereoselectivity. These indicated the effects of specific interactions between the phenol, guanidinium, and carboxylate moieties of the coordinated amino acid and peptide. Similar interaction modes were revealed in the adduct formation constants and crystal structures of guanidinium hydroxybenzoate salts, supporting the presence of interaction of -$HNC(NH_2)_2^+ \cdots COO^- \cdots HO\text{-}C_6H_5$-. Specific interaction toward salicylate(*o*-hydroxybenzoate) was also observed in the adduct formation constants with Pt(phen)(L-Arg) complex. The adduct structure in aqueous solution estimated by H-1 NMR supported the interaction between three functional groups. Such interactions may be intriguing in view of wide pharmacological effects of salicylate, and interestingly the same functional groups are found in the crystal structure of an estrogen-receptor complex.

Acknowledgment. The authors thank the Ministry of Education, Science, Sports, and Culture for a Grant-in-Aid for Scientific Research (COE).

WHAT ROLES DO POLYMERASES PLAY TOWARD THE CYTOTOXICITY OF PLATINUM ANTI-TUMOR DRUGS?

Rathindra N. Bose, Rebecca K. Duman, Wei-Wen Yang and Kristi Allen
Department of Chemistry, Kent State University, Kent, OH 44242, USA,

The platinum antitumor drug, *cis*-diamminedichloroplatinum(II), arrests the cell synthesis in G2 phase of the cell cycle by a mechanism commonly known as apoptosis (1). Although at the molecular level, platinum-DNA adducts are believed to be primary lesions responsible for the antitumor activity (2), other mechanisms including enzyme-platinum bindings have yet to be ruled out. We have examined the activities of human DNA polymerase-α (3)and E. coli polymerase I(4) in the presence of *cis*-DDP and platinum(IV) antitumor drugs. The activity of the enzymes was completely retarded in that they failed to extend the primer strand of the DNA due to the covalent binding to the platinum compounds. The irreversible inhibition process is zero order in platinum and first order in enzyme. The mechanism of inhibition entails a rapid formation of *cis*-DDP-enzyme adduct with a binding constant $>10^5$ M^{-1} followed by the formation of an inhibitory complex through a first order process, with a rate constant, $1.0\ 10^{-3}$ s^{-1}. This first order rate constant is much larger than that for the aquations of *cis*-DDP which control the DNA binding processes. Minimal inhibition was observed within two hours when a template DNA was first bound to platinum(II) followed by the activation with the DNA polymerases. Likewise *trans*-DDP-DNA complex was readily recognized as the template by the polymerase in initiating the DNA synthesis. Furthermore, the *trans* isomer, the inactive form did not inhibit the enzyme activity.

Since Zn(II) is released from the human polymerase-α during the platinum binding, we have examined the NMR structures of the putative DNA binding domain of the enzyme. In this domain, Zn(II) is coordinated to four cysteine residues. The structure consists of a helical region, a type II turn, and an anti-parallelβ-sheet. Two cysteine residues are found to be located in the helix region while the other two are in the anti-parallel β-sheet domain. *cis*-DDP selectively reacts with the two cysteines in the anti-parallelβ-sheet region and unwinds the DNA binding domain. These structural perturbations may be responsible for the lack of recognition of the template DNA and therefore may be related to the mechanism of inhibition of polymerase-α.

1. Sorenson, C.M; Eastman, A., *Cancer Research*, 1988, 48, 6703.
2. Trimmer, E. E.; Zamble, D.B.; Lippard, S.J.; Essigman, J.M., *Biochemistry*, 1998, 37, 352.
3. Kelley, T.J.; Moghaddas, S.; Bose, R.N.; Basu, S. *Cancer Biochem. Biophys.*, 1993, 13, 135.
4. Duman, R.K.; Heath, R.T; Bose, R.N., *FEBS Letts.*, 1999, in press.

STRUCTURAL CHARACTERIZATION OF THE MIXED PHOSPHOLIPID/PROTEIN MONOLAYER AT THE AIR/WATER INTERFACE

Junbai Li, Xiaoli Wang and Hengjian Zhang

International Joint Lab between Institute of Photographic Chemistry and Max Planck Institute of Colloid and Interface Sciences, Chinese Academy of Science, De Wai, Bei Sha Tan, Beijing 100101, China

A mixed protein/lipid monolayer has been constructed by the protein adsorption from subphase into the spread phospholipid monolayer. A precisely controlled pump was used to exchange the protein solution with different pH values after the protein was ensured to reach the less condensed surface.

The domains formed in the coexistence region of dipalmitoylphosphatidylcholine (DPPC) have been recorded by Brewster angle microscopy (BAM) combined with the film balance before and after the penetration of the protein, human serum albumin (HAS). The subphase was exchanged by gradually increasing or decreasing pH value of the solution. Three isotherms of the mixed DPPC/HSA monolayer with the subphase of pH=4.18, pH=7.0 and pH=9.1, respectively, were obtained. It indicated that the area per lipid molecule with protein increased as the subphase pH value was lowed. Simultaneously, morphological dynamic changes caused by the gradual changing of subphase pH were observed. These variations can be ascribed to the conformation change of protein under the fluctuation of pH value. The hydrophobic interaction between DPPC and HAS was considered for the interpretation of domain change based on the current experimental results.

A subphase exchange method has been used to detect the stability of the mixed β-lactoglobulin/DPPC film. The monolayer was formed via the spreading of lipid and the adsorption of protein at the air/water interface by using Brewster angle microscopy (BAM). When the surface pressure remained a constant value after the protein adsorbed into the spread DPPC monolayer the protein solution was totally washed out by pumping into pure water for a longer time. In the fluid phase and the coexistence region of DPPC monolayer with penetrated protein layer BAM images have been recorded for comparing the variation of domains before and after the exchange of subphase. The experimental results have showed no significant change of the domain size and shape. It indicates that the adsorbed protein have a strong interaction with DPPC and remain at the interface. This means by this way that a rather stable mixed protein/lipid monolayer has been constructed. The hydrophobic interaction between DPPC and β-lactoglobulin at the interface may be taken place and makes the mixed layers stable.

COMPARISON OF THE SELF-DIFFUSION PROPERTIES OF ALKALI CATIONS IN CATIONS EXCHANGE MEMBRANE

A.-L. Rollet, J.-P. Simonin, P. Turq
Laboratoire LI2C, Université Pierre et Marie Curie, Boîte 51, 4 Place Jussieu, 75252 Paris Cedex 05, France

The properties of ions and molecules in confined media are being given increasing attention. Diffusion of ions in Nafion membrane constitutes an interesting example[1]. This cation exchange membrane is composed of small spherical cavities of 40Å diameter covered with anionic sites SO_3^-, the ionic concentration in these domains is about 5M[2]. For this study, a novel radiotracer method, based on the rotating electrode technique used in Electrochemistry, has been developed ; it allows good control of hydrodynamics near the membrane.

Two alkali ions were studied, Na^+ and Cs^+, because they present different properties of solvation and of association with anions. The influence of electrolyte concentration and temperature has been investigated. An important influence of the electrolyte concentration has been observed. The results indicate that the diffusion process inside the membrane for Na^+ ion depends linearly on water volume fraction : this phenomenon might be interpreted as no particular interactions occurs between Na^+ ions and the membrane. The results for Cs^+ indicate that this ion has a different behaviour in this charged confined media : stronger interactions with anionic sites SO_3^- seems to occur for this ion as compared to Na^+ ions.

1. G. Pourcelly, P. Siestat, A. Chapotot, C. Gavach, V. Nikonenko, J. Membrane Sci., 1996, **110**, 69.
2. W. Y. Hsu, T.D. Gierke, J. Membrane Sci. 1983, **13**, 307.

PHYSICOCHEMICAL PROPERTIES OF ELECTROLYTE SOLUTION COEXISTING WITH SOLID PHASE

Shigehito DEKI and Minoru MIZUHATA
Department of Chemical Science and Engineering, Faculty of Engineering,
Kobe University, 1-1 Rokkodai, Nada, Kobe 657-8501, Japan

It is well-known that properties and behavior of the electrolyte solution are influenced by the solid phase in the interfacial region. In cases that the liquid phase coexisting with the porous solid phase, as the area of interface extremely increases, the macroscopic properties of the liquid phase vary with an increase in the solid content. We have been studying that changes of the structure and properties of the electrolyte solution coexisting with solid phase.[1]

The electrical conductivities of systems consisting of the inorganic powder, such as α-Al_2O_3, SiC, and SiO_2 and several kinds of aqueous electrolyte solution were measured. The electrical conductivity exponentially increases as the liquid content increases. On the basis of Archie's equation,[2] we classified the range of the liquid content, ϕ, as follows;

I. Macro-geometrically depending range (ca. 0.6 <ϕ) --- The electrical conductivity decreased with the interrupt of the conduction path by the solid phase. Therefore, the electrical conductivity mainly depends on the liquid content and a geometric factor of the solid phase.

II. Morphologically depending range (ca. 0.45 <ϕ< ca. 0.6) --- In this range, the liquid phase does not saturate in the space among the solid particles. The shape of conduction path depends on the surface morphology and the shape of the solid phase.

III. Chemical interaction depending range (ϕ< ca. 0.45) --- In this range, most part of the liquid phase exists on and interacts with the solid surface. The conduction varied by the properties of the solid phase, such as hydrophilicity, electrostatic charge, and pH of the liquid phase. Most of our studies have been carried out for the properties of the electrolyte solution in this range, and we concluded as follows;

- Activation energy of the electrical conductivity increases as the apparent average thickness of the liquid phase decreases.
- The hydration structure of the transition metal complexes, such as Co(II), Ni(II), and Zn(II) aquo-complexes, changes.
- On the hydrophobic surface, little or no increase of the activation energy was observed.

Consequently, the transport properties of the ionic species are influenced by the coexisting solid phase. In the view of the results of our previous research, we are studying the structural change by means of IR and Raman spectroscopy, NMR, and XAFS analysis.[3]

The thermochemical properties of the liquid phase were measured for the α-Al_2O_3 powder/ $CaCl_2 \cdot 6H_2O$ melt coexisting system. The molar enthalpy of fusion and phase transition point of the hydrate decreased as the content of solid phase increased. This change also depended on the specific surface area of the solid phase. The electrical conduction remained even below the melting point. It is suggested that a non-frozen part exists in the hydrate at the lower temperature range than the melting point. However, these changes were not observed in the system containing hydrophobic solid phase. We have obtained the similar results for the system of α-Al_2O_3 powder/ molten alkali nitrates and γ-$LiAlO_2$ powder /molten alkali carbonates utilized in the fuel cells etc.[4]

Considering the circumstances mentioned above, the interaction between solid and liquid phases caused the variation of the physicochemical properties of the electrolyte solutions. We expected that the stabilized liquid materials among the solid phase would be developed and utilized as the "Quasi-solid Materials" showing the anomalous behaviors that are not observed in bulk systems.

A part of these study was supported by the Proposal-Based New Industry Creative Type Technology R&D Promotion Program from the New Energy and Industrial Technology Development Organization (NEDO) of Japan.

1. S. Deki and M. Mizuhata, *Denki Kagaku*, **64**, 867 (1996).
2. G. E. Archie, *Trans. AIME*, **146**, 54 (1942).
3. M. Mizuhata et al., *J. Molecular Liquids*, in press.
4. S. Deki et al., *Molten Salts Forum*, **5-6**, 175 (1998).

ENTHALPY-ENTROPY COMPENSATION PHENOMENON OBSERVED FOR DIFFERENT SURFACTANTS IN AQUEOUS SOLUTION.

Gohsuke SUGIHARA and Mihoko HISATOMI
Fukuoka University, Faculty of Science, Department of Chemistry, Jonan-ku, Fukuoka 814-0180, Japan

Based on the thermodynamic data such as changes of the Gibbs energy (ΔG°_m), the enthalpy (ΔH°_m) and the entropy (ΔS°_m) on micelle formation of more than 15 species of surfactants (including nonionic, anionic and cationic ones) reported in the past, the plots of ΔH°_m *vs.* ΔS°_m (not of ΔS°_m *vs.* ΔH°_m usually done) were made. For each surfactant a linear relation having almost the same slope (1 / 307 K^{-1}) within small error ($\pm 2.3\%$), but a different intercept (σ) depending on the surfactant species:

$$\Delta S^\circ_m = (1/307)\,\Delta H^\circ_m + \sigma,$$

where 1 / 307 (K^{-1}) means that the so called compensation temperature (T_C) is 307K. Strictly describing, T_C ranges from 299 to 315K, depending on species. The intercept corresponds to the entropy change at a specific temperature giving $\Delta H^\circ_m = 0$ at which the driving force of micelle formation comes only from the entropy term; this temperature is characteristic to the surfactant species. On the other hand the compensation temperature has no significant meaning other than a mean temperature studied.

In the process of micelle formation hydrophobic groups, accompanying translation from bulk water to micelle, the large entropy increase ($T\Delta S^\circ_m > 0$) and thus the large negative change in the Gibbs energy ($\Delta G^\circ_m < 0$) take place, and simultaneously the ΔH°_mterm changes in parallel with the entropy term and switches its sign from negative to positive at a certain temperature. Therefore, the behavior of hydrophobic groups of surfactants in water is the case for the compensation rule.

SELF-ASSOCIATION BEHAVIOR OF LOCAL ANESTHETIC DIBUCAINE HYDROCHLORIDE IN THE AQUEOUS SOLUTION

Hitoshi MATSUKI[1], Toshiharu YOSHIOKA[1], Hiromu SATAKE[2] and Shoji KANESHINA[1]
[1] Department of Biological Science and Technology, Faculty of Engineering, and
[2] Center for Cooperative Research, The University of Tokushima, Minamijosanjima, Tokushima 770-8506, Japan

The nerve-blocking potency of local anesthetics in cell membranes is proportional to their partitioning ability into the membranes. The main driving force of the partitioning is the hydrophobic interaction between membrane and anesthetic molecules. Local anesthetics are amphiphilic molecules and some form molecular aggregates as micelles in aqueous solutions.[1] Such self-association of the anesthetics is also caused by the same hydrophobic driving force. In the present study, we characterized two self-association mode of local anesthetic dibucaine hydrochloride (DC•HCl) in the aqueous solution by electrode potential measurements using ion-selective electrodes and by static and dynamic light scattering measurements.

Both activities of dibucaine cation and chloride anion in the aqueous solution were determined as a function of their concentrations. Nernstian response was observed for both activities in the low concentration range, but they deviated from the response with increasing their concentrations. The deviation suggests the formation of pre-micellar aggregate since it begins at concentrations below the critical micelle concentration (CMC). We analyzed the depression of both activities in the concentration range and concluded that DC•HCl forms a trimer with two chloride ions at the concentration below the CMC. The trimer formation may be attributable to the stacking of aromatic quinoline ring and the hydrophobic interaction of butoxy group in the molecule.

The static light scattering measurements were performed on various concentrations of aqueous DC•HCl solutions. The scattered light intensity steeply increased at concentrations above the CMC. This behavior means that the association mode of DC•HCl in the concentration range is typically micellar. From Debye plot of the intensity data, we obtained the aggregation number of 15 for DC•HCl micelle in water. Taking account of the pre-micellar aggregation below the CMC, five trimers associate cooperatively and form micelles above the CMC.

Further, we measured the scattered light intensity in the presence of added electrolyte (NaCl). Addition of NaCl reduced the CMC and enlarged the aggregation number. The results were also consistent with those from dynamic light scattering measurements. The stacking effect of quinoline ring significantly contributes to the micellar growth in solutions of high ionic strength.

[1] Attwood, D.; Fletcher, P., *J. Pharm. Pharmacol.* 1986, **38**, 494.

SOLUBILIZATION OF WATER-INSOLUBLE DYES IN SURFACTANT AGGREGATES

Katumitu HAYAKAWA, Mihoko SATO, Makoto KAWANO, Katsuhiko KAMIO, and Iwao SATAKE
Department of Chemistry and BioScience, Faculty of Science, Kagoshima University, 1-21-35, Korimoto, Kagoshima, 890-0065, Japan.

Solubilization of organic compounds in surfactant aggregates is a phenomenon of great theoretical and practical significance. The physicochemical studies have influenced in improving our understanding of the forces involved in micelle formation and the structure and character of micelles. The applications include pharmaceuticals, detergency, agricultural products, and surface modification of powder and suspension. This paper concerns to the solubilization of water-insoluble 1-pyrenecalbaldehyde (PyA) and α-(o-tolylazo)-β-naphtylamine (oil yellow: OY) by surfactants derived from amino acid. The amino acid surfactants have some excellent and special properties such as mild for skin, environmentally gentle and easy gelation at the low concentration in water. This paper reports the critical micelle concentration (cmc) of N-acylglutamates and the solubilization for PyA and OY as a function of solution ionic strength. The surfactants showed a regular behavior on cmc, that is, the regular dependence on ionic strength and surfactant chain length. They showed lower solubilization power than regular surfactants of a similar chain length and the Gibbs function was determined for the solubilization equilibrium.

N-acylglutamates include sodium salts of dodecanoyl- (C_{12}Glu), tetradecanoyl- (C_{14}Glu) and octadecanoyl-glutamate (C_{18}Glu). They were kindly supplied from Ajinomoto Co., Inc. Electric conductivity was measured for the determination of the surfactant cmc and Krafft point. Solubilization was determined from the absorbance of PyA and OY in the surfactant solutions. The ionic strength of the surfactant solutions was controlled and the pH was adjusted as 9.0–9.5 by ammonia-ammonium chloride buffer in order to obtain the complete dissociation state of two carboxylic groups in the N-acylglutamates. All measurements were carried out at 40 °C.

Table 1 indicates that the cmc decreases with increasing solution ionic strength and hydrophobic chain length as regular surfactants indicate. C_{12}Glu shows a much larger cmc than C_{12}TAB, but C_{14}Glu show a comparable cmc to C_{14}TAB. The ratio of cmc of C_{12}Glu to that of C_{14}Glu is 6.9, while the ratio of C_{12}TAB to C_{14}TAB is 4.2. The dependence of ln cmc on the number of carbon in surfactant chain is lower for divalent ionic surfactant than for monovalent ionic surfactant in regular surfactants. The solubilization of PyA by C_nGlus increases with the hydrophobic chain length. The one by C_{14}Glu is much weaker than regular surfactant, C_{14}TAB, though the cmc (indication of hydrophobic properties of surfactant) is comparable for both surfactants. Thus the amino acid surfactants are different to the regular surfactants. The solubilization equilibrium for PyA and OY will be discussed.

Table 1. The cmc and solubilization constant of amino acid surfactants.

Surfactant	Buffer Concentration (M)	Cmc (mM)	Solubilization Constant for PyA
C_{12}Glu	0.1	28.8	0.0357
	0.3	13.8	0.0357
	0.6	8.4	0.0521
	1.0	6.3	0.0521
C_{14}Glu	0.1	4.2	0.0672
C_{18}Glu	0.1	0.068	0.153
C_{12}TAB [1)]	non	15.2	0.111
C_{14}TAB [2)]	non	3.65	0.178

[1)] Dodecyltrimethylammonium bromide [2)] Tetradecyltrimethylammonium bromide

EFFECT OF SURFACTANTS ON ROTATIONAL DYNAMICS OF OCTADECYLRHODAMINE B AT TOLUENE-WATER INTERFACE

Satoshi TSUKAHARA, Yoshiaki YAMADA and Hitoshi WATARAI
Department of Chemistry, Graduate School of Science, Osaka University, Machikaneyama, Osaka 560-0043, JAPAN

The liquid-liquid interface plays essential roles in various fields, such as colloidal chemistry, ion and electron transport processes, pharmacology, and solvent extraction of metal ions. Rotational dynamics of reagents at the liquid-liquid interface is an important subject, because the reaction kinetics at the interface are strongly affected by the rotational dynamics as well as the orientation. However, few studies on these subjects were reported so far. In this study, we measured the rotational reorientation of *N*-octadecylrhodamine B (C_{18}RB) without and with surfactants, and clarified the effect of the surfactants.

Organic phase was 1.0×10^{-7} M C_{18}RB in toluene. As surfactants, Triton X-100 (nonionic), sodium dodecylsulfate (SDS, anionic), and dihexadecyl hydrogen phosphate (DHP, anionic, $pK_a\approx2$) were used in the concentration range of 1.0×10^{-10}–1.0×10^{-4} M. The pH of the aqueous phase was 1.0 (0.1 M H_2SO_4) for Triton and SDS systems, whereas it was 3.0 (5.0×10^{-3} M H_2SO_4) for DHP system. S- and p-polarized pulsed laser lights (wavelength, 536 nm; pulse width, 1 ns) were irradiated to the interface at the incident angle of 70°, which was larger than the critical angle (63°). The s- and p-polarized fluorescence emitted from adsorbed C_{18}RB were measured, and in-plane and out-of-plane rotational reorientations of C_{18}RB at the interface were obtained from the difference between the time-resolved polarized fluorescences.

At pH 1.0, the cationic form of C_{18}RB, C_{18}RBH$^+$, was dominantly adsorbed. In the absence of surfactant, the in-plane fluorescence anisotropy, r_ϕ, was almost 0 independent of time, and this implied that C_{18}RB molecules rotated very fast (rotational correlation time, τ_ϕ < 1 ns) at the interface. In the nonionic Triton system, C_{18}RB molecules rotated fast (τ_ϕ < 1 ns), but the rotational region was restricted by Triton molecules. In the cases of SDS and anionic DHP, the interfacial concentration of C_{18}RBH$^+$ increased with an increase in the surfactant concentration (1.0×10^{-10}–1.0×10^{-7} M) by an electrostatic attractive force. Typical variations of r_ϕ with SDS and DHP are shown in Figure 1, In these cases, r_ϕ decreased exponentially and τ_ϕ could be obtained. τ_ϕ increased with an increase in the SDS or DHP concentration. These results suggested that the ionic interaction between C_{18}RBH$^+$ and anionic surfactants interfered the rotation of C_{18}RBH$^+$. Furthermore, the interfacial viscosity was evaluated from the r_ϕ value.

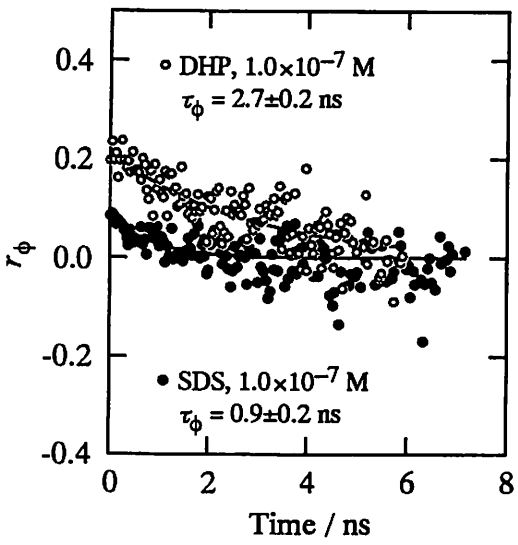

Figure 1 The time resolved in-plane fluorescence anisotropy, $r_\phi(t)$, of C_{18}RB at the toluene/water interface

SELF-ORGANIZATION OF SURFACTANT MOLECULES IN SOLUTIONS

Hironobu KUNIEDA
Graduate School of Engineering, Yokohama National University, Tokiwadai 79-5, Hodogaya-ku, Yokohama 240-8501, Japan

Surfactant molecules form various types of self-organized structures, micelles, vesicles, liquid crystals etc. in solvents. Hydrophile-Lipophile Balance of surfactant is directly related to the shapes of aggregates. In the case of polyoxyethylene-type nonionic surfactant aqueous solutions, the surfactant molecular curvature is changed from negative to positive with the increase in polyoxyethylene (EO) chain length. The surfactant molecular curvature of the aggregates in the liquid crystals would be determined by the balance between the repulsion of the EO chain and the attraction of the lipophilic moieties. Taking into account of this consideration, the self-organization of EO-type nonionic surfactants in water will be discussed using the experimental data of SAXS and phase studies in ordinary hydrocarbon surfactants as well as silicone-type surfactants.

When oil is added to the surfactant self-organized structures in water, the surfactant curvature is changed depending on the types of oils and the amount of solubilized oil. Oil, which tends to be solubilized in the surfactant palisade layers, changes the surfactant curvature negative, whereas the opposite effect is observed if oil is solubilized in the deep core of the aggregates. The effect of added oil on the surfactant curvature will be also discussed in EO-type nonionic surfactant systems.

It is well known to surfactant chemists or engineers that surfactant-functions such as lowering surface and interfacial tensions, stabilizing emulsions, solubilizing insoluble substances, etc. are considerably enhanced by mixing surfactants. Judging from the SAXS data for liquid crystals in the mixed surfactant systems, an effective cross sectional area per surfactant in the aggregates considerably decreases upon mixing, since the reduction in repulsion of the hydrophilic moieties takes place. The result will be compared with the surfactant functions.

STRUCTURE AND DYNAMICS OF CONCENTRATED MICELLAR AND LAMELLAR PHASES IN NONIONIC SURFACTANT-WATER SYSTEMS

Tadashi Kato
Department of Chemistry, Tokyo Metropolitan University, 1-1 Minamiohsawa, Hachioji, Tokyo 192-0397, Japan

Static and dynamic light scattering have been measured on semidilute and concentrated solutions of nonionic surfactants ($C_nH_{2n+1}(OC_2H_4)_mOH$, C_nE_m). The observed concentration dependence of the scattered intensity has been analyzed based on the method proposed by Schurtenberger[1] where the concentration dependence of the micelle aggregation number and intermicellar interactions are combined in a self-consistent way using results from the theory originally developed for entangled polymers. In the dynamic light scattering measurements, we have found the so-called slow mode in addition to the diffusion mode in time correlation function of the scattered field. The relaxation time of the slow mode (τ_s), independent of the scattering angle, first increases with increasing surfactant concentration, goes through a maximum, and then decreases.[2] As the temperature increases, τ_s decreases very rapidly, corresponding to an activation energy of about 200 kJmol^{-1}. The concentration and temperature dependencies of τ_s are strongly correlated with those of the surfactant self-diffusion coefficient (D) obtained from pulsed-gradient spin echo reported before.[3,4] Quantitative analyses of these data suggest that surfactant molecules migrate to another micelles through transient connections between wormlike micelles. In the higher concentration and temperature range, near the lamellar and bicontinuous cubic phases, on the other hand, the surfactant self-diffusion is dominated by the lateral diffusion alone, suggesting the existence of network formed by wormlike micelles.

Small angle X-ray scattering has been measured on a lamellar phase of the $C_{16}E_7$ system. The lamellar spacing d follows the usual swelling law ($d = \delta_{hc}/\phi_{hc}$ where δ_{hc} and ϕ_{hc} are the thickness and the volume fraction of the hydrocarbon layer, respectively) in the higher temperature range. In the lower temperature range, however, the swelling law does not hold and the observed d value decreases with decreasing temperature. By analyzing the scattering curve profile assuming that the electron density is uniform n the hydrocarbon and hydrophilic layers, δ_{hc} has been determined at each concentration and temperature. The obtained δ_{hc} value depends on concentration and temperature only slightly. These results suggest that the bilayer has water-filled defects and that the fraction of the defects increases as the concentration and temperature decrease. As such a defected bilayer can be regarded as two dimensional network formed by cylindrical micelles, the transition from the micellar phase to the lamellar phase may correspond to the transition from three dimensional network to two dimensional network.

1. Schurtenberger, P.; Cavaco, C.; Tiberg, F.; Regev, O., *Langmuir*, 1996, 12, 2895.
2. Kato, T.; Taguchi, N.; Nozu, D., *Progr. Colloid. Polym. Sci.*, 1997, 106, 57.
3. Kato, T.; Terao, T.; Seimiya, T.; *Langmuir*, 1994, 10, 4468.
4. Kato, T.; Taguchi, N.; Terao, T.; Seimiya, T. *Langmuir*, 1995, 11, 4661.

FUSION OF VESICLES WITH OLIGOMERIZED BILAYER LEAFLETS

J.B.F.N. ENGBERTS, B.J. RAVOO and W.D. WERINGA
Department of Organic and Molecular Inorganic Chemistry, University of Groningen, Nijenborgh 4, 9747 AG Groningen, The Netherlands

We have performed a detailed study of the bilayer properties and fusogenic behavior of a series of phospholipid derivatives carrying an oligomerisable and hydrolysable ß-nitrostyrene unit linked to the phosphate head group.[1] The amphiphiles easily form vesicles in aqueous solution. Upon UV irradiation, the lipid head groups undergo oligomerization. Under alkaline conditions and at temperatures below the main phase transition temperature of the bilayer, the ß-nitrostyrene groups can be cleaved specifically exo-vesicularly, providing vesicles with an oligomerized inner-leaflet and an unoligomerized outer-leaflet. The bilayer properties and fusogenic behavior of these three types of surface-differentiated vesicles (unoligomerized, both leaflets oligomerized, solely the inner-leaflet oligomerized) are significantly different.

Particular emphasis has been placed on: phase transition temperatures, permeability of the bilayer, lateral diffusion of the lipid components, rates and extents of aggregation and fusion in the presence of calcium ions and possibilities for directly observing a hemifusion intermediate in the case of vesicles with an oligomerized inner-leaflet.

Finally, a microcalorimetric study has been made of the thermodynamics of calcium-induced fusion. It was found that the driving force for merging of the bilayers is entropic in origin.

1. B.J. Ravoo, W.D. Weringa and J.B.F.N. Engberts, (a) *Langmuir*, 1996, **12**, 5773; (b) *J.Phys.Chem.B*, 1998, **102**, 11001; (c) *Biophys. J.*, **76**, 374.

NMR DETERMINATION OF DRUG DELIVERY SITES IN PHOSPHOLIPID BILAYER MEMBRANES

Emiko OKAMURA, Ryo KAKITSUBO, and Masaru NAKAHARA
Institute for Chemical Research, Kyoto University, Uji, Kyoto 611-0011, JAPAN

Drug delivery (DD) into phospholipid bilayer membranes becomes of great importance, as a primary step of the membrane-drug interaction. The determination of DD sites and orientation of drugs in bilayer membranes is crucial to develop basic concepts of the molecular mechanism of the DD from water to lipid bilayer phase. However, the equilibrium concentration of drugs in the membrane interior is, in general, too low to be detected experimentally. No noninvasive spectroscopic procedures have been established yet. There are no systematic studies providing direct experimental evidence for the structure and dynamics of drugs trapped in membranes. Most recently, we have, for the first time, succeeded in monitoring DD process of benzene derivatives from water to phospholipid vesicles by site-selective ^{1}H and ^{13}C NMR technique.[1]

We categorize three types as molecular mechanisms of the membrane-drug interaction, as shown in the scheme.[1] The type I is that drugs are adsorbed on the hydrophilic surfaces of bilayer membranes by Coulombic interaction or the hydrogen bonding. In this case, drugs are generally polar and water-soluble. No significant effect of drugs is induced in the membrane interior. The type II is the case where drugs are slightly penetrated and trapped at the interfacial site of the membranes. These drugs are less hydrophilic than those of the type I. Membrane structure is perturbed mainly at the interfacial glycerol and carbonyl sites of phospholipids. These drugs do not significantly perturb the inner hydrophobic chains. The type III is that drugs are deeply penetrated into the hydrophobic chain region of the membranes. These drugs are almost insoluble in water nonpolar and highly lipophilic. In this case, the membrane interior can be most remarkably perturbed.

How can we strictly determine these trapped sites of drugs at the atomic-site level from their direct NMR signals?

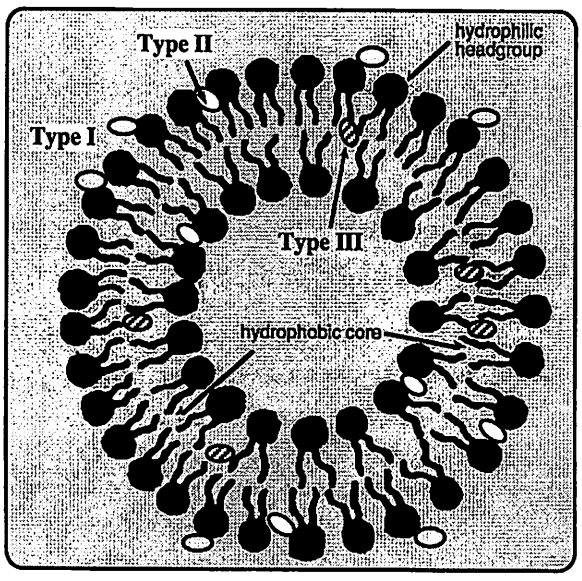

Classification of Drug Delivery Sites

We can rely upon the empirical rule that the NMR signals largely shift to a higher field when molecules are in the nonpolar environment. According to this fact, the NMR signals of the trapped drugs should shift to a higher field in the order, the type I<type II<type III. The bilayer interface and interior as delivery sites are unambiguously specified by taking advantage of the site selectivity of NMR. Delivery sites are also confirmed by the ring current effect of drugs on phospholipid NMR signals.

Delivery site determination is applied to local anesthetics in bilayer membranes. Finally, the application to recent severe problems of endocrine disruptors (EDs) is also proposed, as a basis for the comprehensive understanding of the molecular mechanism of the membrane disrupting action and for the purpose of detoxication and the prevention of ED accumulation.

1. Okamura, E. and Nakahara, M., *J. Phys. Chem.*, in press.

Revised and Expanded Scales of Gas-Phase Lithium-Cation Basicities. An Experimental and Theoretical Study

Ilmar Koppel
Institute of Chemical Physics, University of Tartu, 2 Jakobi St., Tartu 51014, Estonia

The gas-phase lithium-cation basicity (LCB) is defined as the Gibbs free energy associated with the thermodynamic equilibrium of attachment of Li cation to neutral or anionic base. In the present work the previously reported lithiun-cation basicity scale[1] was significantly revised and expanded on the basis of a new experimental and theoretical (G2 calculations) results.

A new anchoring based on the experimental lithium cation affinity value for H_2O is suggested (all earlier reported values of LCB should be reduced by 2.6 kcal/mol). New LCBs for 28 compounds were measured using FT ICR spectroscopy.

The revised LCB scale involves more than 200 neutral bases of various classes and covers the LCB range ca 30 kcal/mol. Two Lewis acids, H^+ and Li^+, present a significant contrast in the nature of the bond formed with the ligand. The proton adds to the base giving a polar covalent sigma bond with a very extensive charge transfer, whereas the bonds formed by Li^+ and other alkali metal cations are largely ionic. Therefore, one of our goals was to make a general comparison of the gas-phase LCBs for widely variable families of Lewis bases with the gas-phase basicities (GB). No general correlation was found for all studied compounds, while fair or satisfactory correlations were found for families with the similar basicity center. The differences in slopes could be traced back to the different sensitivities to structural effects. Large deviations from "normal" linear family-specific relationships are explained either by a different attachment center for Li^+ and H^+, or by a chelation effect towards Li^+.

G2 and G2(MP2) calculations of LCBs for 37 compounds and DFT B3LYP/6-311+G** calculations for LCBs of 63 compounds were carried out. It was found that used levels of theory adequately (but with some systematic error) describe lithium cation binding energies. Calculated structures reveal the origin of the deviations from correlation line between gas-phase proton and lithium-cation basicities.

The present work was accomplished in collaboration of University of Tartu, Universite de Nice, University of California, Irvine, and Instituto Chimica Fisica Rocasolano, CSIC, Madrid.

1 R. W. Taft, F. Anvia, J.-F. Gal, S. Walsh, M. Capon, M. C. Holmes, K. Hosn, G. Oloumi, R. Vasanwala, and S. Yazdani, *Pure Appl. Chem.*, **1990**, *62*, 17.

SOLUTE-SOLVENT AND SOLVENT-SOLVENT INTERACTIONS EVALUATED THROUGH CLUSTERS ISOLATED FROM SOLUTIONS

Akihiro WAKISAKA
National Institute for Resources and Environment, Onogawa 16-3, Tsukuba 305-8569, Japan

Solvent effects on organic chemical reactions, especially those in water-organic solvent mixtures, were found to be closely related to the microscopic molecular clustering structures in the solutions.

If a water-organic solvent mixture seems to be macroscopically homogeneous like water-alcohol mixtures, the water and the organic solvent molecules are hardly mixed homogeneously at the molecular level due to the hydrophobic interaction and the various intermolecular interactions. Such an inhomogeneous microscopic solvent structure was observed as clusters by means of specially designed mass spectrometer.

It is worth to note that the solvation for the organic solute molecules in the water-organic solvent mixtures is controlled by the clustering structure of the solvent mainly, not by the solute-solvent interactions.

Fig. 1 represents the change of clustering structure as functions of the mole fraction of alcohol in water-alcohol mixtures: water-methanol, water-ethanol and water-1-propanol. The monomeric alcohol interacting with the water clusters, the water-alcohol coexisting clusters and the alcohol molecular clusters are predominantly observed in the region A, B and C, respectively. The region A and B become narrow with increase of the alkyl chain length of the alcohol, which indicates that the larger alcohol molecules aggregate more easily in water. It will be presented that the observed solvent-solvent interaction controls solvation properties influencing chemical reactivity.

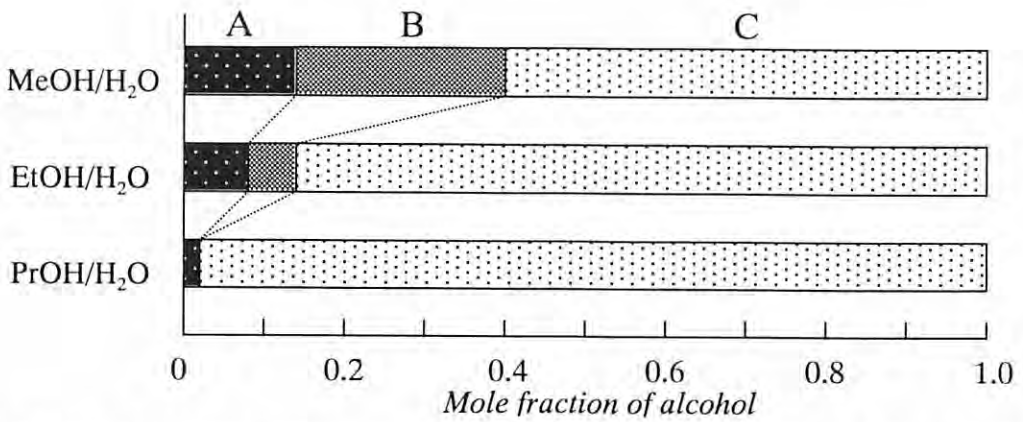

Fig. 1 Change of cluster structures in water-alcohol mixtures as functions of the mole fraction of alcohol. A: monomeric alcohol, B: water-alcohol coexisting clusters, C: alcohol clusters.

EFFECTS OF *ORTHO* NITRO GROUP ON THE NUCLEOPHILIC REACTIVITY OF BENZOATE ION

Yasuhiko KONDO, Hiromi TAKEZAWA, Mari SHIBATA and Tomomi KATSURA.
Department of Environmental Science, Faculty of Science, Osaka Women's University, Sakai, Osaka 590-0035, JAPAN

Chemical reactivity in solution is a composite quantity of intrinsic and solvational terms, and quantitative evaluation of the role of solvational term has been a long-standing subject of physical organic chemistry. In this work empirical evaluation of the role of the solvational term in nucleophilic reactivity of benzoate ion will be carried out through the following procedures; ① comparison of the effects of *ortho*- vs. *para*-substituted nitro group on the rate of nucleophilic substitution of benzoate ion, ② measurements of the relative reactivity of methyl iodide vs. ethyl iodide in acetonitrile, log (k_{MeI} / k_{EtI}) as a function of nucleophile, ③ enthalpy of solution measurements in acetonitrile-methanol mixtures, $\Delta_s H$ for tetralkylammonium salts containing *ortho*- and *para*-nitrobenzoate ion, and its constituent analysis, ④ measurements of the activation parameters for the reaction in acetonitrile-methanol mixtures,

$Nu^- + Et\text{-}I \rightarrow Nu\text{-}Et + I^-$, Nu⁻ ; *o*-nitrobenzoate and *p*-nitrobenzoate ion, and the quantitative analysis of $\Delta H^{\ddagger}$ *vs.* $\Delta S^{\ddagger}$ correlations.

Results and Discussion

Rate constants and activation parameters for the reaction of *p*-nitrobenzoate ion and of *o*-nitrobenzoate ion with ethyl iodide in acetonitrile (30℃) , and specific interaction enthalpy for relevant anion , $\Delta_t H_{SI}^{AN \rightarrow MeOH}$ are summarized in the Table .

Nucleophile	k	$\Delta H^{\ddagger}$	$\Delta S^{\ddagger}$	$\Delta_t H_{SI}^{AN \rightarrow MeOH}$
	10^{-2} dm^3 mol^{-1} s^{-1}	kJ mol^{-1}	J K^{-1} mol^{-1}	kJ mol^{-1}
para-Nitrobenzoate	1.07	68.0	-58.3	-28.0
ortho-Nitrobenzoate	0.608	73.2	-46.0	-31.0

The results indicate that the *ortho*-nitro group gives influences not only on a reaction rate and activation parameters but also on the solvation properties of the anion itself. Furthermore, the pattern of $\Delta H^{\ddagger}$ *vs.* $\Delta S^{\ddagger}$ correlation in acetonitrile-methanol mixtures is much varied by the change of the position of substituent from *para*- to *ortho*-position, and the quantitative discussion will be given on the physical origin of these effects, with emphasis being laid on the solute-solvent interaction at the transition state.

1. Y. Kondo *et. al.*, *J. Chem. Soc. Perkin 2*, 1990, 741.
2. Y. Kondo *et. al.*, *J. Chem. Soc. Perkin 2*, 1995, 1049.

HYDROPHOBIC EFFECT AS A POSSIBLE ORIGIN OF DISPERSION IN THE GRUNWALD–WINSTEIN RELATIONSHIP IN SOLVOLYTIC REACTIONS

Ken'ichi TAKEUCHI, Kenji UEDA, Takao OKAZAKI, Eiji SHIBA and Tomomi KINOSHITA

Department of Energy and Hydrocarbon Chemistry, Graduate School of Engineering, Kyoto University, Sakyo-ku, Kyoto 606-8501, Japan

The Grunwald–Winstein (GW) relationship has played an important role in diagnosis of the mechanisms of solvolytic reactions. In particular, the use of 1- and 2-adamantyl systems as the standard substrates of the solvent ionizing power (*Y*s) provided a methodology to estimate the contribution of nucleophilic solvent assistance and charge delocalization in the transition state of ionization.[1] These effects have been taken as origins of some dispersions in the GW relationship.

Recently, we proposed that the dispersions that are often observed in the solvolysis of highly crowded tertiary alkyl chlorides might be caused by the blend of steric hindrance to Brønsted-base type hydration to β-hydrogens and the hydrophobic effect in aqueous organic solvents.[2] However, it has also been proposed that the results would be explained in terms of concerted elimination reaction[3a] or decreased ion-pair return.[3b]

In the present work, we show that similar dispersions are observed in the GW plot using Y_{Br} for the solvolysis of 1-bromoadamantane derivatives having alkyl substituents on the bridgehead carbons other than C(1). The results indicate that the dispersions are better understood by the solvation effect on the alkyl moieties rather than the proposed[3] mechanistic changes. Similar dispersions have also been observed in the solvolysis of congested secondary alkyl mesylates or tosylates.

1. (a) Bentley, T. W.; Llewellyn, G. *Progr. Phys. Org. Chem.*, 1990, **17**, 121. (b) Kevill, D. N.; D'Souza, M. J., *J. Chem. Soc., Perkin Trans.* 2, **1995**, 973.
2. (a) Takeuchi, K.; Ohga, Y.; Ushino, T.; Takasuka, M., *J. Org. Chem.*, 1997, **62**, 4904. (b) Takeuchi, K., *Pure & Appl. Chem.*, 1998, **70**, 2025.
3. (a) Bentley, T. W.; Llewellyn, G.; Ryu, Z. H., *J. Org. Chem.*, 1998, **63**, 4654. (b) Kevill, D. N.; D'Souza, M. J., *Tetrahedron Lett.*, 1998, **39**, 3973.

STRUCTURE OPTIMIZATION OF GLYCINE IN AQUEOUS SOLUTION: TOWARD SOLUTION CHEMICAL REACTION ERGODOGRAPHY

Naoto OKUYAMA-YOSHIDA[1], Ken KATAOKA[1], Masataka NAGAOKA[2*] and Tokio YAMABE[3]

[1] Research Center, Daicel Chemical Industries, Ltd., 1239, Shinzaike, Aboshi-ku, Himeji, Hyogo 671-1283, Japan

[2] Graduate School of Human Informatics, Nagoya University, Nagoya 464-8601, Japan

[3] Institute for Fundamental Chemistry, 34-4, Takano-Nishihiraki-cho, Sakyo-ku, Kyoto 606-8103, Japan

In order to understand solution chemistry theoretically, we have developed the free energy gradient method (FEGM)[1] to obtain optimaized structures of stationary and transition states (SS and TS) on the free energy (FE) surface[1]. The force vector $\mathbf{F}_{FE}$ on the FE surface (FES) can be calculated as a long time average via the equilibrium molecular dynamics method;

$$\mathbf{F}_{FE}(\mathbf{q}) = -\frac{\partial G(\mathbf{q})}{\partial \mathbf{q}} = -\left\langle \frac{\partial V_{RS}(\mathbf{q})}{\partial \mathbf{q}} \right\rangle \quad (1)$$

where $G(\mathbf{q})$ and $\mathbf{q}$ are the FE and internal coordinate vector, respectively. In the FEGM, the structure is updated by the deviation

$$\Delta\mathbf{q}(I) \equiv C(I)\cdot\mathbf{F}_{FE}(I), \quad |\Delta\mathbf{q}(I)| = \left\{\sum_{i=1}^{3N}(x_i(I+1)-x_i(I))^2\right\}^{1/2} \quad (2)$$

where its amount at the I-th step is estimated presently in proportion to $\mathbf{F}_{FE}(I)$.

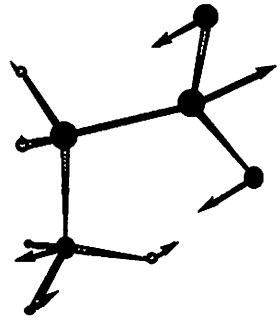

Fig. 1. Force vector (Step 0)

For an example, it was applied to the isomerization reaction of glycine in aqueous solution[2], demonstrating its feasible polar structure of zwitter-ionic form (ZW) in aqueous solution[2]. In Fig. 1, the force vector $\mathbf{F}_{FE}$ on the FES is shown at the ZW structure (step 0) in gas phase. In Fig. 2, the relative energy at each step is plotted at the same time for both the total molecular energy in gas phase and the present FE, *i.e.*, $G(\mathbf{q})$ in solution. The former increases monotonically, while the latter decreases monotonically, showing the efficiency of the FEGM to converge to the stable solvated structure in solution. In the talk, the relation between the dipole moment and $G(\mathbf{q})$ is also discussed in the viewpoint of structural relaxation.

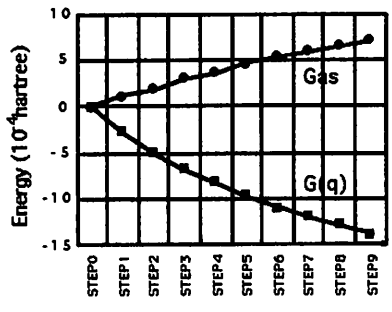

Fig. 2. Energy deviation on structure change along the force vector

1. Okuyama-Yoshida, N; Nagaoka, M.; Yamabe, T., *Int. J. Quantum Chem.*, 1998, **70**, 95.
2. (a) Okuyama-Yoshida, N; Nagaoka, M.; Yamabe, T., *J. Phys. Chem. A*, 1998, **102**, 285; (b) Nagaoka, M.; Okuyama-Yoshida, N.; Yamabe, T., *ibid.*, 1998, **102**, 8202.

EQUILIBRIUM AND NON-EQUILIBRIUM SOLVATION EFFECTS IN ORGANIC REACTIONS. THE DIELECTRIC CONTINUUM SOLVATION MODEL FOR ELECTRON TRANSFER PROCESSES.

Mikhael V. BASILEVSKY[1], Ivan V. ROSTOV[2] and Marshall D. NEWTON[2]
[1]Karpov Institute of Physical Chemistry, ul. Vorontsovo Pole 10, Moscow, 103064, Russia
[2]Department of Chemistry, Brookhaven National Laboratory, Upton, NY 11973, USA

Dielectric continuum models of solvation most efficiently combine a description of the solute electronic structure in terms of recent quantum-chemical methodologies and an explicit treatment of polar environment effects within the linear response approach of statistical mechanics. Advanced theories of this sort include non-equilibrium solvation effects described in terms of collective medium coordinates and can be applied to study kinetics and mechanisms of charge transfer chemical reactions proceeding in polar media. Electron transfer (ET) processes serve as a benchmark for this approach because there non-equilibrium solvation constitutes an essential part of the reaction mechanism. We have applied dielectric continuum models for calculations of solvent reorganization energies and coupling matrix elements, the two basic kinetic parameters of a ET process. It was shown that standard continuum theories fail to consistently describe both equilibrium and non-equilibrium solvation effects. A refined continuum model has been elaborated in which fast electronic and slow orientational polarisation variables are considered separately and are spatially resolved in the vicinity of a ET solute. This new theory has proved to be successful in adequately treating ET reactions.

1. Basilevsky, M.V., Chudinov, G.E., Rostov, I.V., Liu, Y.-P., Newton, M.D., *Theochem*, 1996, **371**, 191.
2. Basilevsky, M.V., Rostov, I.V., Newton, M.D., *Chem. Phys.*, 1998, **232**, 189.
3. Newton, M.D., Rostov, I.V., Basilevsky, M.V., *Chem. Phys.*, 1998, **232**, 201.
4. Basilevsky, M.V., Rostov, I.V., Newton, M.D., *Journ. Electroanal. Chem.*, 1998, **450**, 69.

Solvent Fluctuations and Viscosity-Dependent Rates of Solution Reactions in a Regime Indescribable by the Transition State Theory

Hitoshi Sumi
Institute of Materials Science, University of Tsukuba, Tsukuba, 305-8573 Japan

The standard theory on the rate of chemical reactions is the transition state theory (TST). However, the fundamental assumption of TST concerning rapid thermalization of fluctuations on the reactant-state potential is not satisfied in many reactions in solution.[1] They cover various solution reactions, extending from elementary reactions such as electron-, proton-, excitation- and atom-group-transfer reactions and isomerization reactions, to composite reactions such as enzymatic reactions mediated by biological supramolecules. Therefore, a more general expression of chemical reaction rates has been required, to cover such solution reactions.[1] It is one of the most fundamental subjects in chemistry, since study of solution reactions has been regarded as one of the most traditional and important in chemistry.

It is a priori assumed in TST that thermal fluctuations are sufficiently fast on the reactant-state potential. To be more exact, it is assumed that before reaction occurs, thermal equilibration has already been established on the reactant-state potential, which extends up to the saddle point for the transition state, because of fast thermal fluctuations. Under this assumption, the reactant population at the transition state is determined only by the free energy at the transition state. In this situation, the rate constant should not depend on how fast thermal equilibration is established on the reactant-state potential, being determined fluctuation-speed independent only by how fast reactants at the transition state change to products.

In solution reactions, solvent fluctuations play essential roles in thermalization on the reactant-state potential. The thermalization time becomes slow in viscous solvents, increasing usually in proportion to the solvent viscosity. In solution reactions mentioned earlier, the rate constant was observed to decrease with an increase in the viscosity. Therefore, such reactions are regarded as controlled by the slow speed of solvent fluctuations in a regime indescribable by TST.

Recently, Asano and his collaborators succeeded in covering both the TST and the non-TST regimes in a single reaction system with a viscosity change as wide as 10^8-fold under pressure, measuring the thermal Z/E isomerization of substituted azobenzenes and *N*-benzylideneanilines in viscous solvents.[2] Their data have disclosed not only the isomerization mechanism of these molecules in the non-TST regime but also manifestation of solvent fluctuations in the rate constant of solution reactions, keeping step with the development in theories.[2] Viscosity dependent rates have also been observed in many biological reactions. Such developments enabled us to understand their metabolic meaning in the non-TST regime.

1) Sumi, H., In *Electron Transfer: From Isolated Molecules to Biomolecules*, Part Two: Jortner, J; Bixon, M. Ed.; Wiley: New York, 1999; (*Adv. Chem. Phys.*, 107) pp 601 - 646.
2) Asano, T.; Sumi, H. *Chem. Phys. Lett.* 1998, *294*, 493, and references cited therein.

Kinetics in highly viscous solutions: Dynamic solvent effects in "slow" reactions

Tsutomu Asano
Department of Applied Chemistry, Faculty of Engineering, Oita University, 700 Dannoharu, Oita 870-1192, Japan

For most organic chemists who study thermal reactions in solution, reaction mechanism studied within the framework of the transition state theory (TST) looked satisfactory in most of the cases. In such studies, solute-solvent interactions are considered only in terms of solvation and desolvation in the initial and the transition state and, therefore, the events between the two states are not considered to be the subject of study. For complete understanding of solution reactions, however, it is indispensable to know the roles of solvent molecules in the activation step. To be more specific, whether the structural changes of the reactant are in concert with the solvent reorganizations must be a fundamental question to be answered. In order to obtain such information, we must realize the situation where the reaction rate is regulated by the rate of the solvent thermal fluctuations. In other words, we must study "dynamic" solvent effects. Since thermal fluctuations can be considered to be slowed down with increasing solvent viscosity η, the problem would be reduced to a study of the viscosity effects on the reaction rate. In fact, viscosity dependence has been reported for various isomerizations of molecules in their electronic excited states.[1] However, an agreement is yet to be reached on how to rationalize the observed results. It might be possible to shed light on the problem if we could study dynamic solvent effects in slow thermal reactions. Although several groups reported apparent viscosity dependence of thermal isomerization rates,[2-4] the reactions could be in the TST-valid viscosity region. In order to observe unequivocal dynamic solvent effects, we decided to undertake kinetic measurements in highly viscous solutions. As a measure to increase η, high pressure was used. By selecting liquids with branched structures, such as glycerol triacetate, viscosities higher than 10 Pa s (= 1×10^4 cP) could be easily realized at pressures of several hundred megapascals. As reactions, we selected thermal *Z*/*E*-type isomerizations in C=C, C=N, and N=N bonds in carbocyanine dyes,[5] benzaldehyde and hexafluoroacetone anils,[6-9] and in azobenzenes,[6,7] respectively. The half lives of these reactions were in milliseconds to seconds and the TST was expected to be valid at atmospheric pressure. Indeed, TST-expected pressure effects were observed at the beginning of pressurization. However, such effects were replaced by strong retardations at higher pressures and it was concluded that the reactions were brought into the TST-invalid conditions and dynamic solvent effects were observed. These effects appeared only at $\eta > 1$ Pa s casting doubts on the stochastic analyses in the previous reports.[2-4] Furthermore, from the plots of the observed rate constant against η, it could be concluded that the isoviscosity temperature effects stayed almost constant in the TST-valid region but it decreased rapidly with increasing η at the TST-invalid conditions. It is difficult to rationalize these results on the basis of a one-dimensional reaction-coordinate model where the chemical changes are assumed to take place in concert with the solvent thermal fluctuations. In such a model, the height of the energy barrier for the rate-determining step must be independent of the viscosity and, therefore, we must expect the same isoviscosity temperature effect at all of the viscosities. The decreasing energy barrier strongly suggests the validity of a two-dimensional reaction-coordinate model where the medium and the chemical coordinates are treated independently and the structural changes along the chemical coordinate are preceded by reorganizations of the solvation sphere.

1. For examples see, Drljaca, A.; Hubbard, C. D.; van Eldik, R.; Asano, T.; Basilevsky, M. V.; le Noble, W. J. *Chem. Rev.* **1998**, *98*, 2167. 2. Velsko, S. P.; Waldeck, D. H.; Fleming, G. R. *J. Chem. Phys.* **1983**, *78*, 249. 3. Hara, K.; Akimoto, S. *J. Phys. Chem.* **1991**, *95*, 5811. 4. Campbell, D. M.; Mackowiak, M.; Jonas, J. *J. Chem. Phys.* **1992**, *96*, 2717 and earlier papers cited therein. 5. Kim, J. C.; Ohga, Y.; Asano, T. *Chem. Lett.* **1999**, in press. 6. Asano, T.; Furuta, H.; Sumi, H. *J. Am. Chem. Soc.* **1994**, *116*, 5545. 7. Asano, T.; Cosstick, K.; Furuta, H.; Matsuo, K.; Sumi, H. *Bull. Chem. Soc. Jpn.* **1996**, *69*, 551. 8. Asano, T.; Matsuo, K.; Sumi, H. *Bull. Chem. Soc. Jpn.* **1997**, *70*, 239. 9. Ohga, Y.; Asano, T.; Karger, N.; Gross, T.; Lüdemann, H.-D. unpublished results.

Electrolyte Solutions for Technology - New Aspects and Approaches

J. BARTHEL*; E. CARL; H.-J. GORES, A. SCHMID

*Institute of Physical and Theoretical Chemistry, University Regensburg, 93040 Regensburg, Germany

Electrochemical technologies search for electrolyte solutions with optimized properties for the special tasks which they must fulfil in the investigated system. Chemical models of the electrolyte solution which take into account the long range forces, and short range forces stemming from the non-coulombic interactions in the solution, often permit the construction of suitable solutions on the drawing board and the representation of wanted properties over large ranges of electrolyte concentration, solvent composition and temperature[1,2,3]. A short presentation is given on the features of chemical model based calculations and their information on structure-property relationships.
Lithium battery electrolytes are chosen as an example of technological interest[3,4]. We report on families of methides, imides, chelatoborates and chelatophosphates. The common feature of their anions are

- charge delocalisation by large substituents entailing high conductivity despite large anion diameters,
- large electrochemical windows which can be controlled by suited substituents,
- high thermal stability in comparison to the commonly used Lewis acid-based anions (e.g. $LiPF_6$), caused by the covalent bonds,
- increasing anionic oxidation limits when electron withdrawing substituents are introduced.

The role of the solvent will be discussed.

References:

1. Barthel, J.; Krienke, H.; Kunz, W., *Physical Chemistry of Electrolyte Solutions - Modern Aspects*, Steinkopf, Darmstadt; Springer, New York 1998.
2. Barthel, J. et al., *Electrolyte Data Collection*, Vol. XII of DECHEMA Chemistry Data Series, ed. By G. Kreysa, DECHEMA, Frankfurt (11 vol., to be continued) 1992-1999.
3. Barthel, J.; Gores, H.J., in Mamantov, G.; Popov, A.I. (eds.), *Chemistry of Nonaqueous Solutions - Current Progress*, VCH, New York 1994, Ch. 1.
4. Barthel, J.; Gores, H.J., in Besenhard, J.O. (ed.) *Handbook of Battery Materials*, VCH, New York 1999, Ch.7.

Advanced Electrolyte for Electric Double Layer Capacitor

Y.Takamuku[1], H.Shimamoto[1], Y.Kobayashi[2] and K.Shiono[2]
[1] Capacitor Division, Matsushita Electronic Component Co., Ltd.
25 Nishinaka, Kowata, Uji City, Kyoto 611-8585, Japan
[2] Electronic & Optoelectronic Materials Intracorporation, Sanyo Chemical Industries. Ltd.
11-1 Ikkyo Nomoto-cho, Higashiyama-ku, Kyoto 605-0995, Japan

Electric double layer capacitors (EDLCs) are the electrochemical energy storage devices exhibiting capacitance between conventional capacitors and rechargeable batteries. They are generally prepared employing high surface (1000-2500m^2/g) activated carbon electrodes and non-aqueous electrolytes. Various studies about non-aqueous electrolytes have made because the withstand voltage and the inner resistance of EDLC are strongly related to the electrochemical decomposition voltage and the electric conductivity of the electrolyte respectively[1]. As a result, tetraethylammonium-tetrafluoroborate ($TEABF_4$) in propylenecarbonate (PC) is commonly used as the electrolyte.

In the recent year, in the case of the aluminum electrolytic capacitor using quaternary onium based salts in organic solvents, it is confirmed that quaternary onium hydroxides are formed at the surface of the cathode and the lead attached to the cathode when voltage is applied to the capacitor. Quaternary onium hydroxides degrade a sealing material and electrolyte solution leaks outside the capacitor because it shows strong base as well as potassium hydroxide (KOH)[2]. Therefore a new improved cation (1,2,3,4-tetramethylinidazorinium:TMI) of the electrolyte was developed and has applied to aluminum electrolytic capacitors[3]. However it is difficult to apply TMI cation to EDLC, because electrochemical decomposition voltage of TMI cation is lower than a quaternary onium cation.

We investigate the electrochemical decomposition voltage with cyclic-voltammetry and the electric conductivity of 1-ethyl-3-methylimidazorium tetrafluoroborate ($EMIBF_4$) in PC. The pH changes is determined when sodium hydroxide (NaOH) is added to 1-ethyl-3-methylimidazorium chloride (EMICl) and tetraethylammonium chloride (TEACl) in aqueous solution, in order to obtain the degree of dissociation of base (α) of EMIOH and TEAOH. Furthermore, ^{1}H-NMR spectrogram of the $EMIBF_4$ in PC including NaOH is observed to define the associated structure of EMIOH. As a result of these examinations, it is revealed that $EMIBF_4$ in PC (0.65mol/l) exhibits high electric conductivity (13mS/cm) and high electrochemical decomposition voltage. A pH change of the EMICl solution is smaller than that of TEACl solution. Two new peaks attributed to the associated EMIOH are observed in ^{1}H-NMR spectrogram of the $EMIBF_4$ in PC including NaOH.

1. M. Ue, M. Takeda, M. Takehara, and S. Mori, *Electrochem. Soc. Proc.*, 1996, **96-25**, 289.
2. *Standard of Electronic Industries Association of Japan*, EIAJ RC-2372.
3. K. Shiono, Y. Nitta, *PCT International Publication Number*, WO95/15572.

DROP COALESCENCE BEHAVIOR IN LIQUID- LIQUID EXTRACTION

Takahiko BAN, Fumio KAWAIZUMI, Susumu NII, Katsuroku TAKAHASHI
Department of Chemical Engineering, Nagoya University
Furo-cho, Chikusa-ku, Nagoya 464-8603, Japan

Drop coalescence plays an important role in the liquid extraction process. Numerous workers have reported the coalescence time. However, no clear relationship has been found between the coalescence time and several controlling factors as well as effects of impurities adsorbed at the interface. In the present study toluene (dispersed phase) is constantly fed to the nozzles so as to have a fresh drop interface of toluene in water. The experimental apparatus is shown in Fig. 1. A video camera was used and a time course of coalescence was monitored for toluene droplets formed at the top of adjacent nozzles in water. Several parameters which control the coalescence have been investigated, such as concentration of acetone added to toluene, flow rate of continuous phase, and time for attaining contact of the droplets.

Figure. 2 is a plot of average coalescence times against acetone concentration under three different conditions. Continuous phase is fed upward into the coalescence cell at flow rate 0.29 cm/s. Average coalescence times, $t_{c,av}$, decrease with acetone concentration when the acetone is transferred from dispersed phase toward continuous phase, while they increase with the time for attaining contact, t_0. When the acetone concentration is high, oscillation of droplets was observed.

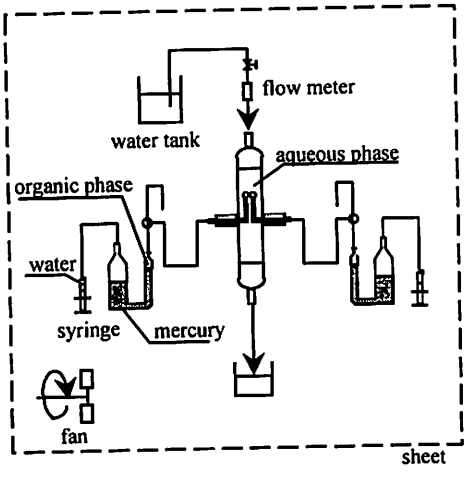

Fig. 1 Schematic diagram of experimental apparatus

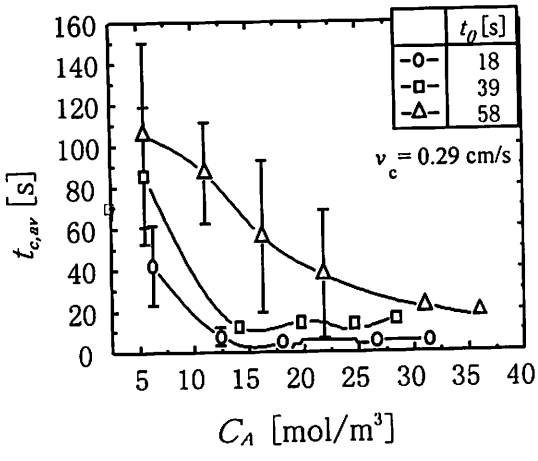

Fig. 2 Effect of acetone concentration on average coalescence time for different t_0

PLASMA PRODUCTS AND SOLUTION CHEMISTRY

T. HAMAMOTO
Department of Blood Products Research, KAKETSUKEN, 1-6-1 Okubo, Kumamoto, 860-8568, Japan

The application areas for plasma products derived from plasma proteins are many indeed. They span from the treatment of severe traumas, to coagulation disorders, to infections following bone marrow transplantations, as well as auto-immune diseases and prophylactic treatment to prevent illnesses due to infections or special immune deficiencies. Specialists in many medical fields depend on the therapeutic advantages of plasma products. In production facilities with state-of-the art technologies for refinement and manufacturing, products are made for the following area.s:

1. Coagulation: Coagulation factor VIII and IX products are essential for the treatment of hemophilia, a rare hereditary disease which affects approximately 300,000 people worldwide. Factor VIII/von Willebrand factor complex, or von Willebrand factor products are currently also prescribed for von Willebrand's disease. To overcome problems caused by inhibitors in hemophilia treatment, activated factor VII products are in high demand and are nowdeveloping. Fibrinogen product is also essential for the treatment of patients with coagulation disorders.

2. Wound healing: Tissue glue (fibrin sealant) is a revolutionary product that assists in the recovery from surgical treatment. Factor XIII product also helps in the recovery from surgical treatment. These products for wound healing are used in many areas of surgery; their function is to stimulate tissue healing and to check bleeding.

3. Anticoagulation: Antithrombin III and activated protein C are used for the treatment of disseminated intravascular coagulation (DIC) and complications due to hereditary or acquired deficiencies.

4. Immune globulins: Immune globulins help to treat hereditary and acquired immune deficiency disorders. They are also applied in order to close gaps within the body's own defense system.

5. Plasma substitute: Albumin or haptoglobin product is used in emergency and first-aid cases, for treating shock conditions and severe burns, and during operations and for controlling blood circulation disorders.

6. Other preparations: C1 inhibitor is used for handling hereditary angioneurotic edema. Alpha 1 protease inhibitor is used to help treat patients suffering from alpha 1 protease inhibitor deficiency, a genetic disorder that can lead to emphysema.

The safety of these plasma products is considered an on-going task requiring continuous adaptation to the latest technical advances and changes in scientific knowledge regarding the nature of plasma related viruses. Furthermore, product handiness is also considered an on-going task requiring continuous improvement.

The talk will focus on viral inactivation technologies and a stable aqueous pharmaceutical formulation comprising a plasma protein, which are a point of contact between plasma products and solution chemistry.

CHEMISTRY FOR MEASURING CELL VIABILITY

Kazumi SASAMOTO[1], Munetaka ISHIYAMA[2], Masanobu SHIGA[2], Hideyuki TOMINAGA[1] and Keiyu UENO[1]

1 Dojindo Laboratories, Tabaru 2025-5, Mashiki-machi, Kumamoto 861-2202, Japan
2 Dojindo Molecular Technologies, 211 Perry Parkway, Gaithersburg, MD 20877, USA

Cell viability assay has been gaining much attention as an alternative to using animals. It is useful, for example, in screening a large number of chemicals for their cytotoxicity for various cells. It has also been used in cancer chemotherapy to select an anti-cancer drug as well as its dose. Measuring the uptake of [^{3}H]thymidine is a common method for assessing cell viability although it requires special facility and produces radioactive waste.[1] As non-radioactive approaches, dyes such as neutral red[2], crystal violet[3] and tetrazolium salts[4] have been applied to colorimetric cell viability assays, where they stain cells at different sites. MTT has been among the most commonly used dye that produces an intense color due to the formazan formation upon cellular reduction by NADH. MTT, however, suffers from a disadvantage that the formazan is extremely water insoluble, which seems to limit the application. The formazan often forms deposits that damage cells and therefore should be solubilized prior to the absorbance measurement. We reported a tetrazolium salt, WST-1[5], that produces a highly water soluble formazan upon cellular reduction, which has found increasing applications for use in colorimetric cell viability assays. In the continuing effort, we have recently synthesized a similar but more sensitive, particularly at neutral pH, water-soluble tetrazolium salt, WST-8[6,7]. In this seminar, the chemistry to measure cell viability using these water soluble tetrazolium sals and the application to drug sensitivity tests will be discussed.

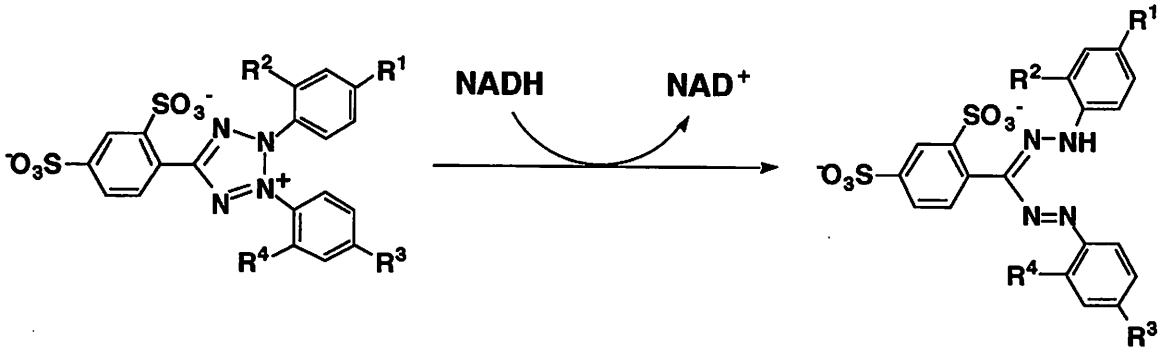

Scheme Reduction of WST compounds by cellular NADH

References

1 J. M. Webb, J. B. Brouwer and E. A. Brouwer, *Toxicol. Appl. Phammacol.*, 1967, **10**, 300.
2 E. Borenfreund and J. A. Puerner, *Toxicol. Lett.*, 1985, **24**, 119.
3 K. Saotome, H. Morita and M. Umeda, *Toxic. In Vitro*, 1989, **3**, 317.
4 T. Mosmann, *J. Immunol. Methods*, 1983, **65**, 55.
5 M. Ishiyama, M. Shiga, K. Sasamoto and M. Mizoguchi, *Chem. Pharm. Bull.*, 1993, **41**, 1118.
6 M. Ishiyama, Y. Miyazono, K. Sasamoto, Y. Ohkura and K. Ueno, *Talanta*, 1997, **44**, 1299.
7 H. Tominaga, M. Ishiyama, F. Ohseto, K. Sasamoto, T. Hamamoto, K. Suzuki and M. Watanabe, *Anal. Commun.*, 1999, **36**, 47.

Characterization of Water in a Variety of Chemical and Biological Milieux: An NMR Approach

Yoji Arata
Water Research Institute
Sengen 2-1-6, Tsukuba 305-0047, Japan
Arata@wri.co.jp

In this talk I will describe a series of water-related NMR studies, which we have been developing in my laboratory. Emphasis will be put on the analyses of 1) the high resolution NMR data obtained by pulsed-field gradient technique on diffusion of water in simple and complicated systems such as protein solutions, and 2) NMR microimaging of the freeze tolerance of flower buds. Relevance of the results obtained to some of the problems of food-chemical interests will also be discussed.

References

Price, W.S., and Arata, Y. (1996) The manipulation of water relaxation and water suppression in biological systems using the Water-PRESS pulse sequence. *J. Magn. Reson.* B112, 190-192.

Price, W.S., Nara, M., and Arata, Y. (1997) A pulsed field gradient NMR study of the aggregation and hydration of parvalbumin. *Biophys. Chem.* 65, 179-187.

Price, W.S., Hayamizu, K., and Arata, Y. (1997) Optimization of the Water-PRESS pulse sequence and its integration into pulse sequences for studying biological macromolecules. *J. Magn. Reson.* 126, 256-265.

Price, W.S., Ide, H., Arata, Y., and Ishikawa, M. (1997) Visualization of freezing behaviours in flower bud tissues of cold hardy *Rhododendron japonicum* by nuclear magnetic resonance micro-imaging. *Aust. J. Plant Physiol.* 24, 599-605.

Ishikawa, M., Price, W.S., Ide, H., and Arata, Y. (1997) Visualization of freezing behaviors in leaf and flower buds of Full-Moon Maple by nuclear magnetic resonance microscopy. *Plant Physiol.* 115, 1515-1524.

Price, W.S., Ide, H., Ishikawa, M., and Arata, Y. (1997) Intensity changes in ^{1}H-NMR micro-images of plant materials exposed to subfreezing temperatures. *Bioimages.* 5, 91-99.

Ishikawa, M., Ide, H., Price, W.S. and Arata, Y. (1998) NMR micro-imaging techniques for the study of freezing behaviours in plant tissues. *Trends in Anal. Biosci.* In press.

Price, W.S., Tsuchiya, F., Suzuki, C. and Arata, Y. (1999) Characterization of the solution properties of *pichia farina* killer toxin using PGSE NMR diffusion measurements. *J. Biomol. NMR.* 13, 113-117.

Price, W.S., Ide, H. and Arata Y. (1999) Self-diffusion of supercooled water to 238 K using PGSE NMR diffusion measurements. *J. Phys. Chem. A.* 103, 448-450.

Price, W.S., Tsuchiya, F. and Arata, Y. (1998) Protein aggregation studies using PFG NMR diffusion measurements. In: *Advances of Magnetic Resonance in Food Science,* (G. A. Webb, Ed.), Royal Society of Chemistry. In press.

STRUCTURE AND DYNAMICS IN SUPERCRITICAL WATER SOLUTIONS

Peter J. Rossky

Department of Chemistry and Biochemistry, University of Texas at Austin, Austin, Texas 78712-1167 USA

For chemical reactions in ambient aqueous solutions, many decades of research has led to the accumulation of a considerable body of knowledge that provides a basis for both qualitative and quantitative "intuition" regarding the rates and outcome of chemical reactions. Due to the relatively more recent emphasis on supercritical conditions, combined with the difficulty of experimental studies under these extremes, corresponding principles are less well developed for these conditions. Hence, theory, modeling, and simulation are even more important tools in this regime. In this presentation, the results of molecular level simulation studies of solutions in supercritical water will be presented and the themes arising in the interpretation of the results will be delineated. Emphasis will be placed on elucidating the solvation structure of ionic solutes and developing the relationship between this structure and corresponding solution properties. Properties to be considered include solvation thermodynamics, chemical equilibrium, reaction activation free energies, and transport coefficients. The important issue of the applicability of simplified representations of solvation in these various contexts will also be discussed.

Key References

L.W. Flanagin, P.B. Balbuena, K.P. Johnston, and P.J. Rossky, "Temperature and Density Effects on an S_N2 Reaction in Supercritical Water," *J. Phys. Chem.* 1995, **99**, 5196.

P.B. Balbuena, K.P. Johnston, and P.J. Rossky, "Molecular Dynamics Simulation of Electrolyte Solutions in Ambient and Supercritical Water: 2. Relative Acidity of HCl," *J. Phys. Chem.* 1996, **100**, 2716.

L.W. Flanagin, P.B. Balbuena, K.P. Johnston and P.J. Rossky, "Ion Solvation in Supercritical Water Based on an Adsorption Analogy", *J. Phys. Chem.* 1997, **101**, 7998.

P. B. Balbuena, K. P. Johnston, P. J. Rossky, and J-K. Hyun, "Aqueous Ion Transport Properties and Water Reorientation Dynamics from Ambient to Supercritical Conditions", *J. Phys. Chem.* 1998, **102**, 3806.

Charge Polarization Effect on Molecular Processes in Solution

Shigeki Kato
Department of Chemistry, Graduate School of Science, Kyoto University, Sakyo-ku, Kyoto, 606-8502, JAPAN

Electronic polarization in solute and solvent molecules has been recognized to play an important role in dynamical processes of molecules in solution. Several theoretical methods have been proposed to incorporate the electronic polarization effect in molecular modeling for simulation studies. Recently we proposed a method, referred to the charge response kernel (CRK), representing the response of atomic charges to the electrostatic potential acting on each atomic site. The CRK is rigorously defined within the framework of *ab initio* molecular orbital theory and naturally takes account of the nonlocal redistribution of atomic charges as the response to the electrostatic potentials acting on the different sites, *via* the off-diagonal elements of CRK, which is important for polyatomic solvent molecules.

We carried out molecular dynamics (MD) simulation calculations with the intermolecular potentials incorporating the charge polarization effect through the CRK for elucidating the anomalously diffusion constant of pyrazinyl radial in methanol compared to pyrazine and the fast vibrational relaxation of azide ion in aqueous solution. It was found that the experimentally observed slow diffusion of pyrazinyl radical could not be reproduced without taking account of the electronic polarization of solute and solvent molecules and the reductions of diffusion constants for various photochemically generated radicals were well correlated to the lowest eigenvalues of CRKs. The fast vibrational relaxation rate for the asymmetric stretching vibration of azide ion was found to be attributed to the charge polarization in the solute induced by the vibration and the solute anharmonic vibrational effect.

We also studied the effect of solvent electronic polarization on the electronic transitions of solute molecules in solution. For this purpose, we developed a charge polarizable reference interaction site model self-consistent field (RISM-SCF) using the solvent CRKs. The excitation energy for $n\pi^*$ transition of acetone in CH_3CN, $CHCl_3$, CCl_4 and CS_2 solvents were calculated and the solvent electronic polarization effect on the solvation shifts were examined. The solvatochromic shifts in the transitions to low-lying excited states of pyridine were also evaluated in the same solvents.

APPLICATION OF THE RISM THEORY TO ANALYSIS ON CONFORMATIONAL STABILITY OF PEPTIDE IN SOLVENT

Masahiro Kinoshita[1], Yuko Okamoto[2], and Fumio Hirata[2]
[1]Institute of Advanced Energy, Kyoto University, Uji, Kyoto 611-0011, Japan
[2]Institute for Molecular Science, Okazaki, Aichi 444-8585, Japan

The first-principle prediction of tertiary structures (conformations) of proteins in solvents from their primary structures is one of the most challenging problems. The usual Molecular Dynamics (MD) and Monte Carlo (MC) simulations, in which a protein molecule and a number of solvent molecules are simultaneously treated, suffer from extremely heavy computational load. A simulation can be performed only for a very short period, and the final conformation obtained relies heavily on the initial one chosen. A problem of these simulations is that they are unable to sample the configurational phase space. To overcome this difficulty, we have been considering a new methodology. In ours, the MC technique is applied only to the protein molecule, and the solvent effects are incorporated by the reference interaction site model (RISM) theory, a statistical-mechanical approach for molecular fluids, with a robust and very efficient algorithm for solving the RISM equations. The conformational sampling is performed by the simulated annealing technique, and structure of the solvent that is in equilibrium with the protein molecule in each conformation sampled is efficiently calculated by the RISM theory. The target function is the total energy defined as the sum of the conformational energy and the solvation free energy. The conformation that gives the target function the minimum value is chosen from among many conformations sampled.

Our methodology has successfully been illustrated for Met-enkephalin (Tyr-Gly-Gly-Phe-Met) and the C-peptide fragment of ribonuclease A (Lys-Glu-Thr-Ala-Ala-Ala-Lys-Phe-Leu-Arg-Gln-His-Met) in the extended simple point charge (SPC/E) model water. In water the solvation free energy varies greatly from conformation to conformation, while in a simple fluid it remains roughly constant against conformational changes. In water most of the conformations with larger solvation free energies are strongly rejected and the number of probable conformations is drastically reduced, which is suggestive that stable conformations are reached far more rapidly than in gas phase and in the simple fluid. This result is important in the following two respects: water plays essential roles in stabilizing particular conformations of peptides; and in water the number of conformations to be sampled with our methodology is drastically reduced, which would remove computational bottlenecks expected for much larger polypeptides or proteins. The stable conformations obtained in water are quite different from those in gas phase and in the simple fluid.

DENSITY FUNCTIONAL THEORY OF LIQUIDS

– Some Extensions and Applications –

Toyonori Munakata, Department of Applied Mathematics and Physics,

Kyoto University, Kyoto 606, Japan

The density functional theory(DFT) of nonuniform liquids plays an ipmortant role in classical many-body theory because of its simplicity and physical clarity. The theory has contributed a great deal not only to studies on liquid-gas and liquid-solid transformations , including interfacial and nucleation phenomena, but also to elucidation of structures of nonuniform liquids, which is decisive to chemical reaction in solutions.

In this paper we present some extensions of the DFT together with applications thereof to simple and molecular liquids. More concretely, we consider

1) a dynamic extension of DFT so that one can study time-dependent behavior of density field and related dynamical phenomena,[1]

2) liquids composed of deformable molecules by removing constraints of fixed bond-length usually imposed by the RISM theory,[2]

3) fully three-body extension of the HNC theory for static structures of liquids.[3]

As applications we would like to discuss

1) viscosity of simple and molecular liquids,

2) intramolecular correlation and thermal expansion of molecules

3) three-body correlations and bridge function for simple liquids.

(1) Munakata, T.; Phys. Rev. E,1994 **50**, 2347.

(2) Yoshida, S, Hirata, F and Munakata, M; Phys.Rev. E 1996, **54**,1763, 3687.

(3) Munakata, T, Kinoshita, M and Hirata, F; in preparation.

PHASE TRANSITIONS IN ELECTROLYTE SOLUTIONS

G. N. Patey, P. J. Camp and J. C. Shelley
Department of Chemistry, University of British Columbia, Vancouver, British Columbia, Canada V6T 1Z1

If the dielectric constant of the solvent is sufficiently low, ionic solutions may undergo demixing transitions which result in coexisting liquid phases of different ionic concentration. However, despite intense experimental[1] and theoretical[2] study, the critical behavior of these systems is still an unresolved problem. The most recent experiments[1] report exponents which appear to vary from Ising towards mean field as the dielectric constant of the solvent is reduced. We have used Monte Carlo simulations to investigate these transitions at both primitive model (continuum solvent) and molecular solvent levels.

Monte Carlo simulations in the NPT ensemble are used to determine the temperature and pressure (density) dependence of ion association in the restricted primitive model (RPM). It is shown that at temperatures below the critical temperature, T_c, the vapor consists almost exclusively of strongly-bound ion pairs at or near contact. Significant ion-pair dissociation begins at temperatures very near T_c. This, together with the fact that the coexistence curve of charged dumbbells essentially coincides with that of the RPM[3], raises the possibility that compositional fluctuations between strongly-bound and free ions influence the critical behavior. 1:2 and 1:3 primitive model electrolytes are also considered, and ion association into neutral species prior to condensation emerges as a common trend.

Grand canonical Monte Carlo calculations are used to investigate the demixing transition in model ionic solutions where the solvent is explicitly included. Charged hard sphere ions in hard sphere, dipolar hard sphere and quadrupolar hard sphere solvents are considered and the results are compared with the primitive model. For all solvents considered, it is found[4] that the demixing transition is in the same general region of the phase diagram and is roughly described by liquid-vapor equilibrium in the primitive model. However, details such as the precise location of the critical point and the width of the unstable region depend upon the exact nature of the solvent.

1. M. Kleemeier *et al.*, *J. Chem. Phys.*, 1999, 110, 3085, and references therein.
2. D. M. Zuckerman, M. E. Fisher, and B. P. Lee, *Phys. Rev. E*, 1997, 56, 6569, and references therein.
3. J. C. Shelley and G. N. Patey, *J. Chem. Phys.*, 1995, 103, 8299.
4. J.C. Shelley and G.N. Patey, *J. Chem. Phys.*, 1999, 110, 1633.

THE MEAN SPHERICAL MODEL: EXTENSIONS AND APPLICATIONS

Lesser Blum[1]
[1]Department of Physics, University of Puerto Rico, P.O.Box 23343, Rio Piedras, Puerto Rico 00931

The general closure of the Ornstein Zernike (OZ) equation in which the direct correlation function is written as a sum of exponentials is known as the generalized Yukawa closure. The analytical solution of this problem is given in terms (screening or scaling) parameter matrix $\mathbf{\Gamma}$. The thermodynamic properties and correlation functions can be expressed in terms of this matrix. It has been shown that [1] all of these results can be obtained from a simple variational principle

$$\frac{\partial \Delta A}{\partial \mathbf{\Gamma}} = 0$$

Free energy models ΔA can be constructed for rather complex systems, in principle. The simplest case is the MSA for electrolytes, in which this variational method produces a theory that satisfies the Stillinger-Lovett sum rules, the perfect screening theorems, the low density, low coupling Debye-Hueckel limit, the high density high coupling Onsager limits, and more recently the low density-high complete binding limits. Applications to electrolytes[2], polyelectrolytes[3], water[4] and nonspherical ions[5] will be discussed.

References

[1] Blum, L. and Rosenfeld, Y., J.Stat.Phys. (J.K.Percus Festschrift), (1991),**63** 1177.

[2] Simonin, J.P., Bernard, O. and Blum, L., J. Phys. Chem. (1998),**102B**, 4411.

[3] Bernard, O. and Blum, L., Proceedings of the International Conference on Strongly Coupled Plasmas, Kalman, G. , Rommel, M. and A. Budaev, A., editors, Plenum (1998),415.

[4] Blum, L., Vericat, F. and Degreve, L., Physica (1999),**A265**,396.

[5] Velazquez, E.S. and Blum, L., J.Chem. Phys. (1999).

Molecular Processes in Solvation Dynamics

Fumio Hirata
Institute for Molecular Science, Okazaki, Aichi 444-8585, Japan

Solvation dynamics induced by sudden changes in the electronic state of a solute molecule has attracted match attention for the past decade in connection with the ultrafast laser spectroscopy. Theoretical investigations have been made to clarify the molecular processes in the dynamics essentially from a view point of the response of charge density of solvent to electrostatic fields of solutes.[1] The process is primarily related to the rotational motion of solvent molecules, since such motion gives rise to large fluctuation in charge density.[2] There is another type of motion which can play important role in solvation dynamics: the translational motion of solvent molecules, or the number-density fluctuation. The slow component which has been observed in the time-resolved hole burning spectroscopy by Nishiyama and Okada may be due to the number-density fluctuation as has been conjectured by themselves.[3] In fact, in many cases, the rotational and translational motions are coupled together to make contributions to solvation dynamics. In the present paper, I take ion dynamics in water invesitigated by the combined RISM and generalized Langevin theories as an example of such coupling between the rotational and translation motions.[4]

As has been well regarded, the drag force exerted on the alkali-halide ions decreases with increasing ionic radii as opposed to the prediction of the Stokes law. Further increase in ion size turns the behavior into monotonic increase in harmony with the Stokes law. The drag force is realized as the response of solvent on ion displacement, which can be classified essentially into two major contributions: rotational and translational motions of solvent. However, as will be clarified in the lecture, there is non-negligible coupling between those two contributions. The coupling becomes large, and some pecuriority is observed for Li^+ when water used as solvent.[5,6] Physical origin of the coupling and the pecurior behavior will be discussed in the lecture.

1. M. Maroncelli and G. R. Fleming, *J. Chem. Phys.*, 1991, **94**, 2084.
2. H. L. Friedman, F. O. Raineri, F. Hirata, and B-C Perng, *J. Stat. Phys.*, 1995, **78**, 239.
3. K. Nishiyama and T. Okada, *J. Phys., Chem.*, 1997, **A101**, 5729.
4. S. Chong and F. Hirata, *J. Chem. Phys.*, 1998, **108**, 7339.
5. S. Chong and F. Hirata, *J. Chem. Phys.*, submitted.
6. S. Koneshan, J. C. Rasaiah, R. M. Lynden-Bell, and S. H. Lee, *J. Phys. Chem.*, 1998, **B102**, 4193.

MOLECULAR DYNAMICS IN LIQUIDS PROBED WITH TWO-DIMENSIONAL OPTICAL SPECTROSCOPY

K. Duppen and T. Steffen
Department of Chemical Physics, University of Groningen, Nijenborgh 4, 9747 AG, Groningen, The Netherlands

In recent years, a number of two-dimensional nonlinear spectroscopies were employed to obtain both structural and dynamic information on liquids and solutions. These experiments with two (or more) time and/or frequency variables depend on high-order nonlinearities. Such methods provide considerable more information than conventional, one-dimensional techniques. This state of affair in optics at the moment resembles that of the field of NMR about 30 years ago, when multi-dimensional techniques were under development, there.

Two-dimensional vibrational spectroscopy has, so far, been dominated by time-domain Raman techniques. Intermolecular motion in liquids, which is the subject of the paper presented here, was investigated experimentally by fifth-order temporally two-dimensional (2D) Raman scattering[1-3]. In this technique a sequence of five nonresonant laser pulses is applied to the sample. Thereby, the structural dynamics is probed on a microscopic level. Due to the fact that two independently variable delay times are involved, the effects of homogeneous (local) and inhomogeneous (global) processes on the optical response can be separated. This was the original reason to develop the two-dimensional methods[4,5].

Recently, it was realized that these experiments offer more information than originally anticipated. Coupling between different modes in the liquid can be probed, which in principle also provides insight in the dynamics of the local structure in a liquid or solution. For high frequency intramolecular modes this coupling gives rise to cross peaks in the 2D-Fourier transform of the time-domain data, similar to those observed in 2D-NMR. For the overdamped intermolecular motions in liquids such cross peaks are not so clearly visible, but yet the coupling is important in explaning the obtained experimental results.

The experimentally observed 2D Raman signals (for instance for CS_2 and benzene) show a pronounced asymmetry along the two independently variable delay times T_1 and T_2. The signal along the first delay time is governed by slow diffusive motion, while ultrafast (subpicosecond) inertial motion is observed along the second delay time. This interplay of diffusion and inertial motion cannot be understood when the modes propagate independently. When mode coupling due to anharmonicities is taken into account, this hardly improves the description of the experimental results. However, mode coupling by the electronic polarizability provides a much better explanation of the two-dimensional Raman response[6-7].

Fifth-order two-dimensional Raman scattering is a complicated technique, which is still in its infancy. Therefore, it is hard to judge its value in the long run. Surprises in the interpretation of the experimental results cannot be excluded. However, considering how valuable 2D-NMR has proved to be, it seems worthwhile to explore these promising new 2D-optical methods further.

1. Tominaga, K.; Yoshihara, K., *Phys. Rev. Lett.*, 1995, **74**, 3061.
2. Steffen, T.; Duppen, K., *Phys. Rev. Lett.*, 1996, **76**, 1224.
3. Tokmakoff, A.; Fleming, G.R., *J. Chem. Phys.*, 1997, **106**, 2569.
4. Tanimura, Y.; Mukamel, S., *J. Chem. Phys.*, 1993, **99**, 9496.
5. Steffen, T.; Fourkas, J.T., Duppen, K., *J. Chem. Phys.*, 1996, **105**, 7364.
6. Tokmakoff, A.; Lang, M.J.; Jordanides, X.J.; Fleming, G.R., *Chem. Phys.*, 1998, **233**, 231.
7. Steffen, T.; Duppen, K., *Chem. Phys. Lett.*, 1998, **290**, 229.

A ROLE OF SOLVENT IN VIBRATIONAL ENERGY RELAXATION OF METALLOPORPHYRINS

Yasuhisa MIZUTANI and Teizo KITAGAWA
Institute for Molecular Science, Okazaki National Research Institutes, Okazaki, 444-8585, Japan

A role of solvent in vibrational energy relaxation of metalloporphyrins was studied by picosecond time-resolved resonance Raman spectroscopy. The formation of vibrationally excited iron(III) *meso*-tetra(4-sulfonatephenyl)porphyrin via internal conversion from the S_1 state to the S_0 state and its subsequent vibrational energy relaxation was monitored by picosecond anti-Stokes resonance Raman intensities. We measured decays of anti-Stokes ν_4 band of the porphyrin in water and in mixed solvents composed of methanol and benzene, to study a dependence of the decay rate on the thermal conductivity of the solvents (Fig. 1). In water solution, the anti-Stokes ν_4 band showed a single exponential decay, of which time constant is 1.9±0.4 ps. In contrast, the band showed an additional slow decay phase in the mixed solvents. The contribution of the slow phase increased when the volume fraction of benzene increased while the behavior of the fast phase was almost independent of the solvent. Therefore we ascribed the fast and slow phases to the process in which the solute-solvent energy transfer is rate-limiting and the process in which solvent-solvent energy transfer is rate-limiting, respectively. In order to verify this assignment, we calculated the solvent temperature in classical thermal diffusion model. The model qualitatively explained the solvent dependence of the anti-Stokes ν_4 decay. A role of solvent in vibrational energy relaxation will be discussed by comparison of the observed data and the model calculations.

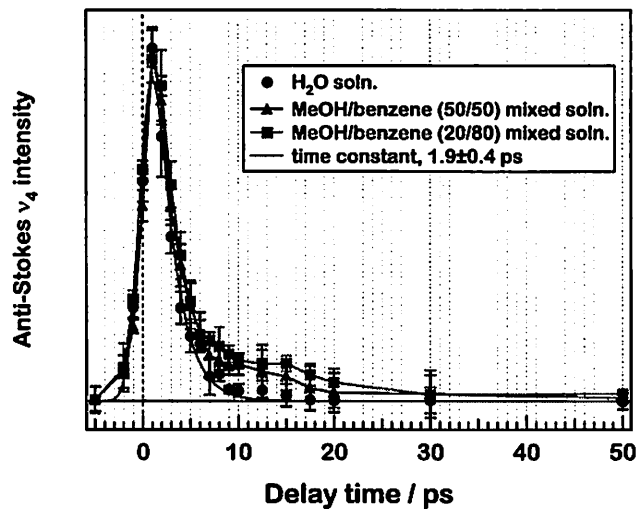

Figure 1. Temporal changes of the Raman intensity of anti-Stokes ν_4 band of iron(III) meso-tetra(4-sulfonatephenyl)porphyrin in water (circles) and in mixed solvents composed of methanol and benzene, 50/50 (triangles) and 20/80 (squares) in volume percent.

FAST ELECTRONIC ENERGY DISSIPATION IN SOLUTION

Masahide TERAZIMA,Toshiya OKAZAKI, Noboru HIROTA

Department of Chemistry, Graduate School of Science, Kyoto University, Kyoto, 606-8502, Japan

mterazima@kuchem.kyoto-u.ac.jp

When excited states relax in solution, most of the energy eventually goes into the translational freedom of the matrix as the thermal energy. The thermal energy affects various molecular dynamics. Although the understanding the initial step of the thermalization processes is important in solution chemistry, it has not yet been established. So far the thermalization in a fast time scale has been studied mainly from a point of view of the energy departure; i.e., the energy loss from the vibrational freedom, by monitoring the depopulational rate of vibrational states. Usually, the vibrational relaxation rate of 10~100 ps were reported using vibrational spectroscopy.[1] On the other hand, researches from a direct temperature detection of the solvent molecules are very limited because of the rather slow temporal responses of the thermal detection methods. In an effort to understand the thermalization from a point of view of the translational energy of the solvents, we recently conducted the transient grating and the transient lens experiments and succeeded in detecting a very fast temperature rise for the first time.[2] The result showed that the temperature rises less than 3 ps in water.

Here, I report fast thermalization processes with a fast time resolution in organic solvents from two novel approaches.[3] First, photophysical and thermalization processes after photoexcitation of 2-(2'-hydroxy-5'-methylphenyl)benzotriazole and 2-hydroxybenzophenone in various solvents were investigated by the transient grating method. From the time profiles of the population grating signals, the populational dynamics in ~300 fs time scale of these molecules are revealed. The thermalization rates of these molecules were measured by the acoustic peak delay method of the TG signal. The results show that in the early step of the thermalization, there is a very fast cooling process (less than a few ps) which is due to the energy transfer from the photoexcited solute to (several) effectively coupled solvent molecule(s), and then the heated solvent molecule becomes cool by the thermal diffusion to the bulk solvents. The thermalization processes depend on both of the solute and solvent properties. The time development of the temperature calculated based on this thermalization model explains the experimental observations.

Second, the thermalization process was also investigated by using a molecular heater-molecular thermometer integrated system. We used azulene and coumarin 151 (C151) as a molecular heater and a molecular thermometer, respectively, and combined them by a methylene chain. The heat flow after photoexcitation of azulene was detected via the hot band absorption of the thermometer (C151). The observed thermalization was described well by the energy transfer from the solute to solvent and the thermal diffusion among the outer solvents. The rate was faster than the reported vibrational relaxation rate previously. An attempt to achieve the high temporally and spatially resolved thermal energy study is reported.

References

1. A.Seilmeier, W.Kaiser in "Ultrashort laser pulses and applications", ed. by W.Kaiser, Springer, 1988, NewYork.

2. M.Terazima, *J.Chem.Phys.*, 105,6587(1996).

3. T.Okazaki, N.Hirota, M.Terazima, *J.Phys.Chem.A*, **101**,650(1997). and *J.Am.Chem.Soc.*, in press.

RELAXATION DYNAMICS OF INHOMOGENEOUS SPECTRAL BAND WIDTH AND AVERAGE ENERGY IN VARIOUS SOLUTE—SOLVENT SYSTEMS

Katsura NISHIYAMA[1] and Tadashi OKADA[2]

[1] Venture Business Laboratory, Osaka University, Suita, Osaka 565-0871, Japan.

[2] Department of Chemistry, Graduate School of Engineering Science, Osaka University, Toyonaka, Osaka 560-8531, Japan.

We have performed subpicosecond transient hole-burning (THB) and picosecond time-resolved fluorescence (TRF) spectroscopy of organic solute molecules in solvents having various polarity for the elucidation of the relaxation of inhomogeneous spectral band widths (relaxation of energy dispersion) in addition to that of spectral peak shift (average energy). We propose that the relaxation process of spectral width and that of average energy of the solute—solvent system should be characterized by different relaxation modes of solvent molecules. In the case of polar solute—polar solvent systems, the relaxation processes of the spectral width detected by both THB and TRF spectroscopy may largely be ascribed to the translational diffusion of solvent molecules. On the other hand the average energy relaxation is achieved by rather fast solvent modes, being attributed to the rotational diffusion and libration of solvent molecules in the closest solvation shell. Even though the distribution of the closest solvation shell is disturbed by the slower translational diffusion mode of solvent molecules, the average energy could be immediately compensated by the fast relaxation of solvent surroundings.

From the viewpoint of fast chemical reaction dynamics in solution, investigation of the relaxation dynamics of energy dispersion should be of crucial importance. The relaxation dynamics of energy dispersion can be experimentally monitored through the time-dependent inhomogeneous broadening of the hole or fluorescence spectral band width. Our results of THB spectroscopy showed that the recovery of the hole spectral width of a polar dye molecule in polar non-viscous fluid solvents was much slower compared with that of the hole peak shift corresponding to the average energy relaxation. In mixed solvents of binary different polarity components, we observed particularly slow dynamics with respect to the relaxation of hole width which was not detected in the case of one component solvents. We interpret this slower dynamics as translational diffusive relaxation of the more polar component of the solvent mixture getting closer to the solute molecule followed with the increase of the solute dipole moment. It is stressed that the relaxation of average energy was not effectively influenced by the solvent mixing, implying that average energy relaxation could be achieved by fast relaxation modes such as rotational diffusion and/or libration of solvent molecules located just around the solute molecule. Results of temperature dependence of TRF spectroscopy of a polar laser dye molecule in ethanol indicated that at room temperature the relaxation of fluorescence spectral width relaxed much slower than that of the spectral peak shift. At lower temperature (while the sample was in the liquid phase) the relaxation time of both processes agreed with each other, which can be explained by the increased contribution from the solvent translational relaxation mode as the decrease of temperature.

In this contribution, we will also discuss our recent results on the THB spectroscopy of nonpolar solute—polar solvent systems for the sake of deeper understanding of solvent modes that should be essentially responsible for the relaxation of energy dispersion as well as that of average energy. In addition, a theoretical approach on the basis of the reference interaction-site model (RISM) will be employed for further interpretation of the obtained experimental results.

VIBRATIONAL COHERENCE IN ELECTRON DONOR-ACCEPTOR COMPLEXES IN SOLUTION

Igor V. RUBTSOV[1,2] and Keitaro YOSHIHARA[1]

[1] Japan Advanced Institute for Science and Technology, Hokuriku, Tatsunokuchi 923-1292, Japan
[2] Institute for Chemical Physics Research, Chernogolovka, Moscow Region 142-432, Russia,

While coherent oscillations were recently observed in real time in systems with different complexity (from gas phase to proteins) and by different spectroscopic methods, very limited information exists about their origin (vibrational mode). In this work we studied different electron donor-acceptor complexes formed by rather large organic molecules in solution with the goal to assign the oscillations to the particular vibrational mode in the complex.

The excited state dynamics of several electron donor-acceptor complexes were studied by a femtosecond fluorescence up-conversion technique. The spontaneous fluorescence of the complexes shows an oscillatory component superimposed with a fast decay component. As an example the fluorescence decay in chloranil-HMB complex detected at 810 nm is shown in Fig.1. Oscillations in fluorescence were observed for complexes with three different electron acceptors: tetracyanoethylene (TCNE), chloranil, and fluoranil. Different frequencies of oscillations were observed for complexes with three different electron acceptors: tetracyanoethylene (TCNE) - ~155 cm^{-1}, chloranil - 178 cm^{-1}, and fluoranil - 212 cm^{-1}. Almost the same oscillatory frequency was observed for the complexes with different donors if the same acceptor was used. The assignment of the oscillatory component to a particular vibration is proposed. It is concluded, that the out-of-plane vibrational mode of the acceptor, having b_{3u} symmetry (D_{2h} group), is responsible for the observed oscillations in all three cases (three acceptors). The time-dependent fluorescence spectrum for the TCNE - HMB complex was reconstructed from the fluorescence dynamics at different wavelengths. The ultrafast relaxation of the fluorescence spectrum is superimposed with oscillatory component. The main component of spectral relaxation of 140 fs was attributed mostly to intramolecular vibrational energy redistribution process in both donor and acceptor parts of the complex. Oscillatory component of fluorescence spectrum demonstrates modulation of transition frequency during vibrations. It should be noted that assignment of the low frequency modes in complex organic molecules is still not full. It is demonstrated that the time resolved spectroscopy can be used to assign some vibrational modes in complicated chemical systems.

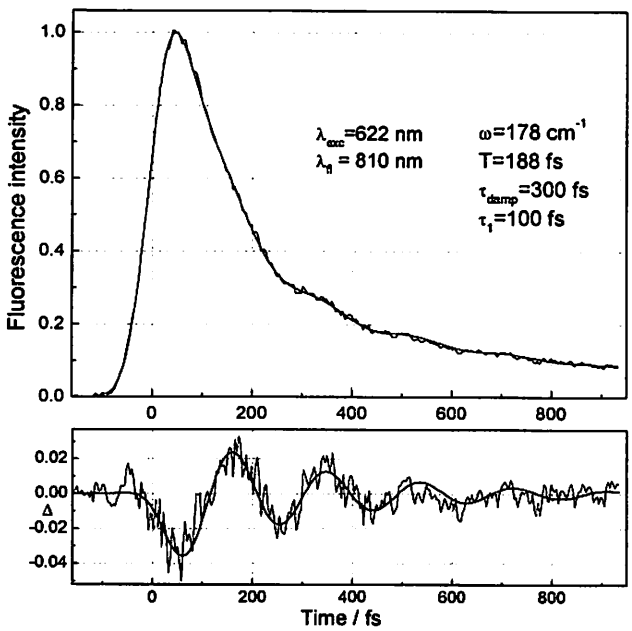

Fig. 1. The fluorescence decay of chloranil - HMB complex in CCl_4 at 866 nm is shown with the best fit. In the lower graph the oscillatory component is emphasized.

HOW DOES NITROGENASE WORK?

David N. Beratan and Igor V. Kurnikov

Department of Chemistry, University of Pittsburgh, Pittsburgh, PA 15260 USA

We are developing theoretical models that describe energy transduction and electron transfer in nitrogenase, the protein responsible for nitrogen fixation. Eight electrons are delivered to reduce each dinitrogen molecule to ammonia. The sequence of electron transport reactions is driven by hydrolysis of ATP, two ATP molecules per electron. Our theoretical analysis provides a mechanism for the displacement of ADP by ATP, redox potential lowering upon protein-protein docking, and electron transfer in the energized complex. From this analysis we have established a working model for energy coupling between ATP hydrolysis and electron transfer in the enzyme. Analogies with other ATP driven processes will be discussed.

STRUCTURE AND INTRAMOLECULAR ELECTRON TRANSFER FUNCTION OF COPPER-CONTAINING NITRITE REDUCTASE

Shinnichiro SUZUKI[1], Kunishige KATAOKA[1], Kazuya YAMAGUCHI[1], Tsuyoshi INOUE[2], Yasushi KAI[2], Kazuo KOBAYASHI[3] and Seiichi TAGAWA[3]

[1]Department of Chemistry, Graduate School of Science, Osaka University, Toyonaka, Osaka 560-0043, Japan
[2]Department of Materials Chemistry, Graduate School of Engineering, Osaka University, Suita, Osaka 565-0871, Japan
[3]The Institute of Scientific and Industrial Research, Osaka University, Ibaraki, Osaka 567-0047, Japan

Dissimilatory nitrite reductase (NIR) is a key enzyme in the anaerobic respiratory pathway of denitrifying bacteria, catalyzing one electron reduction of nitrite ion to NO. Two types of NIR have so far been known; the copper- and the heme-containing enzymes. Cu-containing NIR is a trimer with one type 1 Cu (blue copper) bound in one subunit and one type 2 Cu (nonblue copper) located between the subunits. The type 1 Cu bound by 2His, Cys, and Met accepts one electron from an electron donor protein and shows an intense color, blue or green. The type 2 Cu bound by 3His and a solvent is a reduction center of the substrate.

We have determined the X-ray crystal structures of the oxidized and reduced NIR's from *Alcaligenes xylosoxidans* GIFU1051 (blue AxgNIR) at 2.05 Å and obtained its intramolecular electron transfer rate constants (k_{ET}) from type 1 Cu to type 2 Cu at various pH values with those of the green NIR isolated from *Achromobacter cycloclastes* IAM1013 (AciNIR). The superposition of the oxidized type 1 Cu sites in AxgNIR and the green NIR from *Alcaligenes faecalis*e S-6 (AfsNIR) was carried out on the three strongly ligating residues (His95N(D1), His145N(D1), and Cys136S). In AxgNIR, the displacement of the Cu atom out of the NNS plane defined by 2N(His) and S(Cys) ligands toward S(Met150) is similar to that in AfsNIR (ca. 0.5 Å). The S(Met) ligand of AxgNIR slightly deviates from the axial position of the NNS plane, while that of AfsNIR is in the considerably tilted position. The geometries of type 1 Cu(II) centers in AxgNIR and AfsNIR are distorted tetrahedral and flattened tetrahedral, respectively. Both the Cu(II)-S(Met) distances in these NIR's (ca. 2.6 Å) are shorter than that in the distorted tetrahedral Cu(II) site of plastocyanin by ca. 0.2 Å. The reduced type 1 Cu site of AxgNIR is also distorted tetrahedral. The interatomic distance between the type 1 and 2 Cu's is ca. 12.5 Å and these two Cu's are bound by the Cys-His sequence segment. The observed k_{ET} values of AxgNIR and AciNIR were estimated to be 2100 s^{-1} at pH 6.0 and 25 ℃. The pH-k_{ET} profiles of AciNIR and AxgNIR show the maximum values around pH 6 and those in the presence of nitrite ion approximately coincide with the pH-nitrite reduction activity profiles which show the optimal values of pH 5.5 - 6.0. Therefore, the intramolecular electron transfer process would be closely linked to the following catalytic reduction process of the substrate.

ELECTRON TRANSFER CHEMISTRY OF ORGANOMETALLIC PORPHYRINS AND RELATED METAL COMPLEXES

Shunichi FUKUZUMI
Department of Material and Life Science, Graduate School of Engineering, Osaka University, Suita, Osaka 565-0871, Japan

Homogeneous electron transfer kinetics for generation of iron(IV) porphyrin π radical cations using three different oxidants were examined in deaerated acetonitrile and the resulting data were evaluated in light of the Marcus theory of electron transfer to determine reorganization energies of the rate-determining oxidation of iron(III) to iron(IV).[1] The investigated compounds are represented as (P)Fe(R) where P^{2-} = the dianion of 2,3,7,8,12,13,17,18-octaethyl-5,10,15,20-tetraphenylporphyrin (OETPP) and R = C_6H_5, 3,5-$C_6F_2H_3$, 2,4,6-$C_6F_3H_2$, or C_6F_5, or P^{2-} = the dianion of 2,3,7,8,12,13,17,18-octaethylporphyrin (OEP) and R = C_6H_5, 2,4,6-$C_6F_3H_2$, or 2,3,5,6-C_6F_4H. The first one-electron transfer from (P)Fe(R) to $[Ru(bpy)_3]^{3+}$ (bpy = 2,2'-bipyridine) leads to an Fe(IV) *s*-bonded complex, $[(P)Fe^{IV}(R)]^+$, and occurs at a rate which is much slower than the second one-electron transfer from $[(P)Fe^{IV}(R)]^+$ to $[Ru(bpy)_3]^{3+}$ to give $[(P)Fe^{IV}(R)]^{2+\bullet}$. The reorganization energies (kcal mol^{-1}) for the metal-centered oxidation of $(P)Fe^{III}(R)$ to $[(P)Fe^{IV}(R)]^+$ increase in the order (OEP)Fe(R) (83 ± 4) << (OETPP)Fe(C_6F_5) (99 ± 2) < (OETPP)Fe(2,4,6-$C_6F_3H_2$) (107 ± 2) < (OETPP)Fe(3,5-$C_6F_2H_3$) (109 ± 3) < (OETPP)Fe(C_6H_5) (113 ± 3). Each value is significantly larger than the reorganization energies determined for the porphyrin-centered oxidations involving the same two series of compounds, i.e. the second electron transfer of (P)Fe(R). Coordination of pyridine to (OETPP)Fe(C_6F_5) as a sixth axial ligand enhances significantly the rate of electron transfer oxidation.

Homogeneous electron transfer kinetics for the first reduction of four synthetic manganese porphyrins, [(P)MnCl], three of which have nonplanar macrocycles, were also studied in light of the Marcus theory of electron transfer using a series of semiquinone radical anions as reductants in deaerated acetonitrile.[2] Electron transfer rates for the metal-centered reduction of nonplanar manganese(III) dodecaphenylporphyrins, represented as [(DPPX)MnCl], where X = H, Cl_{12}, or F_{20}, are much slower then the electron transfer rates for reduction of [(TPP)MnCl], which has a planar macrocycle. The effects of bases on the electron transfer rates are also reported.

1. Fukuzumi, S.; Nakanishi, I.; Tanaka, K.; Suenobu, T.; Tabard, A.; Guilard, G.; Van Caemelbecke; Kadish, K. M. *J. Am. Chem. Soc.* **1999**, *121*, 785.
2. Fukuzumi, S.; Nakanishi, I.; Barbe, J.-M.; Guilard, R.; Van Caemelbecke, E.; Guo, N.; Kadish, K. M. *Angew. Chem., Int. Ed. Engl.* **1999**, *38*, 964.

ELECTRON TUNNELING IN INORGANIC MOLECULES

Jay R. WINKLER

Beckman Institute, California Institute of Technology, Pasadena, CA, 91125 USA

Electron-transfer reactions are the simplest chemical transformations: no bonds are formed or broken as an electron migrates from the donor (***D***) to the acceptor (***A***). This simplicity has led to the development of an elegant and powerful theoretical formalism that describes ET rates in terms of a small number of experimentally accessible parameters. Most predictions of semiclassical ET theory have been verified experimentally.

A singular characteristic of ET reactions is that they can proceed at significant rates ($>10^3$ s^{-1}) even when ***D*** and ***A*** are separated by long (>20 Å) distances. Theory suggests that superexchange interactions are responsible for long-range ET: electronic states of the intervening medium (the bridge states) interact with one another and with the states of ***D*** and ***A*** to provide an overall ***D/A*** coupling that is substantially greater than the direct coupling between the isolated states of ***D*** and ***A***. A key element of the superexchange model is that the efficiency of long-range ***D/A*** coupling is predicted to be extremely sensitive to the difference in energy between the bridge states and those of ***D*** and ***A***. As the energy gap decreases, long-range ET efficiency is expected to increase dramatically.

Tunneling-energy effects should be readily observable for electron transfer over very long distances (>20 Å) in systems where the potentials of the redox sites differ only marginally from those of the bridge sites. We have prepared a series of oligoparaphenylene-bridged binuclear metal complexes to examine tunneling-energy effects in long-range ET. A ferrocene moiety is bound at one end of the bridge; diimine complexes of osmium, ruthenium, or rhenium, which serve as photochemical ET sensitizers, are bound at the other end. The tunneling-energy gap decreases from >1 eV to approximately 0.1 eV as the metal changes from Os to Ru to Re. We are testing the theoretical prediction that the distance decay of ET rates should become much more shallow along this series.

ET across solvent bridges is also under investigation. The distance dependence of ET from excited donors to randomly oriented ground-state acceptors can be determined from the donor luminescence decay kinetics. In these studies we are probing the long-range coupling efficiency of rigid aqueous and organic glasses.

If tunneling-energy effects can be better defined, then they can be manipulated to provide an additional level of control in long-range electron transfer. This potentially powerful tuning element could be extremely valuable in designing systems for photochemical energy storage or molecular electronics.

EFFECTS OF CHARGED PEPTIDES ON REACTIONS INVOLVING PLASTOCYANIN AND CYTOCHROME *f*

Shun HIROTA[1], Masaaki ENDO[1], Kozue HAYAMIZU[1], Tomoya TSUKAZAKI[1], Takashi HIBINO[2], Teruhiro TAKABE[3], Takamitsu KOHZUMA[4], and Osamu YAMAUCHI[1]

[1] Department of Chemistry, Graduate School of Science, Nagoya University, Chikusa-ku, Nagoya 464-8602, Japan

[2] Department of Chemistry, Meijo University, Tempaku-ku, Nagoya 468-8502, Japan

[3] Research Institute, Meijo University, Tempaku-ku, Nagoya 468-8502, Japan

[4] Department of Chemistry, Ibaraki University, Mito, Ibaraki 310-8512, Japan

Plastocyanin (PC), a mobile copper protein, and cytochrome *f* (cyt *f*), a subunit of the cytochrome *bf* complex, exist in the electron transfer pathway from photosystem II to photosystem I, where cyt *f* transfers electrons to PC. To gain information on their molecular recognition character and their protein structural changes due to interaction with molecules, we investigated the effects of charged peptides, such as lysine and aspartic acid peptides (Lysptd's and Aspptd's), on electron transfer between reduced cyt *f* or $[Fe(CN)_6]^{4-}$ and oxidized PC and on their protein structures and functions.[1-3] We propose that charged peptides may be useful for molecular recognition and structural studies of electrostatic protein-protein interactions.

Lysptd's and Aspptd's, up to *penta*-Lys and *penta*-Asp, served as competitive inhibitors of electron transfer from reduced cyt *f* to oxidized PC, while Lysptd's promoted electron transfer from $[Fe(CN)_6]^{4-}$ to oxidized PC. The electron transfer inhibitory effects of Lysptd's and Aspptd's are explained as competitive inhibition due to neutralization of the charged amino acid residues at the surface of PC and cyt *f*, respectively, by electrostatic interactions, whereas the electron transfer promoting effects by Lysptd's may be due to formation of PC·Lysptd or Lysptd·$[Fe(CN)_6]^{4-}$ complexes subsequently forming an electron transferring complex, PC·Lysptd·$[Fe(CN)_6]^{4-}$, without repulsion of the negative charges. The inhibitory and promotional effects became significant as the net charge or concentration of the peptides increased, and the effects of Lysptd's decreased as the net charge of the PC negative patch was decreased by mutagenesis. Structural and redox changes of PC and cyt *f* were also observed on adduct formation with Lysptd's and Aspptd's, respectively.

1. Hirota, S.; Endo, M.; Hayamizu, K.; Tsukazaki, T.; Takabe, T.; Kohzuma, T.; Yamauchi, O., *J. Am. Chem. Soc.*, 1999, **121**, 849-855.

2. Hirota, S.; Endo, M.; Tsukazaki, T.; Takabe, T.; Yamauchi, O., *J. Biol. Inorg. Chem.*, 1998, **3**, 563-569.

3. Hirota, S.; Hayamizu, K. Endo, M.; Hibino, T.; Takabe, T.; Kohzuma, T.; Yamauchi, O., *J. Am. Chem. Soc.* 1998, **120**, 8177-8183.

PHOTOINDUCED ELECTRON TRANSFER IN HEMOPROTEINS MODIFIED WITH CHELATORS

Keiichi TSUKAHARA

Department of Chemistry, Faculty of Science, Nara Women's University, Nara 630-8506, Japan

Long-range electron transfer (ET) in proteins is an important subject to elucidate the mechanisms of biological electron transport. The donor-acceptor distances were found to control the ET rates in the protein systems, where a number of donor-acceptor sets were developed on the surface of the proteins by chemical modifications. However, the donor-acceptor set reported previously is limited for a single hemoprotein. Therefore, we have designed myoglobin whose Lys residue is modified with one of the strong metal-chelating reagents, diethylenetriaminepenta-acetic acid (DTPA). In this model, we can easily replace the heme to the other metalloporphyrins and introduce many redox-active metal ions into the DTPA unit. In this symposium the photoinduced ET reactions of zinc-substituted myoglobin modified with DTPA will be presented.

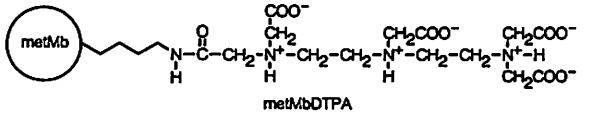

1) Intramolecular ET quenching of the Excited Triplet State of ZnMbDTPA with Cytochrome *c*—ZnMbDTPA can bind cyt *c*(III) and the intramolecular ET quenching occurs from the excited triplet state of ZnMbDTPA to bound cyt *c*(III) within a complex. Both binding constants and intramolecular ET rate constants increased with an increase in the number of DTPA on the surface of myoglobin. The ET pathway is discussed on the basis of the binding site of DTPA.

2) Intramolecular ET Quenching of the Excited Triplet State of Zinc Myoglobin Modified with Co^{III}(dtpa) Complex — Although the excited singlet state of ZnMb{Co^{III}(dtpa)} was not quenched by the bound Co(III), the excited triplet state was intramolecularly quenched by the bound Co(III). The effect of distance and the orientation between donor and acceptor on the ET rates are discussed.

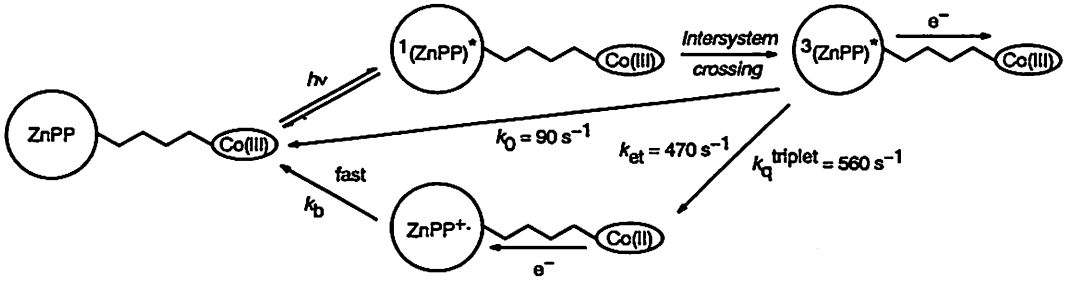

Effect of Chirality in Electron Transfer Reactions between Metalloproteins and Transition Metal Complexes.

Akira NAGASAWA,[1] Masayuki KYOMASU,[1] and Takamitsu KOHZUMA[2]
[1] Department of Chemistry, Saitama University, Urawa, Saitama 338-8570, Japan
[2] Department of Materials and Biological Sciences, Ibaraki University, Mito 310-8512, Japan.

Redox reactions of metalloproteins with optically active cobalt(II) complexes with a chrathrochelate (cage-type) ligand were kinetically studied by stopped-flow spectrophotometry in aqueous solution. The following three systems have been investigated:

(1) Cytchrome *c* (Fe^{III}) + $[Co(sep)]^{2+}$ →
(2) Cytchrome *c* (Fe^{III}) + $[Co(diNOsar)]^{2+}$ →
(3) Plastocyanin (Cu^{II}) + $[Co(sep)]^{2+}$ →

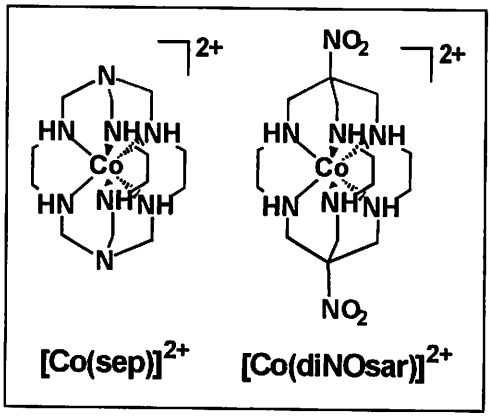

All the reduction processes gave first-order kinetic traces under the pseudo-first-order conditions with the metal complexes in excess, at pH 5.0 (acetate buffer), I = 0.10 M ($Na^+CH_3CO_2^-$), T = 278 – 308 K, and P = 0.1 - 60 MPa. A significant dependence of the rate on the configuration of the metal complex (Δ or Λ) was observed for each system.

Δ-$[Co(sep)]^{2+}$ reduces cytochrome *c* faster than Λ-complex does, (k_f = 9.2 × 10^4 and 8.1 × 10^4 $M^{-1}s^{-1}$ at 298 K, respectively) in the system **1**,. On the other hand, plastocyanin in the system **3** was reduced by Λ-$[Co(sep)]^{2+}$ with a higher rate (k_f = 2.2 × 10^5 $M^{-1}s^{-1}$ at 298 K) than by Δ-form. For the reactions with $[Co(sep)]^{2+}$, the differences with the chirality were seen in the activation enthalpy $\Delta H^{\ddagger}$ (<10 kJ mol^{-1}), but not in other parameters, $\Delta S^{\ddagger}$ (ca.-150 J mol^{-1} K^{-1}), and $\Delta V^{\ddagger}$ (-45 cm^3mol^{-1}). This suggest that the fitness of the complex to the chiral surface residue of the active site of the protein may govern the distance between metal centers, and the electron transfer rate in the encounter complex may be affected.

Δ-$[Co(diNOsar)]^{2+}$ reduces the protein with the 16 % higher rate (k_f = 1.5 × 10^2 $M^{-1}s^{-1}$ at 298 K) than that of Λ-form in the system **2**, and $\Delta H^{\ddagger}$ = 18 and 15 kJ mol^{-1}, and $\Delta S^{\ddagger}$ = -139 and -149 J mol^{-1} K^{-1}, for Δ- and Λ-form, respectively. In this case, the chirality of the metal complex plays a role both in the outer sphere association (the formation of the encounter complex) and in the net electron transfer process.

CHEMICAL INFORMATION VIA A TRANSFERRED ELECTRON: MUON SPECTROSCOPY

Upali A. JAYASOORIYA, John A. STRIDE and Georgina M. ASTON
School of Chemical Sciences, University of East Anglia, Norwich NR4 7TJ, UK

The muon is a sub-atomic particle with a half-life of ca. 2.2 μs. It has a spin of one half and a weight of one ninth of that of a proton. Both positive and negative muon beams are available for experimentation at central facilities around the world, TRIUMF in Canada, RAL in England, PSI in Switzerland and KEK in Japan. Only positive muons were used for the experiments reported here. On implantation in matter, the positive muon can exist either in a diamagnetic state on its own or collect an electron to form the hydrogen atom equivalent, muonium. Muonium may be considered as the lightest isotope of hydrogen. Muonium may then take part in chemical reactions in an analogous manner to a hydrogen atom, and can be studied using Muon spectroscopy. During this presentation, different aspects of Muon spectroscopy are briefly outlined and illustrated with several applications. These applications include electron dynamics of systems of relevance to electron transfer and molecular dynamics of organometallics. The final example will be used to illustrate the potential use of these techniques for the study of hitherto unknown organometallic hydrides.

METAL- AND LIGAND-CONTROLLED MULTISTEP REDOX PROPERTIES OF OXIDE-CENTERED MIXED-METAL TRINUCLEAR COMPLEXES

Maiko TANAKA, Masaaki ABE, and Yoichi SASAKI
Division of Chemistry, Graduate School of Science, Hokkaido University, Kita-ku, Sapporo 060-0810, Japan

Oxide-centered acetate-bridged trinuclear complexes of the general formula $[M_3(\mu_3\text{-}O)(\mu\text{-}CH_3CO_2)_6L_3]^{n+}$ (L = a monodentate terminal ligand) are formed by many transition metal ions, including mixed-metal, mixed-ligand, and mixed-valence complexes. Thermally stable and redox-active mixed-metal complexes $[Ru_2M(\mu_3\text{-}O)(\mu\text{-}CH_3CO_2)_6(py)_3]^{n+}$ (M: various divalent (n = 0) and tervalent (n = 1) metal ions, py = pyridine)[1] are well suited for systematic study of intramolecular metal-metal interactions and ligand-exchange reactions in solution.[2] Here we have prepared new derivatives of Ru_2M trimers (Figure 1) with various terminal ligands (L and L') to investigate tuning effects of metal (M) and terminal ligands upon the redox properties of the clusters.

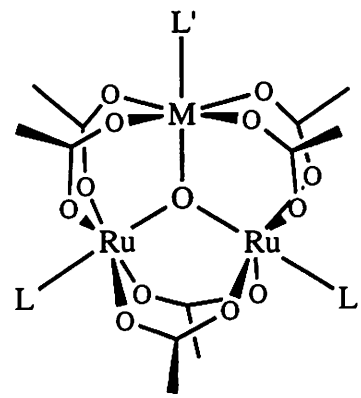

M = Mg^{II}, Mn^{II}, Co^{II}, Ni^{II}, Zn^{II}
L = pyridine derivatives, L' = H_2O or L

Figure 1. Mixed-metal complexes in this study.

The complexes exhibit multistep redox processes including four Ru-based ones and, in some cases, one M-based process (for M = Co) and ligand-based process(es) (for L = (4-cyano)pyridine (cpy) and 1-methyl-4,4'-bipyridinium ($mbpy^+$)). For example, a crystallographically-characterized complex, $[Ru_2Mg(\mu_3\text{-}O)(\mu\text{-}CH_3CO_2)_6(cpy)_2(H_2O)]$ (Ru•••Ru = 3.282(1) Å, Ru•••Mg = 3.408(4) Å), shows four Ru-based waves ($E_{1/2}$ = +1.61, +0.60, –0.89, and E_{pc} = –1.29 V vs Ag/AgCl) and a ligand-based wave (2cpy/2$cpy^{\bullet-}$, $E_{1/2}$ = –1.81 V) in CH_3CN containing 0.1 M $[(C_4H_9)_4N]PF_6$ as a supporting electrolyte. The redox potentials of the Ru-based waves are found to shift negatively with increasing basicity of the terminal ligands for the series of Ru_2Zn and Ru_2Mg complexes. Remote terminal ligand-ligand interactions through the $Ru_2M(\mu_3\text{-}O)$ framework will be discussed for the cpy and $mbpy^+$ analogs.

1. Ohto, A; Sasaki, Y.; Ito, T. *Inorg. Chem.* 1994, **33**, 1245.
2. Abe, M.; Tanaka, M.; Umakoshi, K.; Sasaki, Y. *Inorg. Chem.* in press.

SURFACTANT OLIGOMERS IN AQUEOUS SOLUTION

R. ZANA
Institut C. Sadron (CNRS), 6 rue Boussingault, 67000 Strasbourg, France.

A new class of surfactants, which can be broadly referred to as surfactant oligomers,[1] has recently become available and is receiving much attention in view of its properties in aqueous solution. These surfactants are made up of two or more amphiphilic moieties connected at the level of, or close to, the head groups by a spacer group. The amphiphilic moieties can be identical or different; the spacer group can be hydrophilic or hydrophobic, flexible or rigid; and the head groups can be anionic, cationic, nonionic or zwitterionic. The surfactant oligomers have been found to be much more efficient than the corresponding conventional (monomeric) surfactants as regards the ability to form micelles and to lower the surface tension of water, properties on which are based most utilizations of surfactants. Surfactant oligomers are now presently evaluated in academic and industrial laboratoies in order to assess their possible use on a large scale.

The most investigated surfactant oligomers are of the quaternary ammonium type, as for instance surfactants dimers (gemini) **A** and trimers **B**, which have been obtained in a purified form.

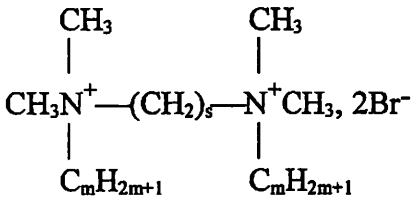

(A) m-s-m,2Br⁻

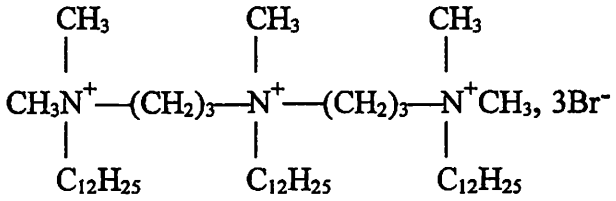

(B) 12-3-12-3-12,3Br⁻

A surfactant tetramer (12-3-12-4-12-3-12, $4Br^-$) has also been synthesized.[2]

This lecture reviews selected aspects of the behavior of surfactant oligomers in aqueous solution: adsorption at the air/solution and silica/solution interfaces; aggregation behavior in water (cmc, aggregation numbers); solution microstructure; rheology; and micelle microviscosity in relation with the surfactant hydrophobicity which is determined by the spacer carbon number the alkyl chain length and the degree of oligomerization (number of amphiphilic moieties). The results are discussed in relation to the behavior of the corresponding conventional (monomeric) surfactants.

1. Zana, R. in *Novel Surfactants: Preparation, Applications and Biodegradability*, K. Holmberg, Ed., M. Dekker, New York, 1998, chapter 8, p. 241.
2. In, M. manuscript in preparation

EXPERIMENTAL ASPECTS OF HYDROPHOBIC INTERACTIONS IN MIXED AMPHIPHILIC SYSTEMS

Ronald E. VERRALL[1], Lee D. WILSON[2], Xiaoguang WEN[1] and Haibo HUANG[3]
[1] Department of Chemistry, University of Saskatchewan, 110 Science Place, Saskatoon, S7N 5C9, Canada
[2] National Research Council (SIMS), 100 Sussex Drive, Ottawa, K1A 0R6, Canada
[3] Alberta Research Council, 250 Karl Clark Road, Edmonton, T6N 1E4, Canada

In recent decades there has been considerable research carried out in an attempt to obtain a clearer understanding of the molecular nature behind the subtle hydration phenomenon occurring between nonpolar solutes and water. The concepts of hydrophobic hydration and hydrophobic interactions have been widely invoked, although not universally applied in a manner consistent with their intended meaning, to explain the unique aspects of interactions between water and biological systems. The important role such interactions play in facilitating the formation of aggregates of amphiphiles in the bulk aqueous phase has also been well documented. Recent research in my laboratory has been focusing, through the use of a wide range of techniques, on a systematic approach to studying the role of small amounts of third components (hydrophobic and/or hydrophilic) on aspects of hydrophobic interactions in complex and organized systems. Some key results of studies of tertiary systems of ethoxylated alcohol-conventional ionic surfactant-water, sodium n-hydro- and n-fluoroalkylcarboxylate-cyclodextrin-water, and triblock copolymer-inhalation anesthetic-water systems will be discussed within the framework of these interactions.

A comprehensive thermodynamic study of mixed micelles comprised of homologous series of sodium n-alkylcarboxylate or n-alkyltrimethyl-ammonium bromide surfactants and ethoxylated alcohols, of chemical formula $C_4(EO)_x$ where $4 \geq x \geq 0$, has shown that there are significant differences between the interactions of an EO group of the alcohol with cationic or anionic micelles. The EO groups behave as though they make a hydrophobic contribution to interactions between the alcohol and the alkylcarboxylate surfactants in the mixed micelles.

Studies of the binding constants, K_I, of cyclodextrin(CD)-surfactant(S) complexes for fluoro- and hydrocarbon homologous series of S have shed new light on the role of hydrophobic effects in the formation, stability, and volumetric properties of CD-S complexes. Apparent molar volume measurements are found to offer new opportunities to probe these binding processes and the results have revealed interesting quantitative information about solvent reorganization during the binding process.

Finally, the role of hydrophobic interactions and anesthetic-induced dehydration of membrane surfaces in the mechanism of anesthesia have been investigated using several model systems. Aggregation studies of aqueous triblock copolymers as a function of temperature and in the presence of small amounts of inhalation anesthetics have provided a means to do this. Polyoxyethylene-polyoxypropylene-polyoxyethylene (POE-POP-POE) triblock copolymers having an appropriate lipophilic/hydrophilic balance readily self-aggregate with increase in temperature or in the presence of small amounts (clinical concentrations) of inhalation anesthetics. They form micelles possessing a hydrophobic core of POP and a surrounding corona of POE segments. The results show that anesthetics can perturb the integrity of the so-called "biological water" of membranes and that dehydration and solvation of membrane surfaces by anesthetic molecules can play an important role in the mechanism of anesthesia.

Isotope Effect in Proton Ttansfer and Association-Dissociation Reactions for Amines by Ultasonic Relaxation Methods

Hua Huang and Sadakatsu Nishikawa

Department of Chemistry and Applied Chemistry, Faculty of Science and Engineering
Saga University, Saga 840-8502, Japan

Ultrasonic absorption coefficients were measured for ethylamine, propylamine and butylamine in heavy water (D_2O) in the frequency range from 0.8 to 220 MHz at 25°C. Two kinds of relaxation processes were observed. One was found in relatively dilute solutions of all amines studied and it was due to a hydrolysis. The rate and thermodynamic parameters were determined from the concentration dependence of the relaxation parameters. Comparing with the results in H_2O, the isotope effect for the reaction was estimated and the stability of the intermediate of the hydrolysis was discussed.

Another relaxation process was observed in the concentration greater than 1 mol dm^{-3} of butylamine. From the profiles of the concentration dependence of the ultrasonic relaxation parameters, thc source of the relaxation was attributed to an association-dissociation reaction, perhaps, associated with hydrophobic interaction. The aggregation number, the forward and reverse rate constants and the standard volume change of the reaction were determined. It was concluded from the comparison with the results in H_2O that the hydrophobic interaction of butylamine in D_2O is stronger than that in H_2O.

Neutron scattering study on dynamics of water molecules in MCM-41

Shuichi TAKAHARA[1], Masatsugu NAKANO[1], Shigeharu KITTAKA[1], Yasushige KURODA[2], Toshinori MORI[2], Hideaki HAMANO[2] and Toshio YAMAGUCHI[3]

[1] Department of Chemistry, Faculty of Science, Okayama University of Science, 1-1 Ridaicho, Okayama 700-0005, Japan

[2] Department of Chemistry, Faculty of Science, Okayama University, Tsushima, Okayama 700-8530, Japan

[3] Department of Chemistry, Faculty of Science, Fukuoka University, Nanakuma, Jyonan-ku, Fukuoka 814-0180, Japan

Introduction. The structure and dynamics of water confined in a nano-space have widely been investigated on the porous materials as silica gels, alumina gels etc. Distributions of pore sizes often brought in an ambiguity in interpretations of the experimental results. Families of MCM-41, which were developed by Beck et al. in 1992,[1] are one of the most suitable model samples for this purpose, because they are composed of highly controlled cylindrical pores with very narrow pore size distribution. In the present study, we have investigated dynamics of water molecules confined in MCM-41 samples with different pore size by quasi-elastic neutron scattering.

Experimental. Three kinds of siliceous MCM-41 samples whose pore radii are 1.07, 1.42 and 1.87 nm were prepared by the method of Beck et al.[1] The neutron scattering measurements were carried out by use of a time-of-flight type spectrometer AGNES installed at the JRR-3M reactor of Japan Atomic Energy Research Institute. Measuring temperature range was 200-300 K.

Results and Discussion. Typical examples of neutron scattering spectra are shown in Fig. 1. The spectra were analyzed by using a model employed by Teixeira et al. in a study for bulk water.[2] This model is composed of two motions of water molecules: rotational and translational diffusions. As regards the translational diffusion, water molecules in MCM-41 were less mobile than those in bulk water, and the mobility was depressed by narrowing of the pore sizes. The residence time of translational diffusion of the confined water molecules showed an Arrhenius type temperature dependence, which is in contrast to the non-Arrhenius type behavior of bulk water. This implies that a growth of hydrogen-bond network of water is hindered by a surface field in a confined space.

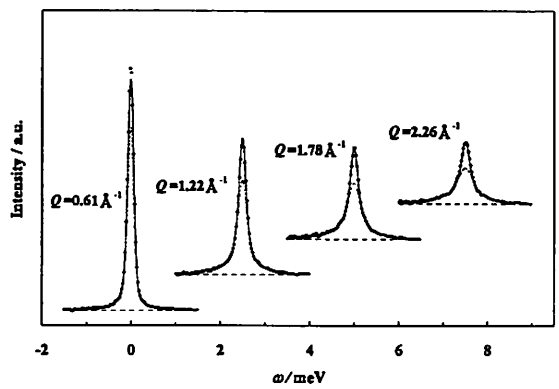

Fig. 1. Q-dependence of neutron scattering spectra for the water-filled MCM-41 sample (pore radius = 1.42 nm) at 300 K.

1. Beck, J. S. et al., *J. Am. Chem. Soc.*, 1992, 114, 10834.
2. Teixeira, J. et al., *Phys. Rev. A*, 1985, 31, 1913.

ORIGIN OF THE LONG-RANGE ATTRACTION BETWEEN CERTAIN HYDROPHOBIC SURFACES

Hugo K. CHRISTENSON, Department of Applied Mathematics, Research School of Physical Sciences, Australian National University, Canberra, A.C.T. 0200, Australia

Between certain macroscopic hydrophobic surfaces across aqueous solutions there is a very long-range, attractive force. This attraction may be up to 100 times stronger than the force predicted by the Lifshitz theory of van der Waals forces, and it is sometimes measurable at surface separations of several hundred nanometres. Although such "hydrophobic" forces have been measured by many groups, there is as yet no consensus on the origin of the interaction. The reported effects of temperature, electrolyte and other additives have been contradictory. Recently, it has become increasingly clear (i) that the long-range attraction is not found between stable hydrophobic surfaces such as smooth, cross-linked polymers, and (ii) that the the nucleation and subsequent persistence of vapour bubbles between the hydrophobic surfaces are often the direct cause of a long-range attraction. There remain, however, a great many experiments where bubbles cannot give rise to the attractive force. I suggest that the long-range ($\geq$ 20 nm) attraction in these cases is related to a lack of stability of the hydrophobic surface, and the possibility of rearrangement of hydrophobic surface groups. For hydrophobic monolayers adsorbed from solution *in situ* , it can be shown that a shift of the adsorption/desorption equilibrium on approach of the two surfaces can lead to a long-range attraction. For those surfaces where no adsorption/desorption equilibrium exists (Langmuir-Blodgett films, silylated surfaces, some polymer surfaces) rearrangement or lateral diffusion of surface groups may be possible. If the *local* density of hydrophobic groups is adjusted to give a decrease in free energy on approach of two surfaces, the result will be an attractive interaction between the surfaces. These ideas explain the presence of a long-range attraction between one hydrophobic surface and one hydrophilic, as well as in nonaqueous solvents. Among the many unresolved issues is the communication between the surfaces - how does one surface "see" the presence of the other?

EFFECT OF PRESSURE ON THE PHASE TRANSITIONS OF DIPALMITOYLPHOSPHATIDYLETHANOLAMINE BILAYER MEMBRANE

Shoji KANESHINA, Hitoshi MATSUKI, Shigeru ENDO, and Takashi HATA
Department of Biological Science and Technology, Faculty of Engineering,
The University of Tokushima, Minamijosanjima, Tokushima 770-8506, Japan

The phase behavior of dipalmitoylphosphatidylcholine (DPPC) bilayer membranes has been most extensively studied by various physical techniques. We have shown the pressure effect on the bilayer phase transitions of a series of diacylphosphatidylcholines containing linear saturated acyl chains,[1,2] and extend these measurements and thermodynamic analysis to another major phospholipid group, i. e., phosphatidylethanolamines. The present study demonstrates the pressure effect on the phase transitions of dipalmitoylphosphatidylethanolamine (DPPE) bilayer membranes.

Synthetic DPPE was obtained from Sigma. The multilamellar vesicle was prepared by suspending DPPE in water. The phase transitions under high pressures were observed by two kinds of optical methods. One is the observation of isothermal barotropic phase transition and the other is the isobaric thermotropic phase transition. The general arrangement of the high-pressure apparatus has been described in detail previously.[1]

The differential scanning calorimetry of DPPE at ambient pressure showed two kinds of endothermic transitions at 63.1 and 64.3 °C. Higher-temperature transition can be assigned as the L_c/L_α transition from the highly ordered lamellar crystalline (L_c) phase to the liquid crystalline (L_α) phase. Lower-temperature transition can be assigned as the so-called main transition from the lamellar gel (L_β) phase to the L_α phase. Both transition temperatures increased linearly with applying pressure. Since the slope of the *T-p* phase boundary for the main transition, 0.264 K MPa^{-1}, is larger than that for L_c/L_α transition, 0.230 K MPa^{-1}, the *T-p* curves for the main transition and L_c/L_α transition intersect each other on the phase diagram at 21.8 MPa. Under high pressures above 21.8 MPa, two kinds of transitions, that is, the L_c/L_β and main (L_β/L_α) transitions, were observed. The slope of the *T-p* phase boundary for the L_c/L_β transition was 0.164 K MPa^{-1}. From the comparison between DPPC and DPPE membranes, the ripple gel (P_β') and interdigitated gel ($L_\beta I$) phases were not observed on the DPPE bilayer membrane. DPPC and DPPE molecules differ only in the polar head groups. Difference in the phase behavior can be attributed to the different interaction in head group between the two types of molecules. Thermodynamic quantities on the phase transitions of DPPE bilayer membrane are discussed.

[1] Ichimori, H.; Hata, T.; Yoshioka, T.; Matsuki, H.; Kaneshina, S., *Chem. Phys. Lipids*, 1997, **89**, 97.
[2] Ichimori, H.; Hata, T.; Matsuki, H.; Kaneshina, S., *Biochim. Biophys. Acta*, 1998, **1414**, 165.

ASSOCIATION REACTION OF SOME FLUOROPHORES WITH SURFACTANT MICELLES

Shinkichi YAMADA, Yasuhiro YAMAMOTO, Sen-ichi AIZAWA and
Motoshi NAKAMURA
Faculty of Engineering, Shizuoka University, Johoku, Hamamatsu 432-8561, Japan

Thermodynamics of the association reaction of 7-hydroxycoumarin(7-OH-C), 4-methyl-7-hydroxycoumarin(4-Me-7-OH-C), 4-phenyl-7-hydroxycoumarin(4-Ph-7-OH-C) and 7-hydroxyflavone(7-OH-F) with surfactant micelles have been studied spectrofluorometrically in 4% methanolic aqueous solution at 25 ℃ by using sodium dodecylsulfate(SDS), Triton X100(TX100) and cetyltrimethylammonium bromide(CTAB) as anionic, non-ionic and cationic surfactants, respectively. Above the critical micelle concentration of respective surfactants, significant change in the fluorescence intensity(F) of protonated(HL) and deprotonated(L^-) fluorophores with slight shift in the excitation and emission maxima was observed in acidic and alkaline media, respectively. Then, the values of F were analyzed as a function of the concentration of each micelle ([M]) to determine the 1:1 association constants, $K_{HL} = [HL \cdot M][HL]^{-1}[M]^{-1}$ and $K_L = [L \cdot M][L]^{-1}[M]^{-1}$ (charges are omitted for simplicity). The results are summarized in Table 1.

The values of K_L are smaller than those of K_{HL} for SDS because of the anion-anion electrostatic repulsion, while the reverse is found for CTAB because of the anion-cation attraction. The values of K_{HL} of 4-Ph-7-OH-C and 7-OH-F are greater than those of 7-OH-C and 4-Me-7-OH-C for TX100 and CTAB probably due to the stronger hydrophobic interaction for the former fluorophores with a phenyl group. Considering that the values of K_{HL} are greater than those of K_L for the non-ionic TX100, it is expected that the stronger solvation of L^- in the bulk solution compared with HL reduces the chemical potential of L^- in the initial state.

Table 1 Association constants of fluorophores with surfactant micelles

Fluorophore	SDS		TX100		CTAB	
	$\log K_{HL}$	$\log K_L$	$\log K_{HL}$	$\log K_L$	$\log K_{HL}$	$\log K_L$
7-OH-C	3.61	2.79	3.64	—[a]	3.62	5.53
4-Me-7-OH-C	3.84	2.22	3.93	—[a]	4.09	6.41
4-Ph-7-OH-C	3.23	1.84	5.76	4.40	5.75	6.96
7-OH-F	3.52	1.93	5.24	4.20	5.55	7.03

a. Change in F is too small to evaluate $\log K_L$.

LOCAL ORDER IN SIMPLE SOLVENTS AND THEIR MIXTURES

T. RADNAI
Chemical Research Center of Hungarian Academy of Sciences, Pusztaszeri út 59-67, Budapest, H-1025, Hungary

A short review of recent results of the investigations on the local order in simple solvents and their mixtures will be presented.

The following methods of investigation were used for revealing various structural features in the target liquids: X-ray and neutron diffraction experiments, Molecular Dynamics, Monte Carlo and Reverse Monte Carlo simulations and, partly, ab initio calculations.

The studies covered a range of the most frequently used solvents of three categories:

- hydrogen bonded solvents as water, some alcohols (methanol, ethanol, 2,2,2-trifluoroethanol), and amides (formamide and *N*-methylformamide),
- aprotic dipolar solvents, examples of which are acetonitrile, acetone, pyridin, *N,N*-dimethylformamide, tetramethylurea and dymethyl sulfoxide,
- diatomic molecular liquids, a representative of which is liquid nitrogen.

The local order is characterized in terms of various microscopic, atomic scale structural properties as structure functions, pair distribution functions, partial correlations functions, some three particle correlations, orientational and angular correlations as well as energies of hydrogen bonds and dimers of molecules.

Our results show that the earlier conceipt according to which aprotic liquids are usually „structurally disordered" compared to those of extended hydrogen bonds has to be reinterpreted. Liquids with molecules of high dipole moment are able to exhibit well defined local order, which, in turn, may fade away rapidly with increasing distance between the molecules. A preliminary report of the phenomenon has already been published[1]. Moreover it has been showed that the extension and strength of the local correlations between the molecules depends on their geometry and the position of the dipoles as well.

However, although the local order is manifested quite differently in various liquids, the interaction energies fall often within the same order of magnitude for dipolar liquids as for hydrogen bonded ones. Therefore one should expect that significant interactions arise between unlike molecules in mixtures of different solvents, which can compete with those between the like ones and as a concsequence, a rather complicated local order can be observed. Examples supporting the ideas of microheterogenity, microscopic phase separations, enhanced dimer formations, reorganized hydrogen bonded networks will be presented for some mixtures: alcohols with water, acetonitrile with water, 2,2,2-trifuoroethanol with dymethyl sulfoxide, acetornitrile and *N,N*-dimethyl formamide, and tetramethylurea with water

1. Radnai, T.; Bakó, I.; Jedlovszky, P. ; Pálinkás, G., *Mol. Sim.*, 1996, **16**, 345.

X-RAY DIFFRACTION STUDY OF ETHANOL-WATER MIXTURES FROM AMBIENT TO FREEZING POINT TEMPERATURES

Toshiyuki Takamuku,[a] Kensuke Saisho,[a] Shuntaro Nozawa,[b] Toshio Yamaguchi,[b] and Nobuyuki Nishi[c]

[a]Department of Chemistry, Saga University, Honjo-machi, Saga 840-8502, Japan

[b]Department of Chemistry, Fukuoka University, Jonan-ku, Fukuoka 814-0180, Japan

[c]Institute for Molecular Science, Myodaiji, Okazaki 444-8585, Japan

Various physico-chemical properties, such as enthalpies of mixing,[1] proton NMR chemical shifts,[2] and freezing process,[3] for ethanol-water mixtures at ambient and undercooled temperatures have shown an anomaly (inflection point) at an ethanol mole fraction of $X_E \approx 0.2$. X-ray diffraction and mass spectrometry measurements have been made from ambient to freezing point temperatures on ethanol-water mixtures as a function of ethanol concentration to clarify an origin of the anomaly on the basis of microscopic structure of clusters formed in the mixtures. It has been revealed that clusters in the ethanol-water mixtures drastically change at $X_E \approx 0.2$. The most likely model of cluster structure has been proposed,[4,5] *i.e.*, at $0.0 < X_E \leq \sim 0.2$ a core of hydrophobic ethyl groups of a few ethanol molecules is hydrogen-bonded by water molecules, while at $\sim 0.2 \leq X_E < 1.0$ inherent ethanol structure of chain type becomes dominant and water molecules are hydrogen-bonded to the ethanol clusters to form sandwich-type structure. These differences of the cluster structures have been clearly observed in X-ray diffraction data at undercooled and freezing point temperatures. The X-ray radial distribution function (RDF) at $X_E = 0.1$ has shown that water structure is gradually strengthened with decreasing temperature and ice I_h is formed at the freezing point temperature. On the contrary, at $X_E = 0.2$ and 0.3 the peaks due to inherent ethanol structure gradually increase with decreasing temperature. At the freezing point temperatures the RDFs at $X_E = 0.2$ and 0.3 are similar to each other and composed of peaks due to pure ethanol structure and new peaks probably due to water structure. On the basis of the microscopic structure of clusters, a possible origin of the anomaly of ethanol-water mixtures is discussed.

1. Franks, F.; Ives, D. J. G. *Q. Rev. Chem. Soc.*, 1966, **20**, 1.
2. Coccia, A.; Inodovia, P. L.; Podo, F.; Viti, V. *Chem. Phys.*, 1975, **7**, 30.
3. Takaizumi, K.; Wakabayashi, T. *J. Solution Chem.*, 1997, **26**, 927.
4. Nishi, N.; Takahashi, S.; Matsumoto, M.; Tanaka, A.; Muraya, K.; Takamuku, T.; Yamaguchi, T. *J. Phys. Chem.*, 1995, **99**, 462.
5. Matsumoto, M.; Nishi, N.; Furusawa, T.; Saita, M.; Takamuku, T.; Yamagami, M.; Yamaguchi, T. *Bull. Chem. Soc. Jpn.*, 1995, **68**, 1775.

Investigation of the structure of liquid acetonitrile-water and pyridine-water mixtures: wide angle and small angle neutron diffraction study

Imre Bakó[1], Gábor Pálinkás[1] John C.Dore[3], Henry Fisher[4] and Marie C. Bellisent Funel[2]

[1] Department of Chemical Phyics, Chemical Research Center, Budapest Pf.,17, 1525, Hungary

[2]Laboratorie Leon Brillouin (CEA-CNRS) CEN-Saclay 91191 Gif-sur-Yvette cedex, France

[3] Physics Laboratory,University of Kent at CanterburyCanterbury,Kent,CT2,7NR,UK

[4] Henry Fischer Institut Laue-Langevin, Avenue des Martyrs F-38042 Grenoble, France

The liquid acetonitrile and pyridine are typical representatives of dipolar liquid. Both of them are able to form hydrogen bonded complexes through their N atoms. They are miscible with water in all proportion. Partial structure factors and pair correlation functions involving the hydrogen atom on the water molecule in the pyridine solution and hydrogen atom on the in the CH_3 group of acetonitrile molecule were determined.

Small angle neutron scattering measurements were carried out on heavy water solutions of these compounds . In the pyridine-water mixture we found by this method a very well defined aggregates with R_g of 4 to 7 Å as a function of pyridine concentration. In the other solution at x_a=0,38 mole fraction we found a critical scattering behavior as we decrease the temperature to the consulate point.

Structure of Mixed Solvents and Preferential Solvation of Metal Ions

Kazuhiko OZUTSUMI and Hitoshi OHTAKI

Department of Chemistry, Faculty of Science and Engineering, Ritsumeikan University, 1-1-1 Noji-Higashi, Kusatsu 525-8577, Japan

Liquid structures of some binary solvent mixtures and preferential solvation structures of metal ions in mixed solvents were studied by the solution X-ray diffraction method.

Dimethyl sulfoxide (DMSO) is a structured liquid owing mainly to dipole-dipole interactions,[1] while *N*,*N*-dimethylformamide (DMF) has a rather disordered structure.[2] In the 4:1, 1:1, 1:2 and 1:4 DMSO-DMF mixtures, the weak dipole-dipole interactions between DMSO and DMF molecules are revealed. The DMSO-DMSO interactions are much stronger than the DMF-DMF and DMSO-DMF interactions in the mixtures, and thus, DMSO forms clusters consisting of a few molecules and DMF molecules almost randomly distribute around the clusters.

The calcium ion has six solvent molecules in the first solvation sphere in neat DMSO and DMF as well as in their mixtures. The DMSO content in the first coordination sphere of the ion is slightly larger than that in the bulk, and thus, the calcium ion is slightly preferentially solvated with DMSO over DMF. Solvation of DMF to the calcium ion may be enthalpically more favorable than DMSO because of the weaker intermolecular interactions of DMF molecules than DMSO molecules in the mixtures. On the other hand, entropy of solvation of DMSO may be less negative than DMF. The loss of entropy of DMSO molecules at solvation to the calcium ion is more or less compensated for the entropy gain at the liberation from the structured clusters of DMSO, while more randomly distributed DMF molecules than DMSO lose more entropy at solvation to the calcium ion. Thus, the preferential solvation of the calcium ion by DMSO occurs entropically.

Liquid structures of other binary mixtures as well as preferential solvation structures of other metal ions in mixed solvents will also be presented.

1. Itoh, S.; Ohtaki, H., *Z. Naturforsch.*, 1987, **42a**, 858.

2. Ohtaki, H.; Itoh, S.; Yamaguchi, T.; Ishiguro, S.; Rode, B. M., *Bull. Chem. Soc. Jpn.*, 1983, **56**, 3406; Radnai, T.; Itoh, S.; Ohtaki, H., *Bull. Chem. Soc. Jpn.*, 1988, **61**, 3845.

PREFERENTIAL SOLVATION OF COBALT(II) ION IN AMIDE–WATER MIXTURES

Haruhiko YOKOYAMA, Yutaka TADA, and Makoto TANABE
Department of Chemistry and Graduate School of Integrated Science, Yokohama City University, Kanazawa-ku, Yokohama, 236-0027, Japan

Water and amides such as formamide(FA) are good solvents to dissolve metal salts due to their strong solvation power. Gutmann's donor number gives useful information of the solvation ability for metal ions in single solvents, but the prediction of the preference solvation in mixed solvents may not be simple because of the presence of solvent-solvent interactions. In the present study the preferential solvation of cobalt(II) ion in various amide-water mixtures has been investigated by X-ray diffraction method. Amides used were FA, *N*-methylformamide(NMF), *N,N*-dimethylformamide(DMF), *N,N*-diethylformamide(DEF), *N*-methylacetamide(NMA), *N,N*-dimethylacetamide(DMA), and *N,N*-dimethylpropionamide(DMP). The X-ray diffraction measurements were carried out for pairs of solutions of cobalt(II) and magnesium(II) perchlorates of the same concentration, using the imaging-plate detector equipped with a zirconium filter to remove the fluorescent X-ray due to cobalt ions. Radial distribution functions(RDFs) including only metal-ion interactions with constituents of solution were derived by supposing the Co(II) and Mg(II) solutions to be isostructural, and were in agreement with those obtained in the usual method using a θ-θ diffractometer.[1]

Six oxygen atoms of solvent molecules were located at a distance around 2.1Å from a cobalt ion in RDFs except for DMP-rich mixtures. The distinct peak located around 3.4Å was assigned to carbonyl carbon of amides and analyzed to estimate the average number of amide molecules existing in the first coordination sphere. The order of the preferential solvation power of solvents was determined to be FA>NMF≧DEF>H_2O>DMF≫NMA≈DMA>DMP by comparing the $X_{amide}(1st)/X_{amide}$ values where $X_{amide}(1st)$ and X_{amide} are mole fractions of amide in the first coordination sphere and in bulk solution, respectively. This order appears to be controlled by the structure and the electron acceptor property of solvents. The poor preference of NMA, DMA, and DMP is dominantly due to the steric hindrance by methyl or ethyl group bonded to carbonyl carbon, suggested by the Co-O-C bond angles(134°-138°) larger than 122°-126° for the other amides. Water molecules disturb the coordination of amide molecules to metal ions by hydrogen-bonding to the carbonyl oxygen atoms, while amide molecules having amino-hydrogen atoms interfere with that of water molecules in a similar manner. The latter effect, closely related to the electron acceptor ability of solvents, probably controls the preferential solvation power of amides in amide-water mixtures.

1. Yokoyama,H.;Suzuki,S.;Goto,M.;Shinozaki,K.;Abe,Y.;Ishiguro,S., *Z.Naturforsch.*,1995, **50a**, 301.

GIBBS ENERGIES, ENTROPIES AND ENTHALPIES OF TRANSFER INTO SOLVENTS AND SOLVENT MIXTURES

Gerhard GRITZNER
Institut für Chemische Technologie Anorganischer Stoffe, Johannes Kepler Universität
A-4040 Linz, Austria

Transfer properties of electrolytes and transfer properties of single-ions derived from electrolyte data provide detailed information on solute-solvent interactions. Such data allow the quantification of solvent properties and yield information on the specific interactions of solutes in solvent mixtures.

Statistical method will be employed to learn about the properties of solvents and ions properties which determine the changes in Gibbs energies, entropies and enthalpies upon transfer from one solvent into another. It will be shown that Gibbs energies of transfer are dominated by the bond formation between the solute and the solvent molecules. The different nature of the chemical bond between the coordination sites of the solvents molecules and the solutes results in preferential solvation in solvent mixtures.

A considerable number of single ion transfer properties of cations into solvents and solvent mixtures have been published in recent years. The changes in the entropies of ions from one solvent into another will be accounted for by the interactions of the solvent molecules coordinated to the ion with the surrounding solvent matrix. Preferential solvation will strongly affect the transfer entropies into solvent mixtures. Transfer properties of cations and anions into the solvent mixtures water-acetonitrile, water-dimethylformamide and dimethylformamide-dimethylthioformamides will be discussed.

A model based on bond formation between the solvent molecules and the solutes and on the interactions between the interactions of the coordinated solvent molecules and the surrounding solvent matrix permits a qualitative and in some cases a quantitative interpretation of solvent-solute interactions not only in neat solvents but also in solvent mixtures.

The large amount of solvent parameters available in literature unfortunately resulted in confusion rather than in clarification of the description of solvent-solute interactions. The contributions of solution chemists over the past decades are in danger of being overshadowed by the huge number of solvent parameters proposed in literature. Single-ion transfer properties permit the evaluation of solvent parameters. They allow to account for the discrepancies between solvent parameters relating to Gibbs energy and those based on enthalpy measurements.

SOLVATION, STRUCTURE AND BONDING OF METAL IONS IN SOME NON-AQUEOUS SOLUTIONS

Magnus SANDSTRÖM
Department of Chemistry, Royal Institute of Technology, S-100 44 Stockholm, Sweden

The solvation of metal ions in non-aqueous solvents has a large influence on their properties. Structural or spectroscopic studies on solutions, e.g. by means of X-ray diffraction and EXAFS techniques or vibrational spectra, can be used to bring out specific bonding and coordination properties. In particular for soft metal ions like mercury(II), these effects depend strongly on and can be used as a measure of the Lewis basicity of the solvent for soft-soft Lewis acid-base interactions. Examples from mercury(II), cadmium(II), zinc(II), copper(I) and (II), silver(I), rhodium(III) solvation, etc will be given. Steric properties are also important with bulky solvent molecules, as e.g. with *N,N'*-dimethylpropylene urea. Examples will be given showing the connection between the metal ion- solvent ligand distances and coordination numbers. Of great importance for the properties of a solvent are the intermolecular solvent-solvent interactions, in particular hydrogen bonding, and several solvent polarity scales based on hydrogen bonding properties are in use. Weak hydrogen bonding interactions have been found to be active even in some "aprotic" solvents like *N,N*-dimethylthioformamide, and are probably of greater importance than hitherto realised for solubility, coordination, thermodynamics etc in many solvation processes and for functional groups e.g. in biological systems. A comparison of the ability of hydrogen bonding in the solvents *N,N*-dimethylformamide (dmf) and *N,N*-dimethylthioformamide (dmtf) will be given.

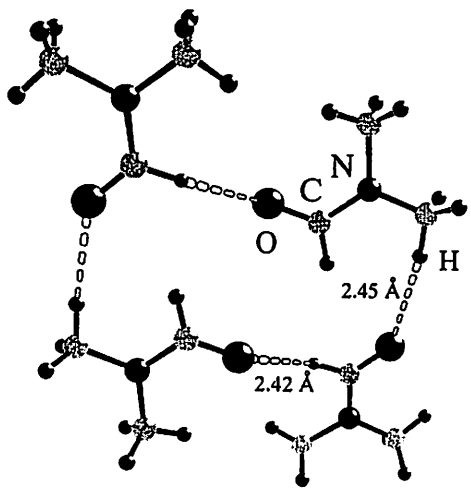

Four-membered ring of dmf molecules

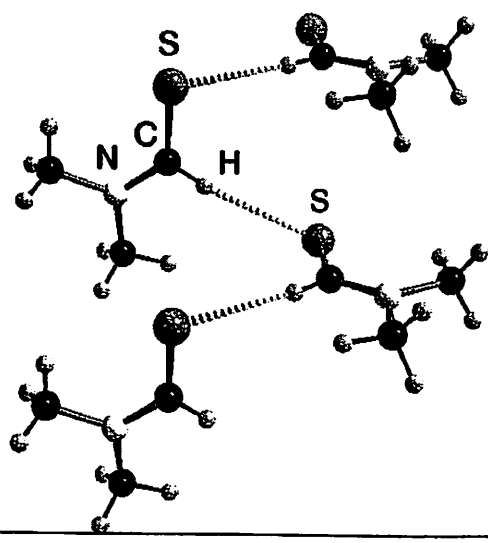

Cooperative hydrogen bonding between dmtf molecules

Solvation Steric Effect and Selective Solvation of Lanthanoid (III) Ions in *N,N*-Dimethylformamide - *N,N*-Dimethylacetamide Mixtures

S. Ishiguro, Y. Umebayashi, K. Kato and I. Mekata
Department of Chemistry and Physics of Condensed Matter, Graduate School of Science, Kyushu University, Hakozaki, Higashi-ku, Fukuoka 812-8581, Japan

Solvation steric effect sometimes plays an important role in chemistry of metal ions in solution. We have so far studied solvation steric effect of a series of lanthanoid (III) ions and the yttrium (III) ion in *N,N*-dimethylformamide (DMF), *N,N*-dimethylacetamide (DMA) and their mixtures from thermodynamic and structural viewpoints.[1-4] Interestingly, it is found for the bromo complexation of these metal ions that an outer-sphere complex is extensively formed in DMF, while an inner-sphere complex in DMA. Furthermore, geometry transition from outer- to inner-sphere bromo complex is observed with increasing DMA content in the DMF-DMA mixture. As complexation behavior depends strongly on the nature of solvation of metal ions, solvation structure has been studied by means of EXAFS and ^{89}Y NMR. It reveals that, for the neodymium (III) ion, the solvation number is kept unchanged up to the DMA content x = 0.8 in the DMF-DMA mixtures, while for the thulium (III) ion with a smaller ionic radius, the decrease of the solvation number starts significantly at lower x. This result indicates that a decrease in the solvation number is not the necessary condition for the transition from outer- to inner-sphere bromo complexation.

Therefore, we then examined selective solvation of lanthanoid(III) ions in DMF-DMA mixture. In order to extract the solvation number of individual solvent in the DMF-DMA mixture, we developed a titration Raman spectrometry system. Raman bands ascribed to a vibration of free and bound solvent molecules are deconvoluted, and the coordination number is finally obtained by analyzing band intensities obtained in solutions of varying concentrations of lanthanoid(III) ions.

Here, we will present a general scope of solvation steric effect of the lanthanoid(III) and yttrium(III) ions studied by calorimetry, NMR and EXAFS, and recent progress on the selective solvation of lanthanoid(III) ions studied by Raman spectroscopy in *N,N*-dimethylformamide, *N,N*-dimethylacetamide and their mixtures.

References:

1) S.Ishiguro, K.Kato, R.Takahashi and S.Nakasone, *Rare Earths*, **27**, 61-77 (1995). 2) S.Ishiguro, K.Kato, S.Nakasone, R.Takahashi and K.Ozutsumi, *J. Chem. Soc. Faraday Trans.*, **92**, 1869-1875 (1996). 3) S. Ishiguro, Y. Umebayashi, K. Kato, R. Takahashi, K. Ozutsumi, *J. Chem. Soc. Faraday Trans.*, **94**, 3607-3612 (1998). 4) S. Ishiguro, Y. Umebayashi, K. Kato, S. Nakasone and R. Takahashi, *Chemical Physics and Physical Chemistry*, **1**, in press.

Raman spectroscopic study on the steric preferential solvation of metal ions in mixed solvents

Yasuhiro UMEBAYASHI, Manabu WATANABE, Shin-ichi ISHIGURO
Department of Chemistry, Faculty of Science, Kyushu University,
Hakozaki, Higashi-ku, Fukuoka, 812-8581, Japan

Aprotic donor solvents *N,N*-dimethylformamide, DMF, and *N,N*-dimethylacetamide, DMA, have similar physicochemical properties such as relative permittivity, ε, donor number, D_N, and acceptor number, A_N. Halogeno and pseudo-halogeno complex formation behavior of metal ions, however, depends strongly on the solvent. The difference is ascribed to steric hindrance of acetyl methyl group of solvated DMA molecules. Solvation steric effect is classified into two groups, *i.e.* ***weak solvation steric effect*** which operates without a significant geometry change or decreasing coordination number, and ***strong solvation steric effect*** accompanying with geometry change or reducing coordination number.[1] In fact, except Zn(II) ions, complex formation of first transition metal ions in DMA is strongly enhanced comparing with that in DMF, though their structures are kept unchanged. Balky aprotic donor solvents such as hexamethylphosphoric triamide, HMPA, and tetramethylurea, TMU, on the other hand, show strong solvation steric effect. In their solutions, metal ions decrease their coordination number and associated with a significant geometry change and remarkable enhancement of complexation.

Now, we have a simple question. ***How does the solvation steric effect operates in mixed solvents?*** In general, coordination number, *C.N.* of metal ions in solution can easily be determined by means of extended X-ray absorption fine structure, EXAFS.[2] However, EXFAS cannot distinguish coordinated atoms provided by different solvent molecules. Raman spectroscopy has a great advantage in this problem. The normal vibration mode of each component of a mixed solvent solution provides the individual solvent *C.N.* of metal ions in mixed solvents. In this presentation, we report Raman spectroscopic study on the individual solvation number of metal ions in mixed solvents, DMF-DMA and DMF-TMU mixtures. The Mn(II) ion in DMF-DMA mixtures shows no appreciable preferential solvation, whilst preferentially solvated by DMF in DMF-TMU mixtures though its D_N is smaller than that of TMU.

1. S. Ishiguro, *Bull. Chem. Soc. Jpn.*, 1997, **70**, 1465.
2. H. Ohtaki and T. Radnai, *Chem. Rev.*, 1993, **93**, 1157.

ANOMALOUS BEHAVIOR OF THE COORDINATION NUMBER CHANGE OF RARE EARTH IONS IN ANHYDROUS METHANOLIC RARE EARTH CHLORIDE SOLUTION

H. Kanno, Y. Yoshimura and S. Namekata
Department of Chemistry, National Defense Academy, Yokosuka 239-8686, Japan

In the previous paper,[1] we reported that the coordination number change takes place in anhydrous alcoholic rare earth chloride solutions. From the frequency change of the Ln-Cl stretching Raman band ($\nu_{Ln\text{-}Cl}$) across the series and the x-ray diffraction data, it is concluded that the coordination number changes from eight for the light rare earth members to seven for the heavy ones. In addition, we have found that the coordination number change shows anomalous chloride concentration dependence: the $\nu_{Ln\text{-}Cl}$ frequency increases with increase in chloride concentration in the solutions of the transition region (Eu ~ Er) where the coordination number change occurs.

In the sequential chloro-complex formation, the $\nu_{Ln\text{-}Cl}$ frequency decreases with increase in the number of coordinated Cl^- ions. Therefore, the $\nu_{Ln\text{-}Cl}$ frequency increase may indicate that the number of the chloride ions coordinated to a rare earth ion decreases with increase in LiCl concentration. Of course, there is another possibility: the equilibrium reaction between the two coordination numbers shifts to the lower coordination number side with LiCl concentration, resulting in the $\nu_{Ln\text{-}Cl}$ frequency increase. In the glassy methanolic $HoCl_3$ solutions, however, the $\nu_{Ln\text{-}Cl}$ frequency decreases with increase in LiCl concentration, which is normal behavior in the sense that higher chloro-complexes are favored at higher LiCl concentrations. Furthermore, the series behavior of the $\nu_{Ln\text{-}Cl}$ frequency changes from the liquid state at room temperature to the glassy state at liquid nitrogen temperature: the former exhibits an extended s-shaped variation while the latter shows an extended z-shaped variation (Fig. 1). We present possible mechanism for this anomalous behavior and compare the results with those for aqueous rare earth electrolyte solutions.

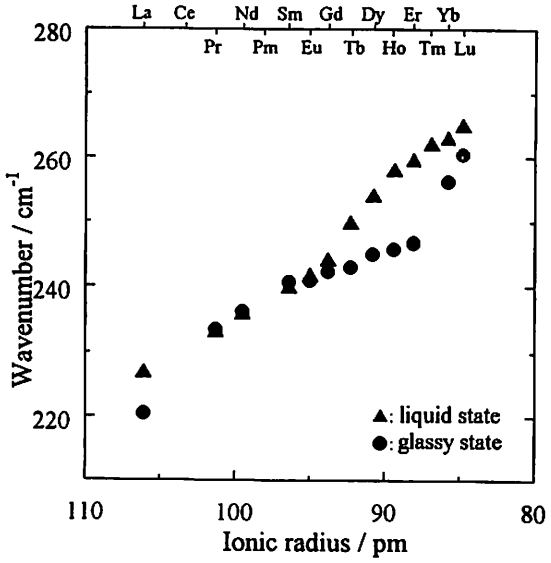

Fig. 1. Variation of the $\nu_{Ln\text{-}Cl}$ frequency across the series.

1. Kanno, H.; Namekata, S.; Akama, Y., *J. Alloy Comp.*, 1998, **275/277**, 868.

NMR STUDIES OF THE POLYETHER COMPLEXES IN NONAQUEOUS SOLVENT

Kiyoshi Sawada, Keiichi Satoh
Department of Chemistry, Faculty of Science, Niigata University, Niigata 950-2181, Japan

The noncyclic polyoxyethylene derivatives (POE compounds) form cationic complexes with the alkali and alkaline earth metal ions and these cationic complexes are distributed to organic solvents with hydrophobic anions in the same manner as cyclic polyether (crown ethers). The study of the complex formation of the noncyclic POE compounds is quite important to understand the interaction of metal ion with the polyoxyethylenes, although the selectivity of their complex formation for cations is inferior to that of crown ethers. That is, the noncyclic polyethers have a flexible structure and the compounds having a long ethyleneoxide (EO) chains are available. We have been studying the thermodynamics, partition and structures of the complexes of cyclic and noncyclic polyethers in nonaqueous solvents. In the present paper, the structures of the POE compound complexes have bees studied by means of H-1 NMR spectrometry.

The NMR spectra of the POE compounds [R-$(OCH_2CH_2-)_n$-OH, R: alkyl or alkylphenyl group] are quite complicated, because the electronic environment of ethyleneoxide groups is quite similar each other. In order to analyze the spectra, H H COSY two dimensional spectra and the spectra of various kinds of derivatives of POE compounds and polyethyleneglycols in dichloromethane-d_2 were measured. An example of the assignment of the signals thus obtained are show in Figure. (Ethyleneoxide region of DEO6; R=$C_{12}H_{23}$, n=6)

The ^{1}H NMR spectra of POE compound complexes of alkaline metal and barium ions at various POE:metal ion ratios. The change of the chemical shift of each proton was determined from the plot of the chemical shift change vs. POE-metal ion ratio. The coordination to the metal ion causes the downfield shift change of the EO proton signals. The effect on the terminal EO is larger than that on middle ones. The water molecules coordinating to the small size metal ion complex affect to the chemical shifts of middle EO protons. The chemical shift change of the barium complexes is much larger than that of alkali metal ions. The effect of counter anion on the chemical shift was studied by using the picrate and sulfonate ions. The position and angle of the picrate ion in the ion pair with the complex cation were estimated from the effect of the ring current of the picrate ion on the chemical shift.

Spin-lattice relaxation time T_1 was measured by means of inversion recovery method. The relaxation time of the EO protons of OH terminal (T_1 = 3.5 s) is much longer than that of middle ones (T_1 = 1.5 s). The relaxation times of all EO protons are shortened by the complex formation and are almost the same among entire EO protons (T_1 = 0.8 s). T_1 of the alkyl group does not change by the coordination. These results offer the direct evidence of the coordination of EO chains to the metal ion.

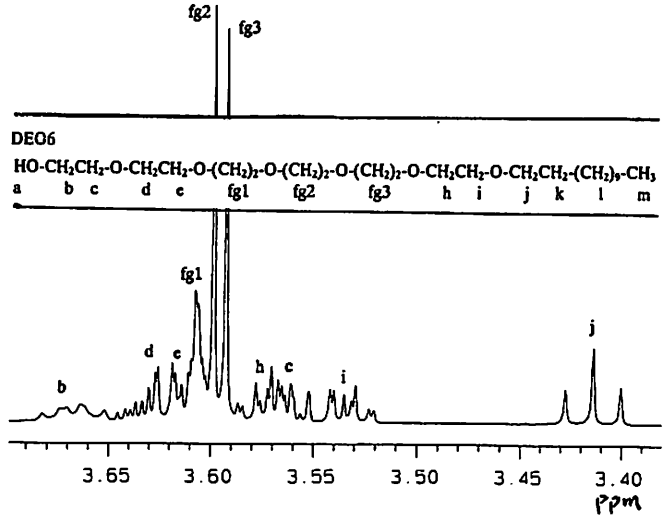

THE WATER MOLECULE AND ITS INTERACTIONS: THE INTERPLAY BETWEEN THEORY, MODELLING, AND EXPERIMENT

John L. FINNEY
Department of Physics and Astronomy, University College London, Gower Street, London WC1E 6BT, UK

Understanding the behaviour of water at the molecular level requires a quantitative understanding of the water molecule and its interactions with other water molecules, and with charged, polar, and nonpolar groups. Since computer simulation methods began to be applied to water in the 1960s, many potential functions have been developed for use in such simulations. The earliest ones tried to take account of the general nature of the hydrogen bonded interaction, usually assuming tetrahedrality, refining the function parameters to give reasonable agreement with known thermodynamic and/or structural data.

As computational power increased, quantum mechanical calculations began to be used to derive potential functions. More recently, in addition to a flood of potential functions, some including manybody terms, *ab initio* simulation methods have begun to be used. Although many current empirical potentials are able to reproduce some of the known behaviour, a case can be made that our understanding of the water molecule and its interactions is not yet sufficient for our modelling to reproduce - let alone explain - much of the subtleness of the water molecule's behaviour in both the pure substance and in solution. For example, we cannot yet explain the phase diagram of ice.

In parallel with increasing computational power, experimental work has begun to play an increasing role in trying to improve our understanding of water interactions. For example, Savage[1] in the 1980s was in effect able to derive experimentally the shape of the - non-spherical - 'van der Waals surface' of the water molecule from crystallographic studies on a range of crystal hydrates, results which were in agreement with quantum mechanical calculations being performed at that time. More recently, neutron diffraction with isotopic substitution, coupled with recently developed modelling procedures such as Soper's empirical potential structure refinement technique[2], has begun to allow us to use experimental data to not only point up some of the deficiencies in current potential functions, but also to lead us to improved representations that can reproduce the behaviour of water molecules in a range of environments and over a range of experimental conditions.

1. Savage, H.J.F., in *Water Science Reviews* (ed. F. Franks), 1986, **2**, 67.
2. Soper, A.K. *Chem. Phys.*, 1996, **202**, 295.

STRUCTURE AND DYNAMICS OF SUPERCRITICAL WATER

M.-C. BELLISSENT-FUNEL
Laboratoire Léon Brillouin, (CEA-CNRS), CEA-SACLAY, Gif-sur-Yvette, 91191, France

Water, the most important solvent in nature, has fascinating properties as a reaction medium in its supercritical state where it behaves very differently from water at ambient conditions. The most interesting property is the high solubility with non-polar organic substances, a property with great application in hazardous waste disposal. The peculiar behavior of supercritical water is thought to be related to the change of the intermolecular structure at elevated temperature, under pressure, especially the change in the hydrogen bond network. This invited lecture reports on the structure and dynamics of supercritical water, at different thermodynamic states, for densities ranging from 0.1 to 0.9 $g.cm^{-3}$, studied by neutron scattering which is a very well appropriate technique.

The variation of the structure factor and of the intermolecular pair correlation function has been investigated as the temperature and the pressure are changed[1]. In combining the results of the neutron isotopic substitution method with that of X-rays[2], it has been possible by using a Monte Carlo Method to reach the partial pair correlation functions[3] $g_{OH}(r)$, $g_{HH}(r)$ and $g_{OO}(r)$. The results are compared with that of molecular dynamics simulations using the extended simple point charge (SPCE) pair potential for water. The results confirm that hydrogen bonding is still present in dense supercritical water and are in good agreement with the recent Raman work of Walrafen et al[4].

H-bond dynamics of supercritical water has been investigated by quasi-elastic neutron scattering from which one got information about translational dynamics and vibrational density of states in supercritical water. The evolution of the width of the quasi-elastic line as a function of the momentum transfer can be described by using a random jump diffusion model. The values of the extracted parameters such as the diffusion coefficient D are in good agreement with that measured by NMR[5].

1. Bellissent-Funel M.-C., Tassaing T., Zhao H., Beyssens D., Guillot B., Y. Guissani, *J. Chem. Phys.*, 1997, 107, 2942.
2. Yamanaka K., Yamaguchi T., Wakita H., *J. Chem. Phys.*, 1994, 101, 9830.
3. Tassaing T., Bellissent-Funel M.-C., Guillot B., Guissani Y., *Europhys. Let.*, 1998, 42, 265.
4. Walrafen G. E., Yang W. H., Chu Y. C., *J. Phys. Chem. B*, 1999, 103, 1332.
5. Lamb W. J., Hoffman G. A., Jonas J., *J. Chem. Phys.*, 1981, 74, 6875.

What is Hydrophobic Hydration?

A.D.J. Haymet
Department of Chemistry and Institute for Molecular Design
University of Houston, Houston, Texas 77204-5641 USA

Water is regarded as an unusual and poorly understood liquid, which possesses a number of anomalous thermodynamic properties: a temperature of maximum density in the liquid phase over a wide range of pressures, an unusually high surface tension, a minimum in the isothermal compressibility as a function of temperature, and a large heat capacity throughout the liquid range. These properties are thought to arise from the ability of water to form tetrahedrally coordinated hydrogen bonds. There remains vigorous debate, however, over the role of hydrogen bonding in the properties of liquid water.

Water is also unusual as a solvent, particularly for nonpolar solute molecules. Unlike simpler solvents, the insertion of nonpolar solutes into water is: (1) strongly unfavorable, (2) strongly opposed by entropy at room temperature, and (3) accompanied by a large positive heat capacity. These properties define the hydrophobic effect. The physical basis for the hydrophobic effect has been the subject of debate. One group holds that the large aversion of oil for water results mostly from the small size of the water molecule, and not from water structuring by the solute. This conclusion arose out of the surprising success of the scaled particle theory (SPT) to account for the free energy of hydrophobic transfers. The proponents of this hypothesis argue that the entropic and enthalpic contributions arising from the structuring of water molecules largely compensate each other. Hence, they proclaim that "structural reorganization is of little importance". Others argue that the large positive heat capacity of insertion of nonpolar solutes is a defining feature of hydrophobicity, and that it results from hydrogen bonding and the ordering of water molecules around the solute. SPT cannot account for this key element. The arguments seem to hinge on whether one assumes that the free energy alone is sufficient to characterize hydrophobic properties of water; or whether one needs to investigate more subtle, derivative properties. We show that the free energy alone masks the underlying physics, and fails to provide predictive power for more complex situations (such as size, shape, and multiple-body effects)[1]. Structural details and mechanisms must be understood before further predictions can be made on these systems.

We have developed a simplified model [2] of the hydrophobic effect, with molecular details stripped away. We show that much of the behavior of pure water, and of the hydrophobic effect, is simply due to a balance between Lennard-Jones interactions and orientation-dependent hydrogen bonding. No other electrostatic terms are included explicitly. Our simple, two-dimensional "toy" model captures the physics and chemistry, not the most-realistic model of the geometry. Its limitations are that it gives up atomic structural detail, and three-dimensionality, but it uses only few parameters, and is computationally simple enough to explore properties that are difficult to study in more realistic models.

1. "Hydrophobic Hydration: Heat capacity of solvation from computer simulations and from an information theory approximation", Arthur, J.W.; Haymet, A.D.J., *Journal of Chemical Physics*, 1999, **110**, 5873 - 5883.

2. "Hydrophobicity in a simple model of water: 1. Solvation and bulk properties", Silverstein, K.A.T.; Haymet, A.D.J.; Dill, K.A., *Journal of the American Chemical Society*, 1998, **120**, 3166-3175.

A theoretical Study of Liquid Water Dynamics; Fluctuation, Relaxation and Chemical Reactions

Iwao OHMINE
Department of Chemistry, Faculty of Science, Nagoya University, Chikusa-ku, Nagoya 464-8602, JAPAN

Various aspects of Water Dynamics will be discussed[1]; (1) Fluctuation and Relaxation in Liquid Water and their Observation, (2) Proton Transfer in Liquid Water and Ice, [2] (3) Solvation Dynamics in Supercritical Water, and (4) Mechanism of Water Freezing.

(1) Water has the rugged potential energy surface involving various deep energy minima with different hydrogen bond network structures. Water undergoes the sluggish dynamics on this potential energy surface. In a short time scale liquid water is thus amorphous gel-like, while in a very longer time scale it exhibits diffusional motion as an ordinal liquid. In between these time scales, the hydrogen bond network rearrangement occurs intermittently and locally in space, involving the local collective motions of tens of water molecules accompanied with the large energy fluctuation. The various experimental techniques to observe the effects of intermittent collective motions in water are discussed. Particular emphasis is on the higher-order nonlinear spectroscopies since these methods deal with the phase-space dynamics of a system. There have been intensive theoretical investigations proposing to apply the echo-type experiment, *i.e.* the off-resonant fifth order (two-dimensional (2D) Raman) spectroscopy to distinguish the homogeneous and the inhomogeneous elements in liquid dynamics.

(2) Proton transfer in water is assisted by Hydrogen Bond Network Rearrangement (HBNR), making some water molecules three-coordinated. Proton transfer takes place on these three-coordinated water molecules. On the other hand, the protonated water molecule is four-coordinated in ice, but its interaction with the fourth coordinated water molecule is repulsive (while those with first three are attractive); four-coordinated geometrically and three-coordinated energetically. Due to this repulsive interaction with the fourth water molecule, O--(H)--O distances with the other three water molecules become short and thus facile proton transfer can take place even in ice without causing a significant HBNR. [2]

(3) We also analyze the mechanism of the water molecule dissociation. A water molecule dissociates to H^+ and OH^- (ionic channel) in liquid water. In the gas phase, however, water is known to separate into two radicals, $H^\cdot$ and $OH^\cdot$. This radical channel is about 290 kcal/mol more stable than the ionic channel. In water the ion channel is extensively stabilized by hydration and thus water yields pH = 7. It is also found that in super-critical water the hydration is stronger than in water in spite of the fact that water molecular density is smaller, and hence the ionic channel becomes even more stable.

(4) We have investigated the freezing mechanism of liquid water was investigated by using molecular dynamics simulation. Placing a small ice-structured unit in a center of a simulation box, the processes of forming a well-ordered hydrogen bond network around it were monitored. It was found that crystallization suddenly takes place after certain induction-time. Various analyses were made to find how the hydrogen bond network grows in this freezing mechanism.

1. I. Ohmine and H. Tanaka, *Chem. Rev.* 93, 2545 (1993);
I. Ohmine, *Feature Article in J. Phys. Chem.* 99, 6767 (1995);
I. Ohmine and S. Saito, *Account of Chemical Reseach* (1999) in press
2. C. Kobayashi, K. Iwahashi, S. Saito and I. Ohmine, *J. Chem. Phys.* 105, 6358 (1996);
C. Kobayashi, S. Saito and I. Ohmine (to be published)

WATER STRUCTURE: GLASSY, NORMAL, AND HTHP WATER

Toshio YAMAGUCHI
Department of Chemistry, Fukuoka University, Fukuoka 814-0180, Japan

Direct structural information of water is obtained through radial distribution functions, OO, OH, and HH, from X-ray and neutron diffraction and computer simulations.

Recent efforts of structural investigations of water by using these techniques have been devoted to water under extreme conditions, such as glassy, supercooled, subcritical and supercritical water, to understand the nature of hydrogen bonding in water, which plays an essential role in various unique properties of water.

Several topics in structure of water will be described, such as low-density and high-density amorphous ice, supercooled water, and subcritical and supercritical water, from which the structure of ambient water will be discussed.

H. Ohtaki, T. Radnai, and T. Yamaguchi, *Chem. Soc. Rev.*, 41 (1997).
M.-C. Bellissent-Funel, *Europhys. Lett.*, **42**, 161 (1998).
A. K. Soper, F. Bruni, and M. A. Ricci, *J. Chem. Phys.*, **106**, 247 (1997).
O. Mishima and H. E. Stanley, *Nature*, **392**, 164 (1998).
N. Yoshii, S. Miura, and S. Okazaki, *J. Chem. Phys.*, **109**, 4873 (1998).

HYDROGEN BONDS BETWEEN WATER MOLECULES: THERMAL EXPANSIVITY OF ICE AND WATER

Hideki Tanaka
Department of Chemistry, Faculty of Science, Okayama University, 3-1-1 Tsushima Okayama 700-8530 Japan

The free energies of two low pressure ice forms are calculated over a wide range of temperatures in order to explain relative stability and their negative thermal expansivities in low temperature regime. Hundred proton-disordered configurations for hexagonal and cubic ices are generated. The Helmholtz free energy is approximated to sum of the minimum potential energy, the harmonic free energy and the configurational entropy arising from the disordered nature of protons. The Gibbs free energy at a given temperature is minimized with respect to the volume of the system. This enables us to evaluate the thermal expansivity at fixed temperature and pressure from only intermolecular interaction potentials. The negative thermal expansivity of ices in low temperature is successfully reproduced. This method is applied to amorphous ice and ice VII, the latter of which has the closest packing among ice polymorphs made from water *molecules*. It is found that low pressure amorphous ice exhibits a similar behavior as hexagonal and cubic ices but the expansivity of ice VII is always positive.

The dilation of the volume from the equilibrium position at 0 K induces normally the shift of mode frequency to lower side so that the vibrational free energy becomes lower while the interaction energy becomes higher. The volume is determined by those two different contributions. However, frequencies of some modes must have different volume dependence in order for the thermal expansivity to change its sign in low pressure ices. We calculate mode Gruneisen parameters to examine their positivity.[1-3] We found that the bending motions of three hydrogen-bonded molecules are responsible for the anomalously negative mode Gruneisen parameter with large mode heat capacity at low temperature.

We will also mention the origin of the large thermal expansivity of clathrate hydrates compared with low pressure ices.[4]

1. H. Tanaka and I. Okabe, *Chem. Phys. Lett.* **259**, 593 (1996).
2. H. Tanaka, *J. Chem. Phys.* **108**, 4887 (1998).
3. H. Tanaka, *J. Mol. Struc.* **461/462**, 561 (1998).
4. H. Tanaka, Y. Tamai, and K. Koga, *J. Phys. Chem.* **B 101**, 6560 (1997)..

Poster Presentations

DYNAMICAL PROPERTIES OF ELECTROLYTE SOLUTIONS FROM BROWNIAN DYNAMICS SIMULATIONS

Marie JARDAT[1], Olivier BERNARD[1], Gerald R. KNELLER[2], Claude TREINER[1] and Pierre TURQ[1]
[1]Laboratoire Liquides Ioniques et Interfaces Chargées, Université P. et M. Curie, boîte 51, 4 place Jussieu, Paris Cedex 05, 75252, France
[2] Centre de Biophysique Moléculaire, CNRS, rue Charles Sadron, Orléans, 45071, France

The dynamics of charged particles in aqueous solutions has been studied in the framework of the continuous solvent model by using Brownian dynamics simulations. Transport coefficients of simple electrolyte solutions (KCl between 0.1 and 2 mol/L) have been firstly computed, and compared to experimental data. The simulation method has been then applied to more complex systems: aqueous cryptate solutions. In the latter case, the experimental conductivity has been measured and compared to simulation results.

Both direct and indirect interactions are taken into account in the simulations: the first ones are modelled by a pairwise effective interaction pair potential and the second ones, the hydrodynamic interactions, are evaluated by using the Rotne-Prager tensor. The Brownian dynamics method includes a smart Monte Carlo algorithm, which allows one to use long time steps and to generate trajectories of several ns in total[1].

It has been shown that hydrodynamic interactions turn out to be crucial to obtain transport coefficients in agreement with experimental data[1,2]. In particular, the self-diffusion coefficients are slightly enhanced and the conductivity is lowered when hydrodynamic interactions are taken into account.

1. Jardat, M.; Bernard O.; Turq P.; Kneller G. R.,*J. Chem. Phys.*, 1999 (under press).
2. Jardat, M.; Durand-Vidal S.; Turq P.; Kneller G. R., .*J. Mol. Liq.*, 1999 (under press)

"Molecular dynamics simulations of aqueous KF solutions, structure breaking effect."

by Y. Laudernet[1], T. Cartailler[1], P. Turq[1], M. Ferrario[2]
[1] *LI2C, CC51, Université P&M Curie, 75252 Paris Cedex 05, France*
[2] *Dipartimenta di Fisica, Univerita degli studi di Modena, 41100 Modena, Italia*

Structural properties of aqueous KF solutions have been studied by molecular dynamics simulations, in isothermal-isobaric ensemble at 298 K. For each concentration, we have used the extended simple point charge (SPC/E) model for water. Density, energy and radial distribution functions have been calculated for highly concentrated solutions (5.500M, 8.405M and 14.120M) and compared to calculated pure water ones. For different KF concentrations, intermolecular O-H radial distribution functions differ, as well as water-water interaction energies, underlining the structure breaking effect of salt. This last effect is quantified by calculating, for both pure water [1] and aqueous solutions, the water-water energies, for a O-O cut-off distance lesser than 3.85 Å. We find decreasing peacs, at -10.0kT, with increasing concentration. Concurrently, we observe increasing peacs, at +3.3kT, with increasing concentration, which do not exist in pure water. This effect may be interpreted as the structuration of water by solvation.

[1] M. Ferrario, A. Tani Chem. Phys. Lett. **121**,182 (1985)

Does the Plasma Oscillation Exist in Concentrated Electrolyte Solutions ?

Taro DODO[1] and Masao SUGAWA
Department of Physics, Faculty of Science, Ehime University, Matsuyama 790-8577
[1]Present address : Eifuku 4-26-7, Suginami-ku, Tokyo 168-0064, JAPAN

The electrical conductivity of alkali halide aqueous solutions increases as the concentration increases and has a maximum at about 5 normal and then *decreases* as the concentration increases. This kind of curious and interesting behaviour of the electrical conductivity is seen in many kind electrolyte solutions. The electrical conductivities of alkali halide in methanol, butanol, and amyl alcohol show maxima at the concentrations of 1.5, 1.0 and 0.85 normal, respectively. Note that the specific dielectric constants of water and these alcohols are 80, 33, 18 and 14, respectively and the Coulomb force between ions is inversely proportional to the dielectric constant ε. This behaviour suggests that mainly the Coulomb interaction between ions governs the electrical conductivity of the concentrated electrolyte solutions. Then, highly concentrated solutions were treated as mass of charged particles interacting with strong Coulomb force (Coulomb interaction energy > thermal energy; *Strongly Coupled Plasma*[1]). The concentration and temperature dependences of electrical conductivities of alkali halide solutions were explained[2] successfully from the above plasma model.

The plasma oscillation, a collective density fluctuation of charged particles, is the characteristic feature of plasma. Radio waves are reflected from or pass through the ionosphere plasma of the earth either their frequencies are below or above the plasma frequency of the ionosphere. The plasma frequency $\omega_p = (n_i e^2/\varepsilon M_{eff})^{1/2}$, where $M_{eff}^{-1} = M+^{-1} + M-^{-1}$ and M+ is positive ion mass, of LiCl aqueous solution of 10 normal is estimated as 700GHz ~1.5THz. The transmitted intensity of far infrared radiation through[3] or reflected intensity from 2~13 normal LiCl solutions were measured in a frequency range 300GHz ~ 1.5THz. Distinct increase of transmitted or decrease of reflected radiation at some frequency were not observed in the surveyed parameter range. It is concluded that the plasma oscillation can not exist in the alkali halide aqueous solutions because of disturbance caused by water. A molecular-dynamics study[4] of molten salt (LiCl) has shown that charge-charge structure factor has a spectral peak at the plasmma frequency. The temperature dependent data of electrical conductivity of molten alkali halides as a function of strongly coupled plasma parameter were alligned beatifully on a single line irrespective of ion species[2].

1. Ichimaru,S. ; Rev. Mod. Phys. **54**(1982)1017.
2. Dodo,T.,Nakagawa,T.A.,Nonaka,E. ; Jpn. J. Appl. Phys. **32**(1993)1236.
3. Dodo,T.,Sugawa,M.,Nonaka,E. ; J. Chem. Phys. **98**(1993)5310.
4. Okazaki,S., Miyamoto,Y., Okada,I. ; Phys. Rev. **B 45**(1992-I)2005.

MOLECULAR DYNAMICS SIMULATION OF BUBBLE FORMATION IN MICROPORES

Tomoyuki Kinjo[1], Guangtu Gao[2] and X.C.Zeng[2]

[1]Department of Engineering Physics and Mechanics,
Kyoto University, Sakyo-ku,Kyoto, 606-8501, JAPAN
[2]Department of Chemistry, University of Nebraska-Lincoln,
Nebraska-Lincoln, USA

We performed molecular dynamics simulations to study the molecular mechanism of bubble formation of confined liquids in slit microscopic pores. The slit pore consists of two flat, semi-finite solid walls separated by a distance h in the direction z. The intermolecular forces in the fluid were modeled with a Lennard-Jones 12-6 potential

$$\phi_{\mathrm{LJ}}(r) = 4\epsilon \left[\left(\frac{\sigma}{r}\right)^{12} - \left(\frac{\sigma}{r}\right)^{6} \right], \tag{1}$$

The fluid-solid interaction at one wall was a Lennard-Jones 9-3 potential [1]

$$\phi_{\mathrm{wall}}(r) = \frac{2\pi}{3}\rho_{\mathrm{w}}\sigma_{\mathrm{w}}^{3}\epsilon_{\mathrm{w}} \left[\frac{2}{15}\left(\frac{\sigma}{z}\right)^{9} - \left(\frac{\sigma}{z}\right)^{3} \right], \tag{2}$$

where ρ_{w} and ϵ_{w} are the density of atoms in the solid wall and the well-depth of the fluid-solid interaction. Three kinds of wall interaction were selected: weakly adsorbing wall (WAW), moderately adsorbing wall (MAW) and strongly adsorbing wall (SAW). The width of the slit pore ranges from about five (the narrow pore) to twenty-four (the wide pore) molecular diameters. We prepared equilibrated liquid states for each systems, and quench or expand them to make metastable states. Markedly different bubble formation behavior is found in pore with WAW, MAW and SAW, for both the narrow pore or wide pore.

References

[1] J.-P.Hansen and I.R.McDonald (1986). "Theory of Simple Liquids" Academic Press, London

CONCENTRATION FLUCTUATION IN 1-PROPANOL AQUEOUS SOLUTION BY MD SIMULATION

N. OHTORI, I. AKIYAMA, K. IGARASHI and K. TAKASE
Graduate School of Science and Technology, Niigata University, Niigata 950-2181, Japan

1-propanol mixed with water forms single-phase aqueous solution at any proportion similarly to methanol and ethanol. A considerable concentration fluctuation will, however, be expected for it since the solution added with a salt[1] and 1-butanol solution without any salts separate into two phases at a given range of composition and temperature. We performed molecular dynamics simulation of 1-propanol aqueous solution at molar fractions of 1-propanol, x_P, of 0, 0.05, 0.17, 0.4, 0.5, 0.6, 0.8 and 1. We examined the composition dependence of liquid structure and concentration fluctuation, based on pair correlation functions $g(r)$, distribution functions of coordination number by nearest neighbor, $P(n)$, and snapshots mainly for O_P and O_W which denote the oxygen atoms of 1-propanol and water molecules, respectively.

All the first peak values of $g(r)$s for O_P-O_P, O_W-O_W and O_P-O_W pairs increased notably with x_P. The behavior for O_W-O_W indicates hydrogen bonds between water molecules considerably remain even at $x_P = 0.8$. The sum of $P(n)$ for O_W-O_W over $n \geq 1$ was more than 0.5 even at $x_P = 0.8$. Moreover, the $g(r)$ for O_W-O_W at $x_P \geq 0.17$ decayed with oscillation $r \geq 4$ Å and the g at $r = 10$ Å decreased as the x_P increased: $g = 0.8$ at $r = 10$ Å and $x_P = 0.8$. These results indicate there exist relatively dilute spatial regions with respect to 1-propanol. The obtained snapshots visualize this picture clearly as shown in Fig. 1. The correlation for O_P-O_W became stronger at higher x_P in spite of the aggregation of water molecules, which suggests 1-propanol and water molecules interact with each other by hydrogen bond between the relatively dilute and concentrated regions. On the other hand, with decreasing x_P, the $g(r)$ for O_P-O_P decreased whereas that between methyl groups increased. At $x_P = 0.05$ the sum of $P(n)$ for O_P-O_P over $n \geq 1$ was only *ca.* 0.1 nonetheless that between methyl groups was more than 0.5. These results imply 1-propanol molecules behave like an extremely small micelle in the dilute aqueous solution.

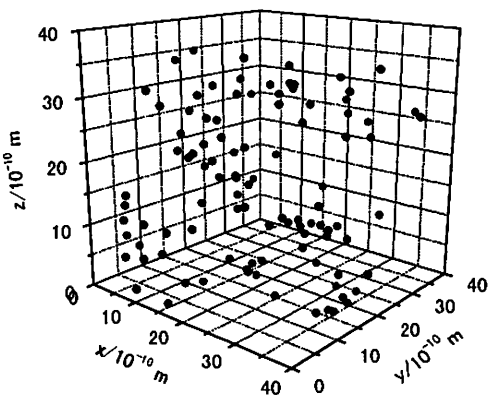

Fig. 1 Snapshot for O atoms of water molecules at $x_P = 0.8$.

1. G. M. Schneider, *Ber. Bunsenges. Physk. Chem.* 1972, **76**, 325.

NONPOLAR SOLVATION DYNAMICS IN THE LENNARD-JONES FLUID

T. YAMAGUCHI, Y. KIMURA, and N. HIROTA
Department of Chemistry, Graduate School of Science, Kyoto University, Kitashirakawa-Oiwakecho, Sakyo-ku, Kyoto, 606-8502, Japan

1. Introduction Solvent fluctuation plays a crucial role in both the static and the dynamic properties of the solute. Due to the rapid developments of the laser technologies, the solvent fluctuation felt by a solute is now experimentally accessible in a time scale of femto second. In these experiments, the fluctuation of either the electronic or the vibrational transition energy is probed, which is called 'solvation dynamics'. Since the polar solvation dynamics (the dipole moment of the solute changes on transition in the polar solvent) is easily observed in experiment due to its large magnitude, the polar solvation dynamics is understood well nowadays. However, our understanding of the nonpolar solvation dynamics is less satisfactory due to its experimental difficulty, and the fundamental concept (i.e. diffusional or viscoelastic) is not solid. Therefore, we devised a molecular dynamics simulation to study the nonpolar solvation dynamics in simple fluids such as the Lennard-Jones (LJ) fluid.

2. Method The system consists of one solute and 499 solvent particles that interact with each other through the LJ potential. The solute-solvent interaction is the same as that of the solvent-solvent interaction in the ground state of the solute, and it increases by the attractive or the repulsive parts of the LJ potential (in the sense of WCA) when the solute is excited. Equilibrium NVT-constant simulations are performed and the time correlation functions of the fluctuation of the transition energy of the solute (solvation correlation functions) are calculated. Keeping the temperature at T=1.5 in the LJ reduced unit (higher than the critical temperature T_c= 1.3), the density of the fluid is varied from the gas-like to the liquid-like ones.

3. Results Figure 1 shows the solvation correlation functions at various densities when the attractive part is changed on excitation. The relaxation rate clearly increases with an increase of the solvent density, which contradicts with the diffusion-based idea on the nonpolar solvation dynamics.

Fig. 1 Solvation correlation functions

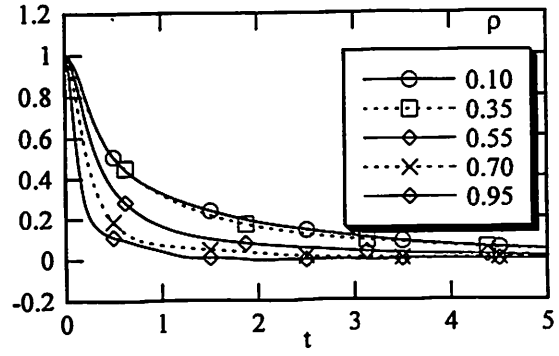

On the other hand, the relaxation time correlates well with the adiabatic sound velocity. We discuss this correlation in terms of the relationship with the static fluctuation and the initial part of the solvation dynamics. The simulations on other systems will be presented at the conference.

COUNTERION-INDUCED CLUSTERING OF MACROIONS

B. Hribar and V. Vlachy
Faculty of Chemistry and Chemical Technology, University of Ljubljana, Aškerčeva 5, Ljubljana, 1000, Slovenia.

Suspensions of charged colloids, solutions of surfactant micelles and other polyelectrolytes play an important role in technology and/or biological processes. The problem of stability of these systems has been considered to be solved in the framework of the DLVO theory[1]. According to this theory, an overlap of the electrical double-layers yields a repulsive interaction and van der Waals forces are responsible for attraction. Some experimental observations e.g., occurrence of large stable voids in homogeneous suspensions and equilibrium separations into two phases are not consistent with the DLVO theory[2-5]. Encouraged by the results of previous studies[6-9] (see[10] for review), we applied the Monte Carlo method to the primitive model solution, containing macroions and counterions. The simulations were performed at constant volume and temperature, with 64 macroions (p) and equivalent number of counterions (c) in the system. The radia of the ions were: r_p = 1.0 nm and r_c = 0.1 nm and the charges were: z_p = -12, and for counterions z_c = +1, z_c = +2 or z_c = +3, respectively. The solvent was treated as a continuum with a dielectric constant equal to that of bulk water at 298 K.
The results for pair correlation functions (pdf) indicate repulsive interaction between the macroions in -12:+1 solutions; these particles are distributed on larger distances from each other. In solutions with divalent ions the macroions share a layer of counterions, but they are not in contact. The results for -12:+3 solutions indicate clustering of macroions: dimers and trimers were observed in solution. Strong correlations yield a nonuniform distribution of macroparticles in solution. The results also reveal a spherically symmetric distribution of monovalent counterions around the macroions in -12:+1 solutions. For -12:+2 solutions, most of the counterions are located in the narrow gap between the two macroions, while for -12:+3 solutions, the highest probability of finding a counterion is in the wedge-shaped space between the two macroions in contact. The contact value of the macroion-macroion pdf (-12:+3 system) first increases with the decreasing concentration, and after passing a maximum, it decreases. Bellow c_p = 0.0005 M no clusters were observed; contact values of the pdf for macroions are close to zero for -12:+3 (as for other) solutions. Simulation results presented in this work show unambiguously, that strong interionic correlations yield an attraction between the equally charged macroions. The correlations depend on the charge densities of counterions and macroions present in the system. Our calculations suggest a mechanism whereby a nonuniform distribution of macroions observed experimentally may occur. These findings may be of importance for understanding practical problems in technology of colloidal suspensions and micellar solutions[11].

1. Verwey, E. J. W.; Overbeek, J. Th., G., Theory of the stability of lyophobic colloids, Elsevier, New York (1948).
2. Ito, K.; Yoshida, H.; Ise, N., *Science, 1994,* **263**, 66.
3. Tata, B. V. R.; Rajalakshmi, M.; Arora, A. K., *Phys. Rev. Lett.*,1992, **69**, 3778.
4. Larsen, A. E.; Grier, D. G., *Nature*, 1997, **385**, 230.
5. Matsuoka, H.; Harada, T.; Kago, K.; Yamaoka, H., *Langmuir*, 1996, **12**, 5588.
6. Kjellander, R.; Marčelja, S.; Pashley, R. M.; Quirk, J. P., *J. Chem. Phys.*, 1990, **92**, 4399.
7. Guldbrand, L.; Jönsson, B.; Wennerström, H.; Linse, P., *J. Chem. Phys.*, 1984, **80**, 2221.
8. Valleau J. P.; Ivkov, R.; Torrie G. M., *J. Chem. Phys.*, 1991, **95**, 520.
9. Hribar, B.; Vlachy, V., *J. Phys. Chem. B*, 1997, **101**, 3457.
10. Vlachy, V., *Ann. Rev. Phys. Chem.*, 1999, **50**, in press.
11. Murray C. A., *Nature*, 1997, **385**, 203.

THEORETICAL INVESTIGATION ON STRUCTURES AND BONDING OF ENVIRONMENTALLY IMPORTANT MERCURY AQUO IONS AND ITS COMPLEXES

S. P. SINHA
SCIENTIFIC RESEARCH & DEVELOPMENT(SRD), 6565 Willowick Place, DAYTON, OH 45459, USA

Mercury and organo-mercuric compounds are extremely hazardous, accumulating in the brain and causing irreversible damage to the nervous system. Methyl mercury cation ($Hg\text{-}CH_3^+$) results as a degradation of mercury compounds, particularly in marine environment. In order to study the behavior of Hg(II) in aqueous solution, we have studied the structure and bonding of its aquo complexes. There is no experimental method available to investigate the structures of the aquo ions. We have carried out theoretical calculations on *mono*, *bis*, *tris*, *tetra* and *hexa* aquo ions of Hg(II) and observed some unusual bonding characteristics. While dichloromercury(II) [Cl-Hg-Cl] is essentially linear and so is dimethyl- mercury [H3C-Hg-CH3], the diaquo ion [$(H2O\text{-}Hg\text{-}OH2)^{2+}$] is non-linear. The angle between the two oxygen is about 118.4°, essentially the same as found in *tris* aquo complex (117.5°). The heats of aquation of Hg(II) ion are as follows: *mono* -109.86, *bis* - 177.43, *tris* -288.67, *tetra* -267.74 and *hexa* -314.08 KCal/mole. We have also studied the aquation of $Hg\text{-}CH_3^+$ cation. The aquo-methylmercury cation is a stable species. Interaction of H3C-Hg-CH3 with water, chloride and carbonate ions are also investigated. These are the main components of marine environment.

Theoretical Studies of the water clusters: $(H_2O)_n^-$ and $M(H_2O)_n$ (M=Li and Na)

Takeshi Tsurusawa[1] and Suehiro Iwata[1]

[1] Institute for Molecular Science, 38 Nishi-Gonaka, Myodaiji, Okazaki, Aichi, 444-8585, Japan

Water cluster anions, $(H_2O)_n^-$, and water clusters containing a group 1 metal atom, $M(H_2O)_n$ (M=Li and Na) were studied with *ab initio* MO methods. In both clusters, we found that in some of the isomers the OH{e}HO structure plays an important role. In the OH{e}HO structure an excess electron in $(H_2O)_n^-$ and an ejected electron from the group 1 metal atom is captured internally by water molecules with their OH bonds (we denote an electron catputed by OH bonds in this way as {e} hereafter).

The experimentally observed ionization threshold energies (ITEs) for the $M(H_2O)_n$ clusters show several peculiar features[1-3]; the observed ITEs are constant for $n \geq 4$, and their limiting value is close to the ionization energy of bulk water, independent of the metal element. To characterize the singly occupied molecular orbital (SOMO) in the calculated isomers, we introduce the indices and classify the isomers into three types; surface (S), quasi-valence (V) and semi-internal (I). The semi-internal cluster has a form of $M(H_2O)_m^+ \cdot (H_2O)_l \cdot (H_2O)_{n-m-l}^-$; the third part $(H_2O)_{n-m-l}^-$ contains a OH{e}HO structure similar to that found in $(H_2O)_n^-$[4]. The structures of the semi-internal type clusters are almost independent of the metal element and their vertical ionization energies converege at n=4 as observed by the experimetalists.

The calculated harmonic vibrational frequencies indecate the strength of the interaction between OH bond and {e} and of the hydrogen bond. The frequency shift for OH{e} is as large as -400 cm^{-1}, which is comparable to the frequency shifts in the OH stretching motion of the single proton donor water molecule within the hydrogen bonding chain of water molecules. For $M(H_2O)_m$, this large shift is found in the similar double proton acceptor water molecules interacting with {e}. We also found the isomers for $(H_2O)_6^-$, which have the double proton acceptor water molecules interacting with {e} and are as stable as the isomers reported by Kim *et al.*[5].

1. Hartel, I.V.;Huglin,C.;Nitsch,C.;Shultz,C.P.,*Phys.Rev.Lett.*,1991,**67**,1767
2. Misaizu, F.; Tsukamoto, K.; Sanekkata, M.; Fuke, K., *Chem.Phys.Lett.*,1992,**188**,241
3. Takasu, R.; Misaizu, F.; Hahimoto, K.; Fuke, K., *J.Phys.Chem.*,1997,**A101**,3078
4. Tsurusawa,T.; Iwata, S.,*Chem.Phys.Lett.*,1998,**287**,553
5. Lee, S.; Kim,J.;Lee,S.J.;Kim,K.S.,*Phys.Rev.Lett.*,1997,**79**,2038

Simulation Studies of Mixtures of Methanol and Carbon Tetrachloride

Philippe A. Bopp[1], Patrick Merkling[2], and M.D.Zeidler[2]
[1]Laboratoire de Physico-Chimie Moléculaire, Université Bordeaux I and CNRS (UMR-5803), 351 Cours de la Libération, F-33405 Talence CEDEX, France
[2] Institut für Physikalische Chemie, RWTH-Aachen, Templergraben 59, D-52056 Aachen, Germany

We have carried out molecular dynamics (MD) computer simulations of liquid mixtures of methanol (CH_3OH) and carbon tetrachloride (CCl_4) at room temperature and mole fractions of x_{CH_3OH}= 0.05, 0.1, 0.3, 0.6, and 1.0. Two interaction models (flexible) have been used, one essentially developed from literature data for the like-like interactions[1,2], and a second one developed from new ab-initio calculations.

We shall focus here our attention mainly on two points:

I) A detailed study on the local structure in the mixtures as a function of composition, also in comparison with data from the literature[3]. Besides radial pair distribution functions (RDFs), an analysis in terms of methanol-clusters and their hydrogen-bonding patterns will be presented. Cyclic clusters are found to play a rather minor role.

II) The determination of the deuterium nuclear coupling constant (QCC) for the hydroxy-Deuterons. Here we use two approaches proposed by Huber et al.[4], one involving ab-initio calculations on configurations extracted from the MD-simulations, and a second one using an empirical formula with fitted parameters. While the absolute values for the QCC are found up to 20% higher than the ones from experiment[5], the concentration dependence is well reproduced by one of the two models; the second one predicts a much weaker dependence.

(1) Pálinkás, G.; Hawlicka, E.; Heinzinger, K., *J.Phys.Chem.* 1987, 91, 4334.
(2) McDonald, I.R.; Bounds, D.G.; Klein, M.L., *Mol.Phys.* 1982, 45, 521.
(3) Veldhuizen, R.; de Leeuw, S.W., *J.Chem.Phys.* 1996, 105, 2828.
(4) Eggenberger, R.; Gerber, S.; Huber, H.; Searles, D.; Welker, M., *J.Chem.Phys.* 1992, 97, 5898.
(5) Ludwig, R.; Gill, D.S.; Zeidler, M.D., *Z.Naturforsch.* 1992, 47a, 857.

MONTE CARLO SIMULATION STUDY OF HYDROGEN-BONDED NETWORKS IN METHANOL AQUEOUS SOLUTION

H. NADA
National Institute for Resources and Environment, 16-3 Onogawa, Tsukuba, 305-8569, Japan

Whether crystal-like structures exist in the solution or not has still been ambiguous, in spite of its importance as an issue of solution chemistry and of crystal growth. In this study, hydrogen-bonded (HB) network structures in methanol aqueous solution were investigated using Monte Carlo (MC) simulations to examine the solid-like molecular arrangements in the HB network structures. It is known that crystals grown from the supercooled methanol aqueous solution change with increasing the methanol concentration (mole fraction, X_M), from ice (X_M<0.56), through water-methanol intermolecular compound (0.56<X_M<0.72), to methanol crystals (X_M>0.72). Therefore, in this study, attention was paid to how the HB network structures in the solution change with increasing the X_M.

The Metropolis sampling method for NPT ensemble was used for the MC simulations. A cubic box with three-dimensional periodic boundary was prepared as a simulation system. The number of molecules included in the system was 250. The temperature and the pressure were set at 298K and 0.1MPa, respectively. The X_M in the system was set with every 0.1 from 0 to 1. The intermolecular potential energies for water-water and methanol-methanol molecules were estimated using a TIP4P model[1] and a model proposed by Haughney *et al.*[2], respectively. The potential energy between water and methanol molecules was estimated using Lorentz-Berthelot combining rules.

The number of HBs in the solution, the size of the HB networks and the molecular arrangements in the networks were analyzed. As a result, it was clearly indicated that the HB network structures drastically change with increasing the X_M. That is, the water-rich networks form at the X_M from 0 to 0.5. However, they drastically changed to the networks including an equal amount of both molecules at the X_M from 0.6 to 0.7. The networks also changed to methanol-rich ones at the X_M from 0.8 to 1.0. It should be emphasized that the X_M dependence of the HB network structure in the solution is much the same as that of the crystal structure grown from the solution. The MC simulation results strongly suggested the existence of the crystal-like structures in the solution.

1. Jorgensen, W.L.; Chandrasekhar, J.; Madura, J.D.; Impey, R.W.; Klein, M.L., *J. Chem. Phys.* 1983, **79**, 926.
2. Haughney, M.; Ferrario, M.; McDonald, I.R., *J. Phys. Chem.* 1987, **91**, 4934.

MOLECULAR DYNAMICS STUDY OF SUPERCRITICAL WATER USING A FLUCTUATING CHARGE MODEL

Noriyuki YOSHII, Ryousuke MIYAUCHI, Shinichi MIURA and Susumu OKAZAKI
Department of Electronic Chemistry, Tokyo Institute of Technology, 4259 Nagatsuta, Midori-ku, Yokohama 226-8502, Japan

In recent years, a number of simulation studies for supercritical water have been reported. Most calculations, there, were based upon fixed charge models assuming a mean electric field on the molecule. The charges on the atoms or interaction sites are constant and thus cannot change in response to the actual electric fields which changes substantially according to the motion of the molecule itself as well as its surrounding molecules.

In the present study, molecular dynamics calculation for supercritical water has been performed using a fluctuating charge model TIP4P-FQ.[1] Since partial charges on atomic sites of the molecule respond to the changing electric field in the fluid, this model is able to describe intermolecular interaction depending on the fluid structure.

First, we improved intermolecular potential function to prevent unphysical behavior of the charge formed in the preliminary calculations. Then, molecular dynamics calculations have been performed for the TIP4P-FQ water at various densities and temperatures in order to determine critical constants of the model and to clarify supercritical region for this model. The critical constants have been evaluated from $P\rho T$-data. They were determined to be T_c = 574 K and ρ_c = 0.33 g/cm^3. Finally, a large-scale molecular dynamics calculation was performed for water near the critical point. The strong intensity of the static structure factor at small wave number region was found. This clearly shows the presence of long-ranged density fluctuation in the supercritical water. Furthermore, the long-ranged and long-time density-density fluctuation in the fluid was analyzed by dynamic structure factor.

1. Rick, S. W.; Stuart, J.; Berne, B. J., *J. Chem. Phys.*, 1994, **101**,6141.

MOLAR EXCESS ENTHALPIES OF LENNRD-JONES FLUID MIXTURES BY MONTE CARLO SIMULATION

Ichiro FUJIHARA1, Mie ASANUMA2, Akio KUBOTA2, Yoshimori MIYANO2 and Koichiro NAKANISHI2
1 Osaka Sangyo University, Daito-shi, Osaka574, Japan
2 Kurashiki University of Science and the Arts, Kurashiki-shi, Okayama712, Japan

Recently, much attention is directed to the industrial application of supercritical fluid(SCF), above all, carbon dioxide. Needs for fundamental studies of SCF are highly recognized. However, experimental approach to SCF is confronted with much difficulties because it involves extraordinary accurate measurements at higher temperatures and pressures. One of the ways to circumvent these difficulties would be the use of molecular simulation.

Interesting problems in applying molecular simulation to SCF studies include the determination of thermodynamic excess functions and dynamic characteristics and both Monte Carlo(MC) simulation and molecular dynamics(MD) calculation can be used. Of various thermodynamic excess functions, the excess volumes(VE) and the excess enthalpies(HE) can be most easily evaluated from NPT ensemble MC calculations.

We have recently carried out extensive MC calculations for model mixtures interacting with Lennard-Jones(LJ) potential in their SCF region(1). Among others, we call attention to the following evidences obtained.

In the case of model mixture named as Lorentz-Berthelot(LB)-2-1 which can be regarded to represent mixtures of nonpolar molecule with weakly polar molecule and nearly equal size, the molar excess enthalpy(heat of mixing) *vs.* molar composition relation at isobaric condition does not show symmetrical "regular solution" like behavior in their SCF region, in spite of the fact that the mixture behaves regular solution like at low temperature and essentially zero pressures(2,3).

B) Furthermore, the magnitude of HE of LB-2-1 model in SCF region is largely positive(endothermic mixing), more accurately, as large as +0.8 kJ•mol. This is to be compared with those at ultra high pressure(up to 4000 atm.) and at essentially zero pressure, which are estimated to be both +0.2 to +0.3 kJ•mol(2,3).

C) Another binary mixture model we studied here is an athermal mixture called At-1-2, for which the energy parameter is common to component and the size parameter is different(1 to 2). This is also a typical example of systems showing "regular solution" like behavior. We have obtained HE values mainly at 180 K and various pressures. Equimolar HE values are slightly positive and almost symmetrical with respect to mole fraction at lower(30 atm.) and higher(1000 atm.) pressures, while drastic change in HE in the SCF region from 60 to 100 atm. has been observed.

It should be mentioned finally that the present observation in MC model calculations is consistent with that obtained by experimental group.

(1)Fujihara, I.; Nakanishi, K.; J. Chem. Phys., 1997, 107, 3121
(2)Fujihara, I.; Nakanishi, K.; Fluid Phase Equi., 1995, 104, 341
(3) Nakanishi, K., et al.; J. Chem. Phys.,1982, 76, 629

COMPUTATIONAL ESTIMATION OF LITHIUM ISOTOPIC REDUCED PARTITION FUNCTION RATIOS OF $[Li(H_2O)_n]^+$

Kazuyo YAMAJI, Yoji MAKITA, Akinari SONODA, Hirofumi KANOH, Takahiro HIROTSU, and Kenta OOI

Shikoku National Industrial Research Institute, 2217-14 Hayashi, Takamatsu 761-0395, JAPAN

We have been interested in the fractionation of lithium isotopes in lithium-isotopic exchange reactions. A lithium-isotopic exchange reaction between an aqueous solution phase and a solid phase is given by eq.1,

$$^6Li^+_{aq} + {}^7Li^+_{solid} \overset{S}{\rightleftharpoons} {}^7Li^+_{aq} + {}^6Li^+_{solid} \qquad \text{eq.1}$$

where S means the lithium isotope separation factor, theoretically represented by reduced partition function ratios (f) as shown in eq.2.

$$\ln S = \ln f_{aq} - \ln f_{solid} \qquad \text{eq.2}$$

In particular, our attention is focused on f_{aq} because the fractionation is mainly due to a great isotopic effect of hydrated lithium ions. According to a theoretical study by Bigeleigen and Mayer[1], the f values can be calculated from frequencies (ν) as shown in eq.3,

$$f = \Pi_i [u_{7i} \exp(-u_{7i}/2)/\{1-\exp(-u_{7i})\}]/[u_{6i} \exp(-u_{6i}/2)/\{1-\exp(-u_{6i})\}] \quad (u_{mi} = h\nu_{mi}/kT) \qquad \text{eq.3}$$

where m denotes a mass number of the lithium element and i denotes a normal mode of vibration.

In this research, we carried out structural optimization and normal vibration analysis of $[Li(H_2O)_n]^+$ by computational chemical methods, an *ab initio* MO method at the RHF/6-31+G(d) level using Gaussian98W and a DFT method at the VWN/DNP using DMol, and made the first attempt to estimate the f values of $[Li(H_2O)_n]^+$ from the wavenumbers.

The Li-O distance in optimized $[Li(H_2O)_n]^+$ increased with an increase in n. From the *ab initio* MO calculation, all of the successive binding energy changes (ΔE_n) for the reaction, $[Li(H_2O)_{n-1}]^+ + H_2O \rightarrow [Li(H_2O)_n]^+$, were negative, where $\Delta E_n = E([Li(H_2O)_n]^+) - E([Li(H_2O)_{n-1}]^+) - E(H_2O)$. Thus, $[Li(H_2O)_4]^+$ is the most stable among $[Li(H_2O)_n]^+$ with n=1-4. The normal vibration analyses were also carried out for optimized molecules for each isotope. Isotopic shifts of $[Li(H_2O)_n]^+$ with n=1-4 appeared between 500 and 700 cm^{-1}, and the corresponding wavenumbers for ^6Li were at least 20 cm^{-1} higher than those for ^7Li. The frequencies were assigned to the normal mode corresponding to the asymmetric stretching of Li-O. The f values of the molecules with n=1-4 optimized by the *ab initio* MO method gave 1.036, 1.062, 1.082 and 1.086, respectively. Similarly the f values with n=1 and 2 by the DFT method gave 1.036 and 1.063 respectively, notably close to those given by the *ab initio* MO method. The f value of $[Li(H_2O)_4]^+$ is close to the value (1.063) derived from the totally symmetric stretching frequency of $Li^+(H_2O)_4$ in the literature[2]. The results will provide a foundation for the design of new materials with a high efficiency for separation of lithium isotopes.

1. Bigeleisen, J.; Mayer, M. G. *J. Chem. Phys.*, 1947, **15**, 261.

2. Oi, T., *Proc. Int. Ion Exch.*, 1995, 147.

Quantum Spin Dynamics in Solution: Effects of External Magnetic Field

H. Nagao[1], K. Kinugawa[2], Y. Shigeta[1], K. Ohta[3] and K. Yamaguchi[1]
[1]Department of Chemistry, Graduate School of Science, Osaka University, Toyonaka, Osaka 560-0043, Japan
[2]Department of Chemistry, Nara Women's University, Nara 630-8506, Japan
[3]Department of Optical Materials, Osaka National Research Institute, Ikeda, Osaka 563-8577, Japan

Molecular dynamics (MD) simulation is a technique to compute the equilibrium and transport properties of a classical many-body system. In this context, the word "classical" means that the nuclear motion of the consistuent particles obeys the laws of classical mechanics. This is an excellent approximation for a wide range of materials and MD simulations are in many respects very similar to real experiments. The ab initio molecular dynamics (AIMD) method pioneered by Car and Parrinello[1] enables one to study the dynamics of condensed phase systems where the internuclear forces are obtained not from fitted potential functions but from the instantaneous ground-state electronic density from density functional theory (DFT). For quantum dynamics, the path integral-based centroid molecular dynamics (CMD)[2] method has been shown to be capable of simulating the dynamics of complicated many-body systems, even for reasonably long times, albeit approximately.

Recently, CMD has been extended to the ab initio CMD (AICMD) method[3], and Pavese et al. have shown some initial results for a 13-atom system which consists of a wire of four water molecules plus an excess proton ($H_9O_4^+$). Centroid properties have also been discussed in relation to Boson or Fermion system[4,5] and path integral molecular dynamics (PIMD) and CMD simulations have been performed for ^{4}He and ideal Bose gas, respectively[4].

In this study, we present a CMD method with nuclear spin space to study quantum spin dynamics in solution. We can expect that when the total effective nuclear spin is a half-interger spin in the extistence of an external magnetic field, the magnetic quantum tunneling rate vanishes as the tunneling events[6] for the electronic spin of Mn_{12} cluster and will discuss the quantum spin dynamics in relation to the quantum computing.

1. R. Car and M. Parrinello, *Phys. Rev. Lett.* 55(1985)2471.
2. J. Cao and G. A. Voth, *J. Chem. Phys.* 99(1993)10070.
3. M. Pavese, D. R. Berard, and G. A. Voth, *Chem. Phys. Lett.*, 300(1999)93.
4. K. Kinugawa, H. Nagao, and K. Ohta, *Chem. Phys. Lett.* in press.
5. P-N. Roy and G. A. Voth, *J. Chem. Phys.*, 110(1999)3547.
6. H. Nagao, S. Yamanaka, M. Nishino, Y. Yoshioka, and K. Yamaguchi, *Chem. Phys. Lett.* 302(1999)418.

Cooperative electron and proton transfer(CEPT) in a pseudo one-dimensional hydrogen bonded network system.

Y. Shigeta, H. Nagao, Y. Yoshioka, J. Toyoda. K. Nakasuji and K. Yamaguchi
Department of Chemistry, Graduate School of Science, Osaka University, Toyonaka 560-0043, Japan.

Water is the most abundant compound on the surface of the Earth and it is the principal constituent of all living organisms. In ice or liquid water, there exists a complex hydrogen bonding network. Particular, structure of ice I is hexagonal and ice I has three dimensional hydrogen bonding structure. Every water molecule is hydrogen bonded to its four nearest neighbors. The proton transfer(migration) occurs cooperatively in the three dimensional network. Theoretical approaches of the proton transfer are mainly based upon the molecular dynamics method and its applications have been carried out with successful results.

On the other hand, intra- and inter- molecular proton transfer reactions play an important role not only in the condensed matter but also in the biological systems. One of the most notable phenomena in the systems is phase transition with respect to the cooperative proton and electron transfer(CEPT) reaction, which are observed in quinhydrone and quinone crystals [1] or the DNA double strand [2,3].

We present a tight binding band structure calculation and its extension to include the electron correlation effects of a model system for the quinhydron crystal. We investigate a relation between pressure induced conductivity of the system and the electron correlation from the phase diagram of the band structure. We will discuss an analogue of CEPT in other systems, for example, in the ice I.

1. K. Nakasuji, K. Sugiura, T. Titagawa, J. Toyoda, H. Okamoto, K. Okaniwa, T. Mitani, H. Yamamoto, I. Murata, A. Kawamoto and J. Tanaka, *J. Am. Chem. Soc.* **113**, 1863(1991).
2. E. Meggers, M. E. Michel-Beyerle and B. Giese, *J. Am. Chem. Soc.* **120**, 12950(1998).
3. I. Saito, T. Nakamura, K. Nakatani, Y. Yoshioka, K. Yamaguchi and H. Sugiyama, *J. Am. Chem. Soc.* **120**, 12686(1998)

PATH INTEGRAL INFLUENCE FUNCTIONAL STUDY OF MULTIPHONON PROCESSES IN VIBRATIONAL ENERGY RELAXATION OF CN^- ION IN THE AQUEOUS SOLUTION

Motoyuki SHIGA and Susumu OKAZAKI
Department of Electronic Chemistry, Tokyo Institute of Technology,
4259 Nagatsuta, Midori-ku, Yokohama 226-8502, Japan

Influence functional theory has been applied to describe vibrational energy relaxation of molecules in the solution based upon harmonic oscillators bath approximation.

First, an algebraic formula of the perturbative influence functional was presented for a number of quantum bath oscillators $\{q_k\}$ nonlinearly coupled to the system x as $\Sigma_k c_k q_k x + \Sigma_k \Sigma_l c_{kl} q_k q_l x + \Sigma_k \Sigma_l \Sigma_m c_{klm} q_k q_l q_m x$. The approach opens a way to molecular based analysis of multiponon processes making usage of a number of techniques and concepts in the field of path integral and quantum field theory. Based upon the functional, we have also derived a computationally tractable expression for the relaxation time by executing the path integral exactly. The theory is of much higher approximation than Fermi's golden rule including perturbations up to the infinite order.

Next, vibrational energy relaxation of cyanide ion in the aqueous solutions has been investigated. Both the solute (CN^-) and the solvent (H_2O or D_2O) were treated quantum mechanically based upon path integral influence functional formalism assuming harmonic oscillators bath. Single- and multiphonon spectral densities were evaluated numerically from the normal modes of the solvent, *i.e.* the bath phonons, and the linear and nonlinear coupling constants between the C-N stretching coordinate and the phonons for 30 different quenched and instantaneous solvation structures generated by molecular dynamics calculations. The method presented not only the time constant of the relaxation but also information about what sorts of the solvent bath modes are responsible for the relaxation process. We have shown that two-phonon process caused by the nonlinear coupling between the C-N stretching mode and two bath phonons are shown to be mostly responsible for the present system. It was found, too, that the coupling of the system with two bath rotational libration modes and the coupling with bath bending mode and bath rotational libration mode are dominant in the relaxation process in H_2O solution, while, in D_2O solution, the coupling with bath bending mode and bath rotational libration mode is most important.

Quantum Chemical and Molecular Dynamics Studyof the Nitrate/Water System

Michael Probst and Christoph Ebner
Innsbruck University, Institute of General. Inorganic and Theoretical Chemistry

The interaction of nitrate anion with water was studied by means of high-1evel ab-initio calculations. For the binary nitrate-water complex a structure with two hydrogen bonds was found to be the most stable one. It is planar but deviates from C_{2v} symmetry. More symmetric structures and singly hydrogen bonded ones are only slightly higher in energy. An analytical interaction potential was calculated by fitting polynomial parameters to quantum chemically calculated energy points. It shows that interaction between nitrate anion and the hydrogen atoms of water near the NO_3^- plane is preferred over on-top conformations and that the directional specificity of nitrate-water hydrogen bonds is rather low.

Using this interaction potential together with terms accounting for intramolecular flexibility, we have performed NVE molecular dynamics simulations on systems consisting of a few hundred molecules of water and one potassium nitrate ion pair. Hydration shell structure as well as energetical and dynamical properties of the systems were analyzed from simulation runs of 10-50 picoseconds. Details of the hydration shell structure as derived from angular and radial distribution functions are discussed. The small changes in the vibrational frequencies of the hydration shell water molecules indicate that water-water and water-nitrate hydrogen bonds have similar strength.

Intramolecular/Intermolecular Excimer Formation in Dinuclear Metal Complexes

Y. YANO, K. HINO, R. NAKATA, H. SEKIYA and Y. MAEDA
Department of Chemistry, Faculty of Science, Kyushu University, Hakozaki 6-10-1, Higashi-ku, Fukuoka 812-8581, Japan

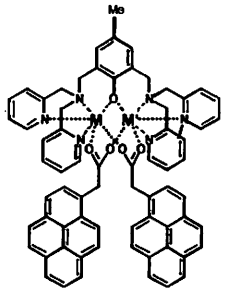

Chart 1 Figure of $[MM'(bpmp)(1\text{-pyac})_2]^{n+}$

The complexes shown in chart 1 were prepared,where Hbpmp is 2,6-bis[bis-(2-pyridylmethyl)-aminomethyl]-4-methylphenol and 1-pyac is 1-pyreneacetic acid (**1**).[1] The intramolecular/intermolecular excimer formation of $[Fe_2(bpmp)(1\text{-pyac})_2](BF_4)_2$, $[FeZn(bpmp)(1\text{-pyac})_2](ClO_4)_2$ and $[Zn_2(bpmp)(1\text{-pyac})_2]ClO_4$ which contain 1-pyreneacetic acid as a chromophore is reported. The fluorescence emission spectra of 1-pyrene acetic acid and its metal complexes were recorded in acetonitrile with the excitation light of 365 nm and are shown in Fig. 1. The spectra of the complexes are different from (**1**) in the intensity and maximum emission wavelength, and are dependent on the nature of the metals. The fluorescence emission spectra are composed of the monomer-like and excimer emissions. The broad excimer emission band pointed at about 490 nm for **ZnZn(1)** is appeared with the strong intensity. The fluorescences of **FeZn(1)** and **FeFe(1)** are very weak in intensity compared to that of **ZnZn(1)**, suggesting that the quenching is due to ferric ions. Formation of an excimer in below 10^{-5} M is believed to result from the intramolecular stacking of chromophores in solvent. Increasing the concentration of the complexes brings about an increase in the formation of the excimer at the expense of monomer-like fluorescence. The observations that the excimer formation takes place predominantly in 10^{-4} M and that it is dependent on the concentration of chromophore are explained by thinking that the formation of micelle/aggregation of the complexes begins in 10^{-4} M: the stacking of two chromophores in micelle/aggregation(enhanced local concentration) brings about the intermolecular emission. Concentration-driven phase transition around the atmosphere of the complexes would be clear by studying the fluorescence of complexes.

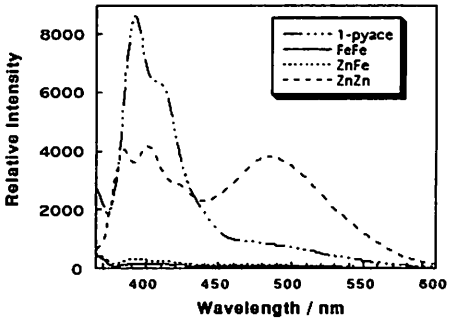

Fig. 1 Fluorescence spectra of the complexes and 1-pyreneacetic acid in acetonitrile (1×10^{-4}M).

1. Y. Maeda, Y. Tanigawa, N. Matsumoto, H. Oshio, M. Suzuki, and Y. Takashima, *Bull. Chem. Soc. Jpn.*, 67, 125-130(1994).

HYDRATION OF CONCAVE HYDROPHOBIC SURFACES

P.-L. Chau

Department of Biochemistry, University of Cambridge, Cambridge CB2 1QW, United Kingdom

Experimental[1] and simulation[2] studies of non-polar solutes in water have shown that the structure and dynamics of water molecules in the immediate vicinity of the solute are altered. However, previous simulation work has used convex[3] or planar surfaces[4] as model systems. As yet, there has been no study of the hydration of concave hydrophobic surfaces. This research aims to investigate the hydrophobic hydration of concave surfaces.

Hemispherical objects of radius from 6.5 Å to 13.5 Å were constructed from tessellated icosahedra[5] where the vertices were hydrophobic "atoms". These hemispheres were hydrated in a periodic box of water, and molecular dynamics simulations in the NVE ensemble were performed on this solution at 320 K. The water molecules were divided into three types: those in the bulk region, those in the first hydration shell of the convex surface, and those in the first hydration shell of the concave surface. The effect of concavity on the structure and dynamics of water molecules in different regions were compared.

[1]E. von Goldammer and H.G. Hertz, *Journal of Physical Chemistry*, 1970, **74**, 3734; K. Hallenga, J.R. Grigera and H.J.C. Berendsen, *Journal of Physical Chemistry*, 1980, **84**, 2381; R. Haselmeier, M. Holz, W. Marbach and H. Weingärtner, *Journal of Physical Chemistry*, 1995, **99**, 2243.

[2]A. Geiger, A. Rahman and F.H. Stillinger, *Journal of Chemical Physics*, 1979, **70**, 263; C. Pangali, M. Rao and B.J. Berne, *Journal of Chemical Physics*, 1979, **71**, 2975.

[3]B. Guillot and Y. Guissani, *Journal of Chemical Physics*, 1993, **99**, 8075.

[4]D.A. Zichi and P.J. Rossky, *Journal of Chemical Physics*, 1986, **84**, 2814; S.H. Lee and P.J. Rossky, *Journal of Chemical Physics*, 1994, **100**, 3334.

[5]P.-L. Chau and P.M. Dean, *Journal of Molecular Graphics*, 1987, **5**, 97.

ON THE EFFECT OF THE SOLVENT NATURE ON THE IONIC SOLVATION AND ASSOCIATION

Igor S. PERELYGIN
Ufa State Aviation Technical University, 12 K.Marx Street, Ufa, 450000, Russia

The IR spectral absorption bands of the anion and solvent molecules, most sensitive to the ion-molecular and interionic interactions, were used to investigate the effect of the solvent nature on the ion association and solvation in the solutions of alkaline and alkaline-earth salts in a wide range of aprotic solvents differing in their physico-chemical nature.

Studied was the effect of different dielectric permittivities and electron-donor capacities of the solvent molecules on the structural diversity of the species formed in the ion associate and solvate solutions, as well as the dependence of this diversity and their relative content on the solution concentration and temperature.

The ion association in solvents that have comparable dielectric permrittivities increases in the order reverse to the electron-donor capacities of their molecules. In a set of solvents with comparable electron-donor capacities the dielectric permittivity effect of the solvent on the ion association is relatively weak compared to the electron-donor capacity t of its molecules. The ion association in solutions depends on the ratio of the electron-donor capacities for the solvent molecules and the anions of the dissolved salt. Those anions having high electron-donor capacities are in competition with the solvent molecules for the site in the cation's coordination shell. The solution temperature effect on the ion association is largely determined by the temperature-dependent variation of the solvent dielectric permittivity.

The character of the changes taking place in the aprotic solvent spectra (the absorption band shifts) caused by the interactions with the cations of the dissolved salts, gives the evidence of appreciable difference in the states of molecules in coordination with cations and in the neat solution. The state of those molecules which solvate cations entering into different ion associates is largely the same as for the molecules solvating free cations.

Ion solvates retain their composition in a wide range of the solution temperature variation.

The details of the dependence on the initial salt concentration and the electron-donor molecular capacities are discussed for the concentration of the free and associated ions as well as the solvent molecules within the solvate complexes of different composition.

NMR STUDY ON ROTATIONAL MOTION OF TETRAMETHYLPHOSPHONIUM ION IN SOLUTION

Haruko Hosoi[1], Akiko Muramoto[2], and Yuichi Masuda[2]
[1] School of Integrated Sciences, Graduate School of Humanities and Sciences, Ochanomizu University, Otsuka, Bunkyo-ku, Tokyo, 112-8610, Japan
[2] Department of Chemistry, Faculty of Science, Ochanomizu University, Otsuka, Bunkyo-ku, Tokyo, 112-8610, Japan

An application of solvent continuum models, such as hydrodynamic and dielectric friction models, is insufficient for representing the rotational relaxation times of small ions, particularly for their solvent dependence, e.g., perchlorate[1] and ammonium[2] ions with ionic radii, r=1.49 and 2.4Å, respectively. The rotational motion of tetramethyl onium ions with larger ionic radius, r=2.93Å will be suitable to probe how solvent, as a continuum or as molecules, produces the rotational friction of an ion.

In the present paper, we present the rotational relaxation times of tetramethylphosphonium ion in various solvents and the results are compared with those for perchlorate and ammonium ions. The rotational relaxation times were obtained from the ^{31}P spin-lattice relaxation rates by the magnetic dipolar interaction between ^{31}P–^{13}C, and the spin-lattice relaxation rates were determined from difference between those rates for the ^{13}C labelled $(^{13}CH_3)_4PI$ and the unlabeled sample.

Figure indicates the rotational relaxation times of tetramethylphosphonium ion in various solvents. As shown in the figure, the obtained rotational relaxation times do not simply follow a hydrodynamic model (Stokes-Einstein-Debye model), and show a fractional power dependence on the solvent viscosity without that in water ($\tau(obs) \propto \eta^{\alpha}$, α=0.54). Such solvent dependence is similar to that for perchlorate ion but the exponent, α, is larger in $(CH_3)_4P^+$ than that in ClO_4^- (α=0.25 for the perchlorate ion).

The rotational relaxation time in water showed a relatively lower value compared with those in other solvents. Such trend is not shown in smaller perchlorate ion and larger alkylammonium ion[3] (alkyl=C_3H_5, n-C_4H_7, n-C_5H_{11}).

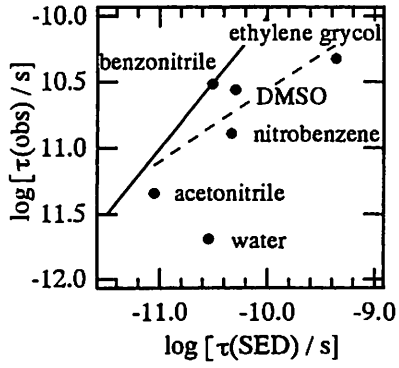

Figure Plot of rotational relaxation times, τ(obs), of tetramethylphosphonium ion against those calculated by SED model at 298 K. $\tau(SED) = \eta(4/3\pi r^3)/kT$, η:solvent viscosity. The solid and the broken lines indicate the calculated values by SED model and the least-squares fitting results except water, respectively.

1 Hosoi, H. Masuda, Y. *J. Phys. Chem. B* **1998**, *102*, 2995.
2 Masuda, Y. The 21th Symposium on Solution Chemistry of Japan. 1998.
3 Masuda, Y. Tobita, J. Muramoto, A. *Bull.Chem. Soc. Japan* **1998**, *71*, 1555.

A neutron diffraction study of intramolecular structure of 2,2,2-Trifluoroethanol in the liquid phase

Imre Bakó[1], Tamás Radnai[1] and Marie C. Bellisent Funel[2]

[1] Department of Chemical Phyics, Chemical Research Center, Budapest Pf.,17, 1525, Hungary

[2]Laboratorie Leon Brillouin (CEA-CNRS) CEN-Saclay 91191 Gif-sur-Yvette cedex, France

2,2,2,-Trifluoroethanol is a peculiar solvent which attracts the interest of chemists of many field due to its unique physico-chemical properties. The intramolecular structure of this liquid has already been studied by the X-ray diffraction (1), electron diffraction and microwave spectroscopic (2) methods as well. Eaerlier. ab initio calculations showed that the most stable rotational isomer is the gauche staggered form.It was also suggested the main association form is the dimer or trimer one in the liquid state

We studied this system by the neutron diffraction method by using isotopic substitution technique. In addition, new ab initio quantum chemical calculations have been performed . Our results show that the structural parameters for the skeleton of the molecules in the liquid phase are similar to those obtained from our ab initio calculations. Since the new calculations were performed on a much more extended basis set compared to the previous one, the good agreement between both theoretical calculations and the experimental results demonstrate that the determination of the main structural form is correct.

1. T.,Radnai,S.,Ishiguro, H.,Othaki., *J.Sol. Chemistry* 1989, 18,771
2. L.,Xu,G.,T.,Fraeser,F.,J.,Lovas,R.,D.,Suenram,C.W.Gillie,H.,E.,Warner,J.,Z.,Gillies, J.Chem.Phys 1995,103,9541

Pressure and temperature effects on the rotational correlation times of water molecules coordinated to monovalent ions

Masakatsu UENO, Junji HORIMOTO, Yoichi KAWABE, Noriaki TSUCHIHASHI, and Kazuyasu IBUKI

Department of Molecular Science and Technology, Faculty of Engineering, Doshisha University, Kyotanabe, Kyoto 610-0321, Japan

Pressure effect on the rotational correlation times (τ_c) of water molecules coordinated to the ions gives us an important information on the ion-water interactions. However, there are only a few studies about the pressure effect on τ_c in aqueous electrolyte solutions.[1,2] Therefore, we measured the spin-lattice relaxation times (T_1) of D nuclei of D_2O molecules in reference (KCl) and other (LiCl, KBr and $LiClO_4$) electrolyte-D_2O solutions at 10, 25, and 45 °C under high pressure up to 300 MPa. T_1' s were measured on JEOL FT-NMR A-300 equipped with a high pressure probe (JEOL) and determined by the inversion recovery method within an error of ±1%.

As shown in Fig. 1, T_1 in LiCl solutions at 10 °C increases with pressure as that in pure D_2O (T_1^0). However, the concentration dependence of T_1 is specific to solutions, and is expressed in dilute solutions by $T_1^0 / T_1 = 1 + Bm$, where B is the NMR B coefficient and indicates the strength of ion-solvent interactions. Assuming an additivity rule of the ionic B coefficient and $B(K^+) = B(Cl^-)$, and applying a two state model,[3] we can obtain the rotational correlation times (τ_c) of water molecules coordinated to the ions under high pressure.

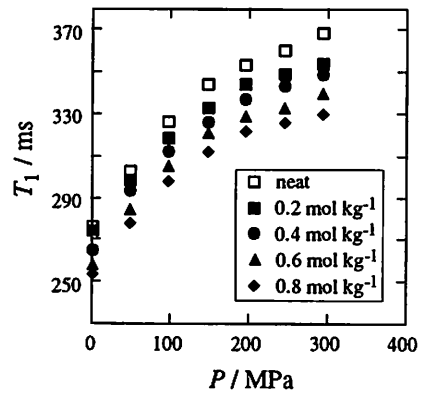

Fig. 1. Pressure dependence of T_1 in LiCl-D_2O solutions at 10 °C.

As shown in Fig. 2, $\tau_c(Li^+)$ is about 2.9 times longer than that of pure D_2O (τ_c^0) at 1 atm, but decreases with increasing pressure as in the case of τ_c^0. It is expected that the ion-solvent interactions are strengthened with pressure and $\tau_c(Li^+)$ increases with pressure. The contradiction suggests that the interactions between water molecules in the first and outer hydration spheres are important in the rotational motion of water molecules in the first hydration sphere. On the other hand, $\tau_c(Cl^-)$, $\tau_c(Br^-)$, and $\tau_c(ClO_4^-)$ show the characteristics of breaking ions: τ_c' s are shorter than τ_c^0 and increase with pressure. These characteristics come to disappear with increasing temperature.

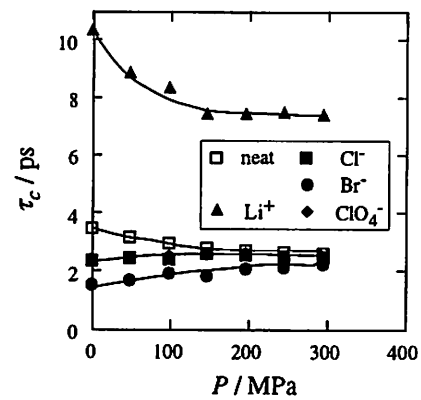

Fig. 2. Pressure dependence of τ_c at 10 °C.

1. Ueno, M. et al., *J. Chem. Phys.*, 1996, **105**, 3662. 2. Ueno, M. et al., *Rev. High Press. Sci. Technol.*, 1998, **7**, 1162. 3. Hertz, H.G., *Water*, ed. by F. Franks (Plenum, 1973), Vol. 3, Chap. 7.

ELEMENT AND SOLVATION STRUCTURE ANALYSES BY TOTAL-REFLECTION X-RAY ABSORPTION SPECTROSCOPY FOR AIR/SOLUTION INTERFACE

Iwao WATANABE[1], Masaharu NOMURA[2], Hajime TANIDA[3], Tomoya URUGA[3], Masao TAKAHASHI[4], and Makoto HARADA[1]
[1]Department of Chemistry, Graduate School of Science, Osaka University, 560-0043, Japan
[2]Photon Factory, Institute of Materials Structure Science, Tsukuba 305-0801, Japan
[3]SPring-8, Japan Synchrotron Radiation Research Institute, Hyogo 679-5198, Japan
[4]The ISIR, Osaka University, 567-0047, Japan

A new method to detect elements at the solution surface has been developed. It is the X-ray absorption spectroscopy (XAS) under the total-reflection condition at solution surface. The penetration depth of X-rays to aqueous solution is less than 10 nm at the incidence angle of 1 mrad (=0.057°) being a half of the critical angle for total-reflection. The X-rays of synchrotron radiation are monochromatized by a double-crystal monochromator and introduced onto a solution surface at a very small glancing angle by adjusting the angles of two mirrors. The X-ray absorption by the elements at the solution surface is detected by measuring total-conversion electron-yield current.

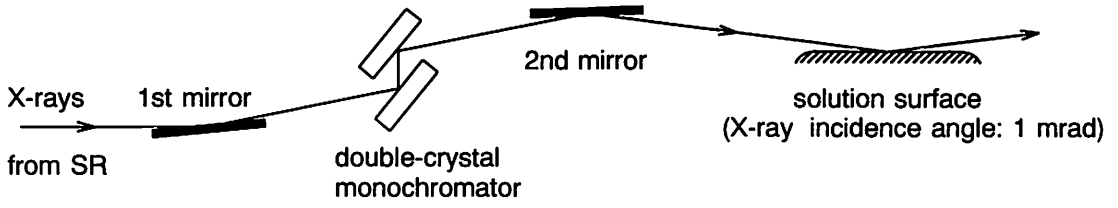

Since each element has its own specific absorption edge energy in the X-ray region, it is possible to perform elemental analysis of liquid surface layer, which is impossible by other known surface sensitive techniques, e.g. visible or infra-red reflectance spectroscopy, SFG or SHG, or surface tension experiments. With this technique surface activity of various molecules and ions can be easily studied. Some of the results will be demonstrated for bromide anions segregated at the aqueous solution surface by surface active alkylammonium cations.

The XAS also provides information on the geometrical structure of a target element (EXAFS and XANES analyses). It is expected that ions at the solution surface may have different solvation structures from those in the bulk. With no surfactant, the metal ions and halide ions so far studied showed identical spectra to those in the bulk, however, some of the ions highly segregated at the solution surface by surfactant did display quite different spectral features indicating different solvation structures at the surface.

EXAFS STUDY OF IODIDE ANIONS IN VARIOUS SOLVENTS

Hajime TANIDA[1] and Iwao WATANABE[2]
[1]Japan Synchrotron Radiation Research Institute (JASRI), SPring-8, Mikazuki, Hyogo, 679-5198, Japan
[2]Department of Chemistry, Graduate School of Science, Osaka University, Toyonaka, Osaka, 560-0043, Japan

Solvation structures for halide anions are not well understood owing to their weak interaction with solvent molecules. The situation is reflected on their hydration numbers as reported to be from zero to seven or eight depending upon methods to determine them. Our previous study on Br^- by EXAFS (Extended X-ray Absorption Fine Structure) method concluded that the method is suitable for determining local structure of the anion dissolved in water or in any other organic solvents, although the EXAFS signals from Br^- are weak and difficult to analyze.[1]

Iodide anion is considered to have even weaker ion-solvent interactions than Br^-, then its solvation structure analysis should be more difficult. This reports the first EXAFS study on I^- in solvents. The I *K*-edge transmission spectra were obtained at BL01B1 station of SPring-8. Figure 1 displays the spectra for 0.1 mol/dm^3 I^- dissolved in several solvents. Their small EXAFS oscillation amplitudes are due to two reasons, firstly weaker interaction of I^- with solvents than other halide anions and secondly short life-time of its core-hole state. Figure 2 shows the interesting correlation of the EXAFS oscillation amplitude with the acceptor number A_N of the solvent. The correlation was already found and reported for Br^- systems.[1] The height h of the peak due to I-O interaction (protic solvents) or I-C (aprotic solvents) in Fourier transform (FT) spectrum, the vertical scale of Fig. 2, is a function of solvation number, ion-solvent distance, and its interaction strength (Debye-Waller-like factor). The result suggests that the EXAFS method is not only a tool to determine geometrical structures in liquids, but can also be used for evaluating solute-solvent interaction strength, similarly to A_N.

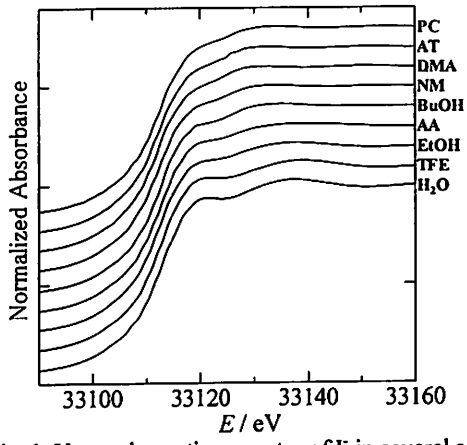

Fig. 1 X-ray absorption spectra of I^- in several solvents.

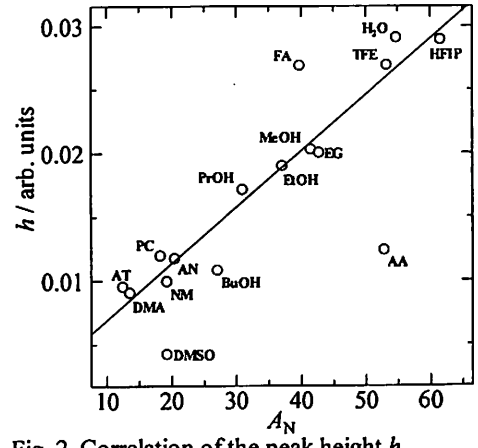

Fig. 2 Correlation of the peak height h in FT spectrum with acceptor number A_N of the solvent.

The solvents are water (**H_2O**), 2,2,2-trifluoroethanol (**TFE**), ethylalcohol (**EtOH**), acetic acid (**AA**), *t*-butyl alcohol (**BuOH**), nitromethane (**NM**), *N*,*N*-dimethylacetamide (**DMA**), acetone (**AT**), propylene carbonate (**PC**), 1,1,1,3,3,3-hexafluoro-2-propanol (**HFIP**), formamide (**FA**), ethylene glycol (**EG**), methyl alcohol (**MeOH**), propyl alcohol (**PrOH**), acetonitrile (**AN**), and dimethyl sulfoxide (**DMSO**).

1. H. Tanida, H. Sakane, and I. Watanabe, *J. Chem. Soc., Dalton Trans.*, 1994, **15**, 2321.

HYDRATION STRUCTURE OF GLYCINE MOLECULE IN AQUEOUS ALKALINE SOLUTIONS

Kentaro SUGAWARA, Yasuo KAMEDA, Takeshi USUKI and Osamu UEMURA
Department of Material and Biological Chemistry, Faculty of Science, Yamagata University, Kojirakawa-machi 1-4-12, Yamagata, 990-8560, Japan

Neutron diffraction measurements for $^{14}N/^{15}N$ and H/D isotopically substituted 2 mol% aqueous glycine solutions in the strongly basic condition have been carried out in order to obtain structural information concerning the hydration structure around both amino and methylene groups within glycine molecule in the $NH_2CH_2COO^-$ form.

Three sample solutions which are identical in all except for different $^{14}N/^{15}N$ and H/D isotopic ratios, a) $(^{14}ND_2CH_2COOD)_{0.02}(NaOD)_{0.02}(D_2O)_{0.96}$, b) $(^{15}ND_2CH_2COOD)_{0.02}(NaOD)_{0.02}(D_2O)_{0.96}$, and c) $(^{14}ND_2CD_2COOD)_{0.02}(NaOD)_{0.02}(D_2O)_{0.96}$, were used in this study. The sample solution was sealed into a cylindrical fused quartz cell (7 mm in inner diameter and 0.55 mm in thickness). Time-of-flight neutron diffraction measurements were carried out at 25°C using the HIT-II spectrometer installed at KENS, Tsukuba, Japan. Data acquisition time was 12h for each sample to keep good statistics. Measurements for an empty cell, vanadium rod (8 mm ϕ), and background were made in advance.

The first-order difference function around the nitrogen atom within the glycine molecule, $\Delta_N(Q)$, was obtained by a combination of the observed scattering cross sections for the sample solutions a) and b). Intermolecular difference function, $\Delta_N^{inter}(Q)$, was derived by subtracting the intramolecular contribution from the observed $\Delta_N(Q)$. Intermolecular structural parameters for interatomic distances, root-mean-square amplitudes and coordination numbers, were determined by the least squares refinement analysis of the observed $\Delta_N^{inter}(Q)$. The first-order difference function around the hydrogen atom of the methylene group in the glycine molecule, was derived by taking a difference between the cross sections observed for sample solutions c) and a). The observed intermolecular difference function, $\Delta_H^{inter}(Q)$ was analyzed using the least squares fitting procedure.

It has been revealed that the nitrogen atom within the amino group forms hydrogen bonds of N-D···OD_2 type with two nearest neighbor D_2O molecules ($r_{N\cdots O}$ = 2.92(7) Å), and forms a hydrogen bond of N···D-OD type with one D_2O molecule ($r_{N\cdots D}$ = 1.97(3) Å) in the present solutions, which are in contrast to the hydration structure around the amino group reported for the aqueous neutral solutions in which the glycine molecule is in the zwitterionic form, $NH_3^+CH_2COO^-$, ($r_{N\cdots O}$ = 2.85(5) Å, $n_{N\cdots O}$ = 3.0(6)).[1] From a least squares fitting analysis of the observed $\Delta_H^{inter}(Q)$ term, the nearest neighbor intermolecular distance and the coordination number around the methylene hydrogen atom were determined to be $r_{H\cdots D_2O}$ = 2.63(1) Å and $n_{H\cdots D_2O}$ = 0.81(6), respectively.

1. Kameda, Y.; Ebata, H.; Usuki, T.; Uemura, O.; Misawa, M., *Bull. Chem. Soc. Jpn.*, 1994, **67**, 3159.

STRUCTURE OF CONCENTRATED AQUEOUS PHOSPHORIC ACID SOLUTIONS

Yasuo KAMEDA, Kentaro SUGAWARA, Takayoshi HOSAKA, Takeshi USUKI and Osamu UEMURA

Department of Material and Biological Chemistry, Faculty of Science, Yamagata University, Kojirakawa-machi 1-4-12, Yamagata, 990-8560, Japan

Raman scattering, X-ray and time-of-flight neutron diffraction measurements have been carried out for highly concentrated aqueous phosphoric acid solutions in order to obtain detailed information on both the intramolecular geometry of the PO_4 unit and the intermolecular hydrogen-bonded structure in the solutions.

Isotropic Raman spectra observed for $(H_3PO_4)_x(H_2O)_{1-x}$, x = 0.1 ~ 0.6, exhibited a single band for the symmetrical stretching vibrational mode of the PO_4 structure unit, the results are in contrast to the case for concentrated aqueous sulfuric acid solutions in which SO_4^{2-}, HSO_4^- and $H_3O^+ \cdot HSO_4^-$ are identified as independent peaks in the S-O stretching region of the observed spectra.[1] The present results for aqueous phosphoric acid solutions indicate that fast proton exchange may occur in the concentrated phosphoric acid solutions.

The molecular geometry of the PO_4 unit in the concentrated aqueous phosphoric acid solution was found to be a regular tetrahedron with intramolecular P-O bond length of 1.539(2) Å, which was determined by a least squares fit to the observed X-ray interference term for aqueous 53 mol% H_3PO_4 solution in the higher-Q region ($9 \le Q \le 17$ Å^{-1}). A least squares analysis of the neutron interference term in the range of $12 \le Q \le 40$ Å^{-1} observed for 53 mol% D_3PO_4 heavy water solution, revealed that the P-O bond length is 1.540(1) Å which is in good agreement with the present X-ray result. Intramolecular parameters within D_3PO_4, r(O-D) = 0.977(1) Å and ∠P-O-D = 113(1)°, were determined.

Structure parameters for intermolecular hydrogen-bonded interactions were obtained by the least squares fit to the observed X-ray and neutron intermolecular interference terms. The observed values of the nearest neighbor intermolecular distances, r(O···D) = 1.77(1) Å and r(O···O) = 2.73(2) Å, are both ca. 0.1 Å smaller than those observed in liquid pure water, indicating that strong hydrogen bonds exist in the concentrated aqueous phosphoric acid solution. The nearest neighbor intermolecular P···P distance, r(P···P), and the coordination number, n(P···P), were determined to be 3.63(2) Å and 3.6(2), respectively. In the present solution, the PO_4 unit is surrounded by on the average four PO_4 units which are hydrogen-bonded. Any indication of $H_5O_2^+$ structure unit which has been found in concentrated aqueous hydrochloric acid solutions,[2] was not observed in the present aqueous phosphoric acid solutions.

1. Ikawa, S.; Kimura, M., *Bull. Chem. Soc. Jpn.*, 1976, **49**, 2051.

2. Kameda, Y.; Usuki, T.; Uemura, O., *Bull. Chem. Soc. Jpn.*, 1998, **71**, 1305.

LIBRATIONAL MOTIONS OF WATER MOLECULES COORDINATED BY METALLIC CATIONS IN CONCENTRATED AQUEOUS SOLUTIONS

Alves Marques, M.; Gaspar, A.M.; Morais, C.M.; Resina Rodrigues, J.; Tomkinson, J. and Margaça, Fernanda.
Centro de Física da Matéria Condensada da Universidade de Lisboa, Av. Prof. Gama Pinto, 2, 1649-003 Lisboa, Portugal and Departamento de Física do Instituto Superior Técnico, Av. Rovisco Pais, 1049-001 Lisboa, Portugal.

A coupling of rocking oscillations of water molecules coordinated by aluminium cations with totally symmetrical vibrations of the hydrate is suggested for concentrated aqueous solutions of the inorganic salts. A weak Raman band observed in the region of about 600 cm^{-1} is plausibly attributable to the activity of some of these coupled motions. This coupling may interpret the low value of the isotopic shift observed, when the ordinary water is substituted by deuterium oxide, in a polarised Raman band attributed to the 'breathing' oscillation of the first coordination shell of this cation (1). Molecular interactions may be estimated if the proposed interpretation is correct. This theme is discussed with reference to magnesium and calcium cations also. Inelastic neutron scattering experiments appear to be useful to precise some attributions.

(1) A. da Silveira, M. Alves Marques and N. Macias Marques, Mol. Phys., 1965, 9, 271.

ROLE OF IONS WITH HIGH POLARIZABILITY IN ELECTRIC CONDUCTANCE IN MOLTEN SALTS

Isao OKADA[1] and P.-H. CHOU[2]

[1]Department of Chemistry, Faculty of Science & Engineering, Sophia University, Kioi-cho 7-1, Chiyoda-ku, Tokyo 102-8554, Japan

[2]Department of Electronic Chemistry, Graduate School, Tokyo Institute of Technology, Nagatsuta 4259, Yokohama 226-8502, Japan

Role of high polarizability ions in dynamic properties in liquids such as self-diffusion coefficients and electric conductivities has not been systematically investigated.

In the present work the effect of cations having high polarizability on the internal mobilities of coexisting cations as well as the cations themselves in binary molten mixtures $(M_1, M_2)NO_3$ has been studied for M_1=Ag^+, Tl^+ and Cs^+ and M_2=alkali ions. The polarizability of these ions is given in Table 1. We have previously found that the internal mobilities, u, of alkali ions, M_1, in molten salts such as nitrates are well expressed by the empirical equation:

$$u_{M_1} = [A/(V_m - V_0)] \exp(-E/RT) \quad , \qquad (1)$$

where V_m is the molar volume, and A, V_0 and E are parameters nearly independent of coexisting cations M_2. However, a perturbation on Eq. (1) should be taken into account in some cases, which could be accounted for in terms of the *agitation effect* (positive deviation) and the *free space effect* and/or the *tranquilization effect* (negative deviation).[1]

It is interesting to note that Ag^+ has the tranquilization effect on the internal mobilities of existing cations except on Li^+, while Tl^+ has the agitation effect, as listed in Table 2. The Cs^+ has the self-agitation effect. This difference with these cations will be discussed.

Table 1. Polarizability α of some monovalent cations.

Cation	Li^+	Na^+	K^+	Rb^+	Cs^+	Ag^+	Tl^+
Ionic radius, $r/10^{-10}$ m	0.59	1.02	1.38	1.52	1.67	1.15	1.50
$\alpha/10^{-30}$ m^3	0.030	0.182	0.844	1.42	2.45	1.72	3.50

Table 2. Effect on u_{M2} caused by M_1 in $(M_1, M_2)NO_3$ melts.

M_1	M_2: Li^+	Na^+	K^+	Rb^+	Cs^+	Ag^+	Tl^+
Ag^+	No effect	⟵ *Tranquilization effect*			⟶	---	*Tranquilization effect*
Tl^+	⟵		*Agitation effect*			⟶	*Self-agitation*
Cs^+	No appreciable effect		⟶	*Self-agitation*		⟵	No effect

1. Okada, I.; Chou, P-.H., *J. Electrochem. Soc.*, 1997, **144**, 1332.

Measurement of Dielectric Relaxation Time of Coordinated Water in Aqueous Solution of HalogenoAlcohols

Masayoshi Ishihara, Shouichi Okouchi, Tomoyuki Nagasawa, Hishashi Uehara
Department of Material Chemistry, Faculty of Engineering, Hosei University,
3-7-2,Kajino-Cho,Koganei-City,184-8584,Japan

Dielectric relaxation measurements were performed on aqueous solutions of halogenoalcohols in the water rich region by the frequency domain reflectometry method that used a vector network analyzer and an open-ended coaxial line probe over the frequency range from 200MHz to 20GHz at 298K.

We have proposed a relaxation model in which there are two motional states of water molecules, those are coordinated water molecules and bulk water molecules with different dielectric relaxation times.

From the concentration dependence of dielectric relaxation times, τ_d, of aqueous solutions of halogenoalcohols we have defined the dynamic hydration numbers, $n^{\varepsilon}_{DHN}(\equiv n^h(\tau_d^h/\tau_d^0-1))$, and the determined the ratios, τ_d^h/τ_d^0, of dielectric relaxation times, τ_d^h, of coordinated water molecules to bulk water molecules, τ_d^0, using the coordination number, n^h, calculated from the water-accessible surface areas of the solute molecule.

The values of τ_d^h/τ_d^0 obtained were largest for ethanol, and decreased in the following order, for β-monohalogenoethanols,

$CH_3CH_2OH>ICH_2CH_2OH>BrCH_2CH_2OH>ClCH_2CH_2OH>FCH_2CH_2OH$,

and for the β-chloro- and –fluoro- ethanols,

$CH_3CH_2OH>Cl_3CH_2OH>Cl_2CHCH_2OH>ClCH_2CH_2OH$,

and

$CH_3CH_2OH>F_3CCH_2OH>FCH_3CH_2OH$,

respectively.

These dielectric results agreed with well ratios, τ_c^h/τ_c^0, of rotational correlation times, τ_c^h, of coordinated water molecules to bulk water molecules , τ_c^0, determined from dynamic hydration numbers, n_{DHN} $(\equiv n^h(\tau_c^h/\tau_c^0-1))$, by the NMR measurements.

Dynamic State of Water in Aqueous Solution of Halogeno-alcohols

Shoichi Okouchi, Yoshimasa Ishihara, Tatsuya Ashida and Hisashi Uedaira
Department of Materials Chemistry, Faculty of Engineering, Hosei University, 3-7-2, Kajino-cho, Koganei-si, Tokyo, 184-8584, Japan

The spin-lattice relaxation times, T_1, of natural abundance $H_2{}^{17}O$ have been measured for aqueous solutions of halogenoalcohols in the water rich region, as a function of the solute concentration at 298K. In order to investigate the effect of halogen atom on hydrophobic hydration, the rotational correlation times, τ_c^h, of water molecules around the solute molecules were estimated and compared with pure water, τ_c^0, from the value of the dynamic hydration number, $n_{DHN} \equiv n_h(\tau_c^h/\tau_c^0-1)$, obtained from the concentration dependence of T_1 and the coordination number, n_h, calculated from the water-accessible surface area of the solute molecules.[1,2]

The values of τ_c^h/τ_c^0 obtained were largest for ethanol, and decreased in the following order, for β-monohalogenoethanols,

$CH_3CH_2OH > ICH_2CH_2OH > BrCH_2CH_2OH > ClCH_2CH_2OH > FCH_2CH_2OH$,

for β-polychloroethanols,

$CH_3CH_2OH > Cl_3CCH_2OH > Cl_2CHCH_2OH > ClCH_2CH_2OH$,

and for β-polyfuluoroethanols,

$CH_3CH_2OH > F_3CCH_2OH > FCH_2CH_2OH$.

The breaking of water structure in the aqueous solution of β-halogenoethanols was considered due to that the orientation of water molecules close to the halogen atom of methyl group substituted for hydrogen atom is different from that of water molecules around the adjacent methylene group, then disturbing the structured layer of hydrophobic hydration. The inhibition of the thermal motions of water molecules around the solutes with increasing the numbers of halogen atom was interpreted in the size increase of the hydrophobic group.

1. Yoshimasa Ishihara; Shoichi Okouchi; Hisashi Uedaira, J. Chem. Soc., Faraday Trans., 1997, 93, 3337.

2. Shoichi Okouchi; Tetsushi Moto; Yoshimasa Ishihara; Haruhiko Numajiri; Hisashi Uedaira, J. Chem. Soc., Faraday Trans., 1996, 92, 1853.

Proton exchange rate in aqueous solution of glucose

Shoichi Okouchi, Yoshimasa Ishihara, Nobuki Asai, Hisashi Uedaira
Department of Materials Chemistry, Faculty of Engineering, Hosei University, 3-7-2, Kajino, Koganei, Tokyo, 184-8584, Japan

Proton exchange rate in aqueous solution of glucose in the water rich region has been investigated from the line width (half width), Hw, of ^{17}O-NMR signals at 298K. The rate represents how fast protons of water molecules are exchanged with one another or those of hydroxyls of glucose molecules, successively. The ^{17}O-NMR half width, Hw, is equal to the sum of the width, ΔHw_{ex}, attributable to the proton exchange rate and the width, ΔHw_{r}, to the rotational motion of water molecules.[1~3)]

The half width observed for the aqueous solution of glucose was widened appreciably in the vicinity of neutrality, being narrow and constant on the acidic and basic side. The maximum half width, ΔHw_{max}, corresponded to the minimum proton exchange rate was determined from the Hw-pH curve of aqueous glucose solution, that is, indicating the increase of the minimum proton exchange rate. On the other hand, for aqueous solution of ethanol the values of ΔHw_{max} increased with the increase of ethanol concentration, then meaning the decrease of the minimum proton exchange rate. The rotational motion of water molecules in the both aqueous solutions was inhibited together with the increase of their concentration. Therefore, the increase of the minimum proton exchange rate was considered due to the tridymite structure of aqueous glucose solution which was different from the hydrophobic hydration of aqueous ethanol solution.

References

(1) S.Okouchi; Y. Ishihara; S. Ikeda; H. Uedaira, Food Chemistry,1998,64,1
(2)S.Okouchi; Y. Ishihara; H. Uedaira, Nippon Nougeikagaku Kaisi,1994,68,1215
(3)S.Okouchi; Y. Ishihara; M Inaba; H. Uedaira, Nippon Nougeikagaku Kaisi,1995,69,679

IN-SITU NMR STUDY OF HYDROTHERMAL REACTIONS OF HAZARDOUS CHLORINATED HYDROCARBONS

Chihiro WAKAI, Yasuo TSUJINO, Nobuyuki MATUBAYASI, and Masaru NAKAHARA
Institute for Chemical Research, Kyoto University, Uji, Kyoto 611-0011, JAPAN

It is recently alerted that many useful chlorinated organic compounds are biologically and environmentally hazardous. It is thus a main goal of environmental chemistry to establish a reaction scheme which provides nontoxic and recyclable organic compounds from chlorinated organic compounds by reducing the C-Cl bonds. To achieve this goal, high-temperature and high-pressure water is a desirable medium since it is clean and safe and dissolves organic compounds. In order to develop an ideal process to recycle hazardous chlorinated compounds, it is important to understand the mechanism of the hydrothermal reaction of the chlorinated compounds. A powerful method to probe the reaction mechanism is the *in-situ* NMR spectroscopy. In this method, the formation and breakage of chemical bonds can be observed in real time and it is possible to characterize not only products but also reaction intermediates. In this work, we perform the *in-situ* NMR observation of the hydrothermal reactions of model chlorinated organic compounds.

Dichloromethane was chosen as a model for the chlorinated hydrocarbons. Dichloromethane was dissolved in 0.5-2 M NaOH aqueous solution at a concentration of 1 M. The hydrothermal reaction was performed in a quartz capillary for 40 h at temperatures of 70-250 °C. The *in-situ* characterization of the reactants, products, and reaction intermediates was made from the proton NMR spectra obtained using the high-temperature probe described in Ref. (1).

We now describe the typical behavior observed at 140 °C of the concentrations of the compounds involved in the decomposition reaction of dichloromethane in water. The major products are formic acid and methanol and their formation reaches a plateau at 20 min after the reaction starts, as shown in Fig. 1. In the plateau period, which lasts up to 300 min, the concentrations of formic acid and methanol are close to each other and the main reaction is the conversion of dichloromethane into methanediol (Scheme (1)).

$$CH_2Cl_2 + 2OH^- \longrightarrow CH_2(OH)_2 + 2Cl^- \quad (1)$$

This shows that methanediol, a hydrated form of formaldehyde, is the main reaction intermediate from dichloromethane and converted into formic acid and methanol through the Cannizzaro reaction (Scheme (2)).

$$2CH_2(OH)_2 \xrightarrow[OH^-]{\text{Cannizzaro}} HCOOH + CH_3OH + H_2O \quad (2)$$

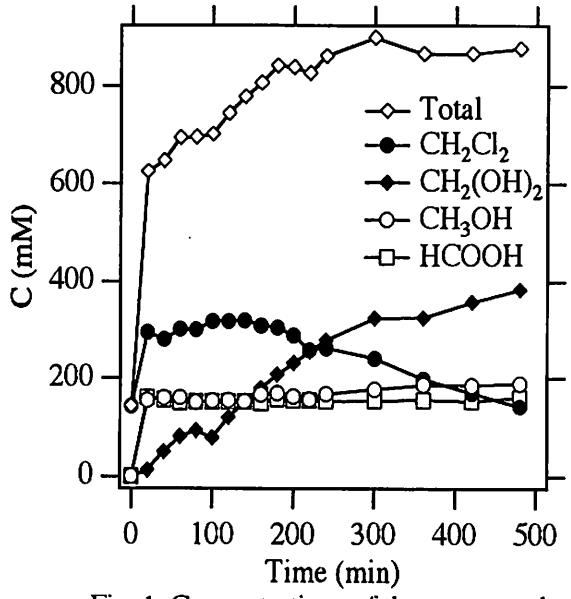

Fig. 1. Concentrations of the compounds involved in the hydrothermal reaction of diclhoromethane at 140 °C.

When more than 300 min passes, the concentration of methanol becomes larger than that of formic acid. This is caused by the cross Cannizzaro-type reaction between methanediol and formic acid, which produces methanol and carbon dioxide.[2] We can also estimate the reaction rate constants of the decomposition and Cannizzaro reations. Detailed temperature effects are to be discussed.

(1) Matubayasi N.; Wakai C.; Nakahara M., *J. Chem. Phys.*, 1997, **107**, 9133.
(2) Tsujino Y.; Wakai C.; Matubayasi N.; Nakahara M., *Chem. Lett.*, 1999, in press.

Electrostatic Effect on the Conformations of Amino Acids Whose Sidechains Contain Ionizable Groups

Tomohiro KIMURA, Nobuyuki MATUBAYASI, Masaru NAKAHARA
Institute for Chemical Research, Kyoto University, Uji, Kyoto 611-0011, Japan

Introduction The conformational distributions of proteins and peptides in aqueous solution at a given thermodynamic state are uniquely determined by the primary amino acid sequences. To understand the protein folding process and the conformation of a peptide, it is helpful to elucidate the factors to control the sidechain conformation of a free amino acid. In this study, we investigate the intramolecular electrostatic effect on the conformational distributions of amino acids whose sidechains contain ionizable groups.

Method D_2O solutions of aspartic acid(Asp), glutamic acid(Glu), lysine(Lys), and arginine(Arg) were prepared and the ionized states of the amino acids were controlled by pD. The distribution on the α-β bond axis was studied from the dihedral-angle dependent vicinal spin coupling constant (equation 1)[1] in the ^{1}H NMR measurement.

$$^3J_{HH} = A + B\cos\theta + C\cos 2\theta \quad (1)$$

In the case of Asp, the gas-phase *ab initio* energy calculation was also carried out at the HF/6-31G* level as a function of the dihedral angle on the α-β bond. In this calculation, the geometry except for the α-β dihedral angle was optimized.

Results and Discussion The spin multiplicity of the α-proton of Lys and Arg are triplet, regardless of the pD, indicating that the electrostatic effect does not play the dominant role in determining the conformational distribution on the α-β bond axis. On the contrary, the two β-protons of Asp and Glu are no longer equivalent, when the two carboxyl groups are both ionized. This is due to the electrostatic repulsion between the negatively charged groups. The result of the *ab initio* calculation for Asp is shown in the Figure. It is seen that one of the staggered conformations is highly improbable due to the large energy difference. Although the three-state model is often assumed to analyze the amino acid and peptide conformations, our result shows that the two-state model can actually describe the conformation of Asp. When the two-state model is applied to the experimentally determined $^3J_{HH}$, the population can be estimated quantitatively. It is found that the distribution is electrostatically controlled when carboxyl groups are ionized, while no electrostatic contribution is seen when they are not ionized.

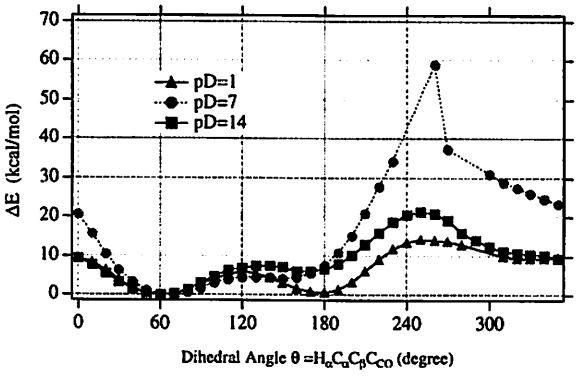

Figure. Calculated energy difference from the energy minimum state (when the dihedral angle θ of $H_\alpha C_\alpha C_\beta C_{CO}$ is 60 degrees) as a function of θ. The pD conditions in which the calculated ionized state predominates are shown. pD=1(▲). pD=7(●). pD=14(■).

1. M. Karplus, *J. Am. Chem. Soc.*, 1963, **85**, 2870.

In-Situ NMR Study of Hydrothermal Decomposition of Formic Acid

Yasuo TSUJINO, Chihiro WAKAI, Nobuyuki MATUBAYASI, and Masaru NAKAHARA
Institute for Chemical Research, Kyoto University, Uji, Kyoto 611-0011, JAPAN

High-temperature and high-pressure (HTHP) water, especially supercritical water, have attracted much attention as a new and novel reaction medium since water is clean and easy to handle compared to many hazardous organic solvents. The development of organic chemical reactions in HTHP water, however, needs to be made in conjunction with the understanding of the underlying reaction mechanisms. To this end, we study C_1 chemistry in HTHP water. Since the carboxylic acid appears as a reaction intermediate of many organic reactions in HTHP water (e.g., the hydrothermal decomposition of dichloromethane), we investigate the hydrothermal reaction of formic acid, the key compound of C_1 chemistry.

Formic acid (Nacalai, 99 %) was dissolved into H_2O to prepare 1.0 M solution. The setup of a sample tube is described elsewhere[1]. The solution was sealed into a capillary made of quartz (I.D. 1.5 mm). This capillary was immersed in the heat medium (DEMNUM S-200) in an NMR sample tube. The solution was *in-situ* measured with NMR (JEOL 270-WB) at 200 °C to 300 °C on the saturation curve, and the hydrothermal decomposition of formic acid was traced in real time by ^{1}H-NMR. In addition, the reaction products obtained by the batch method at 250 °C and 3.8 MPa, 300 °C and 8.6 MPa, and 400 °C and 28.8 MPa of the decomposition reaction of formic acid were characterized with ^{13}C-NMR.

One would expect, from the pyrolytic study of formic acid[2], that there are two reaction pathways for the hydrothermal decomposition of formic acid; (1) HCOOH → CO + H_2O and (2) HCOOH → CO_2 + H_2. According to ^{13}C-NMR, below 250 °C, formic acid is decomposed into CO and H_2O, while above 300 °C, the reaction products are CO_2 and H_2 (although some investigators suggest that formic acid in HTHP water decompose into CO_2 and H_2 dominantly[3-5]). When the pyrolysis of formic acid is concerned, the decarboxylation (2) is the minor process. On the other hand, the decarboxylation (2) occurs in HTHP water above 300 °C since the reaction temperature is high and water lowers activation energy of this decomposition process. *In-situ* ^{1}H-NMR observation of the decomposition reaction of formic acid was performed to estimate the reaction rate constants of the reactions (1) and (2). Figure 1 shows the concentration of formic acid as a function of time. It is seen that the decomposition reaction is of unimolecular nature. The activation energy and results of gas chromatography measurement are to be discussed.

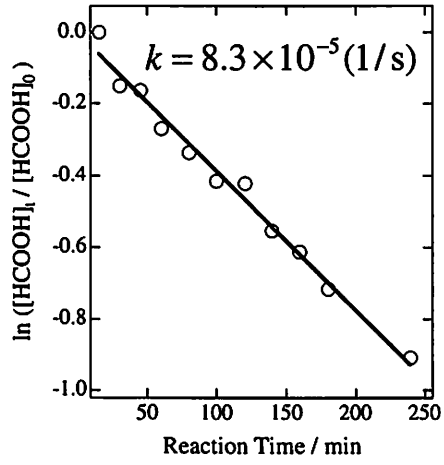

Figure 1. First-order rate behavior of HCOOH in H_2O at 250 °C and 4 MPa.

References

(1) Matubayasi, N.; Wakai, C.; Nakahara, M., *J. Chem. Phys.* 1997, **107**, 9133.
(2) Blake, P. G.; Hinshelwood, C., *Proc. R. Soc. London, Ser. A* 1960, **255**, 444.
(3) Bjerre, A. B.; Sorensen, E., *Ind. Eng. Chem. Res.* 1992, **31**, 1574.
(4) Yu, J.; Savage, P. E., *Ind. Eng. Chem. Res.* 1998, **37**, 2.
(5) Maiella, P. G.; Brill, T. B., *J. Phys. Chem. A* 1998, **102**, 5886.

HYDRATION OF 1,4-DIOXANE, 1,3-DIOXANE, AND 4-METHYL-1,3-DIOXANE PROBED BY NMR AND IR

Shingo IMAFUJI, Teruko FUJIWARA, and Kazuko MIZUNO
Center for Instrumental Analysis, Fukui University, Fukui 910-8507, Japan

We repoprted the blueshifts of the C—H stretching bands of methyl group in IR spectra observed on diluting acetone, DMSO, and *tert*-butanol with water.[1] The concentration dependences of the blueshifts were found to be closely related with the hydrogen-bonding property of the hydrophilic group in the solutes; in DMSO and acetone, the blueshift has a maximum in the water rich region, whereas in aqueous *tert*-butanol it remains almost constant in the region. The results can be explained satisfactorily by considering that a part of the electron about the C—H proton is pushed out into the C—H bond due to a repulsive interaction between the C—H hydrogen and water oxygen to be denoted as C—H•••OH_2(•••OH_2)$_n$, where OH_2(•••OH_2)$_n$ expresses water molecules hydrogen-bonded cooperatively. The more the water content, the stronger the hydrogen bonds, resulting in more blueshifts of the C—H bands. In this paper, we report the hydration of dioxanes, with less hydrogen-bonding hydrophilic group than those in acetone, DMSO, and *tert*-butanol, probed by NMR and IR. The effect of the hydrogen-bonding property of hydrophilic group on hydration is to be discussed.

Experiments. The hydration of 1,4-dioxane and 1,3-dioxane was studied by examining the concentration and the temperature dependences of chemical shifts in NMR, together with the concentration dependences of the frequencies of the C—H streching vibration bands in IR. The chemical shifts were measured by the external double reference method, by which the volume magnetic susceptibilities were also obtained *in situ* for the correction of the chemical shift.[1] To study the temperature dependence of the chemical shifts, the temperature dependences of the volume magnetic susceptibilities of both the sample and the reference solutions should be taken into consideration. In the present paper, all the chemical shifts are referred to the resonance field of liquid TMS at 25°C.

Results and Discussion The ^{1}H chemical shifts of water and the CH_2 protons and the frequency shifts of the C—H streching vibration bands increased monotonically with increasing water concentration in the mixtures. The ^{1}H chemical shifts of water were not larger than the value for pure water even at 1°C in the aqueous 1,4-dioxane and 1,3-dioxane. These results show that the hydrophobic hydration does not occur in the mixtures.[1] The effect of the methyl group introduced into 1,3-dioxane on hydration is to be discussed.

1. Mizuno, K.: Ochi, T.: Shindo, Y., *J. Chem. Phys.*, 1998, **109**, 9502.

SEDIMENTATION OF CHARGED COLLOIDS IN THE GRAVITATIONAL FIELD : RELAXATION TOWARD EQUILIBRIUM

J.F. DUFRECHE, J.P. SIMONIN, P. TURQ
Laboratoire Liquides Ioniques et Interfaces Chargees (LI2C) (UMR CNRS 7612), Universite Pierre et Marie Curie, boite courrier 051, 4 place Jussieu 75252 Paris Cedex 05 FRANCE

The sedimentation of colloidal suspensions has been the subject of interesting studies for a long time. Thus, for infinitely diluted suspensions in the gravitational field, the theoretical concentration profile is simply proportional to the Boltzmann factor $\exp(-mgz / kT)$. This equation allowed Jean Perrin to obtain a estimate of Boltzmann's constant and Avogadro's number in 1910. On the other hand, the influence of Coulomb repulsion and excluded volume has to be taken into account in order to describe concentrated charged colloidal suspensions. Experimental equilibrium profiles have been obtained, which could be recently described theorically[1] by a simple treatment.

In the present work, we give an analytic treatment for the dynamics of charged colloids sedimentation[2]. The process can be described by two different times. The first characteristic time hkT / mgD represents the time required for one particle to travel on distance h by gravity. The second time is the diffusion time h^2 / D. Coupling between gravitation and diffusion effects is due to the presence of boundaries (which define the container). Consequently the relaxation of concentration profiles on long times involves both caracteristic times. In this sense the present study differs from classical sedimentation velocity studies.

Mainly, we deal with salt-free solutions without hard sphere repulsion. The assumptions used are : the colloid particles have a constant charge; the electroneutrality condition is verified locally. It is found that the concentration of the colloidal particles obeys a linear equation. The problem can be studied in terms of relaxation times. The result depends on the initial conditions and the spatial localisation. It is found that it is not a simple relaxation since for exemple the process is not uniform. The result are consistent with experimental studies.

Lastly the effect of added salt and the influence of the hard sphere repulsion are briefly examined. If this repulsion between the colloid sphere is decribed at the Carnahan-Starling level, a numerical study allows to simulate precisely the sedimentation process. Nevertheless the hydrodynamic effects have not be taken into account. They are expected to decrease the sedimentation velocity (like the electrostatic forces), contrary to the hard sphere repulsion that increases the diffusion force. It should be interesting to study the competion between them.

1. Simonin, J.P. *J. Phys. Chem.* **1995**, 99, 5, 1577-81
2. Dufreche, J.F.; Simonin, J.P.; Turq, P. *J. Mol. Liq.* **1999**, 79, 137-149

EFFECTS OF PRESSURE AND SOLVENT ON THE IR INTENSITY FOR O-H VIBRATIONAL MODE OF C_6H_5OH

Hideto ISOGAI, Minoru KATO and Yoshihiro TANIGUCHI
Department of Chemistry, College of Science and Engineering, Ritsumeikan University, Kusatsu, Shiga 525-8577, Japan

【Introduction】 Changes in frequency shift, band-width, and intensity of vibrational bands are reflected by microscopic properties of solutions. A large number of works have been performed on frequency shift and band-width. In contrast, there are few works of intensity, particularly for the effect of pressure. One reason is due to the difficulty of the quantitative calculation.

In general, the internal electric field acting directly on molecules is different from the applied external electric field. The intensity of the aimed IR band in a solution must be firstly corrected for the effect of the internal electric field. In order to know the pressure dependence of IR intensity, we calculated the integrated molar absorption coefficient for O-H vibrational mode of C_6H_5OH.

【Experiment】 The IR spectra of C_6H_5OH in CS_2 were recorded on a Perkin-Elmer system 2000 FT-IR spectrometer at 293.2 K. The concentration of C_6H_5OH-CS_2 solution was ca. 3×10^{-3} mol/l. The pressure dependence of the density of the solution is estimated from the compressive stress [1] of solvent CS_2 because of the very low concentration. The solvents used in the work for the effect of solvent were C_6H_{14} (2,2-dimethylbutane), *c*-C_5H_{10}, CCl_4, and CS_2. The cell used in this work was a quartz cell. For high-pressure measurements up to 200 MPa, we used hydrostatic cell [2], the optical path length of which can be directly measured with a point micrometer.

【Results and Discussion】 Figure 1 shows the relationship between the relative values of the integrated molar absorption coefficients and the Polo-Wilson (PW) factor [3]. The subscript *0.1* and *p* refer to 0.1 MPa and the measured pressure, respectively. It is shown that we could reproduce the change of IR intensity for the effect of pressure by the PW equation. We first found that the increase of the internal electric field up to 200 MPa can be explained by the PW equation.

By comparing the effect of pressure with that of solvent, we will discuss the effect of pressure on the IR intensity for the aimed vibrational mode.

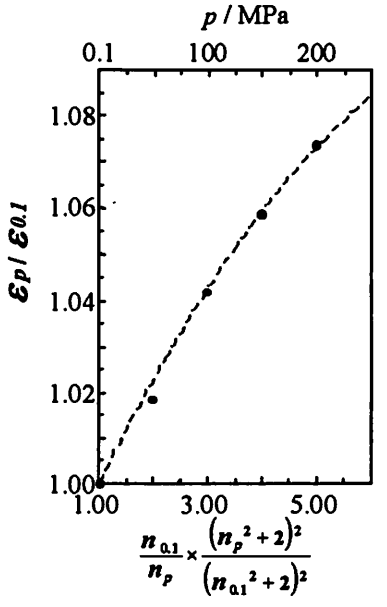

Fig.1. Relationship between the relative values of the integrated molar absorption coefficients and the Polo-Wilson factor. The dot line is the calculated equation by Polo and Wilson.

【References】

1. Isaacs,N.S., *Liquid Phase High Pressure Chemistry*, Wiley & Sons, Chichester,1981, Chap.2.
2. Kato,M.; Taniguchi,Y., *Rev. Sci. Instrum.*, 1995, **66**, 4333.
3. Polo,S.R.; Wilson,M.K., *J. Chem. Phys.*, 1955, **23**, 2376.
4. Bauer,E.; Magat,M., *J. Phys. Radium.*, 1938, **9**(7), 319.

PRESSURE AND TEMPERATURE EFFECTS ON RADICAL DIFFUSION IN ETHANOL

T. OHMORI , Y. KIMURA, M. TERAZIMA, and N. HIROTA
Department of Chemistry, Graduate School of Science, Kyoto University, Kyoto 606-8502, Japan

Since the finding of the slow diffusion of pyrazinyl radical in 2-propanol produced by the hydrogen abstraction reaction,[1] the extraordinary slow diffusion of transient radical molecules have been investigated experimentally for various reaction systems by the transient grating (TG) spectroscopy. In this work we present a new experimental study on the pressure and the temperature effects the diffusion of the ketyl radical created by a hydrogen abstraction reaction of benzophenone in ethanol. By changing the pressure at the elevated temperature, it is possible to change the solvent density widely. It is an interesting issue how the slowness of the radical diffusion will change with the solvent density.

The TG measurement has been performed using a 355nm laser pulse for the excitation and a high pressure optical cell with temperature regulated. Figure 1 shows a typical TG signal at 200MPa and 350K. The signal can be interpreted as the sum of the contributions of the thermal grating, and the species gratings due to the unidentified species, the parent and the radical molecules, as is the case in the ambient conditions. We have fitted the slower part of the signal, and estimated the diffusion constants of the parent and the radical molecules by comparing the decay constants determined at the ambient conditions. Figure 2 shows the comparison between the diffusion constants of the solvent[2], benzophenone, and benzophenone radical thus estimated. It seems that the ratio becomes smaller with increasing the diffusion constant of the solvent. And elevating temperature brings decrease of the both proportions of them. Results in the higher temperature including the supercritical region will be discussed in the presentation.

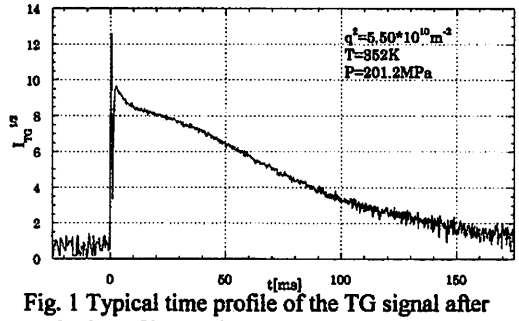

Fig. 1 Typical time profile of the TG signal after excitation of benzophenone at 201.2MPa and 352K.

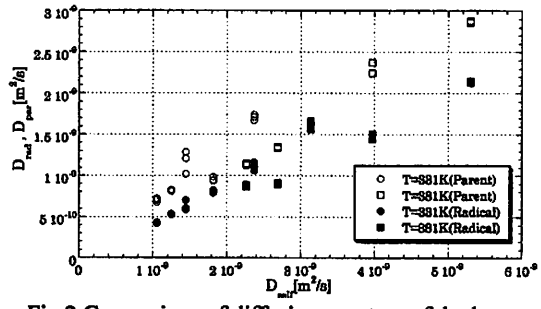

Fig.2 Comparison of diffusion constant of the benzophenone (Parent) and benzophenone ketyl radical (Radical) with that of the pure solvent at various pressure (0.1-200 MPa) and the temperature (331,381 K).

1. M. Terazima and N. Hirota, *J. Chem. Phys.* 1993, **98**, 6257.
2. N. Karger, T. Vardag, and H.-D. Lüdemann, *J. Chem. Phys.* 1990, **93**, 3437.

THE STUDY OF DIELECTRIC RELAXATION IN SUPERCOOLED ETHYLENEGLYCOL-WATER MIXTURES

Seiichi Sudo, Naoki Shinyashiki, and Shin Yagihara
Department of Physics, Tokai University, Hiratsuka, Kanagawa 259-1292 Japan

Water is known as a liquid with abnormal behaviors caused by molecular clusters and network structures through hydrogen bonds. The glass transition temperature, Tg, achieved by conventional method for water is quite lower than the melting point. Then the dynamical behavior of water related to the glass transition has not been clarified, yet. However, aqueous solutions of organic compounds bring enough lower freezing points as we can observe the dynamics around Tg. We examined the dynamics concerning the glass transition for Ethyleneglycol (EG)-water mixtures and the dependency of dielectric property on the water content.

The complex permittivity of EG-water mixtures with concentrations of 60, 70, and 80 wt% of EG were measured in the frequency range between 1mHz and 30GHz in the temperature range between 140.5K and 298K. Alternate Current Phase Analysis Method, LCR meter, and Time Domain Reflectometry were used to measure the dielectric permittivity in the frequency ranges of 1mHz-100Hz, 20Hz-1MHz, and 10MHz-30GHz, respectively.

Dielectric absorption curves for the aqueous solution of 60wt% EG at various temperatures are shown in Figure 1. One relaxation peak is observed at all the temperatures and concentrations. The temperature dependence of the frequency of the relaxation peak is described by the Vogel-Fulcher-Tammann (VFT) equation. Width of the absorption curve gradually increases with decreasing temperature. This increase in the width occurs suddenly below Tg+30K. Relaxation curves observed in higher temperatures are described by the Kohlrausch-Williams-Watts (KWW) function. However, in the lower temperature range, the relaxation curve cannot be described by a single relaxation process. It can be described by a sum of two relaxation processes of the KWW and the Cole-Cole equations. This result suggests that the Johari-Goldstein relaxation is separated from the α -relaxation around Tg. The frequency of the separation, is lower than any other glass forming materials. Temperature and water content dependence of cooperating motion of water and EG molecules will be discussed.

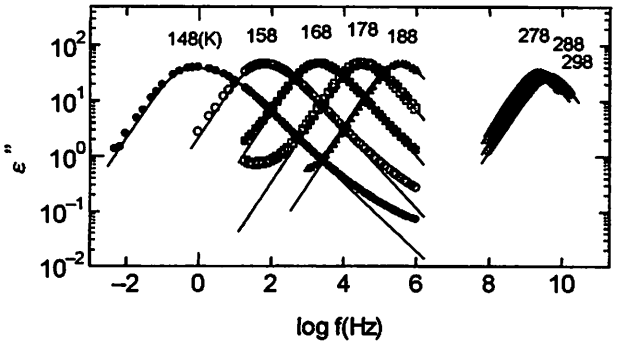

Figure 1. Dielectric absorption curves of aqueous solution of 60wt% EG at various temperatures.

DIELECTRIC PROPERTIES OF ALCOHOL-WATER MIXTURES RELATED TO THE MOLECULAR STRUCTURE OF ALCOHOL

Seiichi Sudo, Naoki Shinyashiki and Shin Yagihara
Department of Physics, Tokai University, Hiratsuka, Kanagawa 259-1292 Japan

The dynamics of water and alcohol are complex caused by cluster and network structures formed through hydrogen bond. The principal dielectric relaxation process of water exhibits a Debye-type relaxation. On the other hand, the principal relaxation process of polyhydroxyl alcohols exhibits asymmetric curve empirically described by the Kohlrausch-Williams-Watts(KWW) function. The various studies on alcohol structure dependence for the dynamics of alcohol-water mixtures have been carried out. However, these works were done only part of various kinds of alcohol.

In order to explain the universal rules for the dielectric properties of alcohol-water mixtures, we made measurements of dielectric complex permittivity for alcohol-water mixtures by Time Domain Reflectometry in the frequency range from 10MHz to 30GHz at 25°C. Seventeen kinds of aliphatic alcohols with various molecular structures were employed. Mole fraction of water, X_W, was varied from 0 to 1 for all the alcohol-water mixtures.

One relaxation peak is found for all the mixtures in the frequency measured, and the relaxation curve can be well described by the KWW function. Distribution of relaxation time depends strongly on the structure of alcohol and water content in particular, and every water mixtures show the broadest distribution of relaxation time in certain concentration range of $0.6 \leq X_W \leq 0.9$. Cooperative motion of water and alcohol molecules will be discussed in relation to the structure of alcohols.

AQUO IONS OF SOME TRIVALENT LANTHANIDES AND ACTINIDES. EXAFS DATA AND THERMODYNAMIC CONSEQUENCES.

F. David[1], R. Revel[2], B. Fourest [1], S. Hubert[1], J.F. Le Du[1], C. Den Auwer[2] , C. Madic[2], L.R. Morss[3], J.C. Berthet[4], M. Ephritikhine[4]

1: IPN, 91406 Orsay Cedex, France ; 2: CEA Marcoule, DCC/DRRV/SEMP, 30207 Bagnols sur Cèze Cedex, France ; 3: Argonne National Laboratory, Chem. Technology Division, Argonne, IL 60439, USA, 4 CEA, DSM/DRECAM/SCM, CNRS URA 331, 91191 Gif sur Yvette, France.

In order to understand the chemical properties of aquo ions the knowledge of their structure is essential. We have, for instance, to determine the distance d, between the cation and oxygen from the water molecule in the first coordination sphere, as well as the coordination number N. For this purpose, X-ray Absorption Spectroscopy is a powerful tool. We have achieved a systematic research to obtain bond distances and coordination number N for all trivalent lanthanide elements (except Pm^{3+}), Y^{3+}, and several trivalent actinides: U^{3+}, Np^{3+}, Pu^{3+}, Am^{3+} and Cf^{3+}. Some experiments were carried out with as little as 1 mg of actinides. Experiments were performed for 1M HCl solution and Zn amalgam was used to stabilize trivalent state of U^{3+}, Np^{3+} and Pu^{3+}.

The Fourier Transform of all X-ray absorption spectra show a single peak, which indicates that no formation of inner-sphere chloro complex occurs. The d_{exp} values have been precisely measured, but N values are more doubtful and we have considered for all ions the data deduced from transport property[1].

We have compared these values of d_{exp} to those that can be evaluated from an ionic model[2] d_i. The results of this comparison show a decreasing difference $\Delta d = d_i - d_{exp}$, as the atomic number of the lanthanide and actinide increases. This result is consistent with the more covalent character of the M-O bonds for the light actinide elements in comparison with the heavy actinides and for La^{3+} and Ce^{3+} in comparison with other trivalent lanthanide ions. The Δd value for californium and for lanthanide ions heavier than Pr^{3+} which are essentially zero, confirms our evaluation of the size of the water molecule in the vicinity of the cation and the dominant ionic character of the M-O bonds for Cf^{3+} ion. As expected, the Δd values correlate with Δq, the difference between +3 and the calculated effective charges of the cations[2].

Finally, we have calculated the free hydration energies of the cations on the basis of a model that takes into account the Born term, the influence of dipole and quadrupole interactions, the dispersion effect, the formation of a cavity, the influence of water molecules in the second hydration sphere, the electrostriction effect, and the packing factor for water molecules.

[1]Structure of Trivalent Lanthanide and Actinide Aquo Ions, David F., Fourest B., *New J. of Chemistry*, 1997, 21, 167.
[2]Water Characteristics Depend on the Ionic Environment. Thermodynamic and Modelisation of the Aquo Ions, David F., Vokhmin V, Ionova G., 26ICSC Fukuoka, Japan, 26-31 July 1999.

Solvation of Tris(acetylacetonato)metal Complexes in Organic Solvents

H. Ikeuchi,[1] and M. Kanakubo[2]

[1] Department of Chemistry, Faculty of Science and Technology, Sophia University, 7-1, Kioicho, Chiyoda-ku, Tokyo 102-8554, Japan

[2] Tohoku National Industrial Research Institute, 4-2-1 Nigatake, Miyagino-ku, Sendai 983-8551, Japan

Structure of solvation sphere of tris(acetylacetonato)metal(III) complex in organic solvents was studied by means of the densities and the viscosities of the solutions, and the NMR-relaxation time of the central metal for the Co-complex–organic-solvent systems.[1] Cobalt-complex was mainly used for these measurements, but some other metal complexes were also used for the special purposes. The NMR-relaxation times of ^{13}C's and ^{1}H of the solvent were measured for the Cr-complex–acetonitrile solution.[2] Diffusion coefficient of the Co-complex in acetonitrile solution was also measured by means of NMR field gradient method.

The partial molar volumes (V_c) of the complexes were obtained from the densities. If we apply the rigid sphere–continuum fluid model to these complex–solvent systems, we can derive volumes of the solute complexes: V_E from viscosity B-coefficient by means of Einstein equation, V_{SED} from NMR-relaxation time by means of Stokes-Einstein-Debye equation, and V_{SE} from diffusion coefficient by means of Stokes-Einstein equation. Some of the results are shown in Fig.1.

Fairly strong solvation of this complex in these solvents can be concluded from the negative temperature dependence of V_E, V_{SED} and V_{SE}.

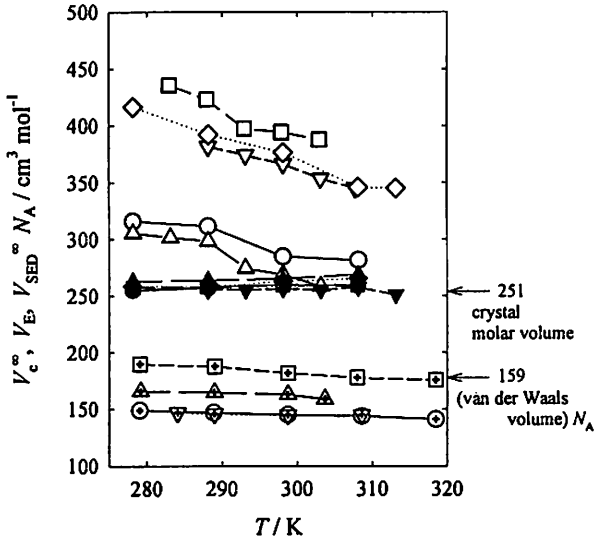

Fig.1. Temperature dependences of V_c^∞, V_E and V_{SED}^∞ of $[Co(acac)_3]$ in various solvents

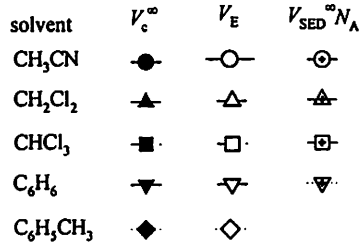

1. Kanakubo, M.; Ikeuchi, H.; Satô, G. P., J. Moleclar Liquids, 1995,65/66 273

2. Kanakubo, M.; Ikeuchi, H.; Satô, G. P., J. Phys. Chem. B, 1997, 101,3827

X-RAY DIFFRACTION, SMALL-ANGLE NEUTRON SCATTERING, MASS SPECTROSCOPY, AND ^{17}O-NMR RELAXATION OF HEXAFLUOROISOPROPANOL-WATER MIXTURES

Koji YOSHIDA[1], Nobuyuki NISHI[2], Hisanobu WAKITA[1] and Toshio YAMAGUCHI[1]
[1]Department of Chemistry, Fukuoka University, Jonan-ku, Fukuoka, 814-0180, Japan
[2]Institute for Molecular Science, Myodaiji, Okazaki, 444-8585, Japan

Hexafluoroisopropanol (HFIP)-water mixture is one of the attractive solvents in biochemistry to transform the β-sheet to the α-helix structures of proteins. In ethanol-water binary mixture, it has appeared that the microscopic structure of the mixture is related to protein denaturation in our previous CD study of chymotrypsin-inhibitor II in the mixture. Therefore, it is important to elucidate the microscopic structure of HFIP-water mixture in order to reveal the mechanism of protein folding in the view of the structure change of solvent as a function of alcohol concentration. We report the results of X-ray diffraction, mass spectroscopy, small-angle neutron scattering, and NMR relaxation time measurements of HFIP-water mixtures.

X-ray diffraction measurements were made on HFIP-water mixtures on a rapid liquid X-ray diffractometer (MAC Science) combined with an imaging plate (Fuji Film Co.). The clusters generated by adiabatic expansion of HFIP-water droplets were analyzed on a double focus spectrometer with electric and magnetic sectors (Kratos Analytical, Propile). Small-angle neutron scattering measurements were made on a WINK instrument at the National Laboratory for High Energy Physics (KEK). ^{17}O-T_1 of HFIP-$H_2{}^{17}O$ mixtures was measured with a FT-NMR GSX-400 (JEOL).

Figure 1 depicts the radial distribution functions at various mole fractions of HFIP at 25°C. The dashed lines show the experimental results, whereas the solid lines were obtained by subtraction of the contribution of intramolecular interactions up to 2.6 Å. The peaks at 4.5Å and 7Å, characteristic of water structure, decrease with addition of HFIP to $X_A \cong 0.1$. In the results of small-angle neutron scattering, the correlation length and the radius of gyration have a maximum at $X_A = 0.1$, suggesting evolution of clusters of HFIP and water. Mass spectra revealed that a HFIP molecule is hydrated by water molecules up to 10 in contrast with 2-propanol-water mixtures, in which almost no water molecule surround the alcohol. The T_1 value of $H_2{}^{17}O$ in HFIP-H_2O firstly decreased with increasing HFIP concentration up to X_A= 0.1 and then became constant with further increase in HFIP concentration. The NMR result indicates that water structure in the mixtures is broken at $X_A \cong 0.1$, consistent with those from the other methods.

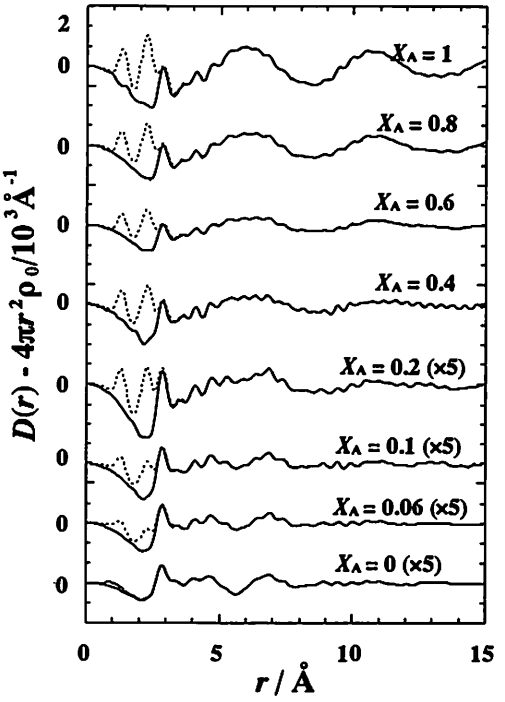

Fig. 1. Radial distribution functions at various mole fractions of HFIP (X_A) at 25°C.

INTERACTIONS BETWEEN A TETRAANIONIC PORPHYRIN AND THE METHYLVIOLOGEN DICATION IN METHANOL STUDIED BY FLUORESCENCE QUENCHING REACTION

Sanjay PANT, Hiroyasu SAIKI and Toshihiro TOMINAGA
Department of Applied Chemistry, Okayama University of Science, 1-1 Ridai-cho, Okayama 700-0005, Japan

Previously we analyzed the transient effect of the bimolecular fluorescence quenching reaction between 5,10,15,20-tetrakis(4-sulfonatophenyl)porphine ($TPPS^{4-}$) and methylviologen (MV^{2+}) in water.[1,2] The effective reaction distance decreased with increasing ionic strength and approached the contact distance of the reactants while it increased with decreasing ionic strength and approached the Onsager distance defined as

$$r_c = z_F z_Q e^2/(4\pi\varepsilon_0\varepsilon k_B T) \quad (1)$$

where z_F and z_Q are the charges of the fluorophore and quencher, respectively, ε_0 and ε are the dielectric constant of a vacuum and the reaction medium, respectively, k_B is Boltzmann's constant, and T is the absolute temperature.

We have studied the above reactants in methanol, where the electrostatic attraction is magnified. The ionic strength was adjusted by adding tetramethylammonium chloride (Me_4NCl). When the Me_4NCl concentration was higher than 0.1 mol dm^{-3}, fluorescence decays could be fitted by

$$I(t) = I(0)\exp\left(-At - Bt^{1/2}\right) \quad (2)$$

which was the case in water.[1,2] When the Me_4NCl concentration was lower than 0.1 mol dm^{-3}, the decays could not be fitted by eq. 2 but could be fitted by

$$I(t) = I_1(0)\exp(-k_1 t) + I_2(0)\exp(-k_2 t) \quad (3)$$

Figure 1 shows the fluorescence decay curves in 0.01 mol dm^{-3} Me_4NCl. The faster rate constant increased slightly with increasing MV^{2+} concentration (k_1 = 0.81 - 1.1 x 10^9 s^{-1}) and the slower rate constant decreased with increasing MV^{2+} concentration (k_2 = 0.84 - 1.6x 10^8 s^{-1}). Assuming that the faster components reflect the electron transfer rate from $TPPS^{4-}$ to MV^{2+} in the solvent-separated ion-pair, we calculated the ion-pair formation constant K. As expected, the K values decrease with increasing ionic strength. They increase slightly with increasing concentration of MV^{2+}, which might indicate the 1-2 ion-pair formation at higher MV^{2+} concentration.

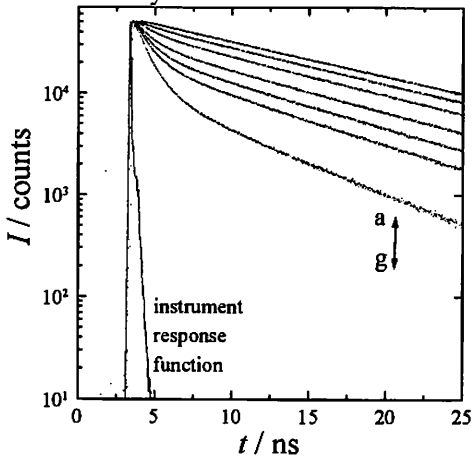

Fig. 1. Fluorescence decay curves for $TPPS^{4-}$ in methanol containing 10 mmol dm^{-3} Me_4NCl at 298.2 K. $[MV^{2+}]$ = (a) 0, (b) 0.1, (c) 0.25, (d) 0.5, (e) 0.75, (f) 1, and (g) 2 mmol dm^{-3}.

1. Scully, A. D.; Hirayama, S.; Hachisu, D.; Tominaga, T., *J. Phys. Chem.*, 1992, **96**, 7333.
2. Scully, A. D.; Hirayama, S.; Fukushima, K.; Tominaga, T., *J. Phys. Chem.*, 1993, **97**, 10524.

BIMOLECULAR FLUORESCENCE QUENCHING REACTION ON ONE-DIMENSIONAL DNA

Makoto Takezaki and Toshihiro Tominaga
Department of Applied Chemistry, Faculty of Engineering, Okayama University of Science, 1-1 Ridai-cho, Okayama, 700-0005, Japan

There are many studies of fluorescence quenching reactions for three- and two-dimensional systems to understand mechanisms of energy transfer and bimolecular reactions. In order to study a one-dimensional system, fluorescence decays were measured for a cationic porphyrin, 5,10,15,20-tetrakis{4-N-(trimethyl)ammonio-phenyl} porphine ($TTMAPP^{4+}$), in the presence of a cationic quencher, methylviologen (MV^{2+}), both adsorbed on Calf Thyms DNA as a one-dimensional media.

The fluorophor was excited at 415 nm and the fluorescence decay was measured using a home-made single-photon counting apparatus. Because the interaction between cationic porphyrins and DNA is very strong,[1] essentially all $TTMAPP^{4+}$ are adsorbed on DNA at our experimental condition. The fluorescence decays can be described by the one-dimensional Smoluchowski model as,

$$F(t) = F_0 \exp(-At - Bt^{1/2}) \qquad (1),$$

where $A = \tau_0^{-1}$, $B = 4(D/\pi)^{1/2} N_A [Q]_{1D}$ and $[Q]_{1D}$ is the one-dimensional quencher concentration.

The fluorescence decay curves are shown in Fig. 1. A and B values obtained from eq. 1 are plotted in Fig. 2. A values are seen to be independent of $[Q]_{1D}$ as expected from eq. 1. The one-dimensional diffusion constant was calculated to be about 5×10^{-11} m^2s^{-1} from Fig. 2. Comparison of this value with those obtained for two-dimensional media[2] and more detailed discussion will be made at the conference.

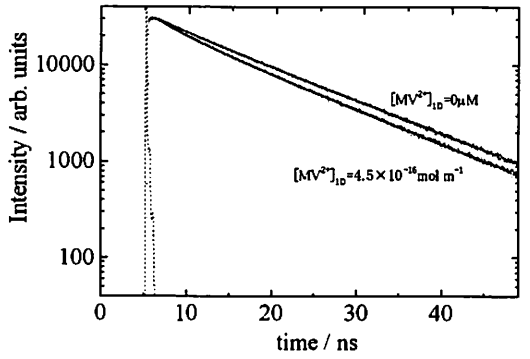

Fig. 1. Fluorescence decay curves of $TTMAPP^{4+}$ on DNA at 25 °C (dots), response curve (broken line) and fitted curves (solid lines).

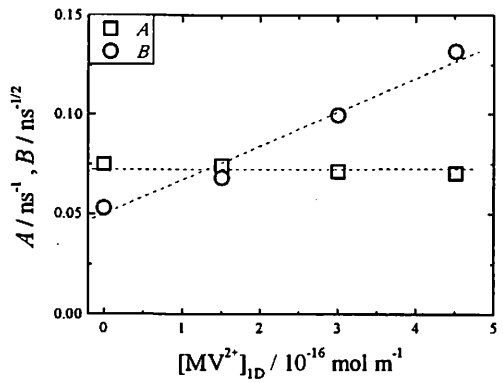

Fig. 2 Plots of A and B vs. $[MV^{2+}]$. Open square, A; open circle, B. The broken lines are least squares linear fits to the data.

1. (a) Fuhrhop, J. H.; König, J., *Membranes and Molecular Assemblies*, The Royal Society of Chemistry, 1994. (b) Pasternack, R. F.; Gibbs, E. J.; Villafranca, J. H., *Biochemistry*, 1983, **22**, 2406.
2. For example, (a) Hammarström, L.; Norrby, L.; Stenhagen, G.; Mårtensson, J.;Åkermark, B.; Almgren, M., *J. Phys. Chem B.*, 1997, **101**, 7494. (b) Zhang, G.; Thomas, J. K.; Eremenko, A.; Kitktev, T.; Wilkinson, F., *J. Phys. Chem. B*, 1997, **101**, 8569.

COMPLEXATION AND IONIC ARRANGEMENT IN Na_3ErCl_6 AND K_3ErCl_6 MELTS ANALYZED BY X-RAY DIFFRACTION

Yasuhiko IWADATE[1], Kazuko FUKUSHIMA[1], Ryuzo TAKAGI[2] and Marcelle GAUNE-ESCARD[3]

[1]Department of Materials Technology, Faculty of Engineering, Chiba University, Yayoi-cho 1-33, Inage-ku, Chiba 263-8522, Japan

[2]Research Laboratory for Nuclear Reactors, Tokyo Institute of Technology, Ookayama 2-12-1, Meguro-ku, Tokyo 152-8550, Japan

[3]Institut Universitaire des Systèmes Thermiques Industriels, Université de Provence, Technopôle Chateau-Gombert, 5 rue Enrico Fermi, 13453 Marseille Cédéx 13, France

It has so far been reported that the nearest neighbour chloride coordination number of a lanthanide ion (Ln^{3+}) changed from 9 in the UCl_3-type crystal (hexagonal) to 6 in the melt, allowing for octahedral geometry around the lanthanide ions. The melt structure of lanthanide trichlorides with $AlCl_3$-type crystal structure (monoclinic; six-fold coordination) has been studied for YCl_3 and $ErCl_3$. It is of much interest to add the typical ionic crystals NaCl and KCl to $ErCl_3$ and to study the Cl^- coordination around Er^{3+} on melting. In the present work, the short range structure of Na_3ErCl_6 melt at 973 K and K_3ErCl_6 melt at 1053 K was studied by X-ray diffraction and the medium range structure was also discussed on the basis of cluster orientation.

Melting behavior such as the changes in molar volume and nearest neighbor coordination on melting between $ErCl_3$ crystal and its melt was confirmed to be similar to that of YCl_3. The volume change was quite a little and the coordination number of Cl^- ions around Er^{3+} ion in melt was estimated at about 6 by integration of the area under the peak of $D(r)$, being nearly equal to 6 in crystal.

In order to refine the short range structure of Na_3ErCl_6 and K_3ErCl_6 melts, the structural parameters for each ionic pairs were optimized by the radial distribution analysis and the correlation method, using the non-linear least squares fitting between the original intensity data and the model structure. The nearest neighbor distance of Er^{3+}-Cl^- and the coordination number of Cl^- around Er^{3+} in Na_3ErCl_6 melt, for instance, were estimated to be 2.61 Å and 5.7, respectively. The Er^{3+}-Er^{3+} and Cl^--Cl^- distances were evaluated at 5.15 Å and 3.90 Å, respectively. These results imply the existence of octahedral $ErCl_6^{3-}$ complex anion. The average Er^{3+}-Er^{3+} pair-distance in pure $ErCl_3$ melt was 4.05 Å, indicating that there is some specific configuration in the melt, which would be well interpreted by an edge-sharing model assuming flexible octahedra with variable Er^{3+}-Cl^- and Cl^--Cl^- bond lengths. The average Er^{3+}-Er^{3+} pair distances in Na_3ErCl_6 and K_3ErCl_6 melts were, however, 5.15 and 5.17 Å, respectively. These distances are elongated extremely from the distance 4.05 Å corresponding to pure $ErCl_3$ melt. This finding is due to that the edge-sharing and/or corner-sharing octahedra of the type $Er_2Cl_{10}^{4-}$, $Er_2Cl_{11}^{5-}$, and so on are decomposed into the discrete octahedra of the type $ErCl_6^{3-}$ and the alkali cations tend to be located among the discrete octahedral complex ions.

EFFECT OF ELECTRIC FIELD ON THE RHEOLOGY OF FERROELECTRIC LIQUID CRYSTALS

Shigeru Fukayama and Keishi Negita

Department of Chemistry, Faculty of Science, Fukuoka University, Nanakuma 8-19-1, Jonan-ku, Fukuoka, 814-0180, Japan

When an electric field of a few kV/mm is applied to complex fluids such as colloidal suspensions and liquid crystals, there appears a change of the rheological properties. This phenomenon is called an electrorheological (ER) effect and has been extensively explored in recent years.[1] In liquid crystals, depending on the characteristic structures of the respective liquid crystalline phases, a variety of ER effects are observed. In the nematic phase having a positive dielectric anisotropy, the electric field gives rise to an increase of the viscosity, which is understood by an orientational change of the director, unit vector specifying the orientation of the liquid crystal.[2] While in smectic A phase, a decrease of the viscosity occurs, and this is interpreted as an induced orientational change of the smectic layer.[3] The ER study on the liquid crystals, thus, gives us interest results on the relationship between the structure and the rheology. In the present study, the ER effect in ferroelectric smectic C* phase is studied, focusing on the role of the spontaneous polarization characteristic to this phase.

Ferroelectric liquid crystals used for the measurements is 4-(6-methyl)octyl-resorcylidene-4'-octylaniline (MORA 8), which has a phase sequence of crystal(K)- smectic C*(SmC*) - isotropic(Is). For comparison, 4-n-octyloxyphenyl-4-(2"-methylbutyl)biphenyl-4'-carboxylate (8OBE) is also studied. The ER effect is measured using a viscometer of a double cylinder type, which is possible to apply a high voltage of a few kV to the gap (1mm) between the inner and outer cylinders. The electric field, thus, is applied perpendicular to the flow. The temperature of the specimen is controlled within 0.1 K.

Temperature dependence of the shear stress, which is proportional to the viscosity, measures for MORA 8 is given in Fig. 1. The shear stress in SmC* phase does not show a strong temperature dependence and decreases at the SmC*-Is phase transition point, resulting in the low shear stress in Is phase. The flow in SmC* is characterized by a non-Newtonian flow and that in Is phase by a Newtonia flow. The application of the electric field induces a change of the rheology. The result of shear stress vs. electric field is depicted in Fig. 2. At higher shear rates, the shear stress increase monotonously with the amplitude of the electric field. On the other hand, at low shear rates, the shear stress decreases at medium electric fields of around 2 kV/mm and increases again at higher electric fields. Such rheological behaviors are characteristic to the SmC* phase, and will be discussed on the basis of structural change, direction of the spontaneous polarization, field induced phase transition, and comparison with the result of 8OBE.

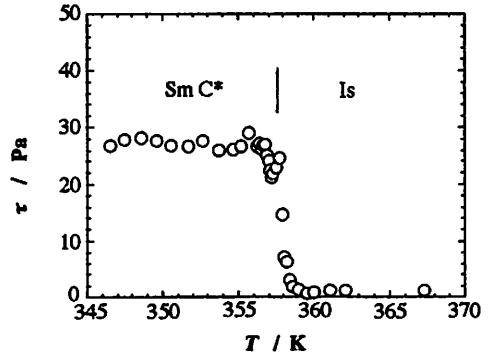

Fig. 1: Temperature dependence of the shear stress measured at a shear rate of 65.9 s^{-1}.

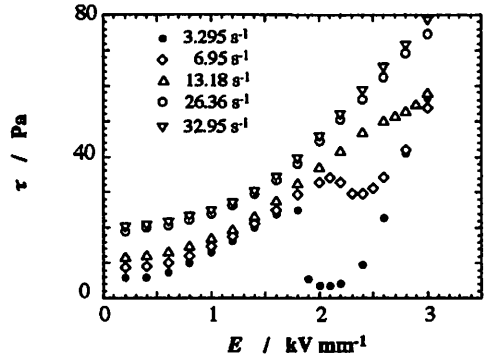

Fig. 2: Shear stress vs. electric field (20 Hz) at various shear rates (345.9 K).

[References]

1. M. Nakano and K. Koyama (eds.), "Electro-rheological fluids, mageto-rheological suspensions and their applications", (World Sci. , 1998).
2. K. Negita, *J. Chem. Phys.* 1996, 105, 7837.
3. K. Negita, *Mol. Crys. Liq. Crys.*, 1997, 300, 163.

Determination of Solvent Reorganization Energy by Charge-Transfer Exchange Interaction in Short Lived Radical Ion Pairs

Yasuhiro KOBORI[1,2], Kimio AKIYAMA[1] and Shozo TERO-KUBOTA[1]
[1] Institute for Chemical Reaction Science, Tohoku University, Sendai, 980-8577, Japan
[2] PRESTO, Japan Science and Technology Corporation (JST)

According to the electron-transfer (ET) reaction theory, the reorganization of the solvent molecules has a quite important factor to determine the ET reaction probability in a liquid media. If the solvent reorganization energy (λ_S) is determined in an electron acceptor-donor (AD) system, one can discuss the own structure of a radical ion-pair (RIP) including the solvent molecules around the RIP. In this study, we propose a novel method to determine the total reorganization energy (λ) precisely by monitoring the dependence of the sign of the charge-transfer exchange interaction (singlet-triplet energy difference of the RIP: J)[1] on the energy gaps ($-\Delta G_{CR}$) for the charge-recombination process.

We observed the time-resolved electron paramagnetic resonance (TREPR) spectra of duroquinone anion radical generated by the photoinduced ET reactions from 1,2,4-trimethoxybenzene (TMB) to excited triplet duroquinone (DQ) in polar solvents. The signs of the J were clearly determined from the phases of the chemically induced dynamic electron polarization (CIDEP) caused by the radical pair mechansim.[2] In dimethylsulfoxide (DMSO), negative J was obtained, while in benzonitrile (BN), the J was positive in the RIP. In DMSO:BN = 8:2 (v/v) mixture, J could not be defined and J~0 was resulted. Taking into account the charge-transfer exchange interaction[1], the sign of the J is negative when the solvent separated RIP potential surface crosses with the ground state AD pair at the normal region ($-\Delta G_{CR}<\lambda$). The J is positive when the level crossing occurs at the inverted region ($-\Delta G_{CR}>\lambda$). $-\Delta G_{CR}=\lambda$ leads to an optimum condition for the charge-recombination process of the RIP. In this case, magnitude of the J becomes zero. Consequently, we are able to obtain the λ by using the redox potentials of DQ-TMB system in the solvents, in which J=0 is observed. λ=1.80(±0.1) eV was determined as the total reorganization energy for the charge recombination in the DQ-TMB system. The λ is composed of the intramolecular vibration reorganization energy (λ_V) and λ_S. From the estimated λ_V value, λ_S = 1.35 eV was obtained in the DQ-TMB system. Structures of the RIPs including the solvent molecules will be discussed from λ_S values.

References

1. Sekiguchi, S.; Kobori, Y.; Akiyama, K.; Tero-Kubota, S. *J. Am. Chem. Soc.* 1998, **120**, 1325.
2. Adrian, F. J. *Rev. Chem. Intermed.* 1979, **3**, 3.

HYDROPHOBIC MOLECULAR CLUSTERING OF AMIDE COMPOUNDS OBSERVED THROUGH IR AND MASS SPECTROSCOPY

Hayato ISHII[1], Kazuko MIZUNO[1] and Akihiro WAKISAKA[2]

[1]Center for Instrumental Analysis, Fukui University, Fukui 910-8507, Japan

[2]National Institute for Resources and Environment, Onogawa 16-3, Tsukuba, Ibaraki 305-8569, Japan

The hydrophobic effect plays important role in the molecular self-assembling process. Especially, the organic molecule with a hydrophilic group such as hydroxyl, carboxyl, amide group, etc., forms ordered structure due to the balance between the hydrophobic and hydrophilic effect, as depending on the size of hydrophobic group and the concentration in water.

As a new experimental approach to see the molecular self-assembling through the hydrophobic effect, molecular clustering of *N*-methyl alkylamide derivatives (*N*-methylformamide (NMF) and *N*-methylpropionamide (NMP)) was studied by IR and Mass spectrometry.

By the mass spectrometric analysis of clusters isolated from aqueous NMF and NMP solutions, the molecular clustering structure was found to be roughly divided into three groups depending on the amide concentrations. Fig. 1 shows the amide concentrations in which the three types of cluster structure were observed. In the region A, the amide molecules exist as monomeric molecules which interact with water clusters; on the other hand, in the region C, the amide molecules are easy to form self-aggregation clusters. The region B corresponds to the intermediate region where the self-aggregation of the amide was promoted through the dehydration with increase of the temperature. Fig. 1 demonstrates that the amide with larger alkyl group forms self-aggregation clusters more easily.

Furthermore, it will be reported that the change of cluster structure in each region is in good agreement with the frequency shift of the C-H streching vibration band for the amide on dilution with water.

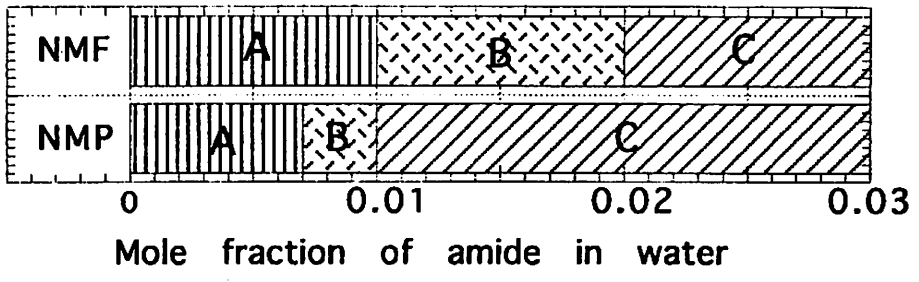

Fig. 1 Effect of concentrations of *N*-methylformamide (NMF) and *N*-methylpropionamide (NMP) on the amide clustering in water. In the region A, B and C, the solutions have the characteristic cluster structure, A: monomeric amide molecule, B: intermediate state, C: amide self-aggregation cluster.

EXAFS and X-ray Diffraction Study on Concentrated Gallium(III) Bromide and Perchlorate Solutions in Liquid and Glassy State

Pavel SMIRNOV and Toshio YAMAGUCHI
Department of Chemistry, Faculty of Science, Fukuoka University, Nanakuma, Jonan-ku, Fukuoka 814-0180, Japan

The supercooled state of aqueous solutions has attracted much attention in connection with various special properties of solutions such as nucleation of ice, crystallization of solutions, glass transition, and so on. Aqueous gallium(III) halide solutions are especially interesting because Ga^{3+} has a highly positive charge 3+ and a trend of complex formation.

X-ray absorption fine structure (XAFS) measurements have been performed on 2.43M $GaBr_3$, 1.83M $GaBr_3$ - 5.5M LiBr and 2.92M $Ga(ClO_4)_3$ (M=mol dm^{-3}) aqueous solutions in the liquid state at room temperature and in the glassy state at liquid nitrogen temperature. X-ray absorption spectra for the sample solutions were measured in transmission mode at the BL10B station of Photon Factory (typical operating conditions were 2.5 GaV and 160 mA). X-rays were monochromatized by an Si(311) channel-cut monochromator. The absolute X-ray photon energy was not calibrated, but the energy of a small peak in the edge of metallic copper was assumed to be 8980.6 eV. The energy resolution of the optical system was ca. 0.8 eV and the energy reproduced within ±0.2 eV. Reproducibility of the EXAFS spectra was checked carefully. The XAFS data have revealed that there are hexaaqua gallium(III) ions in the $Ga(ClO_4)_3$ solution with the Ga^{3+} - OH_2 distance of 196 pm. The equilibrium $Ga(H_2O)_6^{3+} \Leftrightarrow [GaBr_4]^-$ is present in the $GaBr_3$ solutions. The average distances in the solutions are Ga^{3+} - OH_2 = 196 pm and Ga^{3+} - Br^- = 233 pm. Addition of excess of bromide ions shifts the equilibrium to the right-hand-side. Cooling of the solutions leads to the shift of the equilibrium to the left-hand-side.

X-ray scattering measurements have been performed on aqueous 1.85M $Ga(ClO_4)_3$, 2.01M $GaBr_3$, and 1.48M $GaBr_3$ - 4.05M LiBr aqueous solutions over temperature range of – 30°C - 60°C. Experiments have been made with a Rigaku θ-θ type diffractometer using MoKα radiation. Cooling of the solution was made on a specially designed cryostat. It has been shown that in the perchlorate solution Ga^{3+} forms the first coordination shell consisting of six water molecules at a distance of 195 pm and the second coordination shell at a distance of 403 pm. Solvent-separated ion pairs are present in the solution in the temperature range studied. In both $GaBr_3$ solutions there are hydrated Ga^{3+} ions with Ga^{3+} - OH_2 distance of 195 pm and tetrabromogallate complex with Ga^{3+} - Br^- distance of 234 pm, which exist in equilibrium $[Ga(OH_2)_6]^{3+} \Leftrightarrow [GaBr_4]^-$. Addition of excess Br^- shifts the equilibrium to the right-hand-side. Cooling of the solution leads to decreasing of the amount of the gallium bromide complex. These conclusions are in good agreement with EXAFS results.

An *in Situ* X-ray Absorption Fine Structure Study of Different Oxidation States of Mixed-Metal Trinuclear Complexes in Acetonitrile Solution

Akihiro KIKUCHI[1], Takaaki TOKUNAGA[2], Toshimi TAKEUCHI[2], Yoichi SASAKI[1] and Toshio YAMAGUCHI[2]

[1] Division of Chemistry, Graduate School of Science, Hokkaido University, Sapporo 060-0810, Japan

[2] Department of Chemistry, Fukuoka University, Fukuoka 814-0180, Japan

Oxo-centered trinuclear complexes with bridged carboxylates are common to a wide variety of transition metal ions. Among them, mixed-metal trinuclear complexes containing diruthenium(III) moiety such as $[Ru^{III}_2M^{II}(\mu_3\text{-}O)(\mu\text{-}CH_3COO)_6(pyridine)_3]$ (M = Co (**1**), Ni (**2**), Zn (**3**) Mg (**4**); Figure) are important because they play an important role in understanding the nature of metal-metal interaction.

Although X-ray crystal structures for **1** and **2** have been previously reported,[1] all metal ions are statistically disordered within the trinuclear core. On the other hand, X-ray absorption fine structure (XAFS) is an element-specific structural technique that does not depend on the presence of long-range order, and it has been widely used to determine metal-atom environments. Here, we will report an XAFS study of the trinuclear complexes **1** – **3** in acetonitrile solution at both the ruthenium and divalent metal K-edges so as to circumvent the disoder problem.

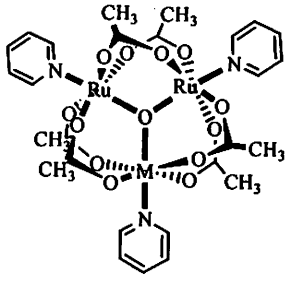

Figure Schematic structure of the trinuclear complex

In addition, XAFS spectra have been recorded for one and two-electron oxidized forms of the complexes **1** - **4** in acetonitrile solution by using a newly developed *in situ* electrochemical cell. The Ru-O_{bridge} distances in the complexes **1** - **4** decrease upon oxidation, indicating that the oxidation sites are ruthenium ions. This trend is good accordance with our previous XAFS study of relevant oxo-bridged ruthenium dimers.[2] However, the absorption peaks of the divalent M^{II} K-edge also shift to higher energy. Thus, it is difficult to derive a conclusion whether the redox centers are localized only on the portion of $Ru_2(\mu_3\text{-}O)$ in the mixed-metal trinuclear complexes, or only on the divalent center. It is likely that some delocalization of redox equivalence to the whole mixed-metal core occurs.

1) Ohto, A. et. al., *Inorg. Chem.* 33, **1994,** 1245

2) Valli, M. et. al., *Inorg Chem.* 36, **1997**, 4622

ROLES OF SOLVATION IN VARIABILITY FOR LIGAND FIELD AND CONFORMATIONAL DYNAMICS OF Cr(III) COMPLEXES AS REVEALED BY DEUTERON NMR SPECTRA

Sumio KAIZAKI
Department of Chemistry, Graduate School of Science, Osaka University, Toyonaka, Osaka, 560, Japan

There have been a number of spectroscopic studies on d-d transitions or ligand field and stereochemistry of metal complexes. Among them, paramagnetic NMR have been one of the most potential.[1] Most targets were labile complexes such as Ni(II). However, they were limitedly applicable to mixed ligand complexes in contrast with inert complexes such as Cr(III) of which ^{2}HNMR spectra were found to be suitable to determining solution structures.[2] In the present paper, solvatochromic and solvent dependent stereochemical phenomena are analyzed from ^{2}HNMR spectra observed for Cr(III) complexes. The solvation around the second coordination sphere in the complexes is found to result in the bond length variation leading to the solvatochromism and in chelate ring conformational change. Solvent- and/or temperature-dependent ^{2}HNMR spectra will demonstrate the usefulness to elucidate the ligand field splitting and the conformational dynamics of the amino acidato and diamine chelate rings of mixed ligand Cr(III) complexes in solutions.

1) Solvatochromism and Ligand Field Splitting:[3]

On the basis of the spectroscopic findings for *trans-* and *cis*-$[CrF_2(N)_4]^+$ type complexes,[4,5] the solvatochromism or solvent-dependent ligand field bands of *fac*-$[CrF_3(tpa)]$(tpa=tri(2-pyridyl)amine) demonstrated the sensitivity of the Cr-ligand bond length or the angular overlap model parameters to the embedding solvents with the solvents' electron acceptor number, and revealed the trigonal splitting in the first $^4T_2 \leftarrow {}^4A_2$ ligand field band owing to the anisotropic Cr-pyridyl π interaction in spite of the holohedrized octahedral symmetry. This was also supported by the solvent dependent ^{2}H NMR contact shifts, of which the inverse correlation for 4- and 3-deuterons of the pyridyl in the tpa complex with the solvents' acceptor number gives direct evidence for the strong acceptor to weak donor π interaction depending on the solvents.

2) Conformational Dynamics of Chelate Rings in Solutions:[6]

Solvent dependent ^{2}H NMR spectra of five-membered α-amino acidato mixed ligand Cr(III) complexes with deuterated methylene, $[Cr(acac)_2(am\text{-}d_2)]$, demonstrated that the solvation toward to the amino proton(s) induce the amino acidato chelate ring conformational change leading to nonplanarity analogously to the cases of the *N*-substituted amino acidato complexes; *i.e.*, the chelate ring conformational rigidity of the edta-like complexes,[7] the existence of the diastereomers of the *N*-Megly(sarcosine) and *N*-Phgly complexes due to the asymmetric coordinated nitrogen atom and the puckered ring in the *N*-Me_2gly complex. Variable temperature ^{2}HNMR spectra of the am complexes suggested the ring puckering for the *N*-Megly and *N*-Phgly complexes and fairly rigid conformations for the gly and *N*-Me_2gly complexes in solutions.

On the other hand, the ethylenediamine analogue $[Cr(acac)_2(en\text{-}d_n)]$ showed more profound solvent and counter ion dependent ^{2}HNMR spectral changes, substantiating more puckered chelate rings due to solvation and/or ion-pairing with counter ions toward the amino protons. The *N*-substituted homologues showed somewhat different NMR behavior from the corresponding am compelxes; the ^{2}HNMR spectra of the *N*-Meen complex exhibit the diastereomers like the *N*-Megly and *N*-Phgly complexes, whereas *N*-Me_2en complex show only one NMR signals arising from the planar ring or rapid puckering unlike the *N*-Me_2gly complex. The thermodynamic parameters for the conformational equilibrium of the en chelate ring estimated from variable temperature ^{2}HNMR spectra will be discussed in connection with the difference in solvation.

1. Bertini, I.; Luchinat, C., *Coord. Chem. Rev.*, 1996, **150**.
2. Wheeler, W. D.; Kaizaki, S.: Legg, J. I., *Inorg. Chem.*, 1982, **21**, 3248.
3. Terasaki, Y.; Fujihara, T.; Schönherr,T.; Kaizaki, S.; *Inorg. Chim. Acta*, 1999, to be accepted.
4. Kaizaki, S; Takemoto, H., *Inorg. Chem.*, 1990, **29**, 4960.
5. Terasaki, Y. ; Kaizaki, S., *J. Chem. Soc., Dalton Trans.* **1995**, 2837.
6. Kaizaki, S; Misaki, N.; Fukushima, T.; Motoki, S.; Ohomori, H.; Fuyuhiro, A., Manuscript in preparation.
7. Kaizaki, S.; Hayashi, M., *J. Chem. Soc. Dalton Trans.*, **1989**, 1947.

LIGAND-EXCHANGE EQUILIBRIA OF BERYLLIUM(II) ION AND HYDROGEN-BONDING INTERACTION IN ITS SECONDARY SOLVATION SPHERE AS STUDIED BY ^{9}Be NMR AND AB INITIO MOLECULAR ORBITAL METHODS

Yoshihisa NAKAYAMA[1], Yasuhiro INADA[2] and Shigenobu FUNAHASHI[1]

[1] Laboratory of Analytical Chemistry, Graduate School of Science, Nagoya University, Chikusa, Nagoya 464-8602, Japan

[2] Research Center for Materials Science, Nagoya University, Chikusa, Nagoya 464-8602, Japan

The investigation of ligand-exchange behaviors for Be(II) ion in solution is important in the biological point of view because of its high toxicity. For the solvation structure of the Be(II) ion in aqueous solution, it has been characterized experimentally and theoretically that the Be(II) ion has the 4-coordinate tetrahedral structure. The widely investigated kinetics of solvent exchange and complexation reactions for the Be(II) ion in solution have been characterized by the relatively slow rate and the associative mode of activation. In this study, we have determined the equilibrium constants of the ligand-exchange reactions (equation 1) of the

$$[BeL^{1}_{5-i}L^{2}_{i-1}]^{2+} + L^{2} \rightleftharpoons [BeL^{1}_{4-i}L^{2}_{i}]^{2+} + L^{1} \quad (i = 1\text{–}4) \qquad (1)$$

Be(II) ion with some unidentate oxygen-donating ligands, such as water, *N*,*N*-dimethylformamide, and 1,1,3,3-tetramethylurea, by means of the ^{9}Be NMR spectroscopy and *ab initio* molecular orbital calculation. We focused on the elucidation of the bonding characteristic of the Be(II) center and the interaction with water molecules in the secondary solvation sphere affecting the ligand-exchange thermodynamics.

The ligand-exchange thermodynamic parameters were determined by the variable-temperature ^{9}Be NMR measurements as a function of concentrations of Be(II) ion and ligands in propiononitrile (PN) as a solvent, in which the PN molecule does not coordinate to the Be(II) ion directly. The electronic properties and the isotropic nuclear mangetic shielding tensor of the component species in the ligand-exchange equilibria were evaluated by means of the *ab initio* molecular orbital calculations using the *Gaussian 94* program in the RHF/6-311++G(3d,2p) level.

It was found that the chemical shifts of ^{9}Be NMR varied to the higher field with the coordination of the more electron-donating ligand to the Be(II) center. According to the molecular orbital calculations, the more electron-donating ligand makes the electron density on the Be(II) ion larger, while the isotropic nuclear magnetic shielding becomes smaller. This means that the electrons on the Be(II) ion interact more strongly with the coordinating oxygen in the more electron-donating ligand. Thus, the chemical shift of ^{9}Be NMR becomes the measure of the strength of the electronic interaction between the Be(II) ion and the ligand.

The values of chemical shifts were affected by the concentration of the free water, *i.e.*, the resonance in the lower field was observed under the higher concentration of free water. The formation of the hydrogen bond in the secondary solvation sphere between the coordinating and bulk water molecules polarizes the coordinating water molecules on the Be(II) ion. The interaction between the electrons on the Be(II) ion and coordinating oxygens becomes more effective due to the polarization owing to the hydrogen bonding and, thus, it is interpreted that the ^{9}Be NMR peak is down-field shifted with an increase in the content of free water.

Speciation of Copper(II) Complexes in Aqueous Solution as Trapped on Exchange Resins by Electron Paramagnetic Resonance Spectroscopy.

Young-Ho MOON[1,2], Yutaka MIURA[1,3], Masahiko TACHIBANA[1], and Akira NAGASAWA[1]

[1] Department of Chemistry, Faculty of Science, Saitama University, Shimo-Okubo, Urawa 338-8570, Japan

[2] Forensic Science Division ,National Institute of Scientific Investigation, Yangchun, Seoul 331-1, Korea

[3] Present Address: Department of Chemistry, Tokyo Metropolitan University, Hachioji 192-0397, Japan

Electron paramagnetic resonance (EPR) was applied to the determination of total concentration and the speciation of copper adsorbed on exchange resins with model solutions of environmental samples.

A number of solutions containing copper(II) complexes including tetraamminecopper(II) ion $[Cu(NH_4)_3]^{2+}$ (sulfate), bis(2,2'-bipyridine)copper(II) ion $[Cu(bpy)_2]^{2+}$ (chloride), bis(glycinato)-copper(II) $[Cu(gly)_2]^0$, and bis(oxalato)cuprate(II) ion $[Cu(ox)_2]^{2-}$ (potassium salt) were treated by a chelating resin Chelex 100, having iminodiacetate residue as a functional group. The EPR spectra of the blue colored copper-adsorbed resins were recorded at ambient temperature, which were analyzed as inhomogeneously dispersed Cu(II) center in axial symmetry.

The $g_{//}$ and $A_{//}$ values were not identical with those of the original copper complexes in mother liquor, but similar with that of Chelex 100 treated with aqueous $CuSO_4$. This observation suggests that the original ligands in solution were at least partially substituted by iminodiacetate residue of Chelex 100 .

Taking the peak to peak height of the g perpendicular region of the spectra as a measure of strength of the signal, the influence of pH, concentration of the Cu complexes, and mass of resins have been studied. In conclusion, when the mass of the resins and the pH of the solution had set constant, the concentration of Cu complexes in mother liquor and the spectral strength had a good linear relationship. These results show that Chelex 100 can be used as determination of concentration of total Cu(II) in aqueous solutions, utilizing high affinity of Chelex 100 resin to Cu(II).

The results of species-sensitive analysis of copper complexes employing cation and anion exchange resins, which may preserve the chemical forms in solution, will be also presented.

SOLVATOCHROMIC BEHAVIOR OF COPPER(II) COMPLEXES OF CYCLAM AND ITS ANALOGS AS SOLVENT PARAMETER INDICATOR

Y. MORIGUCHI[1], Y. CHAN[1] and K. SAKATA[2]

[1] Department of Chemistry, Fukuoka University of Education, Munakata, 811-4192, Japan

[2] Department of Applied Chemistry, Faculty of Engineering, Kyushu Institute of Technology, Kitakyushu, 804-8550, Japan

The some interesting relations between solvent effect on UV-Vis absorption spectra of amine metal complexes and solvent parameter have observed in solvatochromism of mixed diamine-β-diketone Cu(II) chelate[1)] and ion-pair formation of 1,4,8,11-tetramethylcyclam Ni(II) chelate[2)]. The authors have reported linear relation between stability constants for Cu(II) complexes of cyclam and 2,3,9,10-methyl or cyclohexyl substituted cyclams and λ_{max} of their visible spectra in some organic solvents[3)]. In this report, the authors report results of that preparing Cu(II) complexes of cyclam and 2,3,9,10-dicyclohexyl cyclams, $[Cu(L)]X_2$,(X=Cl^-,Br^-,ClO_4^-,$BPhe_4^-$) and observing their ligand-field band for D4h symmetry in various solvents, water(**1**,W), propylenecarbonate(**2**,PC), acetone(**3**,AC), methanol(**4**,MeOH), formamide(**5**,FA), N,N-dimethylformamide (**6**,DMF), dimethylsulfoxide(**7**,DMSO), and acetonitrile(**8**,AN). The maximum absorption wave number,$\tilde{\nu}_{max}$, shifts depending upon solvent parameters, dielectric constant(Dc), donor number(Dn), acceptor number(An) and good linear relationship has been found in case of $[Cu(L)](ClO_4)_2$ as shown in Figs. and Eqs. The Eqs. are applied as solvent parameter indicator to predict unknown solvent parameter. This solvatochromism effect is assumed to be caused by perturbation axially-elongated ligand field through axial approach of solvent to D4h Cu(II) complex.

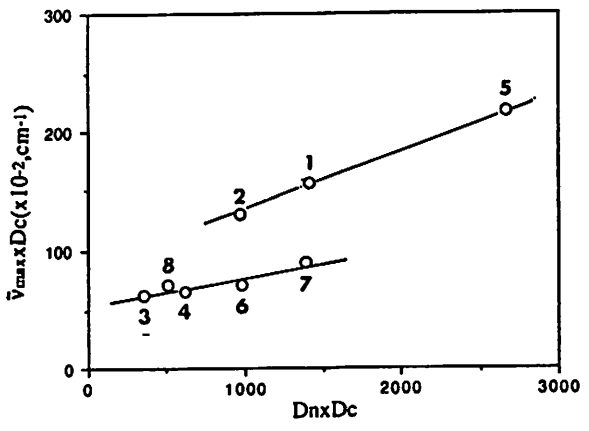

$\tilde{\nu}_{max}xDc = \alpha_1 DnxDc + \beta_1$

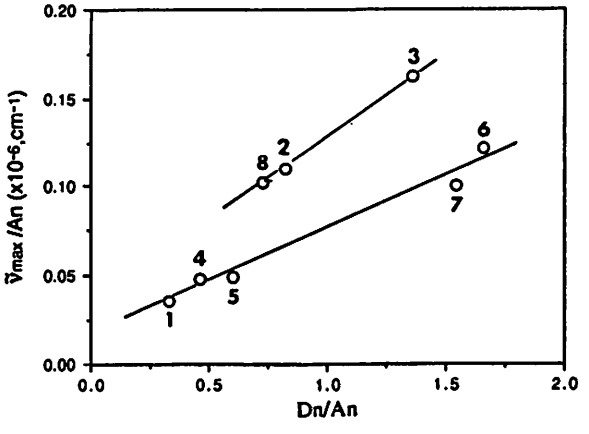

$\tilde{\nu}_{max}/An = \alpha_2 Dn/An + \beta_2$

1) K.Sone and Y. Fukuda, "Inorganic Thermochromism", Spring-Verlag, Heizenberg(1987).
2) E. Iwamoto, T. Yokoyama, S. Yamasaki, T. Yabe, T. Kumamaru, and Y. Yamamoto, *J. Chem. Soc., Faraday Trans.* 1988, 1935.
3) Y. Moriguchi, K. Sakata, K. Kobiro and Y Tobe, *J Coord. Chem.*, 1997, **42**, 143.

STABILITY CONSTANTS IN WATER AND TRANSFER ACTIVITY COEFFICIENTS FROM WATER TO NONAQUEOUS SOLVENTS OF 15,15-DIMETHYL-16-CROWN-5 COMPLEXES WITH UNIVALENT METAL IONS

Shoichi KATSUTA[1], Yoshihiro KUDO[1], Yasuyuki TAKEDA[1] and Mikio OUCHI[2]

[1] Department of Chemistry, Faculty of Science, Chiba University, 1-33 Yayoi-cho, Inage-ku, Chiba 263-8522, Japan

[2] Department of Applied Chemistry, Faculty of Engineering, Himeji Institute of Technology, 2167 Shosha, Himeji, Hyogo 671-2201, Japan

Lariat ethers, which possess cation-ligating side arms, were originally designed to enhance the cation-binding ability of the parent crown ethers. However, it was shown that the complex stability constants in water of 15-(2,5-dioxahexyl)-15-methyl-16-crown-5 (L16C5) with several metal ions are comparable to the corresponding values of 16-crown-5 (16C5), and that the total effect of the side arms (methyl and 2,5-dioxahexyl groups) on the complexation is very small.[1] The stability of 15,15-dimethyl-16-crown-5 (DM16C5) complexes serves to evaluate the effects of the side arms of L16C5 separately. In this study, the stability constants (K_{ML}) of the 1:1 complexes of DM16C5 with Na^+, K^+, and Ag^+ in water have been determined at 25 °C by conductometry. The transfer activity coefficients (${}^{S}\gamma^{H2O}$) from water to nonaqueous solvents (S) [S = acetonitrile (AN), propylene carbonate (PC) and methanol] of DM16C5-Na^+ and -K^+ complexes have been calculated in order to discuss the solvation of the complexes

The selectivity order of DM16C5 in water for the univalent metal ions is $Ag^+ > Na^+ > K^+$, which is the same as that of L16C5 and 16C5. However, the K_{ML} values of DM16C5 are smaller than the corresponding values of 16C5 and L16C5. This leads to the conclusions that the methyl group as a side arm decreases the complex stability and that the 2,5-dioxahexyl arm increases. The decrease in log K_{ML} from 16C5 or L16C5 to DM16C5 is especially large for the K^+ complex, and the Na^+/K^+ selectivity of DM16C5 in water is higher than that of 16C5 and L16C5.

The values of ${}^{S}\gamma^{H2O}$ expresses the relative strength of solvation in S and water. In all the S/H_2O systems, the complexes of these three crown ethers with Na^+ and K^+ are more lipophilic than the free crown ethers in spite of the marked hydrophilicity of the metal ions. This is attributable to not only the dehydration of the metal ions upon complexation but also the reduced hydrogen bonding between the ether oxygen atoms and water as a result of metal–oxygen bonding. Although Na^+ is much more hydrophilic than K^+ in the AN/H_2O and PC/H_2O systems, the Na^+ complexes of 16C5 and L16C5 are always less hydrophilic than the corresponding K^+ complexes. This indicates that Na^+ in the complexes is more effectively screened from water than K^+. On the other hand, the ${}^{S}\gamma^{H2O}$ value of the DM16C5 complex varies with the central metal ion in the same way as that of the free metal ion. Na^+ in the DM16C5 complex is less effectively screened from water than in the complexes of 16C5 and L16C5.

1. Takeda, Y. *et al.*, *J. Chem. Soc. Faraday Trans.*, 1995, **91**, 4079; *J. Incl. Phenom.*, 1991, **11**, 159.

Fluorescence Lifetime of Pyrene and Naphthalene in Acetonitrile-Water Mixtures

Jun Nishimoto[1], Kazuo Inoue[2], Toshiyuki Takamuku[2], and Masaaki Tabata[2]
[1] Instrumental Analysis Center, Saga University, Honjo-machi, Saga 840-8502, Japan
[2] Department of Chemistry, Faculty of Science and Engineering, Saga University, Honjo-machi, Saga 840-8502, Japan

Acetonitrile (AN)-water mixtures at various mole fraction of acetonitrile X_{AN} are widely used in many cases such as HPLC, solvent extraction, etc. We have investigated structure of acetonitrile-water mixtures by X-ray diffraction and IR spectroscopy over a wide range of acetonitrile mole fractions.[1)] We have concluded that microheterogeneity, in which both acetonitrile and water clusters coexist, occurs in the mixtures. In the present study, microheterogeneity in acetonitrile-water mixtures ($0.0 < X_{AN} < 1.0$) has investigated by a fluorescence lifetime method with using pyrene and naphthalene as probes.

Figure 1 shows fluorescence lifetimes ($\tau_{1/2}$) of pyrene and naphthalene in the acetonitrile-water mixtures as a function of mole fraction of acetonitrile. The lifetime values for both pyrene and naphthalene increase with increasing acetonitrile mole fraction at $0.0 < X_{AN} < 0.3$ and show plateau at $0.3 \leq X_{AN} \leq 0.7$. However at $0.7 < X_{AN} \leq 1.0$ the lifetime value for pyrene decreases with increasing acetonitrile mole fraction, while that for naphthalene decreases. These findings indicate that pyrene and naphthalene are dissolved in acetonitrile clusters at $0.3 \leq X_{AN} \leq 0.7$. On the other hand, the aromatic probes are partially hydrated at $0.0 < X_{AN} < 0.3$, leading to decreases of lifetime values. At $0.7 < X_{AN} \leq 1.0$, the different behavior of lifetime between pyrene and naphthalene probably arises from the difference of solvation energy by acetonitrile.

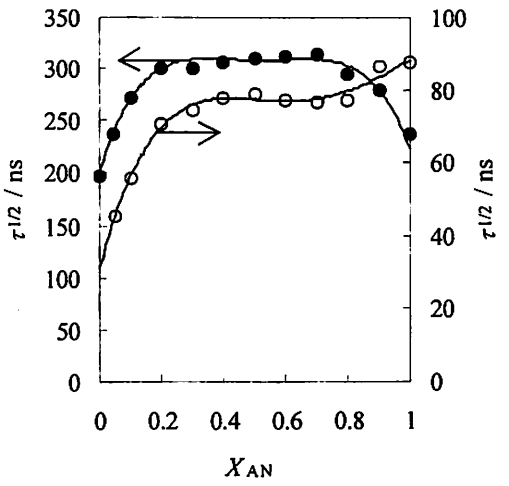

Figure 1. Fluorescence lifetimes of pyrene (●) and naphthalene (○) in acetonitrile-water mixtures.

1. Takamuku, T.; Tabata, M.; Yamaguchi, A.; Nishimoto, J.; Kumamoto, M.; Wakita, H.; Yamaguchi, T., *J. Phys. Chem.*, 1998, **102**, 8880.

Solvation and Metalloporphyrin Formation of Cu(II) Ion in Aqueous Acetonitrile

Masahiko INAMO[1], Naruhisa KAMIYA[1], Yasuhiro INADA[2], and Shigenobu FUNAHASHI[3]
[1] Department of Chemistry, Aichi University of Education, Kariya 448-8542, Japan
[2] Research Center for Materials Science, Nagoya University, Nagoya 464-8602, Japan
[3] Department of Chemistry, Faculty of Science, Nagoya University, Nagoya 464-8602, Japan

Metalloporphyrin formation reaction is an important process in biological systems, especially in relation to the biosynthesis of heme. Although metalloporphyrin formation reactions have been studied for many decades, the reaction mechanism has not yet been fully elucidated. Reaction intermediate which has been proposed to exist in the metalation reaction (a sitting-atop complex) was recently confirmed spectrophotometrically in pure acetonitrile.[1] In the present study, the electronic and steric effects of the porphyrin on the metalation reaction was studied using various types of porphyrins in acetonitrile containing various amount of water up to 1 M in order to elucidate the reaction mechanism.

EXAFS measurements were performed for the solution containing *ca.* 0.1 M Cu(II) triflate in aqueous acetonitrile in the vicinity of the Cu K-edge using the BL-12C station at the Photon Factory of the National Laboratory for High Energy Physics. By using the $k^3\chi_{obs}(k)$ values obtained from the EXAFS spectra, the overall equilibrium constant β for the reaction of the Cu(II) ion with water molecules in the solvent was determined: $\log \beta_1 = 1.32 \pm 0.25$, $\log \beta_2 = 1.49 \pm 0.31$ (25°C).

Metalation reactions of tetraphenylporphyrin (TPP), tetramesitylporphyrin (TMP), tetrakis(4-chlorophenyl)porphyrin (TCPP), and octaethylporphyrin (OEP) with the Cu(II) ion were studied spectrophotometrically. In acetonitrile-water mixed solvent, a sitting-atop complex, in which two pyrolenine nitrogen atoms coordinate to the Cu(II) ion and two hydrogen atoms still bind to the two pyrrole nitrogens, is produced after mixing the Cu(II) triflate and porphyrin solutions. Rates of the reaction were followed under the pseudo-first-order conditions where the Cu(II) ion was in large excess over the porphyrin. Reaction is first order with respect to both porphyrin and Cu(II) ion. Dependence of the conditional second-order rate constant k on $[H_2O]$ indicates that the k value decreases with increasing in $[H_2O]$ according to equation 1.

$$k = (k_1 + k_2\beta_1[H_2O] + k_3\beta_2[H_2O]^2)\,(1 + \beta_1[H_2O] + \beta_2[H_2O]^2)^{-1} \quad (1)$$

Values of k_1 was determined as $(4.2 \pm 0.1) \times 10^5$ M^{-1} s^{-1} (TPP), $(1.2 \pm 0.1) \times 10^5$ M^{-1} s^{-1} (TCPP), and $(5.2 \pm 0.1) \times 10^3$ M^{-1} s^{-1} (TMP) at 25°C. The reaction mechanism will be discussed on the basis of electronic and steric effects of porphyrins as well as the solvation of the Cu(II) ion.

1. Y. Inada, Y. Sugimoto, Y. Nakano, Y. Ito, and S. Funahashi, *Inorg. Chem.*, 1998, **37**, 5519.

PROTECTION OF IMINES COORDINATED IRON(II) FROM HYDROLYSIS BY ACETONITRILE COORDINATION

Masafumi Goto, Tamaki Yamashita, and Hiromasa Kurosaki
Faculty of Pharmaceutical Sciences, Kumamoto University, Oe-honmachi, Kumamoto, 862-0973, Japan

Though imine bond formation is one of the most successful way to construct multidentate ligands, the stability of the imines coordinated to metal ions has not been explored fully. An iron(II) chelate (acetonitrile)[3-(1-iminoethyl)-2,4-bis(2-pyridylmethylimino)pentane=L] iron(II), **2**, obtained from **1**[1] cleaves DNA efficiently in the presence of hydrogen peroxide[2] and has the structural characteristic of three imines not delocalized to each other. In order to investigate the relevance of the identity of **2** in aqueous solution, the decomposition of **2** in acidic or neutral aqueous solution was examined.

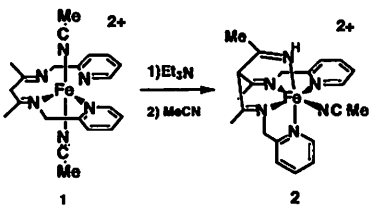

1 2

The decomposition of **2** was followed by the spectral change in near UV region in the presence of acetonitrile. Absorption at 420 nm decreased but absorption at 318 nm was increased in the initial stage but decreased in the later stage. The decrease in absorbance at 420 nm followed a first-order rate law with k_{obs}. The rate was greately dependent on [MeCN] as shown in Figure 1. This dependency was consistent with a mechanism:

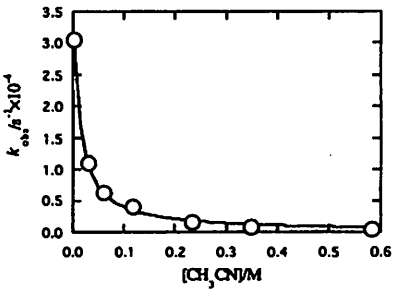

Fig.1 Plots of kobs against [MeCN].pH 7.0 100 mM MOPS buffer at 25 °C

$$Fe(L)\text{-}NCMe + H_2O \rightleftarrows Fe(L)\text{-}OH_2 + MeCN \quad (1)$$

$$Fe(L)\text{-}OH_2 \rightarrow \text{decomposed product} \quad (k_2) \quad (2)$$

$$K = [Fe(L)\text{-}NCMe]/[Fe(L)\text{-}OH_2][MeCN]$$

From the plot of $1/k_{obs}$ against [MeCN] gave a straight line and k_2 and K were estimated to be 4.1×10^{-4} s^{-1} and 85 M^{-1}. Below pH 3, the decomposition was catalyzed by H^+. k_{obs} was proportional to $[H^+]^2$. In 0.1 M aqueous $HClO_4$ solution, similar plots gave k_2= 0.124 s^{-1} and K=50 M^{-1}. These results show that the decomposition of **2** occur exclusively through aquo complex and the coordination of acetonitrile to the sixth coordination site retards the hydrolysis of imine ligands.

1) M. Goto, Y. Ishikawa, T. Ishihara, C. Nakatake, T. Higuchi, H. Kurosaki and V. L. Goedken, *J. Chem. Soc., Dalton Trans*, 1998,1213-1222. 2) Y. Ishikawa, Y. Morishita, T. Yamamoto, H. Kurosaki, M. Goto, H. Matsuo, and M. Sugiyama, *Chem. Lett.* 1998, 39-40.

Outer-sphere Electron Transfer Reactions of Bis(2,9-dialkyl-1,10-phenanthroline)copper(II/I) in Acetonitrile: alkyl = methyl and phenyl

Nobuyoshi Koshino, Yoshio Kuchiyama, Hideo D. Takagi, and Shigenobu Funahashi
Graduate School of Science, Nagoya University, Chikusa, Nagoya 464-8602, Japan

In this study, we evaluated self-exchange rate constants, k_{ex}, for electron transfer reactions of the $Cu(dmp)_2^{2+/+}$, $Cu(bcp)_2^{2+/+}$ and $Cu(dpp)_2^{2+/+}$ couples in acetonitrile from the direct measurements by the ^1H NMR line broadening method and from the cross reactions by application of the Marcus cross relation. The k_{ex} values of $Cu(dmp)_2^{2+/+}$ and $Cu(bcp)_2^{2+/+}$ estimated from the oxidation reactions of $Cu(dmp)_2^{+}$ and $Cu(bcp)_2^{+}$ with $Ni(tacn)_2^{3+}$ were consistent with those determined by the NMR method. In contrast, the values of k_{ex} calculated from the reduction reactions of $Cu(dmp)_2^{2+}$ and $Cu(bcp)_2^{2+}$ with $Co(bpy)_3^{2+}$ were 10^3 times smaller than those obtained by the NMR method. The pseudo-first-order rate constant for the reduction of $Cu(dmp)_2^{2+}$ and $Cu(bcp)_2^{2+}$ by $Fe(Cp)_2$ was not linear against the concentration of $Fe(Cp)_2$ in excess. These findings indicate that the electron transfer reactions of $Cu(dmp)_2^{2+/+}$ and $Cu(bcp)_2^{2+/+}$ proceed through Path B in Scheme 1[1]: a slow conformational change of Cu(II) species from tetragonal $Cu^{II}L(O)$ to tetrahedral $Cu^{II}L(Q)$ takes place prior to the outer-sphere electron transfer process. The preference of Path B for the $Cu(dmp)_2^{2+/+}$ and $Cu(bcp)_2^{2+/+}$ was explained by the relative instability of $Cu^{I}L(P)$ compared to $Cu^{II}L(Q)$. Furthermore, using $Fe(PMCp)_2$ as a reductant, the mixing of Path A and Path B became evident. The result confirmed that the mixing of the two pathways occurs by lowering the energy level corresponding to the less favorable $Cu^{I}L(P)$ species.

On the other hand, k_{ex} of $Cu(dpp)_2^{2+/+}$ calculated from both oxidation and reduction cross reactions were in good agreement with each other. This finding indicates that the redox reaction of $Cu(dpp)_2^{2+/+}$ takes place in a *concerted* manner by considering the pseudo-tetrahedral structure of $Cu(dpp)_2^{2+}$ and $Cu(dpp)_2^{+}$ due to much bulkier phenyl groups at the 2- and 9-positions.[2]

Scheme 1

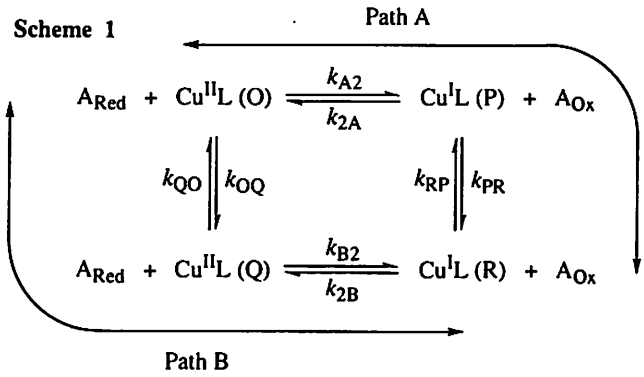

Abbreviations: dmp = 2,9-dimethyl-1,10-phenanthroline, bcp = 2,9-dimethyl-4,7-diphenyl-1,10-phenanthroline, dpp = 2,9-diphenyl-1,10-phenanthroline, tacn = 1,4,7-triazacyclononane, bpy = 2,2'-bipyridine, Cp= cyclopentadienyl, PMCp = pentamethylcyclopentadienyl.

1. Martin, M. J.; Endicott, J. F.; Ochrymowycz, L. A.; Rorabacher, D. B., *Inorg. Chem.*, 1987, **26**, 3012.
2. Miller, M. T.; Gantzel, P. K.; Karpishin T. B., *Inorg. Chem.*, 1998, **37**, 2285.

Reduction and Oxidation Reactions of Tetrakis(acetylacetonato)Cerium(IV) and -(III) Complexes in Acetonitrile: Change in the Reaction Pathways with the Driving Force of the Reaction

M. Matsumoto, H. Kodama, S. Funahashi, and H. D. Takagi
Graduated School of Sciences, Nagoya University, Furo-cho, Chikusa-ku, Nagoya, 464-8602, Japan

It is well known that the most of the outer-sphere redox reactions involving lanthanide ions proceed through the non-adiabatic pathways. Such a tendency in the lanthanide ions has been attributed to the effective shielding of the *f*-orbitals by the outer *s*- and *p*-orbitals. The hydrolytic problem as well as the instability of certain oxidation states of lanthanide species prevented us from detailed analyses of the redox reactions.

In 1981, Balzani *et al* investigated the reactions of $Eu_{aq}^{3+/2+}$ and reported that the reaction pathway may vary with increasing the *driving force* of the cross reactions.[1] The involvement of an excited electronic state, which accordingly affects the coordination geometry, was suggested to open up a kinetically more favorable pathway for the electron transfer. Such a new pathway with a lower activation barrier than that for the ordinary non-adiabatic reaction prompted us to consider the *directional* electron transfer reactions observed in certain biological systems,[2] in which a switch from a slow non-adiabatic process to a pathway involving a low-λ excited state of the reaction product.

In this study we investigated the rather stable $Ce(acac)_4^{0/-}$ (acac=acetylacetonato) couple in acetonitrile, in which an effective shielding of the *f*-orbitals by the outer orbitals and the ligands causes non-adiabaticity. By varying the redox reagents for the cross reactions, the apparent second-order rate constants were obtained, from which electron self-exchange rate constants for the $Ce(acac)_4^{0/-}$ couple were estimated for each cross reaction (Table 1). It is obvious that the *apparent* self-exchange rate constant increases with increasing the driving force of the reaction, K_{12}, and reaches a constant value when K_{12} is large. Such a tendency will be explained on the basis of the theory of the *directional* electron transfer.

Table 1. The thermodynamic and kinetic parameters of the redox reactions of $Ce(acac)_4^{0/-}$

Direction	reagent[a]	k_{11}[b]	k_{12}[b]	K_{12}	k_{ex}[b]
Reduction	dmFc	3.5×10^{7}[c]	9.4×10^{4}	13	3.2
	$Co(sep)^{2+}$	8.7×10^{-2}	7.7×10^{3}	6.6×10^{4}	8.7×10^{2}
Oxidation	$dmFc^{+}$	3.5×10^{7}[c]	2.8×10^{3}	7.7×10^{-2}	5.5
	$Co(phen)_3^{3+}$	2.3×10^{-1}	3.9×10^{5}	9.9×10^{6}	2.5×10^{4}
	$Co(bpy)_3^{3+}$	6.3×10^{-1}	2.6×10^{5}	9.6×10^{5}	2.6×10^{4}

T = 298.2±0.1 K, I = 0.1 mol kg^{-1}(n-*t*BuNClO$_4$), [a] dmFc=decamethylferrocene, sep= 1,3,6,8,10,13,16,19-octaazabicyclo[6.6.6]eicosane, phen=1,10-phenanthroline, bpy=bipyridilne, [b] mol^{-1} kg s^{-1}, [c] ref. 3.

1. V. Balzani, F. Scandola, G. Orlandi, N. Sabbatini, and M. T. Indelli, *J. Am. Chem. Soc.*, **103**, 3370 (1981). 2. R. Bechtold, C. Kuehn, C. Lepre, and S. Isied, *Nature*, **322**, 286 (1986). 3. G. E. McManis, R. M. Nielson, A. Gochev, and M. J. Weaver, J. Am. Chem. Soc., **111**, 5533 (1989).

DIFFUSION COEFFICIENTS OF CHLOROCOMPLEXES OF METALS AND THEIR PROCESSES OF WATER-LIGAND REPLACEMENT IN AQUEOUS SOLUTIONS

Michihisa UEMOTO
Tokyo Metropolitan Industrial Research Institute, Nishigaoka, Kita-ku, Tokyo 115-8586, Japan

Diffusion coefficients of ions in aqueous solutions reflect effective radii of diffusing ions on transport phenomena, which radii depend on their intrinsic sizes and interactions with surrounding water on motion. Halogenocomplexes of metals have relatively simple structures with monatomic ligand, on which hydrated water replaces stepwise by halide ion. This study is concerned with measurements of diffusion coefficients of halogenocomplexes of divalent metals in aqueous solutions in order to investigate the processes of water-ligand replacement on complex formation.

The diaphragm cell with thin membrane filter [1] was used with a modification. A filter made of hydrophilic PVDF resin with a pore size of 0.65 μm was selected instead of the cellulose-made one originally tested[1]. The cell was calibrated with a 0.5 moldm^{-3} KCl solution diffusing into pure water. Aqueous solutions containing 2 x 10^{-3} moldm^{-3} of $Pd(NO_3)_2$ or $Hg(NO_3)_2$ were prepared at an ionic strength of 1.0 adjusted with HNO_3 and KNO_3. They also contained different concentrations of KCl, thereby making some conditions on complex equilibria. They were poured into lower compartment of the cell, while those without KCl were in the upper, allowing to diffuse for 1-1.5 h in a thermostat maintained at 298.2±(5 x 10^{-3})K. At the end of each run the solutions in both compartments were sampled and analyzed separately with chelatometry. Figure shows the diffusion coefficients of the above complexes at some molar ratios of chlorine over the metal. They became greater with an increase of the ratio as for the $PdCl_n^{2-n}$, which suggests that weakening of the interactions occurs between the complexes and solvent water with complex formation, considering that chloride ion replaced is larger in radius than water molecule. As for the $HgCl_n^{2-n}$, the coefficients in the ratio 2 were at their maximum, implying a change of the coordination structure. Diffusion coefficients of the individual complexes have been estimated using stability constants for discussion.

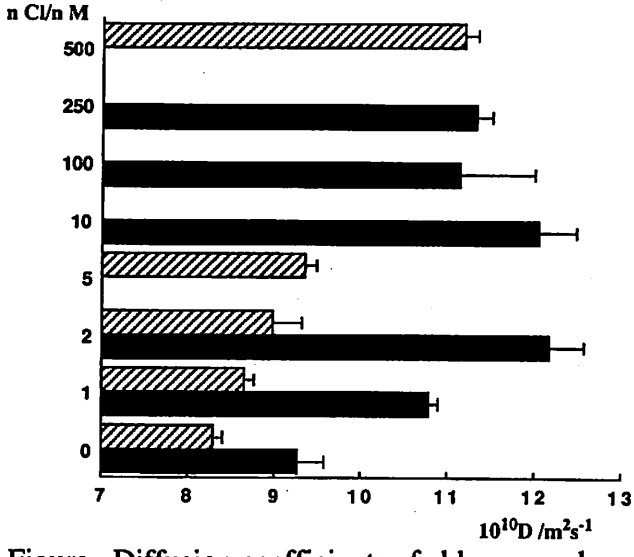

Figure Diffusion coefficients of chlorocomplexes of Pd(II) and Hg(II) at different molar ratios
▨ $PdCl_n^{2-n}$ ■ $HgCl_n^{2-n}$

1. Hashitani, T.; Tamamushi,R.; *Trans. Faraday Soc.*, 1967, **63**, 369.

PERMEATION RATES OF METALLIC IONS THROUGH ROCK-MATRIX

Bing-Jian ZHANG

Department of Chemistry, Zhejiang University, Hangzhou, Zhejiang, 310027, P.R.China

Rock-matrix permeation phenomenon can be applied to modifying such characteristics of rock as color and mechanical performance. It is a serious problem in environmental protection, however, as waste discharged from chemical factories can permeate through soil and rock into the ground water, which may be drunk by people. Thus, it is important to investigate the permeation rates of the metallic ions through. rock-matrix

In this paper the permeation equation involved with the influence of current has been derived based on the standard diffusion theory and by using the concept of ion electrical transport in electrochemistry.

$$C_r = \frac{D_i t}{l^2} \pm \frac{t_+ I t}{C_0 l z F} - \frac{\alpha}{6} - \frac{2\alpha}{\pi^2}\sum_{n=1}^{\infty}\frac{(-1)^n}{n^2}\exp\left(-\frac{D_i n^2 \pi^2 t}{l^2 \alpha}\right) \qquad (1)$$

where D_i is the intrinsic diffusion coefficient; C_0 is the concentration at inlet; t is time; V is the volume of the solution in the measurement cell; l is the thickness of the rock sample; I is the current density; α is the rock capacity factor; z and t_+ are, respectively, the valence and transport number of measured ion; F is Faraday constant; $\pm$ express the directions of electrical transport.

A technique is described for measuring the permeation rates of the metallic ions through. rock-matrix in the laboratory. Permeation rates of nickel ions (Ni^{2+}) through the Fujian 603 granite samples, each with different thicknesses, are measured with and without current. Consequently, when the direction of electrical transport was identical to that of Ni^{2+} diffusion, permeation rates with a current greatly increased. The application of 2.4 mA cm ^{2} current density increased the Ni^{2+} permeation rate by about 40 times as compared with measurements with no current. The results, in general, agee well when comparisons between the experimental data and the predictions from the theory (Eqn.(1)). If the directions of two kinds of transport are contradictory, the total permeation rate decreases and the permeation will even disappear. The experimental result indicates that the application of 0.16 mA cm^{-2} reversed current density makes permeation of 1mol L^{-1} Ni^{2+} unobservable in the measurement cell, which is what the theory predict on.

The studies indicate that: (1) A simple experimental technique has been presented for measuring permeation rate of an aqueous phase through porous rocks. (2) The permeation equation involved with the influence of current has been derived from standard diffusion theory and electrochemistry. It gives a good quantitative prediction of metallic ion permeation rates.

Pentacoordinate carbon atom in solutions and solvents

Alexey K. Baev

The Byelorussian State Technological University
Sverdlov Str. 13a, Minsk, 220050, Republic of Belarus

Refusal from sp^3-hybridyzation worked out the problem of dative bond of aklyl compounds of Main Group elements and substantiation of participation of pentacoordinate carbon atom in intermolecular interaction in liquid compounds and them solutions provides development of theory of solutions. Availability of fifth coordination at carbon atom is provided by essential nondevide $2s^2$-electron pair of this atom of methyl group of alkyl ligands wich is enriched by display of electron density from atom of elements II-IV group or impoverished by display of electron dencity from carbon atom to atom of element V-VI group in them alkyls compounds.

As the result of this carbon atom has donors or acceptors properties in dependence from interacted with them of atom main groupe elements. ability to form specific intermolecular interaction of covalence type of fifth coordination. The dissociation energy of them have been prepared from thermodinamic properties.

In this lecture we are discussed two important problems. The first of them we discuss of pentacoordinate carbon atom in solvation of alkyls of second, third or six group with isoelectron molecular structure. of the same group element. With use of therodinamic properties of evaporation process of solutions as process of destruction the solvats structure. We are discussed the limit of existance of different solvates structures and substantiated specific intermolecular interaction between molecules at solute and solvent on all composition of binary system. We substantiate four type of specific intermolecular interaction with pentacoordinate carbon, determined the dissociation energy of them wich changes in wide interval and exceed value the dissociation energy of H-bonds in liquid ammone and water (11 kJ/mol).

The second problem puts with participation of pentacoordinate carbon atom in intermolecular interaction in liquid solvents of formamide, N-methylformamide and N-N dimethylformamide. We discuss and substantiate specific intermolecular interaction pentacoordinate carbon dissociation energy of wich is quite near and more H-bonds.

Preparation, Redox, and Substitution Dynamics of the Trinuclear Molybdenum(IV) Complexes with an Oxo and an Ethylidyne Capping Ligands and Bridging Carboxlates, $[Mo_3(\mu_3\text{-}O)(\mu_3\text{-}CCH_3)(\mu\text{-}RCO_2)_6(L)_3]^+$

Akira NAGASAWA, Takayuki MURAUCHI, and Takashi FUJIHARA
Department of Chemistry, Faculty of Science, Saitama University, Urawa, Saitama 338-8570, Japan

The trinuclear molybdenum complex ion of this type has metal-metal direct bonds, and ethylidyne (CCH_3^-) as a capping ligand.[1] We have recently prepared acetate-bridged complexes (R = CH_3) with various unidentate nitrogen donors (L = substituted pyridines, and 1-methylimidazole(1-Meim)), and new complexes with various bridging carboxylates (R=H, C_2H_5, $(CH_3)_3C$, $(C_2H_5)_2CH$, and $C_6H_5CH_2CH_2$, L = pyridine(py)) as BF_4^- salts.

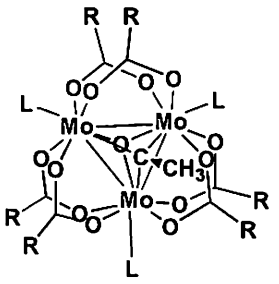

Electrochemical properties of those complexes have been investigated by cyclic voltammetry in CH_3CN. One electron reduction process was reversible or quasi-reversible in the potential range $E_{1/2}$ = 0.58 (R = CH_3, L = 1-Meim) − 0.83 (R = H, L = py) V vs Ferrocene /Ferricenium couple. Linear relationships between the redox potential and σ-electron donating abilities of RCO_2^- and L were observed for the class of complexes, *i.e.*, the smaller protonation constant pK_a, the more positive value of $E_{1/2}$, although the magnitude of the variation is smaller than those for trinuclear iron(III) complex with no direct metal-metal bonds, $[Fe_3(\mu_3\text{-}O)(\mu\text{-}RCO_2)_6(L)_3]^{n+}$.[2]

Dynamic properties of the substitution was elucidated by ^{1}H NMR using isotope labeling method. The exchange of the terminal pyridine (L = py) in a series of complexes with various carboxylate-bridges (R = H, CH_3, C_2H_5, $(CH_3)_3C$, $(C_2H_5)_2CH$, and $C_6H_5CH_2CH_2$) with the solvent deuteriated pyridine (py-d_5) was studied kinetically at 283 − 303 K. Activation parameters, $\Delta H^{\ddagger}$ (122 − 171 kJ mol^{-1}) and $\Delta S^{\ddagger}$ (+101 − +274 J mol^{-1} K^{-1}), suggest that the reaction proceeds via a dissociative mechanism (D or I_d). The rate constant depends linearly upon Taft's parameter of the substituent on the bridging carboxylate, indicating that both the electronic (σ-donating strength) and the steric (hindrance) factors play roles on the substitution at the terminal position.

1. K. Nakata *et al.*, *Inorg. Chem.*, **30**, 1575 (1991).
2. K. Nakata *et al.*, *Chem. Lett.*, **1989**, 753.

Kinetic Studies on the Ligand Exchange Reaction of the Terminal Pyridine in the Trinuclear Chromium(III) Complexes, $[Cr_3(\mu_3\text{-}O)(\mu\text{-}RCO_2)_6(py)_3]^+$. The Substituent Effects of Bridging Carboxylate Ligands

Takashi FUJIHARA, Makiko YASUI, Junko OCHIKOSHI, and Akira NAGASAWA
Department of Chemistry, Faculty of Science, Saitama University, Urawa, Saitama 338-8570, Japan

A remarkable labilization by the *trans* effect of the central oxide ion was found in the substitution for the terminal ligands in the carboxylate-bridged trinuclear Ru, Rh,[1] Mo, W,[2] and Cr complexes.[3] We report here the kinetics and the mechanism of the exchange of the terminal pyridine (py) in the carboxylate-bridged trinuclear chromium(III) complex $[Cr_3(\mu_3\text{-}O)(\mu\text{-}RCO_2)_6(py)_3]ClO_4$ by isotope labeling using deuteriated pyridine (py-d_5).

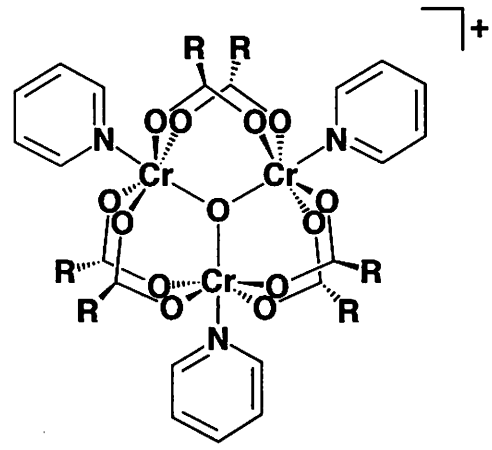

$$[Cr_3(\mu_3\text{-}O)(\mu\text{-}RCOO)_6(py\text{-}d_5)_3]^+ + 3py \rightarrow [Cr_3(\mu_3\text{-}O)(\mu\text{-}RCOO)_6(py)_3]^+ + 3\ py\text{-}d_5$$

Since the complex is paramagnetic, the exchange was monitored by change in the peak intensities of ^2H NMR in nitromethane at 298−333 K. The rate constant k at 328 K varied from 3.2×10^{-6} s^{-1} (R = CH_2Cl) to 1.6×10^{-3} s^{-1} (R = CH_3) depending on the substituent R on the bridging carboxylates. Large positive activation parameters $\Delta H^{\ddagger}$ (116−136 kJ mol^{-1}), $\Delta S^{\ddagger}$ (51−90 J K^{-1} mol^{-1}) suggested a dissociative activation mode (D or I_d mechanism) for the reaction. Examination of the substituent effects in terms of Taft's equation $\log(k / k_0) = \rho^*\sigma^* + \delta Es$ accounting for the electronic and steric parameters gave a critical clue to establishing the reaction mechanism.

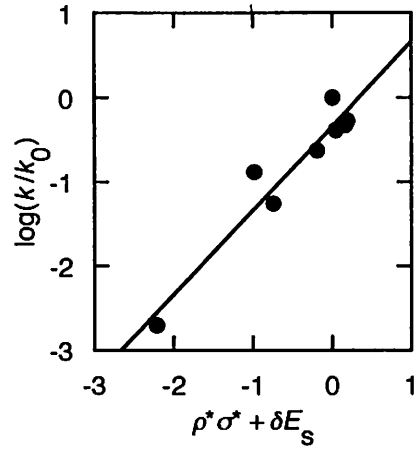

1. K. Nakata *et al.*, *Inorg. Chem.*, **30**, 1575 (1991).
2. Y. Sasaki *et al.*, *Inorg. Chim. Acta*, **212**,175 (1993).
3. T. Fujihara *et al.*, *Inorg. Chem.*, **37**, 1234 (1998).

KINETIC STUDY ON THE REACTION OF HEAD-TO-HEAD α-PYRIDONATE-BRIDGED *cis*-DIAMMINEPLATINUM(III) DIMER WITH SODIUM *p*-STYRENESULFONATE

Nami Saeki, Noriko Nakamura, Koji Ishihara, and Kazuko Matsumoto
Department of Chemistry, School of Science and Engineering, Waseda University, Okubo, Shinjuku-ku, Tokyo, 169-8555, Japan

Substantial number of diplatinum(III) complexes have been reported.[1] It has been shown that most of the complexes, which are usually derived from "platinum blues", have catalytic activity for olefins.[2,3] However, little is known about the reactivity of the trivalent platinum complexes.

We have studied kinetically the axial ligand substitution of head-to-head (HH) and head-to-tail (HT) α-pyridonate-bridged diammineplatinum(III) dimers with halide (Cl^- and Br^-). The results show that the platinum(III) complexes are much more labile than platinum(II) or platinum(IV) complexes.

We report here kinetics on the reaction of the HH dimer (**1**) with Sodium *p*-styrenesulfonate (**2**) in acidic aqueous solution.

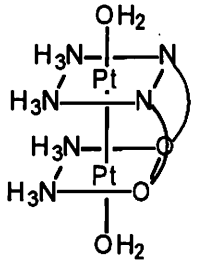

(**1**) HH α-pyridonate-bridged diammineplatinum(III) dimer

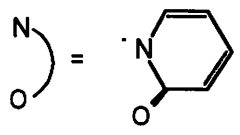

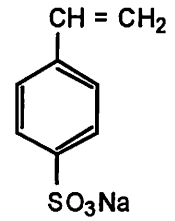

(**2**) Sodium *p*-styrene-sulfonate

A four-step reaction was observed under the pseudo-first order conditions ($C_L \gg C_{Pt2}$). The first three steps were first order with respect to C_{Pt2}. And the pseudo first-order rate constants (k_{obs}) for the three steps depended on the excess ligand concentration C_L as shown in Figs. 1-3.

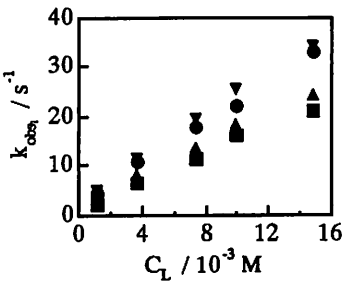

Fig. 1 $k_{obs\,1}$ vs. C_L

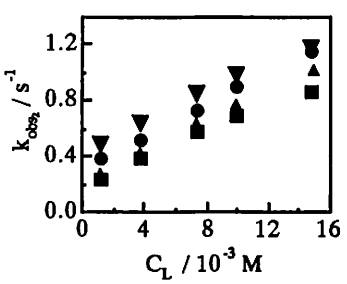

Fig. 2 $k_{obs\,2}$ vs. C_L

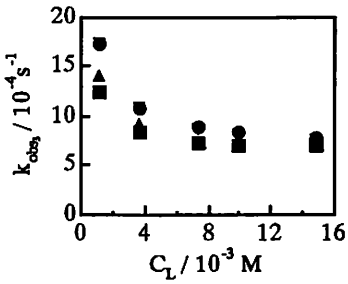

Fig. 3 $k_{obs\,3}$ vs. C_L

$[H^+]$ / M = 0.0318 (▼), 0.0508 (●), 0.102 (▲), 0.152 (■); C_{Pt_2} = 2×10^{-5} M, I = 2.0 M, 25 ℃, λ = 350 nm

1. Abe, T.; Moriyama, H.; Matsumoto, K., *Inorg. Chem.*, 1991, **30**, 4198.
2. Matsumoto, K.; Mizuno, K.; Abe, T.; Kinoshita, J.; Shimura, H., *Chem. Lett.*, 1994, 1325.
3. Matsumoto, K.; Nagai, Y.; Matsunami, J.; Mizuno, K.; Abe, T.; Somazawa, R.; Kinoshita, J.; Shimura, H., *J. Am. Chem. Soc.*, 1998, **120**, 2900.

MECHANISTIC STUDIES ON THE REACTION BETWEEN IRON(III) AND D-PENICILLAMINE IN BASIC AQUEOUS SOLUTION

SUNG-NAK CHOI[1], YOUNG-INN KIM[2] and HEUNG-JAE PARK[1]

[1] Department of Chemistry, Pusan National University, Kumjeong-Ku, Pusan 609-735, Korea

[2] Department of Chemistry Education, Pusan National University, Kumjeong-Ku, Pusan 609-735, Korea

The reaction of iron(III) by excess D-penicillamine, $HSC(CH_3)_2CH(NH_2)COOH$ (H_2Pen) was studied in aqueous solution over the pH range of 8.0～11.0 using a stopped-flow spectrophotometer. The reaction at the initial stage is biphasic with a rapid complexation of 1:2 complex $[Fe(OH)(Pen)_2]^{2-}$, followed by the reduction of this intermediate into iron(II) species and D-penicillamine disulfide $[Pen\text{-}Pen]^{2-}$.

$$Fe(OH)^{2+} + 2\,Pen^{2-} \underset{k_2}{\overset{k_1}{\rightleftharpoons}} [Fe(OH)(Pen)_2]^{2-} \qquad (1)$$

$$[Fe(OH)(Pen)_2]^{2-} + H^+ \xrightarrow{k_3} FePen + 1/2\,[Pen\text{-}Pen]^{2-} \qquad (2)$$

Assuming steady state condition for $[Fe(OH)(Pen)_2]^{2-}$, and since the reaction is carried out in the basic condition ($[H^+] \ll k_1$ and $k_3[H^+] \ll k_2$), the overall rate can be expressed by equation 3 where $[Fe_T] = [FeOH^{2+}]/[1+[H^+]/k_1]$.

$$Rate = (k_1k_3/k_2)[Fe_T][Pen^{2-}]^2[H^+] \qquad (3)$$

The rates of formation and decay the transient intermediate $[Fe(OH)(Pen)_2]^{2-}$ are pH dependent and are also affected by the presence of chloride ion; the rate of overall reaction increases as the concentration of chloride ion increases. This is attributable to the formation of low charged iron(III) species, $FeCl^{2+}$ and/or $Fe(OH)Cl^+$ which, in turn, enhance the rate of formation of $[Fe(OH)(Pen)_2]^{2-}$.

The reaction mechanism described by equations 2 and 3 is valid only in the absence of chloride ion. In the presence of chloride ion, another reaction pathways involving $FeCl^{2+}$ and $Fe(OH)Cl^+$ seem to exist for the formation of transient intermediate.

METAL ION EFFECT ON THE DEGRADATION RATES OF CONDENSED PHOSPHATE OLIGOMERS

G. KURA and J. KAWAGUCHI
Department of Chemistry, Fukuoka University of Education, Akama, Munakata, Fukuoka 811-4192, Japan

Condensed phosphate oligomers are very interesting polyvalent electrolytes which carry a high charge within their relatively compact molecules.[1] It has been known that P-O-P linkages in the oligomers are degraded in the aqueous solutions and their degradation rates strongly depend on the acidity, basicity, cations present and the concentration of the cations.[2] In this study, the effect of Al^{3+} ion on the degradation rates of linear and *cyclo*-polyphosphate oligomers was quantitatively investigated. Catalytic effect of Al^{3+} ion can be considered to be ascribed to the complex formation between Al^{3+} ions and the phosphate anions. Therfore the stability constants of the complex formed were estimated by the cation-exchange method .The apparent rate constants of the oligomers were analyzed using the stability constants determined.

The rate can be expressed as Eq.1

$$-\frac{dc}{dt} = k_0[P] + k_1[AlP] + k_2[Al_2P] \quad (1)$$

, where P, AlP and Al_2P denote free phosphate, 1:1 complex and 2:1 complex, respectively. Finally the apparent rate constant can be written as Eq.2.

$$k_{obs} = \frac{k_0 + k_1\beta_1[Al^{3+}] + k_2\beta_2[Al^{3+}]^2}{1 + \beta_1[Al^{3+}] + \beta_2[Al^{3+}]^2} \quad (2)$$

The apparent rate constants for linear tri- and tetra-phosphate degradations varied with the concentration of Al^{3+} ion as shown in Fig.1. The k_1 and k_2 for each phosphate were determined by a curve fitting method.

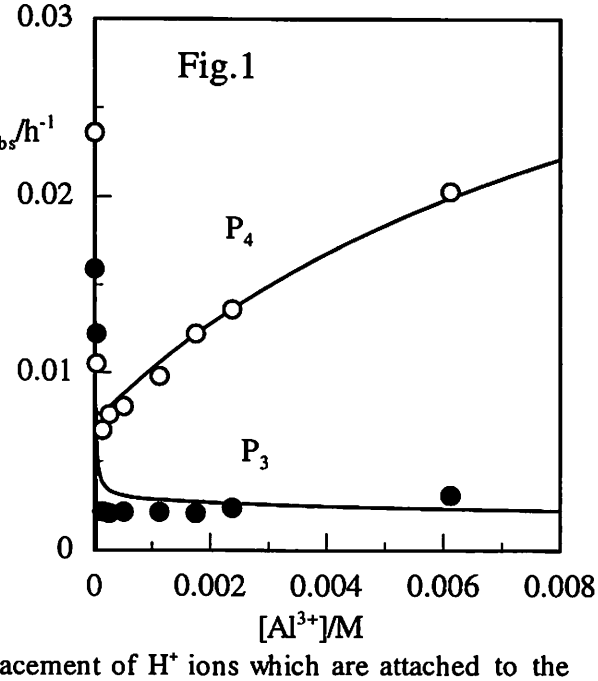

For both phosphates, k_1 were smaller than k_0. Replacement of H^+ ions which are attached to the phosphates, with Al^{3+} ion reduced the degradation rates. For other linear and *cyclo*-polyphosphates, the k_{obs} increased simply with the increase in the concentration of Al^{3+} ion added.

1. J.R.van Wazer, *Phosphorus and Its Compounds,* Vol.I, Interscience, New York(1958).
2. G.Kura, *Recent Research Developments in Pure & Applied Chemistry,* **1**, 17(1997).

ON THE MICROSCOPIC COMPLEXATION BEHAVIOR OF A SERIES OF *CYCLO*-μ-IMIDOTRIPHOSPHATE ANIONS

Hideshi Maki[1], Masahiko Tsujito[1], Hiroyuki Nariai[1], Itaru Motooka[1] and Tohru Miyajima[2]

[1]Department of Chemical Science and Engineering, Faculty of Engineering, Kobe University, 1-1 Rokkodai-cho, Nada-ku, Kobe 657-8501, Japan

[2]Department of Chemistry, Faculty of Science and Engineering, Saga University, 1-Honjo, Saga 840-8502, Japan

Due to slow chemical exchange of Be^{2+} ion in the complexes in aqueous solution, ^9Be NMR technique is expected to give most straightforward evidence for information on the coordination structures. Separate peaks for respective coordination structures of the complexes can be observed in the ^9Be NMR spectra. In this study, microscopic complexation behavior of Be^{2+} ion with cyclic imidotriphosphate ligands, involving P-O-P and/or P-NH-P linkages, i.e., *cyclo*-μ-monoimidotriphosphate, $cP_3(NH)$, *cyclo*-μ-diimidotriphosphate, $cP_3(NH)_2$, and *cyclo*-μ-triimidotriphosphate, $cP_3(NH)_3$ anions(Fig. 1) has been investigated by ^9Be NMR technique. The stability constants of monodentate and bidentate complexes, K_1 and K_2, as well as the microscopic stability constants of O-coordinating and N-coordinating monodentate complexes, $K_{1,O}$ and $K_{1,N}$ have been determined by the peak area ratio analyses of ^9Be NMR spectra(Table 1). Since the basicity of non-bridging O atoms increases with replacement of P-O-P linkage by P-NH-P linkage in the ligand, $K_{1,O}$ increases in the order of $cP_3(NH)_3 > cP_3(NH)_2 \gg cP_3(NH)$. On the other hand, the magnitude of the increase is much more pronounced in the case of N-coordinating monodentate complexes. The fact that N-coordination in Be^{2+}-$cP_3(NH)_3$ system is much more favored than O-coordination is unexpected because hard Be^{2+} ions usually favor harder oxygen atoms than nitrogen atoms to coordinate. The present result shows that electron-crowded donor N atoms in the ring center of these ligands form a specific binding site and this enables hard ions to coordinate directly to soft N atoms.

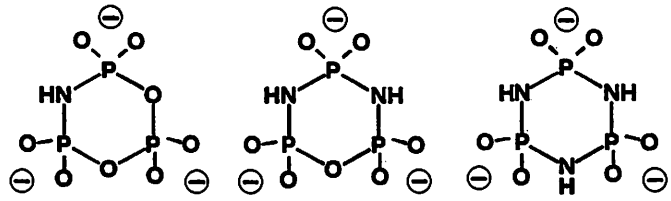

$cP_3(NH)$ $cP_3(NH)_2$ $cP_3(NH)_3$

Fig.1 Structural formulas of $cP_3(NH)_n$ (n=1~3) anions.

Table 1 Logarithmic macroscopic and microscopic stability constants for the interaction of $cP_3(NH)_n$ (n=1-3) anions with Be^{2+} ion.

	$\log K_1$	$\log K_2$	$\log K_{1,O}$	$\log K_{1,N}$
$cP_3(NH)^{3-}$	**2.79**	—	**2.71**	**1.97**
$cP_3(NH)_2^{3-}$	**3.34**	**1.11**	**3.08**	**3.00**
$cP_3(NH)_3^{3-}$	**3.92**	**1.18**	**3.11**	**3.85**

COMPLEXATION OF BORIC ACID WITH CROSSLINKED POLYSACCHARIDE ANION EXCHANGER

C. SHAO[1], Y. MIYAZAKI[2], S. MATSUOKA[1], K. YOSHIMURA[1] and H. SAKASHITA[3]
[1]Department of Chemistry, Kyushu University, Fukuoka 810-8560, Japan
[2]Department of Chemistry, Fukuoka University of Education, Fukuoka 811-4192, Japan
[3]The Center of Advanced Instrumental Analysis, Kyushu University, Fukuoka 816-8580, Japan

Boron adsorption behavior on QAE-Sephadex gel, which is an anion-exchange Sephadex containing diethyl(2-hydroxypropyl) quaternary amino groups, was examined in detail by distribution studies and ^{11}B NMR measurements. Its adsorption onto QA Cellulose anion-exchange gel having a similar structure with QAE-Sephadex was also investigated. For the QAE-Sephadex gel system, the chemical shift values of borate complexes with glucopyranoside residues of the gel matrix are identical with those for the Sephadex gel system. The signal at -13.4 ppm is due to 1:1 complex with an α,β-diol moiety of the glucopyranoside residue, where hydroxyl groups are on adjacent carbon atoms, and that at around -18 ppm is due to the 1:1 and/or 1:2 complexes with the α,γ-diol moieties (hydroxyl groups on alternate carbon atoms). Since the cellulose gel is 1,4-linked polymers of the glucopyranoside residues, only the signal of a 1:1 complex of borate with α,β-diol moiety of the glucopyranoside residue was observed at -13.4 ppm. For both the systems, the signals due to 1:2 complex with α,β-diols were not observed unlike Sephadex gel. The formation constants of the borate complexes, estimated by the signal intensities of ^{11}B NMR, were almost the same in the anion exchangers and Sephadex gel. The adsorbability of borate was not so much enhanced by the presence of charged functional groups, because both the ion-exchange selectivity toward borate and formation constants of borate complexes with the gel matrix are not so high. A kind of cation-exchange property can be revealed for the crosslinked polysaccharide anion exchanger as a result of the fixation of anionic borate onto the gel matrix by the complexation and can influence the concentration of hydrogen ion in the anion exchanger. The pH in the anion exchanger phase is higher than that in the external equilibrated solution, however, is a slightly lower than the value expected from the Donnan relation. The boron adsorption behavior on the polysaccharide anion exchangers could be well understood on the basis of such properties.

1. Yoshimura, K.; Miyazaki, Y.; Ota, F.; Matsuoka, S.; Sakashita, H., *J. Chem. Soc., Faraday Trans.*, 1998, **94**, 683.
2. Yoshimura, K.; Miyazaki, Y.; Sawada, S.; Waki, H., *J. Chem. Soc., Faraday Trans.*, 1996, **92**, 651.

Polynuclear hydoxocomplexes of aluminium(III) with a number of 3d-metals: formation and distribution in water solutions

Maximilian N. Kopylovich, Alexey K. Baev

The Byelorussian State Technological University
Sverdlov Str. 13a, Minsk, 220050, Republic of Belarus

On the basis of research of more than thirty systems with participation of cations of 3d-metals by a set of various methods we represent results of study of joint hydrolysis of metal ions from quantitative positions. In this connection the influence of the various factors on heteronuclear hydroxyl complexation, distribution of the cationic forms, application of kinetics methods for determination of the schemes of processes of their formation and definition of activation energies of these processes is discussed. The mechanism of homopoly and heteronuclear hydoxocomplexes formation, diagrams of distribution of the complex forms is discussed in view of formation of their polynuclear forms in systems containing ions of aluminium(III) and a number of 3d-metals. Thermodynamic numbers of probability of homo and heteronuclear hydroxodimer formation are determined under the obtained diagrams and executed accounts and the scheme of formation of the complex hydrolytic forms is offered.

Using results of the executed researches by various methods we have proved the formation of polynuclear hydoxocomplexes is realized through organization of structures with hydrogen bonds, for example:

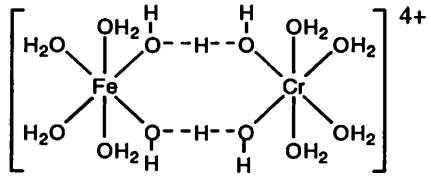

The kinetic schemes of a heteronuclear hydroxyl complexation in solutions of double systems of aluminium(III) with three-valent cations of scandium(III), chrome(III), iron(III), with divalent cations of a cobaltous(II), nickel(II), copper(II), zinc(II) are offered. It is shown the formation of heteronuclear polymers has kinetic advantage before formation of their homopolynuclear analogues because of asymmetry of the intermediate complex with hydrogen bridges.

Activation energies of the homopolynuclear hydrolisis in water solutions of three and two-charged cations of a number of 3d-metals are determined. It is shown that the value of activation energy of the homonuclear hydrolisis of zinc(II) acts as limiting value ensuring formation of stable heteronuclear hydoxocomplexes of aluminium with three and two- charged ions of 3d-metals.

References:

1. M.N. Kopylovich, E.V. Radion, and A.K. Baev // Russian Journal of Inorganic Chemistry.. 40 (1995). #6. p.1037.
2. M.N.Kopylovich, A.K.Baev, A.A.Chernik // Catalysis today 43 (1998). p.339.

COPPER(II) ION-ASSISTED SELF-ASSEMBLY OF BIS-*N, O*-BIDENTATE SCHIFF BASES: FORMATION OF MULTINUCLEAR DOUBLE-HELICAL COMPLEXES

Noboru YOSHIDA[1], Hiroki OSHIO[2] and Tasuku ITO[2]

[1] Division of Material Science, Graduate School of Environmental Earth Science, Hokkaido University, Sapporo 060-0810, Japan

[2] Department of Chemistry, Graduate School of Science, Tohoku University, Sendai 980-77, Japan

Noncovalent interactions such as hydrogen bond are essential for the formation of host-guest complexes and supramolecular architectures in solution. A recent attractive application of aromatic π–π and CH-π interctions is a general synthetic strategy for the construction of many types of supramolecular motifs.[1, 2] Some metal ions with a specific geometrical preference have often been used in order to assist the formation of organized structures by self-assembly of target ligands. However, the relationships between the effect of the noncovalent bond on the structure and the role of the metal ion in the self-assembly of ligands are not always clear.

Developing of simple synthetic methods in the self-assembling process using commercially available starting meterial is also important to extend the wide range of different supramolecular structures in the solid state. From this synthetic strategy, we have focused on semi-*N, O*-bidentate and bis-*N, O*-bidentate Schiff base ligands which can be electronically and configurationally controlled, leading to a systematic study of the self-assembly process in solution.[3]

Here we describe a novel strategy for the construction of Cu(II) ion-assisted supramolecular architectures using ligand L8. This architecture is prepared readily utilizing the weak aromatic interactions between the bridging groups of the bis-bidentate Schiff bases such as L8, L16 and L22.

Reaction of L8 with $Cu(MeCO_2)_2{\cdot}H_2O$ in a molar ratio in hot ethanol afforded a light green solid **1**. Positive-ion electrospray MS (*m/z* = 2073.5) suggested the existence of a 4 : 4 complex for **1**. Single crystals were obtained from chloroform-diethyl ether. An X-ray diffraction study confirms the formation of the L8 : Cu^{II} = 4 : 4 structure. The tetranuclear double helical structure appears to be stabilized by π– π and CH-π aromatic interactions (3.2 - 3.9 Å) between the bridging groups (-$C_6H_4SO_2C_6H_4$-).

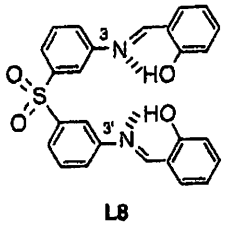

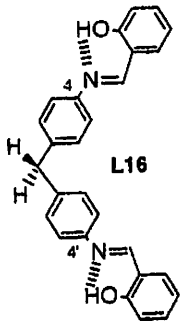

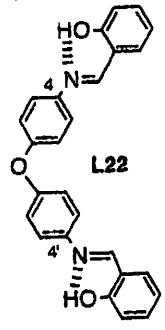

Complex **1** contains four Cu^{II} ions and four ligand L8. Two Cu^{II} ions at the top [Cu(1)] and bottom [Cu(4)] of the tetranuclear $(CuL8)_4$ core adopt a square-planar (SP) coordination geometry, whereas the two remaining Cu^{II} ions [Cu(2) and Cu(3)] in the middle adopt a tetrahedral (T_d) coordination geometry. Each Cu^{II} ion is coordinated by *N, O*-bidentate sites originating from two different ligands. Each ligand L8 interacts with two Cu^{II} ions with a different coordination geometry. Flexible coordination geometry (SP or T_d) of Cu^{II} ion and the flexible conformational freedom in the bridging group of L8 would lead to the tetranuclear double-helical structure.

1. J. S. Fleming, K. L. V. Mann, C.-A. Carraz, E Psillakis, J. C. Jeffery, J. A. McCleverty and M. D. Ward, *Angew. Chem. Inet. Ed.* **1998**, 37, 1279.
2. N. Yoshida and K. Ichikawa, *Chem. Commun.*, **1997**, 1091.
3. N. Yoshida, H. Oshio and T. Ito, *Chem. Commun.*, **1998**, 63.
N. Yoshida, N. Ito and K. Ichikawa,, *J. Chem. Soc., Perkin Trans. 2*, **1997**, 2387.
N. Yoshida, H. Oshio and T. Ito, *J. Chem. Soc., Perkin Trans. 2*, **1999**, 975.

FLUORESCENT SENSING FOR TEMPERATURE AND *p*H USING AMINO-CYCLODEXTRINS HAVING NAPHTHALENE CHROMOPHORE

Yasushi TAKENAKA and Noboru YOSHIDA
Division of Material Science, Graduate School of Environmental Earth Science, Hokkaido University, Sapporo, 060-0810, Japan

The molecular recognition in aqueous solution by modified cyclodextrins have been a subject of special attention in the field of solution chemistry[1], chiral discrimination,[2] photophysical probe[3] and fluorescent sensor for noncovalent interactions.[4] Although the modification at the C6 position by fluorophre of cyclodextrins allows for the photochemical and electrochemical switching of their binding and sensing capabilities for guest molecules, the temperature and/or pH control of the inside-outside binding equilibrium in the appended chromophore has resulted in failure.[3b]

We report here the synthesis and the pH and temperature-dependent fluorescent behaviour of amino-β-cyclodextrin (β-$CD_{xennap-1}$,1) amide-linked a naphthalene probe. Mono-[6-[(2-amino-ethyl)amino]-6-deoxy]-β-cyclodxtrin was coupled in DMF with 1-naphthoic acid by the dicyclohexylcarbodiimine (DCC) method. Recrystallization from water and cation-exchange chromatography gave the derivative **1**. Fig. 1 shows the temperature dependence (20 - 80 °C) of the fluorescent spectra in the absence (the inset in Fig. 1) and the presence of $NaClO_4$ (2 mol dm^{-3}) . The emission intensity at λ_{max} increased rapidly with decreasing temperature. This fluorescent change was amplified in the presence of inorganic salt such as Na_2SO_4, NaCl, KCl and $NaClO_4$. The pH dependent fluorescent spectra was also observed. ^1H NMR data and Cirular-dichroism spectra support clearly the presence of the in-out equilibria of the naphthalene probe of **1** depending on temperature and pH in aqueous solution. These findings suggest that β-$CD_{xennap-1}$, **1** will be one of the excellent CDx-based optical sensor for temperature and pH.

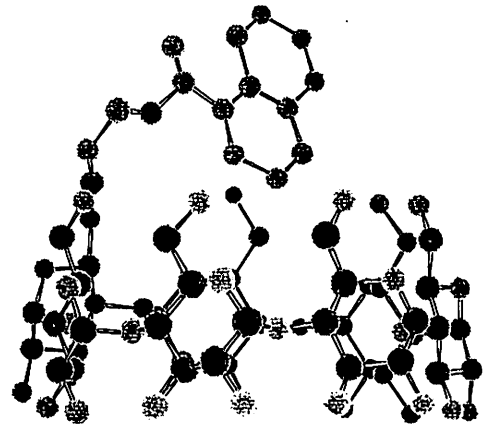

1

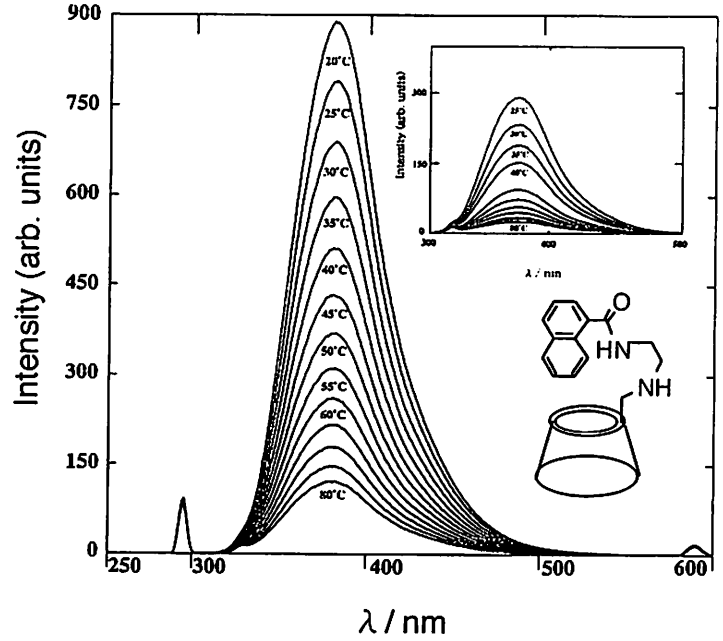

Fig 1. Temperature dependence of the Fluorescence spectra of **1** in the absence (the inset) and the presence of $NaClO_4$ (2 mol dm^{-3}), [1] = 1.25 x 10^{-5} mol dm^{-3}, pH =7.0.

1. N. Yoshida, *J. Chem. Soc., Perkin Trans. 2*, **1995**, 2249.
P. Bugnon, P. G. Lye, A. A-.Hamdan and A. E. Merbach, *Chem. Commun.*, **1996**, 1787.
2. T. Kitae, T. Nakayama and K. Kano, *J. Chem. Soc., Perkin Trans. 2*, **1998**, 207.
N. Yoshida, K. Harata, T. Inoue, N. Ito and K. Ichikawa, *Supramol. Chem.*, **10**, 63, (1998).
3. (a) F. Hamada, S. Minato, T. Osa and A. Ueno, *Bull. Chem. Soc. Jpn.*, 70, 1339, (1997).
(b) S. R. McAlpine and M. A. G-. Garibay, *J. Am. Chem. Soc.*, **1996**, 118, 2750.
4. N. Ito, N. Yoshida and K. Ichikawa, *J. Chem. Soc., Perkin Trans. 2*, **1996**, 965.

STABILITY OF MOLYBDENUM PORPHYRIN DIOXYGEN COMPLEXES IN SOLUTION

Tetsuaki Fujihara, Yoichi Sasaki, and Taira Imamura
Division of Chemistry, Graduate School of Science, Hokkaido University, Sapporo, 060-0810, Japan

Oxomolybdenum(IV) porphyrin having bulky substituents such as $Mo^{IV}O(tmp)$ (tmp = 5,10,15,20-tetramesitylporphyrinato dianion) in solution reacts with O_2 to give a corresponding dioxygen complex, $Mo^{VI}O(tmp)(O_2)$, reversibly.[1] However, the reaction of $Mo^{IV}O(tpp)$ (tpp = 5,10,15,20-tetraphenylporphyrinato dianion) having no bulky substituents with O_2 yields a paramagnetic μ-oxo dimer of $[Mo^{V}O(tpp)]_2O$.[2] A recent finding that $Mo^{IV}O(tmp)$ in the solid state reacts with O_2 to give $Mo^{VI}O(tmp)(O_2)$ suggests that a dioxygen complex can be prepared in the solid state even when the porphyrin ring of a Mo(IV) complex has no bulky substituents.[3] Actually, in the specific mesopores of FSM-16 (Folded-Sheet Mesoporus Material-16), $Mo^{IV}O(tpp)$ forms a respective dioxygen complex.[4] In this conference, we will report the stability of the dioxygen complexes, $Mo^{VI}O(ttp)(O_2)$ **1** (ttp = 5,10,15,20-tetra(*p*-tolyl) porphyrinato dianion) and $Mo^{VI}O(tpp)(O_2)$ **2**, which were discretely prepared by the solid state reactions (Figure 1).

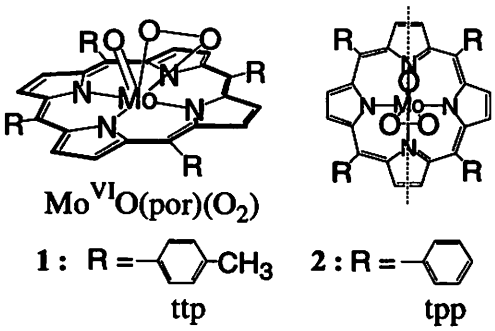

Fig. 1. Structure of the complexes

$Mo^{IV}O(por)$ (por = ttp, tpp) in the solid state was allowed to stand in a dioxygen atmosphere at room temperature for two weeks to give new molybdenum porphyrin dioxygen complexes **1** and **2**. In the case of the $Mo^{VI}O(tmp)(O_2)$ solution system, the dioxygen complex liberates dioxygen by photoirradiation and is recovered quantitatively in the dark.[1] However, in the **1** and **2** systems in solution, the reoxygenation of $Mo^{IV}O(por)$ in the dark proceeded differently, i.e., besides the formation of the dioxygen complexes without the recovery of the initial intensity of the Soret band, an extra absorption band appeared around 450 nm. The solution after repeated reaction cycles gave the characteristic ESR signals of paramagnetic oxomolybdenum(V) porphyrin complexes, i.e., the reactions of O_2 with $Mo^{IV}O(por)$ afforded the Mo(V) complexes such as $[Mo^{V}O(por)]_2O$ or $Mo^{V}O(por)OH$. Side reactions to go to Mo(V) complexes are preferable routes if the porphyrins have no bulky substituents. The reaction mechanisms in solution will be also discussed.

1. a) Tachibana, J.; Imamura, T.; Sasaki, Y., *J. Chem. Soc., Chem. Commun.*, **1993**, 1436. b) Tachibana, J.; Imamura, T.; Sasaki, Y., *Bull. Chem. Soc. Jpn.*, 1998, **71**, 363.
2. Hoshino, M.; Iimura, Y.; Konishi, S., *J. Phys. Chem.*, 1992, **96**, 179.
3. Osada, M.; Tachibana, J.; Imamura, T.; Sasaki, Y., *Chem. Lett.*, **1996**, 713.
4. Tachibana, J.; Chiba, M.; Ichikawa, M.; Imamura, T.; Sasaki, Y., *Supramol. Sci.*,1998, **5**, 281.

ADDITION AND ELIMINATION EQUILIBRIUM OF ANIONS ON A CARBONYL CARBON IN Pt(II)-HFAC CHELATES

Seichi OKEYA[1], Masato HASHIMOTO[1] and Yoshiaki KUSUYAMA[2]

[1] Department of Advanced Material Science and Chemistry, Faculty of Systems Engineering, Wakayama University, Wakayama 640-8510, Japan

[2] Faculty of Education, Wakayama University, Wakayama 640-8510, Japan

$[Pt(hfac)_2]$ **1** (hfac = hexafluoroacetylacetonate) reacts with the primary amine/ROH in CH_2Cl_2 to give an unidentified orange powder **2**, which converts to nitromethyl adduct (red crystals) **3** in $MeNO_2$. Complex **2** also gives a similar CH_2CN adduct **4** in MeCN, OR adduct **5** in ROH, and OH adduct **6** in acetone. Complex **6** was isolated as red crystals from the reaction of complex **1** and tertiary amine or 2-methylpyridines in CH_2Cl_2. These anionic parts; CH_2NO_2, CH_2CN, OR, and OH, on the carbonyl carbon easily eliminate or exchange with the other anions. For example complex **3** liberates $MeNO_2$ in $MeNO_2$ to reproduce complex **1** and in MeOH to afford complex **5**, respectively. All these reactions occur at room temperature. Such an easy C-C bond formation and elimination behavior is very unusual.

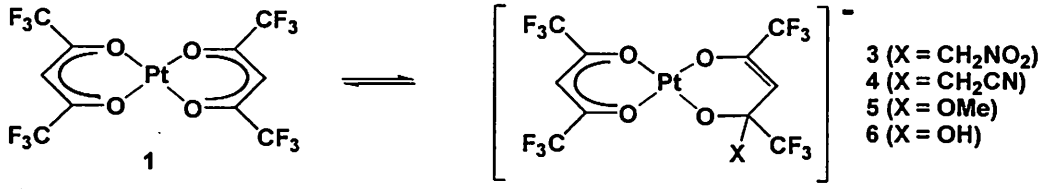

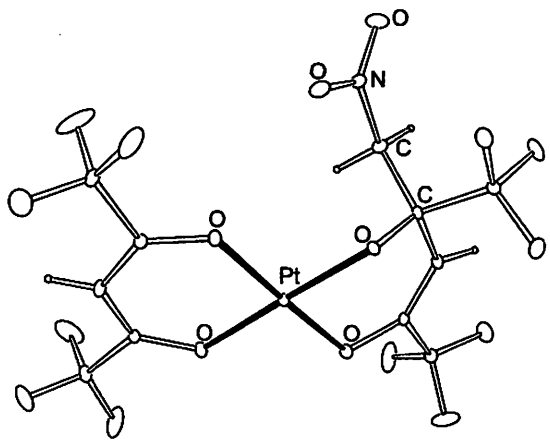

Structure of **3**

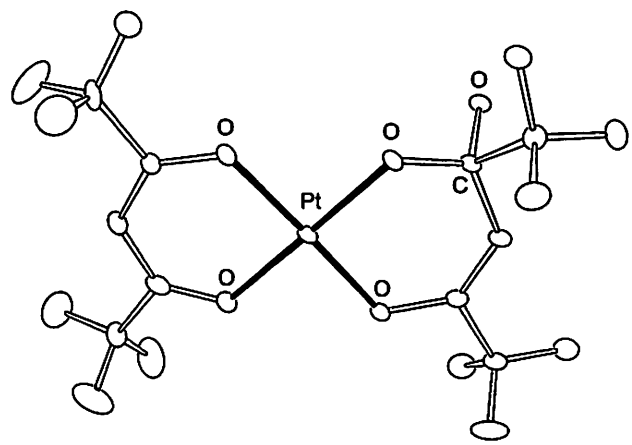

Structure of **6**

COORDINATION BEHAVIOR IN (5,10,15,20-TETRA-PHENYLPORPHYRINATO)ZINC(II) DISPERSED AS A PROBE IN REVERSED MICELLAR SOLUTIONS

Toshiyuki NAKASHIMA[1], Terufumi FUJIWARA[1] and Takahiro KUMAMARU[2]
[1] Department of Chemistry, Hiroshima University, Kagamiyama, Higashi-Hiroshima 739-8526, Japan
[2] YASUDA Women's University, Yasuhigashi, Asaminami-ku, Hiroshima 731-0153, Japan

We have observed that some neutral metal complexes are incorporated by reverse micelles into their water pools easily and decomposed immediately to catalyze a chemiluminescence reaction. In the uptake (or extraction) process of the complexes, the interactions between the complexes and the interface of reverse micelles or bulk solvents are important. In this work, these interactions have been investigated spectrophotometrically using (5,10,15,20-tetraphenylporphyrinato)zinc(II), Zn(tpp) as a probe of donor acceptance. The influence of water-to-surfactant molar ratio (R=[H_2O]/[Surfactant]) and bulk organic solvents on the coordination behavior in Zn(tpp) dispersed in reversed micellar solutions has been examined.

Reversed micellar solutions were prepared by dispersing an appropriate amount of aqueous solution (pH=6.0) buffered with 2-(N-morpholine)ethanesulfonic acid (MES) into chloroform or 6:5(v/v) chloroform-cyclohexane using cetyltrimethylammonium chloride (CTAC) as a surfactant. By adding a Zn(tpp) solution, the CTAC reversed micellar solution containing 1.2×10^{-6} M Zn(tpp) was prepared. Visible absorption spectra were recorded on a Shimadzu UV 2200 spectrophotometer equipped with thermostatted 1 cm quartz cells at 25.0±0.1℃.

When the four-coordinate complex, Zn(tpp) accepts only one axial ligand to form a five-coordinated complex, Zn(tpp)L, a red shift of the entire spectrum relative to that of Zn(tpp) is observed in proportion to the charge and polarizability of the axial ligand. The overlapping Soret bands observed in the CTAC reversed micellar solutions should be the result of four bands, which correspond to Zn(tpp), Zn(tpp)(H_2O), [Zn(tpp)OH]$^-$ and [Zn(tpp)Cl]$^-$. The fractions of the four complexes were calculated from the spectral data using a regression method and the respective molar absorptivities. The coordination behavior of Cl^- in reversed micellar systems was discussed in terms of the phase separation model (Fig. 1). This model provided the following parameters at various R values: the distribution coefficient of Zn(tpp) between bulk organic phase and interface, K_D, the formation constant of [Zn(tpp)Cl]$^-$ in bulk organic phase, K_F and the saturated concentration of CTAC monomer in bulk organic phase, $C_{Saturated}$. With increasing R values, K_D decreased, i.e., the distribution of Zn(tpp) to interface decreased. This is attributed to the hydration of Cl^- at the interface, which lead to masking the nucleophilicity of Cl^- to Zn(tpp). No variation of K_F with R values was observed, suggesting that Cl^- of CTAC located at the bulk organic phase is negligibly hydrated. Furthermore, $C_{Saturated}$ decreased with increasing R values. This indicates that the hydration of Cl^- of CTAC promotes the formation of reverse micelles. The effects of bulk solvents on K_D, K_F and $C_{Saturated}$ will be also reported.

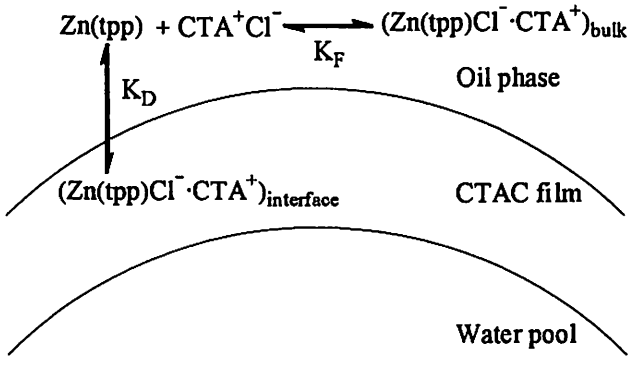

Fig. 1 Schematic representation of the interaction between Zn(tpp) and CTAC reversed micellar system.

UNUSUAL CHANGES OF RATE-DETERMINING-STEP IN FORMATION/EXTRACTION OF IRON(III) WITH TRIFLUOROACETYLACETONE IN TRITON X-100 MICELLAR SOLUTIONS

Kazuho INABA
The National Institute for Environmental Studies, Onogawa, Tsukuba, Ibaraki 305-0053 Japan

Micellar biphasic solution system can dissolve water-insoluble solutes in its pseudophase without toxic and/or flammable organic solvent, seems to be an "environmentally friendly" extraction/separation medium. To learn possibilities of the system for analytical uses, we have investigated both equilibria and kinetics of extraction behaviors in the system.[1-3] During the studies it has been found that the rate of formation/extraction of iron(III) with β-diketones having a trifluoromethyl substituted group is sometimes slower than that of complex formation in single aqueous solutions.[2] In the present study, the rate of formation/extraction of iron(III) with trifluoroacetylacetone (Htfa) in Triton X-100 (CMC = 2.4×10^{-4} M) micellar solutions was measured at 298 K to clarify the slow extraction mechanism.

The rate of complex formation of iron(III) with Htfa in aqueous solutions was firstly measured; the rate was observed to be first order with respect to the metal and the ligand while inverse first order to the hydrogen ion. Since the dependencies, it is concluded that the whole formation reactions in the aqueous solutions are controlled by the formation of mono-complex ($Fe(tfa)^{2+}$) and the value of rate constant for the reaction, $Fe(OH)^{2+} + Htfa_{(enol)}$, is $10^{3.36}$ M^{-1} s^{-1}. It is also concluded that coexisting 2×10^{-4} M Triton X-100 monomer does not affect the rate of complex formation in the aqueous solution. The rate of formation/extraction of iron(III) with Htfa in 0.2 - 10 % Triton X-100 micellar solutions was, on the other hand, somewhat different from that of formation in the aqueous solutions. When the Triton X-100 concentration was low and/or the ligand anion concentration in the bulk aqueous phase ($[tfa^-]$) was low, the reactions were controlled by the formation of mono-complex in the bulk aqueous phase and the value of rate constant was similar to that obtained in the aqueous solutions. However, the rate became slower, and the dependencies on the extractant and the hydrogen ion were not similar to those expected from the values in the aqueous solutions when the Triton X-100 concentration was high and/or the ligand anion concentration was high. The Htfa is not surface-active and the bulk aqueous phase contains no additional salt to extract the metal as ion-pair, the formation reactions should occur only in the bulk aqueous phase. The observed slow reactions may be due to a slow transport of the tris-complex, $Fe(tfa)_3$, from the bulk aqueous phase to the micellar phase. The kinetic data were recalculated as if only the equilibria among three complex species in the bulk aqueous phase were established and no extraction was proceeded in the early stage of the reaction. By the correction, the dependencies of the rate on the ligand and the hydrogen ion became similar to those in the aqueous solutions, and the value of the rate constant was $10^{3.37}$ M^{-1} s^{-1}.

From the results, it is concluded that the deceleration observed during the formation/extraction of iron(III) with Htfa in Triton X-100 micellar system is due to the slow extraction of the tris-complex formed in the bulk aqueous phase. The micellar biphasic system is potentially useful in many analytical applications, however, the extraction behavior is, as shown in the present study, not always similar to that in a conventional liquid-liquid system. Precise discussion on the fundamentals of the extraction behavior of the system is necessary to utilize for separation and analytical applications.

1. Inaba, K.; Muralidharan, S.; Freiser, H., *Anal. Chem.*, **65**, 1510-1516 (1993).
2. Inaba, K., in "*Value Adding Through Solvent Extraction*" ed. D. C. Shallcross, R. Paimin, L. M. Prvcic; University of Melbourne, Vol. 1, 57-62 (1996).
3. Inaba, K., *Langmuir*, **13**, 1501-1509 (1997).

THE COMPUTATIONAL AND EXPERIMENTAL EVIDENCES FOR REMARKABLE LITHIUM ION-π INTERACTIONS IN ORGANIC SOLVENTS.

Takaaki SONODA, Shin-ya IKEDA*, and Akira MORI
Institute of Advanced Material Science, Kyushu University, Kasuga 816, Japan
*Interdiciplinary Graduate School of Sciences, Kyushu University, Kasuga 816, Japan

The cation-π interactions of alkali metal ions with organic molecules have been recognized as one of strong noncovalent binding forces in many areas of mofern chemistry from materials design to molecular biology.[1] The cation-π interactions of alkali metal ions have been so far established by gas-phase experiments and high level theoretical studies for simple aromatic compounds and by X-ray structure analysis of metal ions complexes of biological systems and artificial supramolecular receptors such as cyclophanes, while there have been very few examples of such cation-π interactions of alkali metal ions with simple aromatic hydrocarbons in organic solvents.

We report here some computational and experimental evidences for the remarkably storong cation-π interactions of lithium ions with simple aromatic hydrocarbons such as azulene and 6,6-diphenylfulvene in dichloromethane and hexane solutions, where lithium ions are loosely ion-paired with weakly coordinating TFPB anions and strogly stabilized by the cation-π interactions with such dipolar aromatic hydrocarbons in the low dielectric and low donor-number solvents.

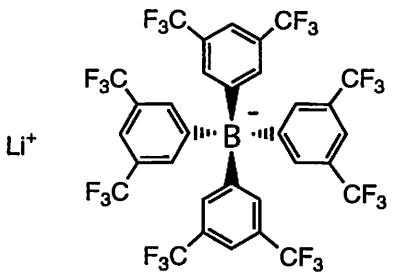

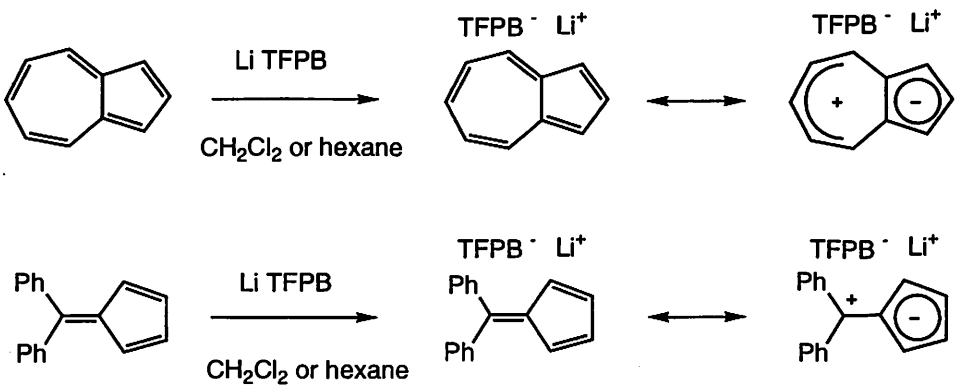

1) J. C. Ma, D. A. Dougherty, Chem. Rev., 97, 1303(1997)

CALCULATING THERMODYNAMIC PROPERTIES FROM PERTURBATION THEORY.
II. AN ANALYTIC REPRESENTATION OF SQUARE-WELL POTENTIAL HARD-SPHERE-CHAIN PERTURBATION THEORY

Bing-Jian ZHANG

Department of Chemistry, Zhejiang University, Hangzhou, Zhejiang, 310027, China

In the preceding paper [1,2] the Barker-Henderson macroscopic compressibility approximation of the second-order perturbation term is improved by assuming that the numbers of molecules in every two neighbour shells are correlated, based upon the original assumptions. The results are better than those for the original macroscopic compressibility and local compressibility approximation, especially at high densities. A simple analytic representation of square-well potential hard-sphere perturbation theory is derived based upon this improvement. The method is tested by calculating thermodynamic properties with the four-term truncated form, and the results are in good agreement with those of Monte Carlo and Molecular Dynamics simulation.

In this paper the method had been expended to fluids of hard-sphere-chains. We present an analytic representation of square-well potential hard-sphere-chain perturbation theory. For a system formed by N chain-like molecule, chain length r, segment diameter σ in a densities ρ at a temperature T, and if the perturbation energy is given by the sum of square-well pair interactions between segments ε/k, the Helmholtz energy of the system can be expressed.

$$\frac{A-A_0}{NkT} = -12\cdot\alpha\cdot r\left[\exp\left(\frac{\beta\varepsilon}{\alpha}\right)-1\right]\sum_{j=1}^{5} C_j\left(\frac{\eta}{1-\eta}\right)^j \qquad (1)$$

where $\alpha = \frac{1}{1+2K\eta^2}\left(\frac{\partial P}{\partial \rho}\right)_0$; $g_0(R) = \frac{1}{\eta}\sum_{j=1}^{5}\bar{g}_{0j}\left(\frac{\eta}{1-\eta}\right)^j$; $C_j = \int_1^{\lambda}\bar{g}_{0j}R^2 dR$ and $\eta = \pi\rho\sigma^3 r/6$

By usual derivations, one obtains the other thermodynamic properties, such as the equation of state, the internal energy and the constant-volume heat capacity. The equation of state, excess internal energy, and constant-volume heat capacity of the square-well potential hard-sphere-chains fluid calculated from analytic formula are compared with computer simulation data. The agreement is good for densities below that of freezing. The results are promising in view of application to mixtures of refrigerants and long-chain hydrocarbons.

1. Zhang Bing-jian, An improvement of the macroscopic compressibility approximation, *Chemical Physics Letters*, 1998, 296, 266
2. Zhang Bing-jian, Calculating thermodynamic properties from perturbation theory (I), *Fluid Phase Equilibria* , 1999, 154, 1-10

DEUTERIUM ISOTOPE EFFECTS ON VOLUMETRIC PROPERTIES IN BINARY MIXTURES OF WATER WITH VARIOUS DIPOLAR APROTIC SOLVENTS

Pirketta Scharlin[1] and Krister Steinby[2]
[1] Department of Chemistry, University of Turku, FIN-20014 Turku, Finland
[2] Department of Physical Chemistry, Åbo Akademi University, FIN-20500 Åbo, Finland

Volumetric properties of liquid mixtures are an important and useful source of information for the characterization of the interactions between components. One of the major motivations for studying binary aqueous mixtures is the belief that the results obtained will shed light on the problem of the structure of liquid water and aqueous solutions - the problem which has attracted considerable attention over the years.

Dipolar aprotic compounds as the organic component in binary aqueous mixtures are interesting for instance because of their solvent effect on rates of reactions.[1] Many of them, like *N,N*-dimethylformamide (DMF), *N,N*-dimethylacetamide (DMA), and *N*-methyl-2-pyrrolidone (NMP), are also versatile solvents in various industrial processes.

Volumetric properties of binary mixtures of H_2O with DMF, DMA, and NMP have been extensively reported by many workers. However, studies on the properties of corresponding systems containing D_2O instead of H_2O are scarce.[2]

In the present work, densities of binary mixtures of H_2O or D_2O with DMF, DMA, and NMP have been measured over the entire mole fraction range at temperatures from 277.13 K to 318.15 K. Results of these measurements have been used in calculating excess molar volumes, partial molar volumes and their derivatives with respect to temperature. Knowledge of these properties and the isotope effects on them provide a basis for understanding some of the molecular interactions in the binary mixtures of water with dipolar aprotic solvents.

1. Kankaanperä, A.; Scharlin, P.; Kuusisto, I.; Kallio, R.; Bernoulli, E., *J. Chem. Soc., Perkin Trans. 2*, 1999, (2), 169.

2. Miyai, K.; Nakamura, M.; Tamura, K.; Murakami, S., *J. Solution Chem.*, 1997, **26**, 973.

THERMODYNAMIC PROPERTIES OF SOME NITRILES IN DIMETHYL SULFOXIDE

Takayoshi KIMURA, Takanori MATSUSHITA and Sadao TAKAGI
Department of Chemistry, Kinki University, Kowakae, Higashi-osaka 577-8502, JAPAN

A series of thermodynamic measurements of vapour pressures, excess enthalpies and excess volumes for the binary mixtures containing amphiphilic solvent have been studied by the present authors,[1-3] to clarify the correlation between thermodynamic properties of such mixtures and molecular structure of their components.

In this paper, the excess enthalpies of alkylnitriles {$CH_3(CH)_nCN$, n=0 to 12} in dimethyl sulfoxide have been measured at 298.15 K and 310.15 K. Measurements of enthalpies of solution($\Delta_{sol}H$) of alkylnitriles at very dilute solutions under 0.001 in mole fraction were performed by Thermal Activity Monitor (Thermometric AB, Järfälla, Sweden) with a modification of reaction vesel.[4] Instrument was calibrated by dissolution of propane-1-ol in water. Alkylnitrile{$CH_3(CH_2)_nCN$, n=0 to 12} and propane-1-ol were fractionally distilled over freshly activated molecular sieves 4A which had been evacuated at 453 K for 12 h under 10^{-2} to 10^{-3} Pa. G.l.c. results showed merely some trace-impurity peaks less than 10^{-7}. The water content of samples measured were 0.01 mole per cent or less.

The results of enthalpies of solution for alkylnitriles were expressed in terms of the virial coefficients expansion according to the McMillan-Mayer theory:

$$\Delta H^E(m)=h_{xx}m + h_{xxx}m^2+ \cdots\cdots \quad (1)$$

where $\Delta H^E(m)$ is the molar excess enthalpy for the solute at molality m.
Enthalpies of solvation $\Delta_{solv}H$ of alkylnitriles were calculated from

$$\Delta_{solv}H=\Delta_{sol}H^{\infty}-\Delta_{vap}H \quad (2)$$

where $\Delta_{vap}H$ is the enthalpies of vaporisation of nitriles.
Partial molar excess heat capacities at infinite dilution were determined from differentiation of temperature dependence on enthalpies of solution.
McMillan-Mayer's parameter, enthalpies of solvation and partial molar excess heat capacities will be discussed with previous reported results.

1. T. Kimura and S. Takagi, *Netsu Sokutei*, **23**(1996) 53.
2. T. Kimura, K. Suzuki and S. Takagi, *Fluid Phase Equilibria*, **136** (1997) 269.
3. T. Kimura, Y. Sugihara and S. Takagi, *Fluid Phase Equili.*, **136**, (1997) 323.
4. T. Kimura and S. Takagi, To be published.

Thermodynamic properties of binary mixtures containing hydrofluoroether II

Takashi Minamihounoki[1], Takayo Takigawa[1], Katsutoshi Tamura[2] and Sachio Murakami[2]

[1] Faculty of Engineering, Osaka Institute of Technology, 5-16-1 Omiya, Asahi-ku, Osaka 535-8585 Japan
[2] Graduate School of Science, Osaka City University, 3-3-138 Sugimoto, Sumiyo-shiku, Osaka 558-8585, Japan

Hydrofluoroethers are solvents developed as a substitution solvent of chlorofluoro carbons. Nonafluorobutylmethylether(FBME) is a representative substance in the hydro fluoroethers. We have investigated this material for the possibility of utilization as a rinse and a vapor desiccant in the cleaning processing of semiconductors, etc. This material has been scarcely found about thermodynamic properties. In this report, mixing enthalpies and densities measurement were performed about FBME + heptane, butylmethylether, 1-propanol, 2-propoxyethanol systems, in order to obtain the knowledge about the solvent properties of FBME. Excess molar enthalpies (H_m^E) and excess molar volumes (V_m^E) were caluculated from the measured values.

Experimental results of H_m^E and V_m^E for these mixtures were shown in Figs.1 and 2. The full lines in the graphs are calculated from the equation of the Redlich-Kister type (1).

$$X^E / F = \chi (1-\chi) \Sigma A_i (1-2\chi)^{i-1} \qquad (1)$$

X^E is the excess thermodynamic function, F is the unit, and χ is the molar fraction of FBME.

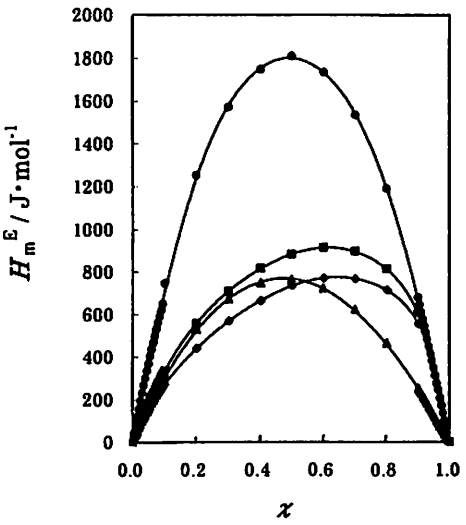

Fig.1 Excess molar enthalpies at 298.15K.
● ; χ FBME + (1 − χ) heptane ,
■ ; χ FBME + (1 − χ) 1-propanol,

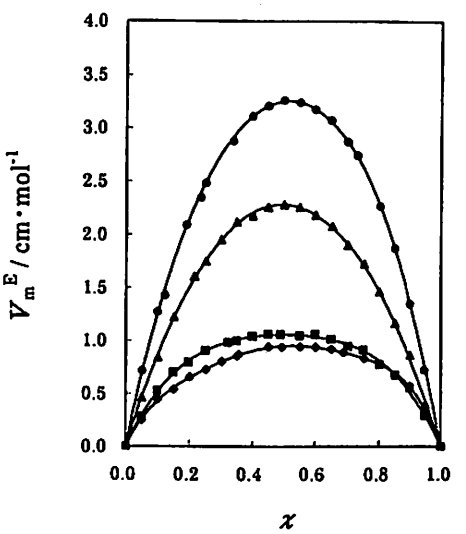

Fig.2 Excess molar volumes at 298.15K.
▲ ; χ FBME + (1 − χ) butylmethyl ether,
◆ ; χ FBME + (1 − χ) 2-propoxyethanol .

The H_m^E was endothermic in whole concentration range of the above systems. The V_m^E was also positive in whole concentration range of the above systems. We will discuss the results from the thermodynamic point of view.

THERMODYNAMIC PROPERTIES OF BINARY MIXTURES {A 2-ALKOXYETHANOL + *n*-OCTANE}: DENSITIES AT 298.15 K AND 303.15 K, SPEEDS OF SOUND AT 298.15 K.

Katsutoshi TAMURA[1], Atsushi OSAKI[1], Sachio MURAKAMI[1], Benoit LAURENT[2], and Jean-Pierre E. GROLIER[2].

[1] Department of Chemistry, Graduate School of Science, Osaka City University, 3-3-138, Sugimoto, Sumiyoshi-ku, Osaka 558-8585 Japan

[2] Laboratoire de Thermodynamique et Genie Chimique, Université Blaise Pascal, 63177, Aubière, France

Densities and speeds of sound of the mixtures {x 2-ethoxyethanol(EE), or 2-propoxyethanol(PE), or 2-isopropoxyethanol(IPE), or 2-butoxyethanol(BE), or 2-isobutoxyethanol(IBE) + (1-x)n-octane}were measured at 298.15 K; densities were also measured at 303.15 K. Excess molar volumes, excess isentropic and isothermal compressibilities, excess isochoric heat capacities and excess thermal expansion factors were estimated therefrom. The excess molar volumes V^E are positive and rather large as predicted from the excess enthalpies of the corresponding systems. The magnitude of V^E decreases along the following sequence IPE≥EE>PE≥IBE>BE as for the excess molar enthalpies H^E,[1)] although an inversion of PE and IBE is observed in the case of enthalpies. This shows the influence of hydrogen bond braking on both V^E and H^E. The temperature dependence of V^E is positive, up to about 0.005 $cm^3\ mol^{-1}\ K^{-1}$ at most. The excess thermal expansion factors are positive and large (in the order of $10^{-5}\ K^{-1}$) as usually for mixtures containing one associated species. The excess isentropic compressibilities excepted in the case of IPE and EE systems, for which, which they are rather positive, are small and change sign from positive to negative with the increase of the mole fraction of alkoxyethanol. Excess isothermal compressibilities are larger than the excess isentropic compressibilities; they are positive except for the BE system where a change of sign from positive to negative with increasing the alkoxyethanol concentration is also observed. Excess isochoric heat capacities are large and almost identical for all systems.

Excess heat capacities (both isochoric and isobaric) from experimental determinations will be compared with UNIFAC and UNIQUAC calculations.

1. K. Tamura, A. Osaki, S. Murakami, H. Ohji, H. Ogawa, B. Laurent, J.-P. E. Grolier, Fluid Phase Equilibria, in print.

ENTHALPY AND ENTROPY CHANGES ON MOLECLULAR INCLUSION OF HEXANOL INTO β-CYCLODEXTRIN CAVITIES IN AQUEOUS SOLUTIONS

Masao FUJISAWA[1], Takayoshi KIMURA[2] and Sadao TAKAGI[2]

[1] School of Biology-Oriented Science and Technology, Kinki University, Uchita-cho, Wakayama 649-6493, Japan

[2] Department of Chemistry, School of Science and Engineering, Kinki University, Kowakae, Higashi-osaka 577-8502, Japan

Cyclodextrin includes various kinds of guest molecules into its cavity recognising the difference in structure of guest molecules in aqueous solution. To clarify the mechanism of molecular recognition and discrimination in aqueous solutions, thermodynamic functions have been determined systematically for the molecular inclusion of alcohols into α-and β-CD cavities in aqueous solutions by the present authors. The alcohols measured are methanol, ethanol, 1-propanol, 1-butanol, 1-pentanol, 2-propanol, cyclohexanol, and 1,3-, 2,3-and 1,4-butanediols.

Importance of the increase in entropy was discovered from quantitative consideration of these thermodynamic functions. In this paper, the enthalpy and entropy changes on inclusion of hexanol molecules into β-CD cavities in aqueous solutions at 298.15 K are reported to show the correlation between molecular interaction and molecular structure of hexanol.

Hexanol molecules are stabilised largely on inclusion into α-CD cavities in aqueous solution, accompanying a large entropy decrease. To explain this phenomenon, the authors have proposed that hexanol molecules take gauche - gauche - ••• conformation or trans - gauche - ••• conformations in the cavities in stead of ordinary trans - trans - ••• conformation. The former conformations may result in some tight inclusion complexes in which the hexanol molecules can not rotate.

On the other hand, the enthalpies of inclusion of hexanol determined with β-CD are endothermic. The enthalpy of inclusion of hexanol into β-CD cavities from gas phase has a normal correlation with the number of CH_2 radicals in normal chain alcohols.

THERMODYNAMIC RESEARCH OF THE REACTIONS OF THE LIQUID-PHASE REDOX-PROCESSES OF ELEMENTARY SULPHUR FROM HYDROGEN SULPHIDE DEPOSITION

V. NESTERENKO and V. GLYBIN
Belarusian State Technological University, 13-a, Sverdlov Str., Minsk, 220050,
Republic of Belarus

Reaction thermodynamic of the liquid-phase deposition of the elementary sulphur from hydrogen sulphide and hydrogen sulphide-containing gases presents interest for development of the technological processes of hydrogen sulphide-containing gases from hydrogen sulphide purification with simultaneous elementary sulphur obtaining.[1-4]

The ferro-ferrisulphate and iodide-thriiodide redox-processes, based on using following reaction:

$$H_2S_{gas} + Fe_2(SO_4)_{3\,aq} = S_{rhomb} + 2FeSO_{4\,aq} + H_2SO_{4\,aq}, \quad (1)$$

$$H_2S_{gas} + H[I_3]_{aq} = S_{rhomb} + 3\,HI_{aq}, \quad (2)$$

are carried out in this paper by two methods – calorimeter and electrochemical.

Studying of the hydrogen sulphide oxidation by Fe (III) sulphate and complex iod $H[I_3]$ solutions is carried in solute isoperibolic calorimeter at standard conditions.[5,6] Following volumes of reaction (1) and (2) enthalpies ($J \cdot mol^{-1}$) are obtained by the special selectived thermochemical cycles:

$$\Delta H^0_{298}(1) = -52700 \pm 7400, \quad \Delta H^0_{298}(2) = -92400 \pm 5200.$$

On its base along with using reference data on entropy of reaction products and original substances are obtained temperature relation between the Gibbs ($J \cdot mol^{-1}$) energies and the equilibrium constant of the hydrogen sulphide oxidation processes:

for ferro-ferrisulphate system –

$\Delta G^0_T = (-52700 \pm 7400) - (184 \pm 3.3)\,T$; $\quad \ln K_c = [(6339 \pm 891)/T] + 22.1 \pm 0.4$;

for iodide-thriiodide system –

$\Delta G^0_T = (-92400 \pm 5200) - (79 \pm 3.31)\,T$; $\quad \ln K_c = [(11114 \pm 626)/T] - 9.5 \pm 0.4$.

Electrode potential method are used for estimating of temperature on equilibrium constant volumes relation of studied reactions.

It is found, that temperature greatly influences on equilibrium constant volumes. Increasing of temperature from 273 to 373 K is accompanied by reducing of K_c volume on several orders. Therefore, this reactions are practically irreversible even at 373 K.

1. *Patent France* № 2222510. Method of gases purification from hydrogen sulphide (1976).
2. *Patent USA* № 4014983. Removal of hydrogen sulphide from gases (1977).
3. *Patent Japan* № 53-31587. The purification of gases from hydrogen sulphide (1978).
4. *Patent Japan* № 54-39235. Method of gases purification from hydrogen sulphide (1979).
5. V. P. Nesterenko. A device for introducing reagent into calorimetric liquid. *Copyright Certificate* № 1644615 (1990).
6. V. P. Nesterenko, V. P. Glybin. *Scientific Bulletin of Lodz Technical University,* 1998, № 23, 111.

Thermodynamic and Viscometric studies of Interactions in concentrated aqueous binary electrolytic solutions.

J.D.Pandey, Y.Akhtar, Ashish K. Sharma
Department of Chemistry
University of Allahabad, Allahabad- 211 002
India

It has been found by number of workers that addition of electrolytes either breaks or makes the structure of liquids. Viscosity and density of Binary electrolytic solutions of different compositions have been measured at 298.15K . Using viscosity and density data the values of apparent molal volume (φ_v) ,relative viscosity (η_{rel}), and free energy of activation ($\Delta\mu^{0\neq}$) have been deduced .The making and breaking of the structure of fluid has been considered as a measure of solute - solvent and solute - solute interactions.

The results show that : (1) there are short range and weak interactions in these binary systems and (2) ions such as Na^+ , K^+ ,Mg^{+2} ,Cl^- ,CH_3COO^{-2} ,SO_4^{-2} , and NO_3^- are structure makers in water in the order of
$Na^+ > Mg^{+2} > K^+ > Cl^- > CH_3COO^{-2} > NO_3^- > SO_4^{-2}$.

ANOMALOUS HIGH-PRESSURE SOLUBILITY OF C_{60} IN ORGANIC SOLVENTS

Nobuyuki FUJITA and Seiji SAWAMURA
Department of Chemistry, Ritsumeikan University, Kusatsu, Shiga, 525-8577, Japan

Generally when a molecular crystal such as naphthalene melts, the molar volume increases by the thermal motion in the liquid phase. Therefore the pressure thermodynamically depresses the melting. In a similar way, it should do the dissolution of the crystal in solvent. This is the fact in the solubilities of several aromatic crystals such as phenanthrene in organic solvents and water. Their solubilities decrease with increasing pressure. On the contrary, we found that the solubility of fullerene (C_{60}) steeply increased with increasing pressure. The details are introduced here.

High-pressure solubility was measured using a clamp-type high-pressure optical cell designed by us.[1] A small amount of C_{60}, solvent, and a stirring ball made of polyethylene tetrafluoride, were put in the cell before the application of pressure. The absorption spectra of the solution in the cell was measured after it was shaken for a long time.[2]

The solubility of C_{60} in n-hexane increased by 7 times at 400 MPa. From the fact the volume change accompanying the dissolution is estimated to be -40 ± 6 cm^3 mol^{-1}. It does not differ much from the difference between the partial molar volume of the C_{60} in organic solvents, *e.g.*, 360 ± 10 cm^3 mol^{-1} in toluene and 355 ± 6 cm^3 mol^{-1} in carbon disulfide, and the molar volume of the crystal, 429 cm^3 mol^{-1}. The solubility in toluene increased at first and then decreased suggesting a phase transition. Enhancement of the solubility by pressure is ascribed to a large vacancy in the crystal of C_{60} compared with C_{60} in toluene as well as that in n-hexane. On the other hand, the phase transition corresponds to that from C_{60} crystal (fcc) to solvated one.

1. Sawamura, S.; Kitamura, K.; Taniguchi, Y., *J. Phys. Chem.*, 1989, **93**, 4931.
2. Sawamura, S.; Fujita, N., *Chem. Phys. Lett.*, 1999, **299**, 177.

UNDERSTANDING VOLUME-SOLUBILITY RELATIONSHIPS IN WATER

P. Ruelle and U.W. Kesselring
University of Lausanne, Section of Pharmacy, BEP, CH-1015 Lausanne, Switzerland

In order to stress the origin of the quantitative solubility dependence of nonelectrolytes on their molar volume, the solubility of aprotic substances of varying size and chemical structure are predicted from the solubility model derived from the mobile order and disorder (MOD) theory. The quantitative development of MOD theory is indeed at the basis of a new thermodynamics for real solutions. The development led in particular to a general solubility equation [1] which, on the basis of a correct description of the enthalpy and entropy changes accompanying the whole solubility process, completely describes the free energy change when a substance is dissolved in a solvent. Negelcting the polarizability/dipolarity effects upon mixing, this equation applied to liquid inert and proton-acceptor substances (B) in water (W) reduces to the sum of three terms: 1) the correction factor for the entropy of mixing related to the difference in size between the water and solute molecules (term B), 2) the hydrophobic effect which accounts for reduction in solubility that originates from the loss of mobile entropy of the water molecules when these are brought into a larger volume (term F), and 3) the increase in solubility due to solute solvation in water (term O).

$$\ln \Phi_B = B + F + O \qquad \text{with}$$

$$\text{term } B = 0.5\, \Phi_W\, (V_B/V_W - 1) + 0.5 \ln(\Phi_B + \Phi_W V_B/V_W)$$

$$\text{term } F = -2.0\, \Phi_W V_B/V_W$$

$$\text{term } O = \ln[1 + K_O(\Phi_W/V_W - \Phi_B/V_B)]$$

Rearranging the equation for low concentrated solutions at saturation ($\Phi_B << \Phi_W$ and $\Phi_W \cong 1.0$) and setting $V_W = 18.1$ cm^3 mol^{-1} lead to a simple expression for the molar solubility prediction.

$$\log S_B = [\ln(10)^{-1} \ln(1 + K_O/18.1) + 2.154] - 0.0360\, V_B - 0.2174 \ln V_B$$

Derived on a thermodynamic basis, this equation provides explanation for the relatively constant slopes (-0.03 to -0.04) and altering intercepts of all empirical volume-solubility straight lines observed for different chemical series of compounds.[2] Indeed, depending on the type of proton-acceptor group (ester, ether, ketone), and on the strength of its interaction with water (K_O), the above equation gives rise to a set of parallel nearly linear equations relating, for different chemical series, the aqueous solubility of a congener to its molar volume.

Although the foregoing solubility model closely resembles the regression equations obtained from experimental data, it entirely differs in essence and origin. The use of the molar volume as the main descriptor in most empirical LSER studies relies on the enthalpic interpretation of the solution process, and reflects the need to create a cavity in water to host the solute: the larger the solute, the higher the energy required to break H-bonds, and the lower the solubility. In contrast, the dependence of the aqueous solubility on the solute size in the above equation has a natural but hybrid origin stemming from the balance of two entropic effects, *i.e.*, the hydrophobic effect and the exchange entropy correction factor. Although both contributions increase with the growing size of the solute, the hydrophobic-related term is always greater and rises far more faster, hence becomes rapidly responsible for the lowering of the solubility in water as the solute gets bigger and bigger.

In water, both the ephemeral character and the mobility of the H-bonds make needless the breaking of the hydrogen-bond network to dissolve a foreign substance, and the formation of a cavity of the solute dimension does not constitute a needed thermodynamic step in the dissolution of a compound in H-bonded or non H-bonded liquids.

1. Ruelle, P.; Rey-Mermet, C.; *et* al. *Pharm. Res.*, 1991, **8**, 840.
2. Lande, S.S., Banerjee, S., *Chemosphere*, 1981, **10**, 751.

HIGH-PRESSURE SOLUBILITY OF $NaCl \cdot 2H_2O$ IN WATER

Yoshihiro SETOGUCHI, and Seiji SAWAMURA
Department of Chemistry, Ritsumeikan University, Kusatsu, Shiga, 525-8577, Japan

NaCl crystal which coexists with NaCl solution at ambient pressure and temperature is transformed into $NaCl \cdot 2H_2O$ at 273.2 K when the temperature decreases. And then the solubility-temperature curve breaks at this temperature. In the present work, we shows the breaking in the form of not the solubility curve but the surface adding another axis of pressure. To do so, we measured the solubility of $NaCl \cdot 2H_2O$ at low temperatures of 273.2, 268.2 and 263.2 K and pressures up to 300 MPa.

$NaCl \cdot 2H_2O$ crystal was prepared by crystallization from the saturated solution in a refrigerater regulated at 258.2 K. The obtained crystal, NaCl solution, and a stirring ball were placed in an inner cell of the pressure vessel which was a piston-cylinder type with an outlet valve designed by us. After the vessel was shaken in a thermostated bath for a long time more than three days, the saturated solution was taken out from the outlet valve dropwise keeping the pressure in the vessel. Concentration of the solution was determined by drying and weighing it.

Obtained solubility is shown in Fig.1. Two planes are observed, *i.e.*, NaCl for high-temperature site and $NaCl \cdot 2H_2O$ for low-temperature site. The solubility of NaCl increases with increasing pressure and that of $NaCl \cdot 2H_2O$ decreases as well as $NaBr \cdot 2H_2O$ [1]. A breaking curve accompanying the phase transition is clearly observed between the two planes. It dose not differ from the one estimated by Adams[2] using the high-pressure density of aqueous solution. Supposing a reaction of $NaCl \cdot 2H_2O$ (s) [I] → NaCl (s) $+2H_2O$ [II] → NaCl *aq* + 2 H_2O [III], the pressure and temperature coefficients of the solubility in Fig.1 thermodynamically suggest that the enthalpic stability is [III] < [II] < [I] and the volume [I] < [III] < [II]. It means that [I] is the most stable in enthalpy and compact in volume.

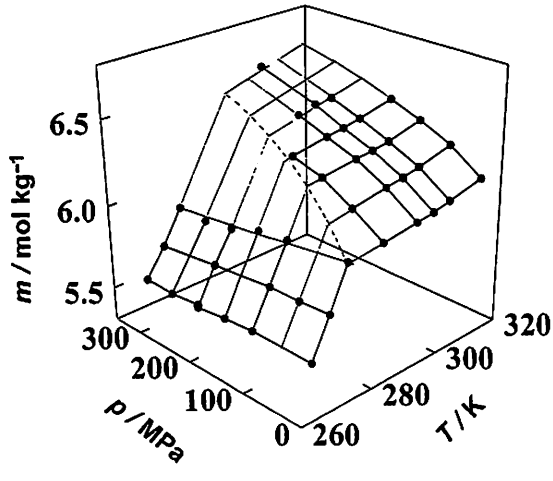

Fig.1. Solubility surface of NaCl and $NaCl \cdot 2H_2O$ in water.

1. Sawamura, S.; Yasuhara, S.; Sugi, S.; Egoshi, N.; *Bull. Chem. Soc. Jpn.*, 1993, **66**, 2406.
2. Adams, L. H.; Gibson, R. E.; *J. Amer. Chem. Soc.*, 1930, **52**, 4252 .

SOLUBILITIES IN THE TERNARY SYSTEM ALKALI METAL HALIDE-GLUCOSE-WATER

Kazuhito KAJIWARA
Department of Biosciences, Teikyo University of Science and Technology,
2525 Yatsusawa Uenohara-machi, Kitatsuru-gun, Yamanashi 409-0193, Japan

A number of authors have established that organic substances have effect on solubility and form of crystals of inorganic substances, which is sometimes of value for carrying out analytical determinations according to the precipitation method. For elucidating the question of the dependence of solubility of inorganic substances on the presence of organic substances and also the effect of inorganic substances on the solubility of organic substances, it was of interest to study the solubility of some organic substances in the presence of salts, over a wide range of concentration. The literature describing the ternary system alkali metal halide-glucose-water is limited. The system sodium chloride-glucose-water[1] has been studied in a point view of its solid phase at 24℃. The system potassium chloride-glucose-water[2] has been studied at 25℃. The present investigation was undertaken with the aim of providing more data of characterisation of the ternary alkali metal halide-glucose-water system and possibly to obtain a study of the solubility of glucose/alkali metal halide in the presence of alkali metal halide/glucose.

The solubility of glucose was measured in saturated alkali metal halide aqueous solutions at 30℃. The solubility of glucose in saturated sodium halide aqueous solutions was lower than that in water. On the contrary, the solubility of glucose in saturated potassium halide aqueous solutions was higher than that in water. The solubility of sodium halide in water is in order NaF<NaCl<NaBr<NaI, and the solubility of glucose decreases with increase sodium concentration except NaI. The solubility of potassium halide in water is in order KCl<KBr<KI, and the solubility of glucose increases with increase potassium concentration. The determinations of solubility of glucose were carried out in the presence of NaCl/KCl at 30℃. In case of NaCl the solubility curve is not simple, the solubility of glucose is nearly constant during lower NaCl concentration and gradually decreases with increase NaCl concentration. In case of KCl the curve is simple, the solubility of glucose increases with increase KCl concentration. The determinations of solubilities of alkali metal chloride were also carried out in the presence of glucose. In case of NaCl the solubility curve is not simple, the solubility of NaCl decreases with increase glucose concentration during lower glucose concentration and gradually increases with increase NaCl concentration. In case of KCl the curve is rather simple, the solubility of KCl is nearly constant during lower KCl concentration and gradually increases with increase KCl concentration.

1. Matsuura, S., *Bull. Chem. Soc. Jpn.*, 1927, **2**, 44.
2. Zhdanov, A. K.; Higai, K. G., *Zh. Obshch. Khim.*, 1956, **26**, 2383.

Raman Study on the Conformational Equilibria of Fluoroacetone in Water

Yosuke Shiratori, Minoru Kato and Yoshihiro Taniguchi
Department of Chemistry, Faculty of Science and Engineering, Ritsumeikan University, Kusatsu, Shiga, 525-8577, Japan

[Introduction] We have reported medium effects on the conformational equilibria of haloacetones in the previous works[1, 2]. For aqueous solutions, an additional band was observed in each conformational key band of chloroacetone[1], bromoacetone[2] and fluoroacetone[2]. We assigned these bands to the *syn* conformer that has a hydrogen bond between the halogen atoms and water molecule (*syn'* conformer). Although pressure effect on the conformational equilibria of chloroacetone has been reported[1], we have not yet done for the other haloacetones. Here, we investigate the hydration structure of fluoroacetone (Fig. 1) using the temperature and pressure turning Raman spectroscopy.

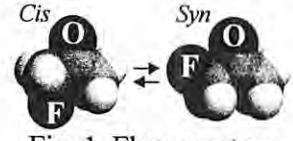

Fig. 1. Fluoroacetone

[Experimental] Raman spectra were recorded using a JEOL-JRS400D. Samples were exited with 90° scattering of 514.5nm radiation from an argon ion laser (Stabilite 2017) with 250~500mW output.

[Results and Discussion] We measured the C-C-C symmetric stretching mode. From temperature dependence of the ratios of the integrated intensities, we calculated thermodynamic values between the conformers. The conformational enthalpy change with the solvent change ($T\Delta\Delta S_{C\to S}$) from C_2Cl_4 to water is quite larger than that to other solvents (Table 1). From pressure dependence of the ratios of the integrated intensities (Fig. 2), we determined the volume differences between the conformers in the aqueous solutions (Table 2). $\Delta V_{C\to S}$ values for the aqueous solutions are significantly positive and $\Delta V_{S\to S'}$ values are significantly negative in comparison with chloroacetone[1]. From these interesting results, we discuss the hydration structure of fluoroacetone by comparing with the results for the other haloacetones.

Table 1. Differences of the thermodynamic quantities (kJ/mol) between the *cis* and the *syn* conformers with the solvent change at 20°C.

Solvent change	$\Delta\Delta G$	$\Delta\Delta H$	$T\Delta\Delta S$
$C_2Cl_4\to$THF	-3.1±2.5	-6.6±1.8	-3.6±3.1
$C_2Cl_4\to$Neat	-5.3±1.5	-5.1±1.1	0.2±1.9
$C_2Cl_4\to D_2O$	-5.8±1.7	2.5±1.2	8.3±2.1
$C_2Cl_4\to H_2O$	-5.7±1.5	3.0±1.1	8.7±1.9

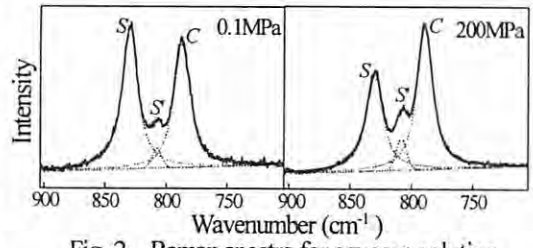

Fig. 2. Raman spectra for aqueous solution

Table 2. Volume differences between the conformers of fluoroacetone (cm^3/mol).

Solvent	*Cis*→*Syn*	*Syn*→*Syn'*
D_2O	6.2±0.4	-12.3±1.2
H_2O	5.1±0.2	-11.0±0.4

1. Kato, M.; Nanba, Y.; Taniguchi, Y., *Chem. Phys. Lett.*, 1998, **30**, 289.
2. Shiratori, Y.; Kato, M.; Taniguchi, Y., 1997 Bunshi-Kouzou Sougou-Touronkai abstract, p. 202.

THERMODYNAMICS OF LANTHANIDES COMPLEX FORMATION IN AQUEOUS SOLUTION

YOUNG-INN KIM[1], SUNG-NAK CHOI[2] and SUN-GUEM PARK[2]

[1] Department of Chemical Education, Pusan National University, Kumjeong-ku,Pusan 609-735, Korea

[2] Department of Chemistry, Pusan National University, Kumjeong-ku ,Pusan 609-735, Korea

The thermodynamic parameters (ΔG_1, ΔH_1, ΔS_1) on the L-prolinate, L-thioprolinate, trans-4-hydroxy-L-prolinate, L-pyroglutamate complexation with lanthanides(III) cations (1:1) in aqueous solution have been determined in the ionic medium of 0.1M $NaClO_4$ at 25℃ using potentiometric and calorimetric methods. The results reveal that the heterocyclic nitrogen atom in proline ring and the carboxylate were involved in chelate formation.

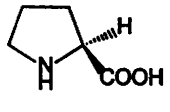

L-proline

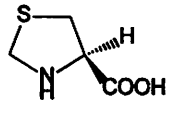

L-thioproline

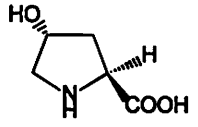

trans-4-hydroxy-L-proline

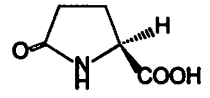

L-pyroglutamic acid

The correlation between the stability constants ($\log\beta_1$) of Eu(III) complexes and the acid constants (pka) of bidentate ligands shows the linear correlation, reflecting the ionic nature of the metal-ligand interaction. The thermodynamic parameters for europium(III) complexes are listed in Table 1, and the complexes are stabilized by the excess entropy effect. The extra stability of the L-thioproline complex comparing to L-proline complex is due to the indirect interaction between the lone pair electrons in sulfur atom in L-thioproline and the large lanthanide metal ion. This is coincident with the result of the rather exothermic enthalpy and the less entropy change in L-thioproline. Moreover trans-4-hydroxy-L-proline complex is more stable than L-proline complex. This increased stability is associated with more positive value of enthalpy change due to the hydration sphere structure of the polarizable lanthanide(III)-trans-4-hydroxy-L-proline complex in aqueous solution.

Table 1. Thermodynamic parameters of the europium(III) complex at 25℃, μ = 0.1M $NaClO_4$

ligand	$-\Delta G_1$ ($kJmol^{-1}$)	ΔH_1 ($kJmol^{-1}$)	ΔS_1 ($kJmol^{-1}$)
L-proline	13.23	11.7	84
L-thioproline	19.06	1.8	70
trans-4-hydroxy -L-proline	15.58	2.2	60
L-pyroglutamic acid	15.03	10.9	87

THERMODYNAICS OF MULTI-COMPONENT SURFACTANT SOLUTIONS

M. TANAKA[1] and Y. MURATA[2]

[1] (Emeritus Professor, Fukuoka University), 5-7-1, Chihara-dai, Ichihara, 290-0158, Japan

[2]Department of Chemistry, Fukuoka University, Nanakuma, Jonan-ku, Fukuoka, 814-0180

Multi-component micellar solutions of surfactants are treated by small system thermodynamics. Firstly we show that in closed solution systems, chemical potentials of interacting solute species can be treated mathematically in the same form of equations as those of ideal solution. Consider a system of two solutions, α and β. The exact differential of the Gibbs free energy of the total system can be written as

$$dG_t = -S_t dT + V_t dP + \sum_{i=1}^{c} \mu_i^{\alpha} dN_i^{\alpha} + \sum_{i=1}^{c} \mu_i^{\beta} dN_i^{\beta} \tag{1}$$

At equilibrium of the total system at given T, P and $N_i^t (= N_i^{\alpha} + N_i^{\beta})$, we have $\mu_i^{\alpha} = \mu_i^{\beta} = \mu_i^{\nu}$.

Then we should have the following equation for the quasi-static process of the total system.

$$dG_t = -S_t dT + V_t dP + \sum_{i=1}^{c} \mu_i^{\nu} dN_i^t \tag{2}$$

in which $N_i^{\nu} = N_i^{\nu}(T, P, N_i^t)$ and $\mu_i^{\nu} = \mu_i^{\nu}(T, P, N_i^t)$. In stead of $\mu_i^{\nu} = \mu_i^{\nu 0}(T, P) + kT \ln x_i^{\nu} \gamma_i^{\nu}$, we use the new expression, $\mu_i^{\nu} = \hat{\mu}_i^{\nu}(T, P, N_i^t) + kT \ln x_i^{\nu}$, where $\hat{\mu}_i^{\nu} = \mu_i^{\nu 0}(T, P) + kT \ln \gamma_i^{\nu}$. We obtain the following equation for the quasi-static process of a solution in closed solution system.

$$d\mu_i^{\nu} = -\hat{s}_i^{\nu} dT + \hat{v}_i^{\nu} dP + \left[d\left(kT \ln x_i^{\nu} \right) \right]_{N_i^t}, \nu = \alpha, \beta \tag{3}$$

Eqn.3 is mathematically of the same form as ideal solution. Analyzing the data obtained from experiments of a series of closed solution systems by the use of eqn.3, we can discuss T, P and concentration effects on the thermodynamic properties of either solution. The same is applicable to the chemical potentials of interacting monomeric and micellar species in surfactant solutions of different solvents constituting a closed multi-phase system. We have for micellar species

$$d\mu^{\square} = -\hat{S}^{\square} dT + \hat{V}^{\square} dP + kTd \ln x_m + \sum_{i=1}^{c} \mu_i d\overline{N}_i \tag{4}$$

We now have a principle that non-ideal solutions can formally be treated as ideal solution when closed. Assumptions of ideality and others are no longer necessary here. Applying the small system thermodynamics together with this principle, for example, to the closed system of aqueous surfactant solution and solid, we can strictly treat the effect of T and P on the solubility of surfactant in water.

Thermal Expansivity of Multicomponent Liquid Systems

J.D.Pandey, S.B.Tripathi & Vinay Sanguri
Department of Chemistry, University of Allahabad, Allahabad,U.P-211002.
India

Various theoretical models viz. Hard-Sphere and Statistical Mechanical Theory have been applied to deduce the values of thermal expansivity of a number of multicomponent molecular liquid mixtures and their binaries. Theoretical formalism has been made.

The values of thermal expansion coefficient (α) of molecular binary and ternary liquid mixtures have been computed at different temperatures by using Flory Statistical theory and seven different hard sphere models due to Thiele-Lebowitz, Thiele, Carnhan-Starling, Guggenheim, Scaled particle theory, Henderson and Hoover-Ree. These values of thermal expansion coefficient are compared with the experimental values.

In prediction of thermal expansion coefficient of aforesaid liquid mixtures by Flory theory the reduced and characteristic parameters are used. These reduced and characteristic parameters are calculated with the help of thermal expansion coefficient and isothermal compressibility of pure components. Except mole fraction no other property of liquid mixture is needed.

Thermal expansion coefficient obtained by seven different hard sphere models using a generalised equation which is a function of packing fraction 'y'

$$\alpha = \frac{1}{T}\,\frac{ab}{by(da/dy)_T - nay(db/dy)_T + ab}$$

where 'a' & 'b' are function of 'y', and 'n' is an integer.
The packing fraction 'y' is defined as:

$$y = (\pi d^3 N/6V)$$

where 'd' is rigid sphere diameterof the molecule.

A careful perusal of results show that Flory theory provides fairly good agreement followed by Scaled particle theory and Henderson model.

Complex formation in polymer solutions—^{11}B NMR studies on the borate-linear and crosslinked polyssacharide systems

Yoshinobu Miyazaki[1], Kazuhisa Yoshimura[2], Yoshinori Miura[3] and Hirofumi Sakashita[3]

[1]Department of Chemistry, Fukuoka University of Education, Akama, Munakata, Fukuoka 811-4192, Japan

[2]Department of Chemistry, Faculty of Science, Kyushu University Ropponmatsu, Ropponmatsu, Chuo-ku, Fukuoka 810-8560, Japan

[3]The Center of Advanced Instrumental Analysis, Kyushu University, Kasuga, Fukuoka 816-8580, Japan

The macromolecule-simple ion complex systems exhibit some very particular features arising from the fact that ligands are fixed on the polymer chain, which greatly limits the analogy with complexation between small molecules. A large number of studies on the complex formation between borate and polyhydroxy compounds had been reported, however, the nature of the complexation of borate with linear or crosslinked polysaccharide has not been clarified. We have employed ^{11}B NMR spectroscopy to elucidate the nature of the complexation of borate with linear dextran consisting of glucopyranoside residues, crosslinked dextran (Sephadex gel) and their monomer derivative (α-methyl-D-glucopyranoside).[1] Well-resolved ^{11}B NMR spectra for Sephadex gel as well as for a solution of dextran or α-methyl-D-glucopyranoside were observed. Five types of borate complexes with α,β- and α,γ-diol moieties of glucopyranoside residues were present. The characteristic ^{11}B chemical shift values were -13 to -14 ppm for the 1:1 complex with α,β-diol, -10 to -11 ppm for the 1:2 complex with α,β-diols, around -18 ppm for the 1:1 and 1:2 complexes with α,γ-diols, and around -14 ppm for the 1:2 mixed ligand complex withα,β- and α,γ-diols, irrespective of linear or crosslinked structure of the polysaccharide. For dextran system, in accordance with the increase in the chain length of polysaccharide the relative stability of 1:1 complex with α,β-diol becomes lower compared to the 1:1 complex with α,γ-diol. This indicates that the glucopyranoside residues in the longer dextran chain prefer the 1C conformation and the interconversion between the C1 and 1C conformers is restricted due to the hydrodynamic and steric hindrance of the linear polymer in aqueous media. It was also found that the intrachain tetradentate complex, in which borate binds with two diol moieties in the same polymer chain, did not form in the case of rigid polymer as polysaccharides. For Sephadex gel system, the lower the degree of crosslinking, the higher the relative stability of 1:1 complex with α,γ-diol. The gel with the lower crosslinking degree exhibits the similar complexation behavior as that for the high molecular weight dextran. The complexation in such heterogeneous aqueous media is discussed in terms of effects of polymerization and crosslinking of saccharides.

1. Yoshimura, K.; Miyazaki, Y.; Sawada, S.; Waki, H., *J. Chem. Soc., Faraday Trans.*, 1996, **92**, 651.

EFFECT OF ORGANIC ACIDS ON THE FORMATION OF Al_{13} AND ALUMINUM HYDROXIDE IN PARTIALLY NEUTRALIZED AQUEOUSALUMINUM SALT SYSTEMS

Chia W. Wu and Ming K. Wang
Department of Agricultural Chemistry, National Taiwan University, 1 Sec, 4 Roosevelt Rd, Taipei, 106, Taiwan, R.O.C.

Aluminum(III) hydrolysis, precipitation and Al_{13} tridecamer formation in the presence of acetic, oxalic, and citric anions have been studied by liquid-state ^{27}Al Nuclear Magnet Resonance (NMR).[2,4]

The typical NMR spectrum of a hydroxy-Al solution, with an Al concentration of 0.02 mol L^{-1} with respect to Al, and the OH/Al mole ratio is 2.2 displays two distinct resonance peaks. The first has a chemical shift of 0ppm, corresponding to the hexaaqua-Al ion $Al(H_2O)_6^{3+}$. The second peak =62.5ppm downfield from the monomer peak has been assigned to the Al_{13} polymeric ion.[1,3,6] Acetate forms weak complexes with aluminum and almost does not affect the hydrolysis of Al. The precipitated phase is hypothesized to be aggregated Al_{13} at 62.5ppm[7,8,9]. Oxalate forms strong multiligand complexes with Aluminum. High oxalate contents (Oxalate/Al = 1.0) inhibit the formation of Al_{13}..and precipitation occurs only at high pH value which has a chemical shift of 16.5ppm[10]. Citrate forms the strongest multiligand complexes with Aluminum. At Citrate/Al = 0.5, the Al-citrate-hydroxyl complexes are formed and has a chemical shift of 12ppm. The aluminate ($Al(OH)_4^-$) is formed when citrate/Al = 1.0 has a chemical shift of 80ppm.[11]

The inhibition tendency of these three organic anions to the hydrolysis of aluminum has shown in the order : citrate > oxalate > acetate. [5]

1. Akitt, J. W.; Greenwood, N. N.; Khandelwal, B. L.; Lester, G. D., *J. Chem. Soc. Dalton.*, 1972, 52, 604-610.
2. Akitt, J. W.; Farthing, A., J. *Magn. Reson.*, 1978, 32, 345-352.
3. Bertsch, P. M.; Thomas, G. W.; Barnhisel, R. I., *Soil Sci. Soc. Am. J.*, 1986, 50, 825-830.
4. Chang, C. M.; Wang, M. K., *J. Chinese Agric. Chem. Soc.*, 1992, 28, 356-363.
5. Hsu, P. H.; Cao, D., *Soil Sci.*, 1991, 152, 210-219.
6. Hunter, D.; Ross, D. S., *Science*, 1991, 251, 1056-1058.
7. Jabor, M.; Bertin, F.; Thomas-David, G., *Can. J. Chem.*, 1991, 251, 1056-1058.
8. Jardine, P. M.; Zelazny, L. W., *Soil Sci. Soc. Am. J.*, 1986, 50, 895-900.
9. Johansson, G., *Acta Chem. Scand.*, 1962, 16, 403-420.
10. Lind, C. J.; Hem, J. D., *U. S. Geol. Surv. Water-Supply Pap.*, 1975, 1827, 83..
11. Ng Kee Kwong, K. E.; Huang, P. M., *Soil Sci. Soc. Amer. J.*, 1977, 41, 692-697.

SOLUTION CHEMISTRY OF ALUMINUM IN THE ACIDIFIED HYDROSPHERE BY ACID RAIN

Tsutomu KURISAKI[1], Takushi YOKOYAMA[2], and Hisanobu WAKITA[1]
[1]Department of Chemistry, Fukuoka University, Jonan-ku, Fukuoka 814-0180, Japan
[2]Department of Chemistry, Kyushu University, Higashi-ku, Fukuoka 812-8581, Japan

Recently acid precipitates have been acidifying soil. The acidification can make aluminum in soils and/or racks dissolve in hydrosphere such as soil water, ground water, river water, and lake water, etc. When present in high amount, aqua aluminum ion exhibits toxic effects against plants. The species that have generally been considered more toxic are the monomers such as $Al(H_2O)_6^{3+}$, $Al(H_2O)_5(OH)^{2+}$, and $Al(H_2O)_4(OH)_2^{+}$. However, aluminum complexes with organic compounds are less phytotoxic than the aqua aluminum ion and its hydrolytic products. Therefore, it is important to investigate the interaction between the aluminum ion and organic ligands in acidic aqueous solution for understanding the phytotoxicity of aluminum.

Fulvic acid is considered to be a typical organic compound in natural water, and is a polymer with carboxylic and phenolic groups which act as binding sites of metal ions in natural water. However, when fulvic acid is used as a ligand for aluminum ions, it is presumed that the experimental results would be very complicated and the interpretation and analysis may be difficult. Consequently, as a preliminary step to understanding the binding properties of aluminum ion for fulvic acid it is essential to investigate the interaction between aluminum ions and simple model compounds including carboxyl, phenolic hydroxyl, and phenolic carboxyl group in acid aqueous solution.

In this study, to elucidate the coordination structure, the interaction between aluminum ion and various organic model compounds (iminodiacetic acid[1], nitrilotriacetic acid[2], tiron[3], salicylic acid[3], phthalic acid[3], quinolic acid[4], etc) which have functional groups contained in fulvic acid is investigated in acidic aqueous solution by the ^{13}C and ^{27}Al NMR spectroscopy and potentiometry. The results show that these organic compounds act as a bidentate ligand to aluminum ion and that the stability of complexes depends on the chelate ring size in order 5>6>7 membered ring.

The formation of aluminum complexes with fulvic acid in acidic aqueous solution probably depends on the number of functional groups which can act as bidentate ligands. The chelate effect will be an important factor to control the formation of aluminum complexes with fulvic acid.

1. Yokoyama, T.; Abe, H.; Kurisaki, T; Wakita, H., *Anal. Sci.*, 1999, **15**,393
2. Yokoyama, T.; Murata, T.; Kinoshita, S; Wakita, H., *Anal. Sci.*, 1998, **14**,629
3. Yokoyama, T.; Abe, H.; Kurisaki, T; Wakita, H., *Anal. Sci.*, 1997, **13** suppl,425
4. Yokoyama, T.; Abe, H.; Kurisaki, T; Wakita, H., 1999, to be submitted

GEOCHEMISTRY OF IRON(III)-SILICIC ACID COMPLEX

Takushi YOKOYAMA[1], Hisanobu WAKITA[2], and Yoshihisa MATSUDA[1]
[1]Department of Chemistry and Physics, Graduate School of Science, Kyushu University, Hakozaki, Higashi-ku, Fukuoka 812-8581, Japan
[2]Department of Chemistry, Faculty of Science, Fukuoka University, Nanakuma, Jonan-ku, Fukuoka 814-0180, Japan

Iron is one of the most insoluble elements in natural water system under oxidizing condition because the extremely low solubility product of iron(III) hydroxide (10^{-36}). However, Goto et al. (1980) reported that ferric ion can be present as soluble species in a neutral well water containing large amount of silicic acid, suggesting an interaction between ferric ion and silicic acid. Weber and Stumm (1965) and Olson and O'Melia (1973) showed the formation of a silicato complex of ferric ion in acidic aqueous solution:

$$Fe^{3+} + Si(OH)_4 \rightleftarrows FeOSi(OH)_3^{2+} + H^+$$

The facts indicate that if the silicic acid concentration is significantly high, ferric ion can be dissolved in natural water. Therefore, it is essential to investigate the interaction between ferric ion and silicic acid in near neutral aqueous solution to elucidate the geochemical behavior of iron in natural water system. In this study we investigated the interaction between ferric ion and silicic acid by spectrophotometry and gel chromatography under two different conditions: [1] when silicic acid was present as monomer and [2] when silicic acid polymerized.

[I] Interaction between ferric ion and monosilicic acid

Sample solutions were prepared as follows. Acidic ferric chloride solution was added to sodium silicate solution at vigorously stirring. Initial ferric ion concentration and silicic acid concentration in sample solutions were 10^{-4} mol dm^{-3} and 0 -100 ppm (as SiO_2), respectively. In the concentration range of silicic acid less than 50 ppm, iron(III) hydroxide (brown deposit) was precipitated in spite of high amount of silicic acid ralative to ferric ion. However, with increasing the concentration of silicic acid, the amount of iron(III) hydroxide precipitated decreased, indicating the formation of soluble species by an interaction between ferric ion and monosilicic acid. Hereafter the soluble species are called " iron(III)-silicic acid complex (ISAC)" . When the silicic acid concentration was 100 ppm, 65.8 % of ferric ion was dissolved at pH 8, while 100 % of ferric ion was dissolved at pH 9 and 10. The Si/Fe atomic ratio of the ISAC ranged from 0.75 to 0.86.

[II] Behavior of ferric ion during the polymerization of silicic acid

The preparation of sample solutions were carried out in a same method described above. The initial concentrations of ferric ion and silicic acid were 10^{-4} mol dm^{-3} and 800 ppm, respectively. In all the experiments brown deposit of iron(III) hydroxide was not apparently observed. In the cases of pH 7-9 at which the polymerization of silicic acid proceeded rapidly, the gel chromatograms of ferric ion were almost same as those of polysilicic acid, suggesting that a major part of ferric ion was preferentially combined with the surface of polysilicic acid because a reaction between monosilicic acid and polysilicic acid was retarded in the presence of ferric ion. The absorption spectra were different between ISAC [I] and [II], suggesting that the structure of ISAC [I] and [II] was different. The proposed structure of ISAC [I] and {II] is as follows: the ISAC[I] consisted of small core of iron(III) hydroxide polymer in size on which the surface was covered with monosilicic acid, while the ISAC [II] consisted of core of silicic acid polymer that ferric ion chemically adsorbed on the surface.

[III] Geochemical implication

Iron is the one of the most immovable elements under oxidizing condition in hydrosphere because ferric ion is easily hydrolyzed and precipitated as iron(III) hydroxide. In hot spring water and deep geothermal water whose concentration of silicic acid is greatly higher than the solubility of amorphous silica, however, ferric ion is possible to be dissolved by the formation of ISAC [I] and/or [II] depending on whether the polymerization of silicic acid occur or not. If the ISAC is stably formed, ferric ion is probably transported for a long distance in hydrosphere.

DEVELOPMENT OF MANAGEABLE REMEDIATION METHOD FOR REMOVAL OF ORGANIC CONTAMINANTS FROM WATER SOLUTIONS

Yu. BASOVA
Carbon Materials Division, Dept. of Energy Resources, National Institute for Resources and Environment, 16-3 Onogawa, Tsukuba-shi, Ibaraki 305, JAPAN

The use of electrochemical method is an effective means to eliminate pollutants from aqueous waste streams [1, 2]. The purpose of this research is to develop and test a technique for controlling the release of unwanted organic compounds on carbon materials tailored to eliminate a range of contaminants from waste as well as to recovery and reuse spent adsorbent. Two approaches have been examined to enhance the separation processes, namely reagent separation and electrochemical potential dependent adsorption-desorption on the surface of synthetic carbons.

The electric conductivity, mechanical and chemical stability of synthetic carbons gives rise to their applications as electrodes for the conventional potential dependent adsorption-desorption of contaminants in aqueous solutions. Organic contaminants include phenol and benzoic acid. Four kinds of synthetic carbon adsorbents with a range of surface areas and functionality have been picked for the observation. Experiments have been carried out at a wide interval of pH and applied potentials to manipulate the interfacial potential and surface adsorptive capacity.

Potential dependent elimination process has been created by using a fluidized layer of carbon bed in a flow-through remediation cell. The fluidizide-bed electrode structure of spherically granulated carbon particles shows a unique combination of high electrochemical accessible surface area and high permeability for solution [3]. The technique that can be used to remove contaminants from aqueous solution is the electrochemical oxidation-reduction or electroadsorption in polarized fluidized carbon layer. This allows significant progress in the reactor optimisation with size and efficiency.

The elimination of phenol studied by cyclic voltammetry and control spectrophtometrically occurs by electrocatalytic oxidation on the surface of carbon electrode. Anode potential applied to fluidizide-bed results in complete electrooxidation of phenol and increase of adsorption capacity towards products of oxidation.

The adsorption of benzoic acid is maximal at the interval of pH where benzoic acid occurs as a molecule while not influenced by competitive adsorption of ions from surrounded solution. Removal efficiency above 95% is observed. After polarization of the electrode by the imposed electric field benzoic acid is removed from the electrolyte and adsorbed on the carbon surface. It has been found that the potential dependent adsorption of benzoic acid is affected by pH of electrolyte solution, surface structure of carbons and their polarizability from external electric field.

Study of an adsorber operated under cathodic polarization showed an improvement in benzoic acid removal from carbon surface. Comparatively with the reagent desorption, in a solvent flushing operation, a cathode polarization appreciably improves and simplifies *in situ* regeneration of carbon adsorbent. The electrochemically-regenerated carbon with intermediate porosity maintains its virgin capacity by applying high cathode potential. The effectiveness of desorption of benzoic acid from spent adsorbent is controlled by interaction between organic compound and carbon surface in adsorption process.

The results show that organic compounds can, under optimized conditions, be reversibly removed from contaminated water solutions. Its simplicity allows economic removal of toxic contaminants in a directly reusable from waste.

1. Rajeshwar K., Ibanetz J.G., Swain G.M., *J. Appl. Electrochemistry*, 1994, **24**, 1077.
2. Golub D., Oren Y. and Soffer A., *Carbon*, 1987, **25**, 1, 109.
3. Basova Yu. *Functional Materials*, 1998, **4**, 5, 586.

A MOBILE ORDER THEORY-BASED MODEL FOR PREDICTING THE POLLUTANTS' DISTRIBUTION BETWEEN IMMISCIBLE SOLVENTS.

P. Ruelle
University of Lausanne, Section of Pharmacy, BEP, CH-1015 Lausanne, Switzerland

Knowledge of the physicochemical property profile of organic chemicals is a prerequisite to assess and model their environmental fate and ecotoxicological risk. In this context, water solubility is often needed to characterize the mobility of xenobiotics in the hydrological cycle as well as their bioavailability in natural waters, and partition coefficients are important indices of the compound's distribution and transport potential in biological and environmental media. In order to describe phase equilibrium behavior correctly, proper weighting must be assigned to the relative importance of the various physical phenomena that determine the partitioning process at the molecular level. Thermodynamically, the partition coefficient, the ratio of two equilibrium concentrations, results from all enthalpy and entropy changes occurring during the transfer of the solute from one phase to the other. It therefore arises from the difference in the compound's stabilization between phases.

As long as the activity coefficient ratio is not concentration dependent, the partition coefficient of a substance B may be calculated from the difference of its volume fraction solubility between the less polar (index 1) and the more polar (index 2) phases: $\log P_{1,2} = (\ln 10)^{-1}\left[\ln \Phi_B^1 - \ln \Phi_B^2\right]$

An in depth understanding of the molecular origin and of the factors that govern partition coefficient may then be achieved by expressing the overall solubility, in each solvent phase, in terms of the various free energy changes taking place during the solubility process. Using the expressions [1] issued from the quantitative treatment of the mobile order thermodynamics, and provided that log P is determined for low concentration ranges, the following model for log $P_{1,2}$ is obtained.[2]

$$\log P_{1,2} = \frac{1}{\ln 10}\left[\Delta B + \Delta D + \Delta F + \Delta(O+OH)\right]$$

with

$$\Delta B = 0.5 V_B\left(\frac{1}{V_1} - \frac{1}{V_2}\right) + 0.5 \ln \frac{V_2}{V_1} \qquad \Delta D = \frac{V_B}{RT}\left(\frac{\left(\delta_B' - \delta_2'\right)^2}{1.0 + \frac{\max\left(K_{O_i}^2, K_{OH_i}^2\right)}{V_2}} - \frac{\left(\delta_B' - \delta_1'\right)^2}{1.0 + \frac{\max\left(K_{O_i}^1, K_{OH_i}^1\right)}{V_1}}\right)$$

$$\Delta F = V_B\left(\frac{r_2}{V_2} - \frac{r_1}{V_1}\right) + \sum_i v_{OH_i}\left\{r_1 - (r_2 + b)\right\} \qquad \Delta(O+OH) = \sum_i v_{O_i} \ln \frac{1 + K_{O_i}^1/V_1}{1 + K_{O_i}^2/V_2} + \sum_i v_{OH_i} \ln \frac{1 + K_{OH_i}^1/V_1}{1 + K_{OH_i}^2/V_2}$$

On the one hand, ΔB and ΔF bring information on the difference between the two phases of both the solute-solvent mixing entropy and the tendency to induce a hydrophobic effect towards the solute. Both terms refers to entropic effects and mainly depend on the volume, V_B, of the partitioned solute. On the other hand, the solvation-related terms, ΔD and Δ(O+OH) account for the difference in the overall interactions formed between the solute and solvent molecules in each phase.

Strictly obtained on a thermodynamic basis, the log $P_{1,2}$ equation may probably be considered as the most general and comprehensive model ever developed for calculating a priori the partition coefficient of a chemical in biphasic systems consisting of two largely immiscible solvents. The predictive ability of the model is demonstrated with the estimation of both the *n*-hexane/water and *n*-octanol/water partition coefficients of a series of environmentally relevant compounds.

1. Ruelle, P.; Rey-Mermet, C.; *et* al. *Pharm. Res.*, 1991, **8**, 840.
2. Ruelle, P.; Kesselring, U.W. *J. Pharm. Sci.*, 1998, **87**, 1015.

SELECTIVE ADSORPTION OF Cu^{2+} AND Pd^{2+} ON A CHITOSAN DERIVATIVE RECOGNIZING PLANAR METAL IONS

Yoshinari BABA, and Hiroshi NOMA
Department of Applied Chemistry, Miyazaki University, Gakuenkibanadai-nishi 1-1, Miyazaki, 889-2192, Japan

In order to improve the selectivity of copper(II)/iron(III), crosslinked *N*-(2-pyridylmethyl)chitosan(PMC) with lower affinity for iron(III) was synthesized[1] by crosslinking the Schiff's base formed in order to prevent amino group to be metal adsorption sites from a attack of 2-(chloromethyl)oxirane. The final chitosan derivative, PMC, was obtained by reducing the imine moiety of the Schiff's base with sodium borohydride. The substituted degree was determined to be over 0.9 by using the C/N ratio of elemental analysis. Figure 1 shows the chemical structure of PMC used in this study.

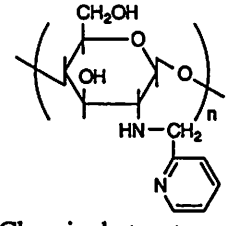

Fig.1 Chemical structure of PMC.

At first, the adsorption order of metal ions was found by measuring the pH dependence of metal ions on the distribution ratio. The experimental result for copper(II) and iron(III) was shown in Fig.2 By comparing the selectivity of PMC for copper(II)/iron(III) with those of the crosslinked copper-complexed chitosan(CLC)[2], it was found that the order of the selectivity towards copper(II)/iron(III) was reversed. Copper(II) was selectively adsorbed on PMC at a lower pH by 4 units compared with on CLC from 1 M aqueous ammonium nitrate solution. PMC selectively adsorbed also palladium(II) and nickel(II) at a lower pH region, while other metal ions such as cadmium(II), zinc(II), cobalt(II) which form an octahedral type of complexes were adsorbed at almost the same pH region as around 3. This suggests that PMC selectively recognized the metal ions that form a planar type of complexes. Figure 3 shows the selective adsorption of copper(II) from the mixture of copper(II) and iron(III). Only copper(II) was selectively adsorbed on PMC even from these mixtures containing 50-fold iron(III). Palladium(II) was also selectively adsorbed from the mixture of palladium(II) and 50-fold copper(II). It was found by examining the adsorption stoichiometrics that copper(II) was adsorbed as a chelate complex accompanied by two nitrate anions as counter-ions.

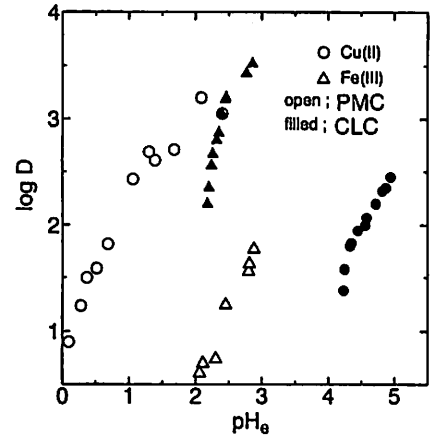

Fig.2 Effect of pH on the distribution ratio of copper(II) and iron(III).

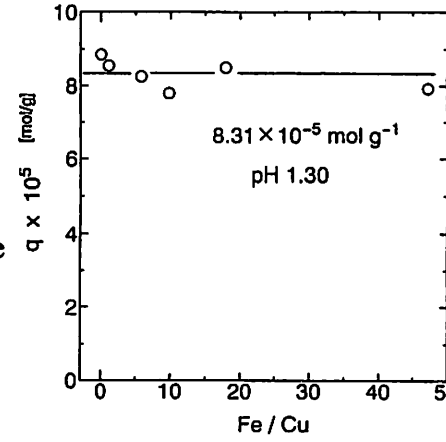

Fig.3 Effect of coexisting iron(III) on the adsorption of copper(II).

1)Baba, Y.; Masaaki, K.; Kawano, Y.; *React & Funct. Polym.*, 1998, 36, 167
2)Inoue, K.; Baba, Y.; Yoshizuka, K.; *Bull. Chem. Soc. Jpn*, 1993, 66, 2915

SELECTIVE EXTRACTION OF PRECIOUS METALS WITH A EXTRACTANT CONTAINING HETEROCYCLIC NITROGEN ATOM

Minako IWAKUMA and Yosinari BABA
Department of Applied Chemistry, Miyazaki University, Gakuenkibanadai-nishi 1-1, Miyazaki, 889-2192, Japan

In order to develop the highly selective extractant for Pd(Ⅱ) and Pt(Ⅳ), di(methylhexyl)-aminomethylquinoline(=DEQ) containing a quinolyl group as a ligand was synthesized by a conventional method. In preliminary experiments, the extraction behavior of various metals ions was examined from hydrochloric acid with DEQ in toluene in a batch method.

Figure 1 shows the effect of the concentration of hydrochloric acid on the distribution ratio of metal ions. Pd(Ⅱ), Pt(Ⅳ) and Au(Ⅲ) were selectively extracted over the whole concentration region of hydrochloric acid, while Cu(Ⅱ), Ni(Ⅱ) and Co(Ⅱ) were almost not extracted.

To elucidate the extraction equilibrium of Pd(Ⅱ), the effects of hydrogen ion, chloride ion and extractant concentrations on the distribution ratio of Pd(Ⅱ) were examined at 303K. Figure 2 shows the effect of the extractant concentration on the distribution ratio. The distribution ratio increases with an increase in the extractant concentration. The plotted points lie on a straight line with a slope of 1. Figure 3 shows the effects of the concentrations of chloride ion and hydrogen ion on the distribution ratio. The distribution ratio decreases with an increase in the chloride ion concentration. The plotted points lie on a straight line with a slope of -1. With respect to the effect of the hydrogen ion concentration, the plotted points in Figure 3 lie on a straight line with a slope of 1 in the lower concentration range of hydrogen ion. From the results mentioned above, it may be concluded that Pd(Ⅱ) is extracted according to the following extraction reactions.

$$RNN + H^+ + Cl^- \rightleftharpoons \overline{RNNHCl}$$

$$\overline{RNNHCl} + PdCl_3^- \rightleftharpoons \overline{(RNNH)PdCl_3} + Cl^-$$

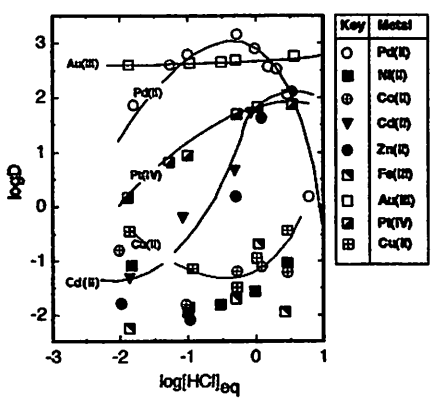

Fig.1 Effect of [HCl] on the distribution ratio of metal ions.

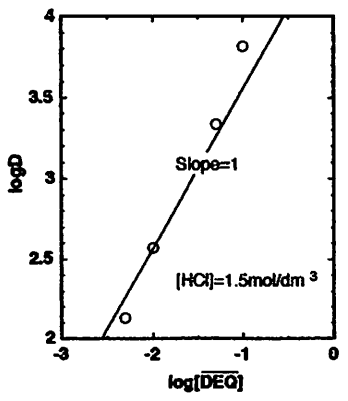

Fig.2 Effect of [$\overline{DEQ}$] on the distribution ratio of Pd(Ⅱ).

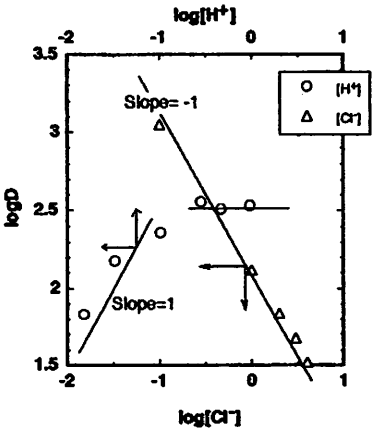

Fig.3 Effects of [H^+] and [Cl^-] on the distribution ratio of Pd(Ⅱ).

SELECTIVE ADSORPTION OF MERCURY(II) FROM HYDROCHLORIC ACID ON CHITOSAN DERIVATIVES

Kenzo OKAMOTO, and Yoshinari BABA
Department of Applied Chemistry, Miyazaki University, Gakuenkibanadai-nishi 1-1, Miyazaki, 889-2192, Japan

In order to develop the selective adsorbent for recovery of mercury(II) from hydrochloric acid, three kinds of chemically modified chitosans, crosslinked *N*-(2-pyridylmethyl)chitosan(PMC), *N*-(2-thienylmethyl)chitosan(TMC), and *N*-[3-methylthio)propyl] chitosan(MTPC) were newly synthesized as selective adsorbents of mercury(II). The amino group of the active adsorption site of chitosan was protected by Schiff's base formation prior to being crosslinked by 2-(chloromethyl)oxirane to prevent the decrease of the adsorption capacity. The final chitosan derivatives were obtained by reducing the imine moiety of the Schiff's bases with sodium borohydride. The intermediates and final products were identified by IR spectra. The substituted degree was determined to be over 0.9 by using the C/N ratio of elemental analysis. Figure 1 shows the chemical structures of chitosan derivatives used in this study.

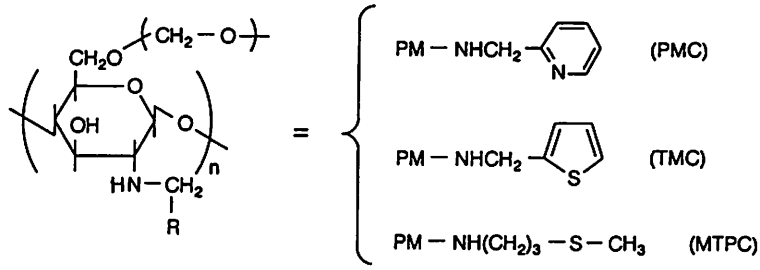

Fig.1 Chemical structures of chitosan derivatives

The adsorption behavior of metal ions on the chitosan derivatives was examined from hydrochloric acid using a batchwise method. Figures 2 and 3 show the experimental results in the adsorption of mercury(II) with PMC, and TMC and MTPC, respectively. PMC exhibited a high adsorption for mercury(II) in the low concentration range of hydrochloric acid, while copper(II), nickel(II), and cadmium(II) were also adsorbed somewhat. On the other hand, TMC and MTPC of sulfur-containing adsorbents exhibited a high selectivity for mercury(II) compared with PMC. The base metals as described above were not at all adsorbed on TMC and MTPC. Among the chitosan derivatives, MTPC especially exhibited a higher selectivity and capacity for mercury(II). The stoichiometric relations in the adsorption of mercury(II) on PMC and MTPC from hydrochloric acid were clarified at 303K.

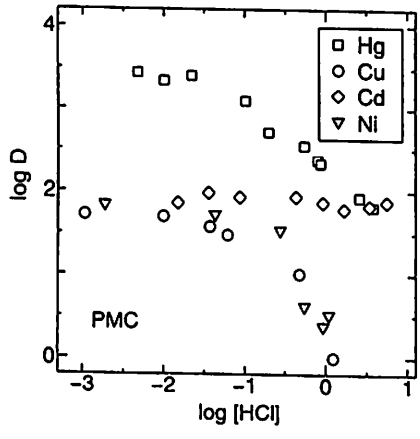

Fig.2 Effect of concentration of HCl on the distribution ratio of mercury(II) (PMC)

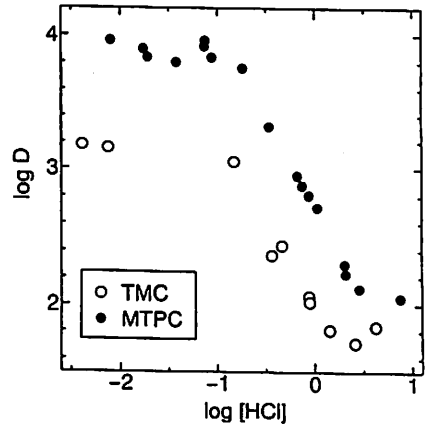

Fig.3 Effect of the concentration of HCl on the distribution ratio of mercury(II) (TMC, PTMC)

EXTRACTION MECHANISM OF COPPER(II) WITH 2-HYDROXY-4-*N*-OCTYLOXYBENZOPHENONEOXIME

Hideto NAGAMI, and Yoshinari BABA
Department of Applied Chemistry, Miyazaki University, Gakuenkibanadai-nishi 1-1, Miyazaki, 889-2192, Japan

2-Hydroxy-4-n-octyloxybenzophenoneoxime (=HOBO) having an octyloxy group at the 4-position of 2-hydroxybenzophenone oxime were synthesized. The introduction of an octyloxy group to 2-hydroxybenzophenoneoxime (HOB) is expected to increase the pKa of HOBO. At first, the extraction selectivity for metal ions with HOBO was examined from 1M-aqueous ammonium nitrate solution by a batch method at 303K. Figure 1 shows the effects of pH on the extraction percent of metal ions. Commercial hydroxyoxime extractants[1] generally extract not only copper ions but also nickel and cobalt ions in the higher pH region, while HOBO exhibited a high selectivity for only copper ions even in the higher pH region.

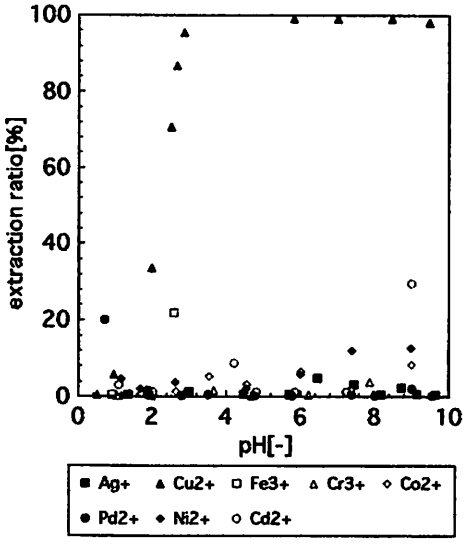

Fig.1. Effect of pH on extraction ratio of metal ions with HOBO.

Next, the extraction rate of copper with HOBO was measured with a stirred transfer cell. The apparent extraction rate was found to be described by the following expression from experimental results of effects of the hydrogen ion, HOBO and copper ion concentrations on extraction rates with HOBO.

$$N = k[Cu^{2+}][\overline{HR}]/[H^+] \quad \cdots \quad (1)$$

The physicochemical properties of the extractant, the interfacial activity and aqueous solubility, were measured in order to elucidate the extraction mechanism of copper(II) ion. Based on the experimental results of the interfacial tension and aqueous solubility of the extraction reagent, the extraction mechanism of copper with HOBO was considered to consist of the following five elementary steps. An extraction rate expression was derived on the assumption that the elementary reaction between the 1:1 intermediate complex adsorbed at the interface and the monomeric species of the reagent in the aqueous phase to form the final chelate is rate-determining step. The extraction rate expression fairly well explained the experimental results over all concentration regions.

$$\overline{HR} \rightleftarrows HR \quad (2)$$

$$\overline{HR} \rightleftarrows HR_{ad.} \quad (3)$$

$$Cu^{2+} + HR_{ad.} \rightleftarrows CuR_{ad.}^{+} + H^+ \quad (4)$$

$$CuR_{ad.}^{+} + HR \rightleftarrows CuR_{2ad.} + H^+ \quad (5)$$

$$CuR_{2ad.} \rightleftarrows \overline{CuR_2} \quad (6)$$

1) G.M.Ritcey and A.W.Ashbrook, "Solvent Extraction part 1", Elsevier(1984)

SOLVENT EXTRACTION OF MONO- AND TRIVALENT METAL IONS BY CALIXARENE-BASED CATION EXCHANGERS WITH HIGH MOLECULAR FLEXIBILITY

S.Kuwata[1a], Nguyen T.K.D[1], R.Ludwig[1] and K.Inoue[2]

[1] Radiochem. Div., Chemistry Institute, FU Berlin, Fabeckstr. 34-36, 14195 Berlin, Germany

[2] Department of Applied Chemistry, Saga University, 1-Honjo-machi, Saga 840-8502, Japan

In this work the solvent extraction of alkali (M^+), lanthanide (Ln^{3+}) and actinide (Am^{3+}) ions with calix[n]arene-based cation exchangers is described (n = 5 to 7). The structures of the extractants (Scheme 1) are characterized by n -O-CH_2-CO_2H groups as well as a higher molecular flexibility, compared with similar ligands bearing *t*-bu at 4-position at the phenyl groups. The aim of this study was to investigate how the extractability and selectivity are influenced by the flexibility of the ligands, and thus by the degree of molecular preorganization. The equilibria for the extraction from weakly acidic aqueous into chloroform solutions were characterized by the corresponding extraction constants and the results are compared with earlier data on the extraction of f-elements by calix[n]arenes with branched alkyl groups at 4-position.[1,2]

The competitive extraction of M^+ (M = Na, K, Rb) from acidic solutions by ligands **1** to **3** as well as by the reference compound **4** has been carried out and the results will be discussed in terms of the relationship between ion radius and macrocyclic cavity.

In case of lanthanide extraction with the ligands **2** to **4**, the distribution ratios decrease with decreasing ion radii within the series of Ln^{3+} (Ln = Nd, Eu, Tb, Dy, Er, Yb) investigated here. With ligand **1** however, the highest extraction is observed for Eu^{3+}. The highest overall distribution ratios are observed with ligand **4**, which also extracts Am^{3+} well. The selectivity Ln^{3+}/Am^{3+} in the different extraction systems is discussed.

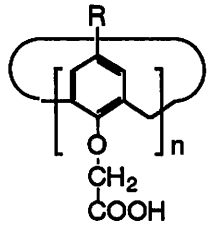

Ligand	n	R
1	5	H
2	6	H
3	7	H
4	7	*t*-bu

Scheme 1

[a] current and permanent address as [2]

1. Ludwig, R.; Nguyen, T. K. D.; Kunogi, K.; Tachimori, S., *Technical Report JAERI-Conf.* 99-04, 1999 (in press).
2. Nguyen, T. K. D.; Kunogi, K.; Ludwig, R., *Bull. Chem. Soc. Japan*, 1999, **72** (in press).

MECHANISM OF URANIUM(VI) TRANSFER ACROSS WATER-NITROBENZENE INTERFACE FACILITATED BY CMPO

Min YING*, Yoshihiro KITATSUJI, Zenko YOSHIDA
Advanced Science Research Center, Japan Atomic Energy Research Institute, Tokai, Ibaraki 319-1195, Japan

Ion transfer across the interface of two immiscible electrolyte solutions is an increasingly attractive subject[1] involved in solvent extraction, phase transfer catalysis, ion-selective electrode, biological membrane transport, etc. For studying interfacial transfer of actinide ions there is an inevitable difficulty due to their high hydrophilicity. Recently, a variety of ionophors such as multidentate phosphine oxide derivatives which can form stable complexes with actinide ions were used to promote the transfer of actinide ions [2].

In the present work, octyl(phenyl)-N,N-diisobutylcarbamoylmethylphosphine oxide (CMPO), one of extractants effective for actinide ions [3], was employed to facilitate the transfer of uranium(VI). The voltammetric characteristics of UO_2^{2+} transfer were investigated using an aqueous electrolyte dropping electrode(AEDE) which was in contact with nitrobenzene solution containing crystalviolet tetraphenylborate as a supporting electrolyte. In the presence of CMPO, the transfer of UO_2^{2+} from 0.1 mol/L $(NH_4)_2SO_4$ (pH 3.0) aqueous solution into nitrobenzene phase was remarkably facilitated. UO_2^{2+} showed a half-wave potential at -0.057 and -0.012 V (referred to TPhE), respectively, when the concentration of CMPO was 0.05 and 0.02 mol/L. The transfer wave showed irreversible characteristics with a slope of 55.8-59.4 mV obtained from log-analysis when CMPO in nitrobenzene was 0.05 mol/L and UO_2^{2+} was 1.0×10^{-3} mol/L. The shift of the half-wave potential with varying the concentration of CMPO from 5×10^{-3} to 0.1 mol/L was determined to be -97.6 mV/dec. The ratio of the half-wave potential shift to transfer wave slope was approximately an integer of 2, indicating that the composition of the complex of UO_2^{2+} with CMPO transferring from aqueous phase into nitrobenzene was 1:2. The limiting current of UO_2^{2+} transfer was almost independent of the flow rate of the aqueous solution constructing the AEDE and of a definite range of the concentration of CMPO, but had a roughly linear relationship with the concentration of UO_2^{2+}, suggesting that the transfer was not of simple diffusion-controlled process. The dropping time t_d of the AEDE was measured at different applied potentials employing the following three solution pairs; CMPO-free nitrobenzene/blank aqueous, CMPO-containing nitrobenzene/blank aqueous and CMPO-containing nitrobenzene/UO_2^{2+} aqueous solution. A fairly long t_d was observed with CMPO-free nitrobenzene/blank aqueous phase system. A significant decrease in t_d when CMPO was present in nitrobenzene phase suggested the adsorption of CMPO at the interface. The t_d with CMPO-containing nitrobenzene/UO_2^{2+} aqueous phase system displayed a further decrease but to a less extent when the applied potential was more positive than -0.09 V. The additional adsorption at the interface was resulted from the formation of the complex of UO_2^{2+} with CMPO. The mechanism of UO_2^{2+} transfer likely includes the following sequential reactions: the distribution of CMPO between the two phases, the formation of the complex of UO_2^{2+} with CMPO, the adsorption of the complex at the interface and the transfer of the adsorbed complex into the bulk of nitrobenzene.

1. Kihara, S.; Suzuki, M.; Maeda, K.; Ogura, K.; Umetani, S.; Matsui, M.; Yoshida, Z.; *Anal. Chem.*, 1986, 58, 2954.
2. Kitatsuji, Y.; Aoyagi, H.; Yoshida, Z.; Kihara, S., *Anal. Sci.*, 1998, 14, 67.
3. Horwitz, E. P.; Diamond, H.; Martin, K. A.; *Solvent Extr. Ion Exch.*, 1987, 5, 447.

On the leaving of the East China Geological Institute, P. R. China, under the STA Scientific Program of Japan.

EXTRACTION EQUILIBRIUM OF GALLIUM(III) WITH HYDROPHOBIC 2-METHYL-8-QUINOLINOL DERIVATIVES IN THE PRESENCE OF 3,5-DICHLOROPHENOL.

S. Y. Choi, H. Imura and K. Ohashi

Department of Environmental Sciences, Ibaraki University, 2-1-1 Bunkyo, Mito, 310, Japan

The molecular design for the highly selective extractants for metal ions has been one of the interesting aspects to develop the more selective separation system.

In this work, the extraction equilibrium of gallium (III) with 2-methyl-8-quinolinol derivatives (HA) such as 2-methyl-8-quinolinol (HMQ), 2-methyl-5-ethoxymethyl-8-quinolinol (HMO_2Q), 2-methyl-5-butyloxymethyl-8-quinolinol (HMO_4Q) and 2-methyl-5-hexyloxymethyl-8-quinolinol (HMO_6Q) into heptane from a weakly acidic aqueous solution in the absence and presence of 3,5-dichlorophenol (DCP) was investigated to get more detailed information about the alkyl substituents effect on the extractability of gallium (III) with 2-methyl-8-quinolinol derivatives. The acid dissociation constants of HA in an aqueous solution, the distribution constants of HA between water and heptane, and the association constants $\beta_{ass,H}$ of HA with DCP in heptane were also determined. The extractability of gallium (III) with HA into heptane increased in the following order of HMQ < HMO_2Q < HMO_4Q < HMO_6Q. This order is agreed with that of the distribution constants of HA. The extractability of gallium (III) with HA was remarkably enhanced by the addition of DCP. The Ga (III)-HA complexes extracted into heptane in the absence and presence of DCP were assigned to be $Ga(OH)(H_2O)(A)_2$ and $Ga(OH)(H_2O)(A)_2 \cdot n$DCP ($n = 1, 2$), respectively. The extraction constants for $Ga(OH)(H_2O)(A)_2$ ($K_{ex} = [Ga(OH)(H_2O)(A)_2]_{org}[H^+]^3 / [Ga^{3+}][HA]^2_{org}$) are $10^{-7.52 \pm 0.38}$ (HMQ), $10^{-4.92 \pm 0.34}$ (HMO_2Q), $10^{-4.02 \pm 0.16}$ (HMO_4Q) and $10^{-3.84 \pm 0.16}$ (HMO_6Q) at I = 0.1 M and 25℃. The stability constants of $Ga(OH)(H_2O)(A)_2 \cdot n$DCP ($\beta_{ass,n} = [Ga(OH)(H_2O)(A)_2 \cdot n\text{DCP}]_{org} / [Ga(OH)(H_2O)(A)_2]_{org}[\text{DCP}]^n_{org}$) in heptane were determined to be $10^{5.36}$ ($n = 1$), $10^{9.89}$ ($n = 2$) (HMQ), $10^{5.41}$, $10^{7.69}$ (HMO_2Q), $10^{5.13}$, $10^{7.54}$ (HMO_4Q) and $10^{4.60}$, $10^{7.02}$ (HMO_6Q) at I = 0.1 M and 25℃. The enhancement effect of DCP should be ascribed to the adduct formation of $Ga(OH)(H_2O)(A)_2$ with DCP by hydrogen bonding formation between the coordinated oxygen atom of HA and OH group of DCP.

1. K. Ohashi.; R. Iwata.; S. Mochizuki.; H. Imura.; K. Hiratani.; H. Sugihara., *Talanta.*, 1996, 43, 1481.

SOLVENT EFFECT ON THE EXTRACTION OF ETHYLENEDIAMINETETRAACETIC ACID COMPLEXES WITH ALKYLAMMONIUM ION

Keiichi SATOH and Kiyoshi SAWADA
Faculty of Science, Niigata University, Igarashi, Niigata, 950-2181, Japan

The anionic complexes of ethylenediaminetetraacetic acid (EDTA) such as $[Fe^{III}(edta)^{-}]$ and $[Ni^{II}(edta)^{2-}]$ as well as ligand itselef are distributed into various organic solvents as an ion-pair with various alkylammonium ions. The analytical method of such complexes as well as ligand itself are quite important since the environmental effect of EDTA and related synthetic complexing agents has much attention in recent years and the development of speciation method is becoming important. In addition, it is interesting to understand the interaction of such hydrophilic metal complex with inert organic solvents as a basic problem of solution chemistry. In the present paper, the distribution behavior of the ion-pair of anionic EDTA complex with various alkylammonium ions into various organic solvents has been studied.

The distribution of Fe(III)-EDTA, Ni(II)-EDTA and EDTA itself was investigated at various pHs for various organic solvents. The distribution of metal complex $[M(edta)^{n-}]$ with tri-*n*-octylmethylammonium chloride (TOMA·Cl) can be written as:

$$n\,\text{TOMA·Cl}_{org} + \text{M(edta)}^{n-} \overset{K'_{ex}}{\rightleftharpoons} (\text{TOMA}^{+})_n\text{·[M(edta)}^{n-}]_{org} + n\,\text{Cl}^{-}$$

where the subscript 'org' denotes the species present in organic phase and K'_{ex} denotes the conditional extraction constant at the constant TOMA·Cl concentration. The distribution with other alkylammonium ion was also analyzed in the same manner.

The distribution of the complexes increased with increasing the number of alkylammonium ion in the ion-pair especially predominant in the case of EDTA itself. It may be due to the increasing hydrophobicity of ion-pair extracted into the organic phase with increasing the number of alkylammonium ion. The species of the most extractable one was determined as $(TOMA^{+})_2\text{·[Fe(OH)(edta)}^{2-}]$, $(TOMA^{+})_2\text{·[Ni(edta)}^{2-}]$ and $(TOMA^{+})_4\text{·[edta}^{4-}]$ and their extraction constants for various organic solvents were determined.

Figs. 1 and 2 show the effect of dielectric constant and $E_T(30)$ values on the distribution of Ni(II)-EDTA system. As can be seen from Fig. 1, the extraction constant increases with decreasing the dielectric constant. It can be explained as the formation of ion-pair. The extrcation constant decreases with increasing the $E_T(30)$ values. It may be interpreted that the solution structure of ion-pair in the organic phase.

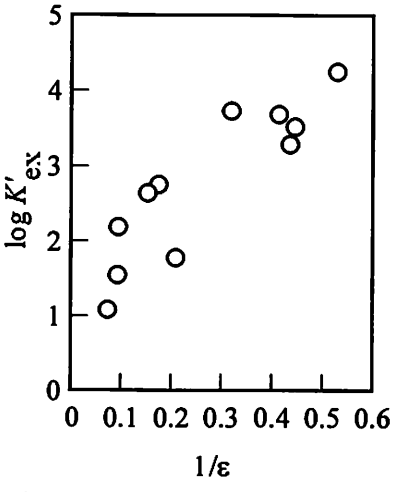

Fig. 1.

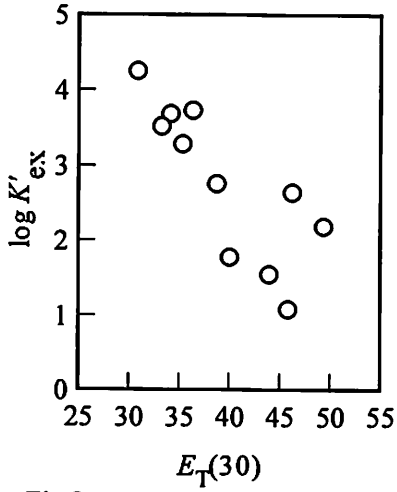

Fig.2.

CALCULATED AND EXPERIMENTALLY DETERMINED HYDROLIPOPHILIC PARAMETERS FOR SOME GUANINE DERIVATIVES

Albin KRISTL and Slavko PEČAR
Faculty of Pharmacy, University of Ljubljana, Aškerčeva 7, Ljubljana, 1000, Slovenia

Partition coefficient in n-octanol/water (P) can be determined by different experimental methods, i.e. shake flask method, filter probes, the generator column method, different reversed-phase (RP) high performance liquid chromatography (HPLC) retention parameters and others. On the other hand, logP values can be predicted also by different estimation techniques; i.e. the calculations based on group contribution according to Hansch or Rekker. There are many different computer programs which have simplified such calculations.

In this study we compared the experimentally determined hydrolipophilic properties of some antivirus guanine derivatives; acyclovir (ACV), deoxyacyclovir (DCV) and their O-acetyl, N-acetyl and N,O-diacetyl congeners; by conventional shake flask method (logP) (1) and by RP HPLC (extrapolated capacity factor to 100% aqueous mobile phase, $\log k_w$) (2) with the calculated ones. The logP values were calculated manually by Rekker's fragmental approach (1). Additionally, some commercially available computer programs were used for the calculations of logP values; i.e. HyperChem Release 5.0, PACO Version 2.9, CLOGP, KOWWIN Version 1.60, MICROQSAR Version 2.0, and PROLOG module of the Pallas system which offers CDR, ATOMIC and ATOMIC5 databases. The module PROLOGP offers also the possibility to calculate a combined logP value, whereby the default values are set to $\log P_{combined} = 0.733 \log P_{ATOMIC5} + 0.267 \log P_{CDR}$.

Rather large discrepancies between calculated and experimentally determined values almost in all cases were observed. The Pearson correlation coefficients obtained by the least - squares linear regression method are relatively low and, in general, show very weak correlation. There are only some correlation coefficients which exhibit significant correlation at the 0.05 level between experimentally determined logP values and the calculated ones. The best correlation and the smallest differences between calculated and experimentally determined logP values were obtained by KOWWIN computations.

Overall one can conclude that the calculations and estimations of logP values for complex molecules such as tested guanine derivatives by different computation and RP HPLC methods do not give reliable results.

1. Kristl, A.; Vesnaver, G., *J. Chem. Soc. Faraday Trans.*, 1995, 91, 995.
2. Kristl, A.; Pečar, S., *Eur. J. Med. Chem.*, 1997, 32, 3.

INTERACTION OF PREMICELLAR AND MICELLIZED SURFACTANT WITH 1,10-PHENANTHROLINE STUDIED BY FLUORESCENCE SPECTROPHOTOMETRY

Ryo KANZAKI [1], Naomi HAYASHIDA [1], Shin-ichi ISHIGURO [1]

[1] Department of Chemistry, Faculty of Science, Kyushu University, Hakozaki, Higashi-ku, Fukuoka, 812-8581, Japan

Interaction of a nonionic surfactant Triton X-100, with a hydrophobic iso-octylphenyl group and a hydrophilic poly-oxyethylene (*POE*) group, with 1,10-phenanthroline has been investigated under the premicellar and micellized condition by potentiometric titration and fluorescence spectrophotometry. Apparent acid dissociation constant of 1,10-phenanthroline decreases in micellar solutions relative to that in an aqueous solution. Fluorescence spectra of 1,10-phenanthroline obtained in aqueous solutions of varying pH show an isosbestic point, and the acid dissociation constant thus determined by fluorescence spectrophotometry agree with that previously obtained by potentiometry. It turned out that fluorescence spectrum of phenanthroline changes drastically by its protonation in an aqueous solution. At neutral pH, although molar fluorescence intensity of monomer Triton X-100 was very weak over 300-500 nm, it was enhanced when the surfactants form micelles. Fluorescence spectrum of phenanthroline hardly changes in dilute surfactant solution, implying that free surfactant molecules hardly form adducts with phenanthroline. In micellar solutions, molar fluorescence intensity of phenanthroline was weakened with increasing the concentration of Triton X-100. Fluorescence spectra of phenanthroline in an aqueous solution and micelles were estimated on the basis of the additivity rule for the fluorescence intensities of Triton X-100 and 1,10-phenanthroline. The molar fluorescence are plotted against the molar fraction of solubilized phenanthroline in micellar solutions calculated by the stability constant of 1,10-phenanthroline and Triton X-100 obtained by potentiometry. It turned out that the fluorescence intensity of micelled phenanthroline is very weak or approximately none. We will also discuss fluorescence spectra of phenanthroline in some nonaqueous solution.

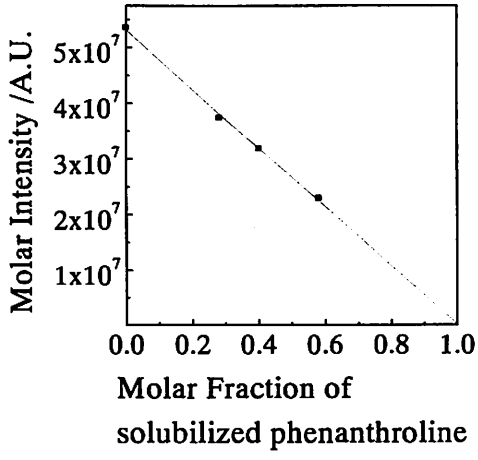

ADSORPTION OF Cr(III), Zn(II) and Ni(II) ONTO BACTERIAL SUBSTRATES

Russell J. CRAWFORD, Elise M. KAVANAGH, Kirsten SCHLIEPHAKE and Greg T. LONERGAN
Centre for Applied Colloid and BioColloid Science, Swinburne University of Technology, P.O. Box 218, Hawthorn 3122, Australia.

Pollution of the natural environment by aqueous heavy metals present in some industrial waste streams is hazardous and causes environmental damage. The process of adsorption has been shown to be one method for successfully removing heavy metals from solution. Water treatment adsorption processes involve the addition of a colloidal substrate to metal solutions, reducing the pH at which the ions can be removed from solution compared to that of hydroxide precipitation. Adsorption has been performed using a wide range of experimental conditions, employing a variety of substrates[1-4]. Metal oxides have been studied extensively, with some exhibiting a greater affinity for some metals over others[3,5]. Carbonaceous substrates have also been used[4,6], with the high levels of adsorptive properties being attributed to the presence of carboxylate surface functionality. Biological substrates have also been shown to be efficient adsorbents of heavy metals[7-9], with associated advantages being that they can be produced relatively inexpensively, are renewable, and in some cases show high selectivity for certain metal types[7]. For bacteria, the substrate surface sites onto which metal adsorption takes place includes hydroxyl, carboxyl and phosphate groups. Whilst it has been shown that the presence of carboxyl (in addition to hydroxyl) surface functionality assists and enhances the metal ion adsorption process[4], it is unclear as to the role that the other surface sites will play.

The pH-dependent adsorptive properties of the aqueous heavy metals Cr(III), Ni(II) and Zn(II) have been measured using Bacillus subtilis and Bacillus licheniformis as adsorbents. In addition, a commercially available bacterial adsorbent product Ecobac® has been used for the same purpose, and compared to the results obtained using the bacterial substrates alone. It was found that the bacterial substrates exhibited an affinity for all of the metals studied, with the extent of metal adsorption increasing with increasing pH. The results indicated that enhancement of Cr(III) removal by the presence of the bacterial substrates was relatively low compared to that of Zn(II) and Ni(II). The amount of metal adsorbed at a given pH was shown to increase as the concentration of bacterial substrate was increased. The Ecobac® provided significantly greater adsorption of all of the metals studied however this was found to be due to the components of the support material rather than the presence of the bacteria.

1. Benjamin, M.M. and Leckie J.O., *Environ. Sci. Technol.*, 1981, 15, 1050.
2. James, R.O. and Healy, T.W., *J. Colloid Interface Sci.*, 1972, 40, 42.
3. Crawford, R.J., Harding, I.H. and Mainwaring, D.E., *Langmuir*, 1993, 9, 3050.
4. Burns, C.L., Cass, P.J., Harding, I.H. and Crawford, R.J., *Colloids Surfaces A*, 1998, (in press).
5. Sen, K.C., *Z. Anorg. Allg. Chem.*, 1929, 182, 118.
6. Mishra, S.P. and Chaudhury, G.R., *J. Chem. Technol. Biotechnol.*, 1994, 59, 359.
7. Volesky, B., (Ed.), Biosorption of Heavy Metals, CRC Press, Boca Raton (1990).
8. Daughney, C.J. and Fein, J.B., *J. Colloid Interface Sci.*, 1998, 198, 53.
9. Leuf, E., Prey, T. and Kubicek, C.P., *Appl. Microbiol. Biotechnol.*, 1991, 34, 688.

AN ALTERNATIVE APPROACH FOR THE INTERPRETATION OF ADSORPTION AT THE HYDROUS OXIDE / SOLUTION INTERFACE

Justin DANN[1], Russell CRAWFORD[1], Eddie BAKSHI[2], Tohru MIYAJIMA[3] and Ian HARDING[1]
[1] Centre for Applied Colloid and BioColloid Science, Swinburne University of Technology, P.O.Box 218, Hawthorn, 3122, Victoria, Australia
[2] Centre for Medical Biophysics and Instrumentation, Swinburne University of Technology, P.O.Box 218, Hawthorn, 3122, Victoria, Australia
[3] Department of Chemistry, Saga University, Honjo-Machi, Saga, 840-8502, Japan

It is well known that one of the main contributors to the control of aqueous heavy metal ions in natural waterways, is the strong binding affinity characteristic to the fine particulate matter present in such systems. Typically, these suspended solids consist of a diverse range of material, including phytoplankton, biological debris, calcium carbonate, aluminium silicates (clays) and various hydrous oxides. Of these, one of the primary contributors to this regulation mechanism is the propensity of hydrous ferric oxide to act as an adsorbent[1] and it is this characteristic which has been extensively studied with the adsorption of cations and anions onto various iron oxide surfaces[1].

Traditionally, adsorption of hydrolysable metal ions at the solid / solution interface, regardless of interfacial morphology, has been described by a number of theoretical models[2]. The more advanced and generally accepted of these models describe the charged interface as a non-porous solid surface where an electrical double layer exists. However, when describing the interaction of ions at the interface of certain hydrated oxides, which are considered to be porous to ion migration[3], the more appropriate model, as suggested by Marinsky[4], is that of a two-phase one. This approach, which utilises Gibbs- Donnan based logic has commonly been used to describe heavy metal complexation with sorbents such as polyelectrolytes[5] and ion exchange resins[6].

In this study, application of the Gibbs – Donnan (two phase) model to describe heavy metal ion adsorption at the hydrous ferric oxide interface will be discussed, also introduced is the concept of Donnan volume applied to colloidal sized particles. A critical appraisal of the Gibbs - Donnan approach and a comparison between this method and the current adsorption models will also be addressed.

1. Dzombak, D.A.; Morel, F.M.M.; "Surface Complexation Modeling. Hydrous Ferric Oxide.", Wiley Interscience, New York, 1990.
2. James, R.O.; Stiglich, P.J.; Healy, T.W.; *Faraday Discuss. Chem. Soc.*, 1974, 59, 142.
3. Yates, D.E.; "The Structure of the Oxide/Aqueous Electrolyte Interface," Ph.D. Thesis. University of Melbourne, Melbourne, Australia, 1975.
4. Marinsky, J.A.; *J. Phys. Chem.*, 1996, 100, 1858.
5. Miyajima, T.; Nishimura, H.; Kodama, H.; Ishiguro, S., *React. Funct. Polym.*, 1998, 38, 183.
6. Miyajima, T.; "Ion-Exchange and Solvent Extraction – A Series of Advances.", Marinsky, J.A.; Marcus, Y.; Eds.; Marcell Dekker, New York, 1995, Vol. 12, Chapter 7.

A SPECTROSCOPIC STUDY OF HEAVY METAL ADSORPTION / COPRECIPITATION AT THE HYDROUS OXIDE / SOLUTION INTERFACE

Justin DANN[1], Russell CRAWFORD[1], Eddie BAKSHI[2], Tohru MIYAJIMA[3] and Ian HARDING[1]
[1] Centre for Applied Colloid and BioColloid Science, Swinburne University of Technology, P.O.Box 218, Hawthorn, 3122, Victoria, Australia
[2] Centre for Medical Biophysics and Instrumentation, Swinburne University of Technology, P.O.Box 218, Hawthorn, 3122, Victoria, Australia
[3] Department of Chemistry, Saga University, Honjo-Machi, Saga, 840-8502, Japan

The process of precipitation, adsorption and coprecipitation of hydrolysable heavy metal ions has received a great deal of attention over the past several decades. These removal mechanisms are responsible for the control of heavy metal ions in natural waterways and hence, play a major role in aquatic ecology. They have also been utilised for the removal of heavy metal contaminants from industrial waste effluent[1]. While the enhancement of removal by adsorption and coprecipitation over simple precipitation is well documented, the relationship between adsorption and coprecipitation is not so clear. Several researchers[2,3] have conducted studies to distinguish between the two closely related processes, for example Crawford *etal*[2] used the James – Healy model for metal ion adsorption to describe both adsorption and coprecipitation. This model determines the free energy of adsorption as a sum of the electrostatic, solvation and chemical free energy components, $\Delta G_{ads} = \Delta G_{ele} + \Delta G_{sol} + \Delta G_{chem}$. In this work the enhanced removal of coprecipitation over that of adsorption was attributed to a lower ΔG_{chem}, but the origin of this term contained some uncertainty and was essentially used as a fitting parameter.

In this study some possible contributions of the ΔG_{chem} term will be discussed. Electron Spin Resonance (ESR) and Mössbauer spectroscopy are used to provide information on the structural environment of the hydroxides as well as the nature of the adsorbed species. It is hoped that this information will lead to a greater understanding of both the distinction made between adsorption and coprecipitation as well as the origins of ΔG_{chem}.

1. Sanciolo, P; Harding, I.H.; Mainwaring, D.E.; *Sep. Sci. Technol.*, 1993, 28(9), 1715
2. Crawford, R.J.; Harding, I.H.; Mainwaring, D.E., *Langmuir.*, 1993, 9, 3050.
3. Charlet, L.; Manceau, A.A.; *J. Colloid Interface Sci.*, 1992, 148, 443.

ON THE EQUILIBRIA OF ACID DISSOCIATION AND COMPLEXATION OF FULVIC ACID - EFFECT OF HYDROPHOBICITY OF SUPPORTING CATIONS

T. MIYAJIMA[1], K. SOHMA[2], S. ISHIGURO[2], and H. KODAMA[3]

[1]Department of Chemistry, Faculty of Science and Engineering, Saga University, Saga, 840-8502, Japan
[2]Department of Chemistry and Physics, Graduate School of Science, Kyushu University, Fukuoka, 812-8581, Japan
[3]Department of Biological Resource Chemistry, Faculty of Agriculture, Kyoto Pref. University, Kyoto, 606-8201, Japan

Fulvic acid(FA) constitutes the main fraction of dissolved organic carbon in natural water systems. FA molecules contain carboxyl and phenolic OH groups, and the complexation behavior controls migration, deposition, and biological activity of hazardous heavy metal ions. A large number of studies have been reported on the acid-dissociation and complexation of the polyfunctional molecules, however, the equilibrium analysis has been hampered by the polyelectrolytic and heterogeneous nature of the molecules.

In the present work, the equilibria of acid-dissociation as well as Ca^{2+} ion complexation of FA standard samples have been studied with an excess of NaCl or $(CH_3)_4NCl$. The apparent binding equilibria are highly sensitive to the degree of dissociation of the polyacids and the concentration level of the added salt. Non-ideality due to the polyelectrolytic effect has been evaluated based on a micro-phase separation model. The bindings of H^+ and Ca^{2+} ions to FA molecules are much more enhanced by the addition of $(CH_3)_4N^+$ ions than Na^+ ions. This enhancement can be explained by the decrease in the degree of hydration of the FA molecules, i.e., hydrophobic $(CH_3)_4N^+$ ions concentrated in the vicinity of the negatively charged molecular assemblies squeeze water molecules from the FA domain. The increase in the mobile ion concentration in the domain leads to the higher degree of ion-binding. The dehydration also assists agglomeration formation of amphiphilic FA molecules, by which intermolecular ion-binding becomes feasible.

SYNTHESES AND STRUCTURES IN SOLUTION AND IN THE CRYSTAL OF TRI-ALKALI METAL SALTS OF BIS(THIOSALICYLATO)AURATE (I)

N. C. KASUGA, R. NOGUCHI, H. YOKOYAMA, AND K. NOMIYA.*
Department of Materials Science, Faculty of Science, Kanagawa University, Tuchiya, Hiratsuka, 259-1293 Japan.

Interest has increased in the coordination chemistry of gold(I) with thiol ligands such as thiomalate, thioglucose, thiosulfate and thiosalicylate, as a result of pharmaceutical activities. Many of these 1:1 type Au(I) complexes obtained have been polymeric or oligomeric and isolated solid powders are difficult to crystallize, [1] so that few structures are known in detail. The molecular structure of the anionic 1:1 Au(I) complex of thiomalate, polymeric and commercially available antiarthritic drug, was reported very recently. [2] We have reported synthesis of 1:2 type of thiosalicylate Au(I) complex as a trisodium salt which also shows antiarthritic activity. [3] Herein we present the preparation of water-soluble tri-alkali metal salts of bis(thiosalicylato)aurate(I), the characterization in solution and the molecular structure of well-characterized tisodium salt in the crystal.

The potassium and cesium salts of 1:2 complex of tsa-Au(I) were prepared from the reaction of $NaAuCl_4$ with thiosalicylic acid (H_2tsa; *o*-$HS(C_6H_4)COOH$) and MOH (M=K and Cs) in the ratio 1 : 4 : 8 in water/EtOH media. All of them were soluble in water. Colorless needle crystals of tisodium salt were obtained from an aqueous/EtOH system. Crystal data: a=21.238 (9) Å, b=22.224 (7) Å, c=8.752(5) Å, V=4131 (3) Å^3, Space group *Ccc2*, Z=8, R=7.5%. The two thiosalicylate ligands coodinate to Au(I) through S atom to make linear S-Au-S geometry (Au−S 2.28 (1) and 2.30 (1) Å, S-Au-S 175.8(3)°). The complex is monomeric in aqueous solution evaluated from the molmass measurement based on the cryoscopic method, however, gold(I)-gold(I) bond formation is observed between the two $[Au(tsa)_2]^{3-}$ in the crystal (the distance between gold(I)-gold(I) is 3.183(2) Å). This weak gold(I)-gold(I) bond formation in the crystal would be due to the interaction of Na^+ with thiolate, carboxylate, and water molecules. The structure analysis of other alkali metal salts of tsa-Au(I) complexes is in progress.

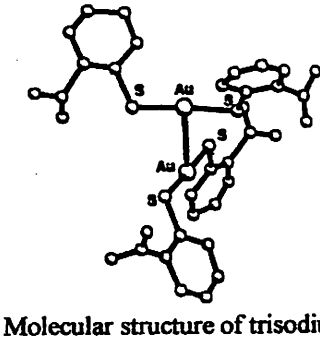

Molecular structure of trisodium salt of Au(I)-tsa complex

1) Pykkö, P., Chem. *Rev.*,1997, **97**,597. 2) Bau, R., *J. Am. Chem. Soc.*, 1998,**120**,9380. 3) Nomiya, K.; Yokoyama, H.; Nagano, H.; Oda, M.; Sakuma, S., *J. Inorg. Biochem*, 1989,**60**, 289.

^{31}P NMR SPECTRA IN THE REACTIONS OF PHOSPHINE CHELATED Pt(II) COMPLEXES WITH AMINO ACIDS, NUCLEOBASES AND RELATIVES

Wakako KANDA[1], Yoshiaki KUSUYAMA[1], Masato HASHIMOTO[2] and Seichi OKEYA[2]

[1] Faculty of Education, Wakayama University, Wakayama 640-8510, Japan

[2] Department of Advanced Material Science and Chemistry, Faculty of Systems Engineering, Wakayama University, Wakayama 640-8510, Japan

In the bioinorganic approach, it is important to determine the structure and equilibrium of the active metallo-species in solution. We have investigated the reactions of the Pt(II) complexes with amino acids, nucleobases and some relating ligands in organic solvents using ^{1}H, ^{13}C, ^{19}F and ^{31}P NMR techniques. The complexes separated from the reaction mixture were recrystallized and employed for the measurements. X-ray analyses of the crystals were also attempted. We found that ^{31}P NMR spectra gave better information of the structure of the complexes. They are classified into three patterns: singlet, AB quartet and multiplet.

1. singlet; The complexes have symmetrical structures, two coordinating atoms are identical each other. Ex. $[Pt(dppf)(1\text{-MeCyt})_2](hfac)_2$ (1-MeCyt = 1-methylcytosine; *N*(3)) and $[Pt(dppf)(Ade)_2]$ (Ade = adeninate anion: *N*(9)).

2. AB quartet; The complexes have unsymmetrical structures and the donor atoms are different from each other. Two types of complexes have been found. One is a complex with an unsymmetrical chelate ligand. Ex. [Pt(dppf)(Cys)] (Cys= Cysteinate anion; *N* ,*S*). The other is a complex such as $[Pt(dppf)(3\text{-MeAde})_2](hfac)_2$ (3-MeAde= 3-methyladenine), in which one 3-MeAde coordinates to Pt(II) through *N*(*C*(6)) and the other 3-MeAde coordinates through *N*(7).

3. multiplet; The complexes have multinuclear structures, but we have not yet confirmed the structures.

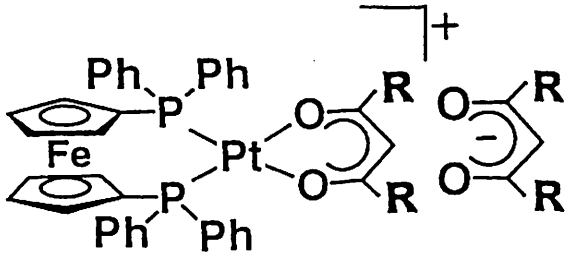

[M(dppf)(ß-dik)](ß-dik)

R= CH_3; (acac), CF_3; (hfac)

dppf: 1,1'-bis(diphenylphosphino)ferrocene

HOMOGENEOUS IDENTIFICATION OF DNA BY USING EUROPIUM FLUORESCENCE ENERGY TRANSFER

Shinji SUEDA, Jingli YUAN and Kazuko MATSUMOTO *
Department of Chemistry, School of Science and Engineering, Waseda University, 3-4-1 Okubo, Sinjuku-ku, Tokyo 169-8555, Japan

DNA hybridization assays have been widely used in the field of molecular biology as a research tool for gene expression analysis and diagnosis of infectious and genetics diseases. Most available methods are, however, time-consuming and tedious because the methods require the immobilization of target DNA on solid support and separation of hybridized DNA duplex from the excess probe DNA. In this work, we developed a new method for identification of target DNA in a homogeneous solution. This method is based on florescence resonance energy transfer from a tetradentate β-diketonate europium complex, BHHCT-Eu(III) to fluorescence organic dye, Cy5. BHHCT-Eu(III) complex is a highly fluorescent complex developed in our group.[1]

The principle of our method is illustrated in Fig. 1. This assay utilizes two DNA probes, one probe containing a biotin label on the 3'-terminus and the other probe containing a Cy5 label on the 5' terminus. Two probes are complementary to contiguous regions of target DNA, such that when hybridized to target DNA the two labels are placed next to one another. After hybridization, streptavidin labeled with BHHCT-Eu(III) complex is added to the same solution. Under this condition, Eu(III) complex is close to the Cy5 so that energy transfer can occur from Eu(III) complex to Cy5, while without target DNA such phenomena cannot occur. Therefore, by monitoring the sensitized emission of Cy5, target DNA can be detected in the homogeneous solution without immobilization and separation steps.

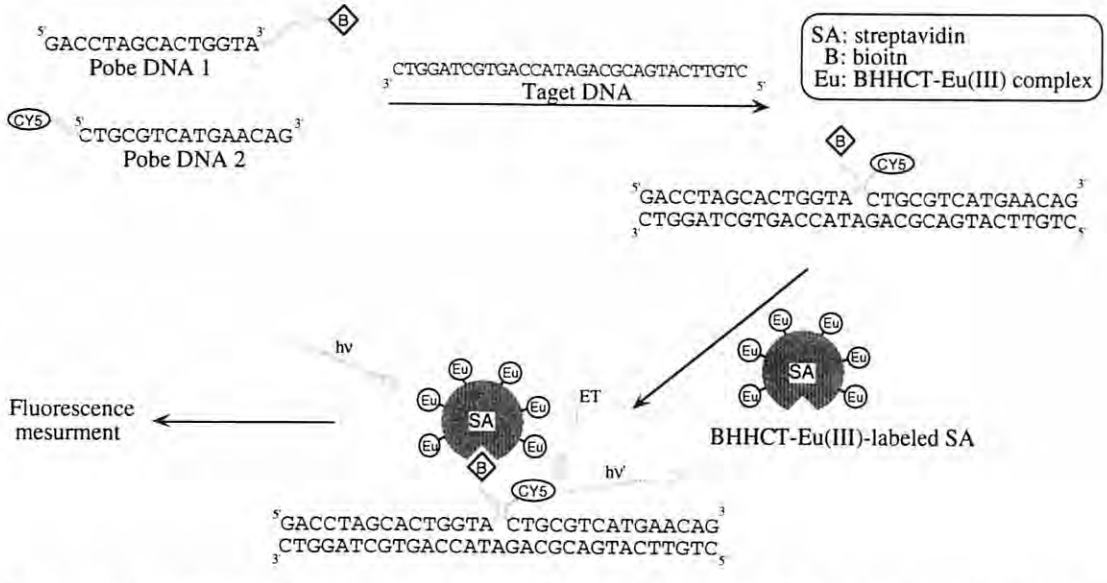

Fig. 1 DNA detection in a homogeneous solution by using europium fluorescence energy transfer.

1. Yuan, J.; Matsumoto, K., *Anal. Chem.*, 1998, **70**, 596.

Photoinduced DNA Cleavage by Amidate-Bridged Pt(III) Dinuclear Complexes

Ryosuke Somazawa, Takuya Ikeda, Jun Matsunami and Kazuko Matsumoto*

Department of Chemistry, School of Science and Engineering, Waseda University, 3-4-1 Okubo, Sinjuku-ku, Tokyo 169-8555, Japan

Studies of compounds with the ability to cleave DNA are of great importance in preparing chemical nucleases and medicinal agents. It is widely recognized that DNA cleavage is often caused by activated oxygen, which is generated by the redox reactions of the metal centers, and by aryl and indenyl radicals originate from, for instance, enediyne.

Recently, we discovered that the pivalamidate–bridged Pt(III) dinuclear complexes generates alkyl and aryl radical species under UV irradiation, and we were prompted to investigate DNA cleavage using the complex.[1]

It was confirmed that supercoiled pBR322 DNA was cleaved to yield both circular and linear DNAs by the pivalamidate-bridged Pt(III) dinuclear complexes under UV irradiation. However, the presence of a spin trapping reagent, 4–OH–TEMPO, or ethanol does not harm DNA cleavage.

The axial substituent dependence on the DNA cleavage efficiency was investigated using the Pt(III) dinuclear complexes with various axial substituents. Among them, the Cl^- substituted Pt(III) dinuclear complex exhibits the highest efficiency. The activity is almost inhibited in the presence of spin trapping reagents such as 4–OH–TEMPO, DMPO, and DBNBS. It was suspected that Cl radical is responsible for DNA cleavage, however, generation of other radical species is also possible. We are currently identifying the radical species by ESR spectroscopy.

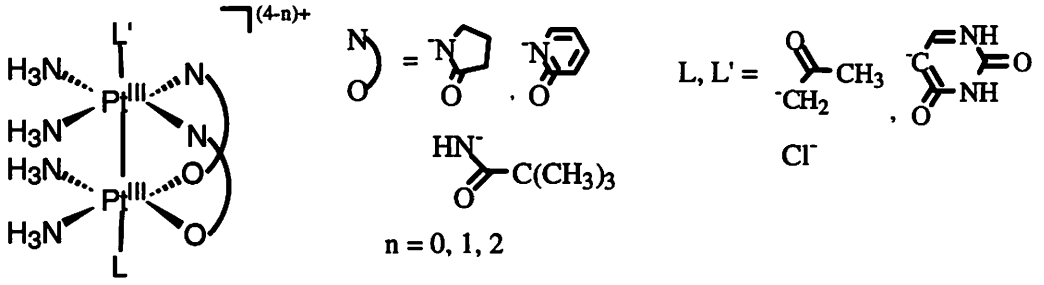

Scheme Structures of amidate-bridged Pt(III) dinuclear complexes

1. Matsunami, J.; Matsumoto, K. *J. Am. Chem. Soc.* **1996**, *118*, 8959-8960

THE REACTION OF CU(II) COMPLEXES WITH BIOLOGICAL REDUCTANTS CAUSE DNA STRAND SCISSION

Jun-ichi UEDA and Toshihiko OZAWA
National Institute of Radiological Sciences, 9-1 Anagawa 4-chome, Inage-ku, Chiba-shi 263, Japan

Oxidative DNA damage from active oxygen species such as hydroxyl radicals (·OH) has been hypothesized to play a critical role in diverse physiological processes including carcinogenesis, radiation damage and cancer chemotherapy. Copper(II) (Cu(II)) is an important metal ion present in chromosomes and is closely associated with DNA bases. Consequently, interest in copper-DNA adducts stems from the possibility that endogenous, DNA-associated copper may be able to promote oxidative damage of DNA. Hydroxyl radicals may be produced by the metal-catalyzed Haber-Weiss reaction, *i. e.* metal-catalyzed reaction of superoxide ($O_2^{\cdot-}$) with hydrogen peroxide (H_2O_2). Since H_2O_2 may be generated *in situ* through the reduction of molecular oxygen by reduced copper ions (Cu(I)), we investigated what kind of Cu(II) complexes can react with biological reductants such as ascorbic acid, glutathione, N-acetylcysteine or hydroquinone in the presence of molecular oxygen to generate ·OH using electron spin resonance (ESR) spin-trapping method and to cause DNA strand scission.

The following Cu(II) complexes were used; $Cu(CyHH)_2$ (CyHH: cyclo(L-histidyl-L-histidyl)), $Cu(OP)_2$ (OP: *o*-phenanthroline), Cu(HGG) (HGG: L-histidylglycylglycine) and $Cu(en)_2$ (en: ethylenediamine). Methyl radical adduct of a-(pyridyl-4-N-oxide)-N-*tert*-butylnitrone (POBN-CH_3) was obtained from the reaction of ascorbic acid with all Cu(II) complexes used here in the presence of a spin trap, POBN, and dimethyl sulfoxide, indicating the generation of ·OH. Glutathione, N-acetylcysteine and hydroquinone reacted with both $Cu(CyHH)_2$ and $Cu(OP)_2$ to generate POBN-CH_3, whereas neither Cu(HGG) nor $Cu(en)_2$ reacted with these reductants.

The DNA strand scission caused by reaction mixtures of Cu(II) complexes with reductants was investigated under the same conditions as the ESR spin-trapping experiments. Addition of ascorbic acid to mixtures of these four Cu(II) complexes and DNA resulted in DNA strand breakage. Hydroquinone plus $Cu(CyHH)_2$ also caused DNA strand scission. In addition, DNA strand breakage was also observed with the reaction of $Cu(OP)_2$ with glutathione, N-acetylcysteine and hydroquinone. In contrast, reaction mixtures of glutathione, N-acetylcysteine, or hydroquinone with Cu(HGG) or $Cu(en)_2$ did not cause DNA strand scission within the concentration range used. Thus, DNA strand scission may be caused by ·OH generated from the reaction of some Cu(II) complexes with biological reductants.

COPPER(II) BINDING TO A MODEL OF PRION PROTEIN; ANALYSIS OF THE STRUCTURE BY ESR SPECTRA IN SOLUTION

Hiromu Sakurai[1], Tomoko Matsuda[1], Jun Fugono[1], Makoto Hiromura[1] and Koich Kawasaki[2]

[1]*Department of Analytical and Bioinorganic Chemistry, Kyoto Pharmaceutical University, 5 Nakauchi-cho, Misasagi, Yamashina-ku, Kyoto 607-8414, Japan*
[2]*Faculty of Pharmaceutical Sciences, Kobe-Gakuin University, 518 Arise, Ikawadani-cho, Nishi-ku, Kobe 651-2113, Japan*

Since the prion protein (PrP) has been found to have a highly conserved octapeptide repeat region (sequence PHGGGWGO) near the N terminus, the functional role of PrP has been proposed to involve the binding of copper(II) ion (Cu(II)). Recently, several groups have reported that the octarepeat peptides bind with Cu(II) in solution. However, the detail binding structure has not been revealed.[1-2)]

Recently, we have proposed that the coordination structure around the Cu(II) in copper complexes as well as copper proteins could be analyzed by ESR spectra in solution, where ESR parameters such as g-values and hyperfine coupling constants, A-values, were found to be correlated with the configuration of the complex. Moreover, linear relationship between ESR parameters and stability constants or half-wave potentials of the Cu(II) complexes were observed. [3-5)]

On the basis of the results on the fundamental investigation, we analyzed the Cu(II) binding structure of PrP using the octarepeat peptide and its related compounds.

The peptides, Pro-His-Gly-Gly-Gly-Trp-Gly-Glu (PHGGGWGQ) and HGGG, were prepared in our laboratory. Other related peptides and bovine serum albumin (BSA) were commercially available. Optical and ESR spectra at room and liquid nitrogen temperatures were measured at the ligand: Cu(II) ratio of 1:1 ~ 3:1 in a collidine-HCl buffer, pH 7.80.

Binding ratio of octarepeat peptide or GGH and Cu(II) was found to be 1:1, similarly to that of BSA and Cu(II), while that of HGGG, HG or GH with Cu(II) was 2:1, as estimated by the molar ratio method.

ESR spectral pattern for the octarepeat peptide-Cu(II) system indicated the presence of a square-planar geometry with a ligand superhyperfine splitting, consisting of a 9-line signal, similarly to the spectrum of BSA-Cu(II) system. While, ESR spectra of HGGG-Cu(II) system exhibited a ligand superhyperfine splitting, consisting of a 7-line signal.

From these results, the octarepeat peptide was concluded to bind with Cu(II) forming CuN_4 configuration, being one prolyl nitrogen, one histidyl(imidazole) nitrogen and two deprotonated amido nitrogen or one deprotonated amido nitrogen and one glutamyl nitrogen.

References

1. Brocon, D. R., et al.: *Nature* **390**, 684 (1997)
2. Viles, J. H., et al.: *Proc. Natl. Acad. Sci.*, USA, **96**, 2042 (1998)
3. Sawada, T., et al.: *Biochem. Biophys. Res. Commun.*, **216**, 154 (1995)
4. Sawada, T., et al.: *Chem. Pharm. Bull.*, **44**, 1009 (1996)
5. Fukumaru, K., et al.: *Chem. Pharm. Bull.*, **44**, 1989 (1996)

CYTOCHROME C PEROXIDASE-LIKE ACTIVITY OF METMYOGLOBIN MODIFIED WITH DIETHYLENETRIAMINEPENTAACETIC ACID

Kimiko KIGUCHI[1], Keiichi TSUKAHARA[1], Naoko KUBOTA[2], Ryuichi ARAKAWA[2], and Takeshi SAKURAI[3]

[1] Department of Chemistry, Nara Women's University, Nara, 630-8506, Japan

[2] Department of Applied Chemistry, Kansai University, Suita, 564-8680, Japan

[3] Division of Life Sciences, Graduate School of Natural Science and Technology, Kanazawa University, Kanazawa, 920-1192, Japan

We have reported that metmyoglobin (metMb) modified with diethylenetriaminepentaacetic acid (DTPA) catalyzes the oxidation of cytochrome *c* (Cyt *c*) with hydrogen peroxide (cytochrome *c* peroxidase (*Cc*P) activity) more efficiently than native metMb.[1] In this work, we report the relationship between *Cc*P activity and the number and the binding site of DTPA.

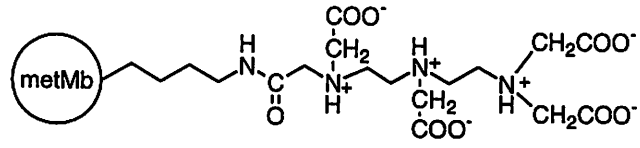

metMbDTPA

Chemically modified metMb (metMbDTPA) was separated by a DE-52 cellulose column chromatography (Fig. 1). The number of DTPA was analyzed by MALDI-TOF MS. Binding site of DTPA was determined by an amino-acid sequential analysis for peptide fragments treated with lysyl endopeptidase.

Fig. 1. Column Chromatography of metMbDTPA on a DE- 52 Cellulose Column

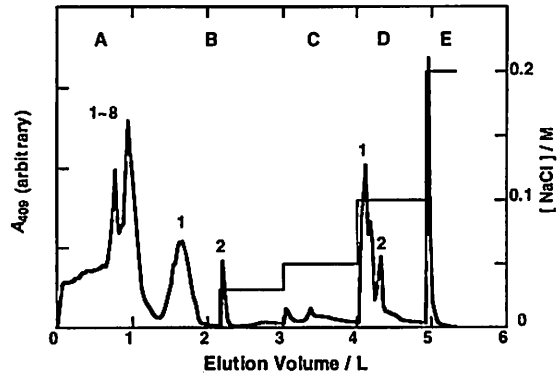

From the *m/z* values of metMbDTPA compared with that of native metMb, metMbDTPA (A, B, C, D, and E) are linked with 1, 2, 3, 4, and 5 DTPA ions, respectively. The binding sites of DTPA are as follows: Lys-87 and Lys-145 for B-2, Lys-47, Lys-87, Lys-145, and Lys-147 for D-1, and Lys-47, Lys-50, Lys-87, Lys-145, and Lys-147 for E.

*Cc*P-like activity of metmyoglobin increased in the following order: native metMb < metMbDTPA (B-1) < metMbDTPA (B-2) < metMbDTPA (D-1) < metMbDTPA (E). The difference in activity arises from the number of DTPA. Therefore, the difference in electrostatic interaction between metMbDTPA and Cyt *c* is important in the *Cc*P-like activity of metMbDTPA.

1. Tsukahara, K; Kiguchi, K., *Chem. Lett.*, **1998**, 913. *Additions and Corrections*: Tsukahara, K; Kiguchi, K., *Chem. Lett.*, **1999**, 189.

Role of NH···S Hydrogen Bond for Cys-Containing Fe(III) and Fe(II)(OEP) Complexes as a Model of the Active Site of Cytochrome P-450

Yukihide KOUSUMI[1], Taka-aki OKAMURA[1], Norikazu UEYAMA[1], Akira NAKAMURA[2]
[1] Department of Macromolecular Science, Graduate School of Science, Osaka University, Machikaneyama-chou 1-1, Toyonaka, Osaka 560-0043, Japan
[2] Faculty of Science, Toho University, Miyama 2-2-1, Funabashi, Chiba, Japan

Cytochrome P450 catalyzes monooxygenation of a variety of hydrophobic substrates. Cytochrome $P450_{cam}$ intermolecularly binds putidaredoxin (Pdx) as a redox partner to transfer electron through an unknown pathway. Using Cys-containing peptide model complexes for $P450_{cam}$, we have demonstrated that the formation of NH···S hydrogen bond between Cys sulfur and amide NH regulates the redox potential of Fe(II)/Fe(III). The change of secondary structure of $P450_{cam}$ by the association with Pdx is thought to affect the reactivity of the metal center. In order to investigate the regulation of the redox potential by intermolecular interaction, molecular association between a $P450_{cam}$ model complex and a multi-amide compound was studied in CH_2Cl_2 at room temperature.

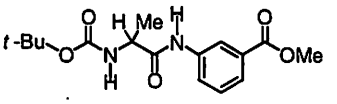

Boc-Ala-**Aba**-OMe

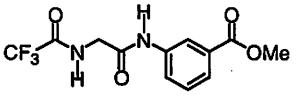

CF_3CO-Gly-**Aba**-OMe

Figure 1. Multi-amide compounds

[Fe^{III}(OEP)(Z-cLGL-OMe)] (**1**) and [Fe^{III}(OEP)(Z-cPAL-OMe)] (**2**) were employed as peptide model complexes having NH···S hydrogen bonds. Multi-amide compounds, Boc-Ala-Aba-OMe (Boc = *t*-butoxycarbonyl, Aba = *m*-aminobenzoic acid) and CF_3CO-Gly-Aba-OMe, possessing a rigid structure (Figure 1). An (1:1) mixture of **1** and multi-amide compound exhibits the negative redox potential shift of 0.02 - 0.03 V from that of **1**. It turns out that NH···S hydrogen bonds are weakened by the complexation. In the case of **2**, an irreversible reduction potential is observed at ca -0.5 V upon addition of a multi-amide compound due to the formation of [Fe^{III}(OEP)Cl] (Figure 2). This decomposition of **2** by the complexation with multi-amide compound results in the formation of [Fe^{III}(OEP)Cl]. The ^1H NMR and ^2H NMR spectra of an (1:1) mixture of **2** and a multi-amide compound also indicate that the intermolecular interaction with multi-amide compounds induces the weakening of NH···S hydrogen bonds and affects the redox potential through the Fe-S bond. The complexation between **2** and a multi-amide compound disrupts the NH···S hydrogen bonds supporting the complex stability. Then the complex dissociates the axial thiolate and alternatively binds Cl^-. Thus, we speculate the regulation of the NH···S hydrogen bond by the molecular association of the amide CO with multi-amide compound is one of the important functions for the $P450_{cam}$ and Pdx interaction.

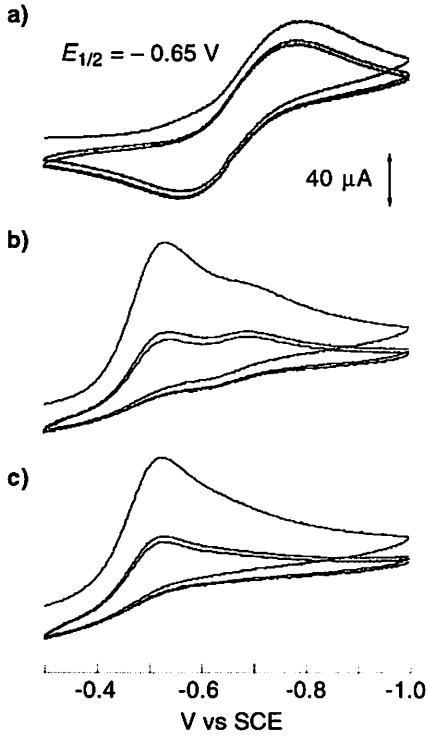

Figure 2. Cyclic voltammograms of a) **2** and b) **2** + 0.5 equive of CF_3CO-Gly-Aba-OMe, c) **2** + 1.2 equive of CF_3CO-Gly-Aba-OMe

Ligand-exchange Reaction in Mononuclear Phosphate Ca(II) Complexes with a Bulky Amide Ligand

Akira Onoda[1], Yusuke Yamada[1], Taka-aki Okamura[1], Norikaz Ueyama[1] and Akira Nakamura[2]
[1]Department of Mocromolecular Science, Graduate School of Science, Osaka University
[2]Faculty of Science, Toho University

Phosphate compounds usually play a crucial role in biological systems and the transportation of these compounds are precisely regulated by phosphotransferases with metal ions. Phosphoinoside specific phospholipase C contains mononuclear Ca(II) ion in the active site and NH···O hydrogen bonds are formed between the side chain NH of Arg, His and phosphate oxygen. A novel hydrogen-bonded phosphate monoester ligand with bulky triphenylacylamino-substituent, 2,6-$(Ph_3CCONH)_2C_6H_3OPO_3H_2$ (**1**) was prepared and mononuclear tris(phosphate) calcium complex, $(NMe_4)[Ca^{II}\{O_2(OH)O\text{-}2,6\text{-}(NHCOCPh_3)_2\}_3(MeCN)_3]$ (**2**), was successfully synthesized.

$$(NMe_4)[Ca^{II}\{(OPO(OH)OC_6H_3\text{-}2,\ 6\text{-}(NHCOCPh_3)_2\}_3(NCMe)_3] + 3\ ArOPO_3H_2$$
$$\rightarrow (NMe_4)[Ca^{II}\{(OPO(OH)OAr\}_3(NCMe)_3] + 3\ 2,6\text{-}(Ph_3CCONH)_2C_6H_3OPO_3H_2 \qquad \text{(eq 1)}$$
$$(\ Ar = 2,6\text{-}i\text{Pr}_2C_6H_3\ )$$

The ligand exchange reactions of **2** with excess 2,6-$(i\text{-Pr})_2C_6H_3OPO_3H_2$ (**3**) , which is defined in equasion 1, were monitored by the chemical shifts of amide NHs detected by ^{1}H NMR spectra. Figure 1 shows the ligand-exchange reaction of **2** with **3** in $Me_2SO\text{-}d_6$ at 30 °C. The amide NH protons apear at 9.67 ppm and 9.69 ppm with 4 and 12 equivalent of **3**, respectively. The chemical shift of amide NH of **1**, which is produced by proton exchange reaction, is 8.49 ppm. The down field shifted NH signals indicate that the NH···O hydrogen-bonded ligands exist in the monoanion state without dissociation from Ca(II) ion. The pK_a values of **1** and **3** are 3.3, 7.9 and 3.6, 8.0 in 50 % THF aqueous solution, respectively. The lowered pK_a value of **1** is due to the NH···O hydrogen bond. The reverse ligand-exchange reactions were also detected and the results indicate that the NH···O hydrogen bonds easily forms Ca–O bond. The NH···O hydrogen bond to phosphate monoanion ligand prevents Ca–O bond from dissociation.

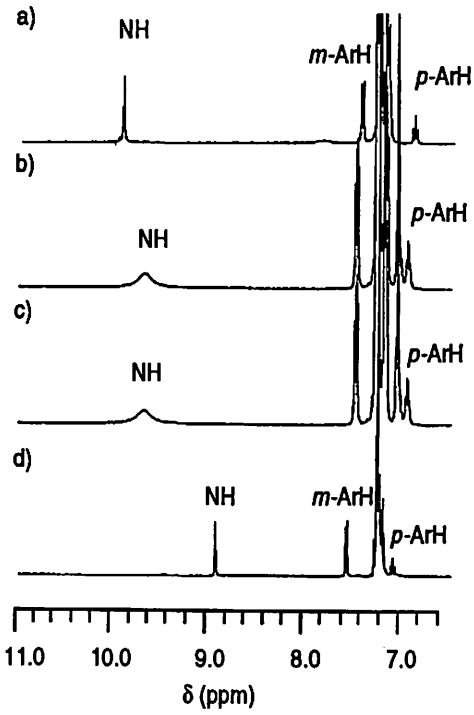

Figure 1. ^{1}H NMR spectra of a) **2**, b) **2** with 3 equiv. (1 equiv. to ligands), c) with 12 equiv. (4 equiv. to ligands) and d) **1** were shown.

ENHANCED STABILITIES OF TERNARY CU(II) COMPLEXES WITH AROMATIC AMINO ACIDS AND TERDENTATE HETEROAROMATIC N BASES

Tasuku MURAKAMI[1], Yoichi KIKUCHI[1] and Yasuhiko YUKAWA[2]

[1]Faculty of Education, Iwate University, Morioka 020-8550, Japan

[2]Department of Environmental Science, Faculty of Science, Niigata University, Niigata 950-2181, Japan

The electrostatic, hydrophobic or steric interaction between the ligands which affects the stability of ternary metal complexes have been extensively studied based on the idea that these ligand-ligand interactions could play an important role in enzyme-metal ion-substrate systems.[1,2] Most of the ternary copper(II) complexes which have been studied so far are four-coordinate planar complexes containing a bidentate heteroaromatic N base, 2,2'-bipyridine (bpy) or 1,10-phenanthroline (phen), as a primary ligand. There have been very fewer studies on the stabilities of five-coordinate ternary copper(II) complexes, although copper ions in biological systems could take on various geometries including the five-coordination.

In this paper, we report on the stabilities of the ternary copper(II) complexes containing linear terdentate heteroaromatic N bases, 2,2'-dipicolylamine (dpa) and N,N-dimethyl-N'-(2-pyridylmethyl)ethylenediamine (pyen), as the primary ligand and various α-amino acids as the secondary ligand. The effect of the side chains of the amino acid ligand on stability will be discussed.

The stabilities were determined by means of the computer processing of potentiometric titration data by use of HYPERQUAD.[3] Some stability constants were also obtained by spectrophotometric titrations. For both the terdentate ligands, the ternary complexes containing aromatic amino acid anions, such as L-tryptophanate and L-tyrosinate, were significantly more stable compared with the ternary complexes of alkyl- and hydroxyalkyl-substituted amino acid anions. This finding indicates that a sort of hydrophobic intramolecular interaction is present between the hydrophobic moiety of dpa or pyen and the aromatic side chains in aqueous solutions. These ternary complexes showed spectral features indicating square-pyramidal five-coorinate geometries.

The X-ray crystal structures of [Cu(dpa)(L-phe)]ClO_4 and [Cu(dpa)(pic)]ClO_4, where L-phe and pic are L-phenylalaninate and 2-picolinate respectively, are also described. There is no intramolecular ring-stacking, while the *inter*molecular stackings are observed between the pyridine rings of dpa of adjacent complex molecules.

1. Sugimori, T., Masuda, H., Ohta, N., Koiwai, K., Odani, A., and Yamauchi, O., *Inorg. Chem.*, 1997, **36**, 576, and refs therein.
2. Bastian, M., and Sigel, H., *Inorg. Chem.*, 1997, **36**, 1619, and refs therein.
3. Gans, P., Sabatini, A., and Vacca, A., *Talanta,* 1996, **43**, 1739.

SPECIATION OF PHYTATE METAL COMPLEXES. AN ENVIRONMENTAL KEY SUBSTANCE FROM GRAIN

Akira ODANI[1] and Osamu YAMAUCHI[1,2]

[1] Department of Chemistry, Graduate School of Science, Nagoya University, Nagoya 464-8602, Japan
[2]Research Center for Materials Science , Nagoya University, Nagoya 464-8602, Japan

Phytate, *myo*-inositol 1,2,3,4,5,6-hexaphosphate, whose mixed salt (phytin) with Ca^{2+}, Mg^{2+}, and a small amount of K^+ is distributed in seed or grain, is believed to play the role of energy source for the plant growth through dephosphorylation by phytase (phytic acid phosphatase). First finding of the necessity of trace element in human was due to Zn-phytate salt. The interactions between phytate and metal ions were usually described as salt formations, but we showed that the nature of the complex formation of phytate was very important for understanding the substrate of phytate hydrolyzing enzyme.[1] Phytase activity is too low in mammalian (swine, horse, fowl) to digest the phytate, which is hydrolyzed by the phytase of the microbe in the ground to liberate phosphate. This causes an environmental problem. This study aims at elucidating the species of phytate metal complexes.

The pKa values and stability constants were determined by the pH titrations carried out at I = 0.1 M (Et_4NClO_4) and 25°C. Phytate (PA, IP6) formed stable complexes $M_p(PA)H_r$ above pH 4 even with Na^+ and K^+ (M: Li^+, Na^+, K^+, Cs^+, Mg^{2+}, Ca^{2+}, Mn^{2+}, Zn^{2+}, Cu^{2+}, p=1-3, r=0-6). For M = Al^{3+} and VO^{2+}, the complex formation started at lower pH, but, at high pH the complexes were decomposed by the hydrolysis of the metal ions. The stability constants were in the order $M^{3+} > M^{2+} > M^{1+}$ for $M(PA)H_r$ complexes, and enabled us to calculate the population and stoichiometry of metal-phytate complexes. For Zn^{2+}-phytate the precipitation occurred above [phytate]/[Zn] = 2, so that the insoluble complex may cause the Zn deficiency in human. On the other hand, phytate formed soluble ternary complexes such as Cu(II)-2,2'-bipyridine-phytate.

1. Odani, A.; Kimura, Y.; Yamada, T.; Yamauchi, O., Anticancer Research, in press.

Acknowledgments. The authors thank the Ministry of Education, Science, Sports, and Culture for a Grant-in-Aid for Scientific Research (COE).

INTERACTION OF A DINUCLEAR PLATINUM(II) COMPLEX DERIVED FROM CISPLATIN WITH DNA

M. CHIKUMA, Y. KIMURA, K. KUMAKURA, T. SATO, M. HIRAI and S. KOMEDA
Department of Pharmaceutical Sciences, Osaka University of Pharmaceutical Sciences, 4-20-1 Nasahara, Takatsuki, 569-1094, Japan

Cisplatin is an effective agent in the treatment of a number of human cancers. Its clinical effectiveness is limited, however, by dose limiting toxicities such as renal failure. Furthermore, acquired resistance to cisplatin is an almost inevitable occurrence even amongest initially sensitive tumors. The need to search for more favorable platinum anticancer drugs is still strong. A new dinuclear platinum complex cis- [$\{(NH_3)_2Pt\}_2(\mu\text{-OH})(\mu\text{-pz})]$ $(NO_3)_2$(pz=pyrazolato, complex I) was found effective against both L1210 murine leukemia cell lines sensitive and resitance to cisplatin. In order to elucidate the reactivity of complex I, kinetic study for the release of bridging hydroxide in the presence of some mineral acids was carried out by potentiometry, and physicochemical study for its interaction with DNA.

The observed rate constants for the release of bridged hydroxide ions in complex I were monitored by potentiometry after the addition of HNO_3, HCl, and HI in the presence of 0.1 mol/l KNO_3. The pH once decreases according to the concentration of acids added, and increases gradually as the bridged hydroxide ions release. The order of the observed rate constant values was $HI > HCl > HNO_3$. These findings suggest that complex I which is a dinuclear complex, obeys the substitution reaction mechanism governing mononuclear square planar platinum(II) complexes. No substitution reaction of pyrazole, another bridging ligand of complex I with the entering ligands such as Cl^- and I^- was confirmed by ^{1}H-NMR.

The interaction of DNA with platinum complexes was examined by measuring r_b(platinum atom number/nucletide) and melting curves of Salmon sperm DNA. The difference of melting temperature of DNA in the presence and absence of platinum complexes, ΔT_m was measured by ultraviolet absorption method in the r_b range of 0.006-0.03. Large postive value of ΔT_m were found in complex I, whereas in cisplatin small negative. These observations indicate that complex I forms interstrand crosslinks predominatly and that cisplatin introduces intrastamd crosslinks in the r_b range.

The conversion of B- to Z-DNA in poly(dC-dG) was monitored by circular dichroism spectroscopy in the presence of platinum(II) complexes. Complex I did not induced Z-form, but its CD spectra were different from those of cisplatin.

In conclusion, complex I binds to DNA with maintaining dinuclear structure and induces different distortion to DNA conformation in comparison with cisplatin.

Synthesis and Characterizations of a New Dinuclear Mixed-valence Manganese(II,III) Complex with an Asymmetric Ligand and Kinetic Study of Hydrogen Peroxide Dismutation

K. Abe,* A. E. M. Boelrigk,** Y. Abe,*** and G. C. Dismukes**
*Department of Polymer, Graduate School of Engineering, Kyoto University, Kyoto 606-8501
**Department of Chemistry, Princeton University, Princeton , NJ 08540, USA
*** Department of Chemistry, Nara Women's University, Nara 630-8506, Japan

Manganese-containing enzymes catalyze the oxidation of water during photosynthesis and disproportionation of superoxide ion and hydrogen peroxide. Hydrogen peroxide, which is readily formed in all aerobic cells by reduction of dioxygen and superoxide, is extremely toxic to living cells owing to oxidative damage. A principle biological defense against hydrogen peroxide is a class of enzymes called as catalases. Spectroscopic studies of the catalases from *T. thermophilus* and *L. plantarum* have revealed that hydrogen peroxide dismutation proceeds by the cycle between the Mn_2(II,II) and Mn_2(III,III) oxidation levels during the normal catalytic cycle.

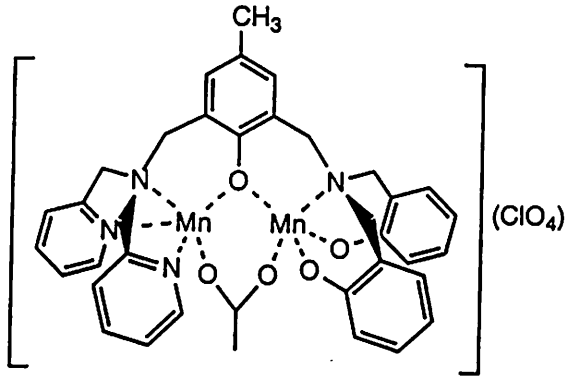

1

The present paper summarizes the synthesis and characterizations of the mixed-valence $[Mn_2^{II,III}L(\mu\text{-}OOCCH_3)](ClO_4)$ [1] derived from an asymmetric ligand. The mixed-valence Mn_2(II,III) complexes have attracted great interest in the oxidation levels compared with the tetranuclear Mn aggregate in Photosystem II (PSII), which cycles between five distinct mixed-oxidation levels labeled S_0, S_1, S_2, S_3, and S_4, including mixed-valence Mn^{II}, Mn^{III}, Mn^{IV}, and Mn^{V}. Futher, the mechanism of the disproportionation of H_2O_2 by the Mn_2(II,III) complex is of interest in comparison of catalytically inactive mixed-valence Mn_2(II,III) and Mn_2(III,IV) species in the catalytic disproportionation of H_2O_2 by the catalase from L. plantarum. The structure of **I** has been determined by IR, ESI-MS, ^{1}HNMR, and EPR spectroscopies, and CV measurement, owing to the formation of poor quality crystals, which is unsuitable for X-ray diffraction studies on the solid. We also report kinetic studies of the catalase activity by the mixed-valence Mn_2(II,III) complex **I**.

The EPR signal of **I** showed the solvent dependence. Although the EPR singal in CH_3OH showed a 6-line signal at 128 K and 6K, the EPR signal in CH_3CN exhibited the 16-line ^{55}Mn hyperfine structure associated with g=2 at lower temperatrure. It indicates that the Mn_2(II,III) exists as the valence-trapped ^{55}Mn nuclei with the S=1/2 ground state. The reaction proceeds mainly by a cycle between Mn_2(II,III) and Mn_2(III,IV) although the EPR signal of Mn_2(III,IV) was not obtained during the reaction. This is based on not only the very small intermediate concentration of Mn_2(III,IV) but also the large intensity of a 6-line signal due to the increased Mn(II) during the reaction, which may be due to the reduction from Mn_2(II,III) to Mn_2(II,II) by H_2O_2 and/or due to the decomposition of **1** and/or the formed Mn_2(II,II). After the reaction stopped, no O_2 evolution occurred by further addition of H_2O_2 and more addition of **1** led to O_2 evolution, which strongly indicates that **1** is converted to the inactive species by H_2O_2 during reaction. The catalytic activity of **1** is less than 100 turnovers in CH_3OH in comparison of the stable catalyst with 5000 turnovers without decomposition of the catalyst which cycles between Mn_2(II,III) and Mn_2(III,IV).[1,2]

* This research was performed at Princeton University.

1) P. J. Pessiki and G. C. Dismukes, *J. Am. Chem. Soc.*, **1994**, 116, 898.
2) A. Gelasco, S. Bensiek, and V. L. Pecoraro, *Inorg. Chem.*, **1998**, 37, 3301.

A STUDY OF ENTHALPY-ENTROPY COMPENSATION PHENOMENON IN MICELLIZATION PROCESS

Hsin-Yi Chang, Cheng-Ying Lee and Li-Jen Chen
Department of Chemical Engineering, National Taiwan University, Taipei, Taiwan 106, Republic of China

A variety of processes of certain solutes in aqueous solution, such as oxidation-reduction, hydrolysis, protein unfolding, etc., exhibit a linear relationship between the entropy change ΔS_m^o and the enthalpy change ΔH_m^o, i.e., $\Delta H_m^o = \Delta H_m^* + T_c \Delta S_m^o$. The slope T_c, known as compensation temperature, can be interpreted as a characteristic of solute-solute and solute-solvent interactions. The intercept ΔH_m^* characterizes the solute-solute interaction This phenomenon is known as enthalpy-entropy compensation. Micellization process of surfactants has been shown also possessing such a compensation phenomenon.[1]

The measurements of critical micelle concentration (CMC) of surfactants were performed over a wide temperature range. According to the mass action model, the temperature dependence of CMC is used to calculate the enthalpies and entropies of micelle formation for six different homologous series of surfactants. The enthalpy-entropy compensation plot exhibits an excellent linearity. It is found that all the compensation lines for surfactants in a homologous series are parallel to one another and the intercept ΔH_m^* of these compensation lines is a linear function of the hydrophobic chain length of surfactants. The value of ΔH_m^* decreases as the hydrophobicity of a surfactant increases. Effects of salt and alcohol on the enthalpy-entropy compensation phenomenon are also discussed.

1. Chen, Li-Jen; Lin, Shi-Yow; Huang, Chiung-Chang, *J. Phys. Chem.*, 1998, **102**, 4350.

CALORIMETRIC STUDY ON MICELLAR SOLUTIONS OF PENTAETHYLENE GLYCOL MONOALKYL ETHERS

Akio Ohta, Takanori Takiue, †Norihiro Ikeda, Makoto Aratono

Chemistry and Physics of Condensed Matters, Graduate School of Science, Kyushu University, Fukuoka 812-8581, Japan

†Department of Human Environmental Science, Fukuoka Women's University, Fukuoka 813-8529, Japan

The micellar solutions of pentaethylene glycol monoalkyl ethers CiE5 (i = 8 or 10) were investigated by employing the high precision isothermal titration microcalorimeter (Thermal Activity Monitor TAM 2277). The enthalpy of mixing of pure liquid of C8E5 with water was negative and decreased with increasing concentration of C8E5 and decreasing temperature. In the case of C10E5, the enthalpy of mixing of aqueous solution of surfactant, instead of pure liquid of C10E5, with water was measured owing to the relatively low cmc and high melting point of C10E5. The enthalpy was also negative. From the thermodynamic analysis of the experimental results, the partial molar enthalpy changes and the enthalpies of micelle formation of CiE5 were obtained. It was taken into account in the analysis that measured heat per small injection divided by the injected mole of surfactant is approximately equivalent to the partial molar enthalpy change of surfactant in the case of C8E5, while it is no longer true in the case of C10E5, because the content of solvent increases with the injection of aqueous solution. The enthalpies of micelle formation of CiE5 were positive and decrease with rising temperature in both systems. Its absolute value of C8E5 is lager than that of C10E5 above 283.15K. However, its temperature dependence of C8E5 is smaller than the one of C10E5. It is clear that these findings are attributable to the difference on the contact area of hydrocarbon with water between them. By analyzing the partial molar enthalpy changes in detail, furthermore, the monomer concentration was evaluated as a function of the total surfactant concentration and temperature, and then the enthalpy of micelle formation was estimated. These values were comparable with those directly obtained by the calorimetry. According to the thermodynamic consideration, it was found that the difference offers information on the temperature dependence of average aggregation number of micelle.

ELECTROCHEMICAL DETERMINATION OF THE SINGLYDISPERSED SURFACTANT ION CONCENTRATIONS IN MICELLAR SOLUTIONS OF BINARYCATIONIC SURFACTANTS

Tamaki MAEDA, Youshun NISHI, Akiko KAMINAGA, Katumitu HAYAKAWA and Iwao SATAKE

Department of Chemistry and BioScience, Kagoshima University, 1-21-35 KORIMOTO, KAGOSHIMA, 890-0025, Japan

The use of the surfactant ion selective membrane electrodes with different selectivity constant permits the electrochemical determination of the singly dispersed surfactant ion concentrations (C_f) in binary cationic surfactant solutions such as dodecyltrimethylammonium chloride (DTAC) and decyltrimethylammonium chloride (DeTAC). For the sake of simplicity, activity coefficients were assumed to be unity. C_f and the micellar composition (x) thus determined were compared with those calculated from an ideal mixing model.

The electrodes used are a carrier-free PVC membrane electrode which is composed of 20 wt.% poly (vinyl chloride) and 80 wt.% plasticizer (Elvaloy L-742, MITSUI-DU PONT POLY-CHEMICAL Co., Ltd.), and an ion-exchange resin (Dowex 50^{w}x4, 20-50mesh) fixed at the pointed end of the electrode. The electrodes were conditioned by soaking the electrodes in 1mM DTAC solution for a day or a month respectively before use. The emf of the electrodes was measured by HORIBA pH METER F-24. The critical micelle concentration (cmc, C_o) was determined from conductivity measurements by using a TOA Conductivity Meter CM-50AT. All of the measurements were carried out at 25℃.

Figure 1 shows the typical change in C_f with the total concentrations (C_t) measured at DTA mole fraction y=0.5. Solid line below the cmc represents the initial concentrations, and those above the cmc represent the concentrations calculated on the basis of ideal mixing model. The x values calculated from C_f are also plotted in Fig.2. The values of C_f are well reproduced below the cmc. It can be seen that this technique provides a simple method to estimate the composition of binary surfactant solutions.

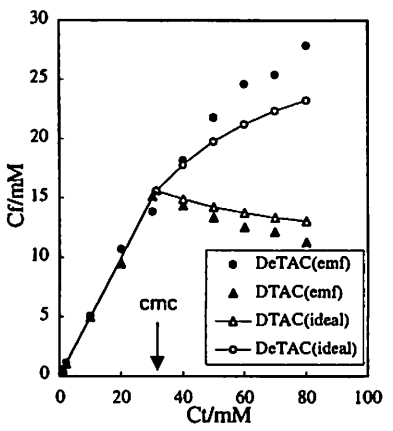

Fig.1 Singly dispersed surfactant ion concentrations at y=0.5.

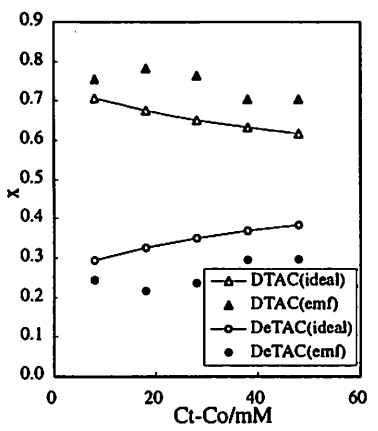

Fig.2 Micellar compositions at y=0.5.

Temperature Dependence of the Surface Adsorption and CMC of Sodium Oleate in Aqueous Solution

Yoshio Murata[1], Kosuke Eto[1], Tohru Inoue[1], Kazuo Onuma[2] and Masao Suzuki[3]

[1] Department of Chemistry, Faculty of Science, Fukuoka University, 8-19-1 Nanakuma, Jonan-ku, Fukuoka, 814-0180, Japan

[2] Inorganic Control Lab. National Institute of Materials and Chemical Research, Higashi 1-1, Tsukuba, 305-0046, Japan

[3] Oleochemical Research Laboratory, Nippon Oil and Fat Corporation Ltd., 1-56 Oohamachou, Amagasaki, 660-0095, Japan

The oleate ester is one of the most important components of the cell membranes. The most striking characteristic of sodium oleate molecule is the cis-double bond located in the center of oleoyl group. Due to the cis-double bond, this molecule has a bent shape. The purpose of this paper is to clarify the influence of this cis-double bond on the surface adsorption and micelle formation of sodium oleate in aqueous solution, comparing with those of some sodium salts of saturated fatty acids.

The purity of oleic acid was more than 99.9% (Nippon Oil and Fat Co. Ltd.). Sodium oleate was prepared by neutralizing the oleic acid in ethanol solution by aqueous solution of NaOH followed by freeze-drying. Surface tension measurements were made at the temperature range from 25 to 60°C by the use of the Wilhelmy plate technique improved for high temperature measurements. Quesi-elastic light scattering measurements were carried out by DLS-7000 (Otsuka Electronics Co. Ltd.)

The adsorption amounts of the fatty acid salts of aqueous solutions(pH11) were obtained from the slope of surface tension vs. log(concentration) curve by applying the Gibbs equation. The inverse of the adsorption amounts gives the area per molecule at the air-water interface (a_0). The temperature dependence of a_0 of sodium oleate at air-water interface is shown in Fig. 1. The value of a_0 of sodium oleate is 230Å^2 below 30°C. This value is about 3 times larger than a_0 of sodium salts of saturated fatty acids at the corresponding temperature. The value of a_0 of sodium oleate decreases rapidly with the increase in temperature, while those of sodium salts of saturated fatty acids tend to increase with temperature. Critical micelle concentration (CMC) in aqueous solutions (pH11) was determined from the bent point in the surface tension vs. log(concentration) curve. The CMC of sodium oleate increases sigmoidally with the increase in temperature (Fig. 2) but the CMC of the salts of saturated fatty acids is almost independent of temperature. These differences in the behavior of surface adsorption and micelle formation will be discussed from the view point of molecular structure of the fatty acids.

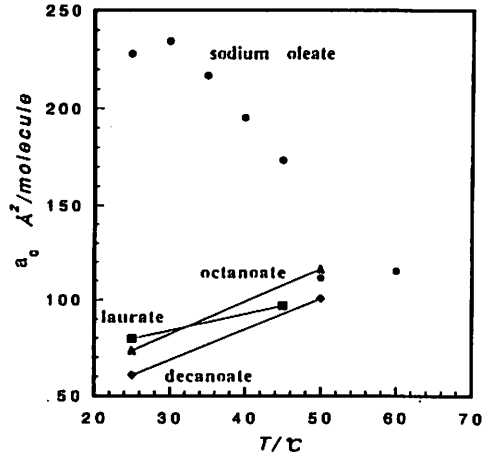

Fig. 1 Temperature dependence of the area per molecule of sodium salts of fatty acids in aqueous solutions(pH 11).

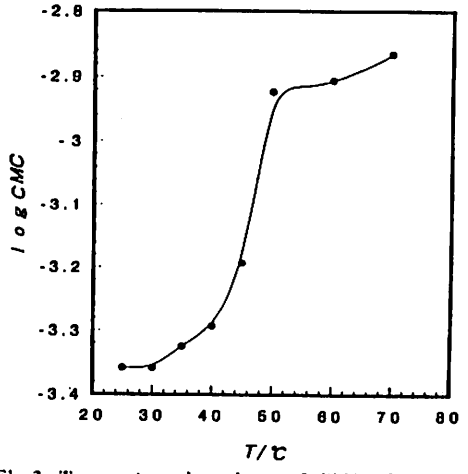

Fig.2 Temperature dependence of CMC of sodium oleate in aqueous solutions(pH 11).

Phase Behavior of Binary Phospholipid Mixtures in Hydrated Bilayer

Tohru Inoue and Yoshinori Nibu
Department of Chemistry, Faculty of Science, Fukuoka University,
Nanakuma, Jonan-ku, Fukuoka 814-0180, Japan

Biomembranes are constituted of various kinds of lipids and proteins, and the physical state of phospholipids and the lipid composition of local regions of biomembranes is relevant to many biological functions of the membranes. Thus, the phase science of hydrated bilayer of phospholipid mixtures is a subject of fundamental interest in relation to membrane biophysics. From this point of view, we have been studying the phase behavior of binary phospholipid mixtures in hydrated bilayer, and have reported for mixtures of several types of phospholipid species having the same head group but different acyl chains.

In the present work, we have studied the phase behavior of hydrated lipid bilayer composed of two phospholipid species chosen from phosphatidic acid (PA), phosphatidylcholine (PC), phosphatidylethanolamine (PE), and phosphatidylglycerol (PG) with the same acyl chains. The pseudo-binary phase diagrams were constructed by a differential scanning calorimetry (DSC).

The phase diagrams exhibited a non-ideal nature of mixing of the two lipid species in both gel and liquid-crystalline phases. These phase diagrams were analyzed based on a thermodynamic model applying the Bragg-Williams approximation for non-ideality of mixing. The non-ideality parameters of mixing, ρ_0, derived from this approach were positive for all mixture systems in both gel and liquid-crystalline phase bilayers. The values of ρ_0 for gel phase bilayer were larger than those for liquid-crystalline bilayer, and increased in the order PG/PE < PC/PA <PC/PE < PG/PA for both gel and liquid-crystalline bilayers. This indicates that (i) the mixed-pair formation is energetically unfavorable compared with the like-pair formation in hydrated bilayers, (ii) the energetical disadvantage for the mixed-pair formation is more pronounced in the gel phase bilayer, and (iii) it increases in the above order for different combination of phospholipid species. In addition, the ρ_0 values increased with the increase in the acyl chain length of the phospholipids. These experimental results were discussed in terms of an intermolecular interaction of the phospholipid species in hydrated bilayer.

Structure of Water under Multi- and Mono-Layer Conditions Confined in MCM-41 over a Temperature Range –50 to +25 °C by X-ray Diffraction

Pavel SMIRNOV[1], Toshio YAMAGUCHI[1], Shigeharu KITTAKA[2], Shuichi TAKAHARA[2], Yasushige KURODA[3]

[1]Department of Chemistry, Fukuoka University, Fukuoka 814-0180, Japan

[2]Department of Chemistry, Okayama University of Science, Okayama 700-8530, Japan

[3]Department of Chemistry, Okayama University, Okayama 700-8530, Japan

X-ray scattering measurements on water confined in the cylindrical pores of MCM-41 with different pore sizes C-10 (diameter = 21 Å) and C-14 (28 Å) have been performed over a temperature range -50 to +25°C. Both samples were sealed in glass capillaries at water vapor pressures p/p_0= 0.3 (monolayer) and 0.6 (multilayer). X-ray measurements were made on a rapid X-ray diffractometer with an imaging plate detector by using MoKα radiation (λ=0.7107 Å). The X-ray radial distribution functions (RDFs) (Fig. 1) showed that for both samples there are three types of notable interactions: H_2O-H_2O interactions at ~2.8 Å and 4.6 Å for the tetrahedral hydrogen bonded network of water, the non-hydrogen bonded H_2O-H_2O interactions at 3.4 Å, and the H_2O - Si interactions at ~3.8 Å between water and silica wall. With decreasing temperature the coordination numbers of the 2.8 Å and 4.6 Å interactions increase for the multilayer samples, showing evolution of hydrogen bonded water structure in the both samples. The amount of the hydrogen bonded water molecules is larger in the C-14 sample than in the C-10 one, showing more hydrogen bonded water structure in the former. On the other hand, the amount of the non-hydrogen bonded H_2O molecules is larger in the latter. It shows that decreasing porous size leads to increasing non-hydrogen bonded interactions in the water structure. It is interesting to note that no DSC curves show ice formation in the C-10 sample. No significant structural change was observed for the monolayer sample with decreasing temperature.

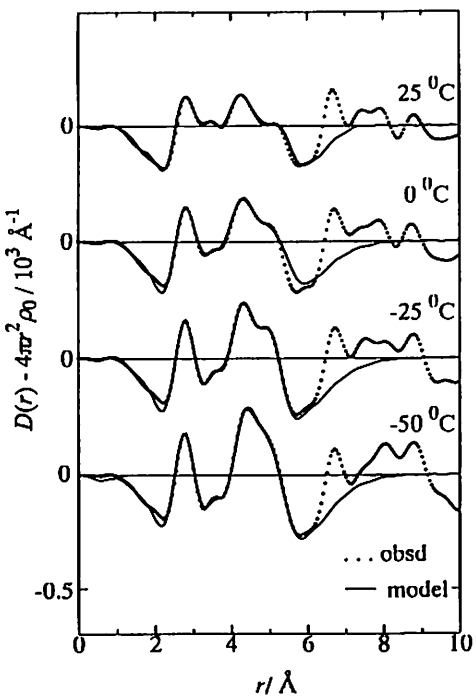

Fig. 1. RDFs of water absorbed at p/p_0 = 0.6 in MCM-41 C-10.

MUTUAL DIFFUSION COEFFICIENTS OF ZWITTER-IONIC AND IONIC MIXED MICELLES : EFFECTS OF COUNTER IONS AND MICELLAR AGGREGATION NUMBERS

Yui NOGAMI, Hiroyasu SAIKI and Toshihiro TOMINAGA
Department of Applied Chemistry, Okayama University of Science, 1-1 Ridai-cho, Okayama 700-0005, Japan

Mutual diffusion coefficients of ionic surfactants are known to increase with increasing concentration above critical micelle concentrations (CMCs). This increase can be interpreted in terms of increasing electrostatic coupling between micelles and counter ions because the concentration of surfactant monomer ions decrease with increasing surfactant concentration. By minimizing surfactant monomer concentrations, mutual diffusion coefficients of surfactants can be increased significantly.[1] In this study we examine the effects of counter ions and aggregation numbers of micelles on the mutual diffusion coefficient of mixed surfactants.

We studied systems containing 10 mM (1M = 1mol dm^{-3}) 3-(N-tetradecyl-N,N-dimethylammonio)-propanesulfonate (C_{14}DAPS) and varying amount of long-chain ionic surfactants such as sodium 1-octadecanesulfonate ($C_{18}SO_3Na$), potassium 1-octadecanesulfonate ($C_{18}SO_3K$), and octadecyltrimethyl-ammonium chloride (C_{18}TACl). Krafft points of all the ionic surfactants are higher than 298.2 K and essentially all of them are solubilized in C_{14}DAPS to form mixed micelles. Figure 1 shows the mutual diffusion coefficients for the mixed surfactants at 298.2 K. If the concentration of monomer ions is negligibly small, the mutual diffusion coefficients of the surfactant, D, can be expressed as

$$1/D = (1/D_{mic} + q/D_c)/(1 + q) \qquad (1)$$

where D_c and D_{mic} are tracer diffusion coefficients of micelles and counter ions, respectively, and q is the number of counter ions per micelle. Figure 1 shows that the D value is larger for the $C_{18}SO_3K$ system than the $C_{18}SO_3Na$ system, which can be interpreted in terms of larger D_c value for K^+ than Na^+. However, the D values are smaller for the C_{18}TACl system than for the $C_{18}SO_3K$ system in spite of the similar D_c values. In order to obtain the q values, we determined micellar aggregation numbers by measuring pyrene fluorescence decays in the mixed micelles. The aggregation number increased when $C_{18}SO_3Na$ was added to C_{14}DAPS, but the change in the aggregation number was very small when C_{18}TACl was added to C_{14}DAPS. Thus the smaller D values for C_{18}TACl can be interpreted by smaller q values.

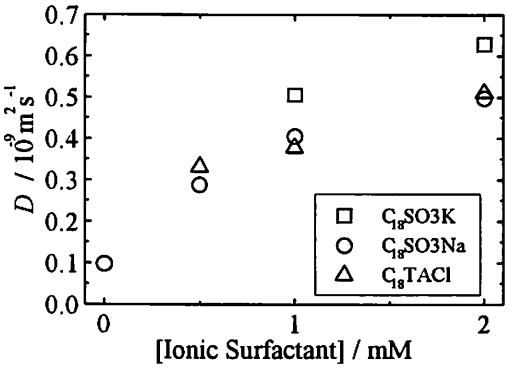

Figure 1. Mutual diffusion coefficients for mixed surfactants of 10 mM C_{14}DAPS and varying concentration of ionic surfactants.

1. Tominaga, T.; Nakamura, T.; Saiki, H., *Chem. Lett.* 1997, **1997**, 979.

MICELLE FORMATION IN AQUEOUS SOLUTIONS OF NONIONIC SURFACTANTS OBSERVED IN SEDIMENTATION EQUILIBRIUM

Keiichi KAMEYAMA[1)], and Hirofumi SHINOYAMA[2)]
[1)] Department of Biomolecular science, Faculty of Engineering, Gifu University, Yanagido 1-1, Gifu 501-1193, Japan.
[2)]Graduate school of Science and Technology, Chiba University, Matsudo 648, Matsudo, 271-8510, Japan.

Expeimental observation of the micellar size distribution and the equilibrium between monomeric and micellar species is important for understanding the micelle forming properties of aqueous solutions of amphiphilic molecules. Application of sedimentation equilibrium is promising for characterizing micellar forming systems in the above respects. In the present study, the micelle forming properties of a nonionic surfactant, *n*-octyl- β-glucoside and *n*-heptyl- β- xyloside in their aqueous solutions were investigated mainly by means of sedimentation equilibrium procedure.

Sedimentation equilibrium experments were performed employing an analytical ultracentrifuge, model XL-I (Beckman Instruments, Inc.) equipped with Rayleigh interference optical system, to determine the change of apparent weight average vuoyant mass, B_w, of the solutes as a function of the concentration for a concentration range including the vicinity of apparent critical micelle concentration (*cmc*), which was estimated from the inflection point in the concentration dependence of B_w. According to the mass-action model for micelle formation, monomer concentration, number, weight and z-average aggregation numbers of micelles were obtained as functions of total surfactant concentration.

For both of the nonionic surfactants, the micellar aggregation numbers and their standard deviations were observed to increase with total surfactant concentration, while the distribution was shown to be quite narrow in the vicinity of the *cmc*. The change of monomer concentration with total surfactant concentration could be also obtained. The monomer concentration was commonly observed to vary significantly even above the apparent critical micelle concentration *cmc*. These results apparently indicate that the phase separation approximation is not adequate for quantitative description of the micellar forming properties. For aqueous octylglucoside solutions, the profiles were obtained for several temperatures to allow an evaluation of the change of the association constant and the *cmc* with temperature. These results for the surfactant indicate that the phase separation approximation appears to be reasonable to describe the thermodynamic properties of the present micellar systems only for the limiting regions where the micellar concentrations are sufficiently low.

Acknowledgement
The authors are grateful to Dr. Masato Shimizu, Biomolecular Engineering Research Institute for his technical assistance in the ultracentrifuge experiments.

ULTRASONICALLY INDUCED BIREFRINGENCE AND THE DYNAMICAL PROPERTIES OF THE WORMLIKE MICELLES

Shinobu KODA, Ken YAMAMOTO, Tatsuro MATSUOKA, and Hiroyasu NOMURA
Department of Molecular Design and Engineering, Graduate School of Engineering, Nagoya University, Nagoya, 464-8603, Japan

Some surfactant molecules form wormlike micelles in aqueous solution with addition of the salts. The dynamics of the wormlike micelles has been investigated by dynamic light scattering, ESR measurements, ultrasonic absorption measurements, and electric and flow birefringence.

The double refraction is induced in liquids and solutions containing a certain amount of nonspherical particles when traversed by ultrasonic waves. This is called the phenomenon of ultrasonically induced double refraction. Compared with other birefringence methods, advantages of the ultrasonically induced birefringence method are that it enables us to investigate the motion of wormlike micelles under flow of high frequency and it is free from the effects of ions or electric double layer of wormlike micelle. The purpose of this work is to investigate the dynamical properties of the wormlike micelles by ultrasonically induced birefringence method. We observed the induced birefringence on the aquaous solutions of hexadecyltrimethylammonium (C_{16}TAB) bromide and sodium salicylate (NaSal) in which the micelles form the entangled networks at composition ratio of NaSal to C_{16}TAB larger than a threshold value. After the onset of ultrasound, the birefringence increased suddenly and approached the steady value after a damped oscillation. The steady value of the birefringence was proportional to the ultrasonic intensity and increased with the ultrasonic frequency. The fact implies that the birefringence is induced by the radiation pressure. The period of oscillation and damping time constant of the birefringence signal is discussed in their relation to composition ratio, micelle concentration and temperature.

PREPARATION AND CHARACTERIZATION OF SURFACTANT-PROTECTED PLATINUM NANOPARTICLES

Hironori Tamaki, Yoshiyuki Sato, Makoto Takezaki and Toshihiro Tominaga
Department of Applied Chemistry, Faculty of Engineering, Okayama University of Science, 1-1 Ridai-cho, Okayama 700-0005, Japan

Metal nanoparticles have attracted many researchers because of their unique properties and potential uses as new materials and catalysts. In order to understand the mechanism of catalysis, it is important to characterize not only metal cores but also protective layers. In this study, we focus on the effect of the protective layer thickness of Pt nanoparticles on the fluorescence quenching reaction rate, where the distance between the fluorophore and the quencher (metal core) is controlled by the length of protective surfactants (see figure 1).

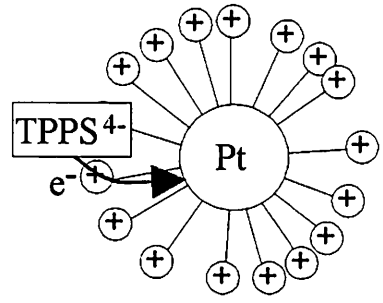

Figure 1. Fluorescence quenching model of $TPPS^{4-}$ by Pt-C_nTAC.

Pt nanoparticles were prepared by photoreducing H_2PtCl_6 using a Hg lamp for one day at 35 °C. Dodecyl-, tetradecy-, and hexadecyl-trimethylammonium chloride (C_{12}TAC, C_{14}TAC and C_{16}TAC) were used as protective surfactants. Fluorescence decays were measured for tetrakis(sulfonatophenyl)porphine ($TPPS^{4-}$) by exciting at 415 nm and detecting by a single-photon counting apparatus at the same Pt concentration.

Figure 2 shows fluorescence decay curves of $TPPS^{4-}$. In the absence of Pt nanoparticles (Pt-C_nTAC), the fluorescence decay (figure 2 a) was expressed by a single exponential function. However, in the presence of Pt-C_nTAC, the fluorescence decays (figure 2 b-d) were expressed by a double exponential function. The slower decay rate constants in the presence of Pt-C_nTAC are those for free $TPPS^{4-}$ as they are very close to the decay constant of $TPPS^{4-}$ in the absence of Pt-C_nTAC. The main component, whose contribution to the decays were larger than 0.9, is the faster component, which indicates that most fluorophores are located at the surfaces of the protective cationic surfactants. Logarithms of the faster decay rate constants are found to increase linearly with decreasing surfactant chain-length. The chain-length dependency, however, is smaller than those for the electron-transfer rate constants across self-assembled monolayers on the gold electrode.

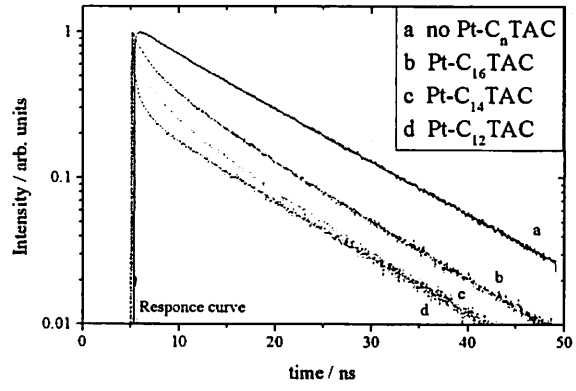

Figure 2. Fluorescence decays of $TPPS^{4-}$ in the absence (a) and the presence (b - d) of Pt-C_nTAC.

EFFECTS OF PROTONATION OF ALKYLDIMETHYL-AMINE OXIDES ON THE SOLUTION PROPERTIES AND THE PHASE BEHAVIOR

Hiroshi MAEDA, Atsushi YAMAMOTO, Hideya KAWASAKI and Norio NEMOTO[1]
Department of Chemistry, Faculty of Science, and Faculty of Engineering,[1]
Kyushu University Fukuoka 812-8581, Japan

Aqueous amine oxide solutions are mixtures of the nonionic and the protonated cationic species and the composition (the degree of ionization of micelles α_M) is determined by pH under a given ionic strength. On dodecyldimethylamine oxide (C12DAO), we have found several interesting and unusual solution properties coupled with protonation [1-3]. For example, the cmc was higher for the nonionic species than the cationic one if the ionic strength is higher than 0.2 M.[2] The observed protonation effects cannot be understood in terms of the introduced electric interaction alone and we have been proposing some short-range attractive interactions between the head groups: not only for the cationic-nonionic pair but also for the two cationic species in micelles.[1, 2]

Two aspects will be discussed in the present report on the protonation effects.

(1) The phase behavior in the solid state is examined. DSC curves of the HCl salts (α_M =1) with C10 - C18 alkyl chain have shown two peaks: the higher and smaller one corresponding to the melting point. The main peak is regarded as the melting of the hydrocarbon chains with intact ionic lattice consisting of the head group and the counterion. Values of ΔH and ΔS of the transition increased linearly with the hydrocarbon chain length: the increments of ΔH and ΔS per mole CH_2 group are 3.3 kJ and 8.7 JK^{-1}, respectively. The ΔH value (3.3kJ) is larger than that of alkyltrimethylammonium chloride (2.4kJ) and alkylammonium chloride (0.50kJ). The results on the mixtures of different compositions have suggested that the only stable complex is 1:1(α_M=0.5). For 1:1 complex, no melting peak was observed for C10 - C18.

(2) Viscoelastic properties of the solution of C14 homolog. Significant viscoelastic behavior is observed on C14 homolog without any additives but simply on protonation. With the 1:1 complex at 0.5M surfactant concentration C_D and 0.1M NaCl concentration C_S, the viscoelasticity can be described in terms of single Maxwell type($\tau \approx 30$ ms, $G_0 \approx 200$ Pa), while the solutions of the cationic or nonionic species show negligible elasticity and low viscosities. The storage modulus G_0 increased with C_D with an exponent 2, consistent with the theoretical prediction(9/4) for the entangled polymer system. The relaxation time did not increase with C_D but showed a maximum, contrary to the predicted behavior of increasing with an exponent 1.5. As to the dependence on C_S, G_0 showed the maximum around 0.1 M NaCl.

References
1. Maeda, H., *Coll. Surf. A*, 1996, **109**, 263.
2. Maeda, H.; Muroi, S.; Kakehashi, R., *J. Phys. Chem. B*, , 1997, **101**, 7378.
3. Imaishi, Y. et al., *J. Colloid Interface Sci.*, 1998, **197**, 309.

SOLUTION PROPERTIES OF TETRADECYLDIMETHYLAMINE OXIDE

Masahiko Miyahara, Yoko Kanakubo and Hiroshi Maeda
Department of Chemistry, Faculty of Science, Kyushu University,
Hakozaki, Higashi-ku, Fukuoka 812-8581, JAPAN

Alkyldimetylamine oxides are weak basic surfactant and the protonation equilibrium exists in aqueous solutions. Some solution properties have been studied on dodecyldimethylamine oxide (DDAO).[1,2] In the present study, solution properties of tetradecylldimethylamine oxide (TDAO) were examined.

1 CMC. Critical micelle concentrations (CMC) were determined by three different methods; the surface tension measurement, H^+-titration, pH-break point, as functions of pH and NaCl salt concentration (Cs).

Effect of the degree of ionization of micelle (α_M) on the CMC were examined at constant Cs (Cs=0.01, 0.1M). At Cs=0.1M the minimum appeared at about α_M=0.5, while at Cs=0.01M the minimum was not found. At Cs=0.1M the interaction parameter β in the regular solution theory is -1.6~-1.2 which is less negative than that of DDAO (β=-2.12).

Effect of Cs on the CMC was examined at constant α_M (α_M=0; the nonionic species, α_M=1; the cationic species). Generally, the logarithm of the CMC_0 for nonionic species linearly decreases with Cs as eq(1), and the slope Ks is closely related to the salting-out effect.

$$\log(CMC_0/mM) = -Ks \cdot (Cs/M) + \text{constant} \quad (1)$$

In the present study, this relation was observed in the range of $Cs < 1.9$M and $Ks = 0.40 \pm 0.01 M^{-1}$ was obtained. This slope was greater than that of DDAO ($Ks = 0.32 \pm 0.01 M^{-1}$) and the increase of Ks per ethylene group (ΔKs) is $0.08 \pm 0.02 M^{-1}$. This is comparable to that found on betain (ΔKs=0.81 ~0.76).[3]

For the cationic species, the plot of $\log CMC_+$ vs $\log Cg$ (counterion concentration) (the Corrin-Harkins plot) generally shows a linear relation at low Cg. This relation was observed in the range of $Cg < 1.0$M with the slope k_{CH} of 0.71 ± 0.01. This is larger than that of DDAO (k_{CH}=0.64 $\pm$0.01). From the point of view that k_{CH} represents the binding degree of counterions to micelle, it is suggested that a higher surface potential of micelles for TDAO than for DDAO at the same α_M.

In the low Cs (up to Cs=0.15) the CMC_0 was lower than the CMC_+, due to the electrostatic repulsion. However, in the range of high Cs (Cs=0.15~1.0M) the CMC_+ was lower than the CMC_0. In other words, cationic micelles were more stable than nonionic in the high Cs.

2 Surface excesses. The surface excesses of the nonionic species (Γ_T) and cationic (Γ_{TH}) were both nearly equal and they increased (from 4 to 6 μ mol m^{-2}) with Cs (0.01 to 1.0 M) in contrast to the nearly constant value (Γ=4 μ mol m^{-2}) in the case of DDAO.

The surface excess of salt (Γ_S) for the cationic species was $40.8 \pm 1.1 \times 10^{-8}$ mol m^{-2}, which is about five times greater than that of DDAO ($\Gamma_S = 8.6 \pm 0.4 \times 10^{-8}$ mol m^{-2}).

3 Size. Radii of the equivalent hydrodynamic sphere R_H were determined with dynamic light scattering as functions of α_M and the surfactant concentration (C).

At Cs =0.1M and C =0.01. R_H had a maximum at α_M=0.5, representing the maximum aggregation number.

In the range of C (C=0.03~0.1M), decrease of R_H with C was observed at α_M=0.5 as $R_H \propto C^{-0.75}$. In this range of C, the micelles are entangled and they form network structure. It is considered that we observed not R_H but ξ the average distance between entanglement points in semi dilute solution.

1. Maeda, H.; Muroi, S.; Ishii, M.; Kakehashi, R.; Kaimoto, H.; Nakahara, T.; Motomura, K., *J. Colloid Interface Sci.*, 1995, **175**, 497.
2. Maeda, H.; Muroi, S.; Kakehashi, *R., J. Phys. Chem. B*, 1997, **101**, 7378
3. Tori; Nakagawa, *K.-Z.Z.-polym.*, 1963, **189**, 50.

The Hydrogen Ion Titration of n-Alkylamine Oxide Micelles -Effect of the hydrocarbon chain length and the polar head group-

Masafumi Takechi[1] , Yoko Kanakubo[1], Kohji Yoshinaga[2] and Hiroshi Maeda[1]

[1]Department of Chemistry, Faculty of Science, Kyushu University,
Hakozaki, Higashi-ku, Fukuoka, 812-8581, JAPAN

[2]Faculty of Engineering, Kyushu Institute of Technology,
Sensuicho, Tobata-ku, Kitakyushu, 804-8550, JAPAN

1. n-Alkylamine oxides are weak basic surfactants and exist in a protonation equilibrium in the aqueous solution. If the surfactant molecules are ionized by the combination of hydrogen ions and the ionization depends on the pH of the solution, the charge on the miceller particles will also depend on the pH. The behavior of miceller solution of this kind of surfactants can be characterized by its hydrogen ion titration. By the hydrogen ion titration of dodecyldimethylamine oxide (C12DAO) in NaCl solutions of different concentrations, $pK_I < pK_M$ was obtained for the intrinsic dissociation exponents of the monomer (pK_I) and the micelle (pK_M). The degrees of ionizations of monomer $<\alpha_I>$ and micelle $<\alpha_M>$ were different and the two titration curves crossed each other. To explain $pK_I < pK_M$, we propose a stabilization mechanism by hydrogen bond between polar head groups.

2. Effect of the polar head group.

The assumed hydrogen bond is expected to be affected by the bulkiness of the polar head groups. The hydrogen ion titration of dodecyldihydroxyethylamine oxide (C12DHEAO) was carried out in which two methyl groups were substituted with two more bulky hydroxyethyl groups. There was some arbitrariness in extrapolating pK_a to $\alpha_M=0$ to evaluate pK_M [pK_a ($\alpha_M \rightarrow 0$)] and the pK_M values ranged between 5.40 and 5.60. These values are greater than pK_I(4.66) and hence two titration curves crossed. Compared with C12DAO, the crossing point differed : $\alpha_M=0.27$ for C12DHEAO, while $\alpha_M=0.45$ for C12DAO. The difference (pK_M - pK_I) was 0.74~1 for C12DHEAO while the coresponding value for C12DAO was 0.72~1. Effect of the ionic strength on the hydrogen titration was also examined.

3. Effect of the hydrocarbon chain length.

To examine the effect of hydrocarbon chain length, the hydrogen ion titration of tetradecyldimethylamine oxide (C14DAO) was carried out and the results were compared with those of C12DAO. In 0.1 M NaCl solution, the pK_M value was 6.45 for C14DAO while it was 5.70 for C12DAO. These unexpected different pK_M values seem to be caused by different shapes of micelles : a rod like one for C14DAO while a spherical one for C12DAO .

SOLUTION STRUCTURE INFLUENCE ON BIOPOLYMERS STRUCTURAL TRANSITIONS

Elene V. Hackl, Yuri P. Blagoi
Institute for Low Temperature Physics and Engineering, National Academy of Sciences of Ukraine, 47 Lenin Ave., 310164 Kharkov, Ukraine; E-mail: hackl@ilt.kharkov.ua

At present the fact is not beyond doubt that solvent is not passive surroundings, in which biomolecules are located. The solution structure defines the biopolymers conformation, influences their functioning. In the present work we consider the solution structure influence on DNA - the one of the most interesting biopolymers from points of view of physics and biology. It is known that DNA *in vivo* exists under the conditions of the decreased water activity, that *in vitro* can be simulated by the addition of less polar than water solvents to the DNA solution. The present work studies DNA structural transitions under the Cu^{2+} ion action in mixed solutions containing alcohol additions.

By IR spectroscopy method, structural transitions of biopolymers (DNA) on the Cu^{2+} ions action are studied in aqueous and mixed solutions containing ethanol, 1,2-propanediol and glycerol (0-20 v.%) at temperature ~30^{0}C. The mobility of water molecules in mixed solutions was measured by SHF-dielectrometry at λ=3 cm.

It was shown that under the Cu^{2+} ions action DNA transits into the condensed state in aqueous and mixed solutions containing alcohol additions. The transition is of high positive cooperativity. The DNA compactisation mechanism involves the Mt^{2+} ion interaction both with DNA nucleic bases and phosphate groups. Sizes of DNA compact particles are estimated, depending on Mt^{2+}/phosphate ratio.

Ethanol and 1,2-propanediol effects on Cu^{2+} ion - induced DNA compactisation are of monotonous character: with the increase of volume contents of these nonelectrolytes in solution the degree of DNA compactisation increases and the copper ion concentration required for the DNA transfer into the compact state decreases. The glycerol effect is of nonmonotonous character. It is stated that in mixed solutions DNA compactisation depends not only on the solution dielectric permeability but on the solution structure.

It was shown that the Cu^{2+} ions interaction with DNA in aqueous-alcohol solutions (up to ~15 v. %) depends strongly on water activity. The less the mobility of water molecules in comparison with pure water (the less water activity) the more the affinity of Cu^{2+} ions to DNA, and the less copper ion concentration is necessary to induce DNA compactisation. Cooperativity of the DNA transition into the compact state at copper ion binding increase at water activity reduction too. As all potential binding sites (in this work we consider only the Cu^{2+} ion interaction with DNA phosphate groups) on DNA surface contact with water molecules, the interaction of DNA with both alcohol and copper ions must result in the displacement of part of water molecules from the DNA surface. Schematically the interaction may be presented as

$$DNA \bullet nH_2O + ligand \leftrightarrow DNA \bullet ligand + nH_2O \qquad (1).$$

According to Le Chatelier' principle, when increasing the concentration of one of reaction components, the equilibrium is shifted to decrease the concentration of this component, and vice versa. Thus, at the decreased water activity the reaction (1) equilibrium will be shifted to the right and ligand binding to DNA (and cooperativity of DNA compactisation) will increase.

The correlation between the water activity and Cu^{2+} ions binding to DNA shown in the present work allows us to suppose that small alcohol additions to DNA aqueous solution may influence the DNA interaction with divalent metal ions through water activity change.

REFORMATION OF THE HELICAL STRUCTURE OF PROTEIN BY SDS AFTER UREA DENATURATION. A DISTINCT DIFFERENCE BETWEEN THE REFORMATION OF C-TERMINAL HELICAL-RODS OF HUMAN AND BOVINE SERUM ALBUMINS

Yoshiko MORIYAMA and Kunio TAKEDA
Department of Applied Chemistry, Okayama University of Science,
1-1 Ridai- cho, Okayama 700-0005, Japan

Upon the addition of small amounts of sodium dodecyl sulfate (SDS), the helicities of human serum albumin (HSA) and bovine serum albumin (BSA), lost in the urea denaturation, were mostly recovered. The profile of the recovery differed depending on the urea concentration. Then the urea concentrations were divided into three ranges: [1] a range below 3M where the helicity only decreased as in the absence of urea (the helicities of HSA and BSA decreased down to 49% and 50%, respectively, in the SDS solution); [2] a range between 4 and 8M where the helicity initially increased and then sharply decreased; and [3] a range above 9M where the helicities of HSA and BSA only increased with an increase in added SDS concentration. When SDS was added prior to the urea denaturation, the same helicities were obtained at each surfactant concentration. Thus the SDS denaturation finally predominated over the urea denaturation. In the middle range, profiles of the structural change were rather complicated. The helicity of HSA initially increased up to 66% (this was the same as in the native state) and then decreased below 3mM SDS. On the other hand, the helicity of BSA increased up to 62% (this was less than that in the native state) and then decreased below 2mM SDS. It is worth noting that the helicities of both the proteins are mostly recovered upon the addition of SDS less than 300μM in the second range except for 8M urea ([protein]=10μM) and the helicity was completely recovered in the case of HSA.

The helicity-recovery profile of HSA differs from that of BSA, although these are just homologous proteins. This difference might be attributed to the fact that the C-terminal helical-rod of HSA is amphiphilic, while that of BSA is hydrophobic as a whole.

X-RAY DIFFRACTION AND DSC STUDIES ON WATER AND SOME ELECTROLYTE SOLUTIONS CONFINED IN THE PORES OF SEPHADEX G-TYPE GELS

Kikujiro UJIMOTO,[a] Shuntaro NOZAWA,[a] Eizo KOGA,[a] Toshiyuki TAKAMUKU[b], Isao ANDO,[a] Hirondo KURIHARA,[a] and Toshio YAMAGUCHI[a]

[a]Department of Chemistry, Fukuoka University, Jonan-ku, Fukuoka 814-0180, Japan

[b]Department of Chemistry, Saga University, Honjo-machi, Saga 840-8502, Japan

Thermal and dynamic properties of water in porous polymer gels have been studied by DSC[1] and NMR[2], respectively, in terms of those in biological tissues. The microscopic structure of water in porous silica[3] and graphite[4] was investigated by X-ray diffraction using a diffractometer with an imaging plate area detector. In this study, Sephadex G-10, G-15, G-25F, and G-50F, commercially available for chromatographic packing, were chosen as a model medium of biological cells, because they have both hydrophilic and hydrophobic sites when swollen in water. The gel matrix consists of dextran chains of high molecular weight crosslinked with epichlorohydrin. An increase in the number following to G- corresponds to a decrease of crosslinkage and to an increase in pore sizes, which have not yet been evaluated under swollen conditions because of their softness.

The water regains, W_r, (amount of water absorbed by 1 g of dry gel) of the four gels were determined by a low-speed centrifugation method. The W_r value, which decreases with increasing crosslink, gives a volume rate of water-filling into the pore of gel beads, R_w. The heat of fusion of ice in the pore, Q, was measured by DSC with partially swollen gels prepared at various R_w values. The relationship between Q and R_w values gave a rate of unfreezable water, $R_{w(uf)}$, that strongly binds to the gel matrix , *i. e.*, 41% for G-10, 19.5% for G-15, 16.5% for G-25 and 6.3% for G-50.

X-ray diffraction data of water confined in the gels with water contents less than $R_{w(uf)}$ at 25°C showed that the second- and third-neighbor distances are slightly lengthened and that the heights of the corresponding peaks are weakened compared with those in bulk water. This suggests hydrogen-bonds in water confined in the pores are distorted to some extents by crosslinked gel matrices. Similar phenomena were observed for ice in the gels at $R_w = \sim 50\%$ at low temperatures. The crystal structure of the ice proved to be I_h by Bragg peak analysis. In addition, considerable amounts of halo-patterns revealed existence of unfreezable water or amorphous ice in the gel pores.

X-ray diffraction experiments were also made for 2 mol dm^{-3} NH_4F, NH_4Cl and NH_4ClO_4 aqueous solutions in the gel pores in order to examine the interaction between the anions and the gel matrix of G-10, since ClO_4^- exhibits strong affinity to hydrophilic gels in contrast to negligible affinity of the former two anions.[5] We will discuss the anion-gel interaction on the basis of the radial distribution functions obtained.

1. Murase, N.; Gonda, K.; Watanabe, T., *J. Phys. Chem.*, 1986, **90**, 5420.

2. Murase, N.; Watanabe, T., *Magn. Reson. Med.*, 1989, **9**, 1.

3. Takamuku, T.; Yamagami, M.; Wakita, H.; Masuda, Y.; Yamaguchi, T., *J. Phys. Chem.*, 1997, **101**, 5730.

4. T. Yamaguchi, *et al.*, unpublished data.

5. Shibukawa, M.; Ohta, N., *J. Chromatogr. Libr.*, 1988, **40**, 91.

ELECTRORHEOLOGICAL EFFECTS OF SOME SUSPENSIONS

Yasuhito MISONO, Takashi YAMAGUCHI and Keishi NEGITA
Department of Chemistry, Faculty of Science, Fukuoka University
Nanakuma, Jonan-ku, Fukuoka 814-0180, JAPAN

Electro-rheological (ER) phenomenon capable of applications in various fields was at first reported by Winslow.[1, 2] According to his reports, the apparent viscosity of some suspensions composed of water-adsorbed particles and electrically non-conductive liquids enhanced more than two orders of magnitude when a higher electric field was applied. In such ER fluids, the rheology of the fluid is modified by the application of electric fields. In the case of suspensions, the shear stress (τ) of the fluid often increases by a static yield stress (τ_0) induced by an electric field (E), and the fluid behaves as a Bingham fluid. The behavior is contrasted to that in the absence of electric field; the shear stress is proportional to shear rate ($\dot{\gamma}$), resulting in a Newtonian fluid. Mechanism for the ER effect is explained as a dipole-dipole interaction among particles induced by applied electric field. The induced dipole is able to be expressed by $\varepsilon_s a^3[(\varepsilon_p - \varepsilon_s)/(\varepsilon_p + 2\varepsilon_s)]E$ (ε_p and ε_s are the dielectric constants of the particle and of dispersing solvent, respectively, and a is the diameter of the particle), well-known as Maxwell-Wagner mechanism.[3] From these points of view, the larger dielectric constant of the particle relative to that of the dispersing solvent, the larger ER effect of suspensions has been expected.

The authors have investigated the ER effects of suspensions composed of anhydrous particles such as Zeolites,[4] rutile TiO_2 [5] and mesophase carbon[6] and silicone oil. For example, despite similar values of ε_p between Zeolite 4A and Zeolite 5A, the ER effect appears in Zeolite 4A suspension, whereas Zeolite 5A suspension exhibits no ER effects. The dielectric dispersion can be observed in Zeolite 4A suspension, while Zeolite 5A suspension is slightly affected by electric field only in the low frequency region of electric field. The result of the dielectric dispersion indicates that the relaxation time of Zeolite 5A suspension is much slower than that of Zeolite 4A suspension by six orders of magnitude. From these studies, it is suggested that the ER effect is associated with the relaxation time of the induced polarization, dielectric and electrical properties of the particle, and the rotation of the particles under the shear stress.

In this study, in addition to above results, some other ER fluids are explored. We will discuss the relationships between the ER effect and the some properties such as the induced polarization, dielectric relaxation, particle's rotation and the effect of the dispersing solvent.

1) Winslow, W. M., *U. S. Patent* 1947, 2417850.
2) Winslow, W. M., *J. Appl. Phys.* 1949, **20**, 1137.
3) Sillars, R. W., *J. Instr. Elect. Eng. (London)*, 1937, **80**, 378.
4) Negita, K.; Osawa, Y., *J. Phys. II France* 1995, **5**, 883.
5) Negita, K.; Osawa, Y., *Phys. Rev. E* 1995, **52(2)**, 1934.
6) Yamaguchi, T.; Negita, K., the 76th National Meeting of Chem. Soc. Jpn. 1999.

Volume phase transition of gel as a mechano-chemical coupling phenomenon

Shigeo Sasaki and Hiroshi Maeda
Department of Chemistry, Faculty of Science, Kyushu University, 33 Hakozaki, Higashiku, Fukuoka 812-8581, Japan

The transitional volume shrinkage of N-isopropylacrylamide (NIPA) gels in rising temperature[1] is known as a volume phase transition. It has been also found that the addition of the salt[2,3] or the saccharide[4] molecule to the solution also induces the volume phase transition. We have revealed[5] that the chemical potentials of water molecules in the solutions at the transition points (temperatures and concentrations of additives) are the same and that the volume changes are well described by the difference of the chemical potential from those at the transition. From these facts we have proposed[6] the theory that the coupling effect of the cooperative dehydration of the chain (unbinding of water molecules from the chain) and the entropy force of chains, both of which shrinks the gel, induces the volume phase transition. The theory also suggests that the gel, which is shrunken by the binding of small molecules, can exhibit the volume phase transition. Recently we have found that the transitional volume shrinkage of ionic poly(acrylate) gel (GAA) was induced with an increase in the concentration of the hydrophobic counterion, dodecylpyridinium chloride (DPC) in the solution at the salt concentration less than 0.4M.

A hysteresis was observed in the transition; there are 2 transition concentrations of DPC (the C_t^i where the gel makes a shrinkage transition in increasing the concentration and the C_t^d where the gel makes a swelling transition in decreasing the concentration). The former was larger than the latter. At a DPC concentration between C_t^i and C_t^d, the binding amount of DPC to the shrunken gel is much larger than that to the swollen gel. The former almost equaled to the binding amount to the gel shrunken in the solution at a DPC concentration outside the region of hysteresis. This indicates that the volume phase transition is the transition-like binding of dodecylpyridinium ion to the gel. The transition concentrations, C_t^i and C_t^d increased with NaCl concentration (C_s) of the solution outside the gel. The transition disappeared at C_s=0.4M. The interesting patterns were observed in the gels when they were transferred from the solution in the swelling condition into that in the shrinking condition. These volume phase transitions described above were interpreted as the mechano-chemical coupling phenomena.

References

(1) Hirokawa, Y.; Tanaka, T., J. Chem. Phys., 1984, 81, 6379.
(2) Suzuki, A., Adv. Poly. Sci., 1993, 110, 199.
(3) Park, T. G.; Hoffman, A. S. Macromolecules, 1993, 26, 50454.
(4) Kawasaki, H.; Sasaki, S.; Maeda, H.; Mihara, S.; Tokita, M.; Komai, T., J. Phys. Chem., 1996, 100, 16282.
(5) Sasaki, S.; Kawasaki, H.; Maeda, H., Macromolecules 1997, 30, 1847.
(6) Sasaki, S.; Maeda, H., Phys. Rev. E 1996, 54, 2761
(7) Sasaki, S.; Maeda, H., Colloid and Interface Science 1999, 211, 204

Swelling of Poly(2-hydroxyethyl methacrylate) Gels in Water-Alcohol (C1-C4) Mixed Solvents

K. Mukae[1], H. Isogai[2], S. Sawamura[2], K. Shirahama ,K. Makino, M. Sakurai and M. Sakai[1]

[1] Department of Industrial Chemistry, Kyushu Sangyo University, Fukuoka 813-8503,Japan

[2] Department of Chemistry, Ritsumeikan University, Shiga 525-8577, Japan

The swelling volume of poly(2-hydroxyethyl methacryle) (PHEMA) gels in alcohol(methanol, ethanol, 1-propanol, and 2-methyl-2-propanol)-water mixtures was measured at 25°C. The gels demonstrated a "convex" swelling phenomenon: the srunken gel in water swelled with addition of the alcohol solvents and then showed a maximum swelling in intermediate Xal region. As the number of carbon atoms in alcohol increased, the swelling maximum moved to lower mole fraction of alcohol.

In previous papers (1), we reported the swelling of poly(N-isopropylacrylamide) gel in alcohol-water mixtures and discussed the relationship between the gel swelling and the solvent properties such as thermodynamic activities and solubility parameters.

In this conference, the swelling behavior of the PHEMA gels was similarly interpretated by correlating with solution properties such as thermodynamic activities of aqueous alcohol mixture and solubility parameters of pure solvents. Namely, it will be important to see how the activities, or the partial free energy of solvent components, affect the swelling behavior in intermediate Xal region. It will be also important to see how the solubility parameters of pure solvents affect the swelling behavior in Xal=1.0 and 0.0 regions.

The strength of hydrogen bonding of hydroxyl and carbonyl group of the linear polymer in aqueous ethanol solution was examined by Fourier transform infrared spectroscopy (FT-IR). Stretching frequencies of the hydroxyl and carbonyl group of the polymer were sensitive to hydrogen bond strength which depend on the alcohol composition. These FT-IR spectroscopic studies suggested that the polymer networks may take a expanded conformation in a " convex" swelling region where PHEMA chains interact with alcohol solution through hydrophobic interaction.

1. Mukae, K.; Sakurai, M.; Sawamura, S.; Makino, K.; Kim, S. W.;Ueda, I.;Shirahama, K. J. Phys. Chem. 1993, 97, 737

Partition of the salt between N-isopropylacrylamide gel and the salt solution

Hideya Kawasaki, Takayuki Mithou, Shigeo Sasaki and Hiroshi Maeda
Department of Chemistry, Faculty of Science, Kyushu University , Hakozaki, Higashi-ku, Fukuoka, 812-8581, JAPAN

Poly(N-isopropylacrylamide)(NIPA) gel in water has been well known to exhibit a discontinuous volume shrinkage (i.e. a volume phase transition) at about 34 °C with increasing temperature.[1] The distribution behavior of solutes between NIPA gel and the external solution has been attracted in the unique character of NIPA gel : the temperature-induced volume shrinkage. We have studied the partition of the salts (LiCl, KCl, NaCl, CsCl, KSCN, KNO_3, K_2SO_4, CH_3COOLi, CH_3COONa, CH_3COOK, CH_3COOCs) between NIPA gel and the external salt solution (1 M) at various temperatures. The gel / solution partition coefficient (Kp) is defined as the ratio of the concentration of the salt in the gel to that in the external solution.

For the swollen gel at 20 °C (below the transition temperature), the Kp value was nearly equal to be unity ($K_p \sim 1$) irrespective of the kinds of the salts. For the completely shrunken gel at 40 °C (above the transition temperature), the Kp value decreased remarkably ($K_p << 1$) except for KSCN and depended on the kinds of the salts. The anions had a more pronounced effect on the Kp value than the cations. The Kp value for a series of potassium salts decreased in the order { $SCN^- > NO_3^- > Cl^- \sim CH_3COO^- > SO_4^{2-}$ }. The sequence of the anions seems to be the same as the Hofmeister or lyotropic series. Only in KSCN solution, we observed that the NIPA gel exhibited no discontinuous volume shrinkage and the swelling ratio of the shrunken NIPA gel was larger than the swelling ratio in water at 40 °C.

Above the transition temperature, the gel's behavior would be dominated by its hydrophobicity due to the dehydrated NIPA chains. The remarkable decrease of Kp value in the completely shrunken gel is considered to mainly originate from the apolar properties in the gel.

1. Hirokawa, Y. ; Tanaka, T., *J. Chem. Phys.*, 1984, **81**, 6379.

Effects of hydrophobic substances on the volume phase transition of N-isopropylacrylamide gel

Shogo Koga, Shigeo Sasaki and Hiroshi Maeda
Department of Chemistry, Faculty of Science, Kyushu University, Hakozaki, Higashi-ku, Fukuoka, 812-8581, Japan

It is well known that poly(N-isopropylacrylamide) (NIPA) hydro gels undergo discontinuous volume shrinkage in raising temperature.[1] This behavior called as the volume phase transition was observed with increase in the concentrations (C_{out}) of hydrophobic substances (benzoic acid (BZA), phenol (PH) and benzene (BZ)) as shown in Figure 1. The transition temperature was found to descend with increase in the concentration as shown in Figure 2. The volume phase transition is also induced by the addition of the salt[2,3] or the saccharide[4] molecule (the concentration ~ 1mol), which is caused by decrease in the chemical potentials of water molecules due to the existence of additives.[5] However, since the concentration of the hydrophobic substance was an order of 10^{-2} mol, the decrease of the chemical potentials of water molecules in the solution was negligible small. Therefore, the mechanism inducing effects of hydrophobic substances on the transition should be different from that of the salt. The degree of binding of hydrophobic substances per NIPA monomeric unit (β) and the degree of swelling were measured against C_{out}. At constant C_{out}, the binding amounts to the shrunken gel chain were larger than those to the swollen one. The strong correlation between the binding of hydrophobic substance and the gel volume was found as shown in Figure 1. The DSC measurement[6] was also carried out for the transitions mentioned above.

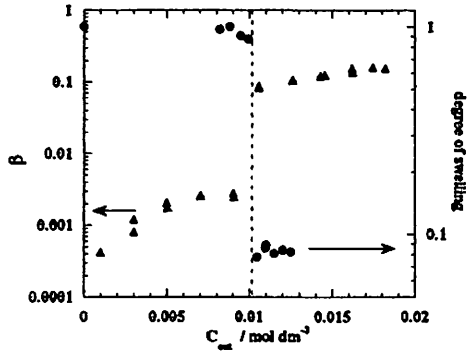

Figure 1 Degree of binding and swelling of gel as functions of C_{out} of BA at 26.5 °C.

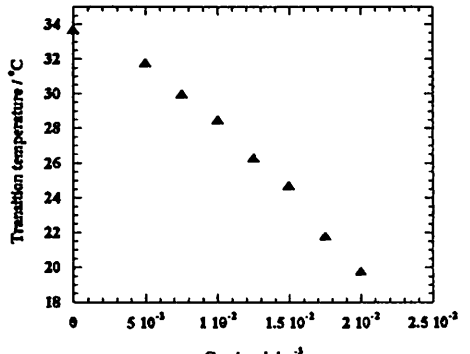

Figure 2 Transition temperature versus C_{out} of BA

1. Hirokawa, Y.; Tanaka, T., *J. Chem. Phys.*, 1984, **81**, 6379.
2. Suzuki, A., *Adv. Poly. Sci.*, 1993, **110**, 199.
3. Park, T. G.; Hoffman, A. S., *Macromolecules*, 1993, **26**, 50454.
4. Kawasaki, H.; Sasaki, S.; Maeda, H.; Mihara, S.; Tokita, M.; Komai, T., *J. Phys. Chem.*, 1996, **100**, 16282.
5. Sasaki, S.; Kawasaki, H.; Maeda, H., *Macromolecules*, 1997, **30**, 1847.
6. Kawasaki, H.; Sasaki, S.; Maeda, H., *Langmuir*, 1998, **14(4)**, 773.

SOLVENT EFFECTS ON THE REACTION RATE OF INTRAMOLECULAR FLUORIDE-ION EXCHANGE OF POLYFLUOROBISSILICATES

Eunsang KWON, Kenkichi SAKAMOTO, Chizuko KABUTO, and Mitsuo KIRA
Department of Chemistry, Graduate School of Science Tohoku University,
Aoba-ku Sendai 980-8578, JAPAN

We report herein solvent effects on the reaction rate of intramolecular fluoride-ion exchange of pentafluorobissilicates determined by dynamic NMR. As shown in eq.1 bissilicates **1a-c** were prepared using reactions of 9,9,10,10-tetrafluoro-9,10-disila-9,10-dihydroanthracene with potassium fluoride in the presence of 18-crown-6, tetraethylammonium fluoride, and tetrabutylammonum fluoride, respectively. We have found that the 1,4-disilacyclohexadiene moieties of **1a-c** take a boat form with a fluorine-bridge between two silicon atoms as determined by X-ray crystallographic analysis.

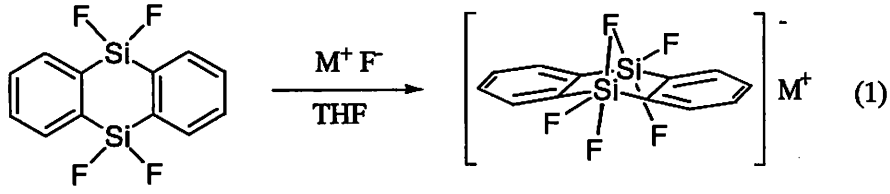

1a (96%, $M^+ = [K^+,18\text{-crown-6}]$)
1b (94%, $M^+ = Et_4N^+$)
1c (100%, $M^+ = Bu_4N^+$)

^{19}F NMR analysis of **1** showed rapid intramolecular fluoride-ion exchange even at low temperatures. The fluoride-ion exchange reaction would be synchronized with a ring inversion motion through a non-bridged intermediate (or a transition state) as shown in Figure 1.[1)]

The fluoride exchange rates were independent of the counter cations but significantly depended on solvent polarity. The rates were larger in polar acetone-d_6 than in relatively non-polar $CDCl_3$. The results suggest that a polar solvent stabilizes more the non-bridged form of **1** than the bridged form due to the negative charge localization on the pentacoordinate silicon moiety in the former.

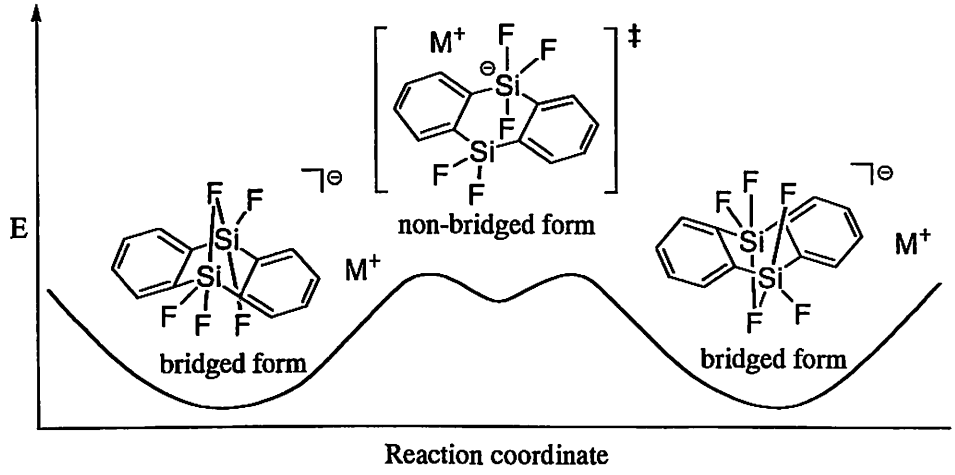

Figure 1. Energy diagram of fluoride-ion exchange reaction.

1) T. Hoshi, M. Takahashi, and M. Kira, *Chem. Lett.*, **1996**, 608.

Molecular Communication in Aqueous Solutions. Understanding and Using Hydrophobic Interactions

Niklaas J. Buurma, Laura Pastorello and Jan B.F.N. Engberts

Stratingh Institute, University of Groningen, Nijenborgh 4, 9747 AG Groningen, The Netherlands.

The hydrolysis of compounds **1a-d** (Scheme 1) is water-catalysed between pH 1.5 and 5.5. The reaction is retarded upon addition of the (hydrophobic) cosolutes EtOH (**2a**), n-PrOH (**2b**) and n-BuOH (**2c**).

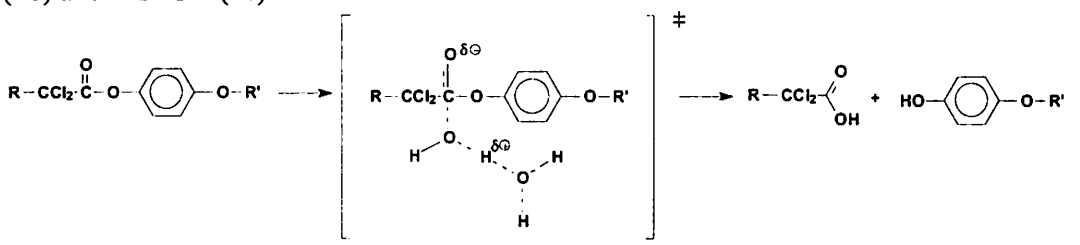

Scheme 1: R=H (**1a**), Me (**1b**), Et (**1c**), nPr (**1d**); R'=Me

Equation 1[1] is used to quantify the rate retardations.

$$\ln\left\{\frac{k(m_c)}{k(m_c=0)}\right\} = \frac{2}{R\cdot T\cdot m_0^2}\cdot\left[g_{cx} - g_{c\neq}\right]\cdot m_c - N\cdot\phi\cdot M_l\cdot m_c \qquad (1)$$

The equation yields the change in activation Gibbs energy [g_{cx}-$g_{c\neq}$], corrected for water activity changes in the solution (second term rhs), normally abbreviated G(C).

The observed rate retardation is interpreted using the concept of hydrophobic interactions. The retardation turns out to be dependent on the hydrophobicity of the cosolutes **2** but also on the hydrophobicity of the hydrolytic probes **1**, as can be seen from equation 2, in which the G(C) values in matrix-form are expressed as a cross-product of probe and cosolute contribution.

$$G(C) = S\cdot \boldsymbol{c}\times \boldsymbol{p} \qquad (2)$$

In this equation, S is a reaction specific scalar, $\boldsymbol{c}$ gives the relative rate retarding efficiency of the different cosolutes **2** and $\boldsymbol{p}$ represents the relative sensitivity of the hydrolytic probes **1**.

The G(C) values that are determined, together with isobaric activation parameters, can be used to increase the understanding of the hydrophobic interactions causing the rate retardation. The observed effects can be understood as resulting from encounter complex formation. The thermodynamics of these encounter complexes is readily explained using current knowledge of the hydration shell structure around apolar solutes.

Possible uses of hydrophobic interactions in simple designer catalysts are also being investigated and will be briefly discussed.

---

[1] Blokzijl, W; Engberts, J. B. F. N.; Jager, J.; Blandamer, M. J., *J. Phys. Chem., 1987, 91, 6022*

REACTION OF MOLECULAR CLUSTERS WITH A VINYL CATION IN ACETONITRILE

Yuji Hori[1] and Shinjiro Kobayashi[2]

[1] Department of Chemistry and Applied Chemistry, Saga University, 1 Honjyo-machi, Higashi-ku, Saga, 840-8502 Japan

[2] Institute for Fundamental Research of Organic Chemistry, Kyushu University, 10-1 Hakozaki 6-chome, Higashi-ku, Fukuoka, 812-8581 Japan

In a solution the solvent- and solute-molecules exchange their position rapidly, and they form clusters with hydrogen bond and dipole moment interaction between the molecules. Formation and disappearance of clusters depends on the size and the strength of the intermolecular bonding. Attack of nucleophilic clusters to a carbocation was investigated to get some information about reactivity of clusters by using laser flash photolysis technique.

Irradiation of laser flash (308 nm, 20 ns) to β,β-diphenyl-α-p-(methoxyphenyl)vinyl bromide in acetonitrile (5 x 10-5 M) in the presence of water gave β,β-diphenyl-α-p-(methoxyphenyl)vinyl cation as the reactive transient species which has the absorption maximum

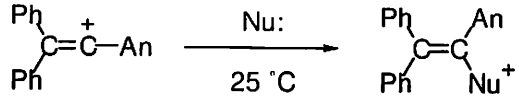

at 350 nm. The decay was followed by first order rate equation and the influence of the amount of the water was shown in figure. There was no linear relationship in the whole range and the second rate constants were calculated as 68,000 $M^{-1}s^{-1}$ and 9,190 $M^{-1}s^{-1}$ in the lower and the higher regions, respectively. This might mean the influence of the clusters of water(s) and acetonitrile.

We will discuss the effects of alchols, too.

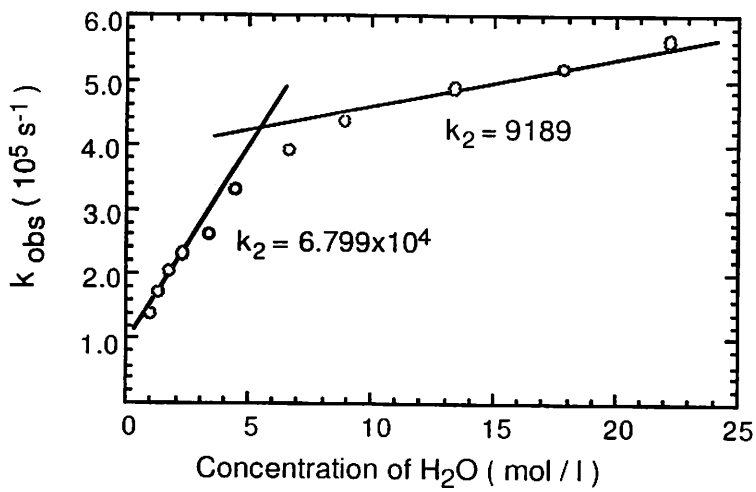

Solvolyses of β-arylethyl esters having strong electron-withdrawing groups at α- or β-position.

Mutsuo OKAMURA, Yoshihiro UMEZAWA, Ken HAZAMA, and Satoshi USUI
Graduate School of Science and Technology, Niigata University, Ikarashi, Niigata, 950-2181, Japan

The nature of carbocations that are destabilized by strongly electron-withdrawing substituents has been studied actively. However, the study of a destabilization in phenonium ion type carbocations was unexamined. We attempted to investigate the solvolyses of 2-aryl-2-(trifluoromethyl)ethyl system[1] where the phenonium ion intermediate must be destabilized by CF_3 group. The solvolyses were followed to 3 half-lives reaction by ^1H and/or ^{19}F NMR. The substituent effect in aryl-assisted solvolysis rates (k_Δ), where the direct π-interaction exists between 2-aryl and carbocationic reaction center, can be generally described by Yukawa-Tsuno Equation (1).

$$\log (k_X/k_H) = \rho(\sigma^\circ + r\,\Delta\bar{\sigma}_R^+) \qquad (1)$$

Enlarged r values (0.77 in acetic acid and 0.63 in 80% aqueous trifluoroethanol; TFE) observed on the solvolysis of 2-aryl-2-CF_3-ethyl nosylates **2** were larger than that of standard aryl-assisted solvolysis by 0.2. This enlargement should depend on a destabilization of aryl-assisted transition-state by an electron-withdrawing CF_3 group. This destabilization is offset a little by a stabilization effect of such enlarged electron-releasing resonance. On the other hand, the stabilization by polar solvent (TFE) makes such resonance smaller. These effects may compensate each other.

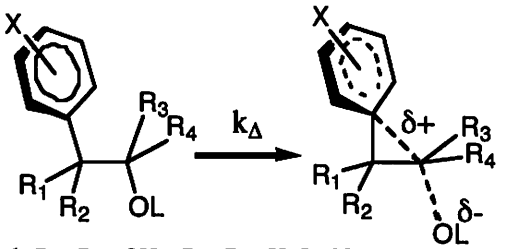

1 R_1=R_2=CH_3, R_3=R_4=H, L=Ns
2 R_1=CF_3, R_2=R_3=R_4=H, L=Ns
3 R_1=R_2=H, R_3=CF_3, R_4=CN, L=Tf
4 R_1=CF_3, R_2=CN, R_3=R_4=H, L=Tf
5 R_1=CH_3, R_2=R_3=R_4=H, L=Ts **a** X=OMe

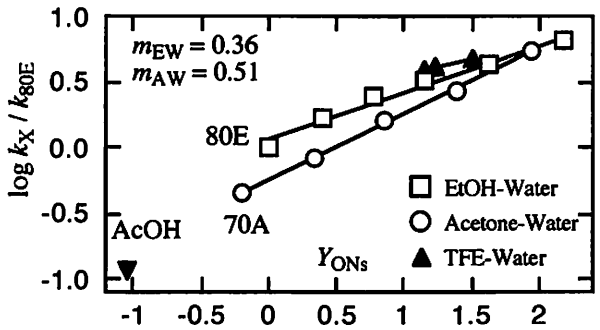

Fig. 1. The mY_{ONs} plots of solvent effect for the solvolyses of β-(*p*-methoxyphenyl)-β-CF_3-ethyl nosylates at 75°C.

Solvolysis rates of *p*-methoxy derivative **2a** were determined in a wide variety of solvents by conductometric method. In Figure 1, the solvolysis rates of **2a** are plotted, on a logarithmic scale, against the corresponding rates of 2-adamantyl nosylate. This split pattern appeared to be quite similar to that of neophyl substrates **1** which were typical examples of the aryl-assisted solvolysis.

Solvolyses of 2-*p*-methoxyphenyl-1-CF_3-1-CN-ethyl triflate **3a** having two strong electron-withdrawing groups were also examined. Interestingly, an aryl-migrated primary acetate **4a**(L=Ac) and triflate **4a** were produced simultaneously by a solvent addition (k_p) or a return (k_r) of the counter triflate anion on the phenonium ion pair in acetic acid. The fractionation factor F=0.67 (k_p/k_Δ) is larger than that of stable phenonium ion systems (e.g. 0.25 in **5a**). This return was not observed in 80% aq. acetone of a nucleophilic solvent and was small in 80% aq. TFE of a high ionization ability. Further investigations of the solvent effects on solvolysis rates and trap mechanisms of highly unstable phenonium ion pair are now in progress.

1. M. Okamura, K. Hazama et. al., *Chem. Lett.*, **1997**, 10, 973.

SOLVENT EFFECTS ON SOLVOLYSES OF β-SILYL SYSTEM

Mai UCHIDA,[1] Hyun-Joong KIM,[1] Ryoji FUJIYAMA,[2] Mizue FUJIO,[1] and Yuho TSUNO[1]

1 Institute for Fundamental Research of Organic Chemistry, Kyushu University, Fukuoka, 812-8581, JAPAN

2 Department of Chemistry, Faculty of Science, Kochi University, Kochi, 780-8520 JAPAN

The β-silicon substituent greatly facilitates the heterolysis of the C-Lv bond by 10^{12}-fold by TMS group in an antiperiplanar conformation. The β-silicon effect has been explained in terms of either the open form, stabilized by hyperconjugation or the bridged form. The difference between these mechanisms may be related to the position of Si atom, i.e., degree of charge delocalization.

The studies of the solvent effects provide the important information to estimate the transition state structure, especially regarding the charge-delocalization. In this study, we carried out the solvolyses of 2-aryldimethylsilylethyl chloride **I** and 2-aryl-2-trimethylsilylethyl chloride **II**, and the solvent effects were analyzed in terms of extended Winstein-Grunwald Equation (1) in order to estimate the charge-delocalization in the reaction center.

$$\log (k/k_{80E}) = m_c Y + m_d Y_{MeOCl} \qquad (1)$$

where Y and Y_{MeOCl} are ionizing power parameters of respective solvents for localized cation model (based on the solvolysis of *t*-BuCl) and delocalized one (based on that of *p*-MeO-*m*-Cl-Ph(*t*-Bu)CHCl), and m_c and m_d are susceptibilities of a given solvolyzing substrate.

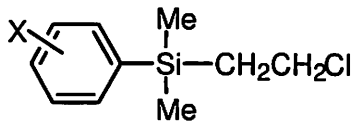

I

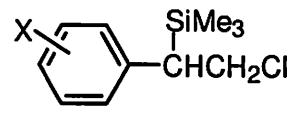

II

An extremely enhanced m_d (or $m_d/(m_c + m_d)$) value for **II** and a moderately enhanced value for **I** indicate large charge delocalization in the β-silyl systems compared with the corresponding β-alkyl systems.

SPECTROPHOTOMETRIC ACIDITY STUDIES OF STRONG NEUTRAL BRÖNSTED ACIDS IN ACETONITRILE AND HEPTANE

Ivo Leito, Ilmar Koppel, Toomas Rodima, Ivari Kaljurand
Institute of Chemical Physics, University of Tartu, 2 Jakobi St., Tartu 51014, Estonia

Spectrophotometric titration technique was used to establish pKa scale of strong acids in acetonitrile [1] and a pKa scale in heptane [2].

A continuous self-consistent quantitative UV-vis spectrophotometric pKa scale of strong neutral Brönsted acids in acetonitrile has been created. The scale consists of 36 compounds (phenols, phenylmalononitriles, sulfonimides, sulfonic acids and sulfonimides modified with Yagupolskii's superacceptor substituents) and 74 independent equilibrium constant measurements. The scale covers pKa range from 4 to 16 in acetonitrile - an acidity region that has been studied only very modestly. The present work together with the pKa data in the range 16 to 27 found in the literature furnish a pKa scale in acetonitrile with pKa values ranging from 4 to 27.

Measurements of acidity are commonly performed in polar media (water, DMSO, acetonitrile) or in the gas-phase. Solvents of low polarity have received only very modest attention as media for acidity measurements. Acidity data in solvents with dielectric constant less than 2 are practically nonexistent to date.

The reason for this low popularity of non-polar solvents as media for acidity measurements are the experimental difficulties, that arise. These solvents almost lack the ability to solvate charged particles, which greatly hampers the formation of ions. If nevertheless the ions are formed, then the very low dielectric constant of the medium causes them to aggregate into associates. Therefore the dissociation is largely masked and the determination of the corresponding dissociation constant is very difficult.

We have succeeded to overcome these difficulties and to develop a method for experimental determination of acidities in a nonpolar solvent heptane and to build a small pKa scale in heptane. The scale contains 6 compounds and 9 independent equilibrium constant measurements.

The experiments in both solvents were carried out as spectrophotometric titration of mixtures of two acids and yielded the difference in their pKa values as the result. To make the results more reliable, multiple overlapping experiments were carried out. This method of measurements eliminates the need for direct determination of the acidity of the medium, which is an important source of error in pKa measurements.

The measurements in heptane can be performed with such acids only, which give large anions with very delocalized charge, otherwise the formation of ion pairs and/or precipitates cannot be avoided. The titrant for the titration in heptane must be a strong base and its protonated form must have delocalized charge. We use phosphazenes - extremely strong bases giving highly delocalized cations - for the titration.

Work is in progress to further extend the pKa scales in acetonitrile and heptane both upwards and downwards. Heptane is particularly promising in this respect, as very high and very low acidities can in principle be studied in this solvent.

1. Leito, I.; Kaljurand, I.; Koppel, I. A.; Yagupolskii, L. M.; Vlasov, V. M. *J. Org. Chem.* **1998**, *63*, 7868-7874.
2. Leito, I.; Rodima, T.; Koppel, I. A.; Schwesinger, R.; Vlasov, V. M. *J. Org. Chem.* **1997**, *62*, 8479-8483.

THE SUPERPROMOTION OF STRONG BROENSTED ACIDS

B.I.Popov. S.G.Hismatullin, V.D.Surkov
Sterlitamak Petrochemical Plant. 453110,Bashkortostan,Russia

The low carbonyl compounds (LCC) are the most active promoters of Specific acidity of hydrocarbons RH or RX solvents (Sol. here: X- = Cl-, Br-, J-. R'Z- or R'C=ZZ-: Z = -O- or -- : R'- = hydrogen, alkyl or aryl), in witch strong Broensted acid $(HA)_nSol$ (aqua complexes of titanium(IV), tin(IV), stibium(V) chlorides, bromine or fluoric hydride, sulphuric, benzene sulphonic, pyrophosphoric, cation exchanger in H-form sulpho resin, high-siliceous zeolites and some other) was soluted, emulsifed or suspended.
In compliance with increase Acidity Ho-function LCC arrange in series: acetaldehide > acetyl acetone > acetone > acetophenone > propylene glycol carbonate > acetic anhydride > acetic ether.

By injection in Sol equimolar (equivalent, relative to $(HA)_nSol$) amount of acetaldehide Acidity -Ho-function increase by 2 - 4 units, that exceeds 1 - 2 unites, when the most active of well-known promoters phenol is injected.

The LCC promotic effect probably is connected with the fast part of$(HA)_nSol$ neutralization in micelle, emulsion or suspension phase according to Hlasko-Usanovitch:

$$(HA)_n\,Sol + p\;O{=}C(R_1)R_2 \;\overset{K_{Sol}}{=}\; p(H^+{---}O{=}C(R_1)R_2 \leftrightarrow \underbrace{H\text{-}O\text{-}C^+(R_1)R_2}_{(HOR^+)}) + A_p^-\,(HA)_{n-p}\,Sol$$

(here: R1 and R2- hydrogen, methyl, phenyl or acetonyl)

with the formation of frue solution of relatively soft by Pearson, that is characterized by considerable activity coefficient value of primare carbenium ions HOR^+, which acidity determines the quantity of Sol Ho-function. Thus, by promotion the interphasal H^+ or D^+ tunneling takes place. The opposite ions $A_p^-(HA)_{n-p}Sol$ stabilization is realized by means of specific interaction inside the micelle, emulsion or suspension.

LCC can be used as promoters of Friedel-Crafts and related reactions.

CONCENTRATED SALT EFFECTS ON THE SOLVOLYSIS RATES IN THE MIXED SOLVENT OF 1,4-DIOXANE AND H_2O

Masashi Hojo, Tadaharu Ueda, Masanori Yamasaki, Sunao Inoue, and Yuri Kawahara
Department of Chemistry, Faculty of Science, Kochi University, Akebono-cho, Kochi 780-8520, Japan

In the mixed solvent of 50 vol% 1,4-dioxane and H_2O, the concentrated salt effects of alkali metal (M^+) and alkaline-earth metal (M^{2+}) perchlorates were investigated on the solvolysis rates of aliphatic halides (RX) and the related compounds. The "pseudo" first-order reaction rates (k/s^{-1}) of typical S_N1 substrates, e.g., adamantyl chloride and bromide, increased exponentially with increasing concentration of the metal salts (cf. Fig. 1). The M^{2+} effects were larger than those of M^+: Li^+, Na^+ < Mg^{2+}, Ba^{2+}. A non-metallic salt, Et_4NBr, of ≥1.0 mol dm^{-3} caused the log k value to decrease, although the log k was slightly increased by the lower concentration of the salt (< 1.0 mol dm^{-3}). The increase in the log k values in the presence of metal ions were explained by the direct chemical interaction between the halide ions and the metal ions in the modified media: X$^-$---M^+ or X$^-$---M^{2+}. The decrease in the log k value in the presence of Et_4NBr seemed to be based on the decrease in the activity of water.

Concentrated salt effects on the solvolyses of S_N1-S_N2 intermediate and typical S_N2 substrates were also examined. The solvolysis rates of ethyl bromide and methyl tosylate were much decreased by the addition of concentrated $LiClO_4$, while the values of benzyl chloride and bromide were slightly increased. Almost no effects were observed on the "apparent" rates of the solvolysis of isopropyl bromide. The salt effects became more positive by the introduction of methyl substituents on benzyl chloride, though negative by the introduction of electron-withdrawning substituents, such as, Cl, NO_2, or CN. The Li^+ effects on 4-methylbenzyl chloride were even similar to those on t-butyl chloride. The S_N1 substrate could be easily differentiated from others by observing a substantial increase in the rate constant in the presence of 1.0 mol dm^{-3} $LiClO_4$ in the mixed solvent. The results in MeOH-H_2O[1] and acetone-H_2O[2] were compared with the present results.

The interactions between carbocations (R^+) and the mother compounds (RX) in acetonitrile observed by ^1H NMR were discussed in this connection.

1. Manege, L. C.; Ueda, T.; Hojo, M.
Bull. Chem. Soc. Jpn., 1998, **71**, 589.
2. Manege, L. C.; Ueda, T.; Hojo, M.; Fujio, M.
J. Chem. Soc., Perkin Trans. 2 1998, 1961

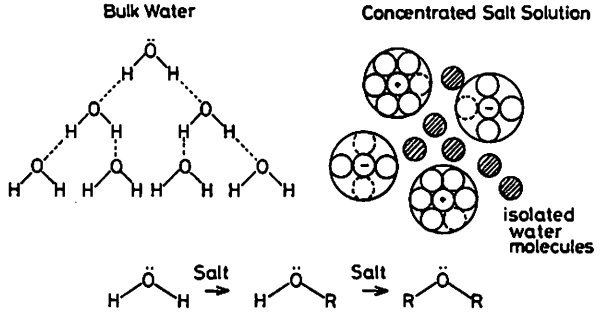

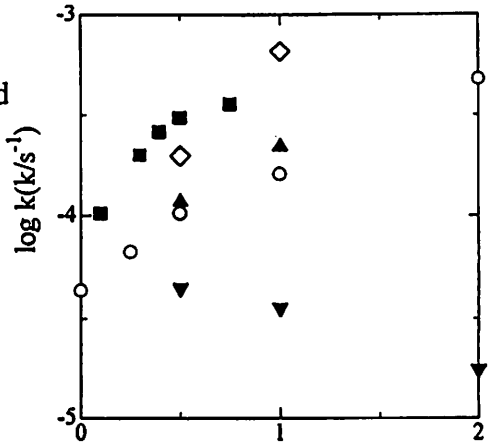

Fig. 1. Changes in the solvolysis rates of 1-adamantyl bromide with the addition of various salts in 50 vol% 1,4-dioxane-H_2O at 35°C: (○)$LiClO_4$; (▲)$NaClO_4$; (■)$Mg(ClO_4)_2$; (◇)$Ba(ClO_4)_2$; (▼)Et_4NBr.

GENERATION OF THE 2,2-DIETHOXYCYCLOPENTANE-1,3-DIYL SINGLET DIRADICAL: ITS ZWITTERIONIC CHARACTER PROVED BY SOLVENT EFFECTS ON THE LIFETIME AND THE CHEMICAL BEHAVIOR

Manabu Abe,[†] Waldemar Adam,[‡] Werner M. Nau[§] and Masatomo Nojima[†]

[†]Department of Materials Chemistry, Faculty of Engineering, Osaka University, Suita 565-0871, Osaka Japan, tel.: +81-6-6879-7930, fax: +81-6-6879-7928, e-mail: abe@ap.chem.eng.osaka-u.ac.jp; [‡]Institut für Organische Chemie der Universität Würzburg, Am Hubland, D-97074 Würzburg, Germany; [§]Institut für Physikalische Chemie der Universität Basel, Klingelbergstrasse 80, CH-4056 Basel, Switzerland

The theoretical prediction of the substituent effects at C-2 position of diradicals **1** on the ground-state spin-multiplicity has been investigated by Borden; a triplet ground state is preferred for X = H, a singlet ground state is preferred for X = F, SiH_3.[1] Although the triplet ground-state for **1a** (X = H) was experimentally confirmed by the EPR measurements, the ground-state spin-multiplicity for **1b** (X = F) has not been experimentally reported until our recent work.[2] Furthermore, we have also discovered the singlet ground-state of the 2-spiroepoxy diradical **3** and its zwitterionic character.[3] In the present poster-presentation, we would like to report our most recent study on the 2,2-diethoxycyclopenatne-1,3-diradical **4**.

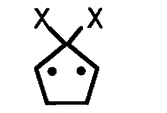

1a(X = H)
1b(X = F)
1c(X = SiH_3)

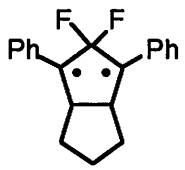

2

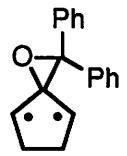

3

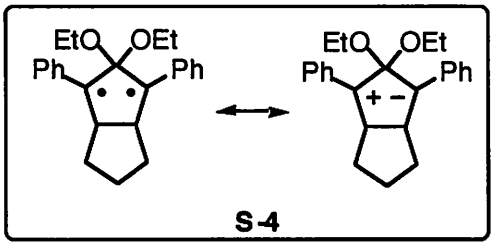

S-4

The diradical **4** was generated by photo-denitrogenation of the corresponding diazene. Under the irradiation of the diazene in a 77 K MTHF matrix, the persistent species (λ_{max} 566 nm) was observed, although the EPR signals were silent. The results strongly suggested the singlet ground-state of the 2,2-diethoxy-1,3-diradical **4**. In order to study the property of the singlet diradical **4**, the lifetime was directly measured by means of time-resolved (ns) flash photolysis. The lifetime of the singlet diradical **4** (λ_{max} 550 nm) increased with increasing solvent polarity ($\tau_{n\text{-}hexane}$ 480 ns, τ_{CH3CN} 835 ns). The strong solvent dependence on the lifetime of the diradical **4** can be explained by its inherent zwitterionic character[4]. The more detailed results will be discussed in the poster presentation.

[1]W. T. Borden et al., *J. Am. Chem. Soc.* (1994 and 1998). [2]W. Adam et al., *ibid.* (1998). [3]M. Abe and W. Adam et al., *ibid.* (1998). [4]L. Salem, *Angew. Chem.* (1972).

ACYL VS. NITROGEN PROTONATION IN CARBOXYLIC AND NON-CARBOXYLIC AMIDES IN THE GAS PHASE AND IN SOLUTION. PATTERNS OF NMR PROPERTIES AND HYDRATION ENERGIES

Alessandro BAGNO,[1] Bogdan BUJNICKI,[2] Sylvie BERTRAND,[1] Clara COMUZZI,[1] Fabrizio DORIGO,[1] Pierre JANVIER,[1] and Gianfranco SCORRANO[1]

[1] Centro CNR Meccanismi Reazioni Organiche, Dipartimento di Chimica Organica, Università di Padova, via Marzolo 1, 35131 Padova, Italy

[2] Center of Molecular and Macromolecular Studies, Polish Academy of Sciences, Lódz, Poland

Amides with the general formula *Acyl*-NR_2, where *Acyl* is a group derived from an organic or inorganic acid (*e.g.* RC(O)O, RS(O), RSO_2, NO, NO_2, CN, etc.), are species of widespread occurrence. All such compounds behave as bases of widely varying strength, and possess more than one site for protonation, *i.e.* the nitrogen atom and a basic atom in the acyl moiety, most often N, S, or O. Therefore, under moderately acidic conditions (*i.e.* only capable of mono-protonation) an ambiguity exists with regard to the preferred site of protonation.

We present the results of a combined experimental and theoretical effort to determine the protonation site of representative amides derived from various acids: carboxamides, thiocarboxamides, sulfenamides, sulfinamides, sulfonamides, nitrosamides, nitramides, cyanamides, phosphorous and phosphoric triamides both in the gas phase and in water.[1] All these compounds may undergo protonation at either the amide nitrogen or at one of the atoms contained in the acyl group (O, N, P, S). Thus, we have monitored the changes in the NMR chemical shifts and longitudinal relaxation rates of ^{14}N , ^{17}O and ^{31}P in solutions containing either the neutral or the protonated form. These are compared with the theoretically calculated nuclear shieldings and quadrupolar coupling constants. Relative energies in water of the possible protonated forms have been calculated with the IPCM continuum method. It is shown that NMR properties and calculated energies allow one to pinpoint the most stable protonated form.

1. Bagno, A.; Bujnicki, B.; Bertrand, S.; Comuzzi, C.; Dorigo, F.; Janvier, P.; Scorrano, G. *Chem. Eur. J.* **1999**, *5*, 532.

THEORETICAL STUDY ON COVALENT HYDRATION ON PTERIDINE (1)

Kazuhide NAKATA[1], Kazuhiko HONDA[2], Kichisuke NISHIMOTO[3] and Kyuji OHTA[1]

[1] Department of Chemistry, Faculty of Liberal Arts, Hosei University, Fujimi 2-17-1, Chiyoda-ku, Tokyo 102-8160, Japan

[2] School of Information Culture, Nagoya Bunri University, Maeda 365 Inazawa-Cho Inazawa, 492-8520, Japan

[3] Osaka City University, Kamotanidai 1-37-10, Sakai, Osaka, 590-0138, Japan

Pteridine (**1**), which is a nitrogen containing heterocyclic compound, has some C-N double bonds where water molecule(s) can be added covalently. Under neutral condition, 1:1 adduct of pteridine and water, i.e., 3,4-hydrated pteridine (**2**), is generated to give equilibrium mixture with non hydrated pteridine (**Scheme 1**).[1,2] Under acidic condition, **2** is generated first, followed by slow formation of 1:2 adduct (5,6,7,8-dihydrated pteridine, **3**) (**Scheme 2**).[3] This hydration reaction is a good object to investigate kinetic and thermodynamic control.

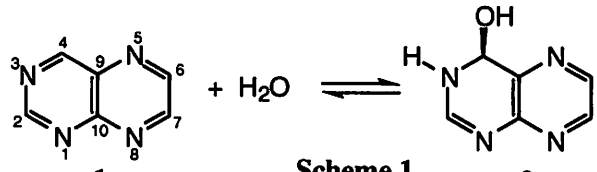

1 **Scheme 1** **2**

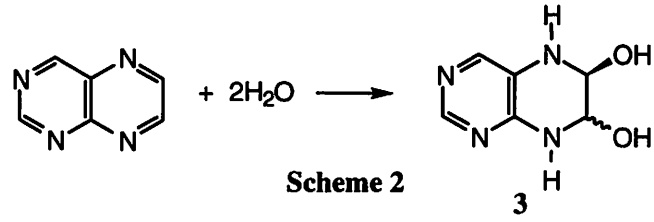

Scheme 2 **3**

It is known experimentally that the reaction proceeds via a mixed mechanism of specific acid (i) and base (ii) and water (iii) catalyses.[4] Therefore, it is important to make clear the effect of solvent on the reaction mechanisms of scheme 1 and 2. In this point of view, geometries of reactants, products, and transition states for possible hydration processes are optimized by means of theoretical calculation with consideration of solvent effect. Geometric features and origin of this reaction will be discussed.

1. D. D. Perrin, *J. Chem. Soc.*, 1962, 645.

2. A. Albert and K. Ohta, *J. Chem. Soc. (C)*, 1971, 2357.

3. A. Albert, T. J. Batterham, and John J. McCormack, *J. Chem. Soc. (B)*, 1966, 1105.

4. Y. Pocker, D. Bjorkquist, W. Schaffer, and C. Henderson, *J. Am. Chem. Soc.*, 5540, **96**, 1974.

ROLE OF SOLVENT IN HYDROLYSIS: AB INITIO MD ANALYSIS

Hiroshi YAMATAKA[1], Misako AIDA[2] and Michel DUPUIS[3]

[1] Institute of Scientific and Industrial Research, Osaka University, Ibaraki, Osaka 567-0047 Japan

[2] Faculty of Science, Hiroshima University, Kagamiyama, Higashi-Hiroshima 739-8526 Japan

[3] Pacific Northwest National Laboratory, EMLS/K1-83, Battelle Blvd, Richland WA 99352 USA

The methyl chloride hydrolysis (eq 1) is a type II S_N2 reaction according to Ingold's classification. The attacking species is a water molecule which loosens a proton to a solvent water

$$nH_2O + CH_3Cl \rightarrow CH_3OH + (n-1)\,H_2O + HCl\,. \qquad (1)$$

molecule, so that the hydroxide ion formally substitutes the chloride ion in methyl chloride. Thus during hydrolysis, bond breaking and bond formation involving both solute and solvent molecules take place. It is essential, therefore, to take the solvent molecules explicitly into consideration in analyzing the methyl chloride hydrolysis. Ab initio MO calculations (HF/3-21G, HF/6-31G, HF/6-31+G*, HF/6-31++G** and MP2/6-31+G*) were carried out in which solvent water molecules up to 13 were considered. The precursor complex, transition state (TS), product complex, and final complex were detected for each of the systems. It was found that the attacking water molecule kept two hydrogen atoms at the TS. The solute and solvent kinetic isotope effects (KIEs) were calculated and compared with the experimental KIEs. The calculated results for the system with 13 water molecules reproduced well the experimental energetics and deuterium KIEs. In this system, CH_3Cl is surrounded by 13 water molecules without any apparent vacant space and there exists hydrogen bonding water networks connecting the nucleophile water molecule and the chloride leaving group.

Ab initio MD simulations at the HF/6-31G level were performed at 298 K on the methyl chloride hydrolysis with explicit consideration of three water molecules. This system was chosen because there also exists a hydrogen-bonding network between the attacking water and Cl^-. In the backward reaction, the system reached the reactant complex region within 50 fs soon after TS. In the forward reaction, different reaction paths were observed. One was a path in which the system reached an intermediate complex (complex-P1) region after nearly concerted proton transfer relay involving the attacking water molecule and the solvent water molecules. The process from TS toward the complex-P1 region was similar to the IRC path, while in the MD trajectories thermal motions of the atoms led the system further to the other intermediate complex (complex-P2) region. The other reaction path was found in which the system reached the complex-P2 region directly after the proton transfers. In all the trajectories, the back proton transfers led the system eventually to the final complex region.

Ab initio Theoretical Study of Chemical Reaction in Solution by RISM-SCF method

Hirofumi SATO[1], Yuuichi HARANO[2] and Fumio HIRATA[1]

[1]Department of Theoretical Study, Institute for Molecular Science, 444-8585, Japan

[2]Graduate School of Science and Technology, Kobe University, 657-0851, Japan

Great development of recent experimental techniques makes it possible to reveal detailed mechanism of chemical processes and provide us various information in the molecular level of description in the gas phase. At the same time theoretical studies have scored great success. Quantum chemical method such as ab initio molecular orbital (MO) method has been able to treat various types of problems.

However, when it comes to molecules in solutions, the situations are completely different. One of difficulties to deal with the liquid system lies in a virtually infinite number of degrees of freedom concerned with a process. Since it is impossible to solve the Schrödinger equation for entire system including about 10^{23} molecules, the most promising approach is a hybrid between quantum solute, which is described in ab initio MO method, and classical solvent.

Recently, we have proposed a new method referred to as RISM-SCF based on the ab initio electronic structure theory and the integral equation theory of molecular liquids (RISM).[1,2] The statistical solvent distribution around solute is determined by the electronic structure of solute, while the electronic structure of the solute is influenced by the solvent distribution. The Hartree-Fock equation and the RISM equation should be solved in a self-consistent manner. We have applied the method to a variety of chemical processes in solution including the coupled solvent and substitution effects on proton affinity, tautomerization in organic solvent, acid-base equilibrium and so on.

The RISM-SCF method has been also successful in exploring a several types of chemical reactions in solution, such as Menshutkin type II SN2 reaction in aqueous solution (Computed free energy curve is shown in the Figure),[3] and Diels-Alder reaction in a various thermodynamical conditions of water. In this presentation, we will report recent theoretical efforts for dealing chemical reaction in solution phase.

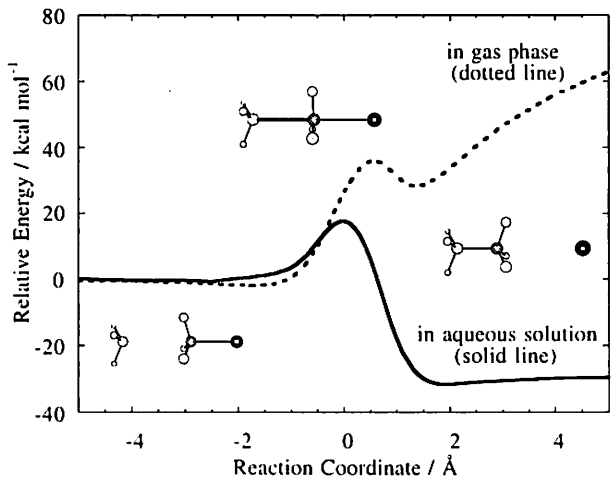

1 Ten-no, S.; Hirata, F.; Kato, S., *Chem. Phys. Lett.*, 1993, **214**, 391.
Ten-no, S.; Hirata, F.; Kato, S., *J. Chem. Phys.*, 1994, **100**, 7443.

2 Sato, H.; Hirata, F.; Kato, S., *J. Chem. Phys.*, 1996, **105**, 1546.

3 Naka, K.; Sato, H.; Morita, A.; Hirata, F.; Kato, S., *Theor. Chem. Acc.*, in press.

ESTIMATION OF ΔS AND ΔV FOR CONFORMATIONAL EQUILIBRIUM BY SCRF-MO CALCULATION

Isao ABE, Minoru KATO and Yoshihiro TANIGUCHI
Department of Chemistry, Faculty of Science and Engineering, Ritsumeikan University, Noji-higashi 1-1-1, Kusatsu, 525-8577, Japan

Solvent effects on conformational equilibrium have been studied for many molecular species to understand geometric property of molecules in solvents and predict the most stable molecular conformation in a solvent. However, most of them focused on free energy of isomerization ΔG, and there have been few studies of solvent effects on entropy ΔS and volume ΔV of isomerization. In general, solvent effect on ΔS was neglected, i.e. solvent effect on ΔG and enthalpy ΔH were assumed to be same amount.

The way we used to estimate ΔS and ΔV of isomerization in a solvent is as follows. First, we calculated Gibbs free energy of isomerization ΔG by IPCM or SCI-PCM SCRF-MO calculation of GAUSSIAN94, like in the work of Wiberg *et al*[1]. In IPCM and SCI-PCM calculation, the solvent effect on ΔG is a function of only two parameters : dielectric constant ε of the solvent and electron density ρ at cavity surface (or cavity volume υ) of the solute.

$$\Delta G = \Delta G_{\mathrm{ref}} + \Delta G_{\mathrm{elec}}(\varepsilon, \rho) = \Delta G_{\mathrm{ref}} + \Delta G_{\mathrm{elec}}(\varepsilon, \upsilon)$$

By differentiating this equation with respect to temperature or pressure, we obtain

$$\Delta S = \Delta S_{\mathrm{ref}} - \frac{3}{(2\varepsilon+1)^2}\left(\frac{\partial \varepsilon}{\partial T}\right)_p\left(\frac{\partial \Delta G_{\mathrm{elec}}}{\partial \mathrm{K}}\right)_\upsilon + \frac{\alpha}{\upsilon}\left(\frac{\partial \Delta G_{\mathrm{elec}}}{\partial \upsilon^{-1}}\right)_\varepsilon$$

$$\Delta V = \Delta V_{\mathrm{ref}} + \frac{3}{(2\varepsilon+1)^2}\left(\frac{\partial \varepsilon}{\partial p}\right)_T\left(\frac{\partial \Delta G_{\mathrm{elec}}}{\partial \mathrm{K}}\right)_\upsilon + \frac{\kappa_T}{\upsilon}\left(\frac{\partial \Delta G_{\mathrm{elec}}}{\partial \upsilon^{-1}}\right)_\varepsilon,$$

where α, κ_T, and K are expansion coefficient, isothermal compressibility, Kirkwood function [$\mathrm{K} = (\varepsilon - 1)/(2\varepsilon + 1)$], respectively. We define the reference system as perfectly non-polar continuum ($\varepsilon = 1$) and estimated ΔS and ΔV from the above equations. All SCRF-MO calculations were implemented on HP EXEMPLAR X-class.

We will show the result for *trans-gauche* rotational equilibrium of 1,2-dichloroethane and discuss the validity of our method by comparing experimental results[2].

1. Wiberg, K. B.; Keith, T. A.; Frisch, M. J.; Murcko, M., *J. Phys. Chem.*, 1995, **99**, 9072.
2. Kato, M.; Abe, I.; Taniguchi, Y., *J. Chem. Phys., in submission.*

Variety of Behavior of Rate in Thermal Isomerization of 6-Nitrospiropyran in Binary Mixtures of Alcohols with Aprotic Solvents

Shunzo YAMAMOTO, Toshio TSUKAMOTO and Yoshimi SUEISHI
Department of Chemistry, Faculty of Science, Okayama University, 3-1-1, Tsushima-naka Okayama, 700, Japan

Jacques studied behavior of some phenomena in CH_3CN/2-propanol mixtures, and found synergistic effects for the $E_T(30)$ parameter and the spiropyran relaxation rate for 6-nitrospiropiran.[1] The synergistic behavior for the $E_T(30)$ parameter was widely investigated in various mixed solvents, and it was explained by the model based on two solvent exchange equilibria.

In the present study, we measured the isomerization rate for 6-nitrospiropyran in various polar aprotic/protic mixed solvents. Fig. 1 shows plots of the rate constant versus the molar composition of the acetonitrile(AN), dimethylacetoamide(DMA) and dimethyl sulfoxide (DMSO)/t-butyl alcohol(TBA) mixtures. In AN/TBA mixtures, the synergistic effects are clearly evidenced. In DMSO/TBA mixtures, the rate constant increases rather monotonously with increasing the mole fraction of TBN. In DMA/TBA mixtures, the rate constant is almost constant in the region of low composition of TBA and then increases with increasing the mole fraction of TBA.

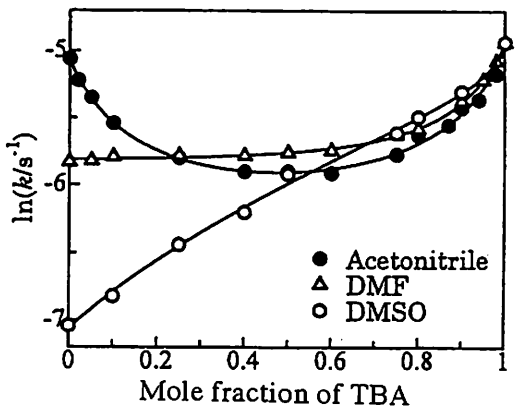

Fig. 1. Plots of $\ln(k/s^{-1})$ *vs.* mole fraction of TBA

Binary mixtures of dipolar hydrogen-bond acceptors (HBA solvents) with hydrogen-bond donors (HBD solvents) often show $E_T(30)$ values higher than those of the two pure solvent components. This synergism is produced by hydrogen bonding between the HBA and the HBD to give a hydrogen-bonded complex, which is more polar than either of the two pure solvents. As is shown in Fig. 1, the k-value decreases with decreasing mole fraction of TBN in all cases. This shows that in this region the hydrogen-bonded complexes are formed bentween aprotic solvents and TBA and these complexes are more polar than TBA. The behavior of the rate constant observed in the region of low TBA composition in the binary mixtures seems to depend on the polarities of the hydrogen-bonded complexes, compared with those of aprotic solvents. For AN, the complex has higher polarity than AN, and in this case, the synergism appeares. For DMSO, the polarity of the complex is lower than that of DMSO, and the rate constant changes monotonously. For DMA, the polarity of the complex is similar to that of pure DMA, and the rate constant does not change in the region of low TBA composition. We discuss the results in term of the model mentioned above.

1) P. Jacques, *Chem. Phys. Lett.*, 1990. **171**, 353..

Solvent Effect on the Solvolyses of β,β'-Disilyl Compounds

Ryoji FUJIYAMA[1], Tetsuya MOTOKI[1], and Mizue FUJIO[2]

1 Department of Material Science, Faculty of Science, Kochi University, Akebono-cho, Kochi-shi, 780-8520, Japan

2 Institute for fundamental Research of Organic Chemistry, Kyushu University, Hakozaki, Higashi-ku, Fukuoka 812-8581, Japan

The ability of β-silyl groups to stabilize cations or to promote the formation of cations is well-known as β-silicon effect. The β-silicon effect has been explained in terms of either hyperconjugation or bridged assistance. Both mechanisms involve the delocalization of cation. Recently, Tsuno and Fujio have been proposed the extended Winstein-Grunwald Equation for estimating of π-delocalization. [1]

$$\log(k/k_{80E}) = m_C Y_{OTs} + m_\Delta Y_\Delta$$

where Y_{OTs} and Y_Δ scales are based on 2-adamantyl and p-methoxyneophyl tosylates as reference substrates, respectively, for a localized cation and an entirely delocalized cation. The adjustable blending parameters m_C and m_Δ reveal the extent to which any substrate approaches adamantyl (m_C=1, m_Δ=0) or p-methoxyneophyl (m_C=0, m_Δ=1) in behavior.

In this study, this extended Winstein-Grunwald Equation was applied to the solvent effect analysis on the solvolysis of 1,3-di(trimethylsilyl)-2-propyl 3,5-dinitrobenzoate without π–electron in the alkyl moiety. The solvolysis rates were determined in a wide variety of solvents (aq.EtOH, aq. MeOH, aq. acetone, and aq. TFE). The extended Winstein-Grunwald analysis gave a good correlation with m_C =0.39 and m_Δ=0.08 , though the leaving group of this substrate is 3,5-dinitrobenzoate and a leaving group also affects solvent effect. Small m values have been obtained for aryl-stabilized carbocation solvolyses. Therefore, these small m values suggest the delocalized cation by β-silyl groups, in the transition state. Tsuno and Fujio have also been proposed $M_\Delta = 0.51m_\Delta/(0.51m_\Delta + m_C)$, that would estimate the degree of charge delocalization into the aryl π system or of the aryl assistance in the solvolysis transition state.[2] The M_Δ value was calculated to be 0.10. This small value corresponds to the simple aliphatic solvolysis (localized cation). Clearly, the delocalization of cation by β-silyl group is different from that by aryl group. This unique behavior of β-silyl compound for m values may be responsible for the Si-C bond hyperconjugation.

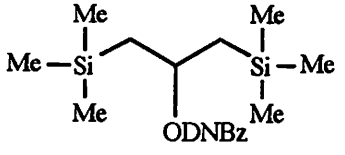

1. Fujio, M; Saeki, Y.; Nakamoto, K.; Yatsugi, K. et al. , *Bull. Chem. Soc. Jpn.*, 1995, **68**, 2603.
2. Fujio, M; Saeki, Y.; Nakamoto, K.; Kim, S.H. et al., *Bull. Chem. Soc. Jpn.*, 1996, **69**, 751.

STRUCTURAL EFFECTS ON THE STABILITY OF HYDROGEN-BONDED COMPLEXES IN THE GAS PHASE

Masaaki MISHIMA and MUSTANIR
Institute for Fundamental Research of Organic Chemistry, Kyushu University, Hakozaki 6-10-1, Higashi-ku, Fukuoka, 812-8581, Japan

Hydrogen bond is a fundamental feature of chemical structure and reactivity. There is much interest in the ability of hydrogen bonds to stabilize ions to understanding a wide variety of phenomena including solvation of ions and enzymatic stabilization of complexes and transition states. Solvation is known to play a large role in both the stability and structure of hydrogen bonded complexes.[1] The intrinsic stability of hydrogen-bonded ionic complexes which is given from gas-phase studies can provide information about the intrinsic character of hydrogen bond. Linear free energy relationships are often observed between the complexation energy and the difference in acidity and basicity of the neutral and ion. However, these relationships are based on a small range of acidity and basicity.

In order to elucidate the intrinsic relationship between hydrogen bond strength and the stability of ion, the thermodynamic stabilities of methanol-bound benzyl alkoxides have been determined by using FTICR spectrometry, as well as the acidities of benzyl alcohols. Methanol bound anions were generated according to Riverose reaction.[2,3] The binding energies between alkoxides and methanol were estimated based on the thermodynamic cycle.

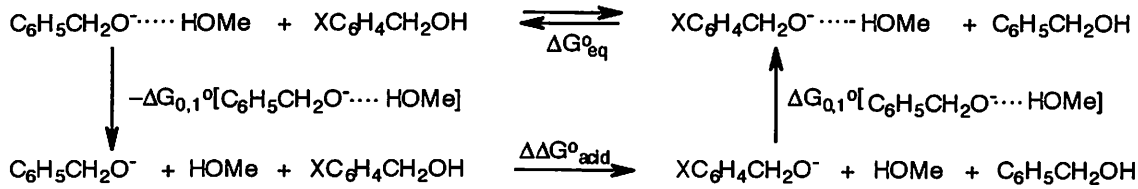

The hydrogen bond strength decreases linearly as the acidity of benzyl alcohol decreases, with a slope quite close to 0.6, corresponding to a hydron shared between the two oxygens. This linear relationship is consistent with that observed for simple alkyl alkoxides including $[MeOHOMe]^-$, suggesting that there is no additional stabilization for symmetric $[ROHOR]^-$.

In addition, ab initio MO calculations using the 6-31+G* basis set were carried out for a comparison with experimental results.

1 Perrin, C. L.; Nielson, J. B. *J. Am. Chem. Soc.* **1997**, *119*, 12734-12741.
2 Caldwell, G.; Rozeboom, M. D.; Kiplinger, J. P. ; Bartmess, J. E. *J. Am. Chem. Soc.* **1984**, *106*, 4660.
3 McIver, Jr. R. T.; Scott, J. A.; Riverose, J. M. *J. Am. Chem. Soc.* **1973**, *95*, 2706.

SOLVOLYSIS OF VINYL IODONIUM SALTS

Tadashi OKUYAMA
Department of Material Science, Himeji Institute of Technology,
Kamigori, Hyogo 678-1297, Japan

1-Alkenyl(phenyl)iodonium ion is a positively charged species with a good leaving group, iodobenzene, that can be a potential precursor of a vinylic cation. Solvolyses of alkenyliodonium salts **1**-**5** are examined in alcoholic and aqueous solutions as well as in acetic acid.

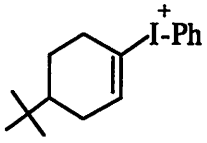
1

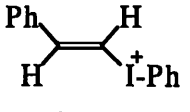
2

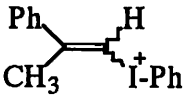
3

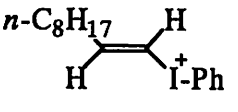
4

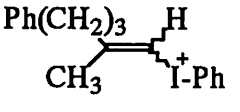
5

All the salts undergo readily solvolysis at about 50-60 °C, but product profiles indicate that several types of reactions are involved, including substitution, α-elimination, β-elimination, rearrangements, and recombination of the vinylic cation with iodobenzene.[1] A 1-cyclohexenyliodonium salt **1** gives both substitution (cyclohexanone derivatives and iodobenzene) and recombination products (mainly 1-(4-*t*-butyl-1-cyclohexenyl)-2-iodobenzene) through a cyclohexenyl cation intermediate. Solvolysis rates are only slightly dependent on the solvent ionizing power Y_{OTs} with m = 0.12, and show that iodobenzene is about 10^6 times as good a nucleofuge as triflate.

(*E*)-Styryliodonium salt **2** solvolyzes via vinylenebenzenium ion due to β-phenyl participation to give the *E* product (retention).[2] The accompanying reactions are the S_N2 substitution to give the product of inversion and α-elimination to lead to phenylacetylene. The *E* isomer of **3** behaves in a similar manner to **2** but is about 200 times more reactive. By contrast, the *Z* isomer reacts much slowly (*E*/*Z* = 200-4000).

Solvolysis of the β-monoalkyl derivative **4** results in substitution (mainly inversion) and α-elimination without any sign of formation of vinylic cation. The β,β-dialkyl derivative **5** readily solvolyzes mainly with β-alkyl participation to extensively give rearranged products of substitution and elimination as well as α-elimination.[3] Rates for solvolyses of **2** and **5** are essentially independent of solvent polarity but seem to increase with solvent nucleophilicity/basicity probably due to the α-elimination.

References

1) Okuyama, T.; Takino, T.; Sueda, T.; Ochiai, M., *J. Am. Chem. Soc.*, 1995, **117**, 3360.
2) Okuyama, T.; Ochiai, M., *J. Am. Chem. Soc.*, 1997, **119**, 4785. *Bull. Chem. Soc. Jpn.*, 1999, **72**, 163.
3) Okuyama, T.; Sato, K.; Ochiai, M., *Chem. Lett.*, **1998**, 1177.

SOLVENT EFFECT ON PHOTOREACTION OF C_{60} WITH DISILIRANE

Yutaka MAEDA,[1] Ryu SATO,[1] Takatsugu WAKAHARA,[1] Takeshi AKASAKA,*[1] Mamoru FUJITSUKA,[2] Osamu ITO,[2] Kaoru KOBAYASHI,[3] Shigeru NAGASE,[3] Masahiro KAKO,[4] Yasuhiro NAKADAIRA[4]

[1] Graduate School of Science and Technology, Niigata University, Niigata 950-2181, Japan
[2] Institute for Chemical Reaction Science, Tohoku University, Sendai, 980-8577, Japan
[3] Department of Chemistry, Graduate School of Science, Tokyo Metropolitan University, Hachioji, Tokyo 192-0397, Japan
[4]Department of Chemistry, The University of Electro-Communications, Chofu, Tokyo 182- 8585 Japan

C_{60} serves as a new electron acceptor and moreover the photoexcited C_{60} is an excellent acceptor in electron transfer process. Meanwhile, it has been known that a Si-Si σ bond can act as a good electron donor. In this context, we already reported the first photochemical bis-silylation of C_{60} with disilirane **1** to afford the 1:1 adduct *in nonpolar solvent.*[1] Recently we have also found a novel metal-free bis-silylation of benzonitrile by the photoreaction of C_{60} with **1** via a photoinduced electron transfer *in polar solvent.* This remarkable solvent effect observed in photoreaction of C_{60} with disilirane **1** will be discussed.

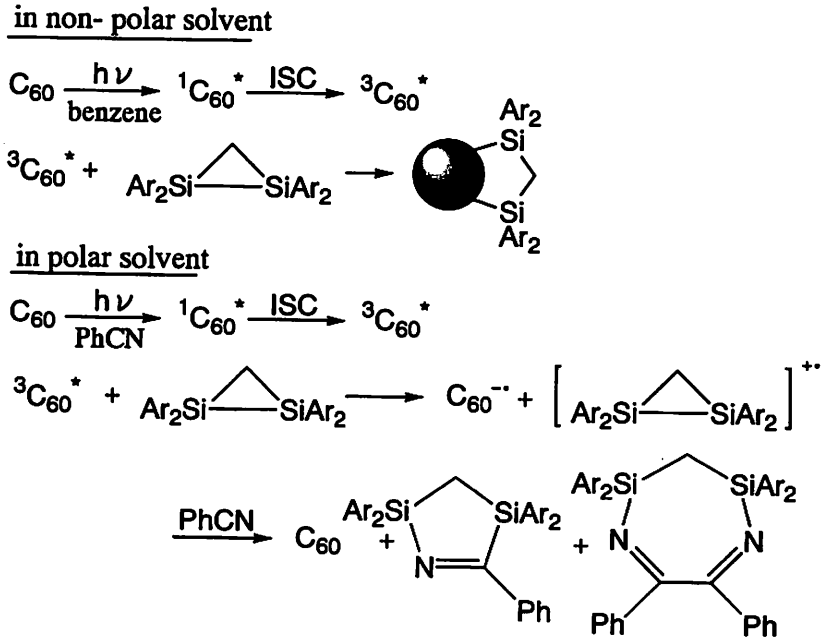

1. Akasaka, T., et al., J. Am. Chem. Soc., 1993, **115**, 1605.

TEMPERATURE EFFECTS ON CONDUCTIVITIES AND ASSOCIATION CONSTANTS FROM -30 TO +10°C OF LITHIUM AND TETRA-ETHYLAMMONIUM SALTS IN SIX ORGANIC SOLVENTS OF HIGH PERMITIVITIES

César A. N. VIANA and Mavitidi DILO
Centro de Electroquímica e Cinética da Universidade de Lisboa, Instituto Bento da Rocha Cabral, Calçada Bento da Rocha Cabral, 14, 1250-047 Lisboa,Portugal

A few non-aqueous solvents of high permitivities and large liquid temperature intervals (low melting points and high boiling points) can be used as good materials to prepare good electrolytic solutions for high energy batteries [1-4] working at very low and high temperatures and high pressures. We have used before propylene carbonate (PC) and γ-butyrolactone (GBL) to prepare lithium and tetra-ethylammonium solutions and all of them have proved excellent behaviour for such purposes [5]. Boiling and melting points of both solvents are between 240°C and 204-205°C and -49 and -44°C, respectively, and permitivities between 65 and 42. So all the solutions have shown very good electrolytic behaviour for both salts, particularly at low temperatures.

In this paper results concerned with limiting molar conductivities and association constants of salt solutions of six organic solvents with similar physical properties are presented.

Generally association constants related to those results show a clear increase with temperature (endothermic behaviour) with an exception which is tetra-ethylammonium bromide in acetonitrile where endothermic behaviour is observed from -30°C to near 0°C and above the isothermic character is shown. Discussions and interpretation of the results are presented. The accuracy of them should be enhanced for their quality and those comparable with some recently published presente very good agreement with them [6].

References

1-Robinson, R. A., Stokes, R. H., "*Electrolyte Solutions*",2nd ed. revised, Butterworths, London, 1970
2-Convington, A. K., Dickinson, T. "*Physical Chemistry of Organic Solvent Systems*", Editors, Plenium Press, London, 1973
3-Popvych, O., Tomkin, R. P. T., "*Nonaqueous Solution Chemistry*", Jonh Willey & Sons, Inc, New York, 1981
4-Barthel, J., Gores, H. J., Wachter, R., *Topics in Current Chemistry*, 1983, 111, 33.
5-Dilo, M., *Tese de Mestrado*, Lisboa, 1997
6-Côte, J-F; Perron, G., Desnoyers, J.E., *J. Solution Chem.*, 1998, 27, 707

DEFINITION OF SOLUTION REACTION SURFACE FOR SOLUTION REACTION

Yoshishige OKUNO

Research Center, Daicel Chemical Industries, Ltd., 1239, Shinzaike, Aboshi-ku, Himeji, 671-1234, Japan

For most of the theoretical studies of chemical reactions in solution, the solution reaction has been simplified from a phenomenological point of view as a barrier-crossing reaction on a potential- or free-energy contour surface in the two-dimensional configuration space spanned by solute reactive and solvent reorganization coordinates. However, these two coordinates have been always identified on the basis of their appeal to intuition rather than as a rigorous definition. Therefore, it should be desirable to formulate these two coordinates from a microscopic point of view. In the present work, we propose a microscopic formulation of the solute and solvent reactive coordinates (the solvent reorganization coordinate is presently referred to as the solvent reactive coordinate).

We define the solute/solvent reactive coordinate as the curvilinear length along the curve that is orthogonal on the intrinsic reaction coordinate (IRC) to the tangential plane of an equipotential energy surface in the solute/solvent coordinate space of mass-weighted Cartesians.[1] Therefore, the configuration changes for displacements along the solute/solvent reactive coordinate coincide with solute-/solvent-configuration changes for displacements along the IRC for the full solute-solvent space. It can be shown that the path along the IRC lies on the two-dimensional configuration space determined by these two reactive coordinates and the IRC for the full solute-solvent space coincides with the IRC for such two-dimensional configuration space.

We termed the two-dimensional configuration space as a solution reaction surface (SRS).[1] The SRS will be regarded as the central surface to the solution reaction, because the reactive motion of the solutes and solvents occurs on the SRS. Therefore, we will capture the characteristics features of the solution reaction by treating the solution reaction as a barrier crossing reaction on a potential energy contour surface in the SRS.[2]

The present formalism was applied to the examination of the contact-ion-pair formation of *t*-BuCl in four waters.[1-3] We found that the reactive motion in the transition state region takes place in a frozen solvent environment, while solvent motion constitutes a relatively large portion of motion along the IRC in the region away from the transition state.

1. Okuno, Y., submitted for publication.
2. Okuno, Y., in preparation.
3. Okuno, Y., *J. Phys. Chem. A*, 1999, 103, 190.

QM / MM TREATMENT OF WATER CLUSTERS

Misako AIDA,[a] Hiroshi YAMATAKA,[b] and Michel DUPUIS[c]

a. Faculty of Science, Hiroshima University, Kagamiyama, Higashi-Hiroshima 739-8526 Japan,
b. Institute of Scientific and Industrial Research, Osaka University, Ibaraki, Osaka 567-0047 Japan,
c. Pacific Northwest National Laboratory,EMLS/K1-83, Battelle Blvd, Richland, WA 99352 USA

Solvent plays an important role in determining rates of reactions in solution and in defining reaction characteristics. In some cases, solvent molecules are actively involved in the activated process. In these cases, the solvent molecules must be treated explicitly in the model. The dependence of computational expense on system size for *ab initio* MO calculations still precludes that a sufficiently large number of solvent molecules could be included. The QM/MM approach includes a quantum-chemical treatment of the (extended) solute system with additional solvent molecules treated at the molecular mechanics (MM) level of theory.

In our study we used the water model for the MM subsystem in connection with a intramolecular vibration force field. It is known that the TIP3P model describes well the essential features of liquid water and has been used successfully in classical MD simulations of solvated organic and biochemical systems. The vibration potential provides the advantage of a simplified treatment of the QM/MM forces and their use in the calculation of reaction pathways and trajectories. We denote this model QM/MM-vib.

We are planning to apply this MD simulation technique to organic reactions in solution. As a first step, we give a preliminary account of the MD simulations based on QM/MM-vib for water clusters $(H_2O)_n$, where n = 2 – 6, with several combinations of QM and MM water molecules. The QM treatment uses the HF/6-31G level of theory, the MM treatment uses TIP3P[1] and the vibrational potential of Bartlett, Shavitt and Purvis.[2] We used the computer code HONDO.[3] We are interested in benchmarking how the hybrid structures of the clusters mimic the full HF/6-31G clusters. Snapshot structures of the QM/MM trajectories are compared with those of the QM trajectories. The characteristics of the vibrational motion in the MM water molecules will be compared with those of the QM water molecules.

1. Jorgensen, W.L.;Chandrasekhar. J; Madura, J.D.;Impey, R.W.; Klein, M.L,. *J.ChemPhys.*, 1983, **79**, 926.
2. Bartlett, R.J.;Shavitt, I.; Purvis, G.D., *J.Chem. Phys.*, 1979, **71**, 281.
3. Dupuis, M.; Marquez, A.; Davidson, E.R., HONDO99.

Solvent Effects on a Diels-Alder Reaction in Supercritical Water: RISM-SCF study

Yuichi Hranao[1], Hirofumi Sato[2] and Fumio Hirata[2]

[1] Graduate School of Sci. & Tech., Kobe Univ., Nada-ku, Kobe 657-0851 , Japan

[2] Institute for Molecular Science, Myodaiji-cho, Okazaki, 444-8585, Japan

The Diels-Alder reaction is the most widely employed synthetic method for the production of polycyclic ring system. In the early 1980's, Breslow et al. reported that using water as a solvent media the rate of the Diels-Alder reaction is dramatically accelerated[1]. However the solubility limits of nonpolar solute to the aqueous solvent restricts the variety of reagents, or requires special additives extra. The unique properties of supercritical water (SCW) would lead us to overcome these matters. Recently, it is reported that by using SCW as an aqueous reaction media the Diels-Alder reaction can be performed cleanly in high yield without any additives extra while increasing the reaction rate[2].

In order to probe this phenomena further, we have carried out the RISM-SCF calculation[3] to study the changes in the solvation free energy and the electronic energy of the solute molecules in reactants, transition states(TS) and products. The DZV basis set was chosen for all molecular orbital calculations. The temperature of the surrounding water is kept at 298 K and 873 K for ambient water and SCW, respectively. We choose the cycloaddition of cyclopentadiene (CP) with methyl vinyl ketone (MVK) ,which is well studied as a prototypical system. In principle, four transition structures are possible for this reaction, corresponding to the dienophile being s-*cis* or s-*trans* and the way of its approaching to diene being exo or endo. Previous ab initio calculations [4] have shown that the endo-*cis* transition structure is the lowest energy in several Diels-Alder reactions, but Assfeld et al.[5] have shown in a recent calculation that the endo-*trans* TS of the reaction of CP and methyl acrylate becomes the more stable form in aqueous solution. Thus, we performed calculation on both endo-*cis* and endo-*trans* reaction, and examined which is the more stable transition structure in water and SCW.

The key results are in the figure, which shows the energy diagram for the reaction through the endo-*cis* transition structure. The activation energy in vacuum is computed at 52.48 kcal/mol, and stabilized by 6.90 kcal/mol in water. On the other hand, through the endo-*trans* transition structure, the activation energy in vacuum is greater than that of the endo-cis TS by 1.77 kcal/mol. However, the activation energy of the endo-trans TS decreases more than that of the endo-*cis* TS by 0.64 kcal/mol. This result indicates that the endo-*cis* TS is still more stable in water at least in this reaction, but the endo-*trans* TS is more influenced in aqueous solvent. Furthermore, this tendency dose not change in SCW. The activation energy for the reaction in SCW through the endo-*cis* transition structure decreases by 2.71 kcal/mol at 873 K. By this decrease in the activation energy, the rate constant in SCW could be estimated, simply by the Arrhenius equation, to be 12.7×10^{13} times greater than that in ambient water.

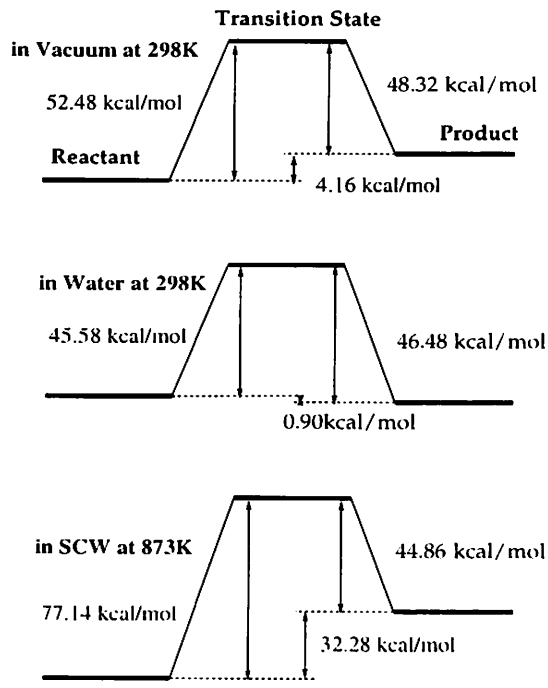

1, Rideout, D; Breslow, R. *J. Am. Chem. Soc.* **1980**,*102*, 741.

2, Korzenski, M. B.; Kolis, J. W. *Tetrahedron.Lett.* **1997**, *38*, 5611

3, Ten-no, S.; Hirata, F.; Kato, S. *Chem. Phys.Lett.* **1993**, *214*, 391

4, Jorgensen, W. L.; Lim.D.; Blake, J. F. *J. Am. Chem. Soc.* **1993**, *115*, 29362.

5, Assfeld, X ; Ruiz-Lopez, M. F. ; Garcia, J. I. *J. Chem. Soc.Commun.* **1995**, 1371.

NONAQUEOUS ELECTROLYTES FOR RECHARGEABLE LITHIUM CELLS

S.TOBISHIMA, K. HAYASHI ,Y. NEMOTO and Y.SAKURAI
NTT Telecommunications Energy Laboratories,
Nippon Telegraph and Telephone Corporation
Tokai-mura, Naka-gun, Ibaraki-ken, 319-1193, Japan

Important issues with regard to lithium (Li) metal cells are cycle life, rate capability and safety. These problems are closely related to electrolyte selection. This work reports the influence of the composition of various mixed solvent electrolytes on the conductivity and charge-discharge cycling efficiency of Li metal anode. The solvents mainly used were ethylene carbonate (EC), propylene carbonate (PC) and 2-methyl-tetrahydrofuran (2MeTHF). $LiAsF_6$ was used as the solute. The purpose of this work is to obtain an electrolyte solution which realizes a high rate capability and a long cycle life of lithium cells.

Figure 1 shows the relationship between the specific electrolyte conductivity (κ) and the 2MeTHF content in EC/2MeTHF binary and EC/PC/2MeTHF ternary mixed solvent electrolytes. At 25 °C, the conductivity exhibits maximum (κ_{max}) at a 40 vol.% 2MeTHF for both mixed systems. The κ_{max} is the result of the total effect of the dielectric constant (number of dissociated ions) and the viscosity (migration rate) by mixing low viscous and dielectric 2MeTHF and high dielectric and viscous EC and PC. The conductivities of EC/PC/2MeTHF is slightly lower than that of EC/2MeTHF with the same 2MeTHF content because EC has a higher dielectric constant than PC. As the temperature is reduced, the EC content exhibiting κ_{max} tends to decrease. When 2MeTHF is increased in mixed solvents, the activation energy (E_A) [1] decreases because 2MeTHF has a lower E_A than EC.

The binary mixed systems tend to have slightly higher lithium cycling efficiency (Ea) values than ternary mixed systems containing the same amount of 2MeTHF. Ea exhibits its maximum value at EC/2MeTHF=50:50 for binary and at EC/PC/2MeTHF=15:35:50 for ternary mixed systems. Based on the above results, we tested EC/2MeTHF and EC/PC/2MeTHF mixed solvent electrolytes containing 2MeTHF from 40 to 70 vol.% for the AA lithium metal cells.

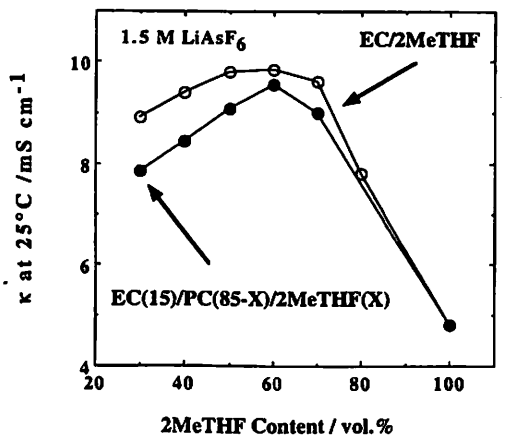

Fig.1 Electrolyte conductivity

1. Raistrick,I.; Ho, C.; Huggins, R. ; *Mat.Res.Bull.*, 1986, **11**, 953.

PHOTOCATALYTIC REACTIONS AS OBSERVED WITH MARINE PLANKTON: EFFECTS OF ADHERING TITANIUM DIOXIDE POWDER ON THE BODY SURFACE

Shuji MATSUO[1], Hisanobu WAKITA[1], Taku MATSUO[1], Tsuneo HONJO[2], Yasuhiro ANRAKU[2], and Sunao YAMADA[3]

[1] Department of Chemistry, Fukuoka University, Jonan-ku, Fukuoka, 814-0180, Japan

[2] Faculty of agriculture, Kyushu University, Hakozaki, Higashi-ku, Fukuoka, 812-8581, Japan

[3] Department of Materials Physics and Chemistry, Kyushu University, Hakozaki, Higashi-ku, Fukuoka, 812-0053, Japan

Photocatalytic reactions provide attractive means for decomposing pollution substances in water. The photocatalytic reactions with titanium dioxide (TiO_2) generate a hole (h^+) - electron (e^-) pair at the TiO_2 surface on irradiation of UV light ($\lambda < 380$ nm). The h^+ oxidizes hydroxide ion (OH^-) to generate a hydroxyl radical (·OH). The highly oxidative ·OH is useful for decomposing organic compounds[1] and destructing bacilli like a phage[2]. In the present paper, we will report effects of the photoirradiated TiO_2 powder on plankton.

Artemia salina (brine shrimp) and *Chattonella antiqua* (noxious red tide flagellate) were used in these experiments. Seawater samples suspending 0.1 ~ 1 mg / ml of the TiO_2 (P25, anatase) were prepared by sonication. An aliquot (2 ml) of the suspension was poured into small beaker (15 mm in radii and 30 mm in height). The light intensity was about 2 mW / cm^2 (λ = 365 nm) at the solution surface. The solutions were occasionally stirred up to disperse the TiO_2 powder during the irradiation. Effects of photoirradiation on the shape and behaviors of plankton were monitored by the aid of magnifiers and microscopes.

As to *A. salina*, the movement was not affected at all for 30 min irradiation period. Then, they began abnormal movement and stopped to swim after ca. 1 hr irradiation. The body surface of the immobilized *A. salina* was covered by TiO_2 powder. In the presence of TiO_2, the photoirradiation for 1 hr was thus concluded to be fatal to *A. salina*.

In the case of *C. antiqua*, the body surface has already been covered by the TiO_2 powder before the irradiation. Behaviors of the plankton were followed for the irradiation period of 100 min: 1) the adhering TiO_2 powder strongly disturbed the plankton movements, 2) the plankton were deformed from elongated to round shapes, 3) the body surface was injured after prolonged irradiation, and 4) the plankton bursts finally. The rounded and injured plankton was transferred to the fresh culture medium in a well plate every 20 min during irradiation, and the number of living plankton was counted after 48 hr elapsed time. The deformed plankton regained the normal activities, while those irradiated for 100 min were completely annihilated.

Photocatalytic action of TiO_2 is thus concluded to cause fatal damage to the body surface of plankton. The reaction appears to take place at the interface between TiO_2 powder and body surface in the presence of seawater.

1. Kraeutler, B.; Bard, A. J., *J. Am. Chem. Soc.*, 1978, **100**, 5985.

2. Lee, S.; Nakamura, M.; Ohgaki, S., *J. Environ. Sci. Health A*, 1998, **33**, 1643.

Self-Consistent, KS DFT and 3D RISM Description of a Metal - Molecular Liquid Interface

Andriy KOVALENKO and Fumio HIRATA
Institute for Molecular Science, Myodaiji, Okazaki 444-8585, Aichi, Japan

Microscopic structure influences the properties of a metal-electrolyte interface significantly. The most consistent description of the interface can be achieved in a unified Car-Parrinello type approach combining the density functional theory in the Kohn-Sham formulation (KS DFT) with molecular dynamics simulation, which takes proper account of many-body quantum effects. However, like all simulations, it becomes problematic in description of processes that take place on a long time scale or involve a great number of solvent particles. An integral equation theory yielding realistic description of molecular liquids of various complexity is the reference interaction site model (RISM), and its three-dimensional generalization for the 3D site distributions of liquid (3D RISM)[1,2].

We have developed a self-consistent combination of the KS DFT for the electronic structure and the 3D RISM for the classical 3D site distributions of liquid at an interface[2]. The electron and classical subsystems are coupled in the mean field and linear response approximations. The procedure takes account of many-body effects of dense fluid on the metal-liquid interactions by averaging the pseudopotentials of liquid molecules over the classical distributions of the liquid. We converge the self-consistent KS and 3D RISM equations simultaneously, by using the dynamical relaxation method[1,2] closely related to dynamical simulated annealing. The electron wave functions are orthonormalized after each relaxation step by the Gram-Schmidt process. The proposed approach is substantially less time-consuming as compared to a Car-Parrinello type simulation.

The calculation[2] has been performed for pure water at normal conditions in contact with the 5-layer FCC (100) metal slab of 80 copper-like atoms modeled similarly to the recent Car-Parrinello simulation[3] for the copper-water interface. The supercell technique is used, bearing in mind further application to description of a solute adsorbed at a metal-water interface. As the input to the 3D RISM equation, we employed the site-site distributions of the simple point charge (SPC) water model. The strong attractive well of the metal-water site potential presents great difficulties for convergence of the 3D RISM equations complemented with the 3D hypernetted chain (HNC) closure. To resolve this problem, we elaborated a hybrid of the 3D HNC and Percus-Yevick (PY) closures.

The results are in good agreement with the Car-Parrinello simulation for the same metal model[3]. The shift of the Fermi level due to the presence of water conforms with experiment. The electron distribution near an adsorbed water molecule is affected by dense water, and so the metal-water attraction follows the shapes of the metal effective electrostatic potential. For the metal model employed, it is strongest at the hollow site adsorption positions, and water molecules are adsorbed mainly at the hollow and bridge site positions[3] rather than over metal atoms[4]. Layering of water molecules near the metal surface is found. In the first hydration layer, adsorbed water molecules are oriented in parallel to the surface or tilted with hydrogens mainly outwards the metal. This orientation at the potential of zero charge agrees with experiment[5].

1. Kovalenko, A.; Hirata, F.; *Chem. Phys. Lett.*, 1998, **290**, 237.
2. Kovalenko, A.; Hirata, F.; *J. Chem. Phys.*, 1999, **110**, (in press).
3. Price, D. L.; Halley, J. W.; *J. Chem. Phys.*, 1995, **102**, 6603.
4. Heinzinger, K.; Spohr, E.; *Electrochimica Acta*, 1989, **34**, 1849.
5. Ataka, K.; Yotsuyanagi, T.; Osawa, M.; *J. Phys. Chem.*, 1996, **100**, 10664.

The local component of solvation thermodynamics and the molecular origin of the dependence on the solute insertion process

Nobuyuki MATUBAYASI [1], Masaru NAKAHARA [1], and Ronald M. LEVY [2]
[1] Institute for Chemical Research, Kyoto University, Uji, Kyoto, 611-0011, Japan
[2] Department of Chemistry, Rutgers University, Piscataway, New Jersey, 08854-8087. U. S. A.

The solvation thermodynamics is closely related to the perturbation of the solution structure caused by the solute. The solution structure is commonly represented by such a quantity as the solute—solvent correlation function and is independent of the condition of solute insertion, i.e., on whether the solute is inserted at constant pressure or at constant volume. It is well known, however, that the partial molar thermodynamic quantities of the solute are, in general, dependent upon the insertion condition. Thus, there is an apparent inconsistency concerning the ensemble dependence of the microscopic solution structure and the macroscopic partial molar quantities. The purpose of this work is to resolve the apparent inconsistency on a rigorous statistical-mechanical basis and to show that a local interpretation is possible for partial molar quantities at constant pressure.

Consider an excess partial molar quantity ΔQ, where Q may be enthalpy, energy, entropy, or volume, and ΔQ is equal to the change in the total Q of the system upon insertion of the solute at a fixed origin. It is in general possible to find a "local estimator" $q(\mathbf{r})$ in the solution and its corresponding value q_0 in the pure solvent in terms of which ΔQ can be expressed as

$$\Delta Q = \int d\mathbf{r}\, \rho(\mathbf{r})\big(q(\mathbf{r}) - q_0\big), \tag{1}$$

where $\rho(\mathbf{r})$ is the density of the solvent at a position $\mathbf{r}$ from the solute. The solvation shell model is introduced by restricting the domain of integration in Eq. (1) to a finite volume called the "solvation shell". Conversely, the exact ΔQ is recovered in the "large shell limit" that the solvation shell approaches the total volume of the solution. In both the canonical and isothermal-isobaric ensembles, Eq. (1) gives the exact ΔQ when the large shell limit is taken first.

The exact ΔQ evaluated by taking the large shell limit first is dependent on the ensemble. The microscopic solution structure represented by $\rho(\mathbf{r})$ and $q(\mathbf{r})$ is, on the other hand, independent of the ensemble in the thermodynamic limit. It then follows that the ensemble dependence of ΔQ is caused by the non-interchangeability of the thermodynamic and large shell limits. It is possible to show that the non-interchangeability is related to the asymptotic behavior of $q(\mathbf{r})$ at distances far from the solute ($\mathbf{r}\to\infty$). Let $q(\infty)$ be the asymptotic value of $q(\mathbf{r})$ at $\mathbf{r}\to\infty$. $q(\infty)$ is different from q_0 by either $o(1/N)$ or $O(1/N)$, where N is the size of the system. Equation (1) is then rewritten as

$$\Delta Q = \int d\mathbf{r}\, \rho(\mathbf{r})\big(q(\mathbf{r}) - q(\infty)\big) + \int d\mathbf{r}\, \rho(\mathbf{r})\big(q(\infty) - q_0\big), \tag{2}$$

where $(q(\mathbf{r})—q(\infty))$ is of $o(1/N)$ at $\mathbf{r}\to\infty$. The main contribution to the first term comes from the solvent molecules closer to the solute. We thus call the first term the local component of ΔQ. The thermodynamic and large shell limits are interchangeable in the local component and the component is independent of the ensemble. In the second term, all the solvent molecules throughout the system contribute equally to it and the term is called the nonlocal component. In the isothermal-isobaric ensemble, it is possible to show that $(q(\infty)—q_0)$ is of $o(1/N)$ and the second term of Eq. (2) vanishes in the thermodynamic limit, irrespective of the order of the thermodynamic and large shell limits. In the canonical ensemble, $(q(\infty)—q_0)$ is of $O(1/N)$. In this case, when the thermodynamic limit is taken first, the second term is simply equal to zero, while when the large shell limit is taken first, the second term is equal to $-\Delta V \partial Q/\partial V$. Thus, the nonlocal component is the origin of the non-interchangeability of the two limits and accounts for the ensemble dependence of ΔQ. Furthermore, the local component is equal to the ΔQ at constant pressure in both the canonical and isothermal-isobaric ensemble.

In the solvation shell model, the shell is commonly of molecular dimension and the thermodynamic limit is taken first. This shows that the solvation shell model is an approximation to the local component. A local interpretation is thus possible for the local component of ΔQ, which is equal to the ΔQ at constant pressure.

SALT EFFECT ON SOLUBILITY AND CONFORMATIONAL STABILITY OF PEPTIDE IN AQUEOUS SOLUTIONS

Takashi IMAI[1], Masahiro KINOSHITA[2], Fumio HIRATA[1,3]

[1] Department of Functional Molecular Science, The Graduate University for Advanced Studies, Okazaki, Aichi, 444-8585, Japan

[2] Advanced Energy Utilization Division, Institute of Advanced Energy, Uji, Kyoto 611-0011, Japan

[3] Department of Theoretical Study, Institute for Molecular Science, Okazaki, Aichi, 444-8585, Japan

Stability of protein depends sensitively on the thermodynamic conditions such as solvent, temperature, pressure, and coexisting solutes. Among those conditions, one of most extensively studied is the salt effects. Concerning the salt effect on stability in aqueous solutions of a certain class of protein, the order of the salt effect called Hofmeister series has been well established. For anions, the series is

$$SO_4^{2-} > CH_3COO^- > Cl^- > Br^- > NO_3^- > ClO_4^- > I^- > CNS^-,$$

and for cations, it is

$$(CH_3)_4N^+ > NH_4^+ > Rb^+, K^+, Na^+, Cs^+ > Li^+ > Mg^{2+} > Ca^{2+} > Ba^{2+}.$$

In above series, the species to the left (right) decrease (increase) the solubility of proteins, namely salting-out (salting-in), or stabilize (destabilize) the native structure of proteins. It has been proven repeatedly that not only protein but also many other substances follows the Hofmeister series. It is generally believed that Hofmeister series is somehow related to the free energy change associated with change in water structure caused by perturbation due to ions. If it is the case, how are those two related? How are the order of salt effect on solubility and conformational stability related?

The reference interaction site model (RISM) theory in statistical mechanics of molecular liquids has the potential capability of investigating the problems described above, i.e. molecular pictures of change in the water structure caused by the addition of salts near a protein and associated change in the solvation free energy. We have investigated the salt effects on the solvation free energy of acetylglycine ethyl ester (AGE) in 1 M LiCl, NaCl, NaBr, NaI, and KCl solutions. We have found the order of the contribution from change in water structure due to the existence of ions for the imaginary peptide whose site charges are set to zero is dominantly reflected in the order of the total free energies. The fact implies that Hofmeister series is closely related to the order of salt effect which manifests through the structural reorganization of water by adding the salt, which comes from excluded volume effect rather than charge effect.

We also try to clarify the relation between the salt effect on the solubility and conformational stability. The study is now in progress.

SOLUTE SIZE DEPENDENCE OF ELECTRICAL POTENTIAL FLUCTUATIONS AROUND A SOLUTE IN WATER

Ryo AKIYAMA[a], Masahiro KINOSHITA[b], and Fumio HIRATA[a]
[a]Institute for Molecular Science, Myodaiji, Okazaki, 444-8585, Japan
[b]Institute of Advanced Energy, Kyoto University, Uji, Kyoto 611-0011, Japan

So much effort has been devoted to characterize properties of ion hydration, because hydration effect plays a crucial role in direction and rate of chemical reactions in aqueous solutions. In 1957 two conceptual models for the ion hydration were proposed by Frank and Wen[1] and by Samoilov[2]. According to the model proposed by Frank and Wen, a small ion (like Li^+) in water has three hydration regions: the innermost " region A" is where water molecules are immobilized due to the electric field exerted by the ion, the second " region B" is that in which water is less " ice-like" ,i.e. more random in organization than " normal" water, and the third " region C" contains normaly polarized water.

According to the Samoilov model, the translational motion of water molecules around an ion can be regarded as the exchange of water molecules that are closest to the ion. S.-H. Chong and F. Hirata discussed the existence of " region A" in terms of the activation energy of O(water) from the first hydration shell of an ion to the outer region using the method based on the RISM theory[3]. Those results are in good accord with the picture of " positive" and " negative" hydration.

When the hydration effects on reactions are discussed, the information of electrical potential fluctuations of water around an ion is important. It is of interest to characterize the solvent fluctuation around ions in terms of molecular picture stated above. Chong and Hirata discussed the effect of molecular symmetry of water on the fluctuation only around Na^+.[4] However, our calculation suggests that the solute size effect is large[5]. We will discuss the solute size dependence of the fluctuation in terms of the solvent (or reaction) coordinate calculated by the RISM theory. The fluctuation is characterized by the second cumlant of the solvation coordinate which is a coefficient of z(external field)-expansion of the solvation free energy[6].

1. H.S. Frank and W.-Y. Wen, Discuss. Faraday Soc. 1957, **44**, 133.
2. O.Y. Samoilov, Discuss. Faraday Soc. 1957, **44**, 141.
3. S-H. Chong, and F. Hirata, J. Phys. Chem., 1997, **101**, 3209.
4. S-H. Chong, and F. Hirata, Chem. Phys. Lett., 1998, **293**, 119.
5. R. Akiyama, M. Kinoshita, and F. Hirata, Chem. Phys. Lett., in press.
6. S-H. Chong, and F. Hirata, J. Chem. Phys., 1997, **106**, 5226.

HYDROPHOBIC INTERACTION IN AQUEOUS UREA SOLUTION

M. IKEGUCHI, S. NAKAMURA and K. SHIMIZU
Department of Biotechnology, The University of Tokyo, 1-1-1 Yayoi, Bunkyo-ku, Tokyo, 113-8657, Japan

To elucidate principles of protein folding, many experimental and theoretical studies are being made. In many experiments on protein folding/unfolding, denaturants such as urea or guanidine hydrochloride are often used to make proteins unfold. However, the molecular mechanism of protein unfolding by adding excess amount of denaturants still remains unclear. In this paper, we attempt to describe the mechanism of urea denaturation of proteins by using molecular dynamics simulations.

There are two mechanisms in the urea denaturation proposed previously. One is that urea weakens hydrophobic interaction of proteins, and the other is that urea weakens the hydrogen bonds of proteins. Solubility experiments showed that urea increases the solubility of both hydrophobic molecules and hydrophilic molecules. The results suggest both mechanisms may be operating. However, recent calculation of potential of mean force between two methane molecules in aqueous urea solutions showed that contacting two methane molecules is stabilized by urea. This indicates that urea enhances the hydrophobic interaction.

To solve the contradiction, we performed molecular dynamics simulation of hydrophobic interactions in aqueous urea solution. Our results of the potential of mean force between two methane molecules are consistent with the previous simulation, that is, urea stabilizes contacting methane molecules. However, by careful examination of calculation and experimental results, we found the calculation agrees with the experiments: the reason of stabilization of two methane association by urea is that small hydrocarbons (less than three carbon atoms) is more soluble in water than in urea solution. There is the size dependence in the influence of urea on the hydrophobic effect.

To understand the size dependence, we performed another molecular dynamics simulation. We divided the hydration process into two parts: the cavity formation and introduction of attractive interaction. We found that the urea enhances the hydrophobic effect in the cavity formation, and that urea decreases the hydrophobic effect in the introduction of attractive interaction. The molecular size changes the balance of two terms.

DENSITY MATRIX AND EIGENSTATES FOR AN EXCESS ELECTRON IN A CLASSICAL FLUID

Ashok Sethia[1],Shinichi Miura[2] and Fumio Hirata[1]
[1]Theoretical Division, Institute for Molecular Science, Myodaiji 444-8585, Okazaki, Japan
[2]Department of Electronic Chemistry, Tokyo Institute of Technology, 4259 Nagatsuta, Yokohama 226-8502, Japan

Density matrix for an excess electron in a classical fluid has been derived[1] using the theory of Chandler, Singh and Richardson (CSR)[2]. Using this density matrix and our earlier developed method[3] we have calculated the eigenstates of the electron in fluid. The results show that the excess electron in a fluid behaves almost like a free particle with effective mass m^* in a constant potential well.
Using the solvent induced interaction of Miura and Hirata[4] we have calculated the eigenstates of electron in water.

1. A. Sethia. F. Hirata and Y. Singh. J. Chem. Phys. (in press).
2. D. Chandler. Y. Singh and D. M. Richardson. J. Chem. Phys. 1984 **81**. 1975.
3. A. Sethia. S. Sanyal and Y. Singh. J. Chem. Phys.1990 **93** 7268.
4. S. Miura and F. Hirata. J. Phys. Chem. 1994 **98**. 9649.

Test of a Fokker-Planck-Kramers Equation Treatment for Short-Time Dynamics of Diffusion-Controlled Reactions by Molecular Dynamics Simulation in Lennard-Jones Fluids

Kazuyasu IBUKI and Masakatsu UENO
Department of Molecular Science and Technology, Faculty of Engineering,
Doshisha University. Kyotanabe, Kyoto 610-0321, Japan

The study of the diffusion-controlled reaction is important for a better understanding of the reaction dynamics in solution. In previous papers,[1] we have proposed a Fokker-Planck-Kramers equation (FPKE) treatment for the rate of diffusion-controlled reaction based on the Harris theory,[2] and pointed out that (1) the inertia effect cannot be ignored, (2) the absorbing boundary condition of the Smoluchowski type is invalid, and (3) the potential of mean force (PMF) should be taken into account. In order to test the validity of the FPKE treatment in realistic systems with attractive interactions, we carry out a molecular dynamics simulation in Lennard-Jones (LJ) fluids.

As in the simulation in hard-sphere fluids by Dong *et al.*,[3] the reaction scheme is A + Q → B + Q, and the A, B, and Q molecules are assumed to be physically identical. First, randomly labeled A (450) and Q (50) molecules is in equilibrium. Then we simulated the survival probability $S(t)$ of A with the condition that the reaction occurs whenever an A molecule approaches a Q molecule within the reaction radius R ($= \sigma$: the distance parameter in the LJ potential).

The theoretical treatment[1] is based on FPKE which corresponds to the Langevin equation with the inertia term. The diffusion coefficient is assumed to be position-independent.

The simulation result at 85 K and 1.34 g cm^{-3} for Ar fluid is shown (black circles) in Fig. 1 together with the theoretical results for three potential functions: (a) PMF obtained from the equilibrium radial distribution function, (b) LJ potential, and (c) $V(r) = 0$.

Our results indicates that the position dependence of the diffusion coefficient are not necessary to explain the dynamics of the diffusion-controlled reaction in the LJ fluid, if PMF is appropriately taken into account.

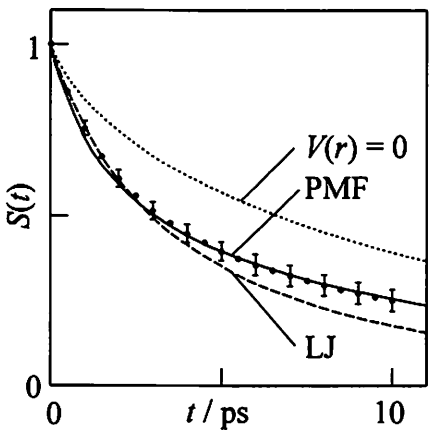

Fig. 1. The Survival probability of A in a LJ fluid.

(1) Ibuki, K; Ueno, M., *J. Chem. Phys.*, 1997, **106**, 10113; **107**, 6594. (2) Harris, S., *J. Chem. Phys.*, 1983, **78**, 4698. (3) Dong, W.; Baros, F.; Andre, J. C., *J. Chem. Phys.*, 1989, **91**, 4643.

ESR STUDY ON INTRAMOLECULAR ELECTRON TRANSFER RATE OF 1,3-DINITROBENZENE RADICAL ANION IN SOLUTION

Haruko Hosoi[1] and Yuichi Masuda[2]

[1] School of Integrated Sciences, Graduate School of Humanities and Sciences, Ochanomizu University, Otsuka, Bunkyo-ku, Tokyo, 112-8610, Japan

[2] Department of Chemistry, Faculty of Science, Ochanomizu University, Otsuka, Bunkyo-ku, Tokyo, 112-8610, Japan

The intramolecular electron transfer rates of the 1,3-dinitrobenzene radical anion in aprotic solvents were determined at various temperatures by means of an electron spin resonance line-broadening method.[1] The rate with negligible ion-ion interaction was determined in acetonitrile, N,N-dimethylformamide, and hexamethylphosphotriamide by addition of a cryptand, 4,7,13,16,21,24-hexaoxa-1,10-diazabicyclo [8.8.8] hexacosane, to capture the sodium counter cation, which was produced in the course of the reduction of 1,3-dinitrobenzene for the preparation of the radical anion.

The obtained rates were 10 times or more compared with those previously reported[2] in the presence of 0.1 M tetra (*n*-butyl)ammonium tetrafluoroborate as supporting electrolyte utilizing an electrochemical reduction method. The decrease in the rate was ascribed to the ion-pair formation, which was confirmed by the calculation of Bjerrum ion association constants.

The ET reaction parameters for each solvent were determined by the measurements of the intervalence transfer band in the near IR region. Some dielectric continuum models were used for the examination of solvent dependence of the reaction parameters as well as the ET rates.

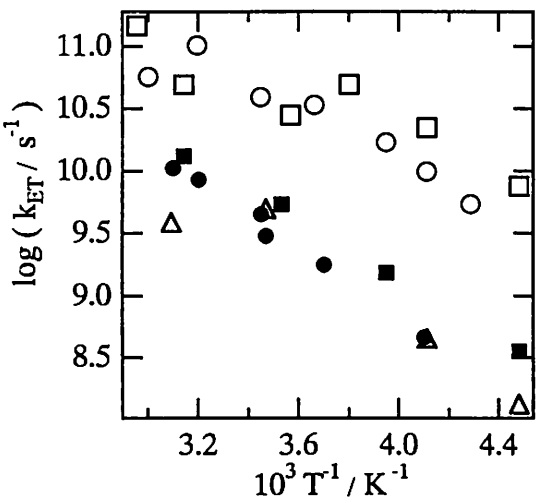

Figure The temperature dependence of the intramolecular electron transfer rates, k_{ET}, of the 1,3-dinitrobenzene radical anion in acetonitrile (circle), N,N-dimethylformamide (square), and tetrahydrofuran (triangle). Open and closed symbols correspond to the rates by us and those by Grampp et al, respectively.

1 Hosoi, H. Mori, Y. and Masuda, Y. *Chem. Lett.* **1998**, 177.

2 Grampp, G. Shohoji, M. C. B. L. Herold, B. J. *Ber. Bunsenges. Phys. Chem.* **1989**, *93*, 580 ; Grampp, G. Shohoji, M. C. B. L. Herold, B. J. Steeken, S. *Ber. Bunsenges. Phys. Chem.* **1990**, *94*, 1507.

CONCENTRATION DEPENDENCE OF RELAXATION PHENOMENA IN BINARY SOLUTIONS STUDIED BY OPTICAL KERR EFFECT SPECTROSCOPY

Masaya SUZUKI, Satoru NAKASHIMA and Tadashi OKADA
Department of Chemistry, Graduate School of Engineering Science, Osaka University,
1-3, Machikaneyama-cho, Toyonaka, 560-8531, Japan

Optical Kerr effect (OKE) spectroscopy is the third order nonlinear spectroscopy that can probe low frequency mode of liquids. In this report, we have studied concentration dependence of binary mixed solvents such as benzonitrile/acetonitrile (BCN/ACN) and benzonitrile/*n*-hexane (BCN/*n*-hex) and compared the two series.

OKE measurements were carried out using home-made self-mode-locked Ti:Sapphire laser, which generates 20fs optical pulse at 780 nm with 400mW of power at 89MHz. Sample liquids were mixed at various concentrations and filtered just before measurements not to contain dust in sample liquids.

The faster component of diffusive response, that analyzed by multi-exponential fitting, gives slowest decay time at around the molar ratio BCN/ACN=7:3. On the other hand, the slower component is not affected by concentration change. Frequency-domain OKE spectra of BCN/ACN mixtures after subtracting picosecond diffusive responses with various mole fractions are shown in Figure.1. Fitting results of librational part of OKE spectra by using antisymmetrized Gaussian are shown in Figure.2. The center frequency of libration also showed the lowest value at around the molar ratio BCN/ACN=7:3. Concentration dependency of density of mixture also shows the inflection point around the same concentration.

From these results, we suggest a model that BCN and ACN molecules take some kind of aggregation in mixed solutions, and the unit of aggregates may not be so large that the size of the aggregates do not affect the bulk diffusive component.

In the case of BCN/*n*-hex binary solutions, on the contrary, uniformly mixed state in every concentration is suggested.

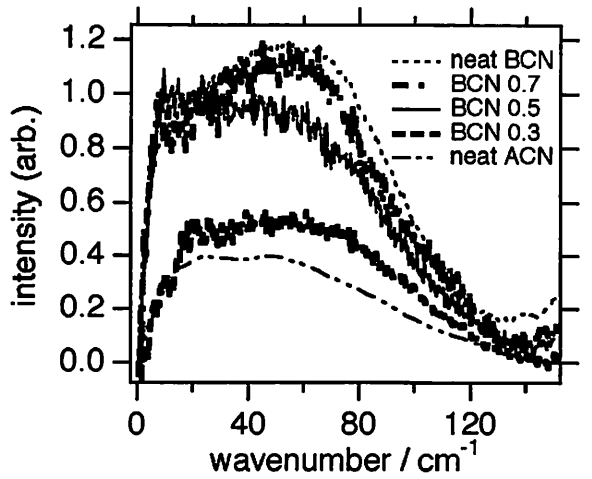

Figure.1 OKE spectra of BCN-ACN binary solutions, after rotational component subtracted. Mole fractions are indicated.

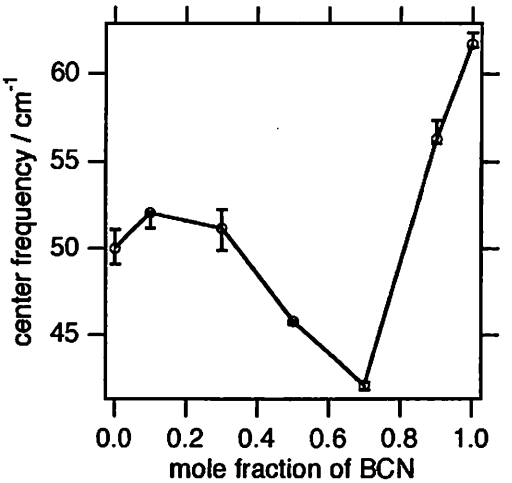

Figure.2 Plot of librational center frequency vs mole fraction of BCN in ACN.

ULTRAFAST NONLINEAR SPECTROSCOPY IN CONDENSED PHASES

Hiroaki MAEKAWA and Keisuke TOMINAGA
Department of Chemistry, Kobe University, Rokkodai 1-1, Nada, Kobe, 657-8501 Japan

In this paper we present our recent results on condensed phase dynamics studied by the ultrafast nonlinear spectroscopy.

1. Vibrational Dynamics in Porous Silica Glasses Studied by Time-Resolved Coherent Anti-Stokes Raman Scattering (CARS).

Porous silica glasses are suitable material to study confinement effect on liquid dynamics because a pore diameter of a nano-scale can be controlled by its preparation and the distribution of the pore size is quite uniform.[1] We have studied pore size dependence on the vibrational dephasing of the CD stretching of $CDCl_3$ in porous silica glasses by time-resolved CARS technique. The CARS signal decay is almost single exponential for all the porous silica glasses, and the decay time constant gets smaller by decreasing the pore size. We explain this behavior in terms of a simple two-state model in which liquid molecules inside the pore are classified into " surface molecules" and " bulk molecules" .

2. Overview of Recent Development of Two-Dimensional Optical Correlation Spectroscopy.

Recently, a new type of two-dimensional correlation spectroscopy has been proposed, which utilizes either visible or infrared optical ultrashort pulses as an excitation electromagnetic field[2-6]. The 2D NMR technique is well-known two-dimensional correlation spectroscopy, which enables us to analyze a complicated NMR spectrum. The same idea of the 2D spectroscopy can be extended to vibrational state and electronic state. However, the time scale of free induction decay of these states are much smaller than that in the NMR experiment, ultrashort pulses with corresponding frequencies are required. We are going to make a brief review on recent development of both theoretical and experimental studies on the optical two-dimensional spectroscopy.

1. Farrer, R. A.; Loughnane, B. L.; Fourkas, J. T., *J. Chem. Phys. A*, 1997, **101**, 4005.
2. Tanimura, Y.; Mukamel, S., *J. Chem. Phys.* 1993, **99**, 9496.
3. Tominaga, K.; Yoshihara, K., *Phys. Rev. Lett.* 1995, **74**, 3061.
4. Tokmakoff, A.; Fleming, G. R., *J. Chem. Phys.* 1997, **106**, 2569.
5. Steffen, T., Duppen, K., *Phys. Rev. Lett.* 1996, **76**, 1224.
6. Hybl, J. D.; Albrecht, A. W.; Gallagher Faeder, S. M.; Jonas, D. M.; *Chem. Phys. Lett.* 1998, **297**, 307.

Solvent dependence of the ultrafast ground state recovery dynamics of triphenylmethane dyes.

Yutaka Nagasawa, Yoshito Ando, and Tadashi Okada
Department of Chemistry, Graduate School of Engineering Science, Osaka University
1-3 Machikaneyama, Toyonaka, Osaka, 560-8531, Japan

Triphenylmethane dyes are known to have remarkably short S_1 excited state lifetime in solution. Torsional motion of the phenyl group is said to be involved in the radiationless relaxation process since the ralaxation becomes faster in lower viscosity solvents. We have measured ultrafast ground state recovery of a dye, Brilliant Green (BG), by single wavelength pump-probe spectroscopy at 635 nm. The SHG of the home-made cavity-dumped Kerr lens mode-locked Cr: forsterite laser at 635 nm with pulse duration of 33 fs was used for the experiment. To our knowledge, this is the shortest pulse ever generated from a cavity-dumped Cr: forsterite laser.

As seen in the figure below, the decay of the signal is highly nonexponential and depends on solvent viscosity as expected. Normally, single wavelength pump-probe signal includes (a) ground state bleach, (b) excited state absorption, (c) stimulated emission, and (d) impulsive-stimulated resonance Raman scattering. Here we ignore the effect of (b), since similar dye is used as a saturable absorber and the anisotropy of BG starts from 0.4. The quantum beats are the effect of (d) of an intramolecular vibration of BG around 210 cm^{-1}. The fastest decay occurs within 100 fs which is due to ultrafast intramolecular relaxation and the solvent inertial response. For slower decays, more than double exponential components were necessary to fit the data. We also observed a plateau or a rising component in the signal which may indicate an existance of an intermediate state. When the molecule is excited to its Franck-Condon state, it may have to relax to a different solvent configuration or to an isomer in either excited or ground state before coming back to its original state. Interestingly, this ultrashort rise time showed linear viscosity dependence which was unexpected for such ultrafast dynamics.

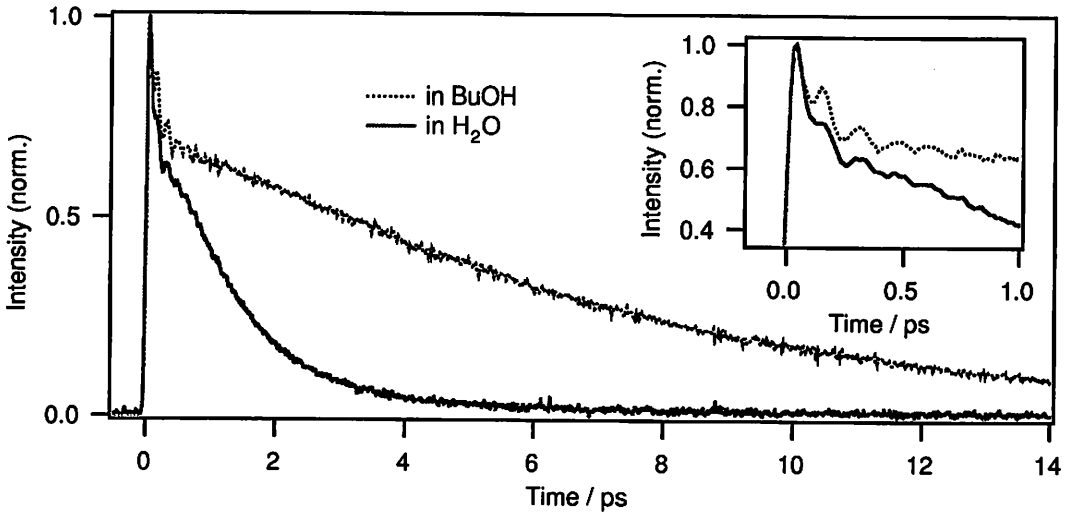

Figure. Normalized single wavelength pump-probe signal of Brilliant Green in butanol and water measured at 635 nm with magic angle configuration. The inset shows the beating part of the signal.

THE REDOX CHEMISTRY OF HEXARHENIUM-SULFUR CLUSTER COMPLEXES

Takashi YOSHIMURA, and Yoichi SASAKI
Division of Chemistry, Graduate School of Science, Hokkaido University, Kita-ku, Sapporo 060-0810, Japan

Since the discovery of an easily accessible preparation method of the face capped octahedral hexarhenium(III) clusters with $Re_6(\mu_3\text{-}E)_8$ core (E = S, Se, Te), their chemistry has developed rapidly both with respect to the synthesis of new complexes and their properties. However, the information of the redox chemistry of these complexes is virtually unknown. We are interested in these complexes as they should have rich redox properties.

Herein, we report the redox properties of mixed-terminal ligand complexes, $[Re_6S_8Cl_{6-n}(L)_n]^{(4-n)-}$ (L = pyridine (py), n = 2-4; L = pyradine (pz), 4-cyanopyridine (cpy), 4,4'-bipyridine (bpy), 4-methylpyridine (mpy), 4-(dimethylamino)pyridine (dmap) , n=2) including geometrical isomers for n = 2 and the ligand-ligand redox interaction through the cluster core for the complexes with redox active pz, cpy, and bpy ligands occupying the terminal sites.

Redox potentials of the mixed ligand complexes. The one-electron oxidation potential for the $Re^{III}_6/Re^{III}_5Re^{IV}$ process of *cis*- and *trans*-$[Re_6S_8Cl_4(py)_2]^{2-}$ and *mer*-$[Re_6S_8Cl_3(py)_3]^-$ are observed at 0.77 and 0.97 V vs Ag/AgCl, respectively, indicating that replacement of the chloride by more basic py makes the hexarhenium core more difficult to be oxidized. The plot of pK_a of the ligands and $E_{1/2}$ for the series of the complexes with n = 2 is linear.

Electron self-exchange between $[Re_6S_8Cl_4(cpy)_2]^{2-}$ and $[Re_6S_8Cl_4(cpy)_2]^-$. Variable temperature ^1H NMR spectra (-90 to +20°C, CD_2Cl_2) of the 1:1 mixture $[Re_6S_8Cl_4(cpy)_2]^{2-}$ and $[Re_6S_8Cl_4(cpy)_2]^-$ shows the exchange behavior. The activation parameters are $\Delta H^{\ddagger}$ = 30.2 ± 2.1 $KJmol^{-1}$ and $\Delta S^{\ddagger}$ = 30 ± $JK^{-1}mol^{-1}$. The second-order rate constant at 298.2 K is 1.2×10^9 $M^{-1}s^{-1}$. The small activation energy is due to small structural difference between the two oxidation states.

Ligand-ligand interaction through the cluster core. The *cis*-, *trans*-$[Re_6S_8Cl_4(L)_2]^{2-}$ (L = pz, cpy, bpy) show ligand centered redox waves ($L \rightarrow L^{\bullet-}$), which split into two one-electron steps. The extent of the peak separation as observed by diffential pulse-voltammetry depend on the kind of the ligand and its coordination geometry. The split for *trans*-$[Re_6S_8Cl_4(bpy)_2]^{2-}$ is comparable to that estimated for the statistical potential difference in noninteracting redox active centers ($\Delta E_{1/2}$ = 36mV), while those for other species apparently exceed the value, indicating the ligand-ligand interaction through hexarhenium core.

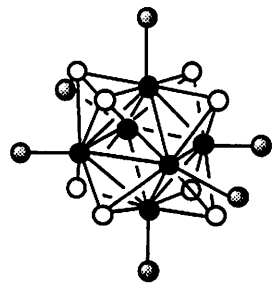

HYDROLYSIS AND SELF-ASSOCIATIONS OF BIS(HEXYL-ETHYLENEDIAMINE)ZINC(II) COMPLEX IN MIXED WATER/ ORGANIC SOLVENTS

Masayasu IIDA,* Keiko ASAYAMA, and Asami GOTOH
Department of Chemistry, Nara Women's University, Nara 630-8506 JAPAN

We have prepared double-chained surfactant of bis(hexylethylenediamine)zinc(II) chloride(= $Zn(HE)_2Cl_2$). Although this surfactant is readily dissolved in water as well as in polar organic solvents such as methanol, ethanol, and chloroform, it is immediately precipitated in water due to a hydrolytic polymerization. However, the hydrolysis does not occur at the concentrations above 0.25 mol/kg in water. In this concentration range, the surfactants extensively aggregate and the aggregation will be favorable to protect the hydrolysis. The hydrolysis was also prevented with an addition of small amounts of alcohols such as methanol, ethanol, propanol and iso-propanol. The prevention of hydrolysis was more effective by the alcohols having more carbons. We described ternary phase diagrams for the stable and transparent solution regions composed of $Zn(HE)_2Cl_2/H_2O$/Organic Solvents. The aggregation behavior was studied using multinuclear NMR relaxation methods, ^1H NMR pulsed field gradient spin-echo(PGSE) method, and vapor pressure osmometry(VPO) in water, methanol, ethanol, chloroform, and water/organic (methanol, ethanol, or chloroform) mixed solvent systems. The extent of the aggregations increased with an increase in the water fraction in the water/alcohol systems. In these systems, water and surfactant tend to move independently. On the other hand, in the water/chloroform system, reversed micelles may be formed and the water molecules tend to move together with the surfactant.

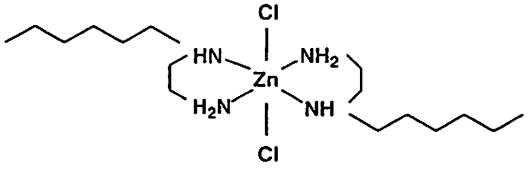

Figure 1. $Zn(HE)_2Cl_2$ Molecule

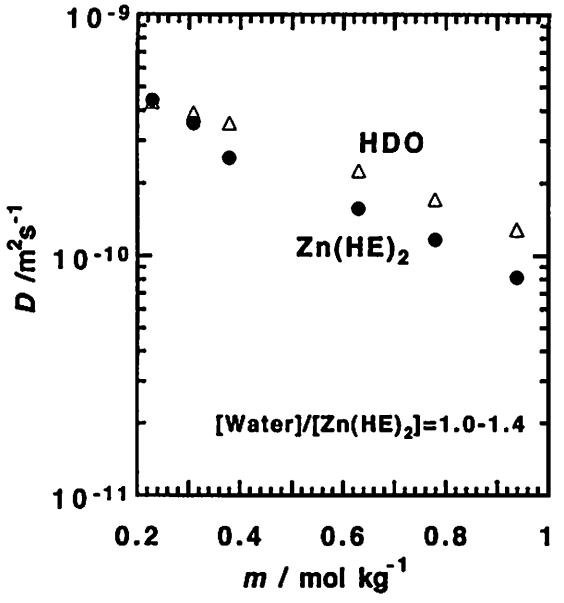

Figure 2. Self-diffusion Coefficients of Water and Surfactant as a Function of Surfactant Concentrations in Water/Chloroform System.

^{1}H-NMR STUDY OF SELECTIVE HYDRATION OF ANIONS IN NITROBENZENE

T. OSAKAI[1], M. HOSHINO[2], M. IZUMI[1], M. KAWAKAMI[2] and K. AKASAKA[2]

[1] Department of Chemistry, Faculty of Science, Kobe University, Nada, Kobe 657-8501, Japan

[2] Graduate School of Science and Technology, Kobe University, Nada, Kobe 657-8501, Japan

Selective hydration of hydrophilic ions in " water-immiscible" organic solvents is a key concept intimately related to ion-transfer processes taking place in solvent extraction, membrane transport, ion-selective electrodes, and cell membranes. It also has a fundamental significance for understanding a role of water molecules in hydrophobic cores in proteins. In this study, we have carried out 400 MHz ^{1}H-NMR measurements for selective hydration of inorganic anions (X^- = Cl^-, Br^-, I^-, NO_3^-, ClO_4^-, SCN^-) in deuterated nitrobenzene (NB-d_5).

Samples for the NMR measurements were prepared by adding stepwise an aliquot of water to a NB-d_5 solution of a tetraalkylammonium salt of X^-. The sample preparation and NMR measurements were carried out at 25 ℃.

Since the exchange of water molecules associated and unassociated with X^- is very fast, the water protons always appeared as a single signal. The chemical sift (δ) changed to lower magnetic fields in the order: $ClO_4^- < I^- < SCN^- < NO_3^- < Br^- < Cl^-$, showing that the ion–water interaction becomes stronger in this order. This sequence agrees well with that of the Gibbs energy of transfer of the ions across the nitrobenzene/water interface. [1] It was also found that the value of δ for every anion depended on concentrations of the ion and water added to NB-d_5, as shown for Br^- in the figure. The dependence could be elucidated not by a one-step reaction mechanism (*i.e.*, $Br^- \rightarrow Br^-(H_2O)_2$), but by a consecutive reactions mechanism ($Br^- \rightarrow Br^-(H_2O) \rightarrow Br^-(H_2O)_2 \rightarrow Br^-(H_2O)_3 \rightarrow Br^-(H_2O)_4$). The simulation curves for the former and latter mechanisms are also shown by broken and solid lines, respectively. The hydration numbers of the anions, which were calculated using the consecutive hydration constants determined, agreed well with those determined by solvent-extraction experiments with the Karl-Fisher method.[2] We will also report the orientational correlation times of water which were obtained by measurements of the spin-lattice relaxation times.

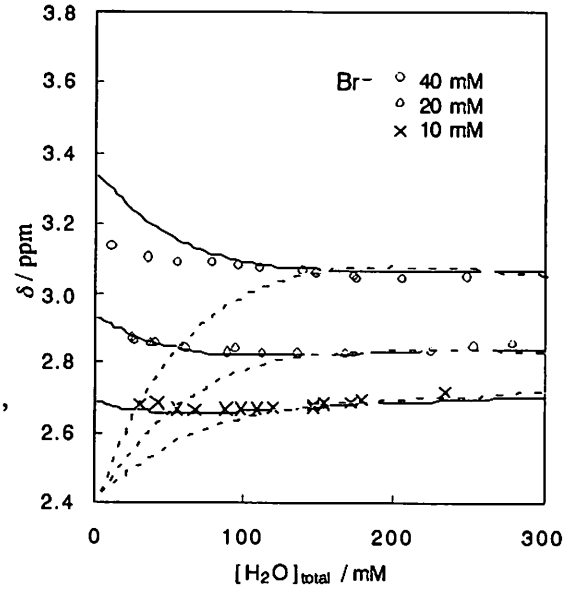

1. T. Osakai, K. Ebina, *J. Phys. Chem. B*, 1998, **102**, 5691.

2. T. Osakai, A. Ogata, K. Ebina, *J. Phys. Chem. B*, 1997, **101**, 8341.

LUMINESCENCE STUDY ON SOLVATION OF LANTHANIDE(III) AND ACTINIDE(III) IONS IN NONAQUEOUS AND MIXED SOLVENTS

Takaumi KIMURA, Ryuji NAGAISHI, Yoshiharu KATO and Zenko YOSHIDA
Advanced Science Research Center, Japan Atomic Energy Research Institute,
Tokai-mura, Ibaraki 319-1195, Japan

The relationship between the luminescence decay constant k_{obs} (i.e., the reciprocal of the excited state lifetime) and the inner-sphere hydration number N_{H2O} (i.e., the number of water molecules in the first coordination sphere) of trivalent lanthanide[Ln][1,2] and actinide[An][2,3] ions has been investigated by Time-Resolved Laser-induced Fluorescence Spectroscopy (TRLFS). The linear correlation of the k_{obs} *vs.* N_{H2O} has been derived and applied successfully for studies on hydration states of Ln(III) and An(III) in various aqueous solutions. In this study, the luminescence lifetimes of Ln(III) and An(III) were measured to evaluate the quenching behavior in nonaqueous solvents and the preferential solvation in mixed solvents.

The luminescence lifetimes of Ln(III)[Ln=Nd, Sm, Eu, Tb, Dy] and An(III)[An=Am, Cm] were measured in dimethylsulfoxide(DMSO), N,N-dimethylformamide(DMF), methanol(MeOH), and water. The luminescence lifetimes in perprotonated and perdeuterated solvents, i.e., τ_H and τ_D, decreased with decreasing energy gap ΔE (Cm>Tb>Eu>Sm>Dy>Nd>Am), respectively for Ln(III) and An(III), where the ΔE is defined as the difference in energy between the emitting state and the next lower lying state. Nonradiative decay rate due to the solvent was estimated from τ_H and τ_D by $1/\tau_H - 1/\tau_D$ and showed the order of the rate, i.e., water>MeOH>DMF>DMSO, indicating that O-H vibrator is more effective quencher than C-H, C=O, and S=O vibrators in the solvent molecules. Maximal lifetime ratios τ_D/τ_H were obtained for Eu(III) in water, for Sm(III) in MeOH and DMF, and for Sm(III) and Dy(III) in DMSO. The ratios τ_D/τ_H are correlated well with the values $\Delta E/\nu$, where ν is the stretching wave number of O-H(D) and/or C-H(D) vibrators of the solvent molecules.

The solvent composition in the first coordination sphere of Ln(III) and An(III) in binary mixed solvents was also investigated by measuring the luminescence lifetime. The N_{H2O} of Ln(III) and An(III) in DMSO-water, DMF-water, and MeOH-water systems were calculated from the luminescence lifetime. Ln(III) and An(III) were preferentially solvated by DMSO in DMSO-water, by DMF in DMF-water, and by water in MeOH-water over the whole range of the solvent composition in the bulk mixtures. The degree of preferential solvation varied considerably with the bulk composition in all the systems. The order of the preferential solvation, i.e., DMSO>DMF> water>MeOH, is in agreement with the relative basicity of these solvents.

1. Kimura, T.; Kato, Y., *J. Alloys Compounds*, 1998, **275-277**, 806.
2. Kimura, T.; Kato, Y., *J. Alloys Compounds*, 1998, **271-273**, 867.
3. Kimura, T.; Choppin, G.R., *J. Alloys Compounds*, 1994, **213/214**, 313.

Inflection Points in the Coordination Number around Ce^{3+} and CeF^{2+} in the Mixed System of Methanol and Water

Hideo SUGANUMA, Makoto ARISAKA, and Naoko TAKUWA

Radiochemistry Research Laboratory, Faculty of Science, Shizuoka University, 836 Ooya, Shizuoka-shi, 422-8529, Japan

The variation in the coordination numbers around Ce(Ⅲ) for Ce^{3+} and CeF^{2+} in the mixed CH_3OH+H_2O solution was examined on the basis of the variation in the stability constants of $CeCl^{2+}$ (monochloride solvent-shared ion-pair) and CeF^{2+} (monofluoro complex).

The stability constants ($\beta_{1(F)}$) of CeF^{2+} and those ($\beta_{1(Cl)}$) of $CeCl^{2+}$ have been determined at 0.10 and 1.00 mol dm^{-3} ionic strengths, respectively. The variation in the Ce^{3+}-Cl^- distance, which was calculated using the Born-type equation and the Gibbs' free energy derived from $\beta_{1(Cl)}$ [1], indicated a change in the coordination number (CN) of Ce^{3+} from CN = 9 to a mixture of CN = 9 and 8 in the vicinity of the mole fraction of methanol (X_s) = 0.23. The variation in ln $\beta_{1(F)}$ [2] with an increase in X_s in the mixed solvent system showed an acute-angled convex inflection point at X_s = about 0.22 and an acute-angled concave inflection point in the vicinity of X_s=0.28. It was concluded that the convex inflection point denoted the same change in the CN of Ce^{3+} from CN = 9 to a mixture of CN = 9 and 8 and the concave point was a change in the CN of Ce(Ⅲ) in CeF^{2+} from CN = 9 to a mixture of CN = 9 and 8.

1. Suganuma, H.; Nakamura, M.; Katoh, T.; Satoh, I.; Omori, T., *J. Radioanal. Nucl. Chem.*,. **223**, 167(1997). 2. Suganuma, H.; Arisaka, M.; Satoh, I.; Omori, T.; Choppin, G. R., *Radiochim. Acta*, **83**, 153 (1998).

Densimetric and calorimetric studies of binary and ternary systems (Water / Dioxane / $NaB(Ph)_4$) "Clathrate" effect and preferential solvation of $B(Ph)_4^-$

J. M'HALLA and S. M'HALLA

Laboratoire d'Electrochimie des solutions, Faculté des Sciences, 5000 Monastir, Tunisie.

In this work we experimentally studied the variation of partial molal volumes and relative partial molal enthalpies of $NaB(Ph)_4$, water and dioxane with the weight-fraction P_D of dioxane ($0 \leq P_D \leq 20\%$) and with the molality m of the salt ($0 \leq m \leq 0.4$) at 25°C and P = 1atm. We also partly achieved the same work for some binary and ternary systems : NaCl / Water / Dioxane, in order to show "clathrate" and preferential solvation effects of $B(Ph)_4^-$. This study shows:

a)- A molecule of dioxane locks into the hexagonal hydrogen bond network of water so that the volume effects remain weak. Each dioxane molecule is surrounded by 8 water molecules, whereas a water molecule is surrounded by 4 H_2O or 3 H_2O and 1 dioxane molecule.

b)- $B(Ph)_4^-$ reinforces the water "clathrate" structure in its vicinity.

c)- Preferential solvation of $B(Ph)_4^-$ by dioxane occurs even at low P_D : $B(Ph)_4^-$ is solvated respectively by 2,3,4 and 5 molecules of dioxane for P_D = 5,10,15 and 20% and it remains hydrated by 2 water molecules for $P_D \leq 20\%$; while Na^+ remains hydrated by 4 water molecules without any dioxane molecules in its first solvation shell. These results agree with those obtained by NMR spectroscopic studies and Ion-solvant mutual transport.

d)- Partial enthalpy of transfer of $NaB(Ph)_4$ at infinite dilution is > 0 whereas partial molal free enthalpy of transfer is < 0 for $P_D \leq 20\%$. So that the irreversible transfer of $B(Ph)_4^-$ from pure water to dioxane-water mixtures ($P_D \leq 20\%$) is due to a positive entropy variation corresponding essentially to the "fusion " of the water "clathrate " structure surrounding $B(Ph)_4^-$.

Effect of pressure on the $\nu_1+\nu_3$ and $\nu_2+\nu_3$ combination bands of water by FT-NIR spectroscopy

Minoru KATO, Hironori KOYAMA, and Yoshihiro TANIGUCHI
Department of Chemistry, Faculty of Science and Engineering, Ritsumeikan University, Kusatsu, Shiga 525-8577, Japan

The effect of pressure on microscopic property of water is of interest since water shows anomalous behaviors of the various dynamic properties upon compression in the temperature range of 0 to approximately 30 °C; for example, the viscosity indicates a minimum at a certain moderate pressure. Vibrational spectroscopies are powerful methods for microscopic studies of water since some vibrational modes prove the strength of hydrogen bond; the frequency of OH stretching mode is well known to be decrease with the strength of hydrogen bond. Near-infrared (NIR) spectroscopy is a unique technique to investigate overtone and combination modes of water, since Raman scattering is extremely weak. There have been several NIR works using dispersive spectrometers. Here we report the effect of pressure on $\nu_1+\nu_3$ and $\nu_2+\nu_3$ combination mode using a Fourier-transform (FT) spectrometer, which provide an accurate peak position determination and a large measurement region.

Near infrared spectra were recorded on Perkin-Elmer Spectrum 2000 FT-IR Spectrometer with TGS detector giving the spectral resolution of 4 cm^{-1}. For each spectrum, 100 interferogams were Fourier-transformed. The diamond anvil cell was used for high-pressure measurements. The pressure of the cell was monitored by the ruby R-line method with error of 30 MPa.

We measured the $\nu_1+\nu_3$ and $\nu_2+\nu_3$ bands under high pressure at various temperatures. Pressure dependencies of both the bands at 313 K shows monotonous decreases in the peak frequencies, indicating -0.053±0.006 cm^{-1}/MPa for $\nu_1+\nu_3$ and -0.020±0.001 cm^{-1}/MPa for $\nu_2+\nu_3$. Walrafen group reported pressure dependencies of fundamental modes: -0.037 cm^{-1}/MPa[1] for the OH stretching band of HOD at 301 K whereas the frequency of ν_2 is nearly independent of pressure at 305 K.[2] Assuming the pressure dependencies of the frequency of combination modes are given by the sum of those of the fundamental modes, we obtained –0.033 cm^{-1}/MPa for ν_1 and –0.020 cm^{-1}/MPa for ν_2, which are comparable with the value for the OH stretching mode. At lower temperatures below 303 K we observed interesting behaviors: with increasing pressure the frequency of $\nu_1+\nu_3$ increases in relatively low pressure region (~300 MPa) and decreases over the pressure, whereas the $\nu_2+\nu_3$ does not show such anomalous behavior. This suggests the frequencies of the ν_1 and ν_3 modes reflect different aspects of the nature of hydrogen bond of water.

1. Walrafen, G. E., *J. Sol. Chem.*, 1973, **2**, 159.
2. Walrafen, G. E.; Abebe, M., *J. Chem. Phys.*, 1978, **68** 4694.

EFFECTS OF PRESSURE AND TEMPERATURE ON THE SOLUBILITY OF NAPHTHALENE IN WATER

Hirotaka YAMASAKI and Seiji SAWAMURA
Department of Chemistry, Ritsumeikan University, Kusatsu, Shiga, 525-8577, Japan

In the previous study, high-pressure solubility of naphthalene in water was measured at 298.2 K and pressures up to 200 MPa and the volume change for a transfer of the solute from hydrophobic solvent to water was estimated to be nearly zero contrary to the negative values generally known to the volume change accompanying the hydrophobic hydraion.[1,2] In the present work, the high-pressure solubility was measured again to confirm the previous rezults shown above using another type of high-pressure vessel and both temperature and pressure regions for the measurement were extended to 273.15-318.15 K and 0.10-300 MPa, respectively.

Previous high-pressure vessel is a piston-cylinder type with a valve. After the saturated solution was prepared using the vessel, the sample solution was taken out from it and the concentration was measured using a UV spectrophotometer. On the other hand, an optical high-pressure vessel[3] was used in the present work. After the saturated solution was prepared in the vessel, the UV spectrum was directly measured at high pressure through the optical windows of the vessel. As a result, the solubility in the present work well coincided with the previous one and supported that the volume change accompanying the hydrophobic hydration of naphthtalene is not so negative as those of alkyl chains.

The volume change accompanying the dissolution of the naphthalene in water was estimated from the pressure coefficient of the solubility and the partial molar volume of the solute in water was estimated using the molar volume of the solid solute. It increases with increasing temperature and the coefficient was estimated to be 1.3×10^{-3} K^{-1}, which is similar to those for alkylbenzenes or alkyl chain, 1.1×10^{-3} -1.35×10^{-3} K^{-1}, though the volume changes accompanying these hydrophobic hydration clearly differ from each other.

1. Sawamura, S.; Tsuchiya, M.; Ishigami, T.; Taniguchi, Y.; Suzuki, K., *J. Solution Chem.*, 1993, **22**, 727.
2. Sawamura, S., *J. Solution Chem.*, to be submitted.
3. Sawamura, S.; Kitamura, K.; Taniguchi, Y., *J. Phys. Chem.*, 1989, **93**, 4931.

VOLUMETRIC PROPERTY OF HYDROPHOBIC HYDRATION FOR ALKYLBENZENES AT HIGH PRESSURE

Seiji SAWAMURA

Department of Chemistry, Ritsumeikan University, Kusatsu, Shiga, 525-8577, Japan

From the measurements of the high-pressure solubility of alkylbenzenes, *i. e.*, toluene, ethylbenzene, and n-propylbenzene, in water and the compression of these pure alkylbenzenes, the volume change accompanying the dissolution of the solutes in water and the molar volume of the pure solutes were estimated respectively. And then the partial molar volume of alkylbenzenes in water was estimated in the range of 273.2−323.2 K and 0.10−400 MPa using these data. The obtained surface of the partial molar volume as a function of pressure and temaprature is considerably distorted in the region of low temperature and pressure. It was previously observed that the partial molar volume increased with increasing pressure to 100 MPa having a negative compressibility at 298.2 K.[1] Present result shows that the phenomenon becomes remarkable at low temperature. The partial molar volume increases with increasing temperature at 0.10 MPa and the expansion coefficient is estimated to be 1.1×10^{-3} K^{-1}. It does not differ from those of organic solvents, $1\times10^{-3}-2\times10^{-3}$ K^{-1} but the sinking of the partial molar volume in the low temperature and pressure region suggests that the expansion coefficient is anomalously large compared with that in high-pressure region. These expansions of the partial molar volume with increasing both temperature and pressure are ascribed to a property of the bulk water whose structure consists of self-association by hydrogen bonding and have a vacant space easy to be broken by pressure and heating. In other words, hydration water is not so vacant nor compressible as the pure water.

1. Sawamura, S.; Kitamura, K.; Taniguchi, Y., *J. Phys. Chem.*, 1989, **93**, 4931.

THE STRUCTURE OF AQUEOUS SOLUTIONS OF TERTIARY BUTANOL

John L. FINNEY[1], Daniel T. BOWRON[2], and Alan K. SOPER[3]

[1]Department of Physics and Astronomy, University College London, Gower Street, London WC1E 6BT, UK

[2]European Synchrotron Radiation Facility, BP 220, 38043 Grenoble Cedex, France

[3]Rutherford Appleton Laboratory, Chilton, Didcot, Oxon OX11 0QX, UK

Using neutron diffraction with isotopic substitution, the structures of aqueous solutions of tertiary butanol have been studied as functions of temperature and pressure. As the behaviour of this system is thought to be driven by hydrophobic interactions, particular attention has been paid to the hydration of the non-polar headgroups and the nature of the intermolecular contacts. The results have been interpreted using the recently developed Empirical Potential Structure Refinement Technique.

As concentration is increased from 0.06 to 0.16 mole fraction tertiary butanol, there is clear evidence for the growth of small clusters of the alcohol molecules, with butanol-butanol co-ordination numbers of 2 to 3 even at the lowest concentration. Orientational pair correlation functions show that the dominant intermolecular contacts between alcohol molecules are between the non-polar head groups, as would be expected for a system whose behaviour is thought to be driven by hydrophobic interactions. As concentration increases, however, there is evidence of mixed polar - nonpolar contacts. The alcohol group's hydrogen bonding requirements appear to be fully met by polar contacts with water molecules: there is no evidence for significant butanol-butanol hydrogen bonding. In comparison, similar measurements in pure liquid t-butanol show significant hydrogen bonding between the alcohol OH groups of neighbouring molecules.

A HYDRATION MECHANISM OF THE ALKYL GROUPS IN ACETONE, DMSO, *tert*-BUTANOL, AND 1,4-DIOXANE

Kazuko MIZUNO
Center for Instrumental Analysis, Fukui University, Fukui 910-8507, Japan

The blueshifts of the C—H stretching band of methyl group were observed on diluting alcohols, acetone, DMSO, dioxane, amines, etc. with water.[1,2] The cause of the blueshifts on a molecular level, however, has not been still presented.[2] We found that the solvation by alcohols do not affect the frequencies of the bands,[3] but that the blueshifts are characteristic of the solvation by water. The blueshifts indicate the electronic depolarization of the C—H bonds, whereas hydration of a solute usually implies an increase in the intramolecular polarization of the solute. Consequently, the blueshifts are contrary to the implication. Thus, we have become to consider that we may reveal the hydration mechanism of the alkyl groups by finding the cause of the blueshifts of the band.[3]

Experiments.

The concentration and the temperature dependences of ^{1}H and ^{13}C chemical shifts in NMR of aqueous binary mixtures of acetone, DMSO, *tert*-butanol, and 1,4-dioxane were studied, together with the concentration dependences of the frequencies of the C—H stretching vibration bands in the IR spectra of the solutes. ^{1}H and ^{13}C chemical shifts were measured by the external double reference method using a capillary with a blown-out sphere at the bottom for tetramethysilane as the external reference substance.[3]

Results and Discussion

On diluting the solutes with water, both the frequencies for the C—H vibration bands of the solutes, ν_{C-H}, and the chemical shift of water protons, δ_{H2O}, increased depending on the concentration almost the same. The chemical shifts of C—H protons also increased slightly.

These results show that the blueshifts of the C—H band may be correlated with the change in the polarization of the water molecules, which increases with increasing water content. The results can be explained satisfactorily by considering that a part of the electron about the C—H proton is pushed out into the C—H bond due to a repulsive interaction between the C—H hydrogen and water oxygen to be denoted as C—H•••OH_2(•••OH_2)$_n$, where OH_2(•••OH_2)$_n$ expresses water molecules hydrogen-bonded cooperatively. The hydrogen-bonding property of the hydrophilic groups in the solutes, >C=O, >S=O, —OH, and —O—, are found to be a predominant factor determining the concentration dependences of ν_{C-H} and δ_{H2O}.

1. Carius, W.: Mockel, K.: Schroter, O.: Thomzik, D., *Z. Phys. Chemie, Leipzig* 1982, **263**, 209.
2. Kamogawa, K.; Kaminaka, S.; Kitagawa, T., *J. Phys. Chem.*, 1987, **91**, 222.
3. Mizuno, K.: Ochi, T.: Shindo, Y., *J. Chem. Phys.*, 1998, **109**, 9502.

Authors Index